

**NASA Contractor Report 181762
DOT/FAA/PS-88/19**

**Analysis of Doppler Radar
Windshear Data**

**(NASA-CR-181762) ANALYSIS OF DOPPLER RADAR
WINDSHEAR DATA Final Report (Sierra Nevada
(cyp.) 189 p CSCl 01C**

N89-20111

**G3/03 Unclassified
 01972E6**

F. Williams, P. McKinney, and F. Ozmen

**Sierra Nevada Corporation
P.O. Box 6900
Reno, NV 89513**

**Contract NAS1-18598
January 1989**



National Aeronautics and
Space Administration

**Langley Research Center
Hampton, Virginia 23665-5225**



TABLE OF CONTENTS

I.	Introduction	1
II.	Objectives	1
1.	Collect Lincoln Laboratory Data For Multiple Events ..	1
2.	Characterize Events And Quantify Key Parameters	2
3.	Obtain Insight Into Lincoln Lab Data Processing Algorithms	2
4.	Perform New Analysis (Correlation Analysis And F- factor)	2
III.	Work Carried Out	3
1.	Obtaining Data	3
2.	Isolating Events	4
3.	Analyzing All Available Data	5
4.	Analyzing Event Data	5
i)	Velocity Profiles	5
ii)	Histogram Analysis	6
iii)	F-factor Profiles and Histograms	6
iv)	Correlation Analysis	6
5.	Interacting With Lincoln Lab Personnel	7
IV.	Results	7
1.	Velocity Profiles	7
2.	Histogram Analysis	9
3.	F-factor Analysis	9
4.	Correlation Analysis	10
V.	Conclusions	10
1.	Comparing Event vs. Non-Event Data	10
2.	Trends Evident In Correlation Analysis	11
i)	SW vs. DZ	11
ii)	SW vs. Range	11
iii)	DZ, SN vs. Range	11
VI.	Recommendations	12
	Appendix A	79

List of Figures

1.	Lincoln Lab Event Description Table	13
2.	Event Data Supplied by Lincoln Lab	14
3.	Radar Parameters Table	15
4.	Event Location Table	16
5.	Color Plot, VE PPI, Event 4	17
6.	Color Plot, SW PPI, Event 4	18
7.	Color Plot, DZ PPI, Event 4	19
8.	Color Plot, SN PPI, Event 4	20
9.	Color Plot, Az=242, Event 4	21
10.	Color Plot, Az=243, Event 4	22
11.	Color Plot, Az=244, Event 4	23
12.	Color Plot, Az=245, Event 4	24
13.	Event 1a-1b Velocity Profiles	25
14.	Event 1c-1 Velocity Profiles	26
15.	Event 2a-2b Velocity Profiles	27
16.	Event 2 Velocity Profiles	28
17.	Event 3a-3b Velocity Profiles	29
18.	Event 3c-3 Velocity Profiles	30
19.	Event 4a-4b Velocity Profiles	31
20.	Event 4c-4 Velocity Profiles	32
21.	Event 5a-5b Velocity Profiles	33
22.	Event 5 Velocity Profiles	34
23.	Event 6a-6b Velocity Profiles	35
24.	Event 6 Velocity Profiles	36
25.	Event 7a-7b Velocity Profiles	37
26.	Event 7c-7d Velocity Profiles	38
27.	Event 7e-7 Velocity Profiles	39
28.	Event 7 Gust Front Examples	40
29.	Peak to Peak Strength Calculations	41
30.	Moving Average Shear Strength Calculation	42
31.	Instantaneous Shear Strength Calculation	43
32.	Non Event Data Histograms	44
33.	Events 1-6 Histograms	45
34.	Mean Data Field Values	46
35.	1st 4 Moments, VE Data	47
36.	1st 4 Moments, SW Data	48
37.	1st 4 Moments, DZ Data	49
38.	1st 4 Moments, SN Data	50
39.	Instantaneous F-factor, No Avg., Event 1	51
40.	Instantaneous F-factor, No Avg., Event 2	52
41.	Instantaneous F-factor, No Avg., Event 3	53
42.	Instantaneous F-factor, No Avg., Event 4	54
43.	Instantaneous F-factor, No Avg., Event 5	55
44.	Instantaneous F-factor, No Avg., Event 6	56
45.	Instantaneous F-factor, No Avg., Event 7	57
46.	Instantaneous F-factor, No Avg., Event 7e	58

List of Figures, Continued

47.	F-factor Histograms, Event 1	59
48.	F-factor Histograms, Event 2	60
49.	F-factor Histograms, Event 3	61
50.	F-factor Histograms, Event 4	62
51.	F-factor Histograms, Event 5	63
52.	F-factor Histograms, Event 6	64
53.	F-factor Histograms, Event 7	65
54.	F-factor Histograms, Event 7e	66
55.	Summary of Correlation Analysis	67
56.	Correlations Plots, Event 1	68
57.	Correlations Plots, Event 2	69
58.	Correlations Plots, Event 3	70
59.	Correlations Plots, Event 4	71
60.	Correlations Plots, Event 5	72
61.	Correlations Plots, Event 6	73
62.	Correlations Plots, Event 7	74
63.	Correlations Plots, All Events	75
64.	Correlations Plots, All Events	76
65.	VE, SW vs. Event Size	77
66.	Event Description Table	78

I. Introduction

The purpose of this program is to perform a statistical analysis of data obtained by MIT Lincoln Laboratory during FLOWS testing at Huntsville, Alabama, in the summer of 1986. The data that was provided by Lincoln Laboratory included mean velocity estimates, spectral width estimates, reflectivity estimates, signal to noise ratio and other key radar parameters. The analysis performed included an evaluation of windshear event spectral characteristics, a statistical summary of the events examined, a correlation analysis among different data fields, and estimation of F-factor for all isolated events. Seven distinct meteorological events were examined, six representative of microburst activity and one representative of gust front activity.

The motivation for such analysis arises from conflicting reports regarding the spectral characteristics of windshear events. In particular, the spectral width estimates are said to lie anywhere from 1 m/s to 4 m/s. As large spectral widths can significantly degrade many processing algorithm's performance, it is important to try to add statistical validity to preliminary results already obtained. An analysis of a single near event as part of a separate SBIR Phase I effort yielded an average spectral width estimate of 1.5 m/s for events¹.

II. Objectives

1. Collect Lincoln Laboratory Data For Multiple Events

The objective of this analysis is to process Lincoln Laboratory doppler radar data to characterize windshear events. The processing includes plotting velocity and F-factor profiles, histogram analysis to summarize statistics, and correlation analysis to demonstrate any correlation between different data fields. The data fields examined include velocity, spectral width, signal to noise ratio and reflectivity.

The first objective in performing the analysis is to obtain data from Lincoln Laboratory. The data was collected using the FL-2 radar in Huntsville, Alabama as part of FLOWS testing during the summer of 1986. A principle objective in trying to add statistical validity to preliminary results is to examine multiple events where each event represents as strong an event as is available. In addition, it is desirable for the events to be well distributed in terms of range from the radar, reflectivity and size.

1. Airborne Weather Radar For Windshear Warning, SBIR Phase I Final Report, Sierra Nevada Corp., F. Williams, 10 July 1987

2. Characterize Events And Quantify Key Parameters

Once the data is obtained, the next objective is to isolate the events. This objective involves more than simply examining the data at the documented time and location, as the available documentation only gives a coarse location during one snapshot of the event's evolution. Each event has multiple scans, at different times, during the event's development. Adding to the difficulty is the large amount of data being examined, and the relatively small portion of the data that contains event activity. For this program, for example, 1.65 GBytes of data were examined to yield less than 50 MBytes of event data, a ratio of only 3%. For these reasons, each meteorological occurrence, an event, is broken down into subevents which have similar characteristics. A **subevent** is a set of well matched rays scanning the event, with similar scan time, azimuth and velocity profile. Velocity profile plots are used to interactively evaluate the shear character of each ray of radar data, and those rays with common profiles, strengths, size, location and time are grouped together as subevents. A **ray** is a single slice of data at any given orientation of the radar. A ray is made up of data points at each range bin, where each data point is a velocity estimate (or other data field) for that range bin. It is estimated that each ray is actually an average of 100 pulsed transmissions from the FL-2 radar.

The primary objective of analyzing the multiple events thus identified is to characterize the spectral width of windshear events, and to compare such estimates with non-event data collected during the same period by the same radar, as well as with preliminary results already obtained. Such a spectral width characterization will help define the turbulent nature of windshear events, which effects the radar signal processing algorithm's ability to calculate accurate velocity estimates, from which shear strength estimates are derived.

A secondary objective is to statistically summarize the range of velocities, reflectivities, signal to noise ratio, F-factor, event size and strength, and other key parameters encountered in windshear events. Such a summarization will add insight into the composition of typical events. These statistics will also be compared to similar results for non-event data.

3. Obtain Insight Into Lincoln Lab Data Processing Algorithms

Another objective is to learn as much as possible from Lincoln Laboratory personnel about their processing technique, including the type of averaging used for data field estimation, the criteria used for calculating event size and strength, and the type of ground clutter filtering used in the FL-2 radar.

4. Perform New Analysis (Correlation Analysis And F-factor)

A final objective is to perform a correlation analysis to demonstrate coupling between different data fields. Such an

analysis shculd demonstrate any dependencies between data fields, and may be used to predict the performance of certain parameters as a function of independent variables.

Included in these analyses is a calculation of F-factor for all identified events and subevents. F-factor is a nondimensional parameter that quantifies the total impact on an aircraft that might encounter the windshear event. F-factor uses both lateral shear estimates as well as downdraft components in its derivation. One approach is to use Range Height Indicator (RHI) color plots at relatively high elevations to calculate the downdraft component of the velocity field using the cosine of the included angle. This crude approach will be attempted in the current analysis.

III. Work Carried Out

1. Obtaining Data

Data comprising nine events with shear strength of 9 m/s/km or greater, covering ranges from 2 km to 60 km, and with a mix of RHI and PPI color plots available, was requested from Lincoln Laboratory. These events are summarized in Figure 1, based on documentation provided by Lincoln Laboratory. Of the nine requested, seven distinct events, with accompanying color PPI and RHI plots, were delivered. The data shortage has been attributed to incorrect information in the documentation supplied to LaRC by Lincoln Laboratory, from which SNC's original request list was generated. According to the technical representative at Lincoln Laboratory that filled SNC's data request, the missing events do not exist. The seven delivered events are summarized in Figure 2, as are the search regions derived from a review of the associated color PPI plots. The seven delivered events cover a range of 3km to 47km, with shear strengths reportedly from 9 m/s/km to 14 m/s/km. The key radar parameters for the FL-2 radar as used during FLOWS testing are summarized in Figure 3. Appendix A includes plots of the scan pattern for each event (azimuth vs. time during event scan periods).

For the seven events analyzed, 20 subevents were identified, with a total of 295 individual azimuth rays. Each subevent averages 42 rays, and each event averages 3 subevents. Note also that for clarity in presentation, within each subevent those rays whose velocity profiles were nearly identical were grouped together, averaged, and plotted as a single line. Thus, although a subevent may average 42 rays of data, the subevent velocity profiles will only show two to four lines. Typically, each line shown on a velocity profile plot is made up of 17 rays of data. Figure 4 summarizes the events locations for the seven events analyzed.

2. Isolating Events

The procedure used to isolate and define the event regions, which for this data comprised less than 3% of the data examined, is outlined below:

- a) Likely areas where events are located are determined based on color PPI plots supplied by Lincoln Laboratory. These designated areas are converted to the SNC data structure and downloaded onto hard disk from tape.

Sample color plots are presented in Figures 5, 6, 7 and 8. These plots show a PPI scan of Event 4, with estimates of velocity, spectral width, reflectivity, and signal to noise ratio, respectively. The event is clearly seen in Figure 5 as the area between the green and red regions of concentrated color, at approximately 20 km and an azimuth of 245 degrees. The different colored regions surrounding a small zero velocity field are indicative of outflow from microburst activity.

- b) Program FILTER examines the designated area and outputs the maximum shear for each ray of data, for all rays whose shear exceeds a minimum threshold input at run time (typically 5 m/s/km). Output includes a filtered window of data demonstrating event trends (as output from a recursive low pass filter, $k=.2$), raw data surrounding the window, and header information. This output is used to more precisely locate the event, in terms of volume and ray numbers (which are needed to search the event data base). The data is also used with color PPI plots and other documentation to verify event location.
- c) Once likely target areas are isolated with FILTER, program FILT_RAY is used to examine these areas more closely. FILT_RAY will output all shear regions that exceed the input threshold, without limiting the number of shear regions per ray. This output is thus much more voluminous than the output from FILTER, and is used to precisely locate the "center" point (in space and time) of the events development.
- d) Once the center point has been determined, data segments of each field are converted to PRO_MATLAB format using GET_DAT. These .MAT files have a limitation of 8188 elements, and as such GET_DAT converts 4143 elements from either side of the isolated center point. In this case, "on either side" refers to before and after the time of the center point, while staying within range bin and ray number constraints. These geometric constraints are also input at GET_DAT run time, and are limited to the more coarse, but similar, limits applied during the initial search with FILTER.
- e) The .MAT files generated using GET_DAT are loaded into PRO_MATLAB for evaluation. This interactive evaluation is used

to isolate the data segments that will define the "event". PRO_MATLAB's graphics, digital filtering, histograms and other tools allow this investigation to be relatively timely. Based on PRO_MATLAB review, the event constraints should be well defined. If, however, the review indicates that there is more event activity outside the current .MAT region, new regions are defined and GET_DAT used to convert the new regions to .MAT format. This iterative process continues until the event is defined.

- f) Once the event is defined, profile plots are generated to aid in analyzing the event. These 2-D plots show independent parameters vs. range (range bin number), with multiple rays overlayed. The overlay allows a more general characterization for a reasonable azimuth slice. Three dimensional mesh plots are also available to characterize the entire event, and are generated to show the velocity field for a range of azimuths.

This procedure is used to define all event segments. Once these segments have been isolated, they are grouped based on time, event character and location, into subevents. To better characterize subevents for moving events, the subevent rays are displaced whatever small range amount is necessary to allow the crossover range positions (where the velocity changes from positive outflow to negative outflow) to coincide.

3. Analyzing All Available Data

As the events and subevents are being identified and downloaded to SNC format, the statistical analysis of all available data, termed the Non-Event Data, is performed.

Histogram analysis of all data received from Lincoln Laboratory is conducted to realize a statistical summary of the type of data being reviewed. This analysis simply runs through all the data received (approximately 1.65 GBytes), ignoring data points annotated as "missing or deleted", or data points whose SNR is less than 10db. Histograms are generated for each field, VE, SNR, SW, and DBZ. The program HIST generates the histogram files and calculates the mean and standard deviation based on selected data regions. The program MERGE_HIST merges multiple histogram files in order to generate histograms for very large data segments, or data from a variety of files. TRANS_HIST translates the histogram data into .MAT format, and scales the data for plotting. The histograms are plotted and printed using PRO_MATLAB.

4. Analyzing Event Data

The next analysis conducted is of the event data, as follows.

i) Velocity Profiles

The events are analyzed on a subevent basis, as well as a composite for each event and for all events.

ii) Histogram Analysis

The histogram analysis performed on non-event data is repeated for the event data. This allows a comparison of the differences in the environment surrounding an event vs. during the event.

iii) F-factor Profiles and Histograms

The F-factor for Delta VE samples between adjacent range bins for each event are calculated and a histogram generated. The histogram shows the number of occurrences for a given range of F-factor, and the maximum F-factor encountered. The F-factor is calculated based on the following formula:

$$F = \frac{\Delta_{VE}}{\Delta_r} * \frac{V}{g}$$

where: **Delta_{VE}** is the change in radial velocity between adjacent range bins;
Delta_r is the change in range between adjacent range bins;
V airspeed (taken to be 150 knots);
g gravity.

Color RHI plots are presented in Figures 9, 10, 11 and 12 of Event 4 at azimuth slices of 242, 243, 244 and 245 degrees. The vertical axis in these plots is height above sea level, in 5 km grids. By examining the zero elevation rays, one can see the outflow region of the microburst (approximately 20 km). By examining the region above this outflow, for example at 20 km of range and 2.5 km of height (~8000 ft), one can try to estimate the velocity vector oriented toward the radar, and from this calculate the downdraft component. However, since the radial velocity component includes both the horizontal and radial components of the downdraft this estimate would be difficult to calculate and may not be accurate.

iv) Correlation Analysis

A correlation analysis is performed to study the effects of the various data fields due to VE, range, DBZ, and storm size. For VE, range and DBZ, the study is performed on a subevent and event basis, with a composite result for all events also generated. For storm size, the study is simply performed for all events. Program CORR determines the following functional relationships:

<u>Dependent Variables</u>	<u>Independent Variables</u>
SW, DBZ, SNR	VE
SW, DBZ, SNR	Range
VE, SW	DBZ
VE, SW	Event Size

TRANS_CORR converts the results to .MAT format, and the plots are generated and printed using PRO_MATLAB.

5. Interacting With Lincoln Lab Personnel

Based on an interaction with Lincoln Laboratory personnel, it was determined that the FL-2 radar uses a 39 pole FIR high pass filter with an estimated cutoff of 1.5 m/s for ground clutter suppression. The coefficients are described in the publication "Ground Clutter Cancellation For NEXRAD"². It was also determined that the criteria Lincoln uses for detecting windshear activity is 2.5 m/s/km. Other criteria, such as how the event size and strength are defined, was not known by the personnel contacted. It has also been estimated that approximately 100 pulsed radar transmissions were averaged for every ray of data estimates.

IV. Results

1. Velocity Profiles

Figures 13 through 27 present the velocity profiles for all 20 subevents making up the seven events. In Figure 13 for example, subevents 1a and 1b are shown. In Figure 14, subevent 1c and a composite of all three subevents that make up Event 1 are shown. For each velocity profile shown, there are two plots. On the left is the actual velocity profile for all rays being examined. Again, note that for clarity of presentation each line shown is typically a composite of 17 rays of data. Note also that these individual lines have been shifted slightly in range so that their positive to negative velocity crossover points coincide. This is to compensate for the movement of the event during its evolution, and for typical microburst activity this adjustment did not exceed one or two range bins. On the right of each set of figures is the average of the individual plots on the left,

2. Ground Clutter Cancellation For The NEXRAD System, J.E. Evans, 19 October 1983, Lincoln Laboratory Report ATC-122

useful for characterizing the shear strength of the event and for F-factor calculations.

Figures 25-27 show the velocity profiles for Event 7. Note that event seven is representative of gust front activity, while the other six events are representative of microburst activity. The differences are readily apparent by examining Figure 28. As shown, the movement of this event during its evolution is substantial. The movement of the event center by three kilometers took less than four minutes. The typical microburst examined would have moved less than one half of one kilometer in the same time.

Also shown in Figure 28 is the aliasing that was evident in Event 7 data. In this event the radar had a PRF of 700 which gave an unambiguous velocity limit of ± 18 m/s. As the velocity estimates exceeded this limit, they would fold over into the other end of the spectrum. Thus velocities of -30 m/s would show up as approximately -6 m/s. This required that for Event 7 an automatic de-aliasing algorithm be incorporated into the data retrieval software.

Though Event 7 is representative of gust front activity rather than microburst activity, it was examined in the same manner, where possible, in order to compare results. Note that the data from Event 7 was not incorporated into the All-Event data.

Different techniques can be used to calculate the event's shear strength and size. Figure 29 summarizes such information based on a peak to peak measurement. The maximum and minimum velocity estimate locations on either side of the divergence are located, and the distance between them used to estimate event size. Their velocity difference divided by the event size gives the shear strength estimate.

Using a peak to peak technique tends to lower the magnitude of both size and strength estimates. A method that bases its estimates on the stronger shear region near the divergence point has been used to generate the tables in Figures 30 and 31. For both tables, the shear strength is measured on a bin to bin basis, starting at the point of divergence, and moving in opposite direction away from that point one pair of range bins at a time. In this manner, the maximum instantaneous shear location can be found (not necessarily the point of peak velocity), and a moving average can be generated to demonstrate the weakening of the shear strength as one moves further removed from the point of divergence. Figure 30 presents such data as a moving average, with each subsequent range bin pair equally weighted in the calculation of the mean. Figure 31 presents the instantaneous shear for any given range bin pair, with no averaging. Using these two tables, an algorithm could be generated to automatically estimate shear strength, perhaps by monitoring the rate of change of the averaged shear strength estimate, or other method.

2. Histogram Analysis

Figure 32 shows the histograms for VE, SW, DZ and SNR for all (Non-Event) data. Figure 33 shows the same histograms for events one through six combined. Appendix A contains the same histograms for each event and subevent. Note that data fields whose SNR was below 10 dB were not included in the analysis.

Figure 34 summarizes the mean values for all data fields, and F-factor, for all event and nonevent data.

Figures 35 through 38 summarize the first four moments for all event, subevents, and nonevent data, for the four data fields analyzed (VE, SW, DZ, and SNR, respectively). These calculations present information about the distribution of the data, as otherwise shown in the histogram plots.

3. F-factor Analysis

Figures 39 through 46 show the instantaneous radial component of F-factor profiles for each event and subevent. These calculations were performed on a bin to bin basis, assuming an aircraft airspeed of 150 knots, with no averaging of multiple adjacent (along a ray) bins. Included in Appendix A are similar plots for all events that show the effects of averaging 2 adjacent range bins (along a ray) per point, and 3 range bins per point. Such averaging is representative of the effects low pass filtering may have on real time F-factor calculations. No azimuthal (spatial) averaging was performed. Note that these F-factor profiles only include the radial component of F-factor.

Figures 47 through 54 show the F-factor histograms for all subevents, as well as the combined histograms for each event. Shown on each histogram are two additional vertical lines; the solid line is the characteristic F-factor for the event or subevent, whose value is also given at the base of each plot, and the dashed line is the approximate F-factor level considered hazardous, given as .12. The radar, however, measures only the radial component of the hazard, while .12 is a threshold level including the vertical component. Therefore, a threshold level for the radial component only would be lower than the hazard level used here. The velocity profiles of Figures 13 through 27 were used to determine the characteristic F-factor for each event, by first determining a characteristic shear strength line. Included in Appendix A are the velocity profile plots showing the shear strength line used to calculate the characteristic F-factor. Note that for this analysis, the characteristic shear strength was found graphically (see Appendix A), rather than using the peak to peak or moving average methods described earlier.

4. Correlation Analysis

Figure 55 contains a table which summarizes the trends evident in the correlation analysis. As described therein, there are only four relationships examined which appear as though they may be correlated, i.e., SW vs. DZ, SW vs. range, DZ vs. range, and SNR vs. range. These four correlation functions are plotted in Figures 56 through 63 for all events. These plots are scatter plots which show the dispersement of the raw data, with an average line overlayed. Appendix A contains two additional sets of correlation plots. The first set contains the same set of correlation functions as in Figure 56 through 63, but for the twenty subevents. The second set contains those correlation functions that were also examined, but appear to be uncorrelated, for all subevents and events. The other correlation functions examined include SW vs. VE, SN vs. VE, DZ vs. VE, and VE vs. DZ.

Finally, Figure 65 contains the remaining two correlation functions that were examined, and are for all events. Shown are VE and SW as a function of event size. All subevents were characterized for average values of VE and SW from the histogram analysis, and their size was characterized from the velocity profile plots.

V. Conclusions

The range of conclusions that can be drawn from the analysis presented herein exceeds the scope of this report, but there are some preliminary conclusions that should be addressed.

1. Comparing Event vs. Non-Event Data

When comparing event data with nonevent data, the mean value of the spectral width estimate does not change appreciably. As shown in Figure 34, the mean value of SW for event data is 2.047 m/s, while for nonevent data it is 1.847 m/s. This result indicates that the 1.5 m/s mean from the Phase I SBIR analysis was slightly lower than for most events. In that analysis, it was speculated that the spectral width estimate, which is made up of components due to antenna motion, turbulence, non-uniform flow fields, and varying sized rain cell volumes, is dominated by the non-uniform flow fields associated with microburst activity in the outflow region. This analysis neither confirms nor rejects such an hypothesis, but the trend of similar or slight increase in spectral width estimate for events when compared to nonevents is confirmed.

Also as shown in the Phase I SBIR study, events tend to have greater reflectivity than nonevents. The mean reflectivity for events for this analysis was 40 dBz, while the mean reflectivity for nonevents was 25 dBz.

Velocity estimates lie within ± 20 m/s for events, with a mean of 2.5 m/s, while nonevents range from ± 20 m/s with a mean of -2.06 m/s. Note that the mean velocity estimates for all events is the average of the absolute value of each events mean velocity, with each event receiving equal weighting. The signed average for events would be -1.2 m/s.

One interesting trend that does differ from the Phase I study is the similarity between distributions of event data and nonevent data for velocity and spectral width estimates. In the Phase I study, the velocity distribution for nonevent data was fairly normal, with a zero mean, while the velocity distribution for event data was skewed toward 10 m/s. In this analysis, both distributions appear normally distributed, centered around zero. This difference is attributed to the larger amount of event data examined, which should tend to have a normalizing effect.

2. Trends Evident In Correlation Analysis

i) SW vs. DZ

As shown in Figures 32 and 33, events have greater SNR than nonevents. The mean SNR estimate for events is 50 dB, while for nonevents the mean is 30 dB. This is attributed to the greater reflectivity apparent during events compared to during nonevents.

ii) SW vs. Range

Figure 63 shows each event's spectral width plotted vs. range. A review of this figure shows that while spectral width estimates do increase with range, the increase is not as great as expected. Such an increase was expected based on the increased volume contained within each range bin and the non-uniform velocity profiles of the outflow. It is difficult to reach a conclusion here because there are so few events and they have such varying ranges.

iii) DZ, SN vs. Range

Figure 64 shows SNR decreasing with range and otherwise following the reflectivity curve. SNR should vary as a function proportional to reflectivity, and inversely proportional to range squared. As range increases, SNR estimates decrease; at the point that DZ drops dramatically (approximately 30 km) SNR also drops at a higher rate than simply due to increasing range. By correlating the SW vs. range graph with the SNR vs. range graph, one can see that as SNR decreases, SW estimates increase, though slightly. Again, the size of the increase (SW only varies by approximately 1 m/s over 45 km) is attributed to the fact that there are many sources contributing to the SW estimate.

VI. Recommendations

Any recommendations derived from this analysis are limited to future use of the processed data, or other work that can be conducted based on the results presented herein. For these reasons, the recommendations given below do not address specific applications of this analysis.

The data processed in this report could be used to develop and test windshear detection algorithms. As the nature of such events has been better characterized, particularly the spectral width estimates, design criteria for detection algorithms in terms of detection thresholds and false alarm rates can be defined.

The data analyzed from FLOWs testing is of course all ground based data. One possible extension to this analysis is the extrapolation of the ground based data to the airborne case. A potential method for doing this would be to generate simulated I,Q data based on the spectral characterization presented. By reverting back to the time domain, assuming a normal noise distribution, one could add in a bias that would model the effects of ground clutter. Additionally, one could add in the effects of a moving platform. Once all these new effects were modeled in the time domain, the simulated data could be used to test pulse pair processing, or other, algorithms for the airborne case.

Should the opportunity present itself, it is highly recommended that real I,Q data be collected of windshear events, allowing different algorithms to be tested for ground clutter filtering, pulse pair processing or FFT type spectral characterization, etc. Raw I,Q data would be a distinct advantage compared to estimates based on pulse pair processing, as complete flexibility would be retained in terms of processing options that could be tried.

Lincoln Laboratory Event Description Data

Date	Time	Range/Azimuth	Size	Reflect.	Strength	RHI/PPI
8/10	0005	5km/275degs	1.7km	50 dBz	18m/s/km	PPI
8/10	2351	3km/007degs	4.3km	55 dBz	09m/s/km	RHI/PPI
5/24	0708	17km/134degs	1.5km	55 dBz	13m/s/km	PPI
9/21	1929	19km/244degs	2.7km	60 dBz	13m/s/km	PPI
7/13	2126	16km/325degs	2.0km	55 dBz	14m/s/km	RHI/PPI
7/31	0252	13km/279degs	2.2km	-	11m/s/km	RHI/PPI
5/24	1802	26km/336degs	2.0km	60 dBz	20m/s/km	PPI
4/12	2020	47km/145degs	4.2km	65 dBz	12m/s/km	PPI
8/06	2059	35km/189degs	2.0km	40 dBz	12m/s/km	RHI/PPI

Figure 1

Event Data Supplied By Lincoln Laboratory

Lincoln Laboratory Documentation Information

Color Plot Search Information

SNC Ev#	Date	Time	Location Range/Azimuth	Time		Range		Azimuth	
				Start	Stop	Start	Stop	Start	Stop
1	8/10	2351	03km/007degs	2346	2353	0km	15km	310	070
2	8/01	0252	12km/279degs	0239	0256	5km	25km	260	320
3	7/13	2126	16km/325degs	2117	2130	10km	25km	270	000
4	9/21	1929	19km/244degs	1925	1938	15km	25km	230	260
5	9/21	1951	21km/208degs	1935	1952	10km	25km	190	220
6	8/06	2059	35km/189degs	2059	2112	25km	40km	170	210
7	4/13	2020	47km/145degs	2015	2021	30km	50km	130	160

The data as originally supplied by Lincoln Laboratory was contained on eleven 6250 bpi magnetic tapes, totaling approximately 1.65 GBytes of data; the actual event data that was recovered from these tapes totaled less than 50 MBytes of data (less than 3 % of the total).

Figure 2

Radar Parameters Table

Event	Date	Time	Unambiguous Velocity (m/s)	Scan Rate (degs/sec)	Ray Separation (degs)
1	8/10/86	23:46:30	+18.23	10.2	1.0
2	8/01/86	02:39:54	+18.23	10.3	1.0
3	7/13/86	21:17:05	+23.44	10.2	1.0
4	9/21/86	19:26:23	+18.23	9.2	1.0
5	9/21/86	19:35:17	+18.23	10.2	1.0
6	8/06/86	20:59:49	+18.23	10.2	1.0
7	3/12/85	02:15:01	+18.23	6.5	1.3

Constant Parameters

Frequency	2.88 GHz
Horizontal Beam Width	.96°
Vertical Beam Width	.96°
Pulse Width	.8 usec
Latitude	20.92°
Longitude	52.31°
Antenna Diameter	28 ft
Transmitter Power	1.1 mw
Pulse Repetition Frequency	700 to 1200

Figure 3

Event Location Table

Event #	Date	Time	Vol	Rays	Azimuths (degs)	Range (Bins)	Range (km)	Elev (degs)
1a	8/10/86	23:46:40	5	291- 295	28.1- 32.2	23- 93	2.76-11.16	0.500
1b	8/10/86	23:52:42	7	275- 281	9.1- 15.2	2- 72	.24- 8.64	0.500
			7	291- 296	25.4- 30.5	3- 73	.36- 8.76	0.500
1c	8/10/86	23:53:45	7	902- 903	3.7- 4.7	1- 71	.12- 8.52	0.391
			7	907- 911	8.8- 12.8	2- 72	.24- 8.64	0.391
2a	8/01/86	2:41:33	1	875- 885	285.0-295.0	93-211	11.16-25.32	0.391
		2:42:42	1	1512-1522	385.0-295.0	87-205	10.44-24.60	0.391
		2:43:51	1	2150-2160	385.0-295.0	82-200	9.84-24.00	0.391
2b	8/01/86	2:48:46	4	921- 931	385.0-295.0	63-181	7.56-21.72	0.391
		2:50:00	4	1621-1630	385.0-295.0	58-176	6.96-21.12	0.391
		2:51:15	4	2320-2330	385.0-295.0	53-171	6.36-20.52	0.391
3a	7/13/86	21:17:11	2	1803-1812	330.8-330.0	87-187	10.44-22.44	2.188
		21:19:20	4	300- 310	334.3-344.6	88-188	10.56-22.56	9.188
3b	7/13/86	21:21:56	5	298- 307	334.5-346.7	51-151	6.12-18.12	0.391
		21:23:10	6	316- 325	350.5-359.7	53-153	6.36-18.36	9.188
		21:24:24	7	56- 66	349.8- 0.0	55-155	6.60-18.60	0.391
3c	7/13/86	21:28:45	10	302- 311	350.4-359.7	59-159	7.08-19.08	9.188
		21:30:48	12	302- 311	350.9-359.3	54-154	6.48-18.48	0.391
4a	9/21/86	19:27:15	9	758- 766	240.9-249.2	100-184	12.00-22.08	0.391
		19:28:07	9	1220-1229	240.0-249.3	105-188	12.60-22.56	0.391
		19:28:59	9	1683-1692	240.2-249.5	111-194	13.32-23.28	0.391
4b	9/21/86	19:32:17	1	759- 767	249.9-249.3	113-196	13.56-23.52	0.391
		19:32:57	1	1221-1230	240.7-249.8	113-196	13.56-23.52	0.391
		19:34:02	1	1689-1698	240.7-249.9	114-197	13.68-23.64	0.391
4c	9/21/86	19:36:13	2	765- 774	240.3-249.5	114-197	13.68-23.64	0.391
		19:37:06	2	1233-1242	240.4-249.2	117-200	14.04-24.00	0.391
		19:37:58	2	1699-1708	240.2-249.5	113-196	13.56-23.52	0.391
5a	9/21/86	19:35:44	2	496- 499	205.3-207.4	134-188	16.08-22.56	18.688
		19:37:47	2	1622-1626	210.4-206.5	140-194	16.80-23.28	23.297
		19:38:20	2	1899-1901	107.1-209.1	150-204	18.00-24.48	11.688
5b	9/21/86	19:36:37	2	967- 969	208.8-210.8	161-215	19.32-25.80	16.297
		19:32:17	2	2089-2094	210.1-205.1	150-204	18.00-24.48	21.000
6a	8/06/86	20:59:51	12	118- 122	183.9-188.2	256-307	30.72-36.84	0.391
6b	8/06/86	20:59:51	12	123- 127	189.2-193.5	271-321	32.52-38.52	0.391
7a	3/13/85	02:16:06	2	327- 331	153.3-157.8	175-274	21.00-32.88	5.000
7b	3/13/85	02:16:18	2	385- 389	159.6-156.1	175-274	21.00-32.88	5.000
7c	3/13/85	02:18:24	3	220- 224	156.2-147.2	195-294	23.40-35.28	1.000
7d	3/13/85	02:19:26	3	556- 559	144.3-147.4	175-274	21.00-32.88	5.000
7e	3/13/85	02:19:40	3	621- 624	158.2-155.2	175-274	21.00-32.88	5.000

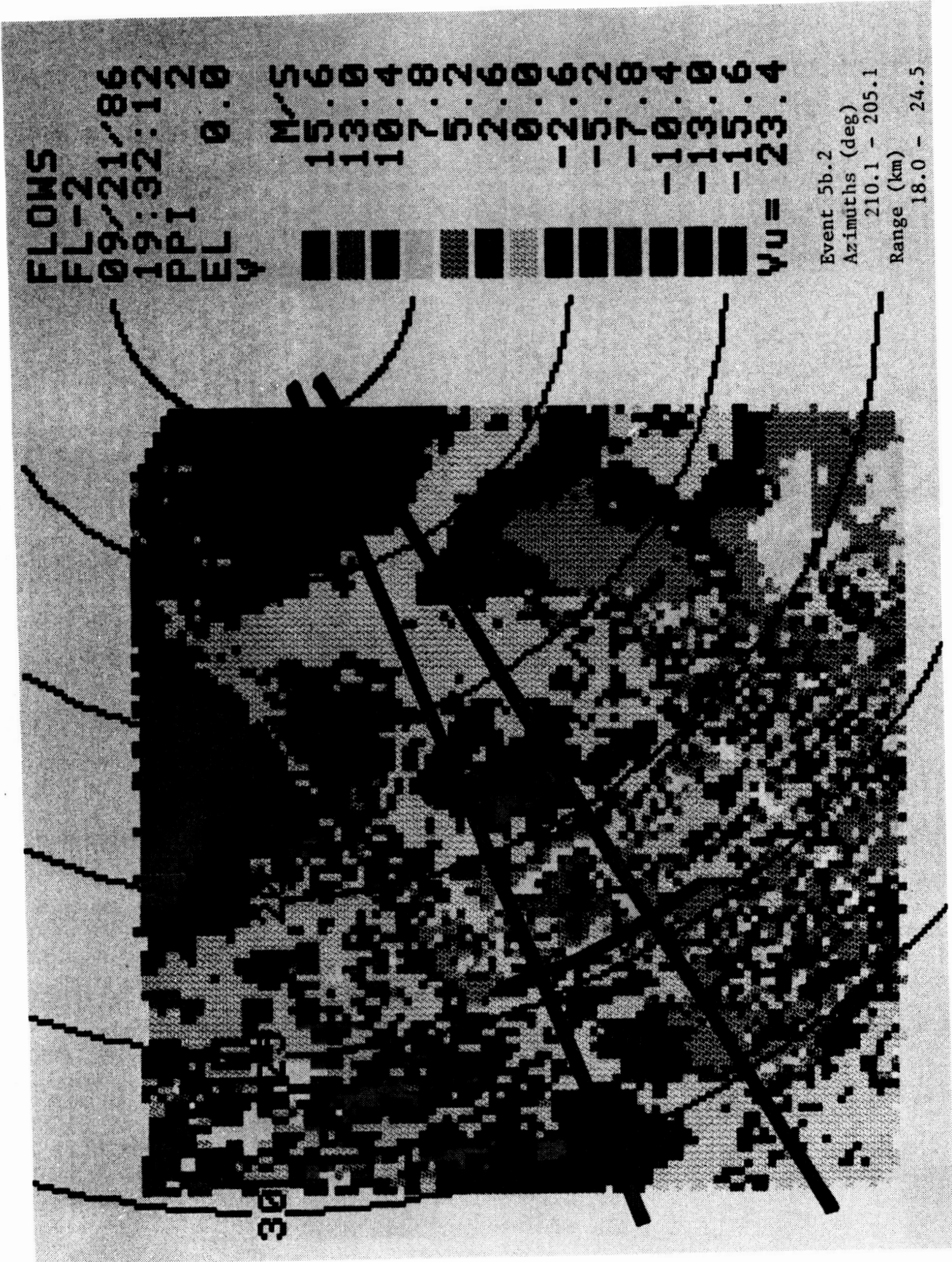


Fig. 5

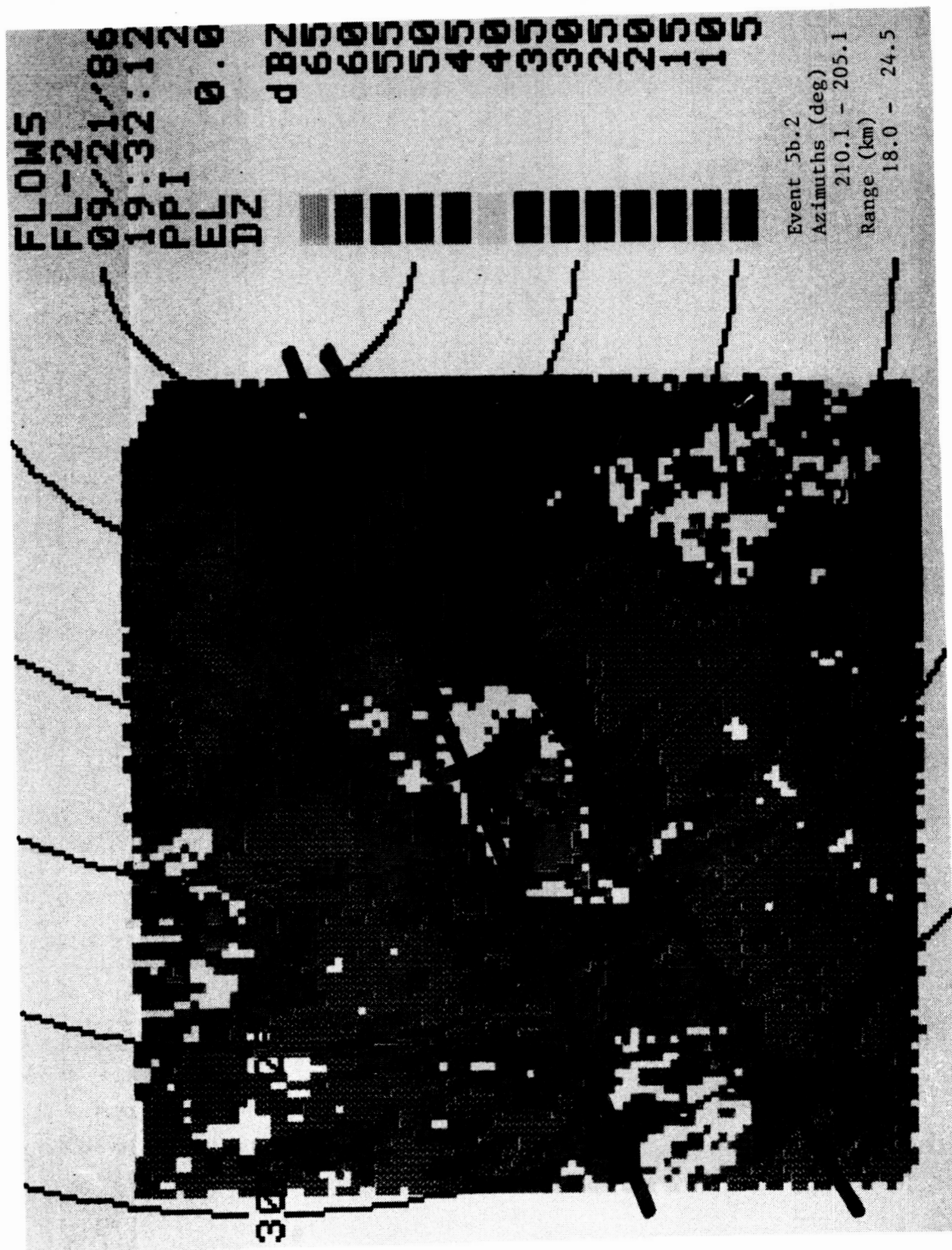


Fig. 6

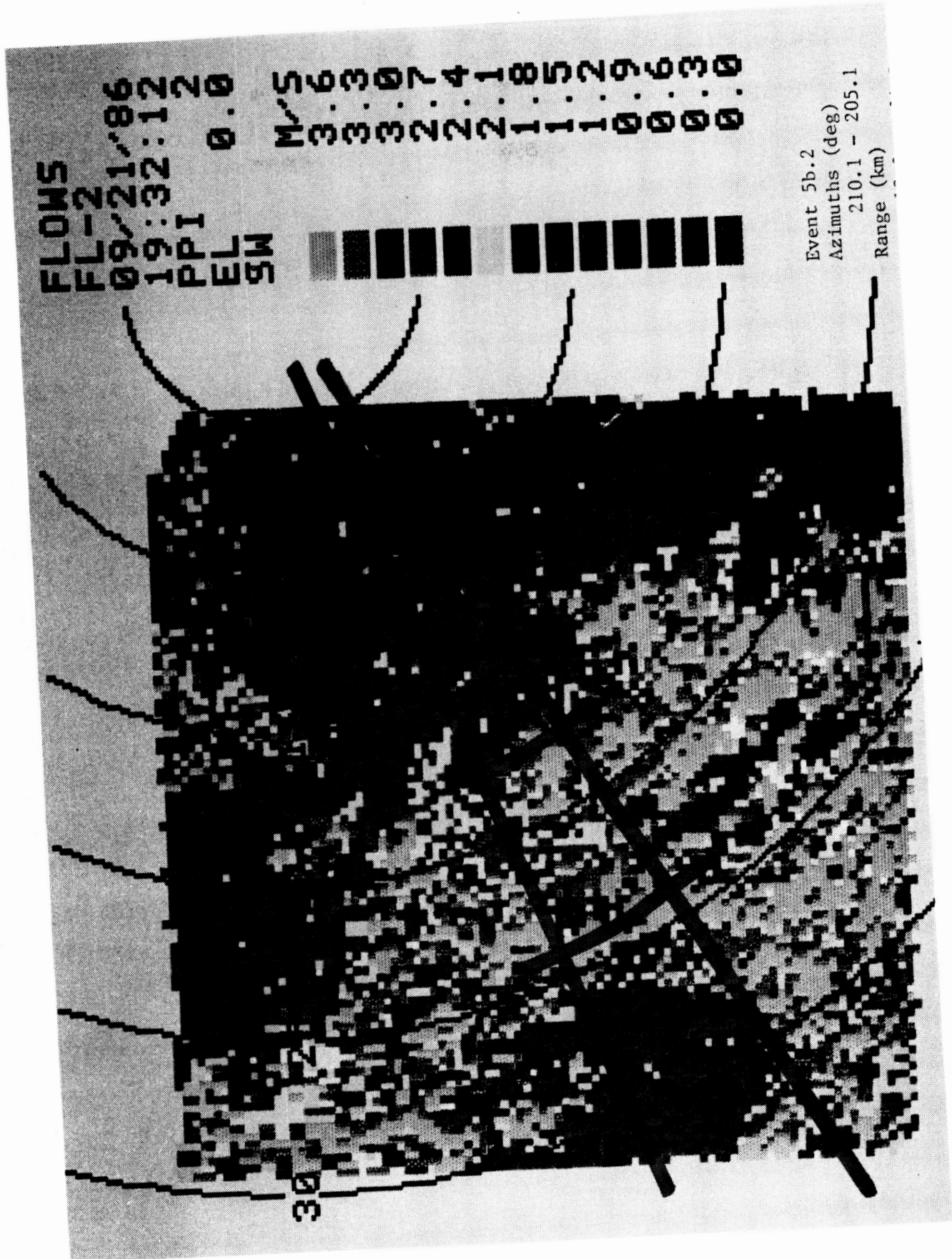


Fig. 7

ORIGINAL PAGE IS
OF POOR QUALITY

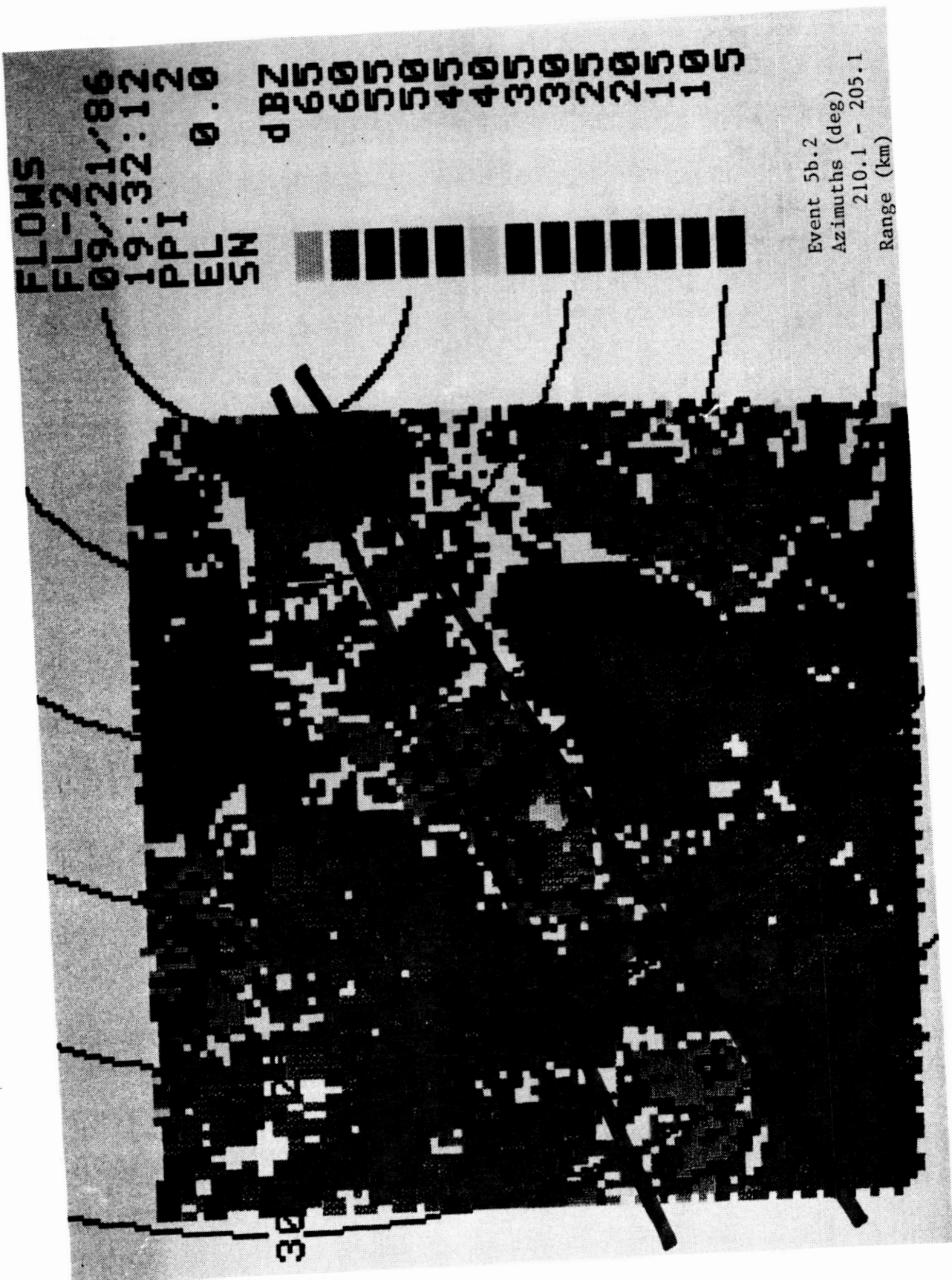


Fig. 8

ORIGINAL PAGE IS
OF POOR QUALITY

ORIGINAL PAGE IS
OF POOR QUALITY

FL0WS
FL-2
199/21/86
19:38:55
RHI
AZ 242.0
V

卷二

Event	5b.2
Azimuths (deg)	
210.1 - 205.1	
Range (km)	
	24.5
	18.0 -

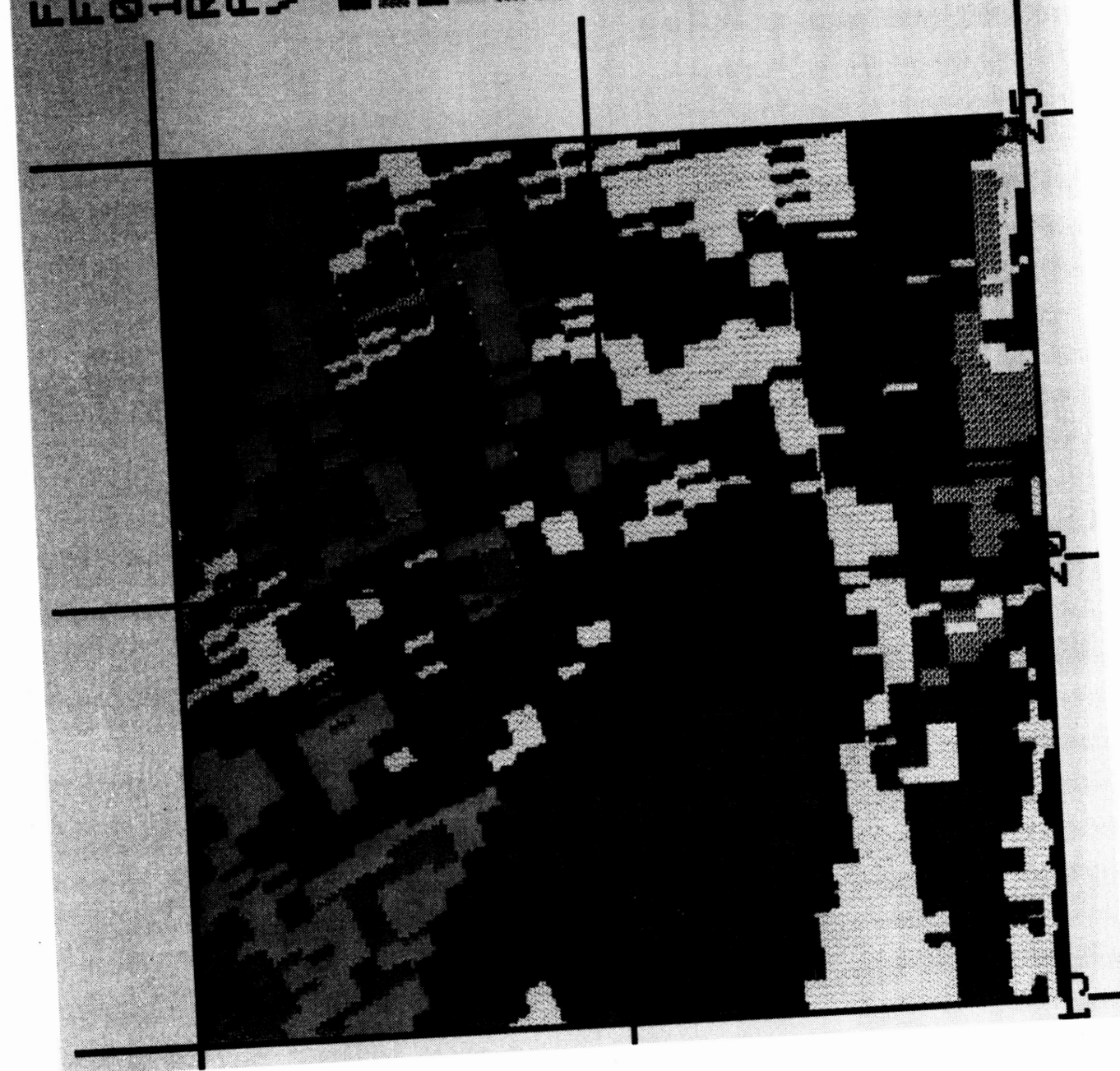


Fig. 9

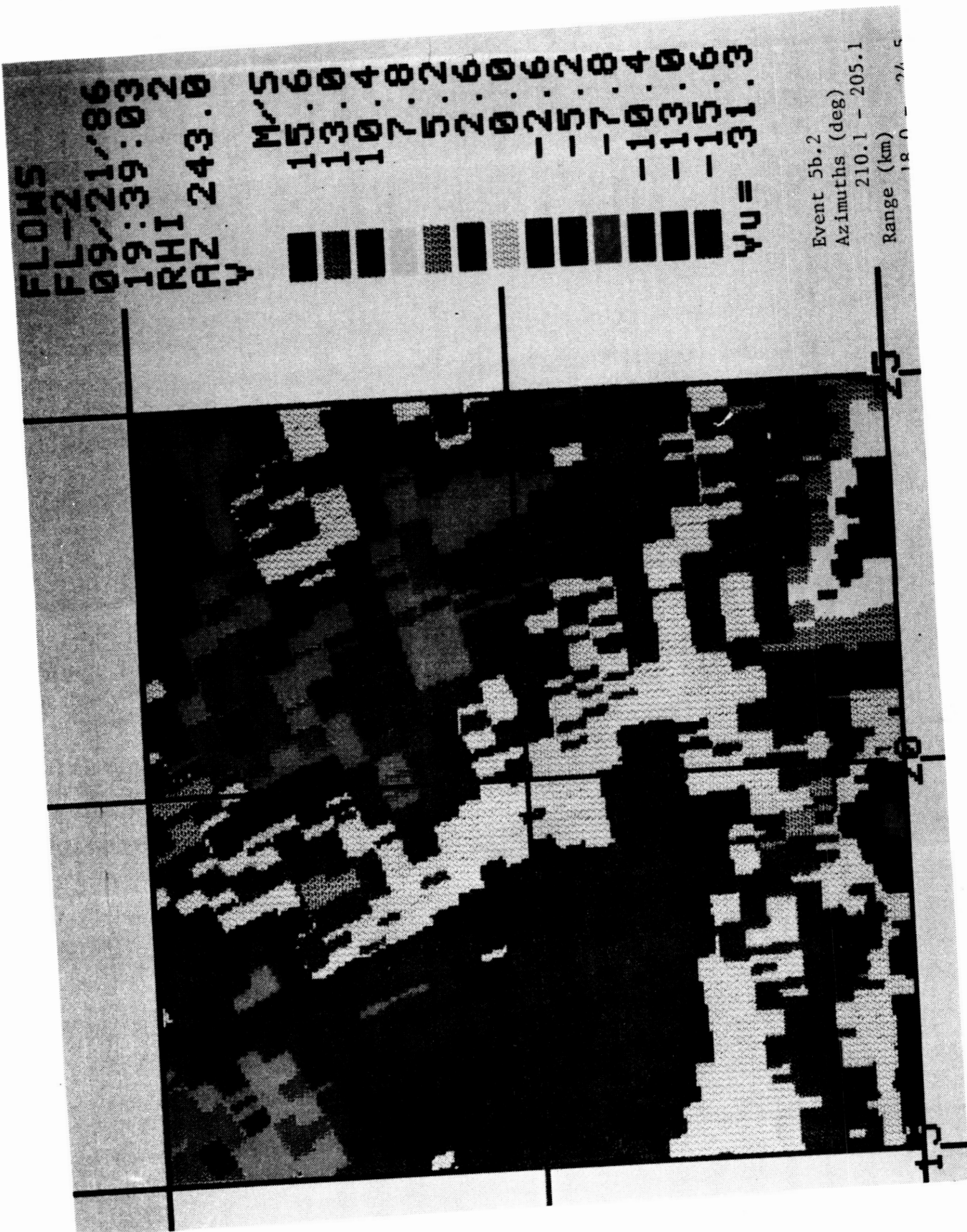


Fig. 10

ORIGINAL PAGE IS
OF POOR QUALITY

ORIGINAL PAGE IS
OF POOR QUALITY

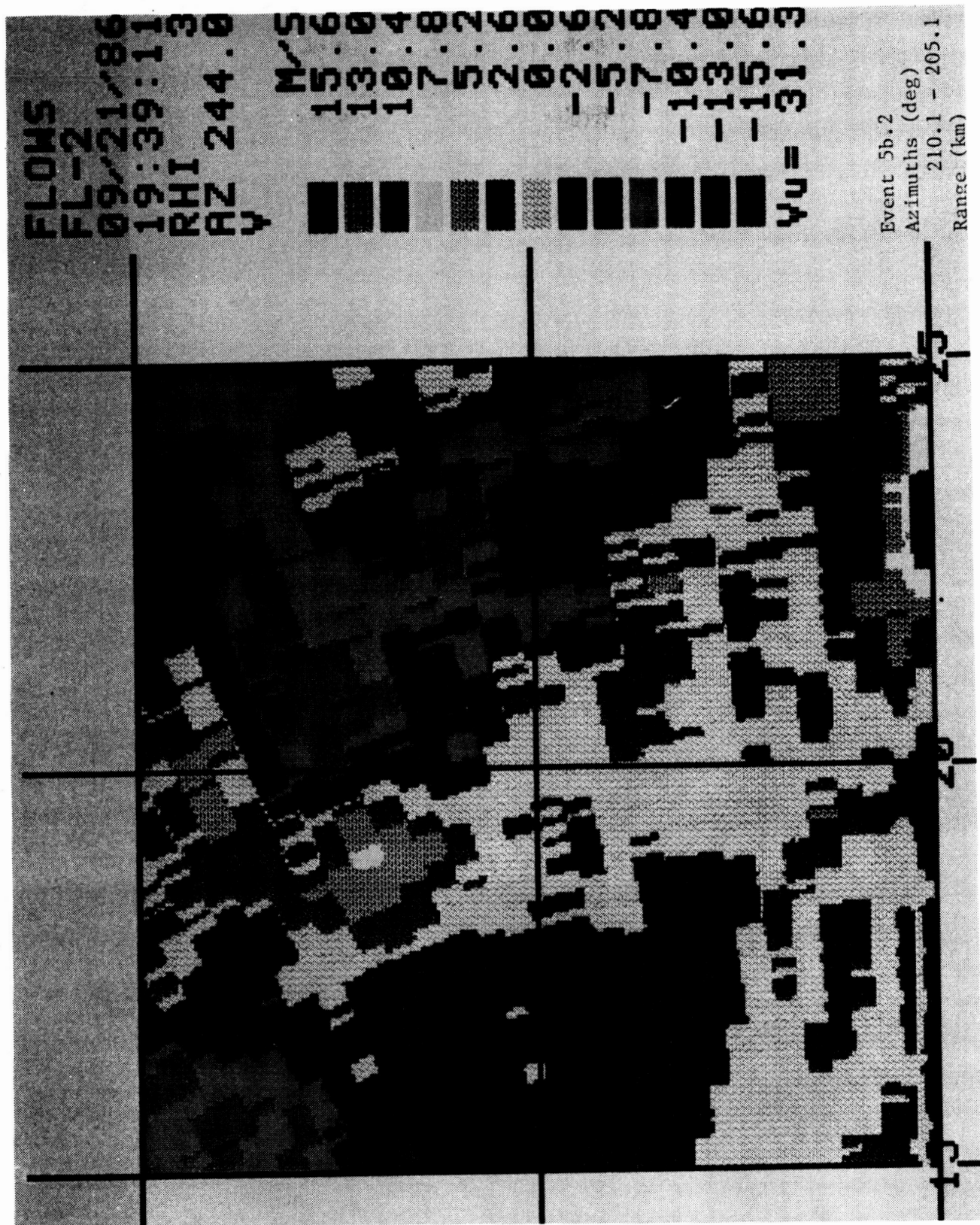


Fig. 11

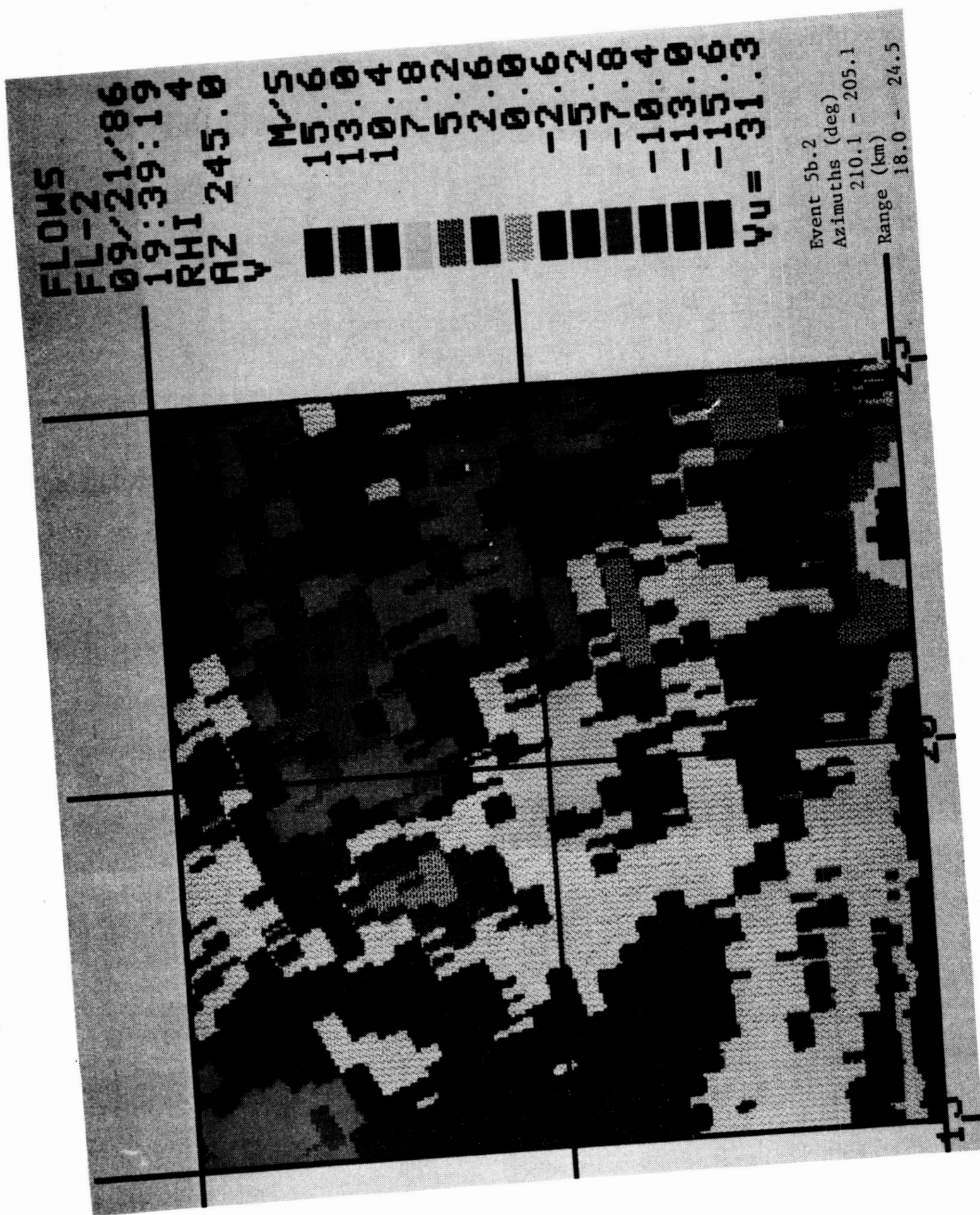
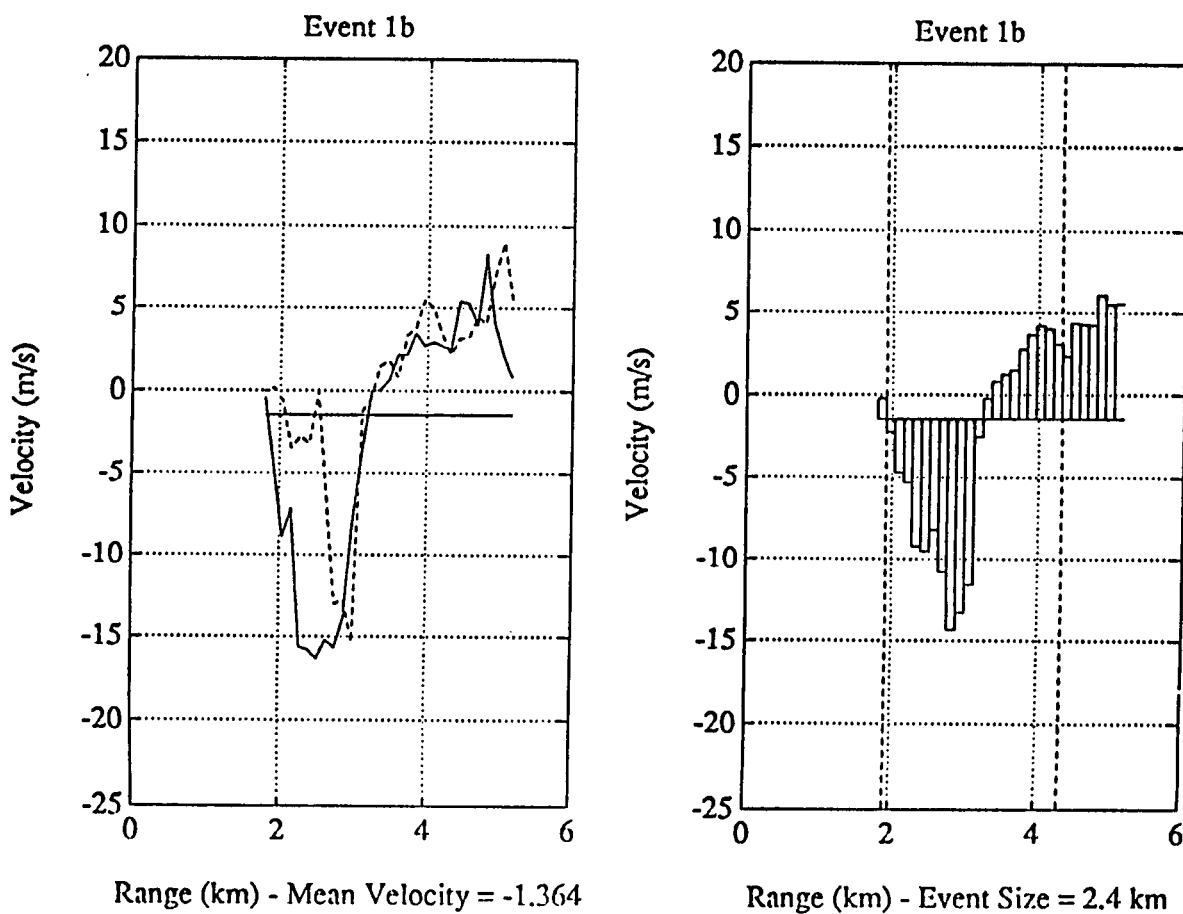
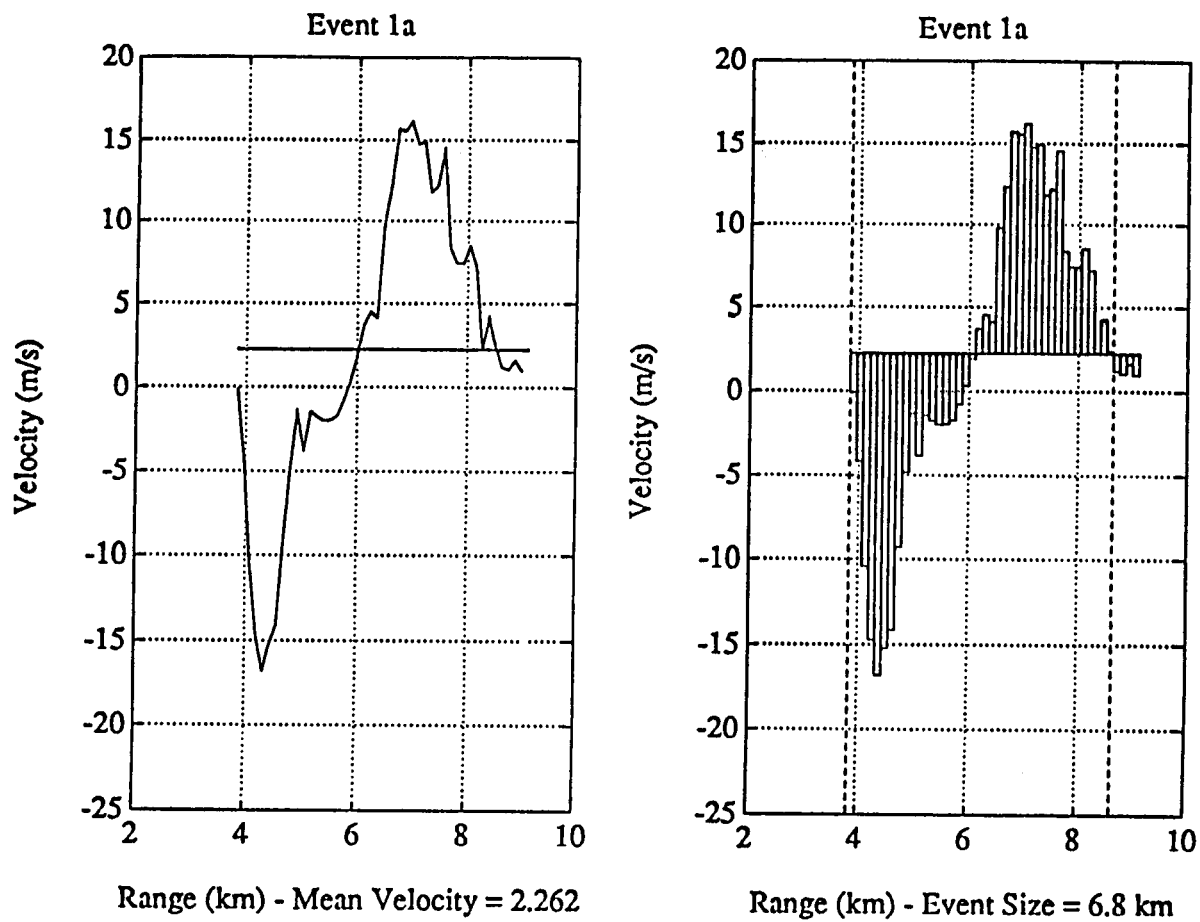
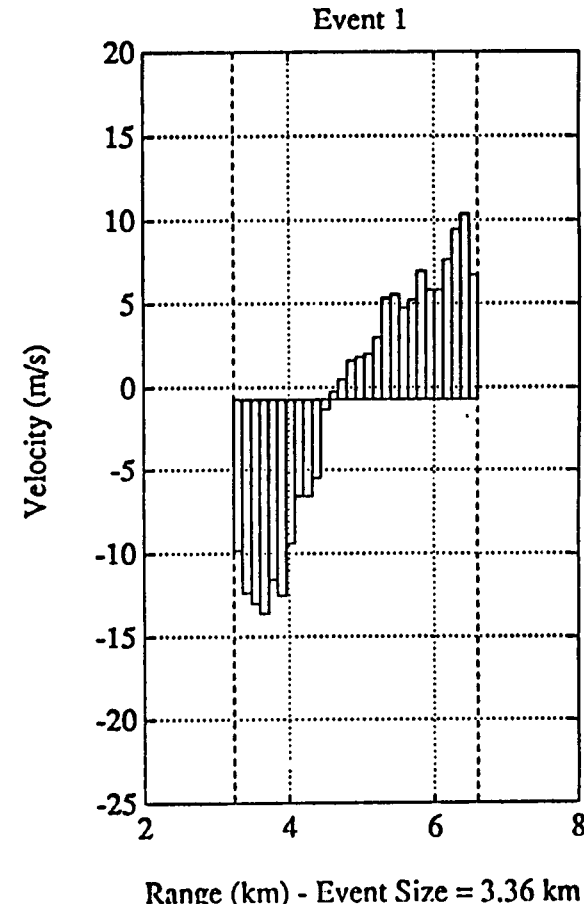
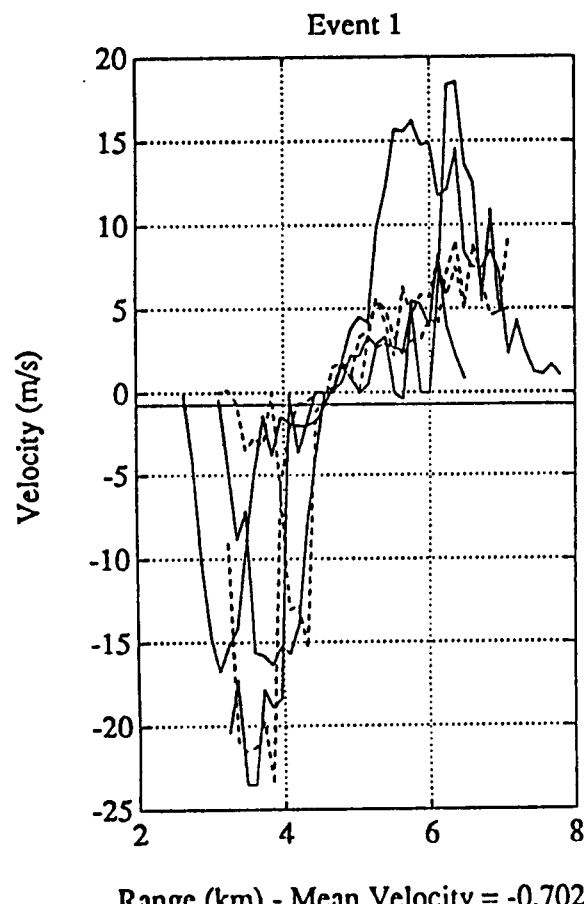
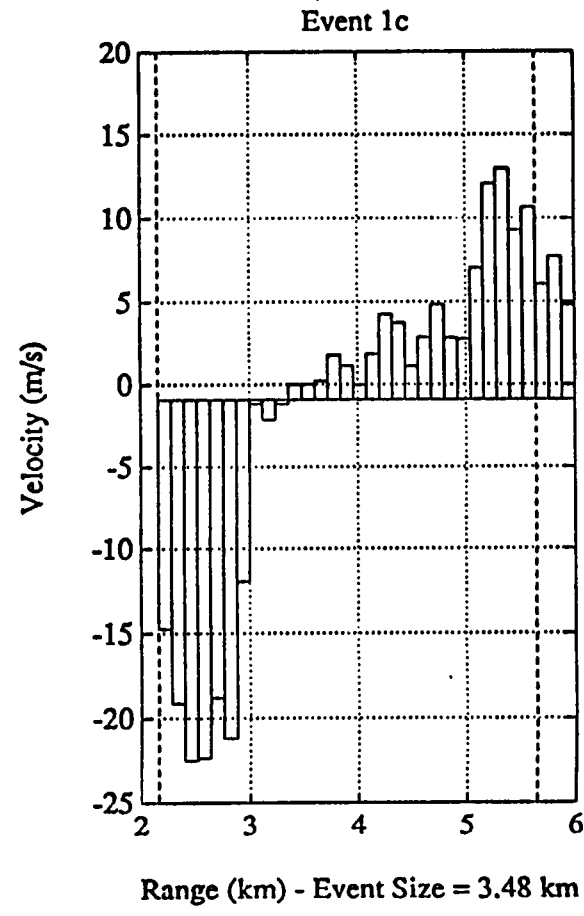
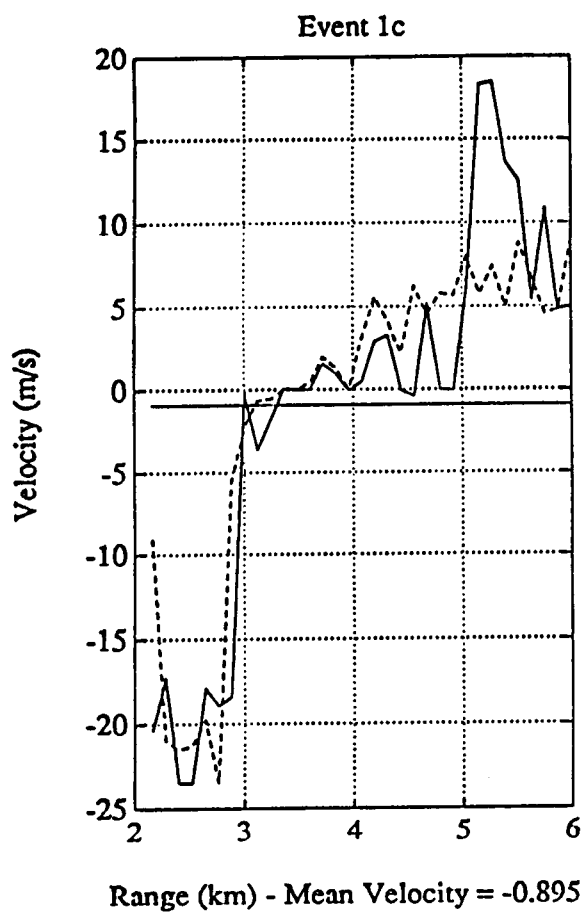
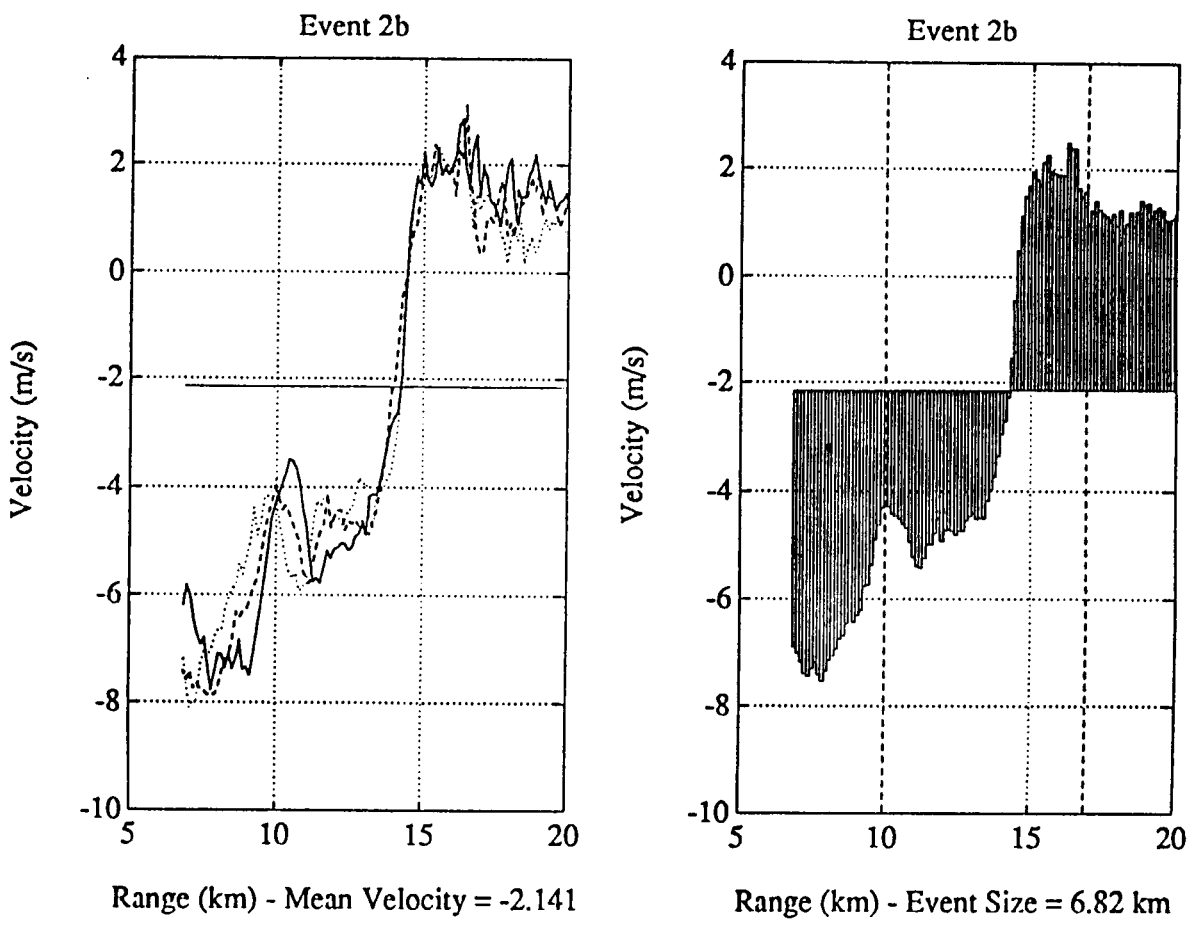
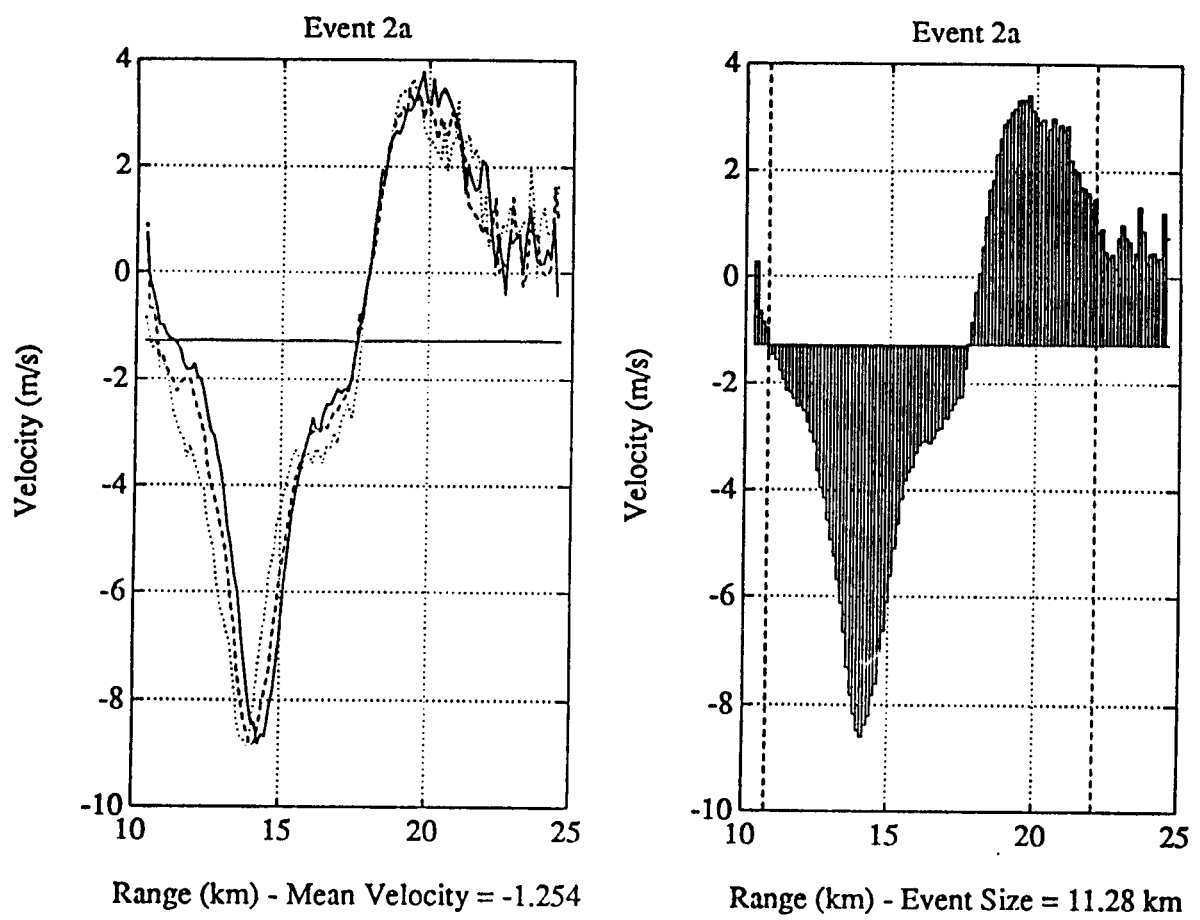


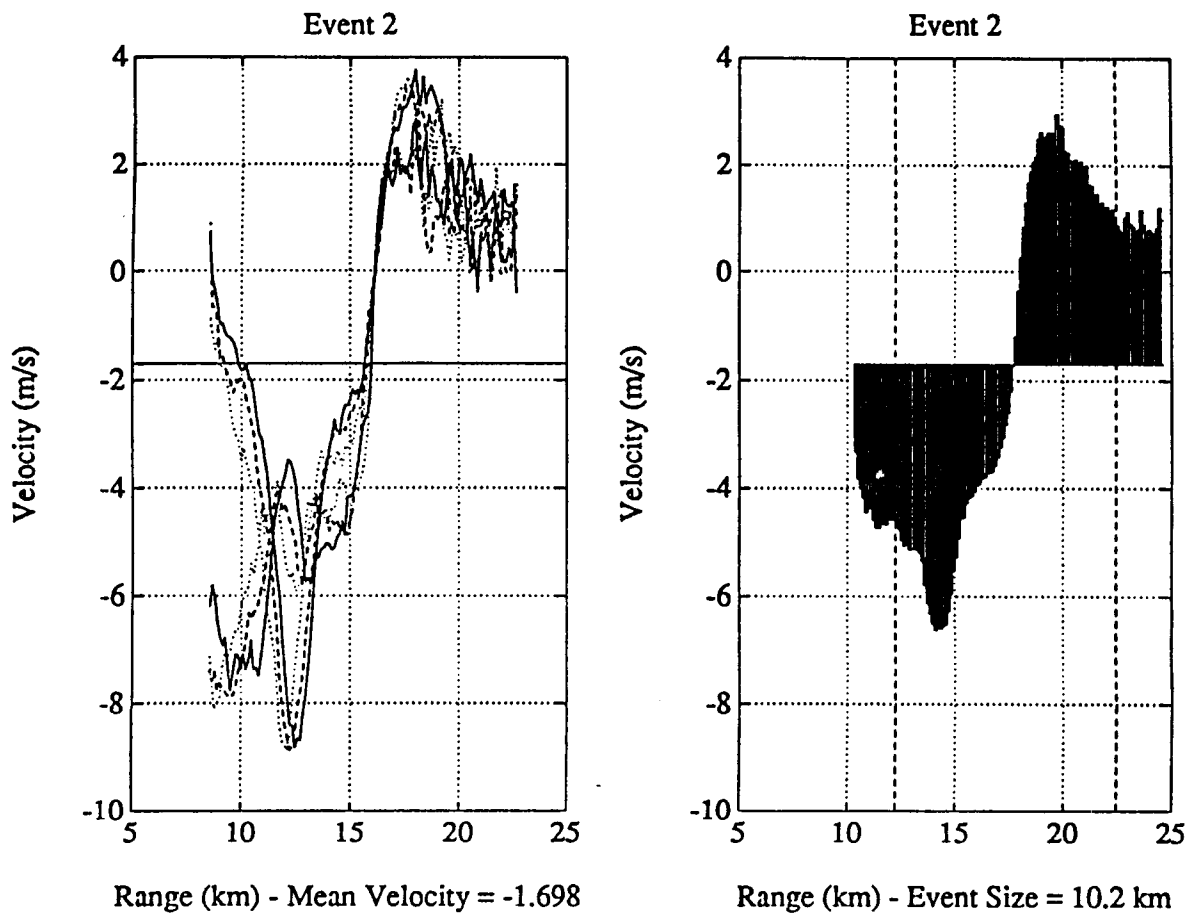
Fig. 12

**ORIGINAL PAGE IS
OF POOR QUALITY**

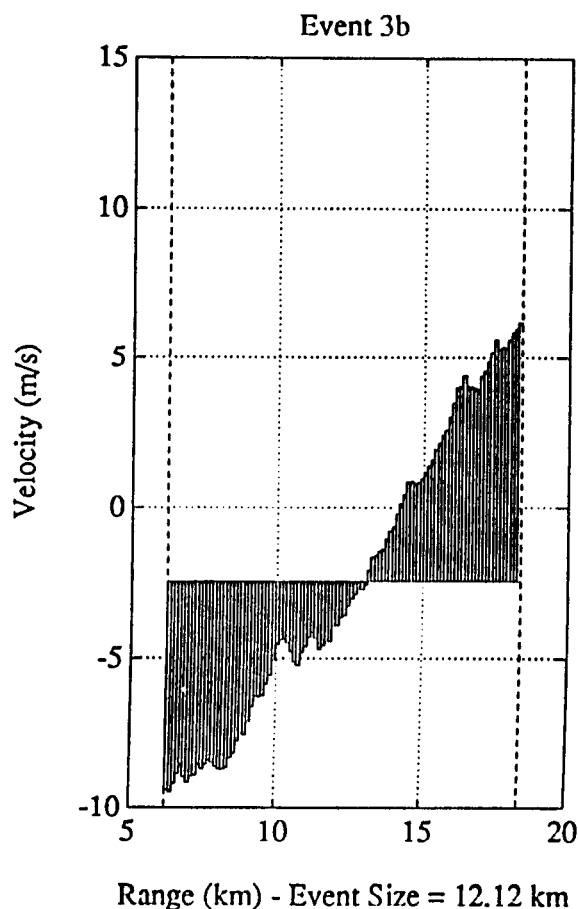
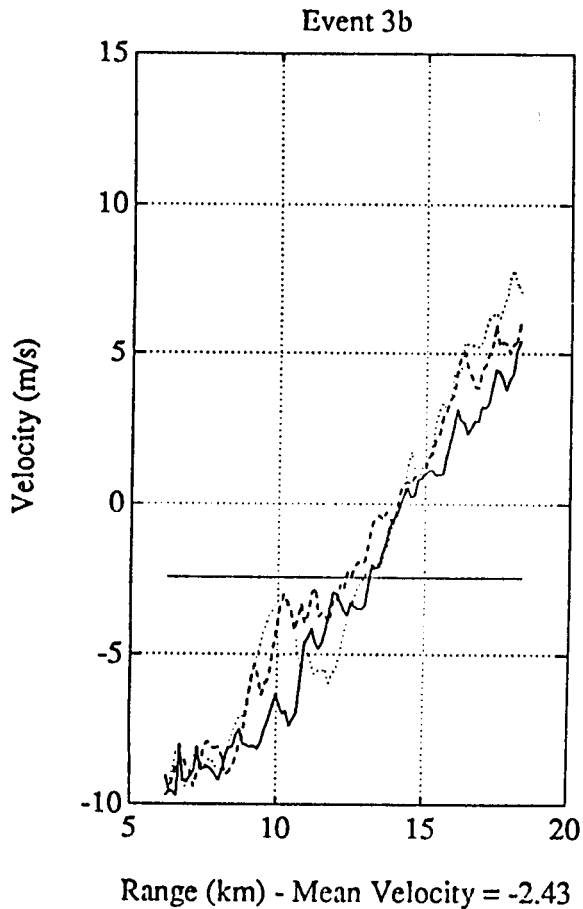
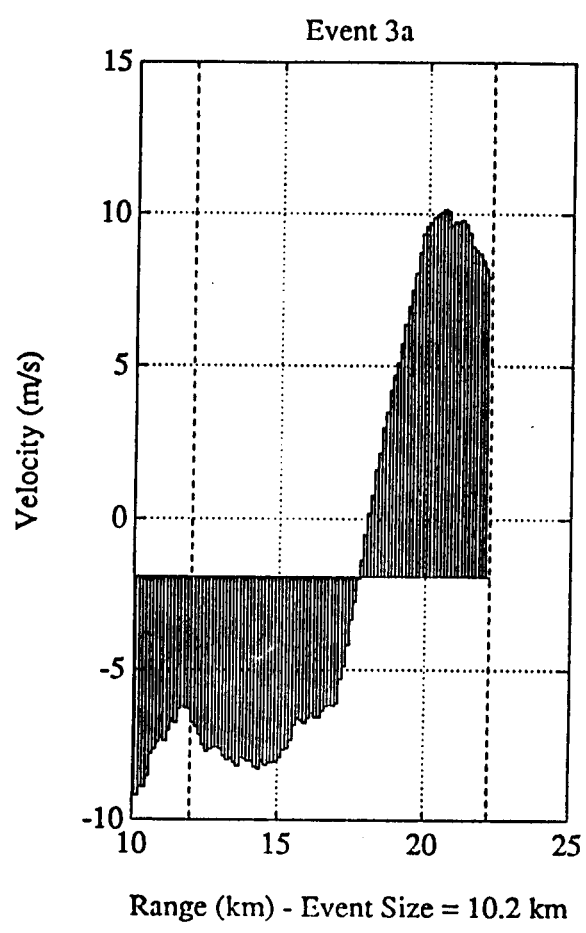
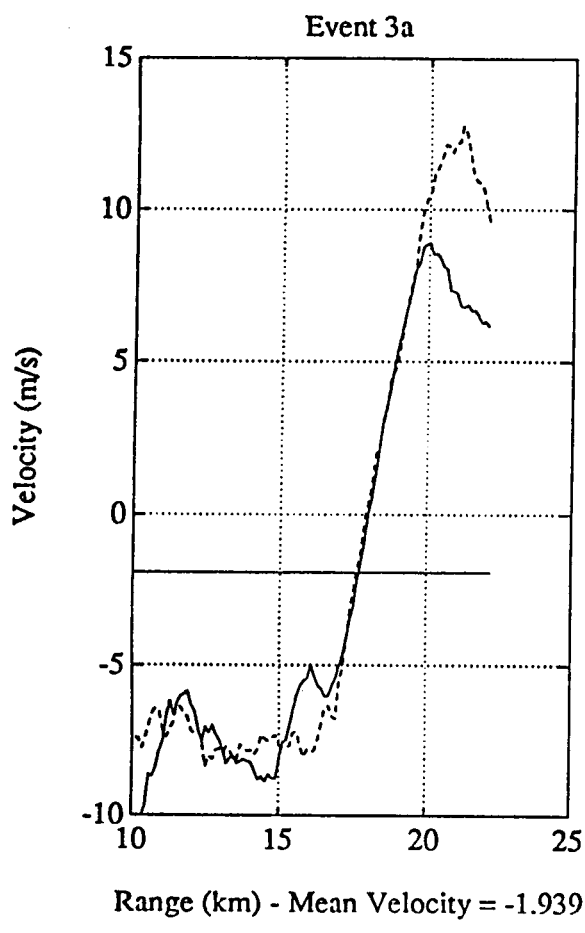


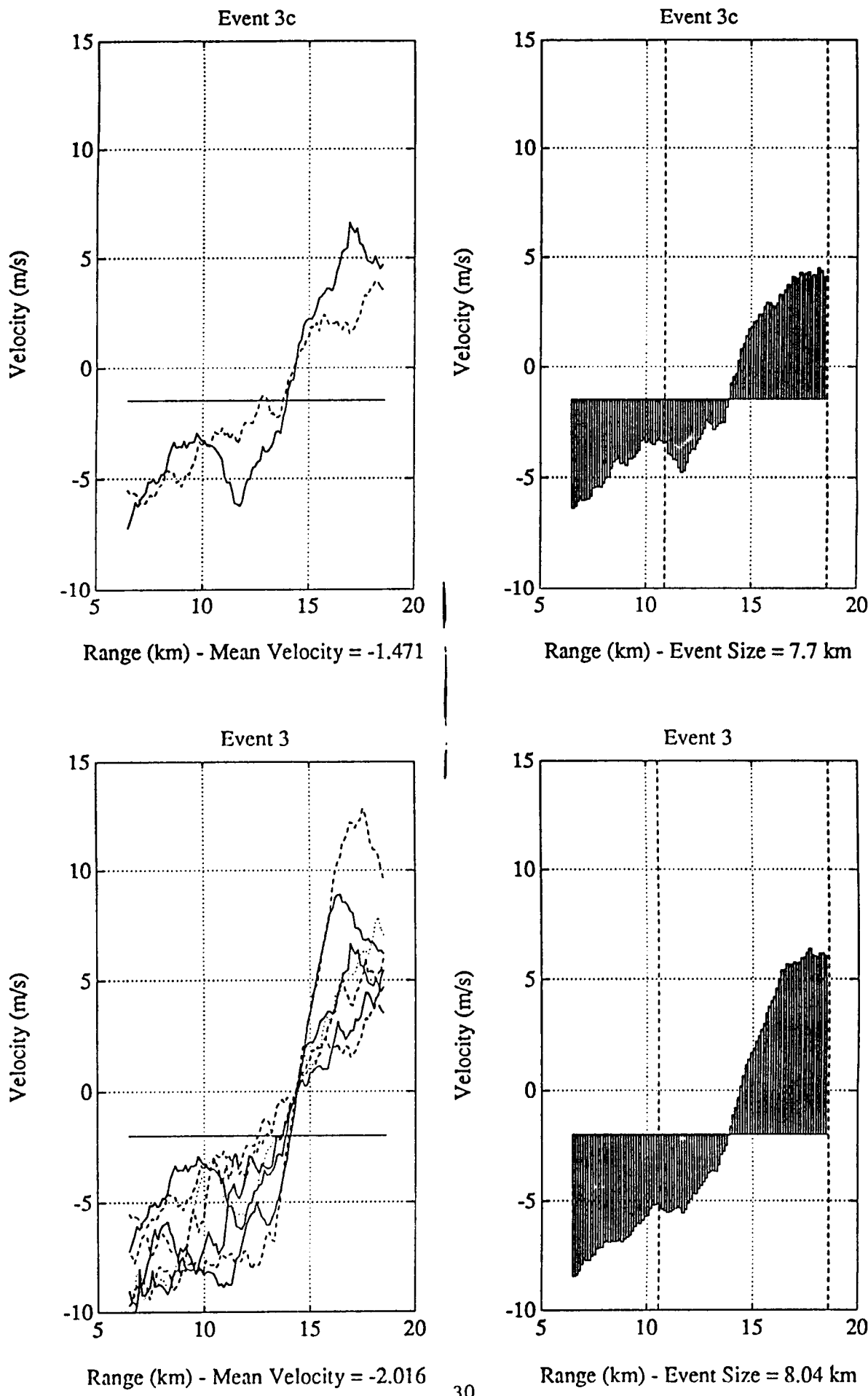


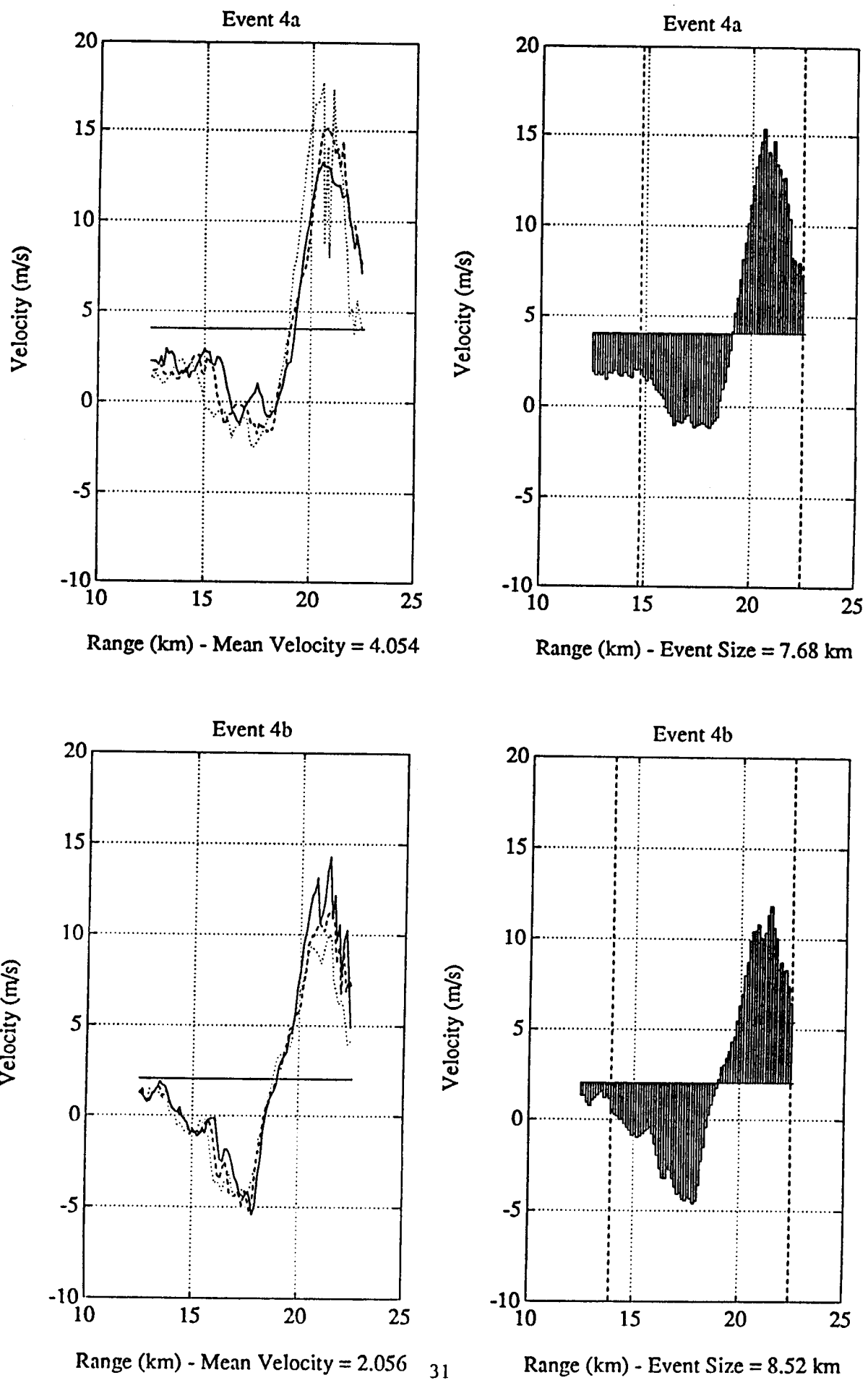


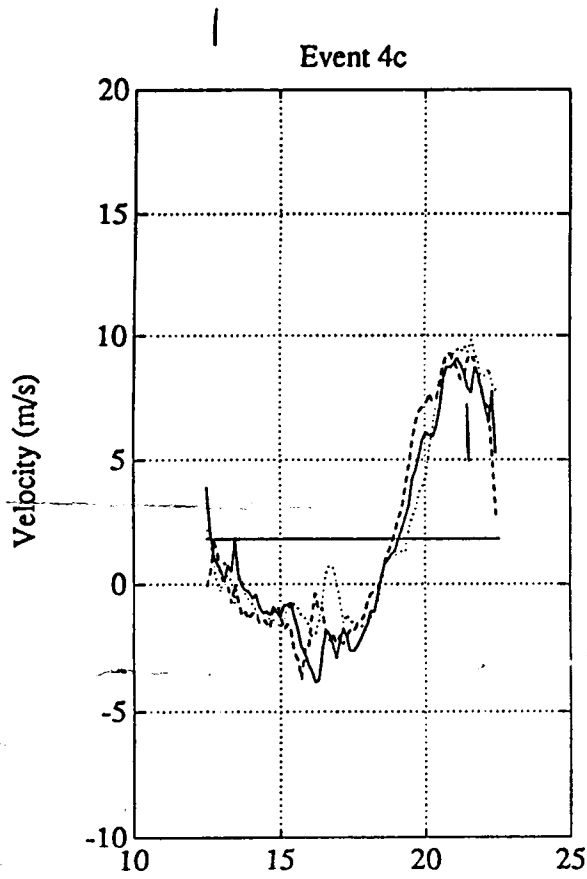


ORIGINAL DATA IS
OF POOR QUALITY

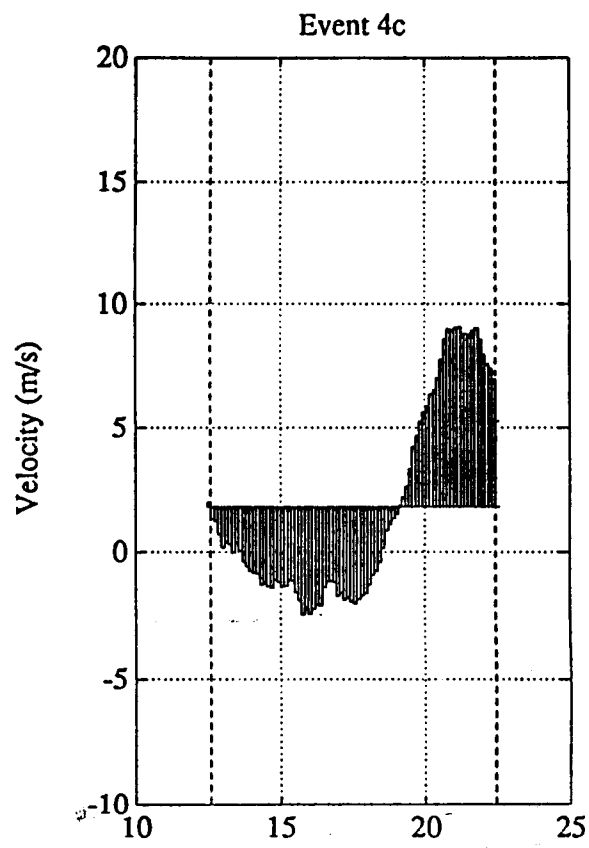




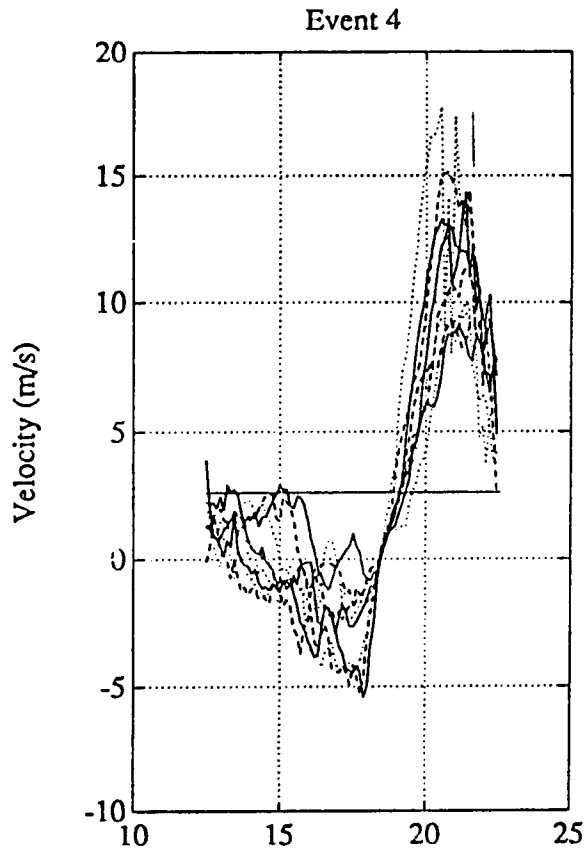




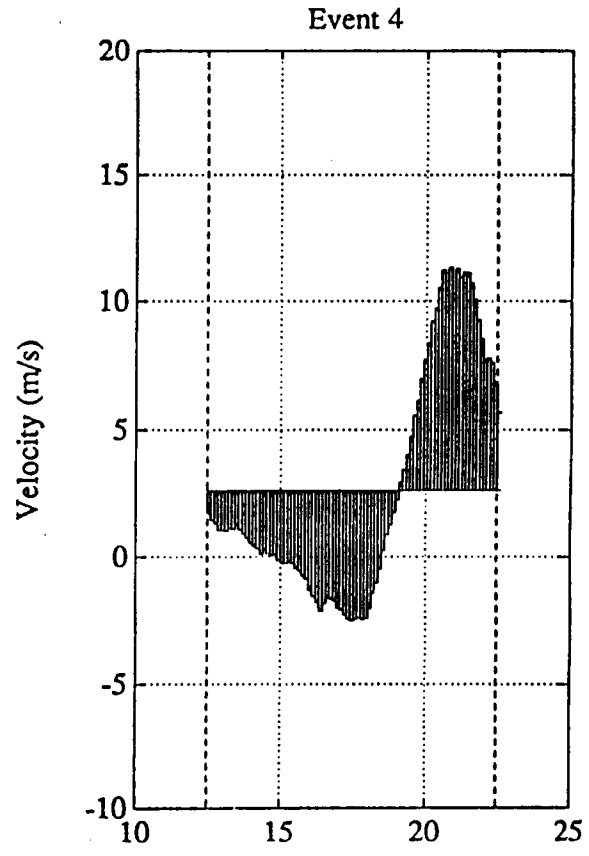
Range (km) - Mean Velocity = 1.788

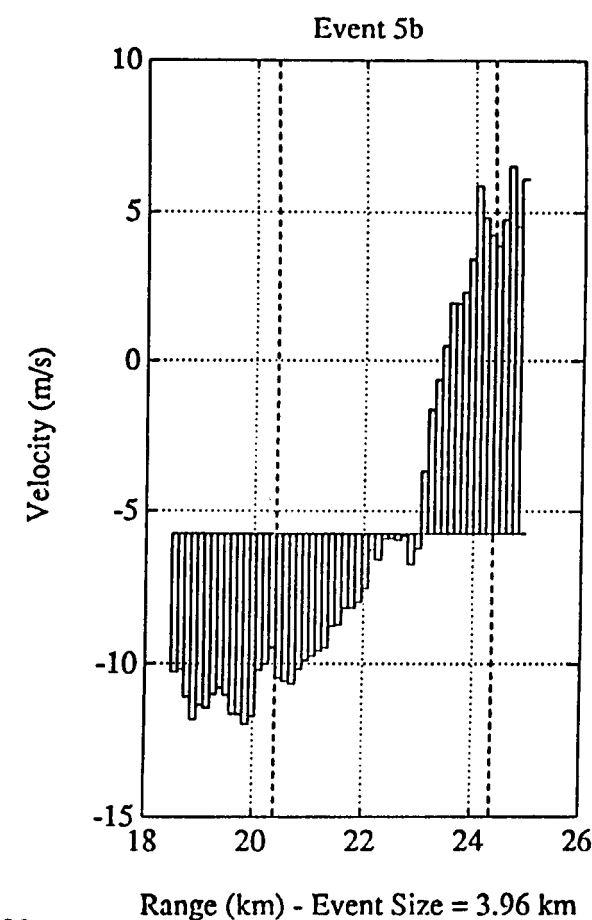
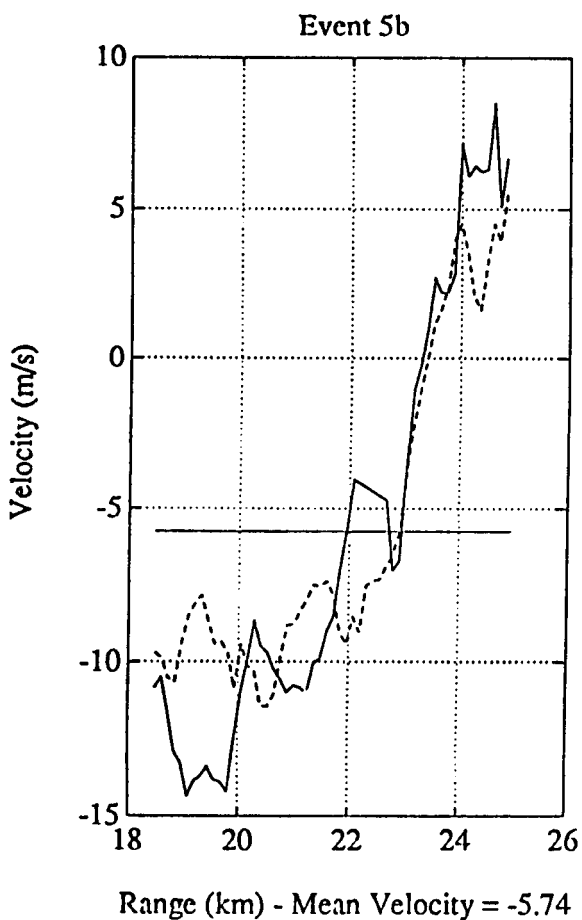
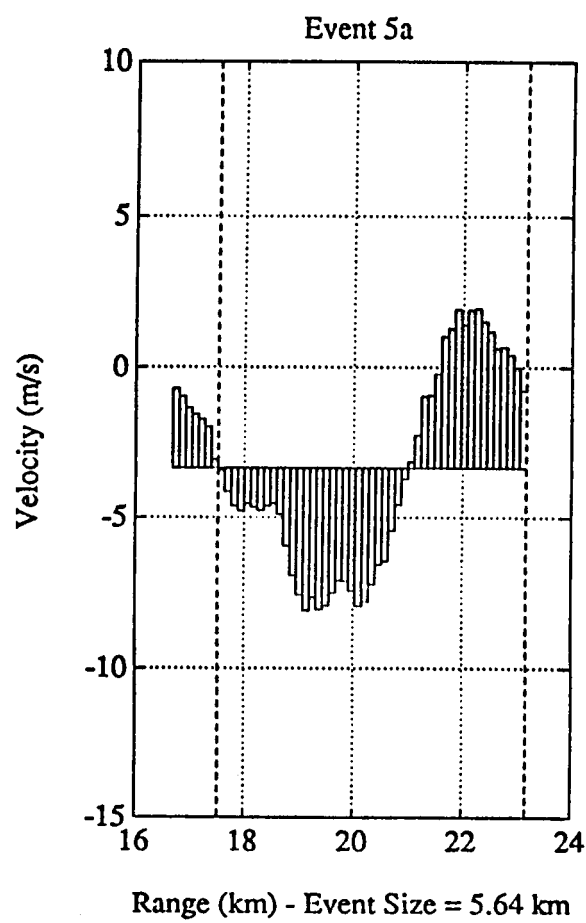
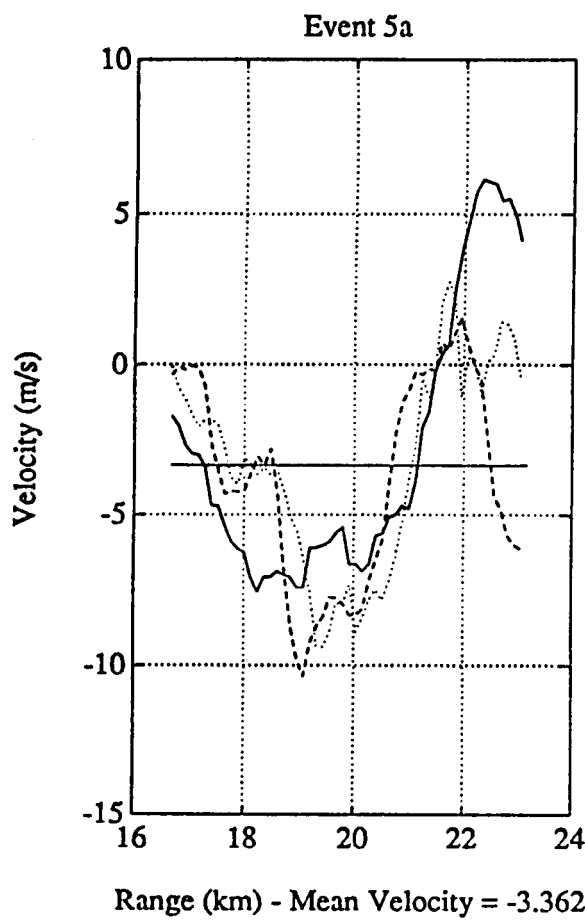


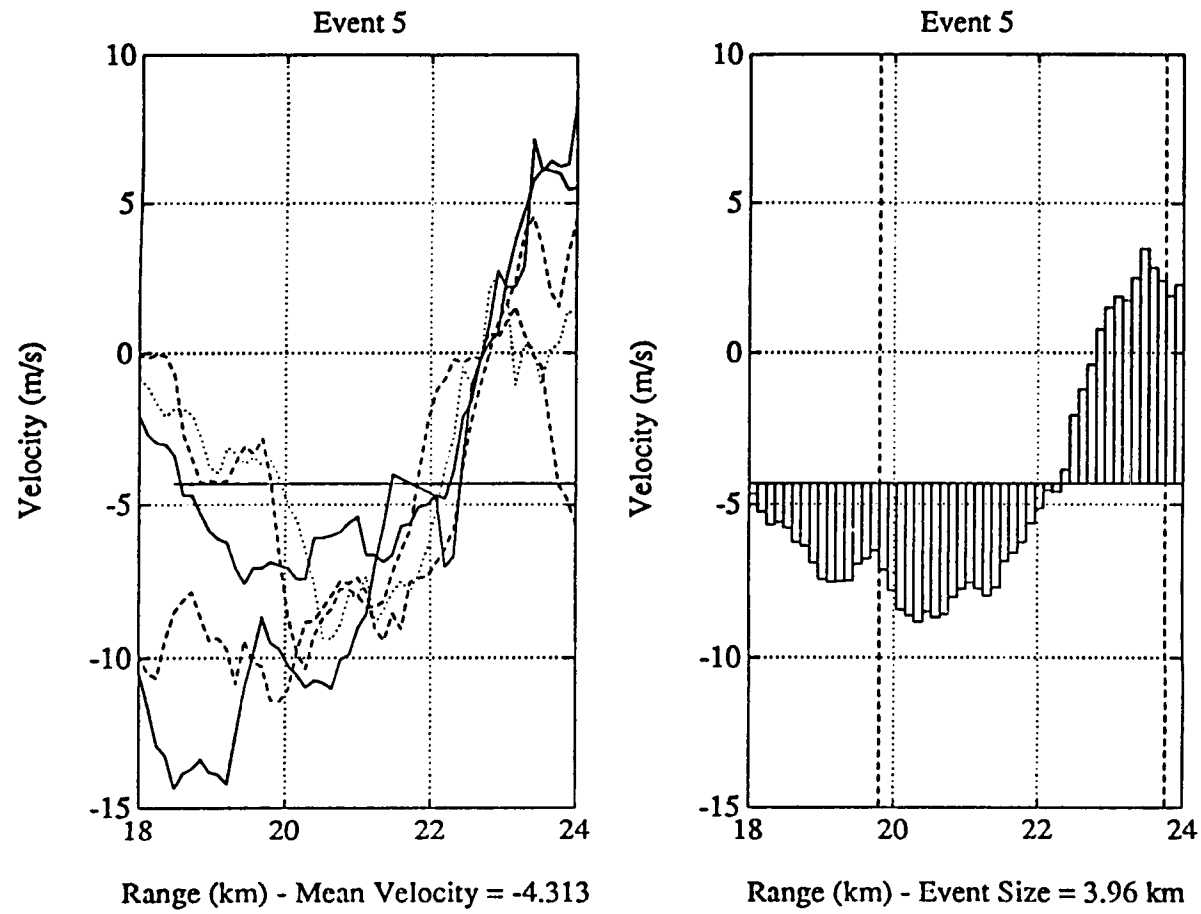
Range (km) - Event Size = 9.84 km

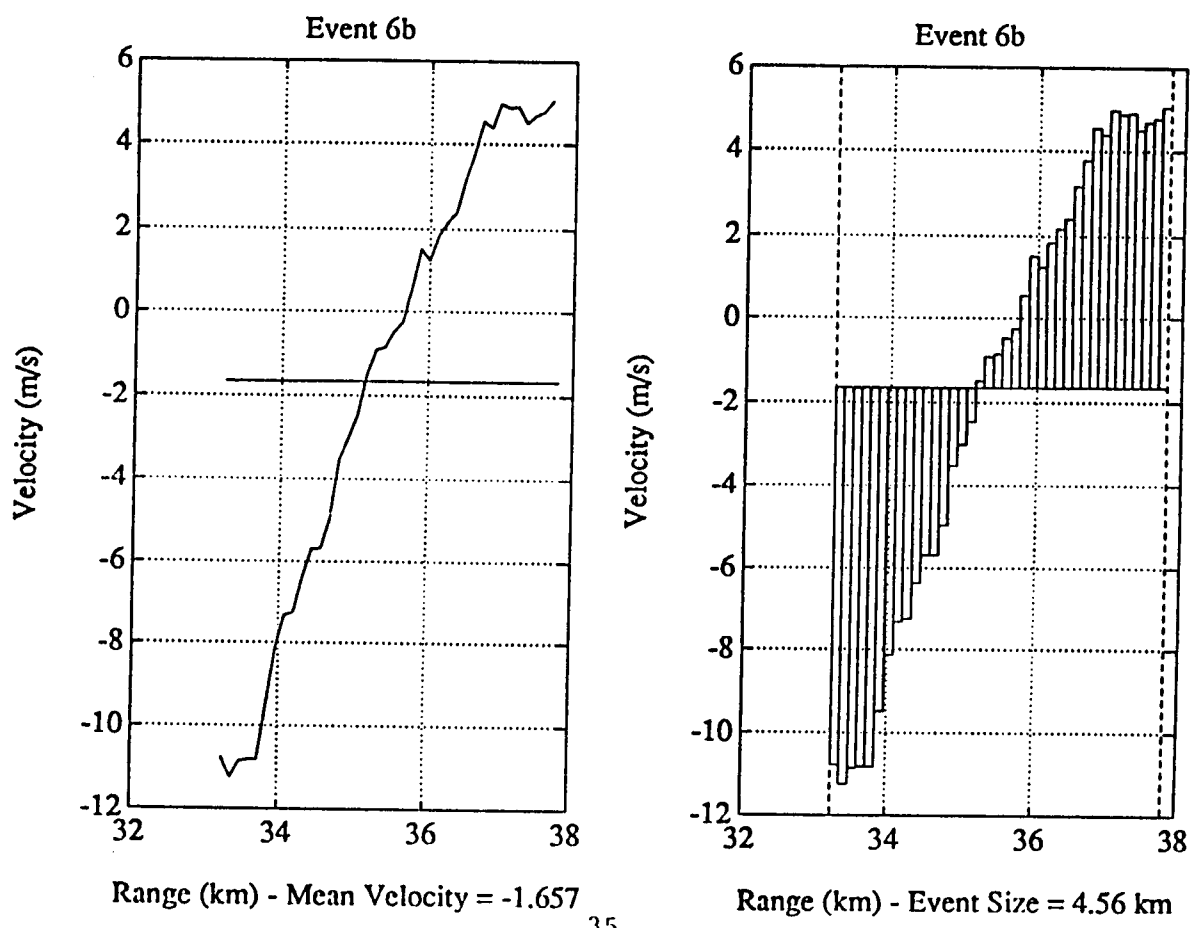
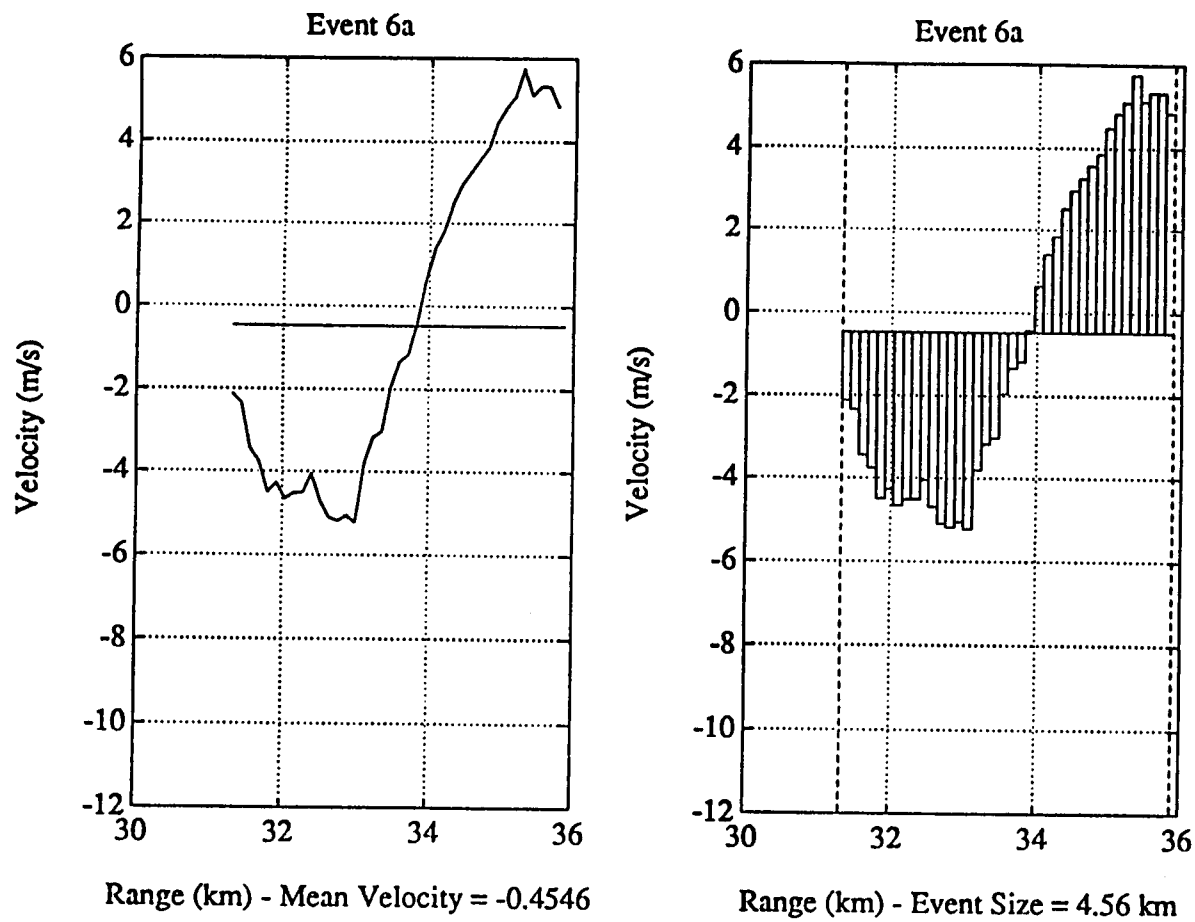


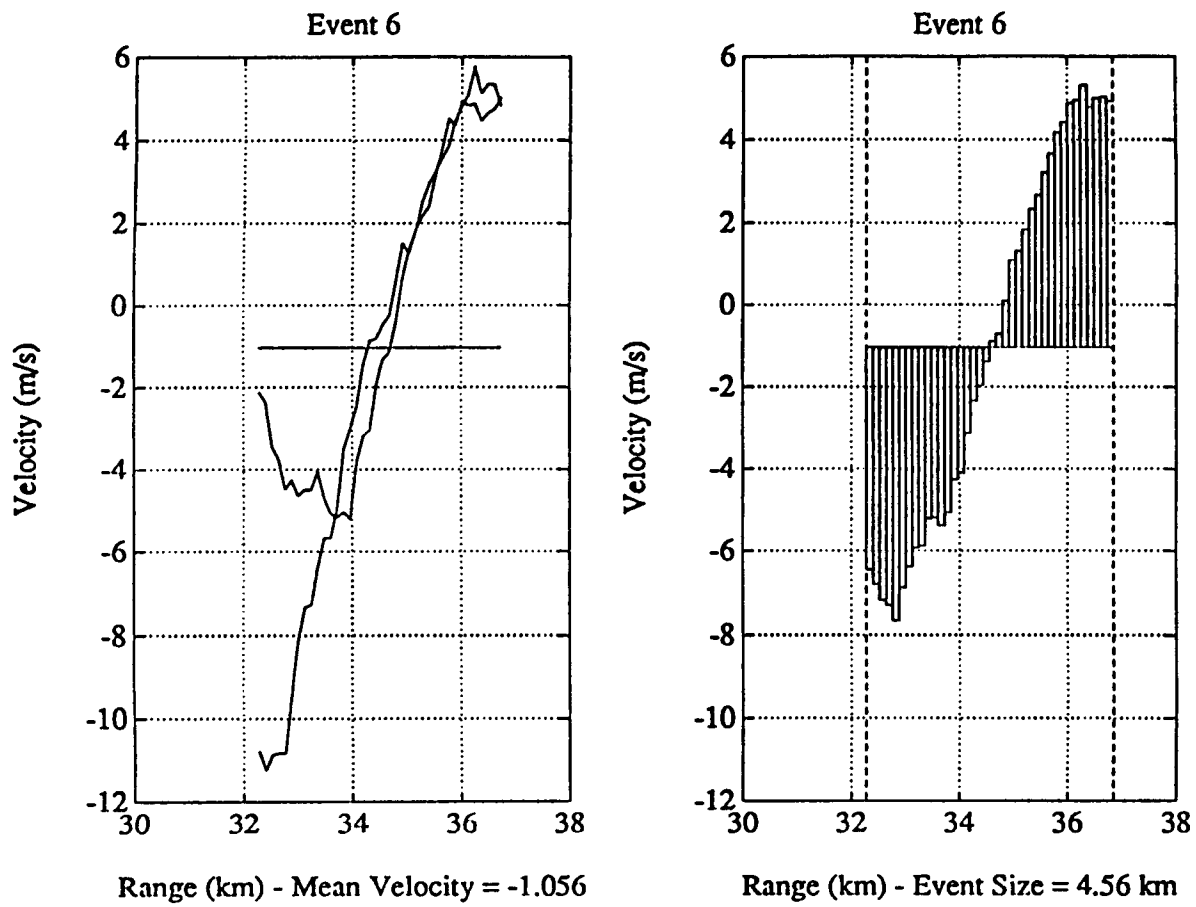
Range (km) - Mean Velocity = 2.633

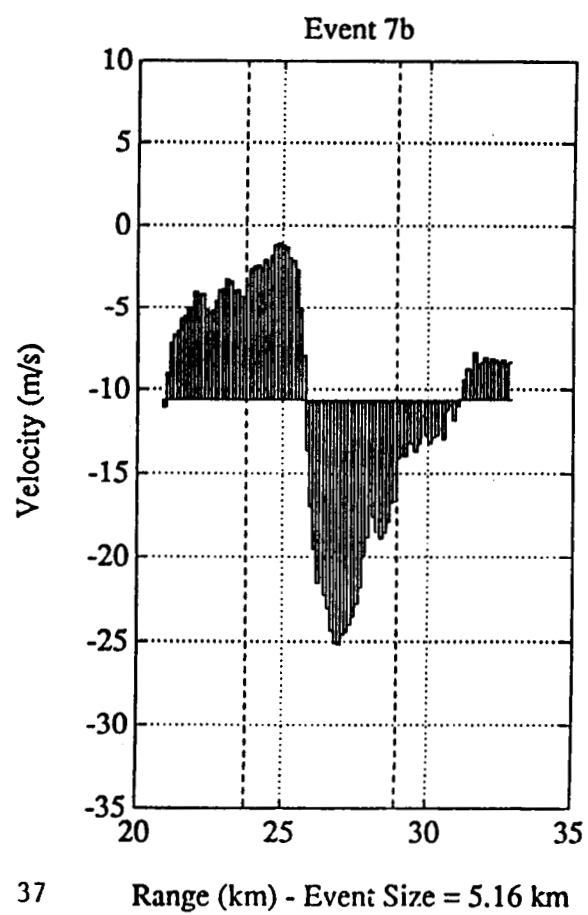
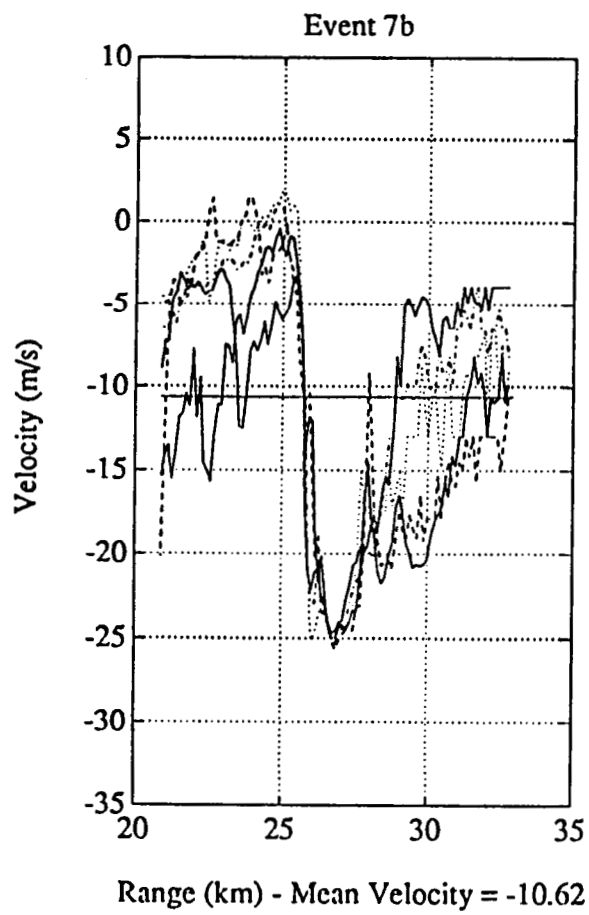
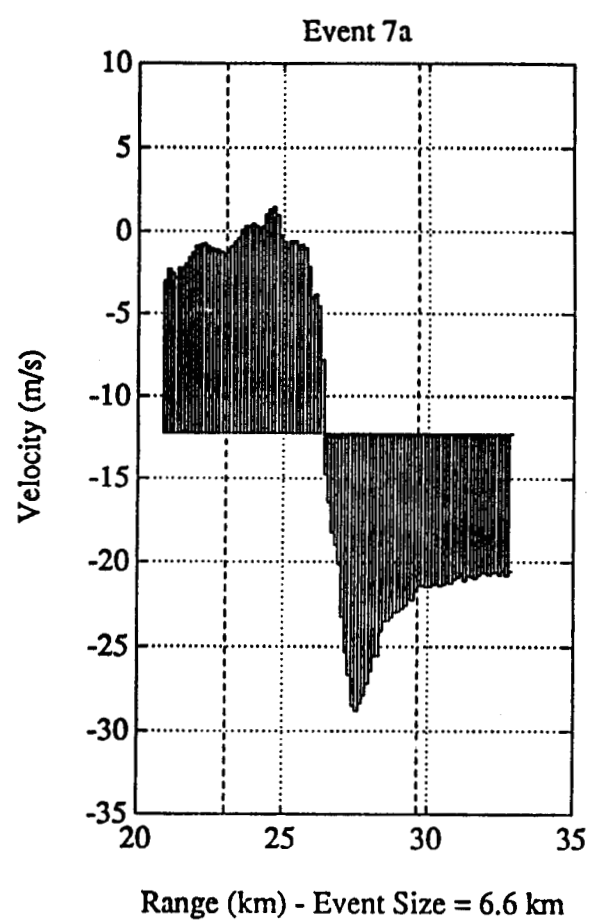
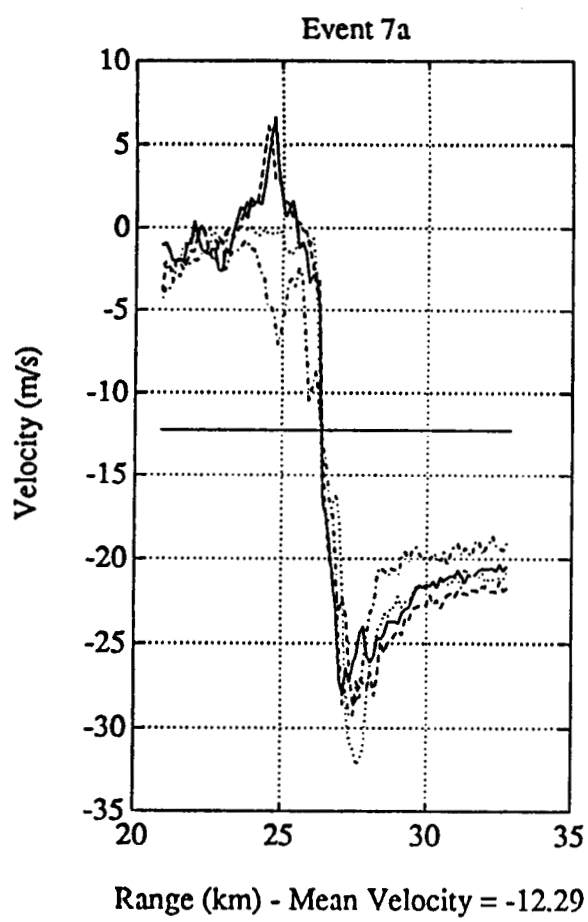












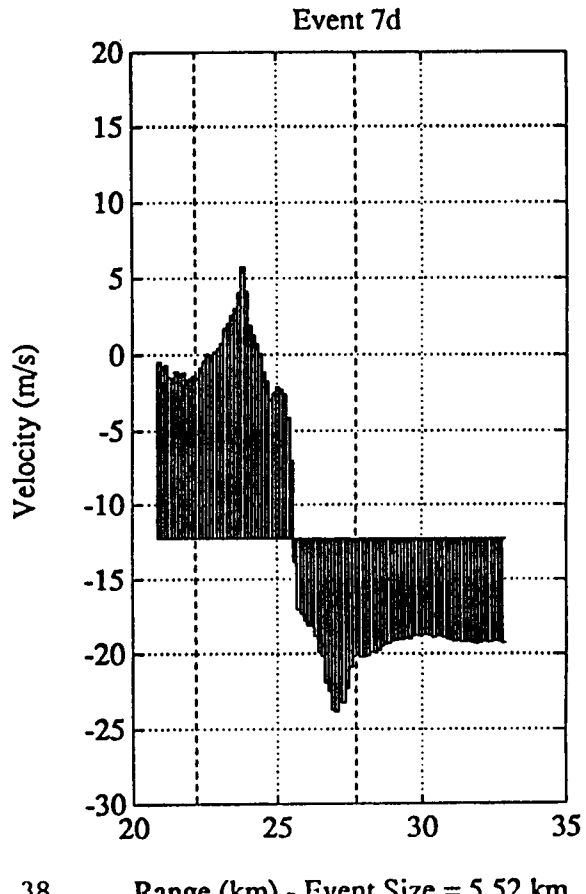
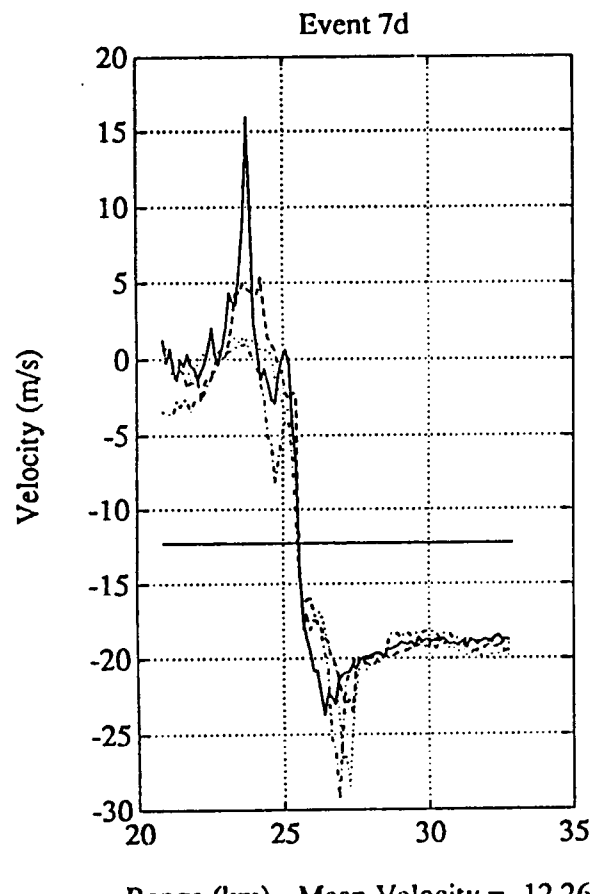
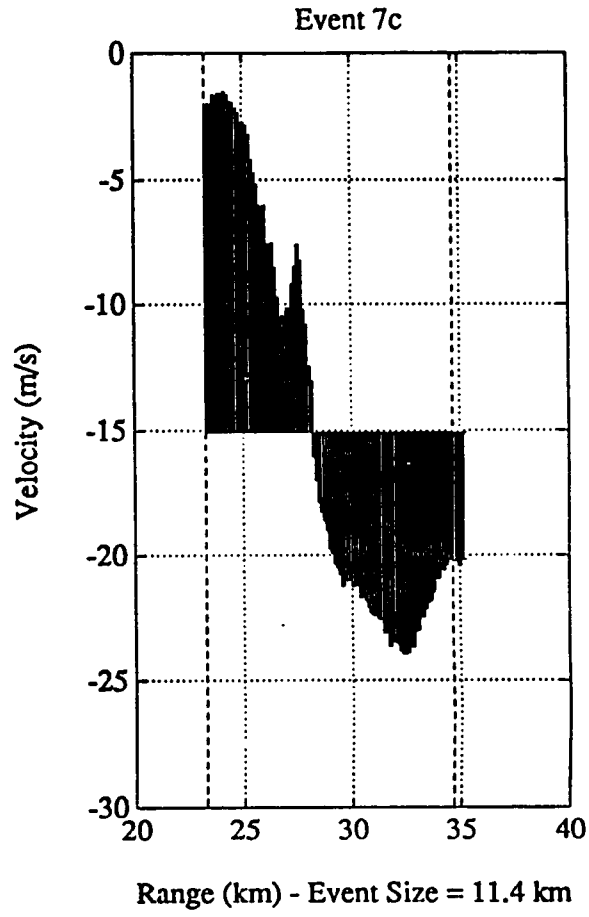
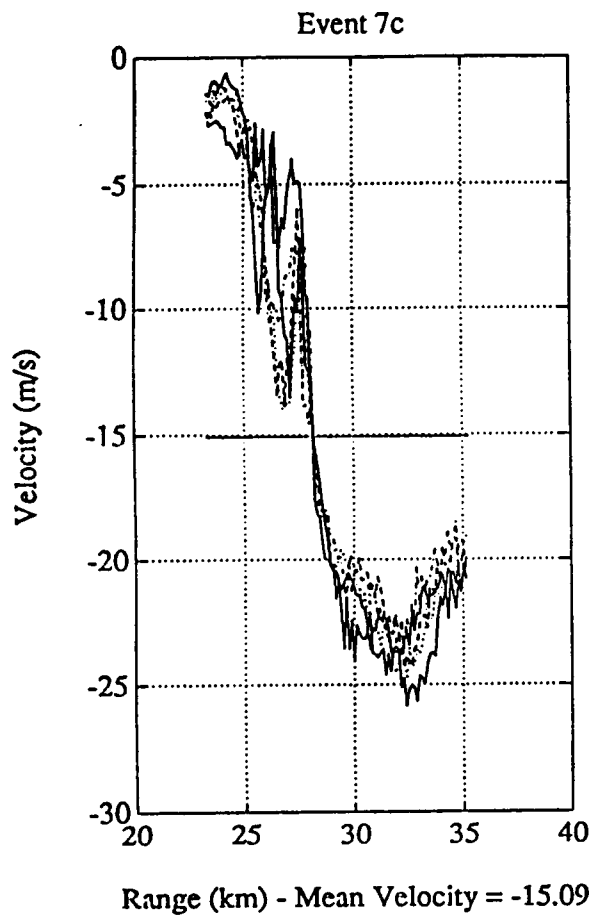
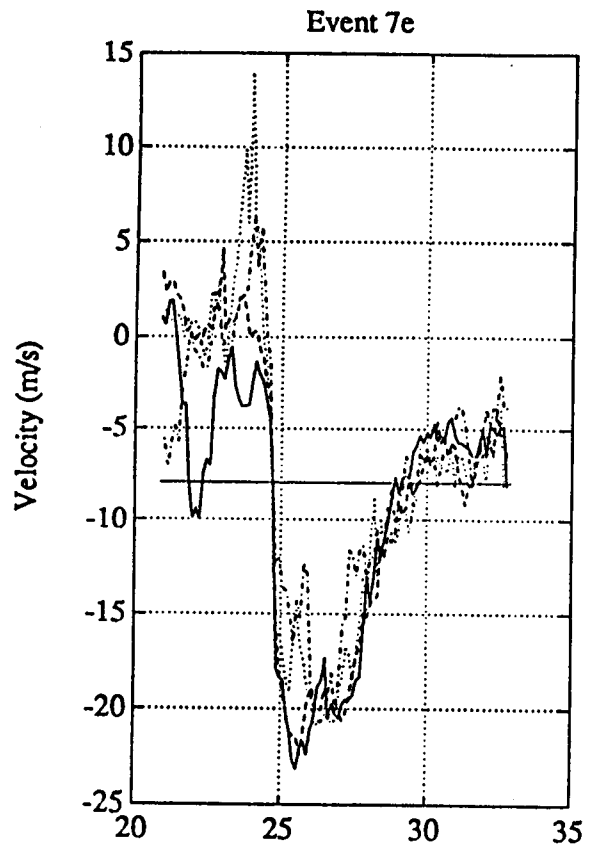
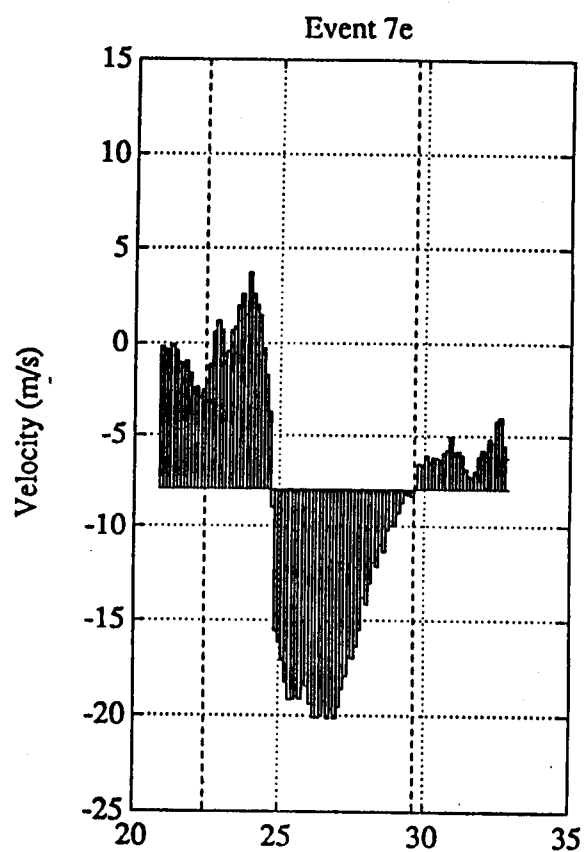


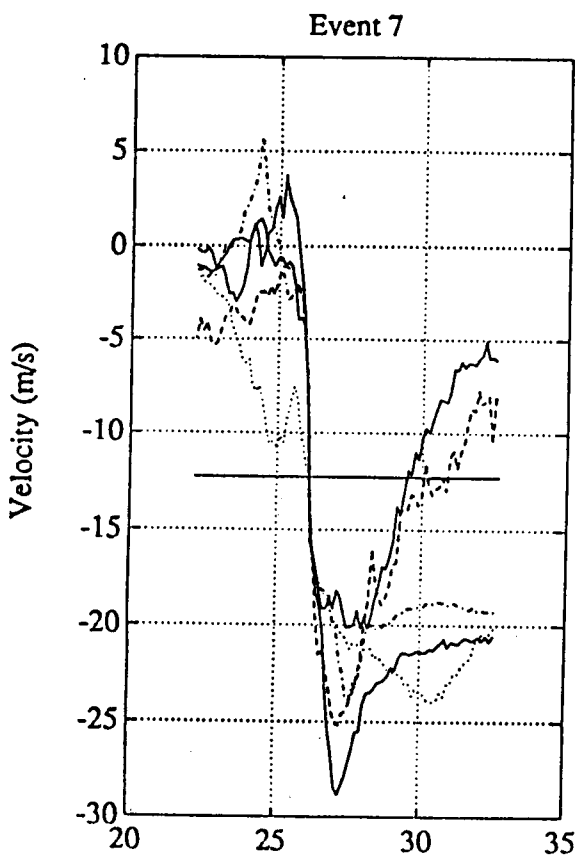
Fig. 26



Range (km) - Mean Velocity = -7.977

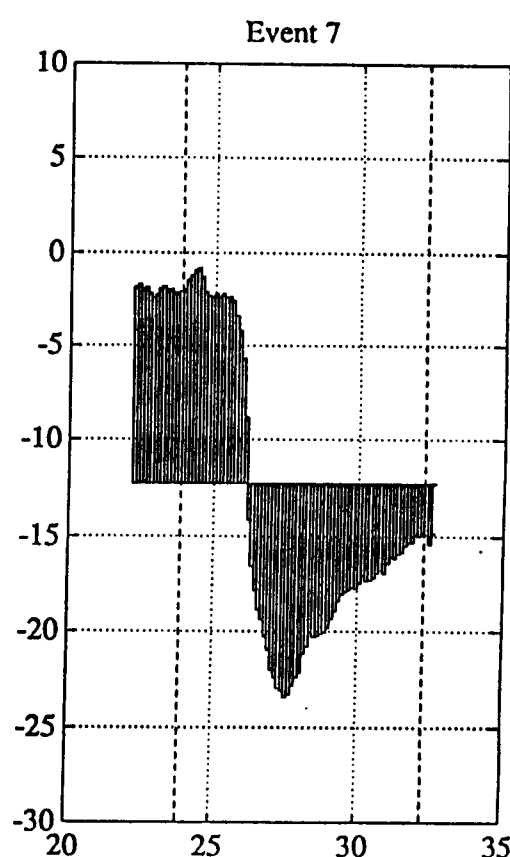


Range (km) - Event Size = 7.2 km



Range (km) - Mean Velocity = -12.3

39

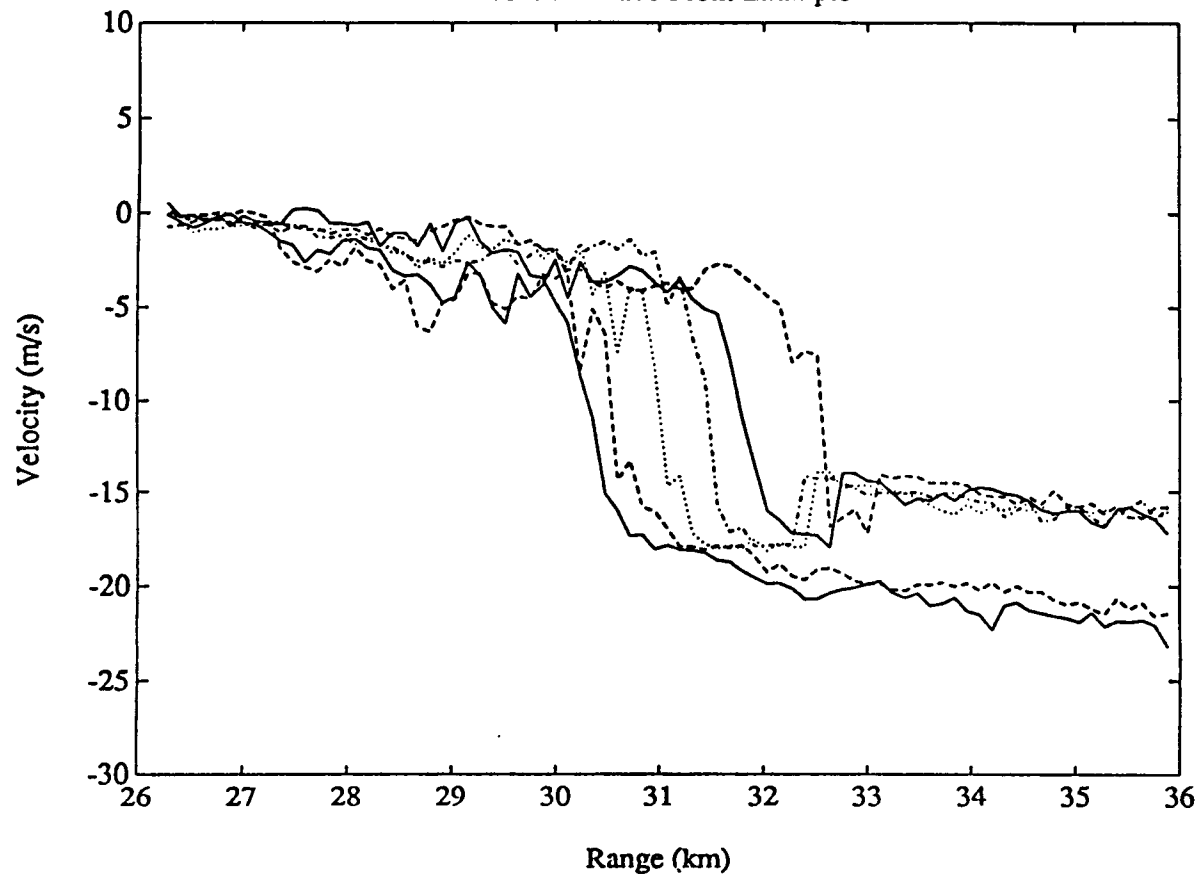


Range (km) - Event Size = 8.42 km

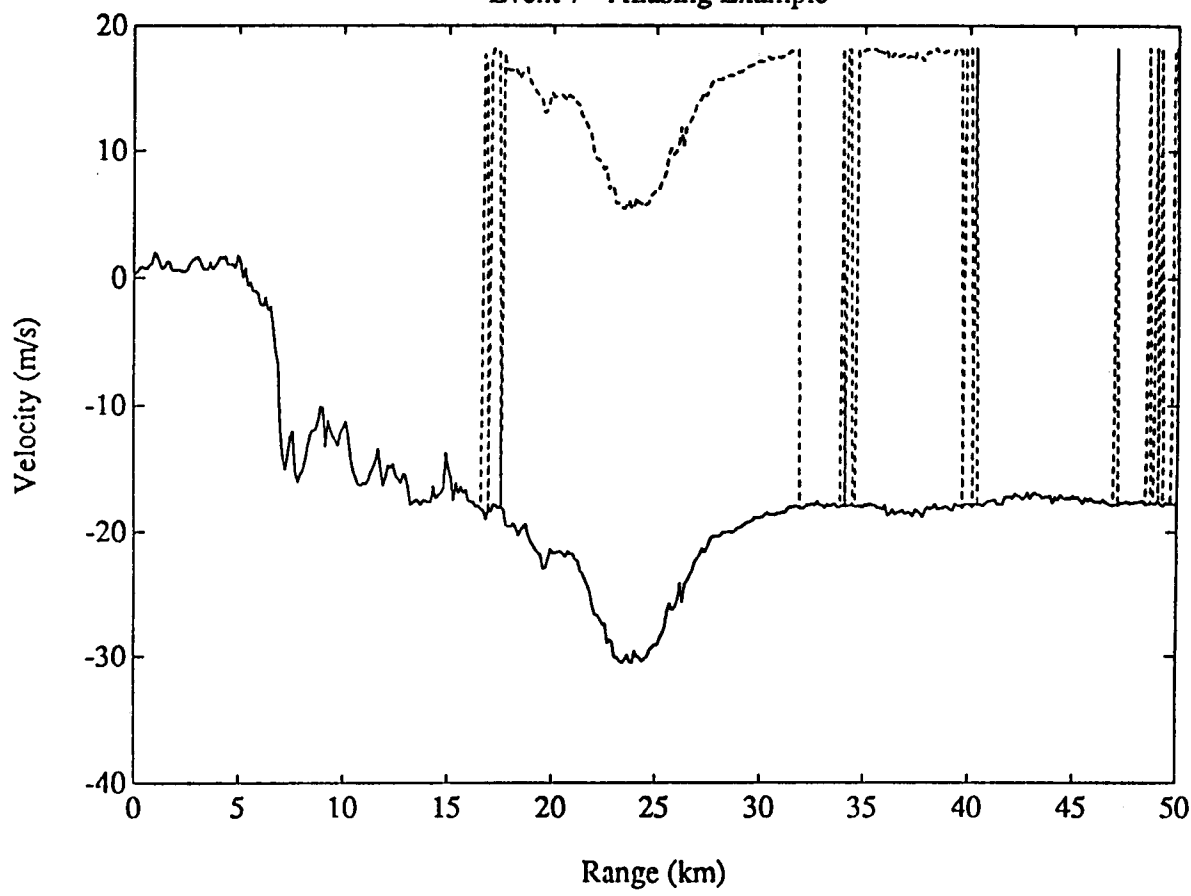
Fig 27

ORIGINAL PAGE IS
OF POOR QUALITY

Event 7 - Wave Front Example



Event 7 - Aliasing Example



Peak to Peak Measurements

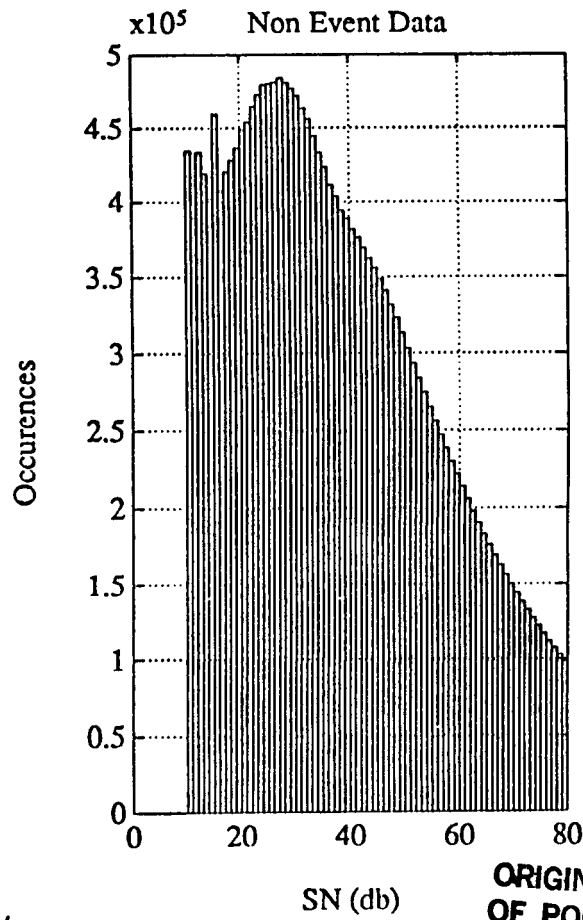
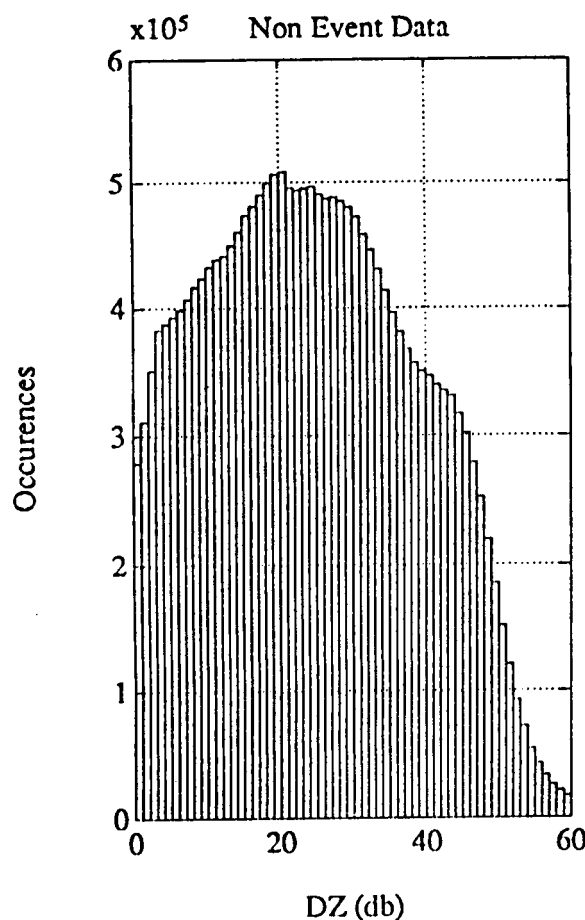
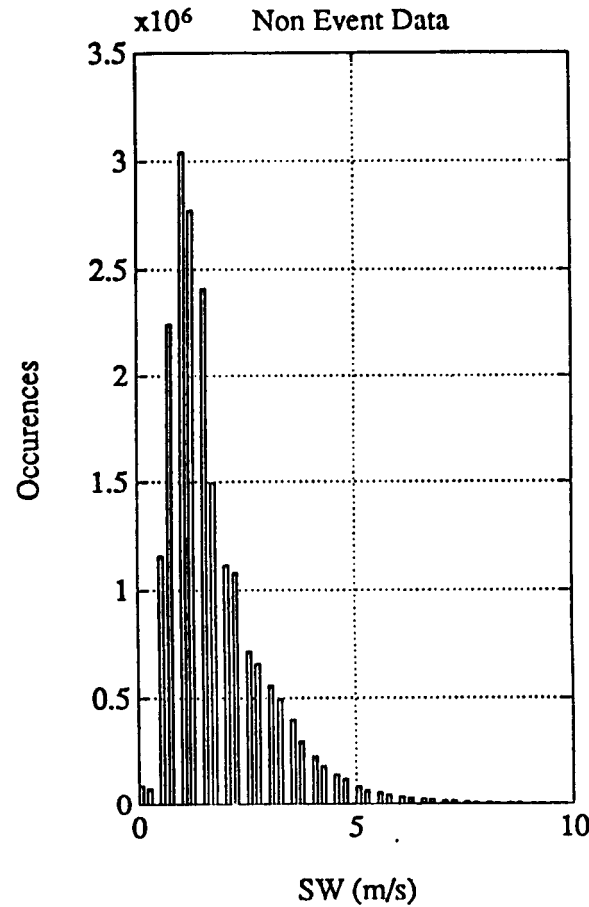
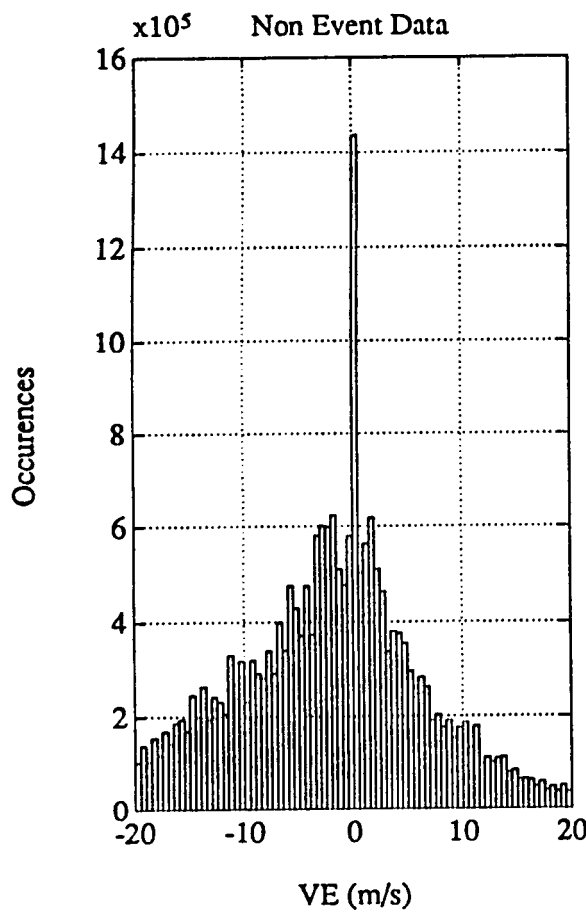
Event #	Minimum		Maximum		Delta V [m/s]	Size [Km]	Strength [m/s/km]
	Velocity [m/s]	Location [Km]	Velocity [m/s]	Location [Km]			
1a	-16.768	4.3200	16.212	6.9600	32.980	2.6400	12.492
1b	-14.350	2.7600	6.1433	4.8000	20.493	2.0400	10.046
1c	-22.530	2.4000	12.986	5.2800	35.516	2.8800	12.332
1	-12.648	3.2400	11.058	6.2400	23.707	3.0000	7.9023
2a	-8.5963	14.040	3.4340	19.680	12.030	5.6400	2.1330
2b	-7.5334	7.8000	2.4696	16.200	10.003	8.4000	1.1908
2	-5.5700	11.040	2.2309	16.800	7.8008	5.7600	1.3543
3a	-9.1884	5.2800	10.146	1.5720	19.334	10.440	1.8519
3b	-9.4715	1.5600	6.1605	13.440	15.632	11.880	1.3158
3c	-6.3770	1.8000	4.5000	13.440	10.877	11.640	.93445
3	-8.3137	2.8800	6.5264	14.040	14.840	11.160	1.3298
4a	-1.1626	18.000	15.352	20.520	16.514	2.5200	6.5533
4b	-4.6116	18.720	11.887	22.320	16.498	3.6000	4.5829
4c	-2.4790	16.920	9.0760	22.320	11.555	5.4000	2.1398
4	-2.4900	18.120	11.320	21.480	13.810	3.3600	4.1101
5a	-8.0817	19.080	1.9482	22.200	10.030	3.1200	3.2147
5b	-11.948	19.800	6.4800	24.600	18.428	4.8000	3.8392
5	-8.9875	19.920	3.8949	23.040	12.882	3.1200	4.1290
6a	-5.2080	32.280	5.7720	34.560	10.980	2.2800	4.8158
6b	-11.242	32.520	5.0340	36.840	16.276	4.3200	3.7676
6	-7.6560	32.040	5.3300	35.520	12.986	3.4800	3.7316
7a	-28.830	27.480	1.4325	24.600	-30.263	2.8800	-10.508
7b	-25.168	26.880	-1.0340	24.840	-24.134	2.0400	-11.830
7c	-23.958	32.400	-1.4030	24.120	-22.472	8.2800	-2.7140
7d	-23.860	27.000	5.7450	23.760	-29.605	3.2400	-9.1373
7e	-20.163	26.640	3.7325	23.880	-23.895	2.7600	-8.6576
7	-23.395	26.160	-.75610	23.040	-22.639	3.1200	-7.2559

Average Event Shear Strength(m/s/km) Starting At Crossover Point

Event	Number of Bin Pairs Averaged									
	1	2	3	4	5	6	7	8	9	10
1a	15.977	11.714	9.088	9.171	9.252	9.452	9.352	9.176	8.856	8.542
1b	18.687	13.852	11.283	9.644	8.682	8.002	7.464	6.977	6.500	6.062
1c	10.048	6.675	5.216	4.786	4.251	3.687	3.435	3.384	3.277	3.047
1	15.977	11.7B4	9.088	9.171	9.252	9.452	9.352	9.176	8.856	8.542
2a	34.694	27.474	24.988	23.174	22.059	21.372	20.877	20.314	19.884	19.474
2b	77.261	62.310	54.021	48.118	43.530	39.969	36.835	34.131	32.012	30.205
2	37.733	34.721	32.418	30.685	29.225	27.922	26.687	25.544	24.472	23.572
3a	5.158	4.648	4.315	4.061	3.921	3.792	3.710	3.628	3.563	3.501
3b	4.359	3.472	2.869	2.485	2.209	2.034	1.906	1.802	1.731	1.675
3c	3.161	3.078	2.813	2.561	2.443	2.370	2.296	2.234	2.179	2.121
3	3.519	3.078	2.758	2.589	2.489	2.417	2.364	2.309	2.257	2.205
4a	8.724	7.252	6.446	6.009	5.741	5.543	5.397	5.282	5.192	5.118
4b	4.015	3.560	3.062	2.783	2.600	2.490	2.393	2.354	2.339	2.333
4c	5.980	5.213	4.627	4.260	3.970	3.725	3.537	3.368	3.235	3.137
4	5.721	4.484	3.946	3.685	3.555	3.448	3.385	3.339	3.299	3.272
5a	4.691	4.341	4.422	4.143	3.960	3.904	3.807	3.723	3.590	3.477
5b	21.366	17.095	14.498	12.871	11.812	10.873	10.106	9.517	9.118	8.691
5	6.051	6.554	6.245	5.931	5.747	5.566	5.368	5.141	4.957	4.816
6a	6.430	5.741	5.252	4.832	4.547	4.309	4.097	3.914	3.752	3.625
6b	8.046	6.191	5.026	4.358	3.893	3.629	3.474	3.297	3.165	3.051
6	4.065	2.974	2.810	2.843	2.77%	2.723	2.675	2.622	2.581	2.544

Instantaneous Event Shear Strength(m/s/km) Starting At Crossover Point

Event	Number of Current Bin Pair									
	1	2	3	4	5	6	7	8	9	10
1a	15.977	7.452	3.835	9.420	9.573	10.452	8.755	7.947	6.294	5.718
1b	18.687	9.017	6.144	4.728	4.834	4.608	4.234	3.564	2.692	2.116
1c	10.048	3.304	2.297	3.498	2.111	.868	1.919	3.028	2.423	.988
1	15.977	7.452	3.835	9.420	9.573	10.452	8.755	7.947	6.294	5.718
2a	4.165	2.431	2.403	2.128	2.112	2.153	2.149	1.964	1.974	1.894
2b	9.274	5.685	4.494	3.650	3.022	2.660	2.164	1.825	1.807	1.673
2	4.529	3.806	3.338	3.059	2.807	2.569	2.314	2.105	1.908	1.857
3a	5.159	4.138	3.650	3.299	3.361	3.151	3.214	3.054	3.045	2.937
3b	4.359	2.585	1.663	1.335	1.108	1.151	1.144	1.074	1.154	1.178
3c	3.161	2.997	2.280	1.807	1.970	2.007	1.852	1.797	1.740	1.606
3	3.519	2.638	2.121	2.077	2.093	2.054	2.052	1.923	1.842	1.731
4a	8.724	5.781	4.834	4.697	4.668	4.556	4.525	4.475	4.471	4.457
4b	4.015	3.106	2.065	1.947	1.869	1.940	1.812	2.076	2.231	2.274
4c	5.980	4.447	3.454	3.160	2.814	2.494	2.413	2.185	2.172	2.262
4	5.721	3.249	2.870	2.901	3.035	2.915	3.009	3.014	2.979	3.040
5a	4.692	3.991	4.585	3.305	3.229	3.622	3.226	3.137	2.525	2.462
5b	21.366	12.823	9.304	7.988	7.574	6.183	5.503	5.395	5.920	4.855
5	6.052	7.056	5.627	4.987	5.016	4.663	4.177	3.549	3.488	3.549
6a	6.430	5.053	4.275	3.570	3.407	3.121	2.827	2.628	2.460	2.481
6b	8.046	4.337	2.695	2.356	2.034	2.308	2.543	2.062	2.104	2.024
6	4.065	1.885	2.482	2.945	2.517	2.443	2.390	2.254	2.251	2.219



ORIGINAL PAGE IS
OF POOR QUALITY

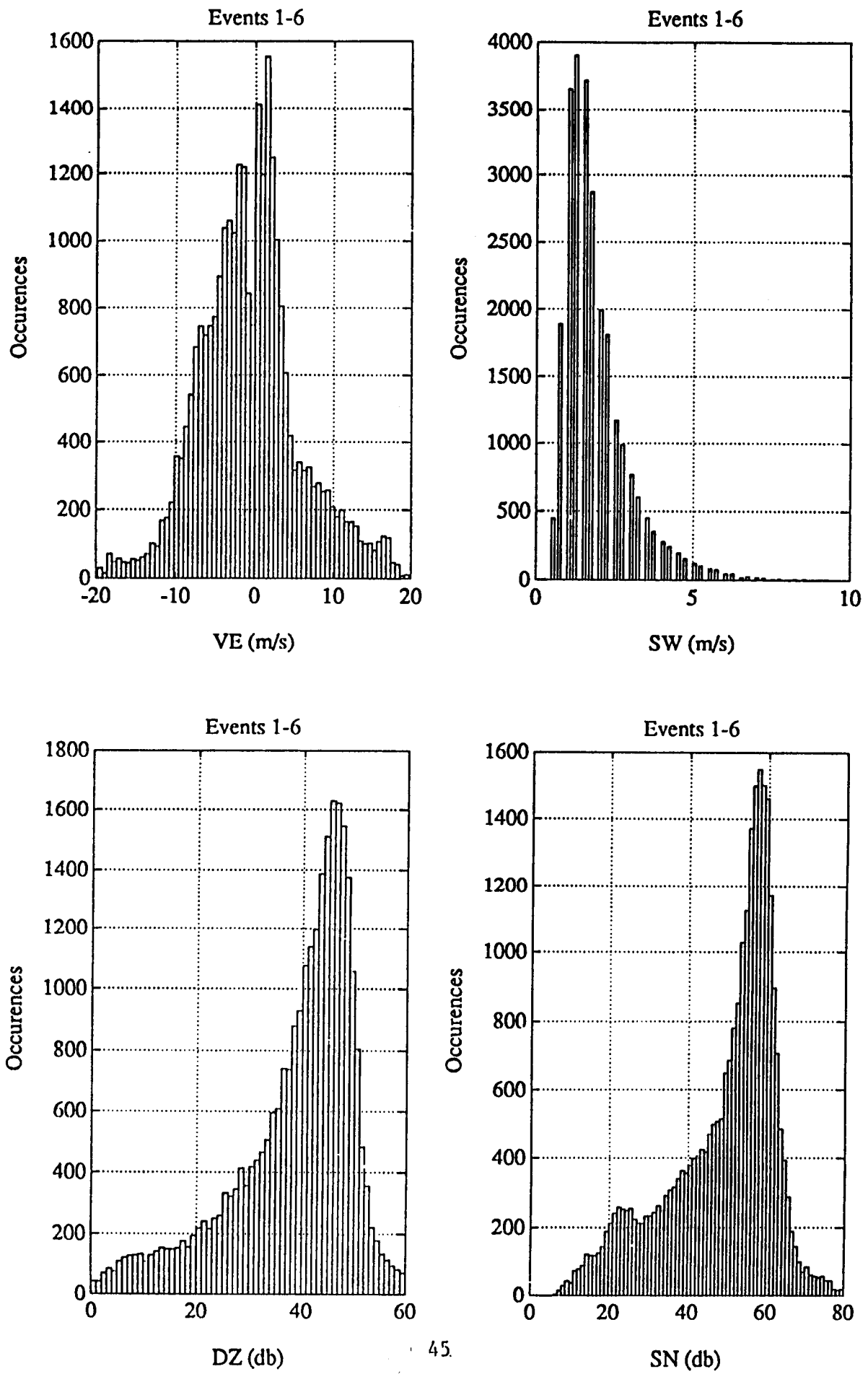


Fig 33

Mean Data Field Values

Event	VE (m/s)	SW (m/s)	DZ (dBz)	SNR (dB)	F-Factor
1	2.408	1.755	41.660	63.843	.139
2	-.836	1.567	30.373	42.517	.047
3	-3.966	1.502	43.512	57.725	.089
4	2.177	1.920	38.205	49.235	.052
5	-4.988	1.920	35.245	44.589	.092
6	-1.566	2.170	44.674	49.766	.069
7	-1.661	3.495	44.896	31.820	.079
All Events	2.515	2.047	39.795	48.499	.081
Non-Event	-2.063	1.847	25.216	29.660	

Event Statistics (VE)

Event	Mean	Variance	Skewness	Kurtosis
1a	1.9497	48.326	-.24369	3.81150
1b	2.2753	34.557	-.57383	3.26580
1c	.4006	46.478	-1.8052	6.17033
1	2.4083	29.646	-.79232	2.87445
2a	-1.2505	9.5866	1.31731	1.7382
2b	-2.1997	10.967	.02102	1.2422
2	-.83617	3.4003	.088726	1.3325
3a	-1.8287	52.415	.67260	1.6819
3b	-3.9794	14.722	.49079	2.54946
3c	-1.5388	12.980	.51146	1.7534
3	-3.9658	10.522	.97701	3.098361
4a	4.0333	25.693	.85642	2.26253
4b	1.4046	18.866	.88153	3.017717
4c	1.1284	11.223	1.1204	3.19435
4	2.1767	15.887	.84464	2.35547
5a	-3.2835	6.3125	.13607	1.8028
5b	-6.3098	22.702	.27026	1.4311
5	-4.9881	7.9810	-.11226	1.4066
6a	-.45458	15.716	.28198	1.3931
6b	-1.2567	29.885	-.45611	1.7856
6	-1.5663	23.426	-.13868	1.3765
7a	-18.805	25.891	-.20979	1.3533
7b	-22.949	9.8414	.95044	2.69892
7c	-15.397	57.793	.51840	1.9754
7d	-11.676	85.455	.47616	1.4357
7e	-23.663	6.3006	1.5017	5.2262
7	-1.661	1.2525	.17993	1.35362
Non Events	5.6864	86.9451	.9026	3.3863

Event Statistics (SW)

Event	Mean	Variance	Skewness	Kurtosis
1a	1.2955	.27650	-.75085	6.4037
1b	1.5632	.39614	-.092647	6.8810
1c	2.1861	.99610	1.4193	5.1907
1	1.7557	.22298	.78531	2.86509
2a	1.6422	.42850	.82111	2.04983
2b	1.4193	.10013	-.04272	1.8736
2	1.5673	.085879	1.2145	3.54299
3a	1.7655	.069488	.54080	3.097786
3b	1.5226	.095633	.56062	2.67983
3c	1.3501	.042799	.29253	2.19454
3	1.5015	.052925	-.60041	2.62021
4a	1.9294	.61756	.19105	1.8462
4b	2.0691	.52487	.21798	1.8877
4c	1.7439	.13086	.93832	3.24405
4	1.9203	.25245	.070823	1.5549
5a	2.2672	.20418	-.035206	2.17768
5b	2.8602	.14586	-.62212	4.3163
5	2.5405	.073804	-.74115	2.88303
6a	1.7947	.19538	.081711	1.9215
6b	2.3467	.12216	.38518	2.27252
6	2.1697	.044844	.025948	2.10578
7a	2.5870	3.1395	-1.0489	2.86882
7b	4.0824	.81505	-.24664	2.68103
7c	2.8203	2.8708	-1.2985	3.67481
7d	3.0110	.34788	.43486	4.3933
7e	3.4379	2.3188	-.54325	2.81113
7	3.4957	.21009	5.7090	8.5135
Non Events	1.8474	1.3754	1.8531	7.8513

Event Statistics (DZ)

Event	Mean	Variance	Skewness	Kurtosis
1a	45.980	26.310	-1.3137	4.7018
1b	42.450	138.11	-1.4495	4.1822
1c	36.329	252.84	-.36440	1.6526
1	41.660	86.576	-.93854	3.30746
2a	32.194	166.04	-.43681	1.6135
2b	32.445	52.772	-.20819	1.9140
2	30.373	40.826	-.83099	2.60674
3a	45.389	11.562	-.80648	2.33874
3b	44.278	1.2162	.72820	3.97395
3c	42.401	3.3873	-.62986	2.76085
3	43.512	1.6363	-.47918	2.63916
4a	39.588	75.875	-.56081	2.01525
4b	38.787	98.332	-.85625	2.24991
4c	36.261	1.2732	-.84593	2.17446
4	38.205	93.103	-.76766	2.14900
5a	38.913	46.583	-.64956	2.16933
5b	32.423	185.79	-.25771	1.5943
5	35.245	117.54	-.39215	1.6774
6a	43.926	34.254	-2.3838	8.7861
6b	44.271	6.4524	-.85804	3.38602
6	44.674	5.9879	-.66302	2.11069
7a	49.503	78.087	-.19041	1.4445
7b	38.503	14.246	-.032071	1.8314
7c	45.994	69.143	.40527	1.6716
7d	46.654	111.70	.19759	1.2382
7e	41.068	54.009	.040807	1.8523
7	44.896	2.6759	-.76838	2.368644
Non Events	25.2157	193.8815	.1684	2.0994

Event Statistics (SN)

Event	Mean	Variance	Skewness	Kurtosis
1a	65.558	35.410	-.35321	2.18416
1b	67.139	82.494	-.56157	2.67771
1c	61.012	283.76	-.51797	2.10476
1	63.843	115.89	-.45807	1.9826
2a	43.329	200.40	-.52574	1.6854
2b	45.972	72.719	-.44655	1.7663
2	42.517	63.229	-.90188	2.80069
3a	57.275	6.5976	-.79084	3.10999
3b	58.669	10.031	.66161	2.03076
3c	56.614	4.4554	-.56871	3.48297
3	57.725	4.1401	.36075	1.7935
4a	50.683	64.591	-.63554	2.23906
4b	49.882	7.6662	-.81133	2.20278
4c	47.211	106.40	-.89170	2.29937
4	49.235	75.263	-.73942	2.09108
5a	48.811	56.713	-.65051	2.09272
5b	41.486	209.45	-.23677	1.5810
5	44.589	136.01	-.37314	1.6726
6a	49.295	31.565	-2.4398	9.1286
6b	49.153	7.7782	-.76235	3.099271
6	49.766	6.4720	-.66439	3.27608
7a	36.424	92.142	-.33034	1.7738
7b	25.414	17.157	-.17242	2.05346
7c	32.168	85.112	.33566	1.5695
7d	33.595	134.25	.19451	1.2541
7e	27.977	5.1359	-.16321	2.19500
7	31.820	3.6354	-.81960	2.26793
Non Events	29.6595	122.9112	.08625	1.9086

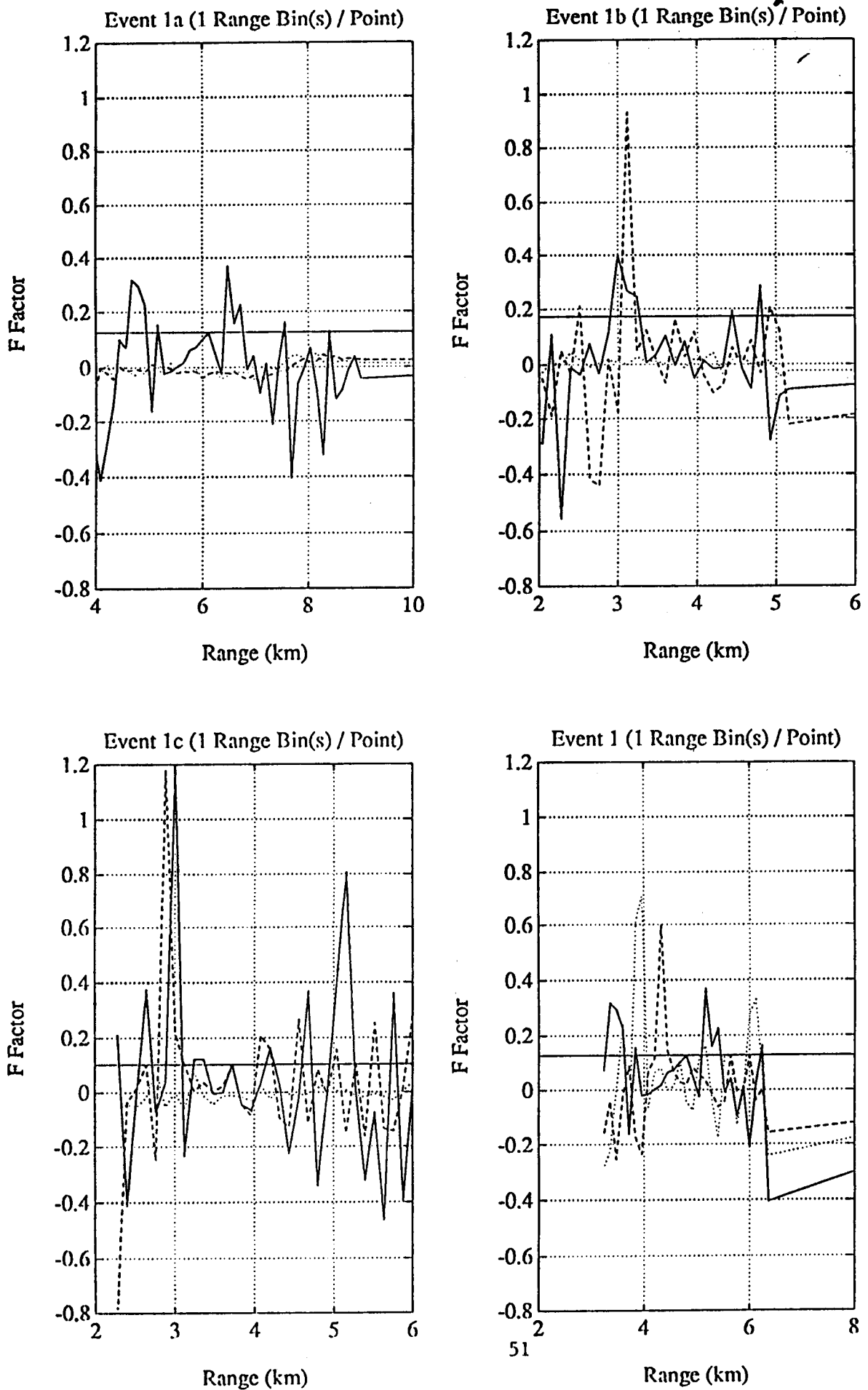
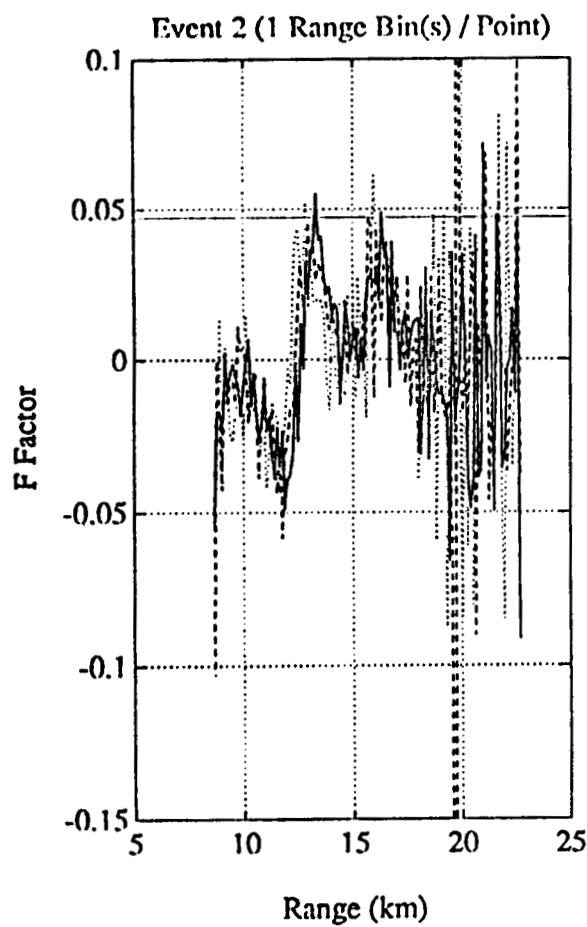
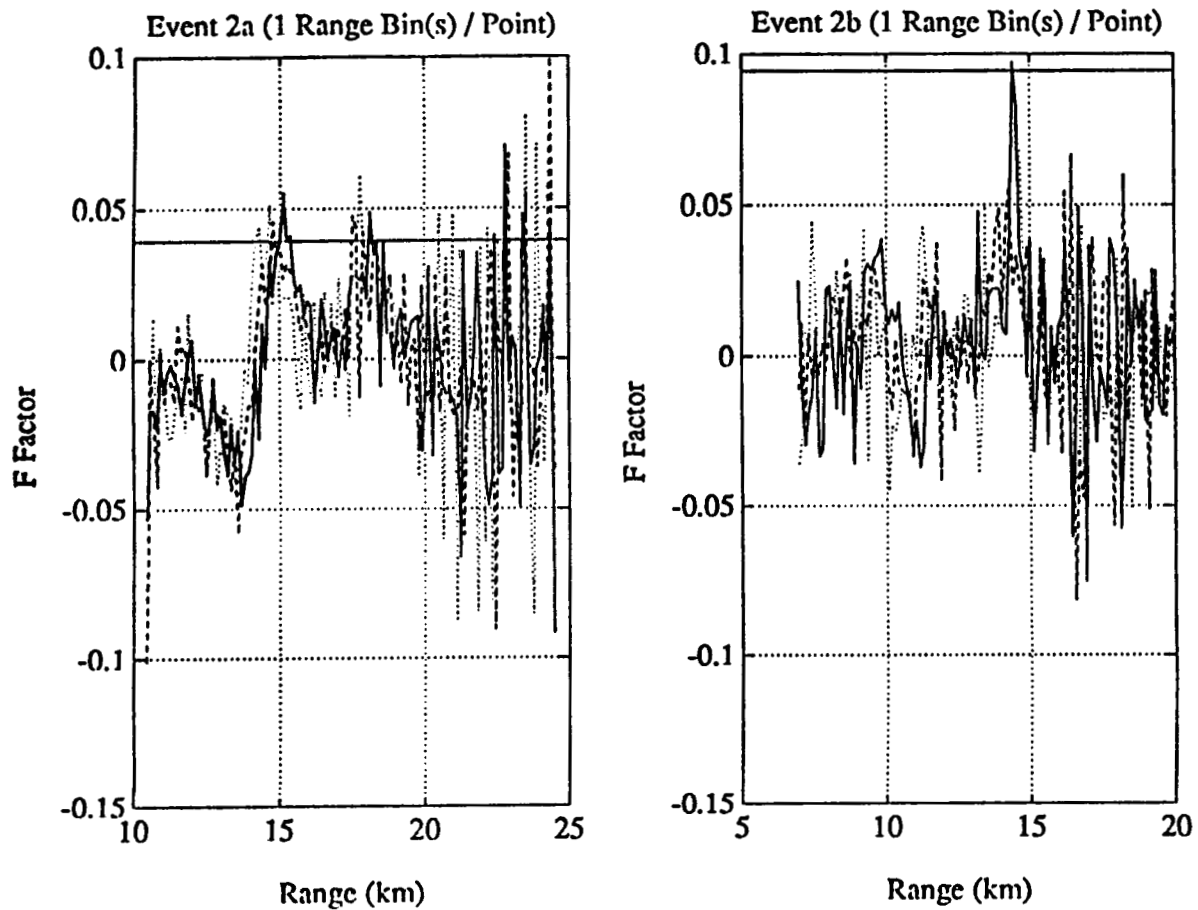


Fig. 39



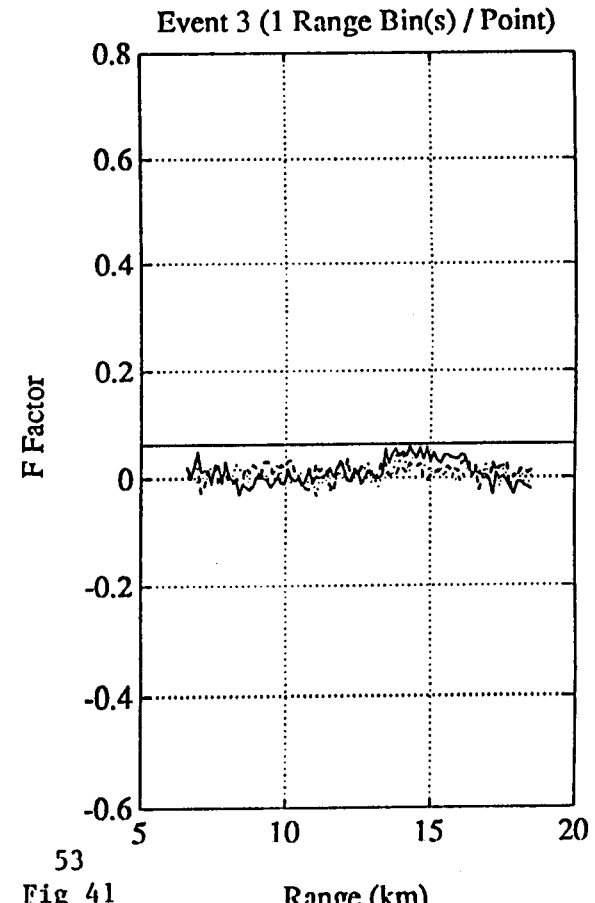
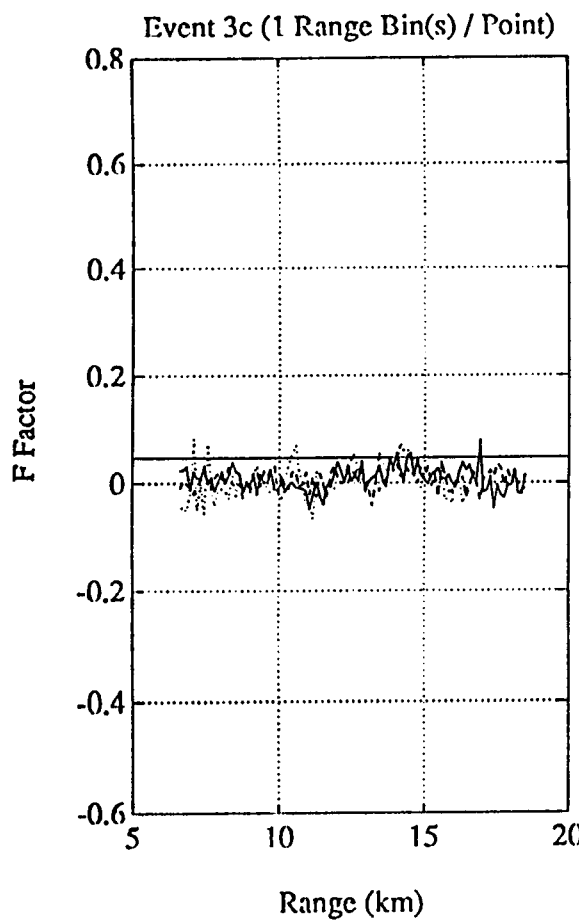
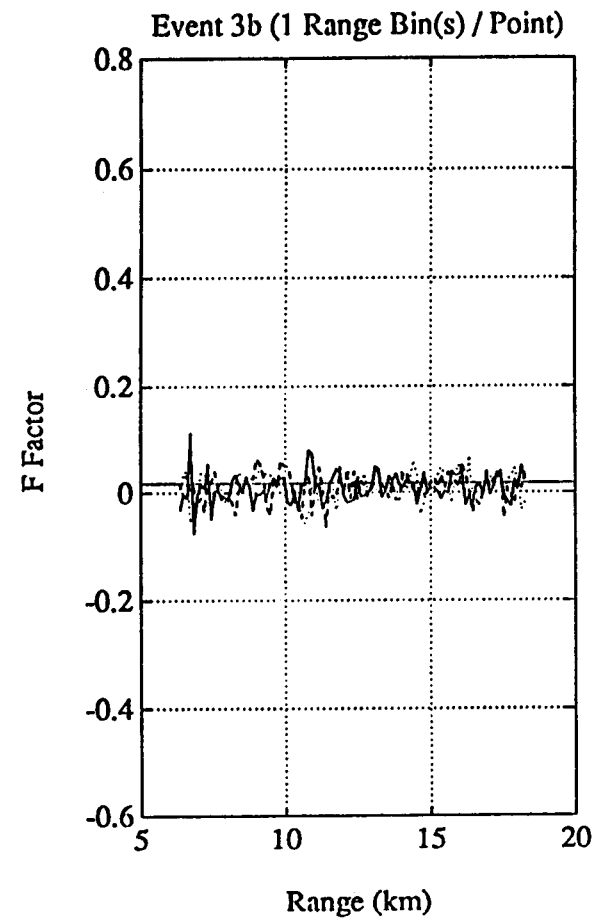
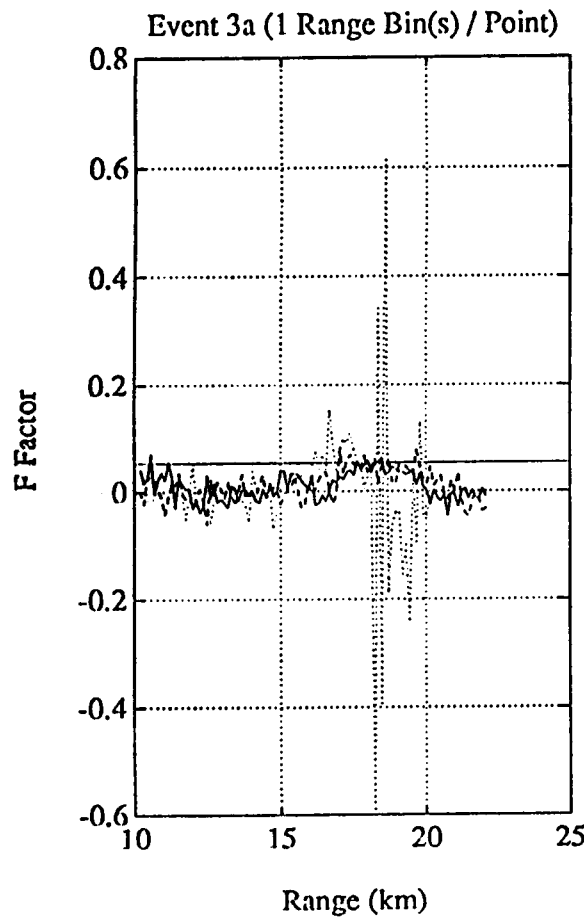
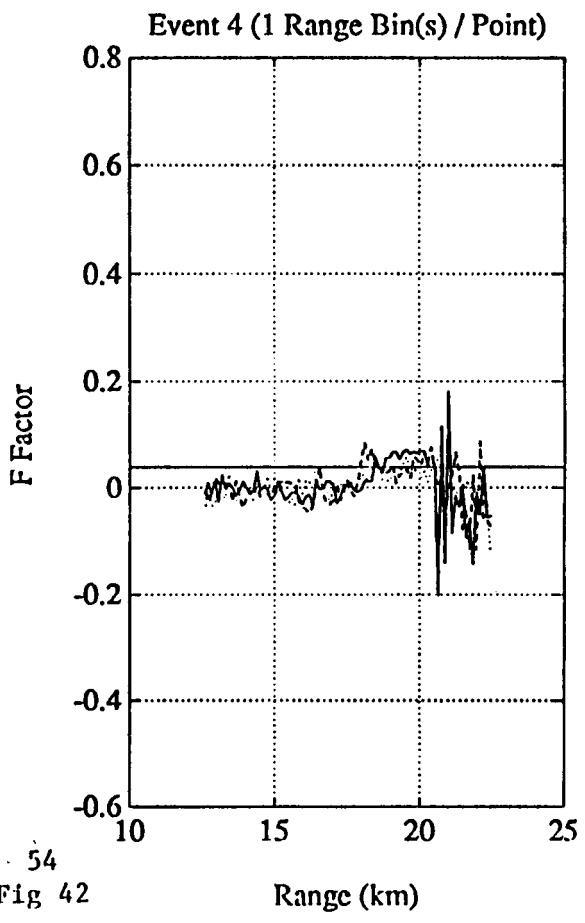
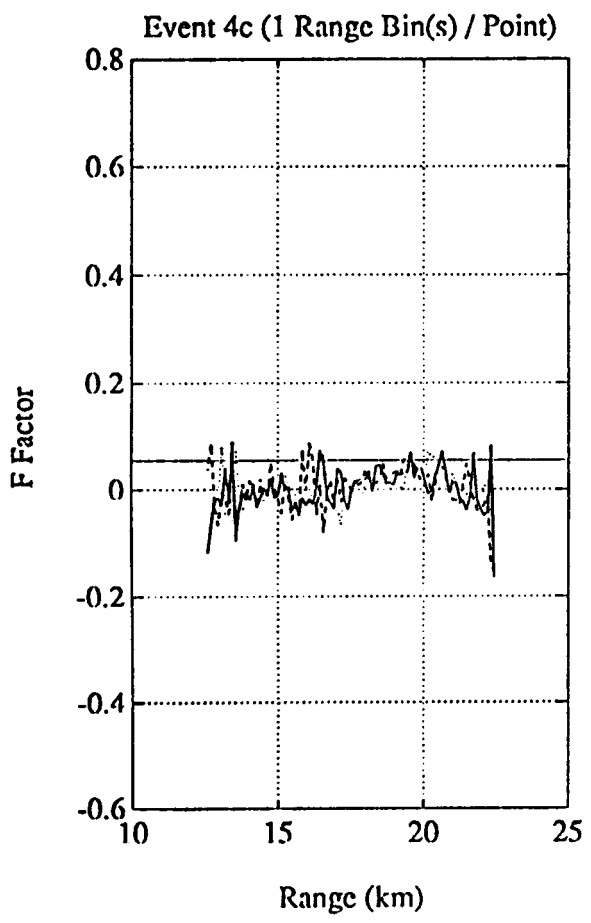
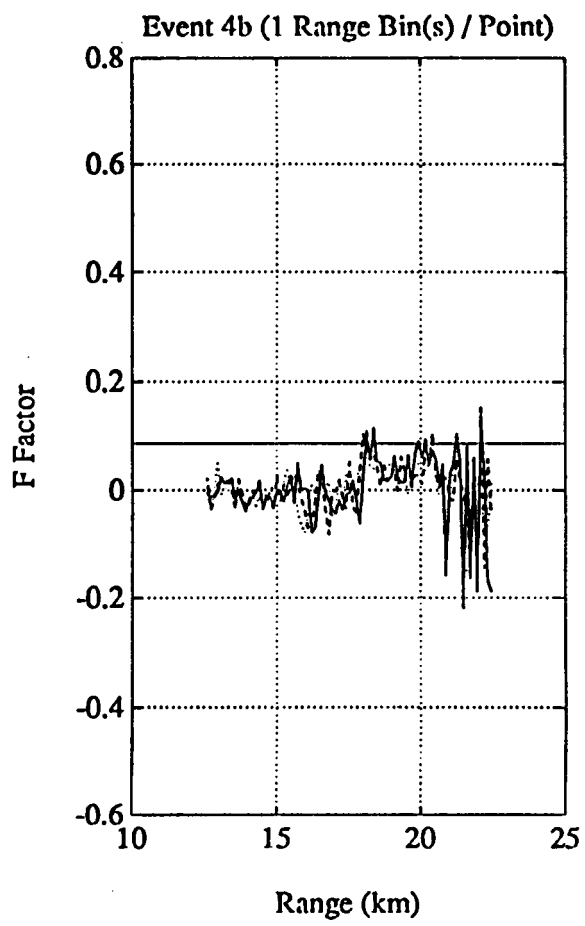
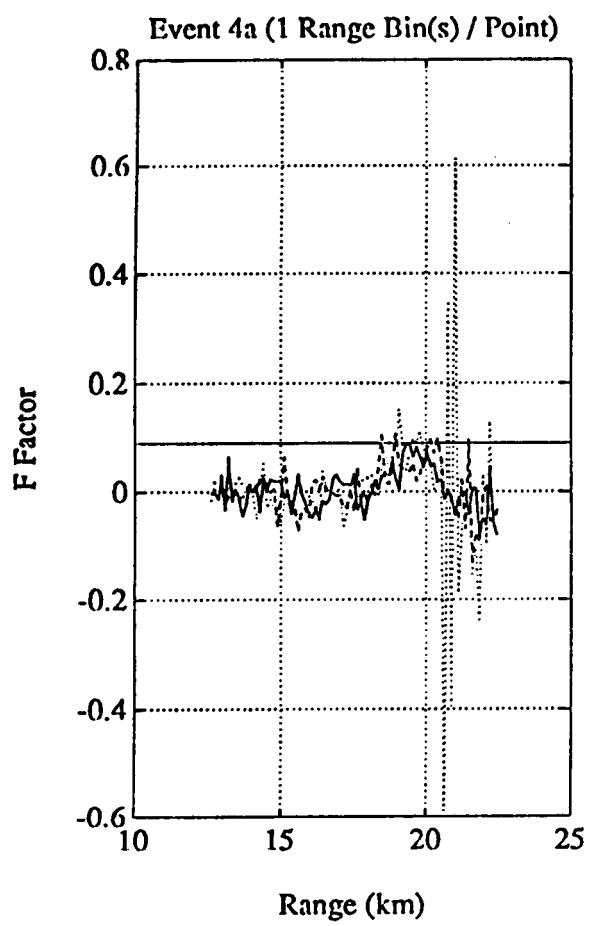
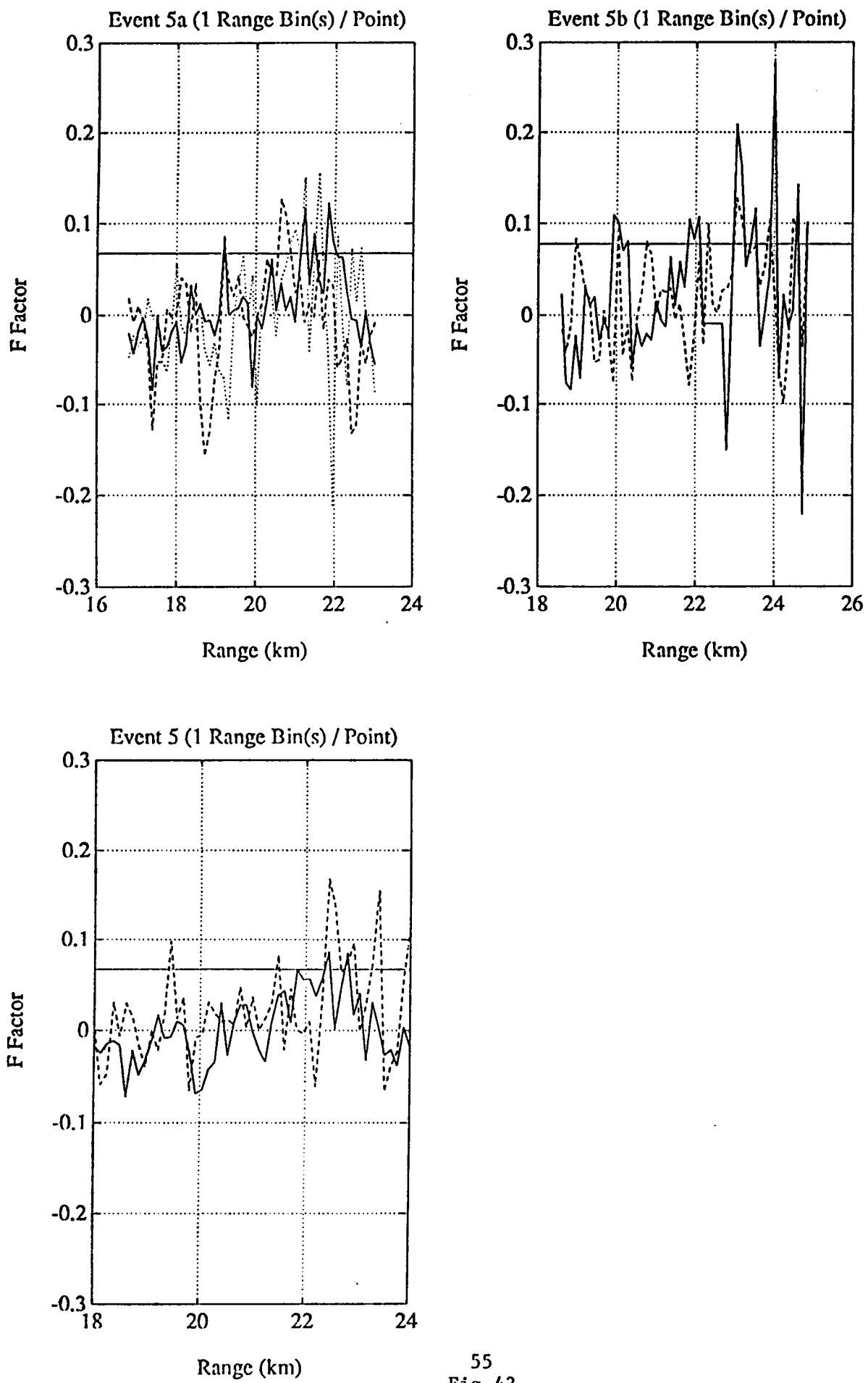


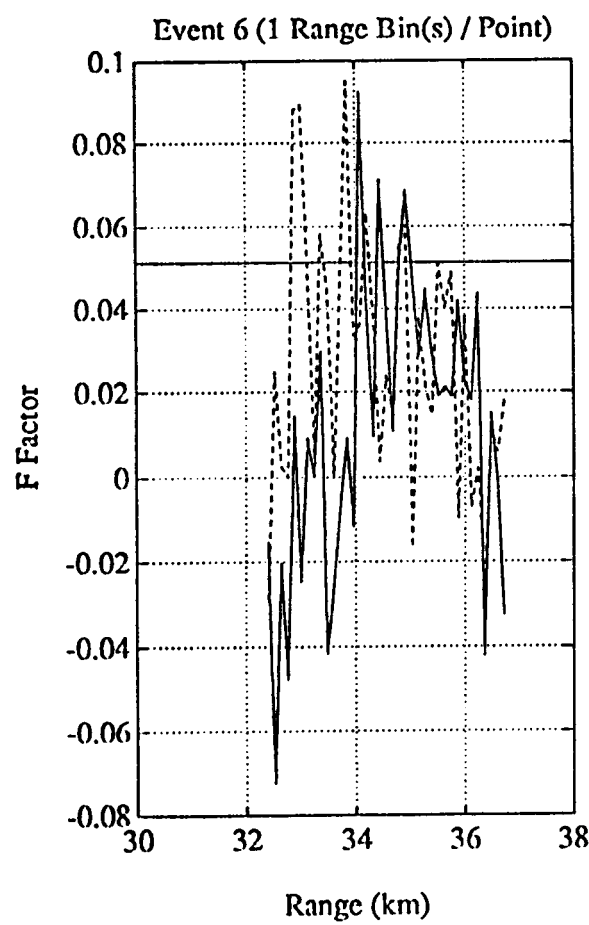
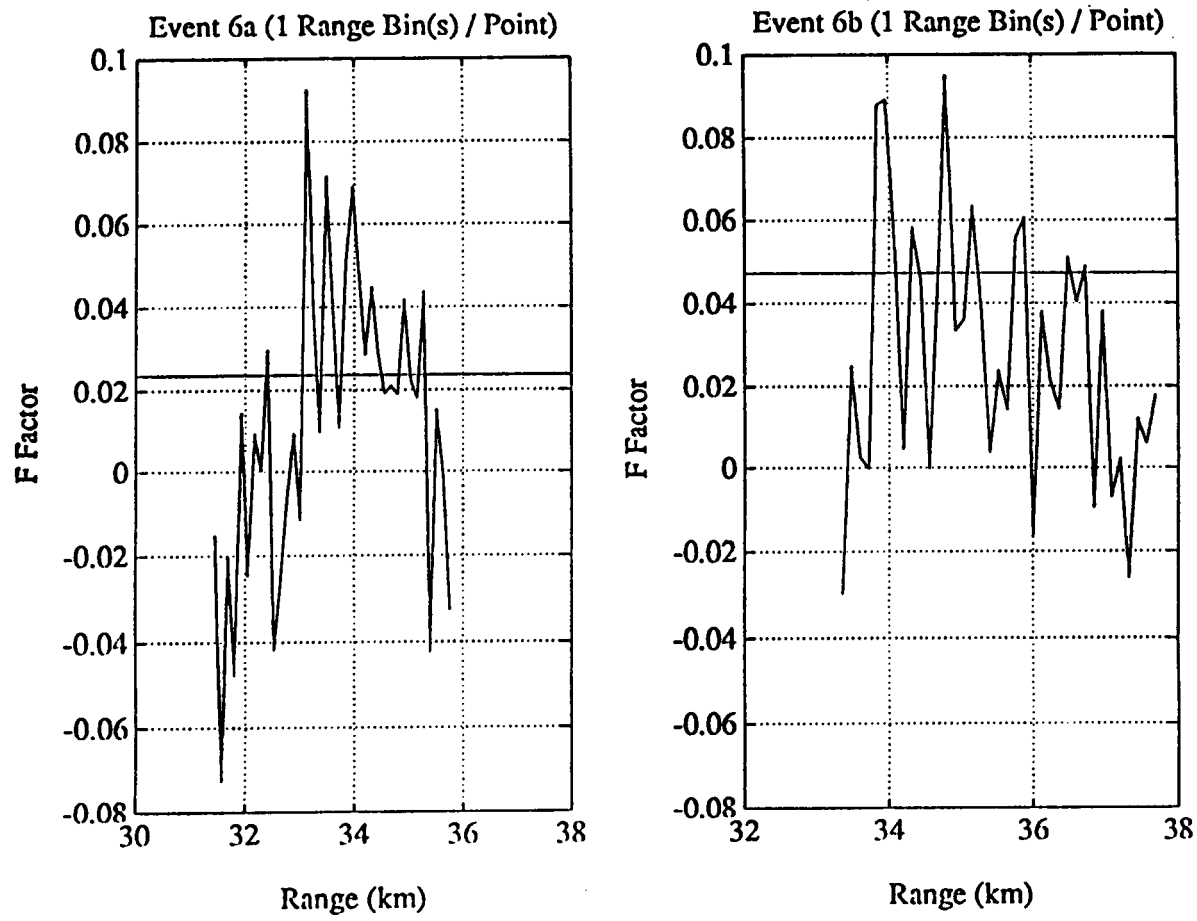
Fig 41

Range (km)





55
Fig 43



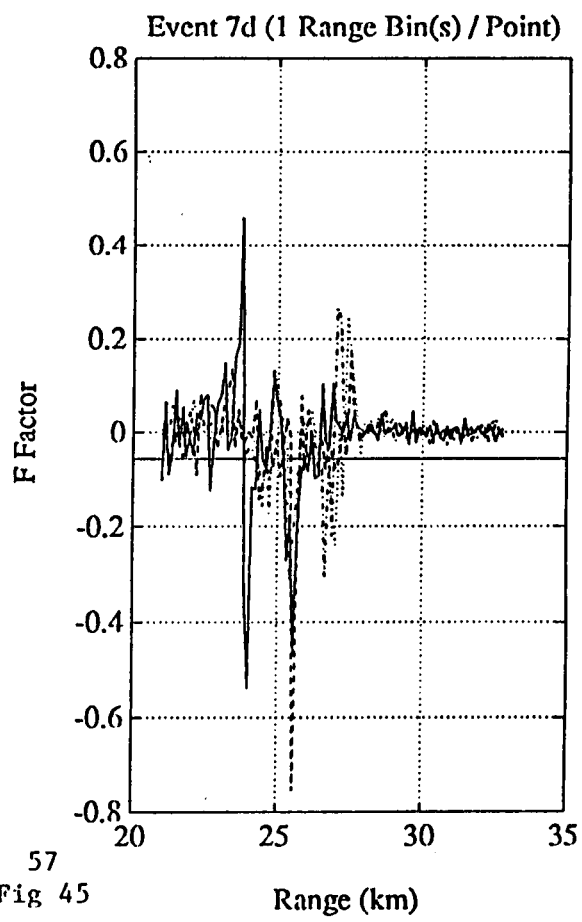
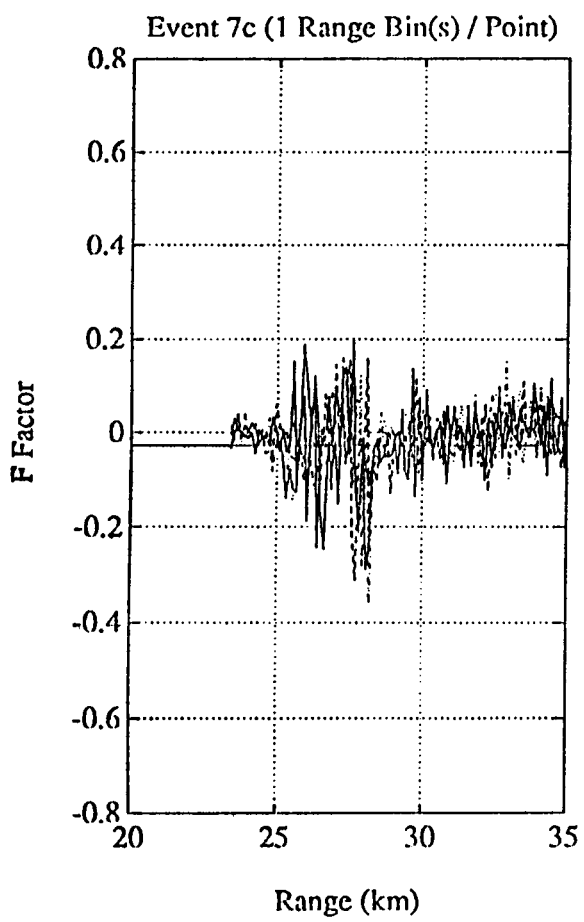
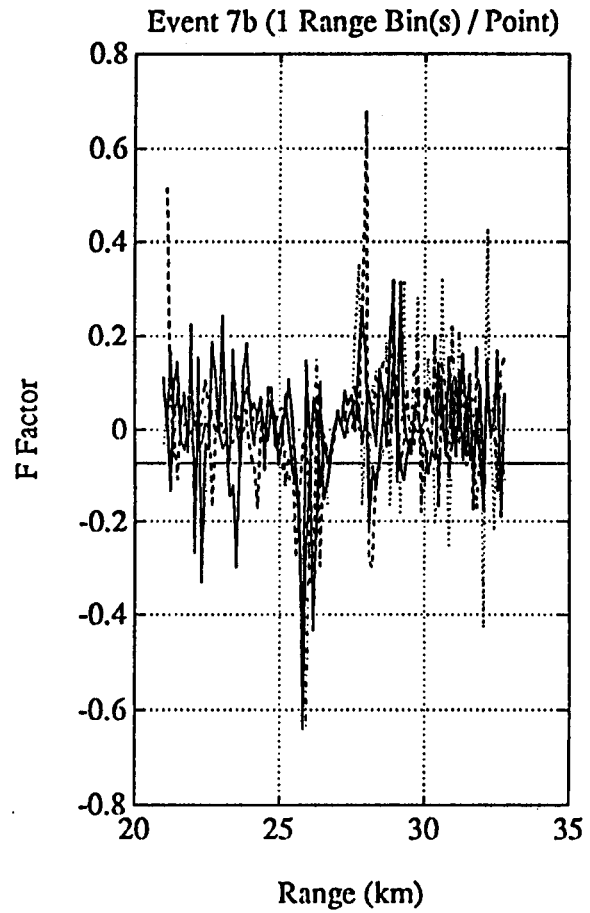
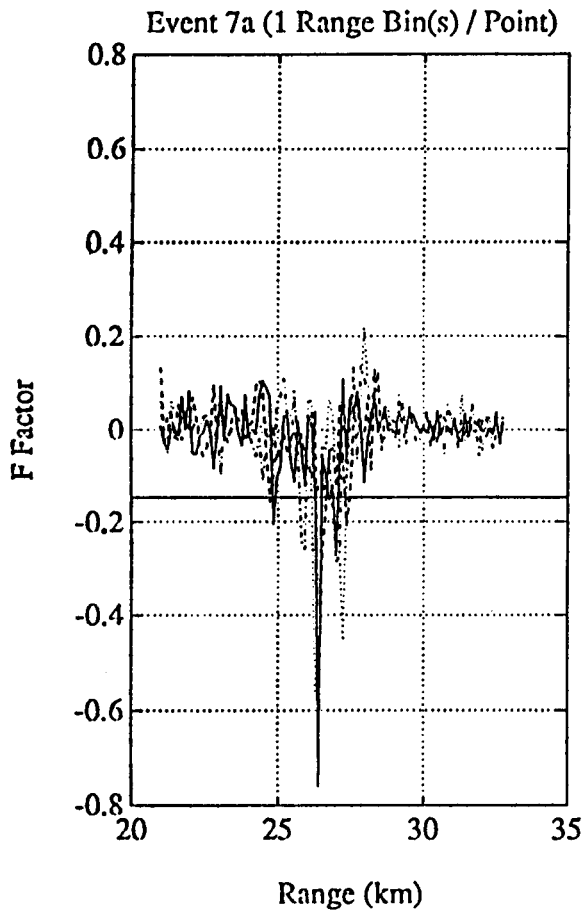
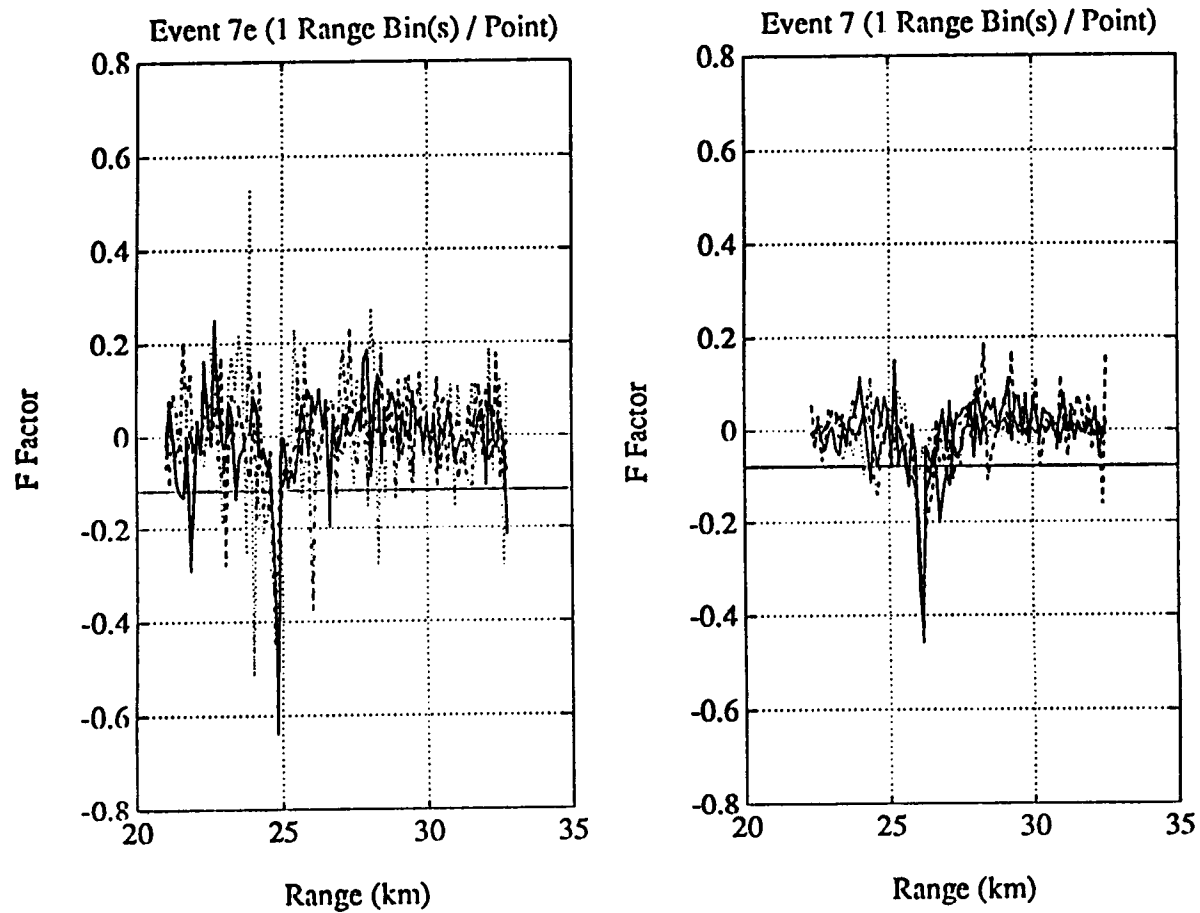
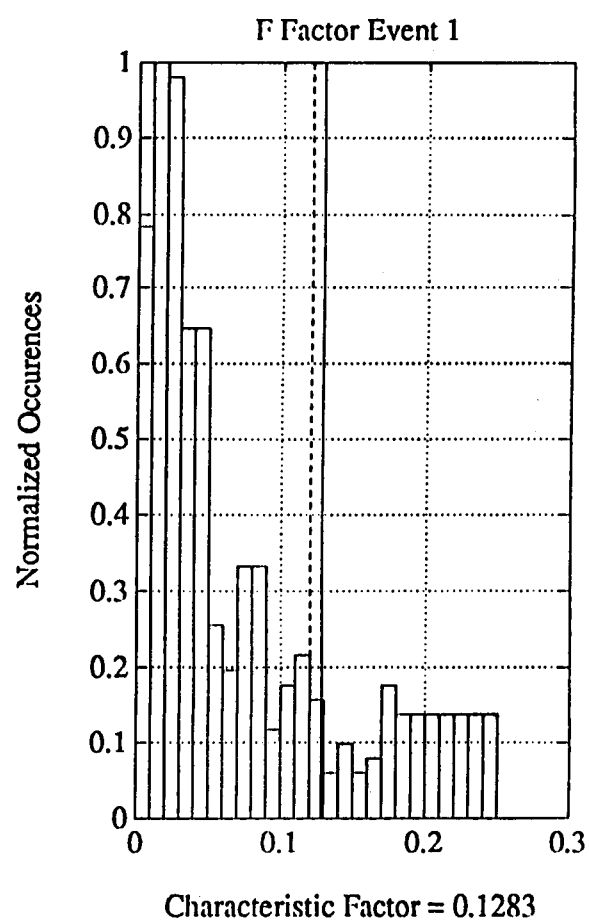
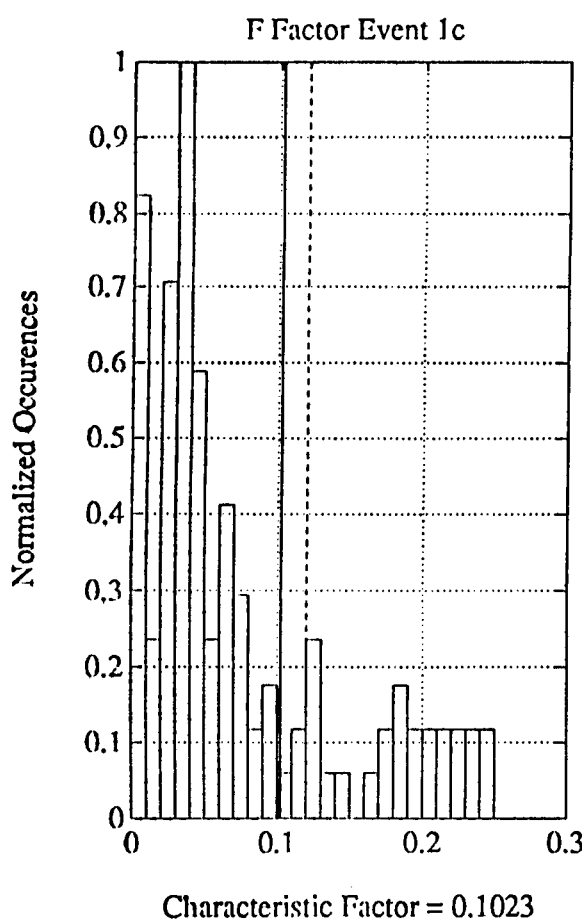
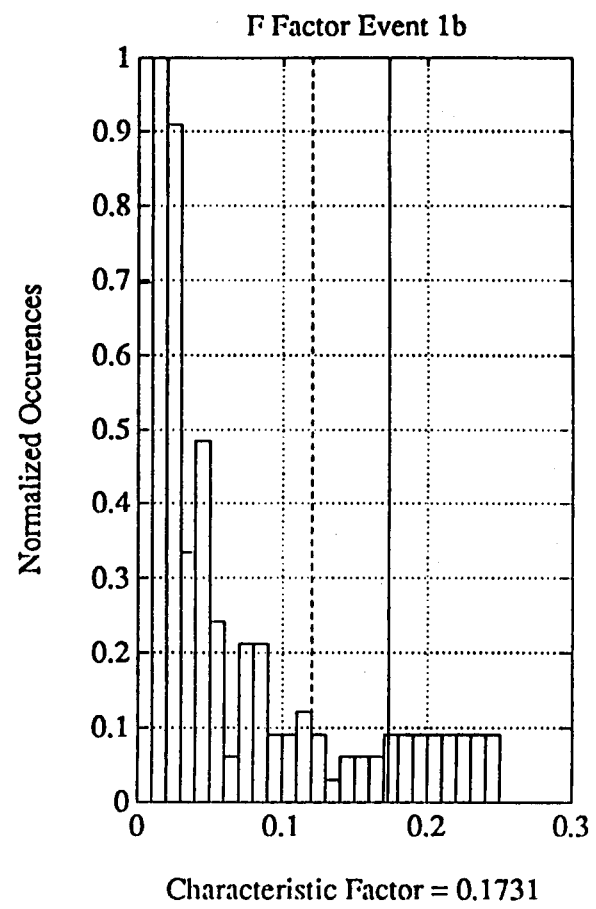
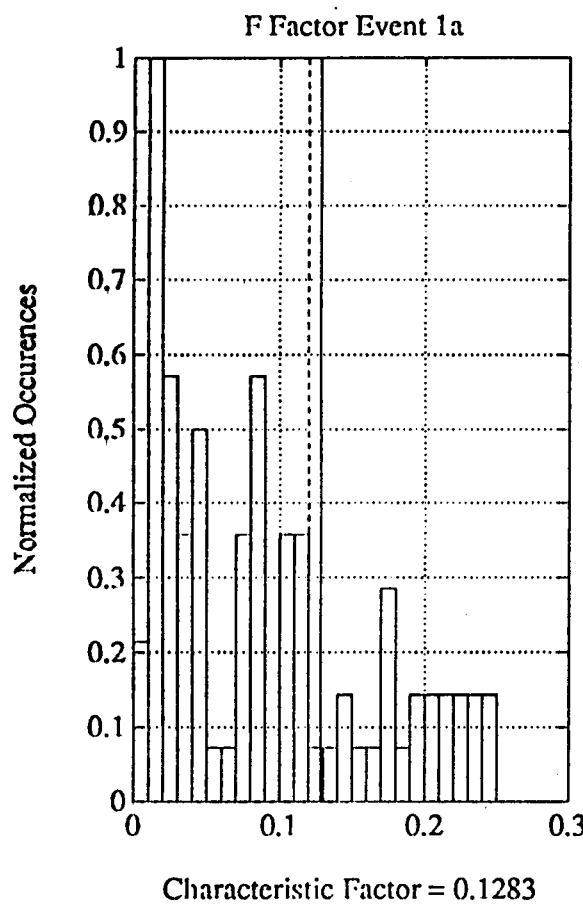
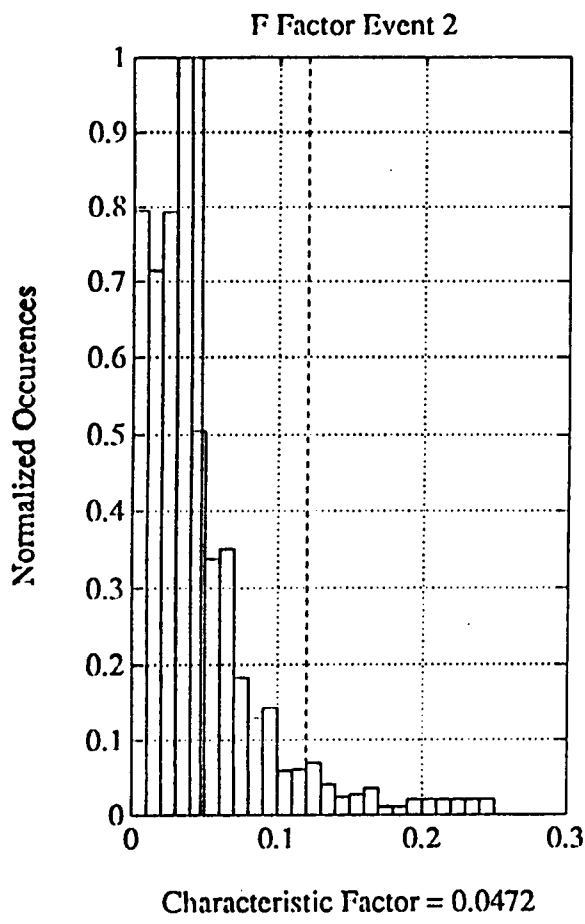
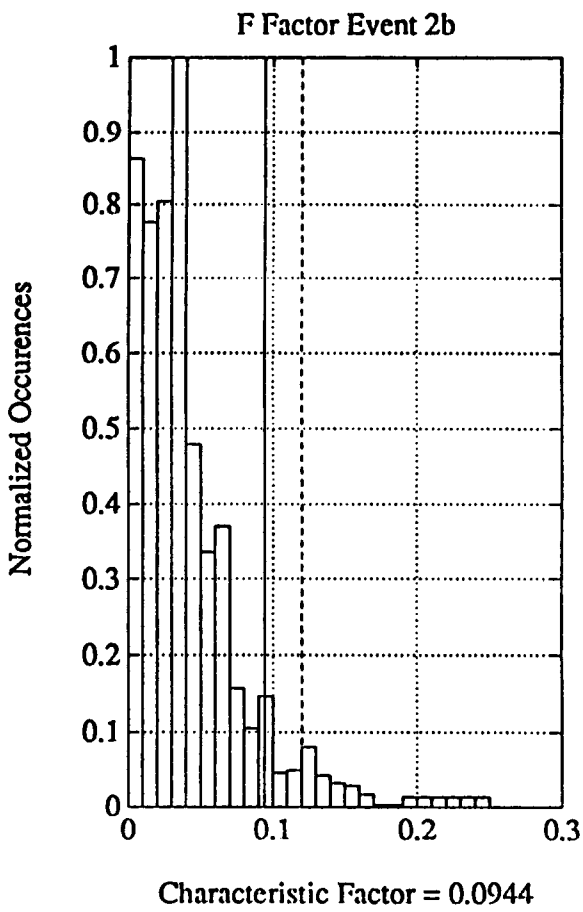
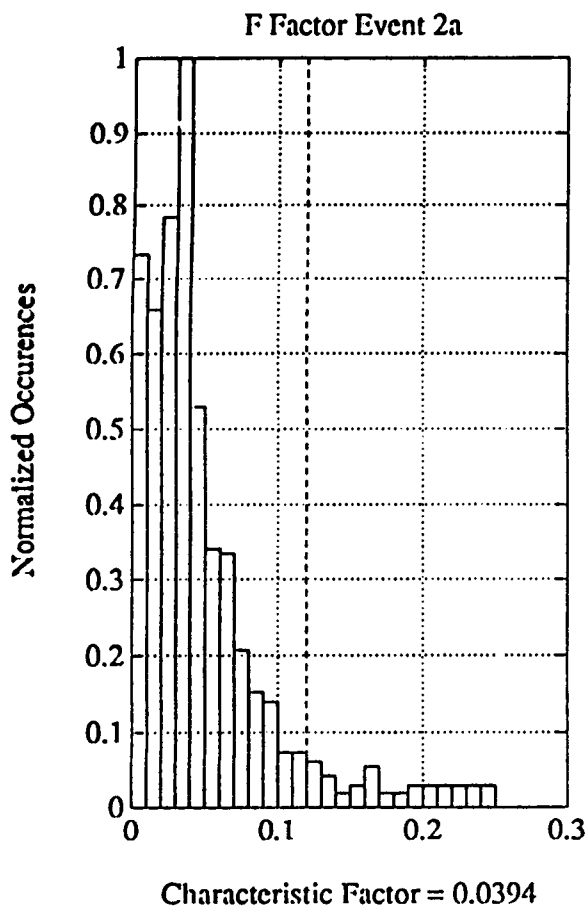


Fig. 45

Range (km)







60
Fig 48

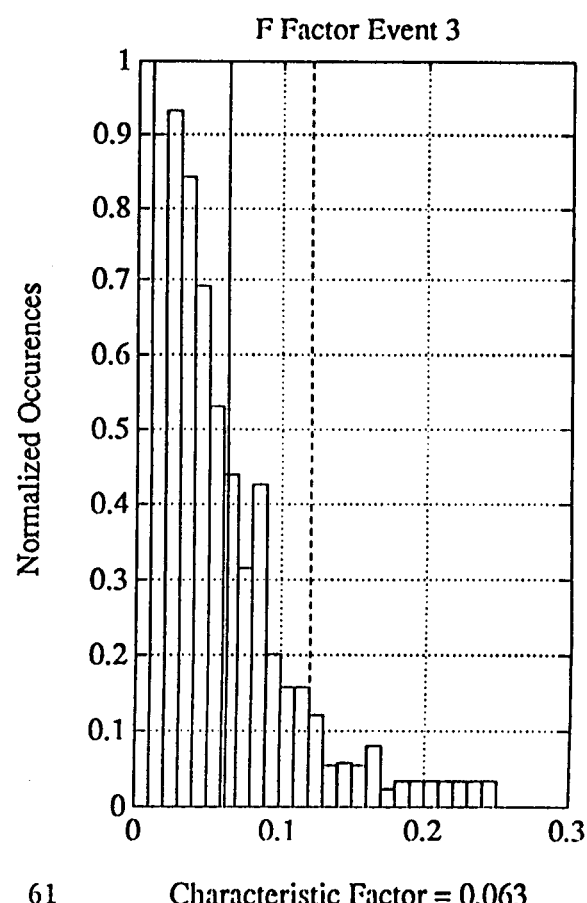
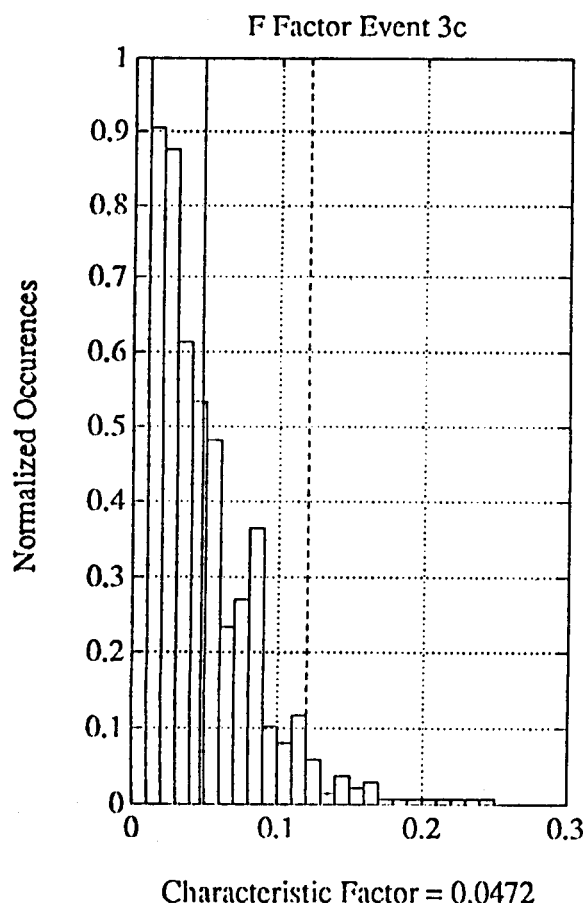
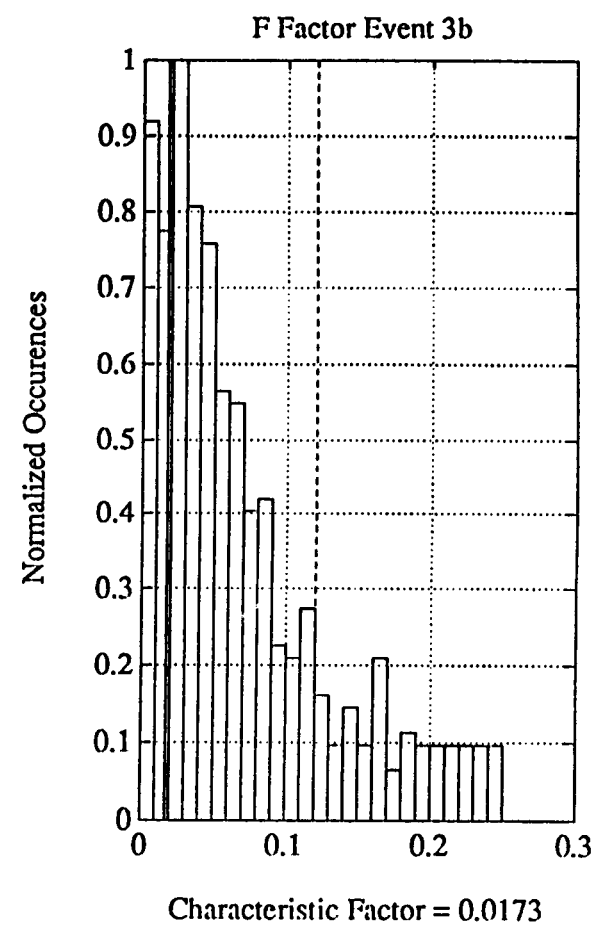
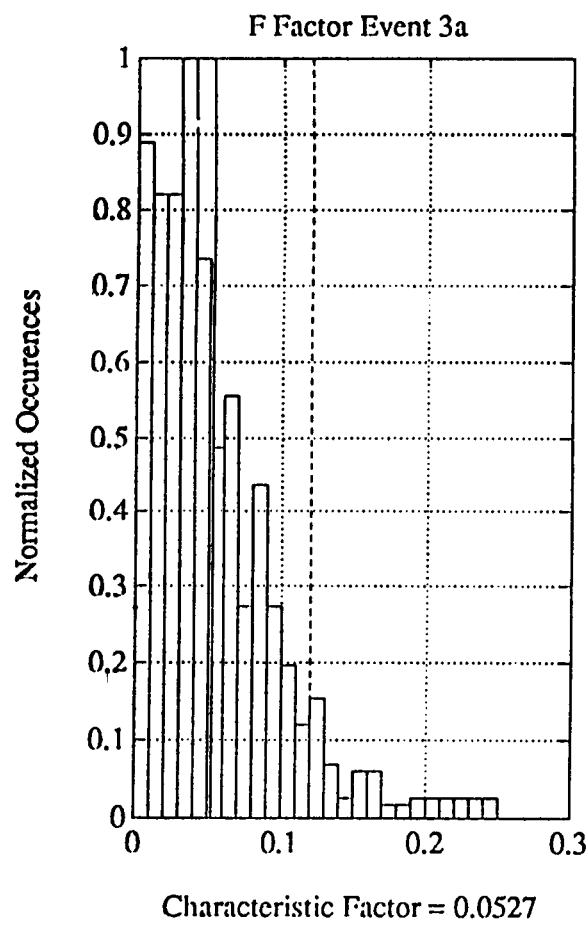
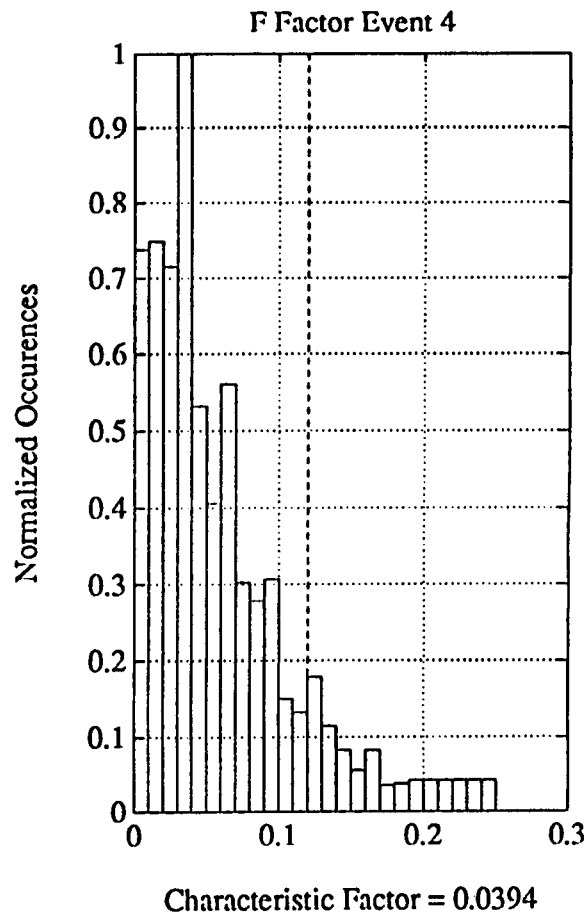
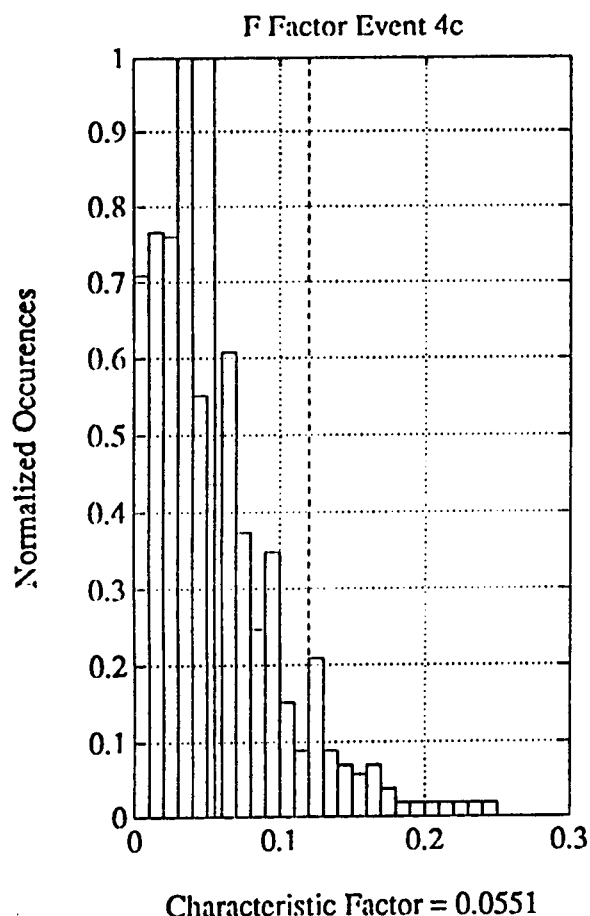
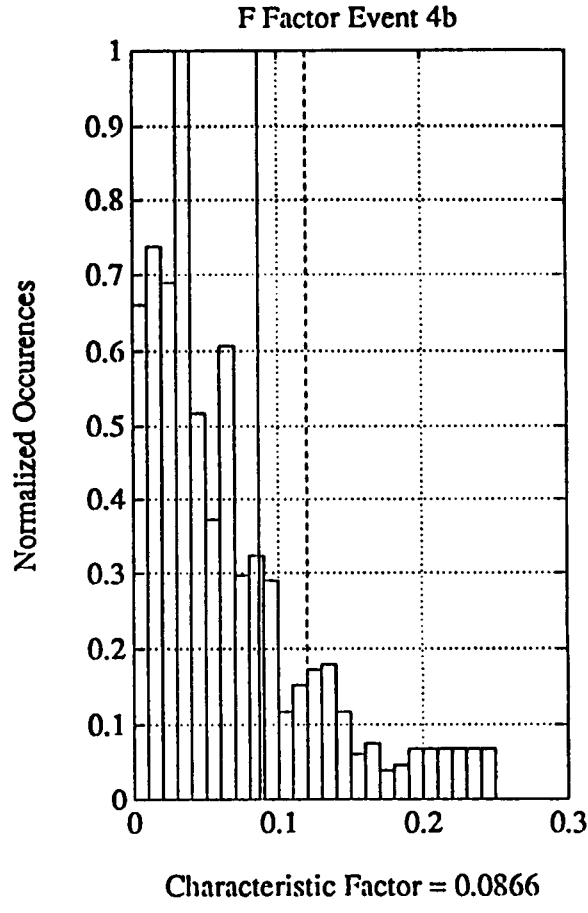
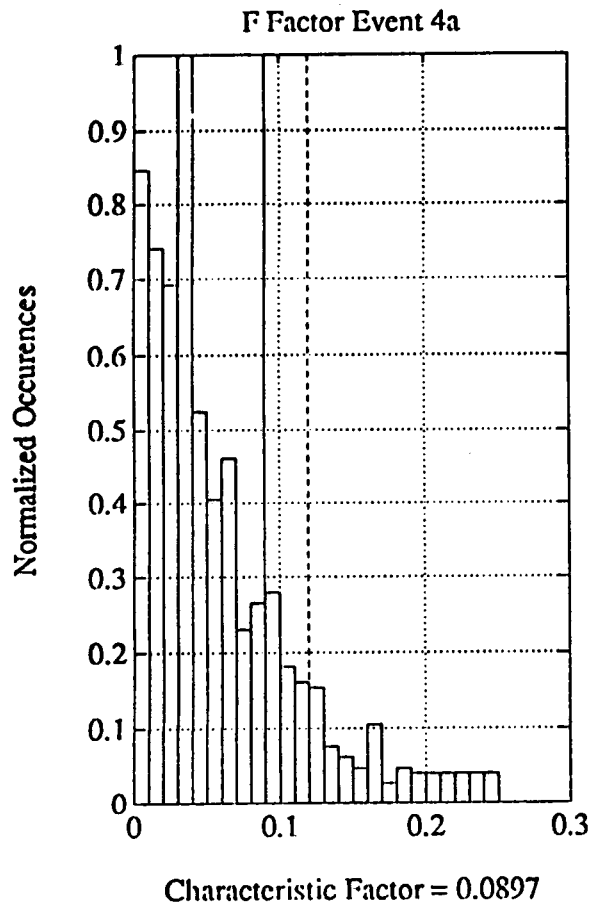
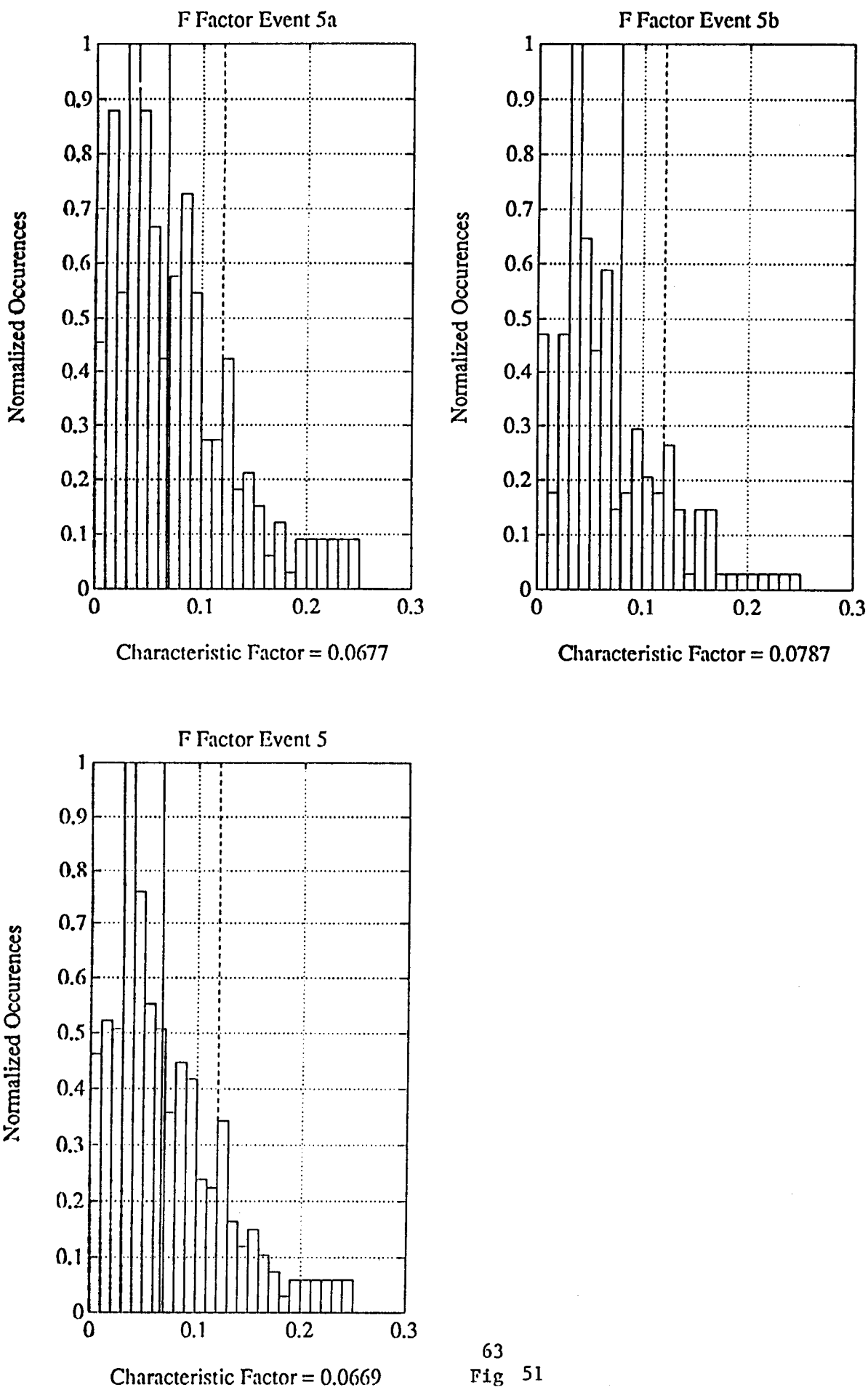
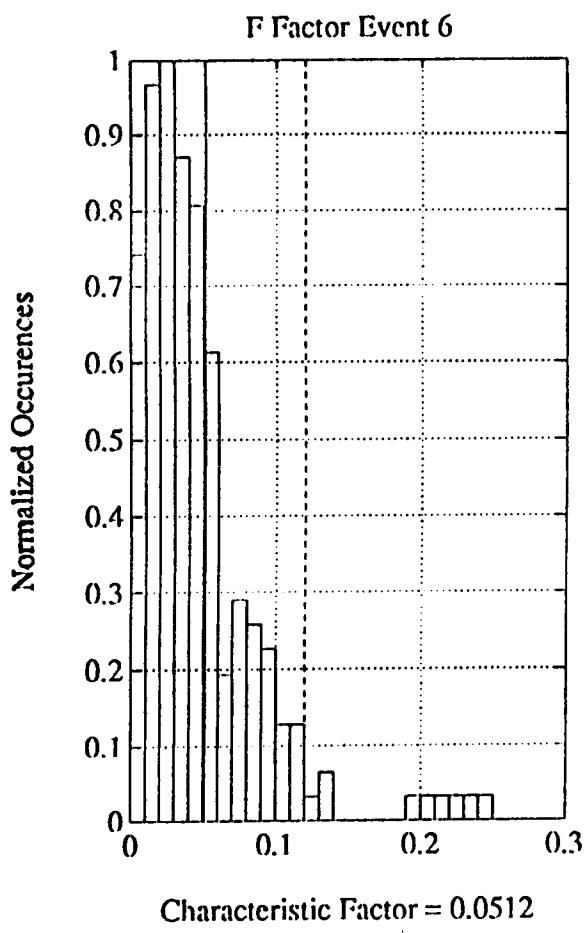
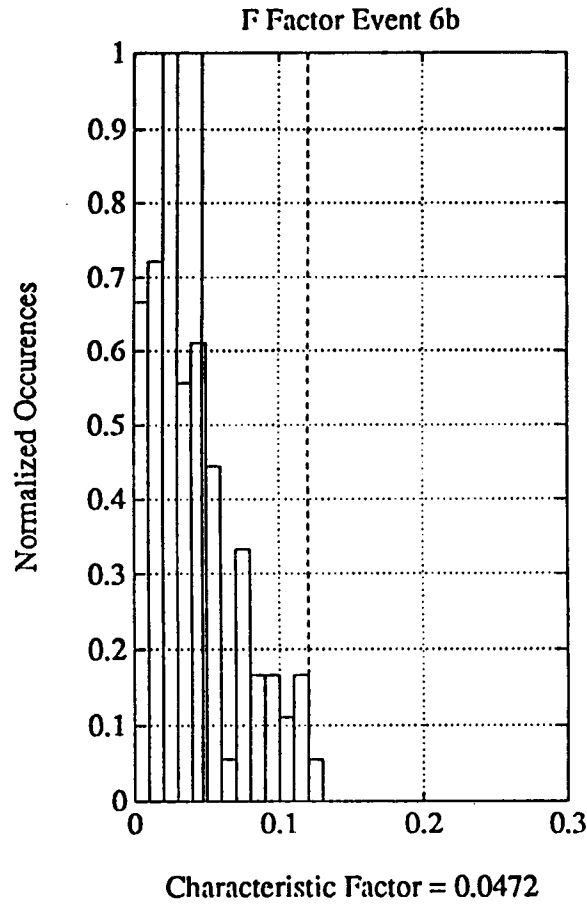
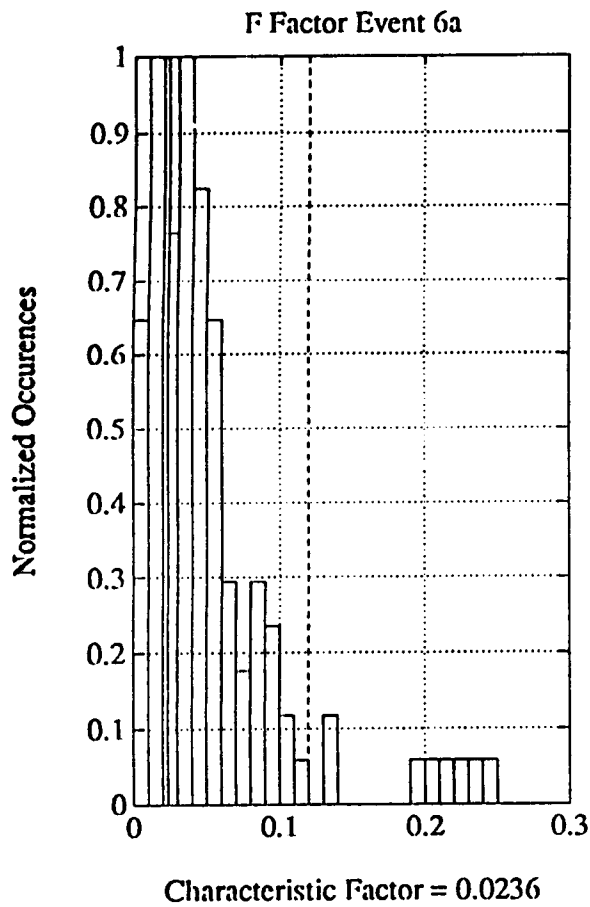


Fig 49







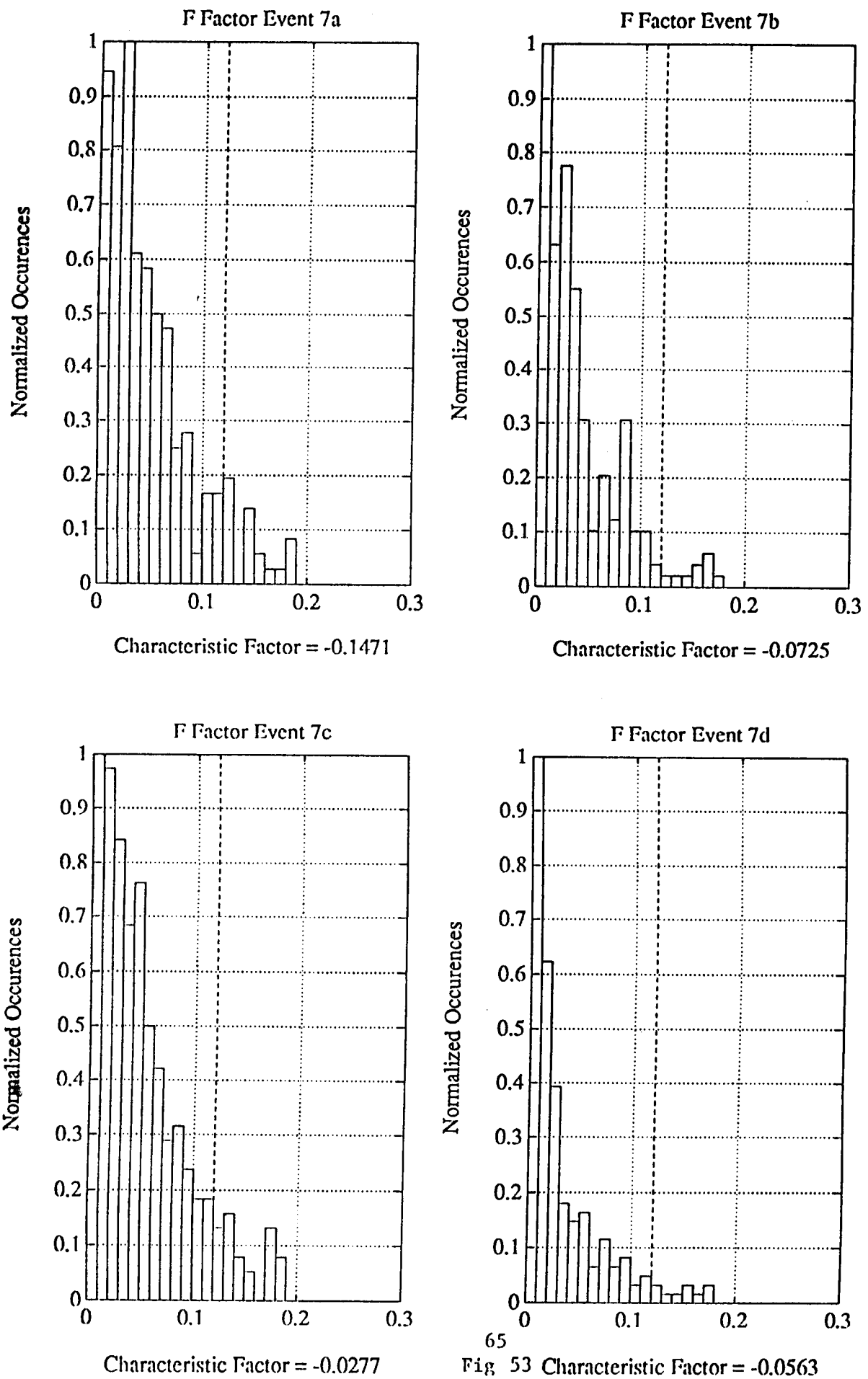
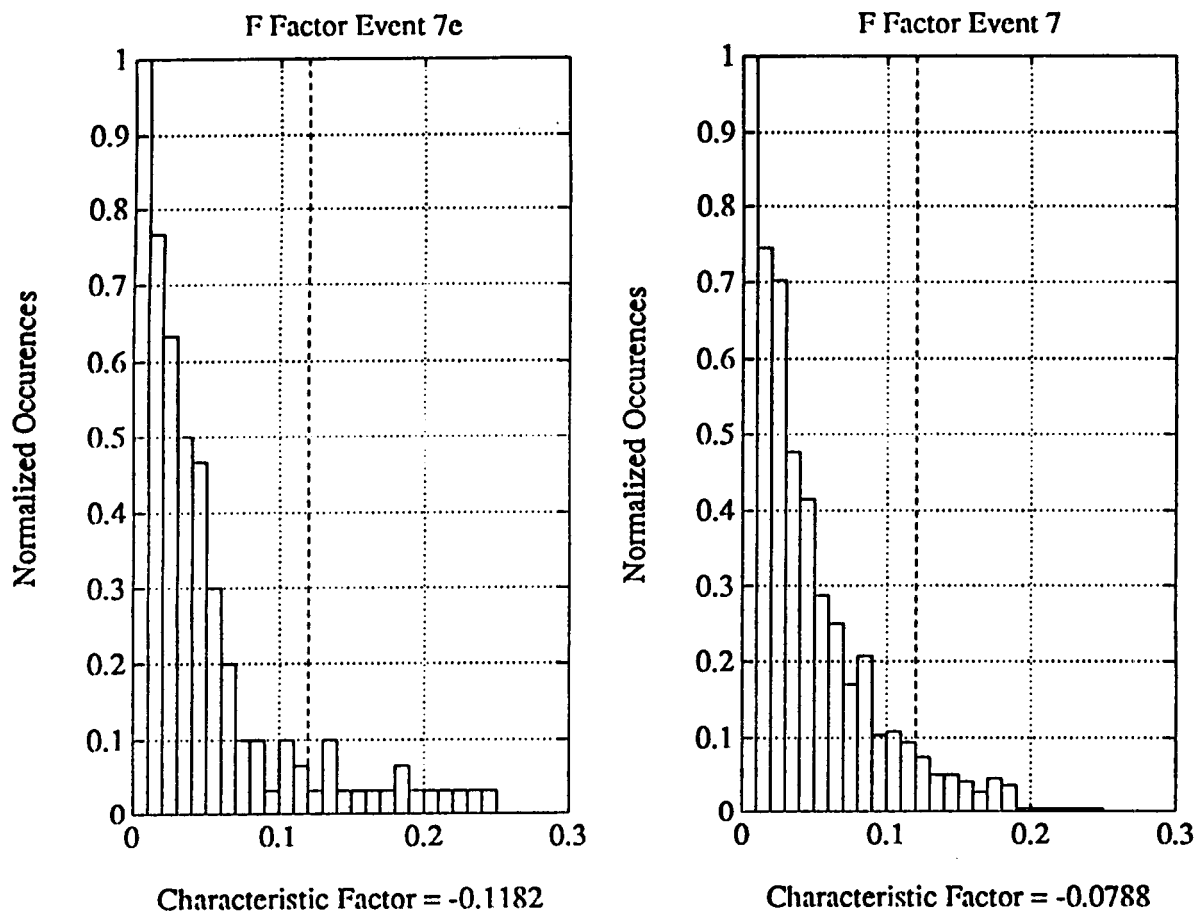


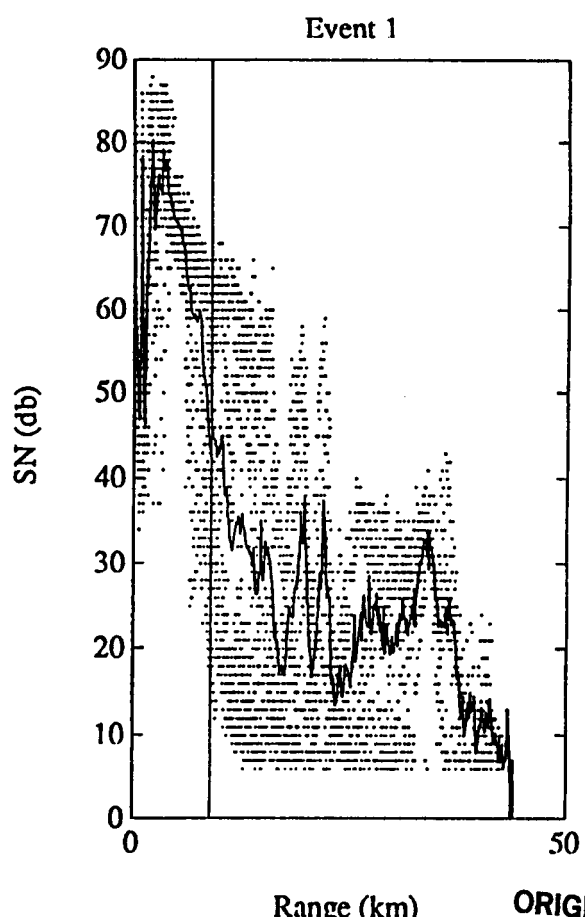
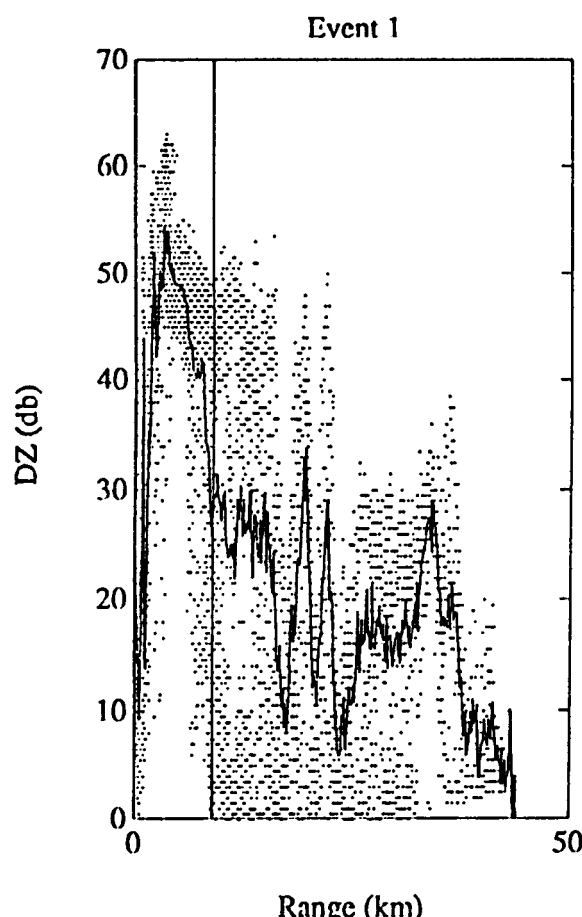
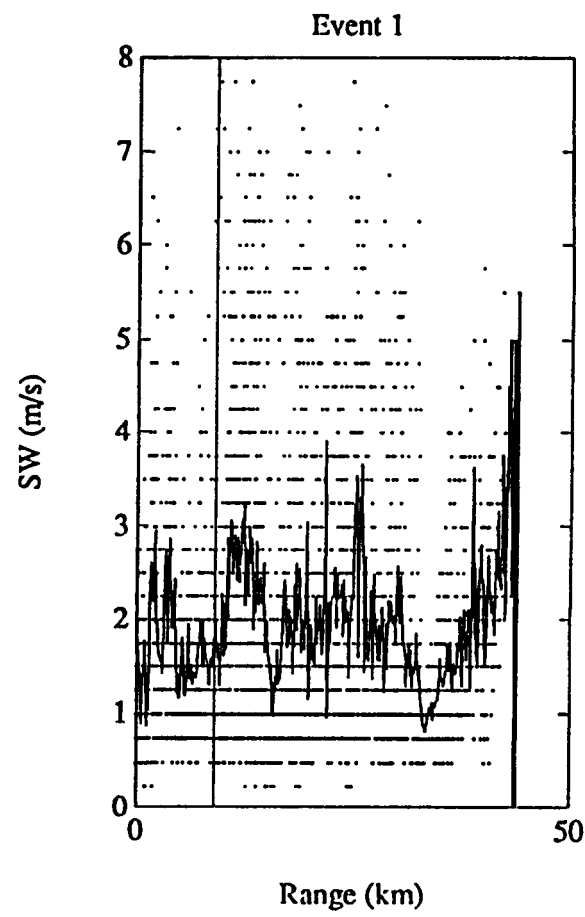
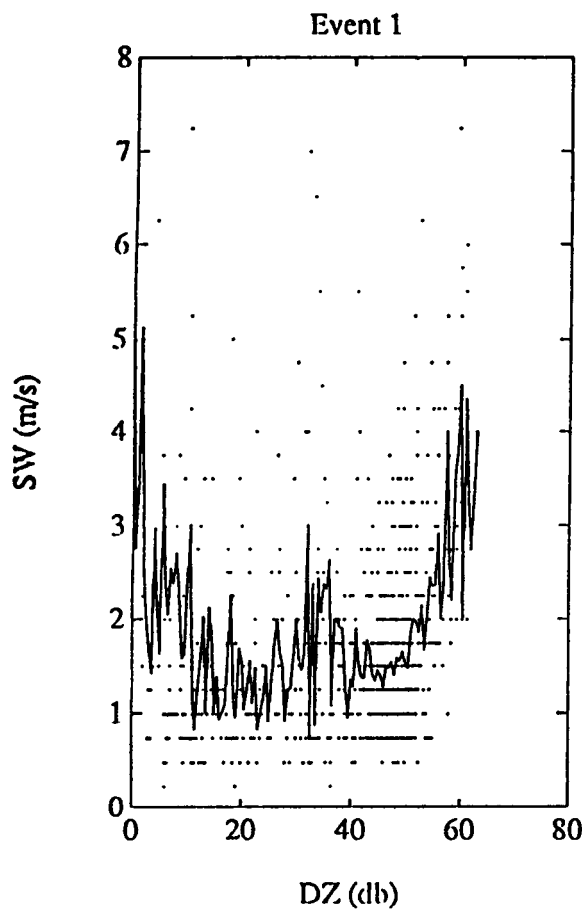
Fig. 53 Characteristic Factor = -0.0563



Evaluation of Trends From Doppler Data Correlation Analysis

Parameters	Trends
SW vs. VE	Symmetric scatter, with uniform distribution for all but Event 2
SN vs. VE	No general trend, appears uncorrelated
DZ vs. VE	Follows SN vs. VE data, and also appears uncorrelated (more specifically, conflicting trends exist)
VE vs. DZ	Two trends appear; i) uniform distribution, ii) positive VE for low DZ flipping to negative VE for high DZ (abs(VE) would likely make distribution uniform).
SW vs. DZ	For approximately 3 events, low DZ has higher SW estimates, while others have uniform or saddle distributions
VE vs. Range	Disregard in favor of SubEvent VE profiles.
SW vs. Range	In general, SW increases with range, as expected, but there are some dips and some uniformity displayed.
DZ vs. Range	Simply reflects where the weather is. No general correlation.
SN vs. Range	Also no general trend, though SN follows DZ vs. Range except for very near ranges, where DZ tends to drop off and SN tends to rise.

Notes: 1) Event 6 appears to have the most erratic behavior (not in scatter as much as in the mean), likely due to substantially fewer points to average when compared to other events.



ORIGINAL PAGE IS
OF POOR QUALITY

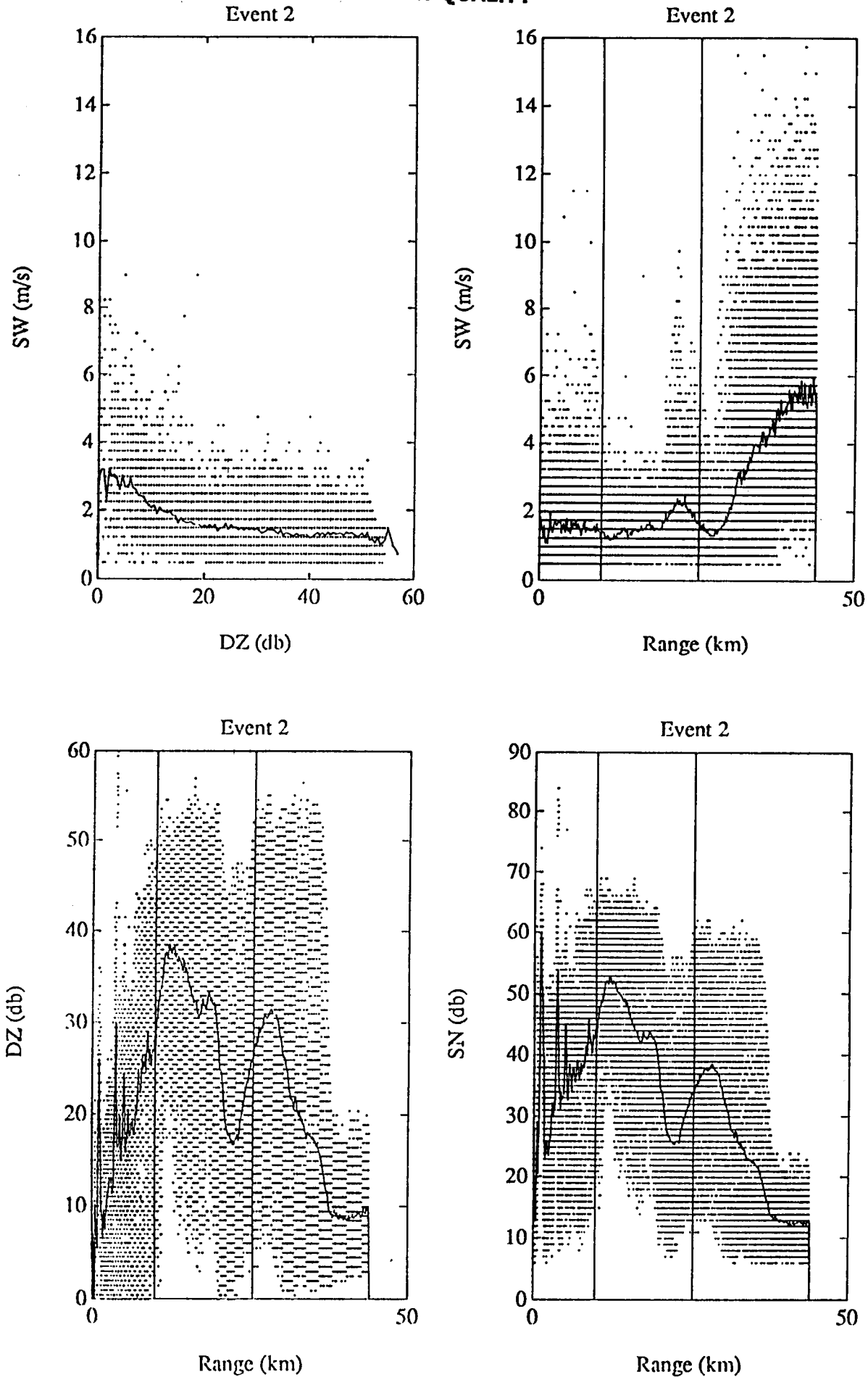


Fig 57

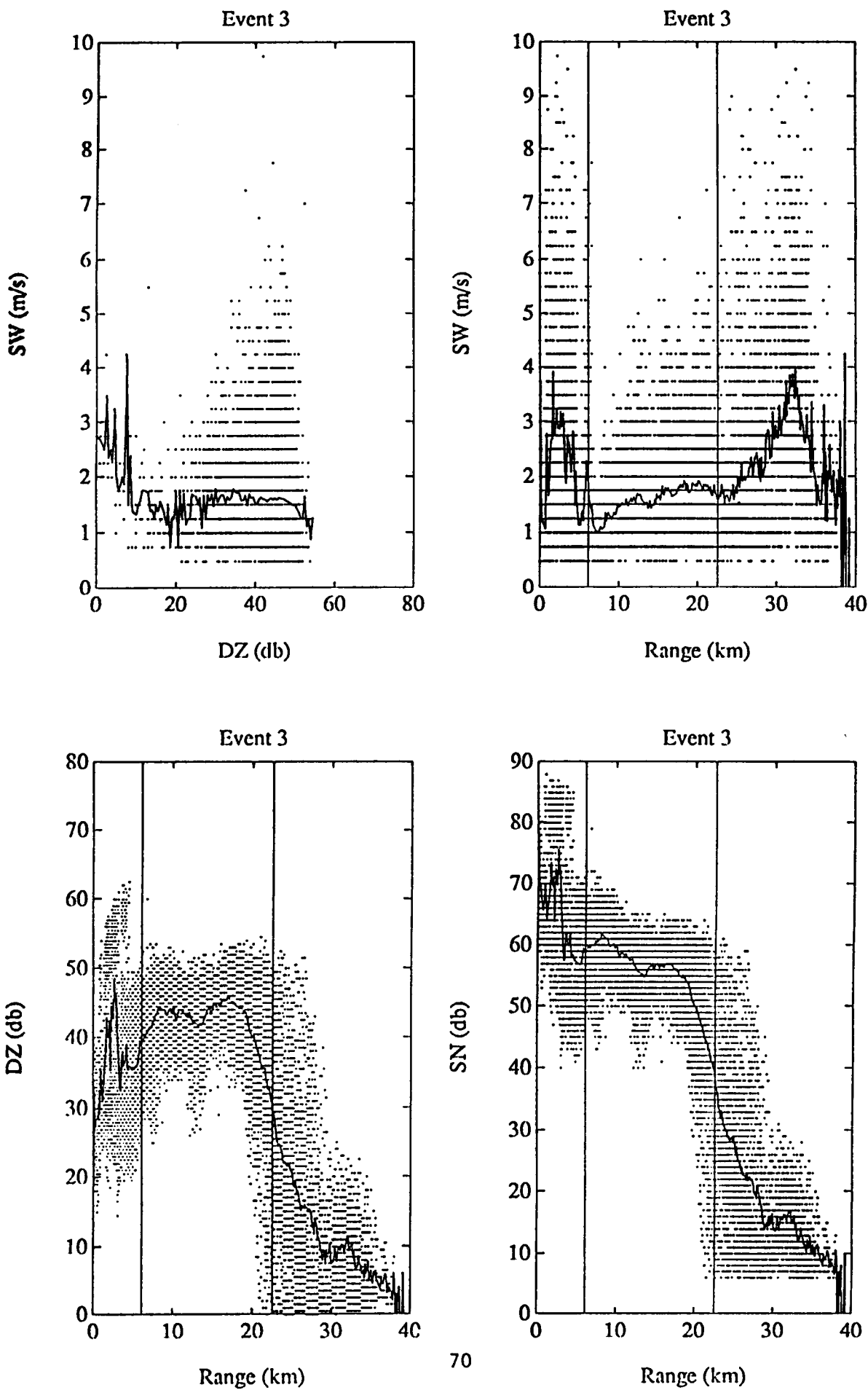
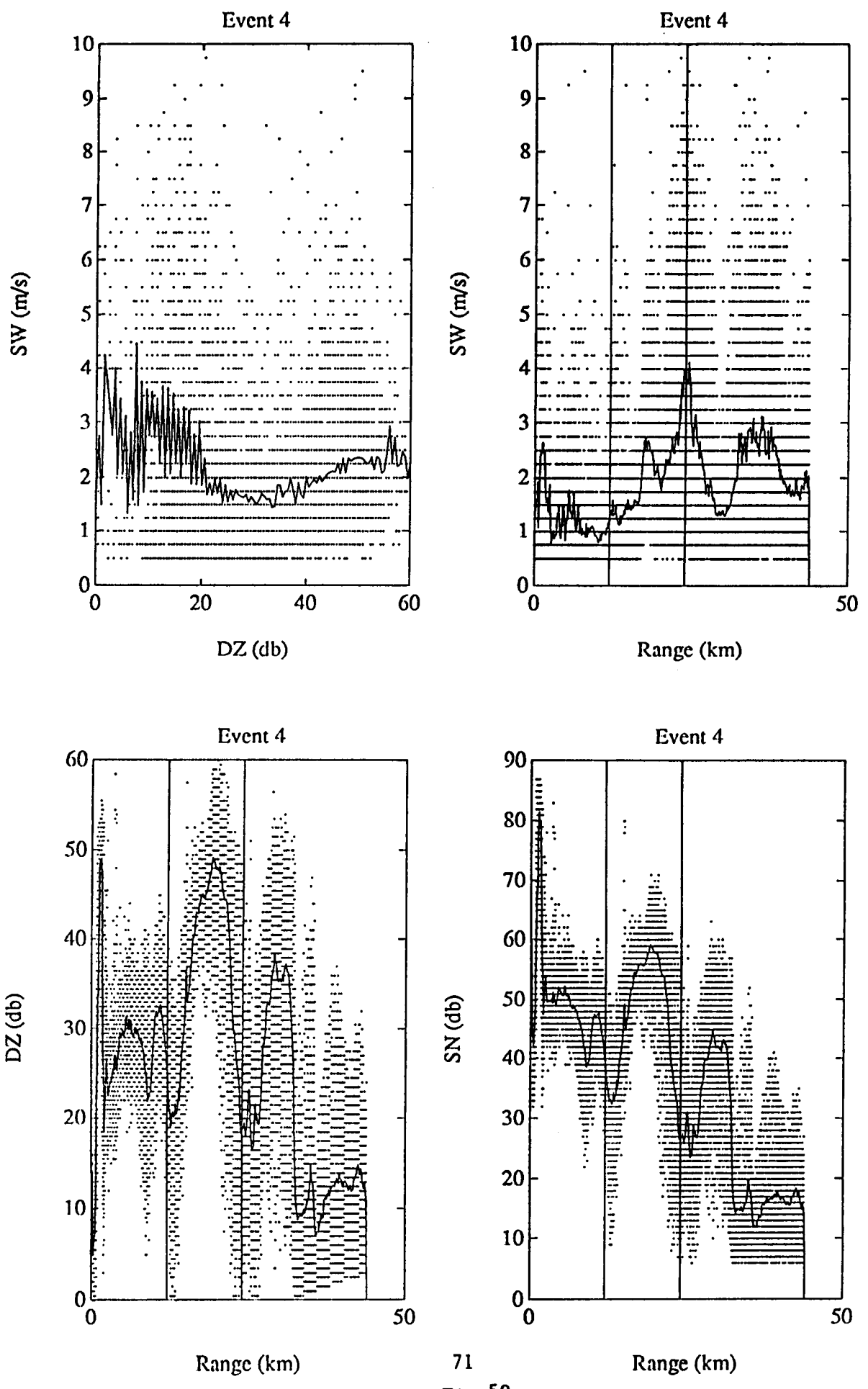
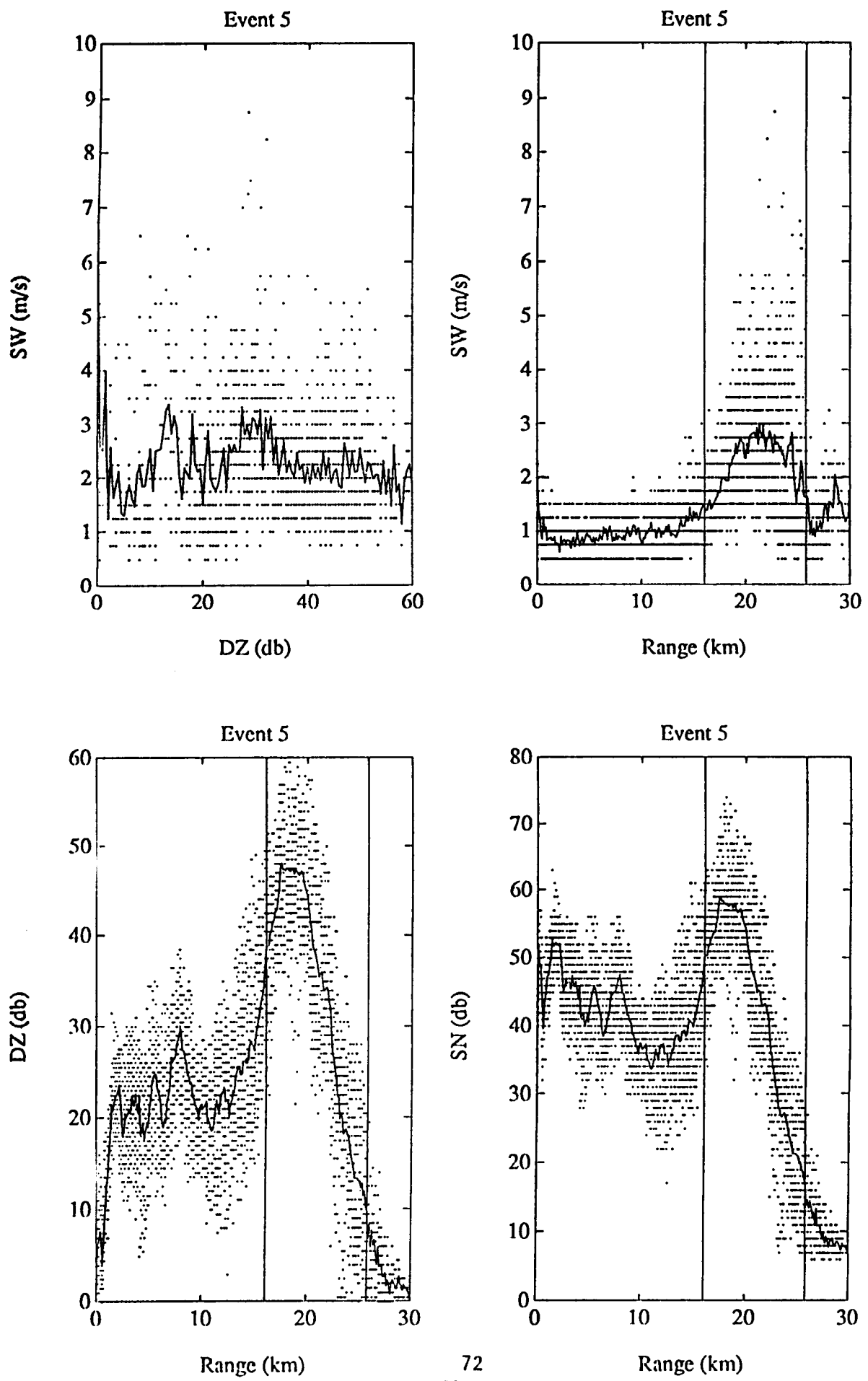


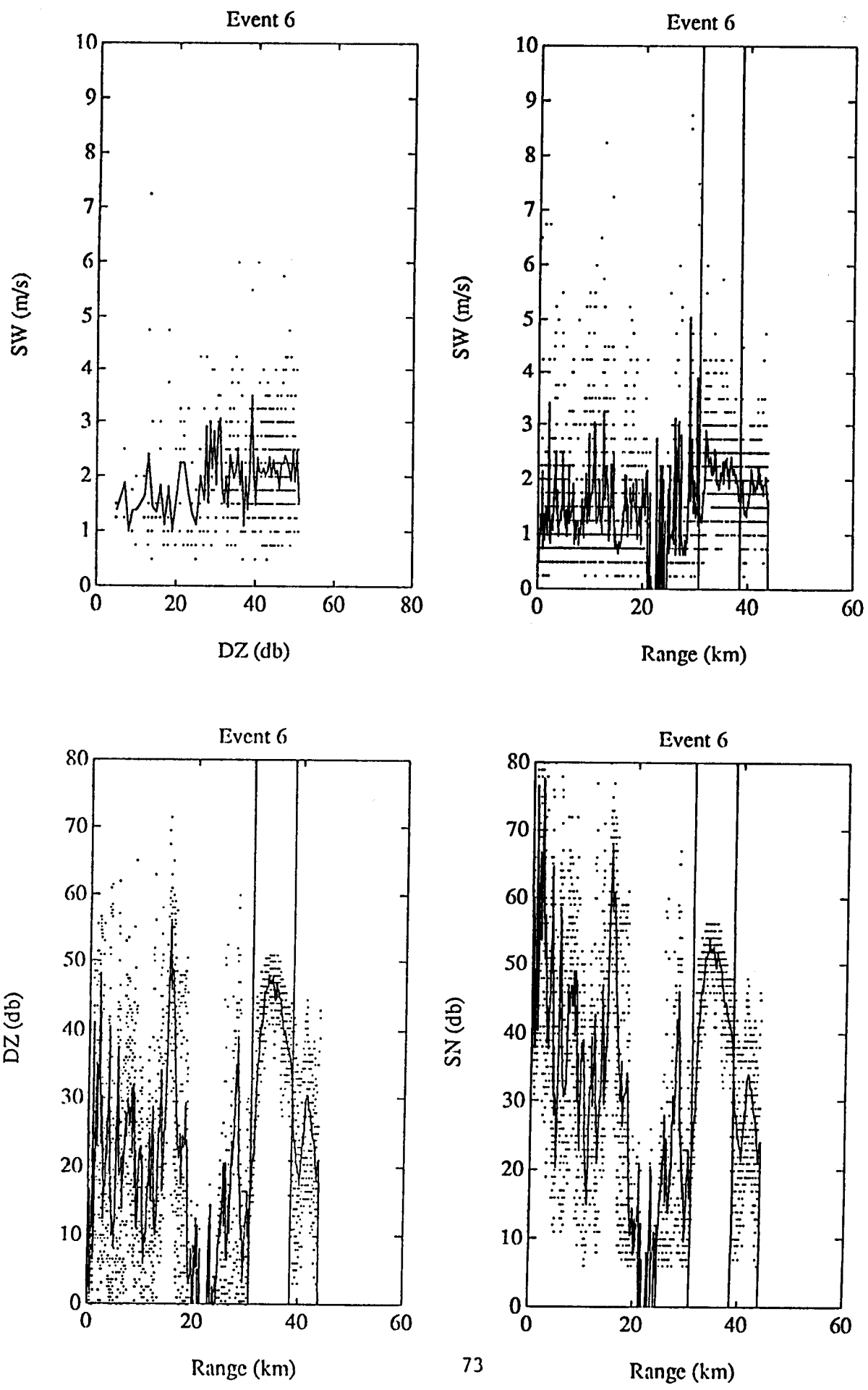
Fig 58

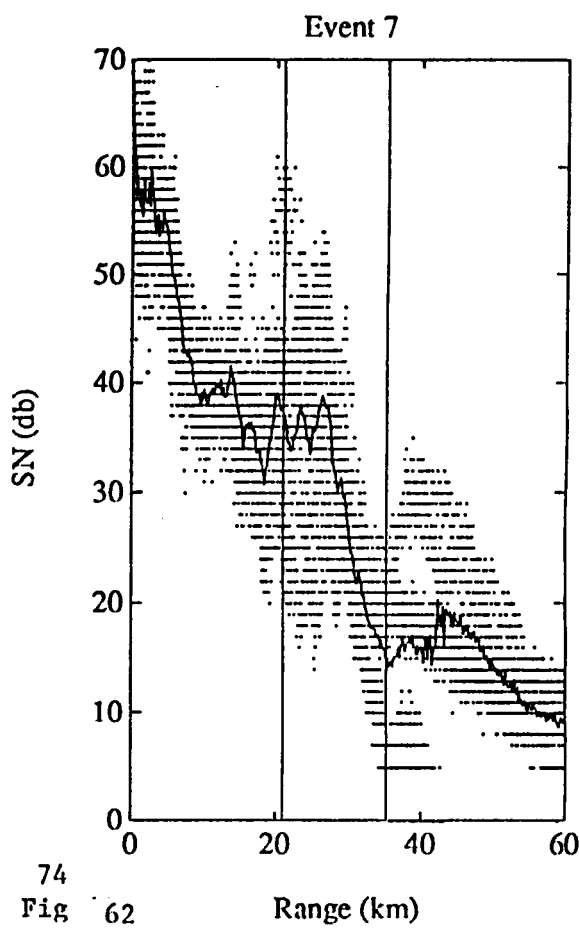
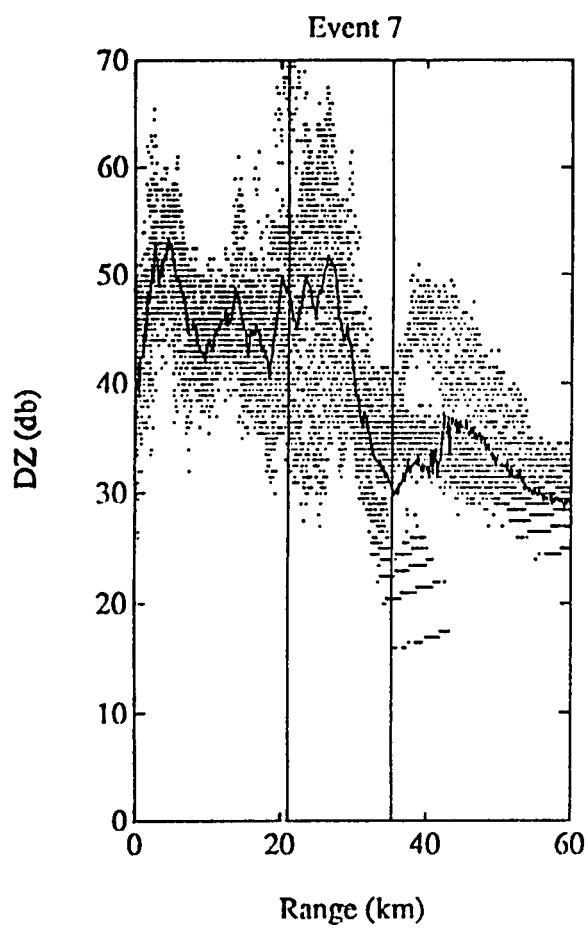
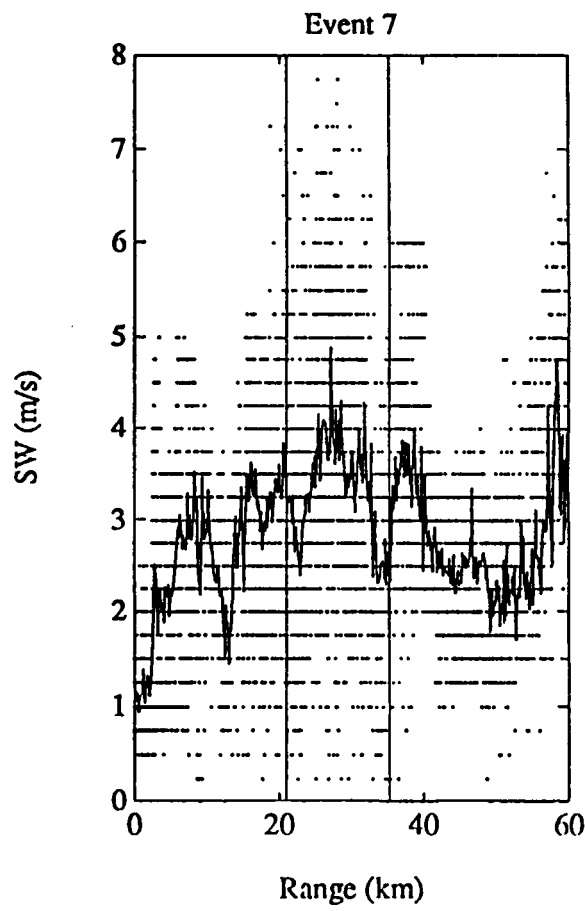
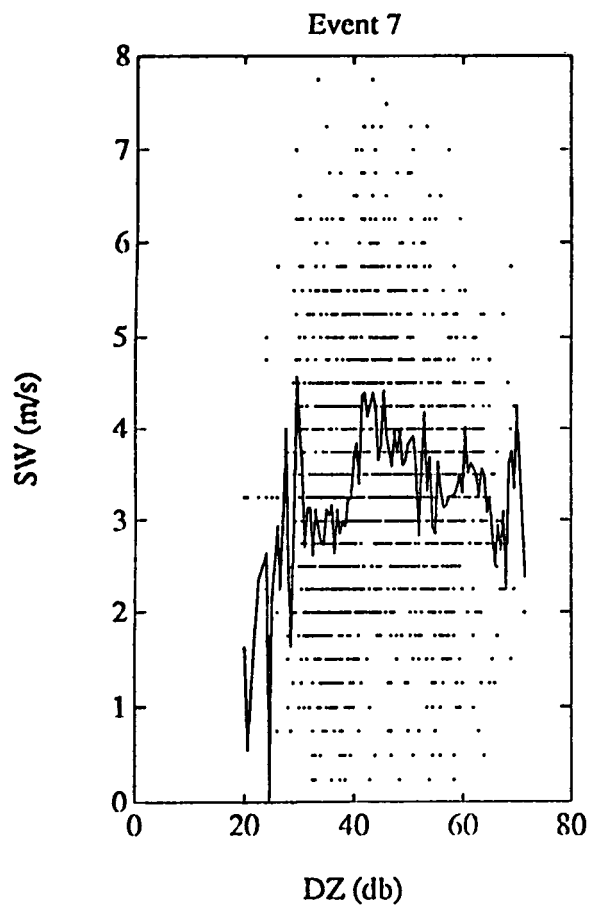


71
Fig 59

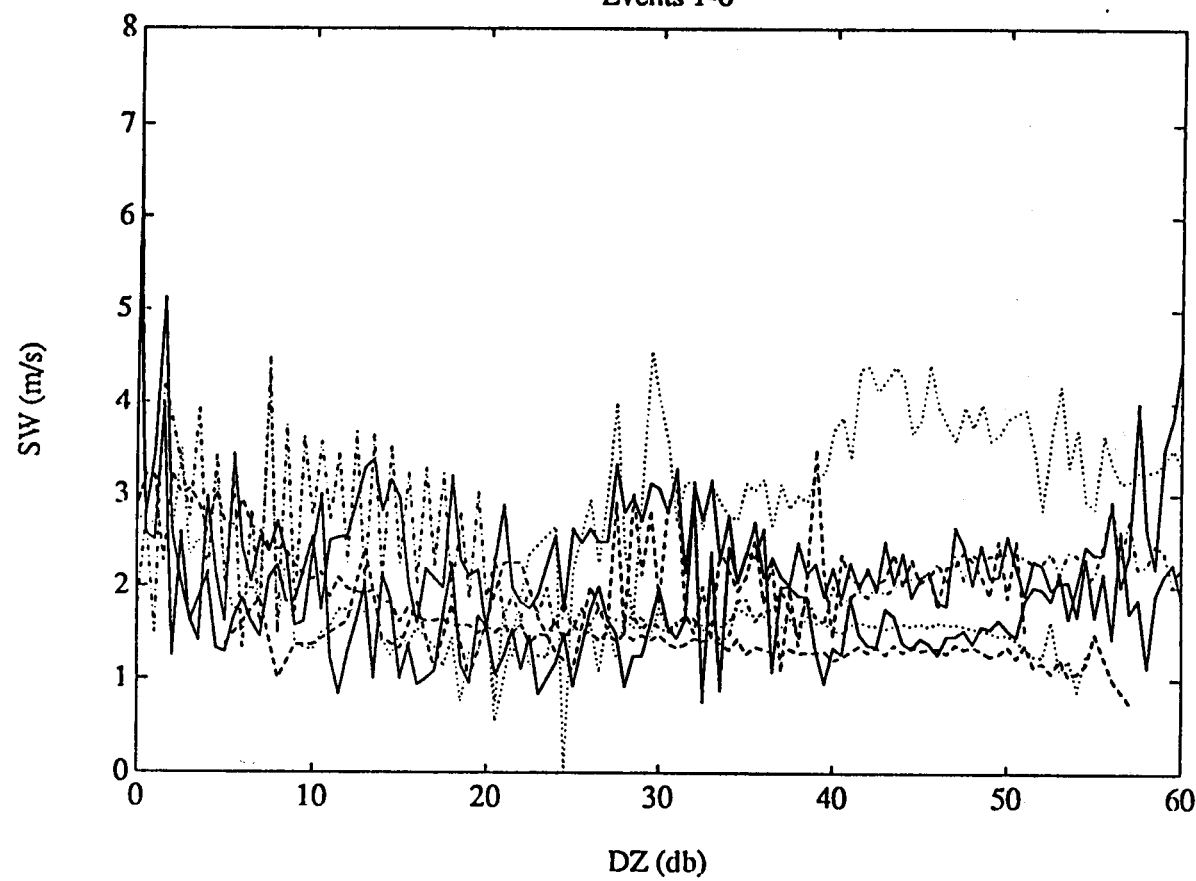


72
Fig 60

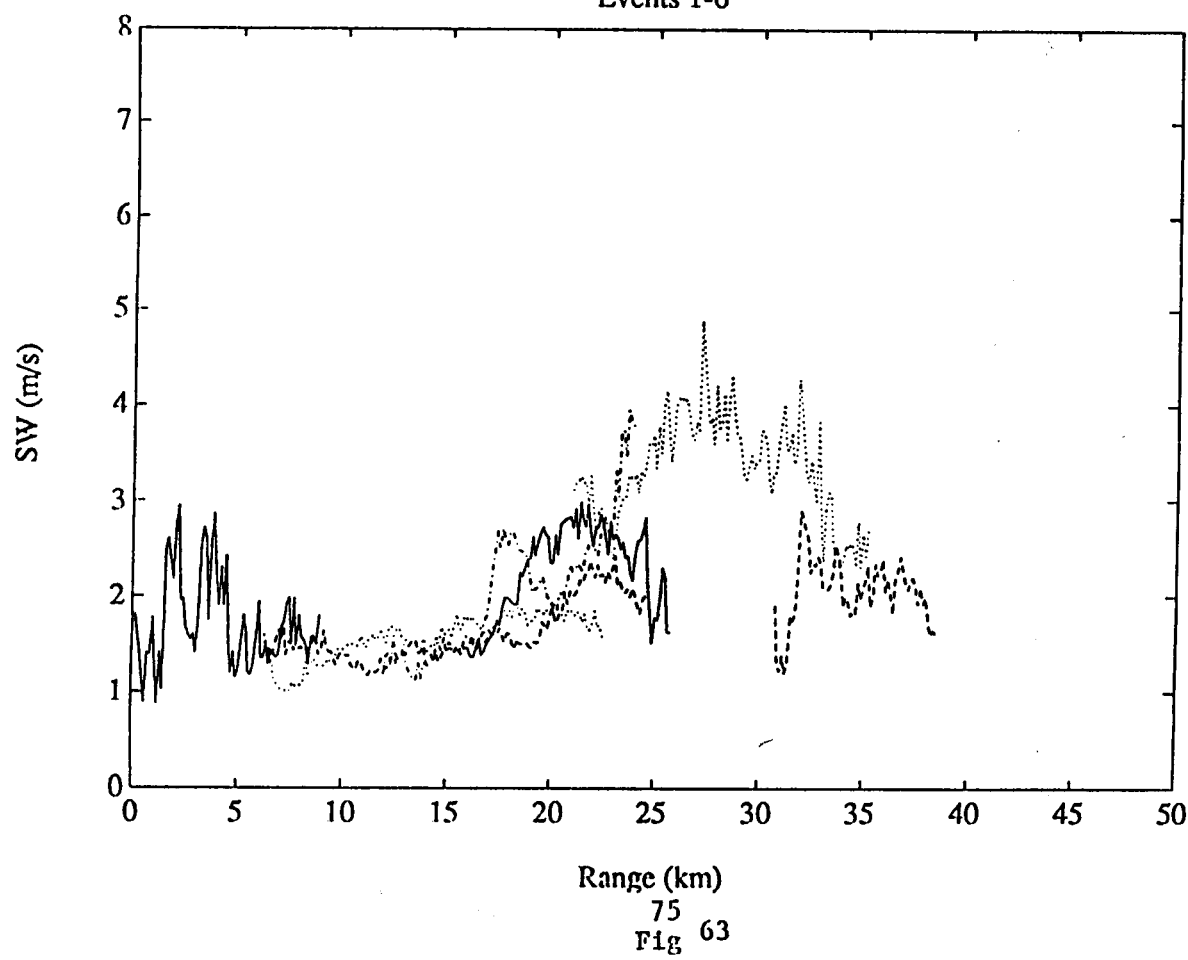


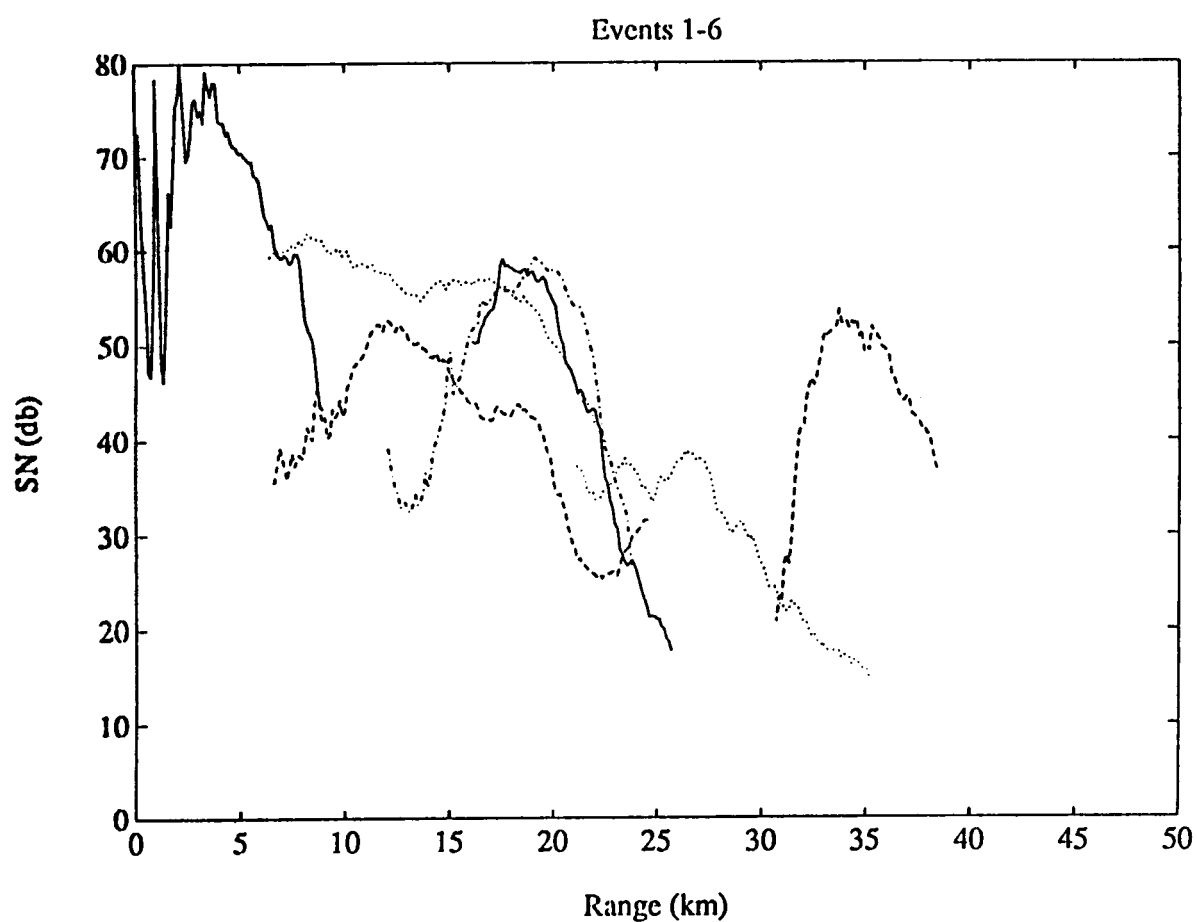
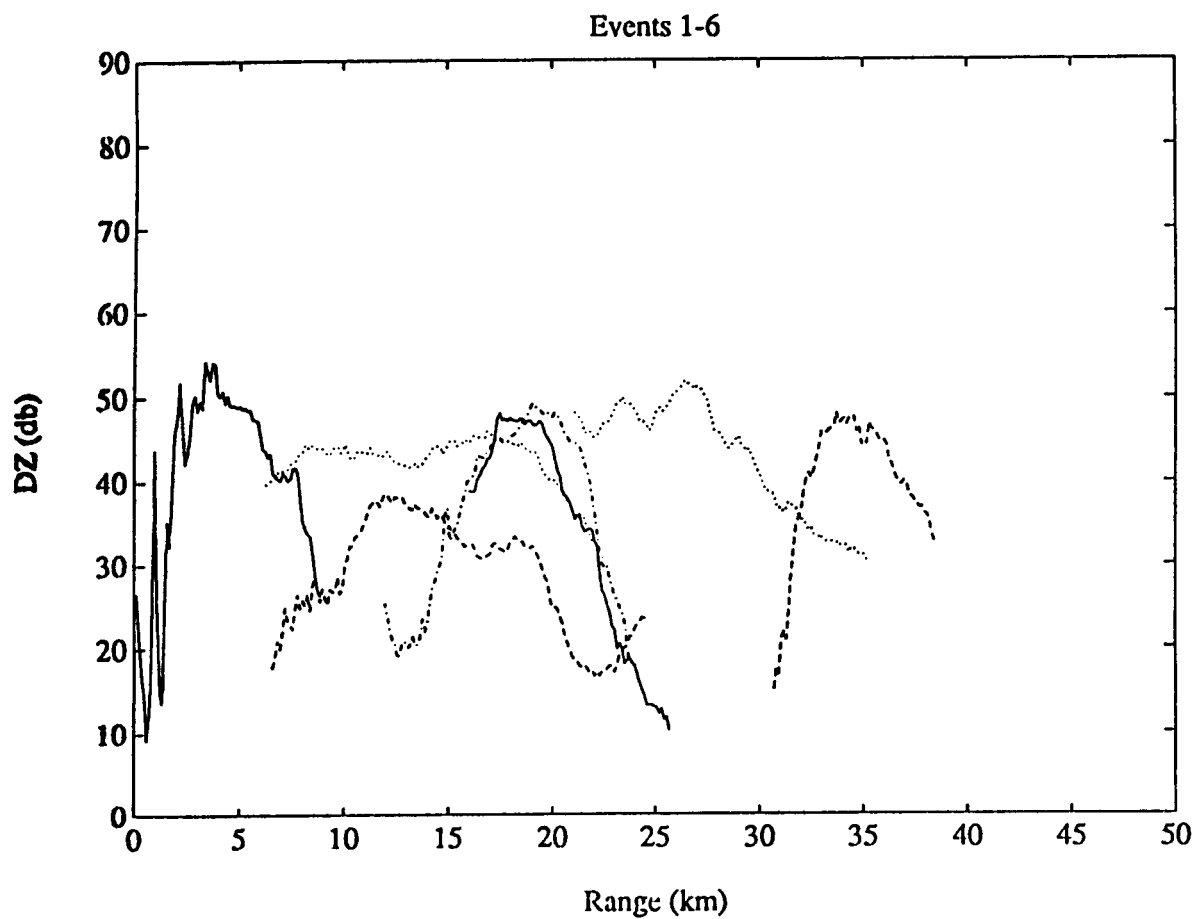


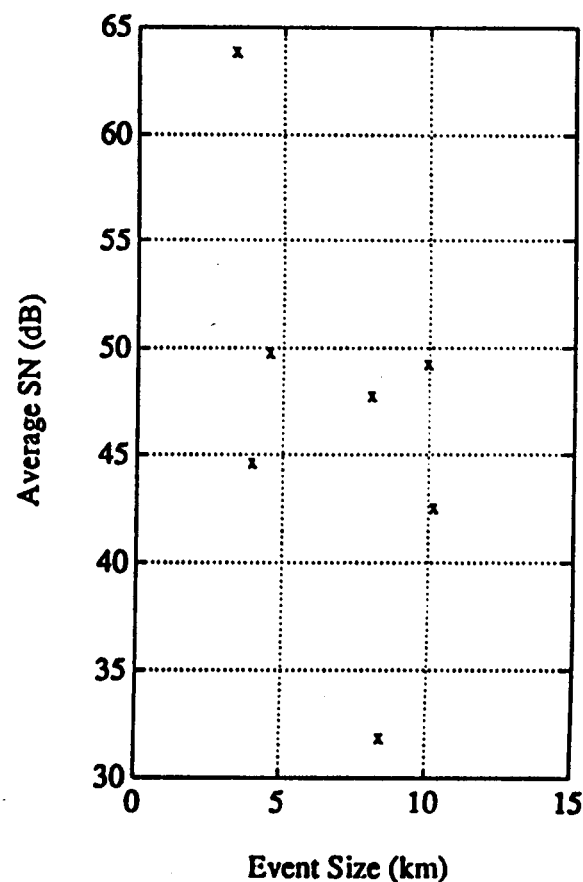
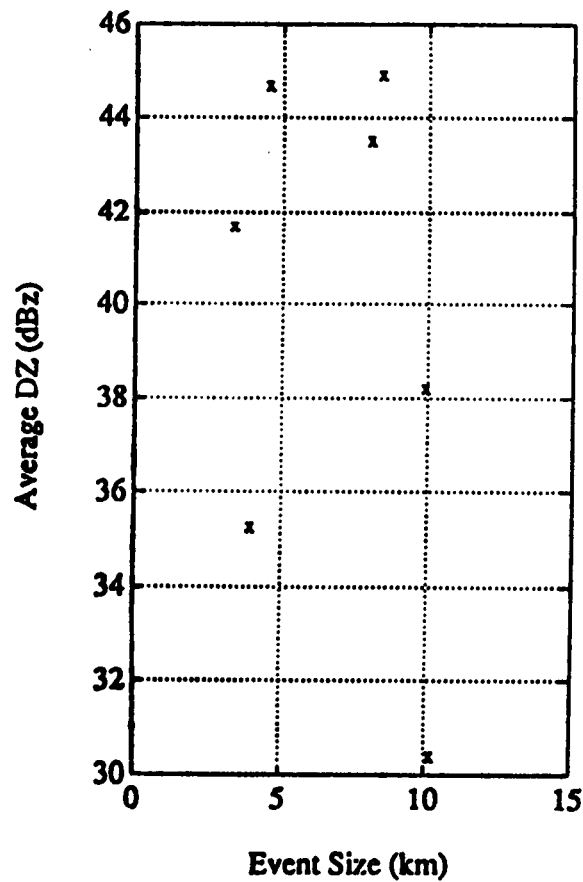
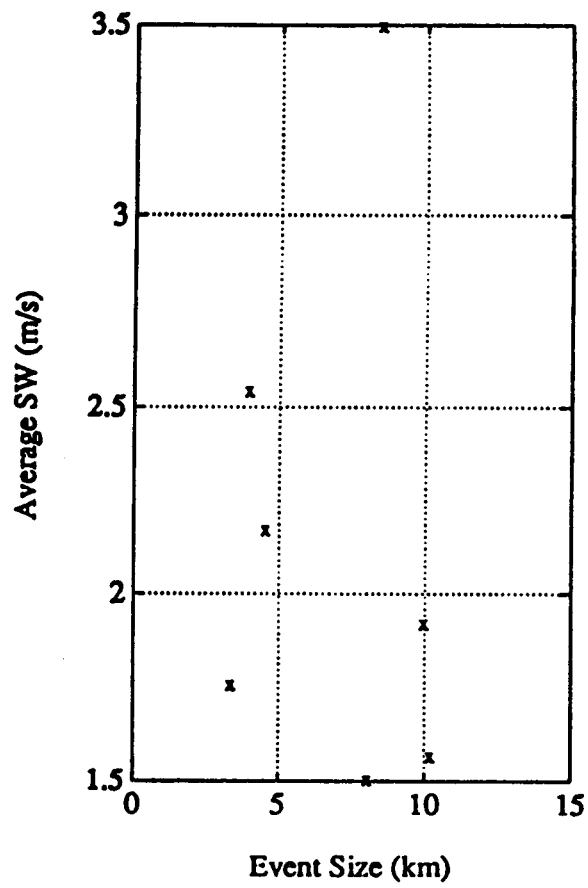
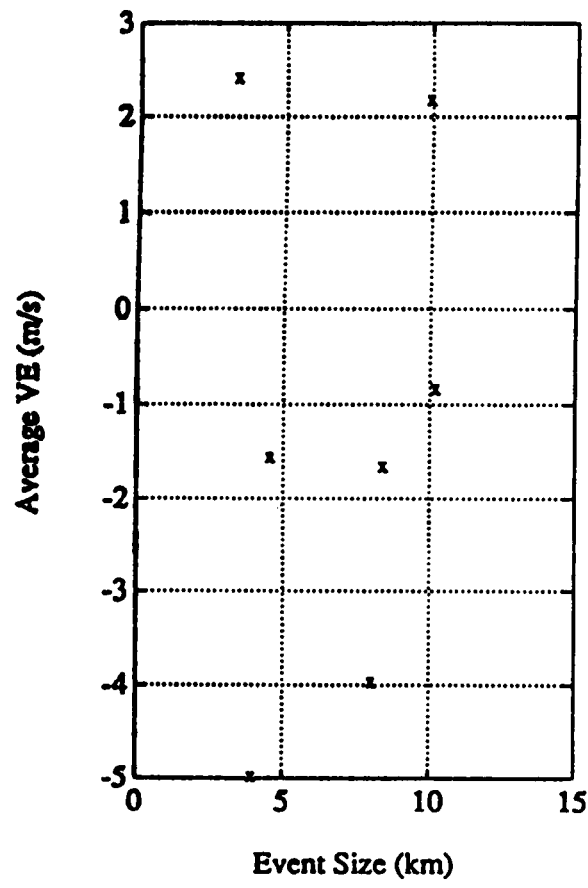
Events 1-6



Events 1-6







Event Description Table

Event	Size [km]	Strength [m/s/km]	Location [km]	\overline{SW} [dB]	\overline{DZ} [dBz]
1a	6.8	xx	6	1.48	27.19
1b	2.4	xx	3	1.87	21.48
1c	3.5	xx	3	2.99	15.97
1	3.4	xx	4	1.97	22.19
2a	11.3	17	17	2.20	22.63
2b	6.8	12	18	2.44	22.30
2	8.4	06	18	2.46	22.11
3a	10.2	07	18	1.84	29.98
3b	12.1	02	14	2.07	30.82
3c	7.7	06	14	2.07	28.35
3	7.6	08	14	1.99	28.46
4a	7.7	11	20	1.96	25.42
4b	8.5	11	19	1.94	20.79
4c	9.8	07	18	1.87	25.01
4	10.0	05	19	1.92	25.81
5a	5.6	13	21	1.42	22.62
5b	2.3	10	24	1.48	23.36
5	4.0	16	23	1.45	22.46
6a	6.1	07	34	1.54	24.62
6b	5.4	06	36	1.74	25.17
6	6.1	07	35	1.64	24.40

Analysis of Doppler Radar Windshear Data

Appendix A

Appendix A

List of Figures

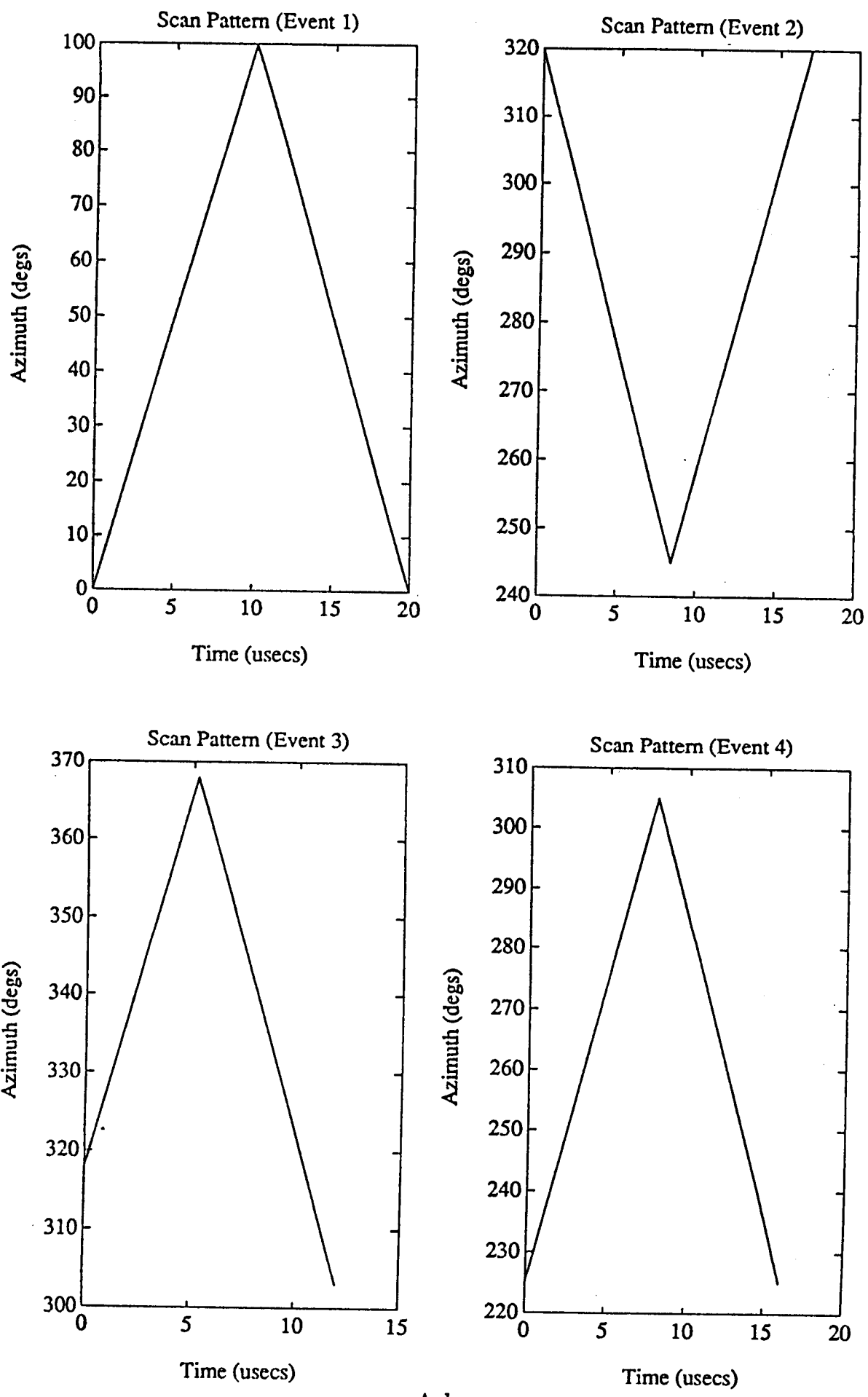
Figure	Description	Page
A1	Scan Pattern Graph, Event 1, 2, 3, 4	A-1
A2	Scan Pattern Graph, Event 5, 6, 7	A-2
A3	Histograms For Subevent 1	A-3
A4	Histograms For Subevent 1a	A-4
A5	Histograms For Subevent 1b	A-5
A6	Histograms For Subevent 1c	A-6
A7	Histograms For Subevent 2	A-7
A8	Histograms For Subevent 2a	A-8
A9	Histograms For Subevent 2b	A-9
A10	Histograms For Subevent 3	A-10
A11	Histograms For Subevent 3a	A-11
A12	Histograms For Subevent 3b	A-12
A13	Histograms For Subevent 3c	A-13
A14	Histograms For Subevent 4	A-14
A15	Histograms For Subevent 4a	A-15
A16	Histograms For Subevent 4b	A-16
A17	Histograms For Subevent 4c	A-17
A18	Histograms For Subevent 5	A-18
A19	Histograms For Subevent 5a	A-19
A20	Histograms For Subevent 5b	A-20
A21	Histograms For Subevent 6	A-21
A22	Histograms For Subevent 6a	A-22
A23	Histograms For Subevent 6b	A-23
A24	Histograms For Subevent 7	A-24
A25	Histograms For Subevent 7a	A-25
A26	Histograms For Subevent 7b	A-26
A27	Histograms For Subevent 7c	A-27
A28	Histograms For Subevent 7d	A-28
A29	Histograms For Subevent 7e	A-29
A30	Averaging 2 Point F-factor, Event 1	A-30
A31	Averaging 3 Point F-factor, Event 1	A-31
A32	Averaging 2 Point F-factor, Event 2	A-32
A33	Averaging 3 Point F-factor, Event 2	A-33
A34	Averaging 2 Point F-factor, Event 3	A-34
A35	Averaging 3 Point F-factor, Event 3	A-35
A36	Averaging 2 Point F-factor, Event 4	A-36
A37	Averaging 3 Point F-factor, Event 4	A-37
A38	Averaging 2 Point F-factor, Event 5	A-38
A39	Averaging 3 Point F-factor, Event 5	A-39
A40	Averaging 2 Point F-factor, Event 6	A-40
A41	Averaging 3 Point F-factor, Event 6	A-41
A42	Averaging 2 Point F-factor, Event 7a-d	A-42
A43	Averaging 3 Point F-factor, Event 7a-d	A-43
A44	Averaging 2 Point F-factor, Event 7e-7	A-44
A45	Averaging 3 Point F-factor, Event 7e-7	A-45
A46	Velocity Profile With F-factor, Event 1	A-46
A47	Velocity Profile With F-factor, Event 2	A-47

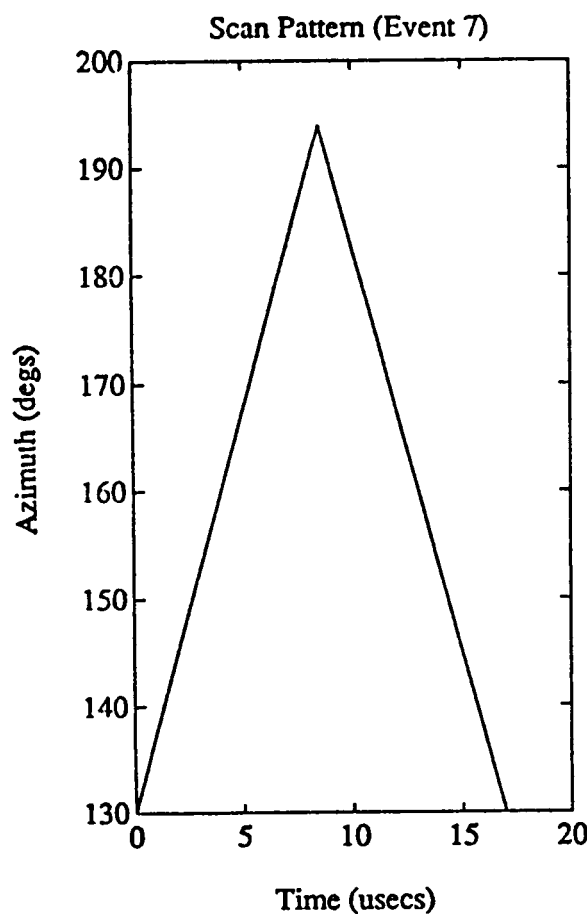
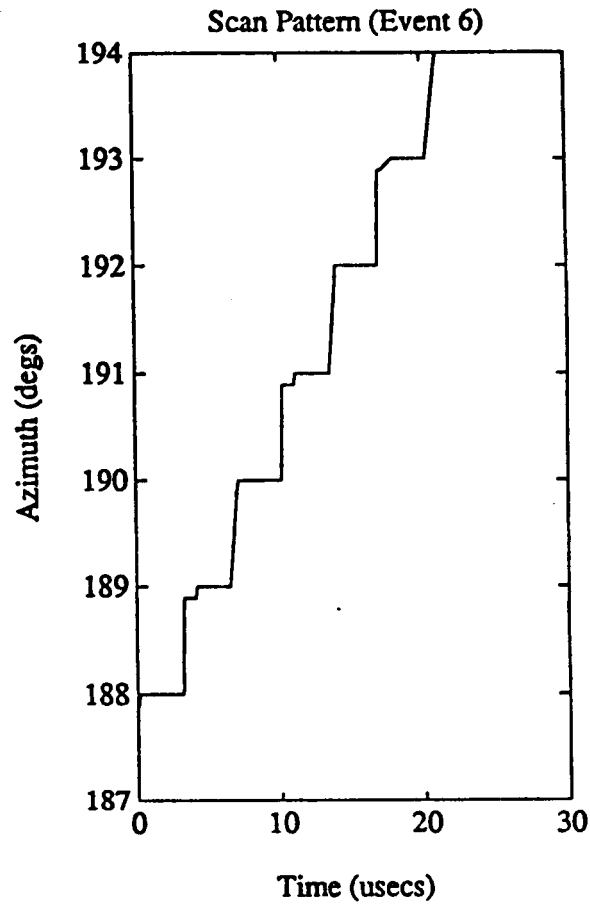
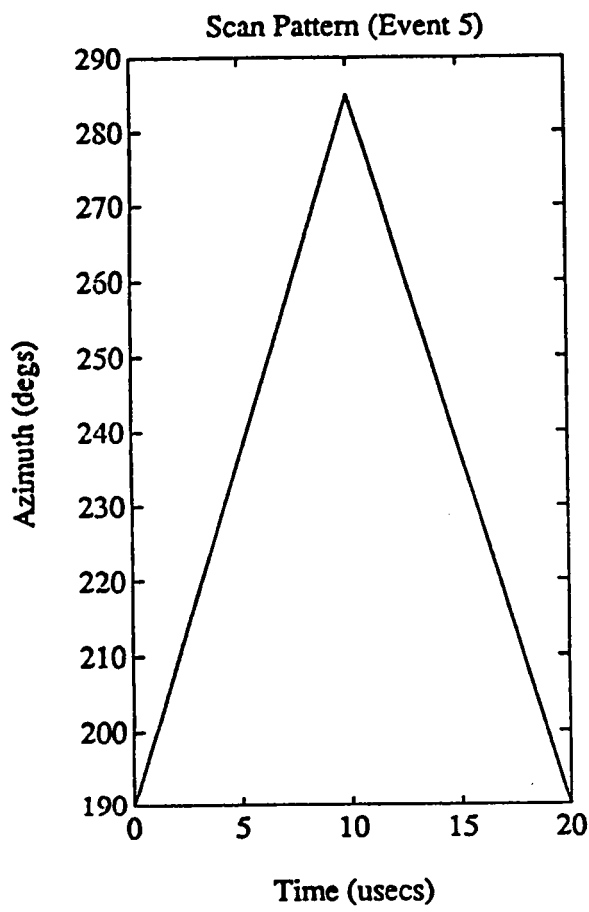
Appendix A
List of Figures, Continued

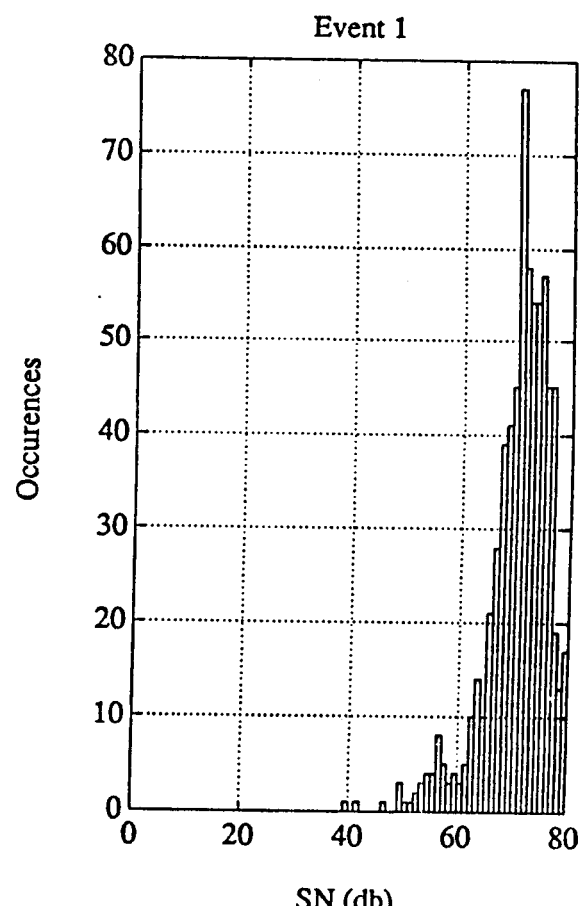
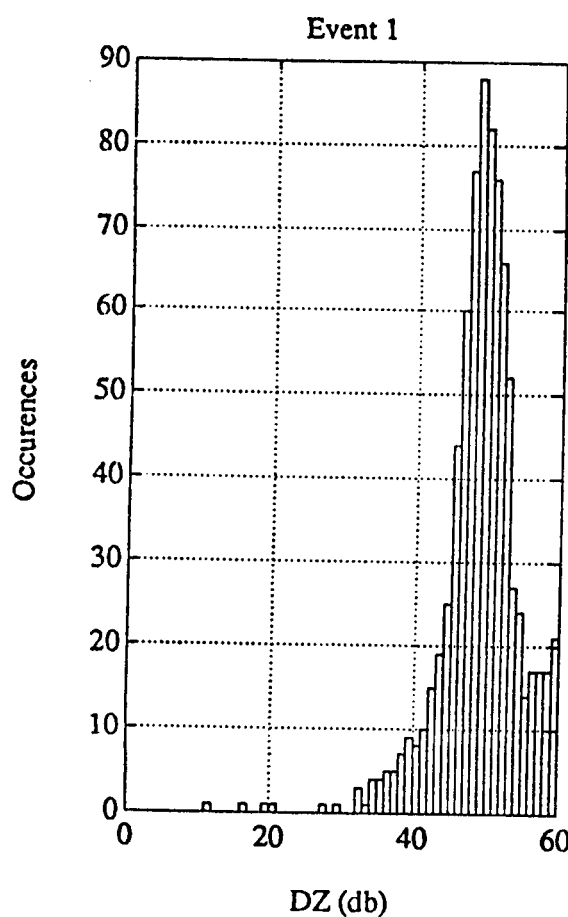
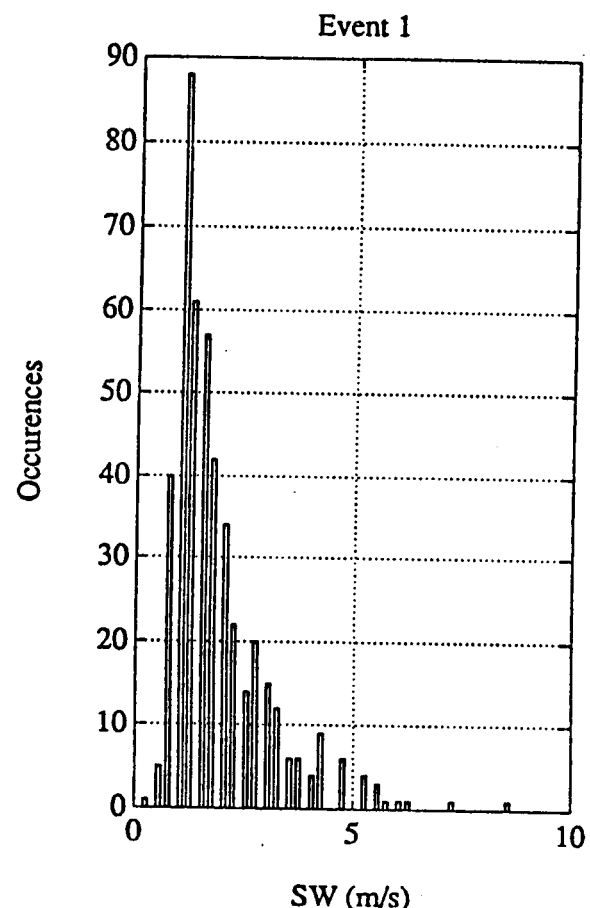
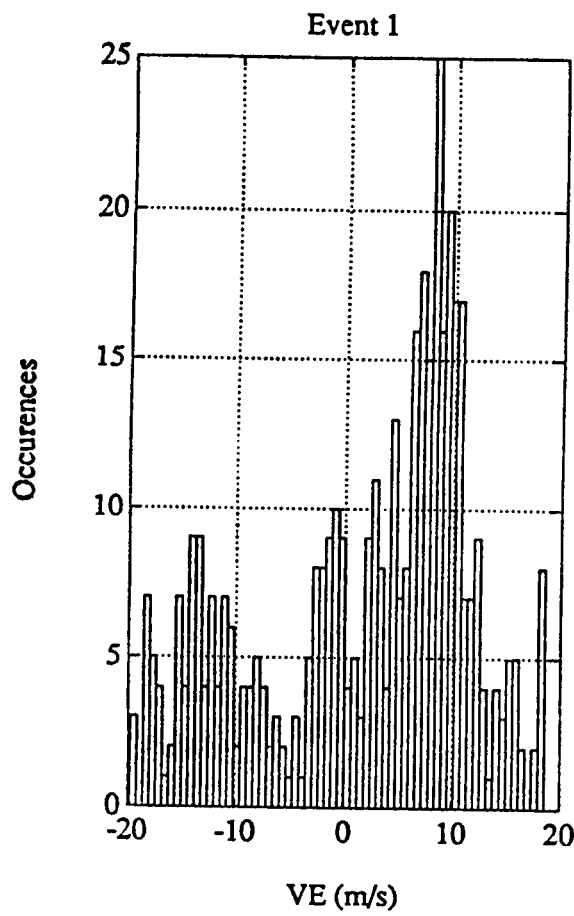
Figure	Description	Page
A48	Velocity Profile With F-factor, Event 3	A-48
A49	Velocity Profile With F-factor, Event 4	A-49
A50	Velocity Profile With F-factor, Event 5	A-50
A51	Velocity Profile With F-factor, Event 6	A-51
A52	Velocity Profile With F-factor, Event 7	A-52
A53	Velocity Profile With F-factor, Event 7 (cont)	A-53
A54	Type 1 Correlation Plots, Subevent 1a	A-54
A55	Type 1 Correlation Plots, Subevent 1b	A-55
A56	Type 1 Correlation Plots, Subevent 1c	A-56
A57	Type 1 Correlation Plots, Subevent 2a	A-57
A58	Type 1 Correlation Plots, Subevent 2b	A-58
A59	Type 1 Correlation Plots, Subevent 3a	A-59
A60	Type 1 Correlation Plots, Subevent 3b	A-60
A61	Type 1 Correlation Plots, Subevent 3c	A-61
A62	Type 1 Correlation Plots, Subevent 4a	A-62
A63	Type 1 Correlation Plots, Subevent 4b	A-63
A64	Type 1 Correlation Plots, Subevent 4c	A-64
A65	Type 1 Correlation Plots, Subevent 5a	A-65
A66	Type 1 Correlation Plots, Subevent 5b	A-66
A67	Type 1 Correlation Plots, Subevent 6a	A-67
A68	Type 1 Correlation Plots, Subevent 6b	A-68
A69	Type 1 Correlation Plots, Subevent 7a	A-69
A70	Type 1 Correlation Plots, Subevent 7b	A-70
A71	Type 1 Correlation Plots, Subevent 7c	A-71
A72	Type 1 Correlation Plots, Subevent 7d	A-72
A73	Type 1 Correlation Plots, Subevent 7e	A-73
A74	Type 2 Correlation Plots, Event 1	A-74
A75	Type 2 Correlation Plots, Subevent 1a	A-75
A76	Type 2 Correlation Plots, Subevent 1b	A-76
A77	Type 2 Correlation Plots, Subevent 1c	A-77
A78	Type 2 Correlation Plots, Event 2	A-78
A79	Type 2 Correlation Plots, Subevent 2a	A-79
A80	Type 2 Correlation Plots, Subevent 2b	A-80
A81	Type 2 Correlation Plots, Event 3	A-81
A82	Type 2 Correlation Plots, Subevent 3a	A-82
A83	Type 2 Correlation Plots, Subevent 3b	A-83
A84	Type 2 Correlation Plots, Subevent 3c	A-84
A85	Type 2 Correlation Plots, Event 4	A-85
A86	Type 2 Correlation Plots, Subevent 4a	A-86
A87	Type 2 Correlation Plots, Subevent 4b	A-87
A88	Type 2 Correlation Plots, Subevent 4c	A-88
A89	Type 2 Correlation Plots, Event 5	A-89
A90	Type 2 Correlation Plots, Subevent 5a	A-90
A91	Type 2 Correlation Plots, Subevent 5b	A-91
A92	Type 2 Correlation Plots, Event 6	A-92
A93	Type 2 Correlation Plots, Subevent 6a	A-93
A94	Type 2 Correlation Plots, Subevent 6b	A-94

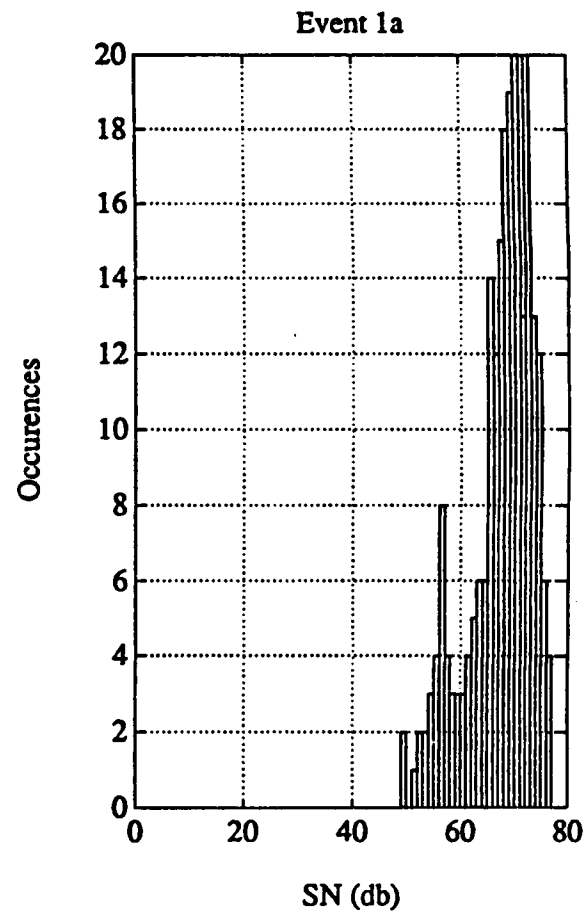
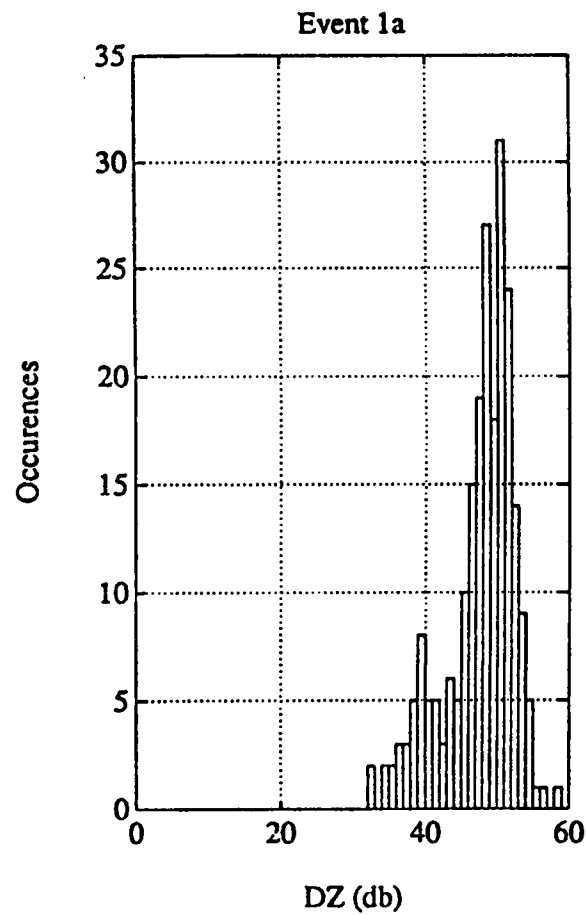
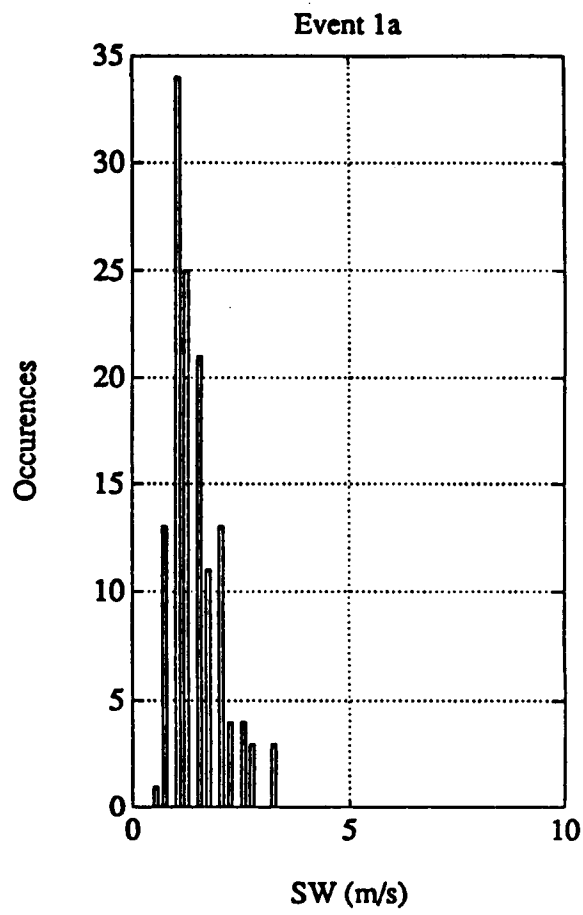
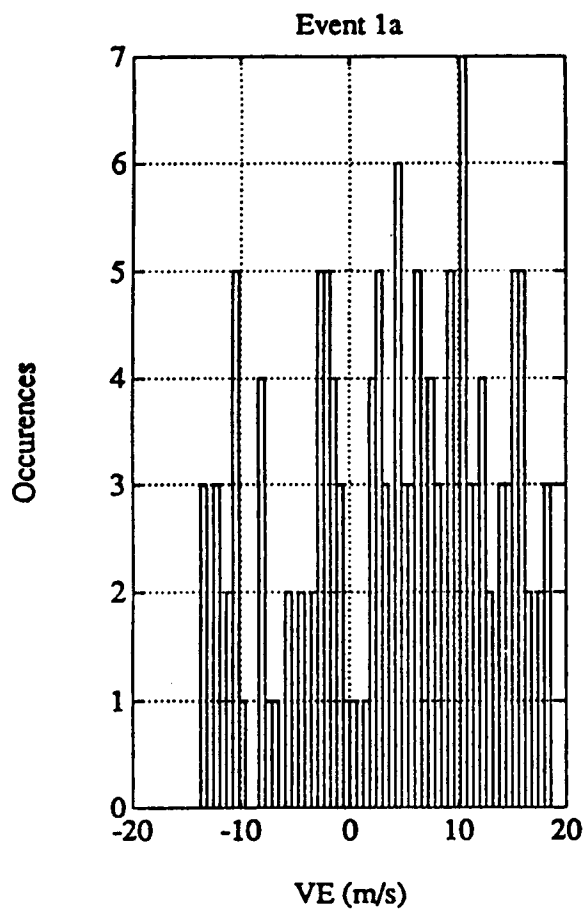
Appendix A
List of Figures, Continued

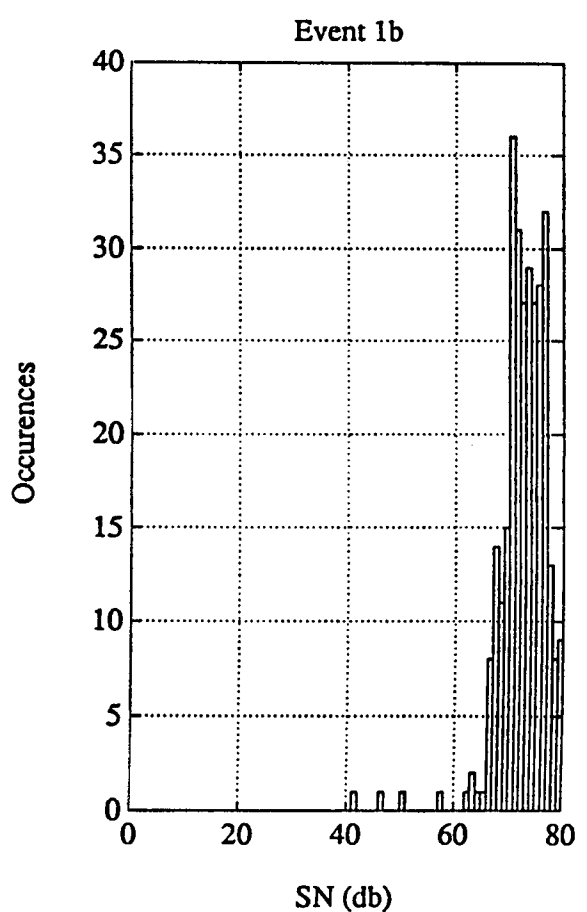
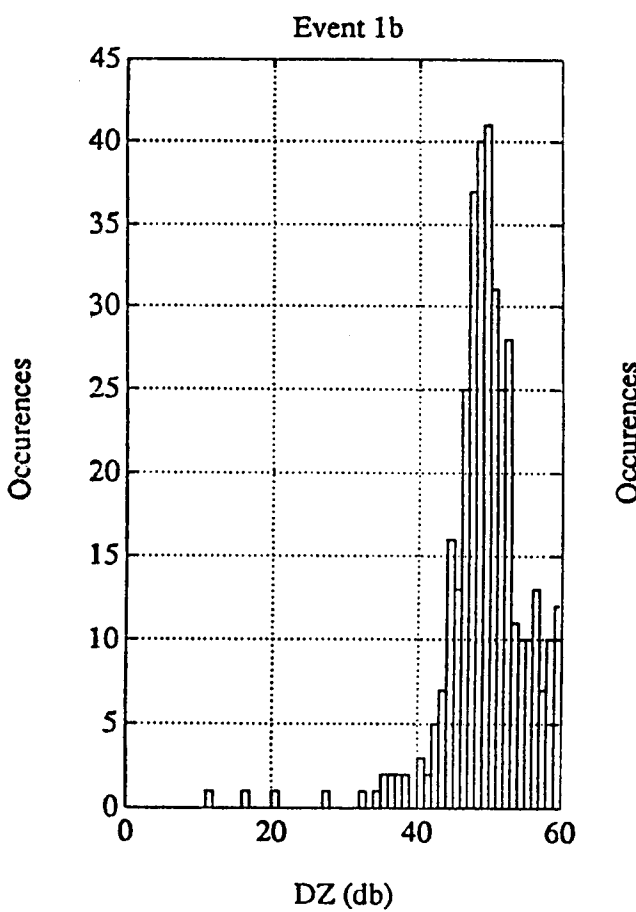
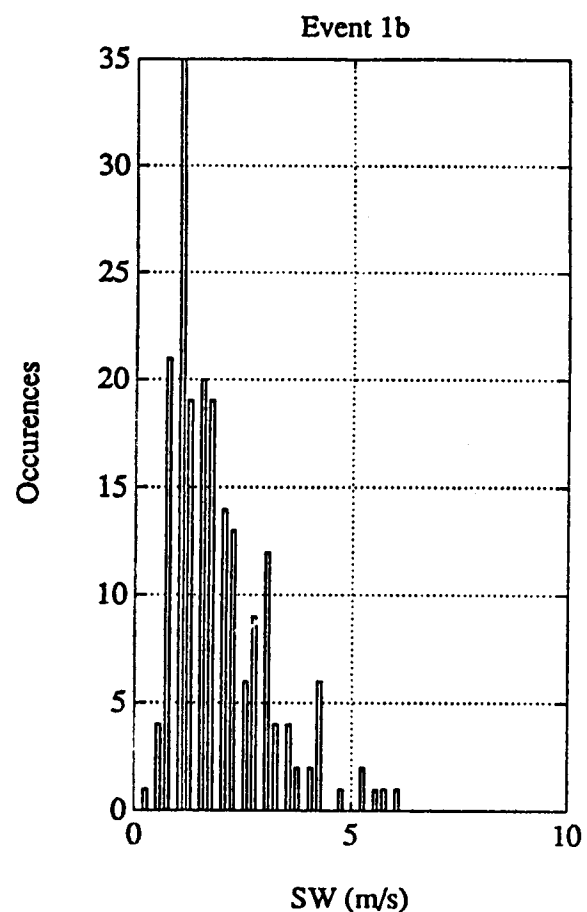
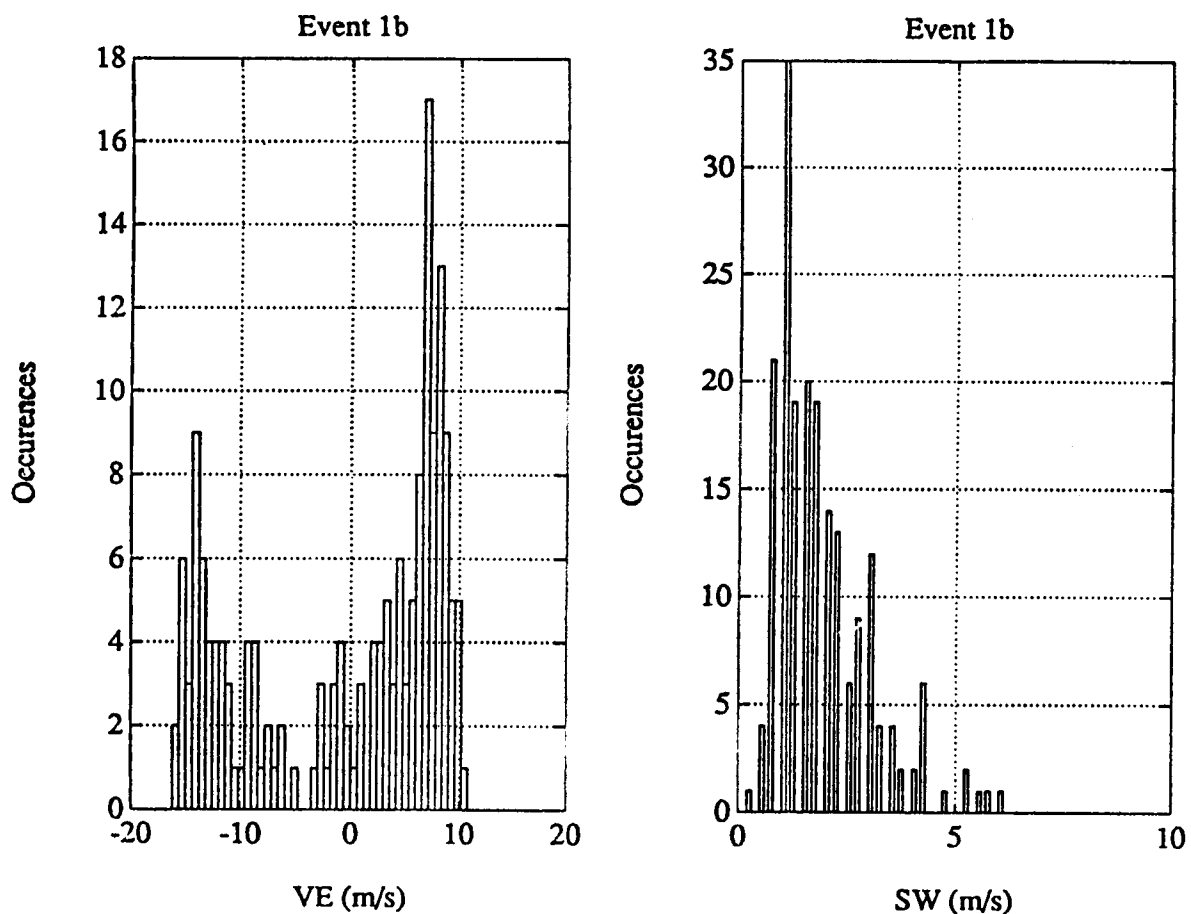
Figure	Description	Page
A95	Type 2 Correlation Plots, Event 7	A-95
A96	Type 2 Correlation Plots, Subevent 7a	A-96
A97	Type 2 Correlation Plots, Subevent 7b	A-97
A98	Type 2 Correlation Plots, Subevent 7c	A-98
A99	Type 2 Correlation Plots, Subevent 7d	A-99
A100	Type 2 Correlation Plots, Subevent 7e	A-100
A101	Type 2 Correlation Plots, Events 1-6	A-101
A102	Type 2 Correlation Plots, Events 1-6	A-102

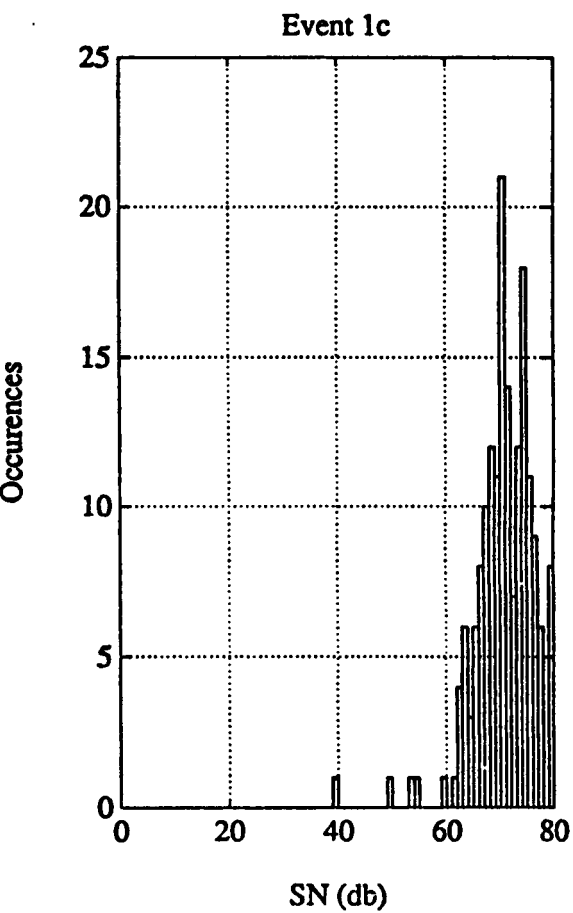
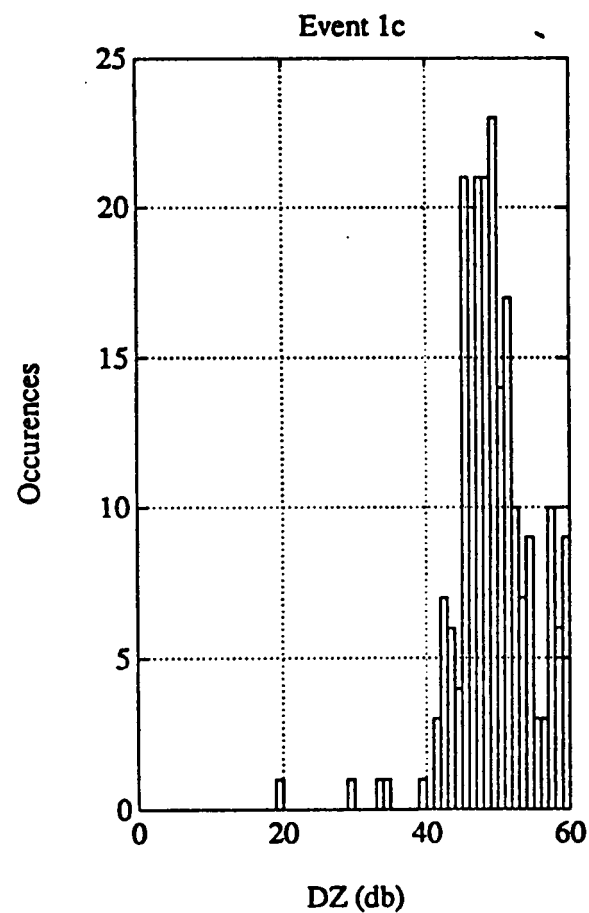
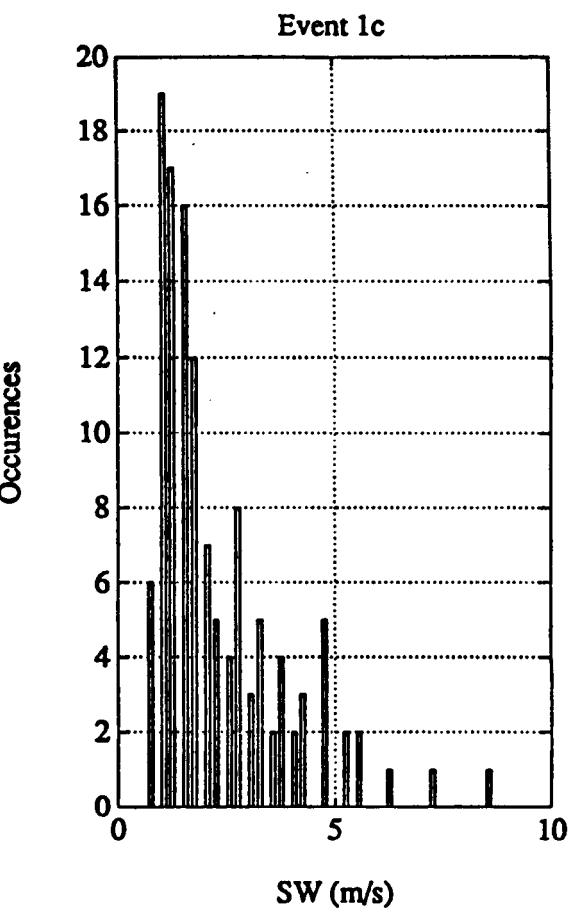
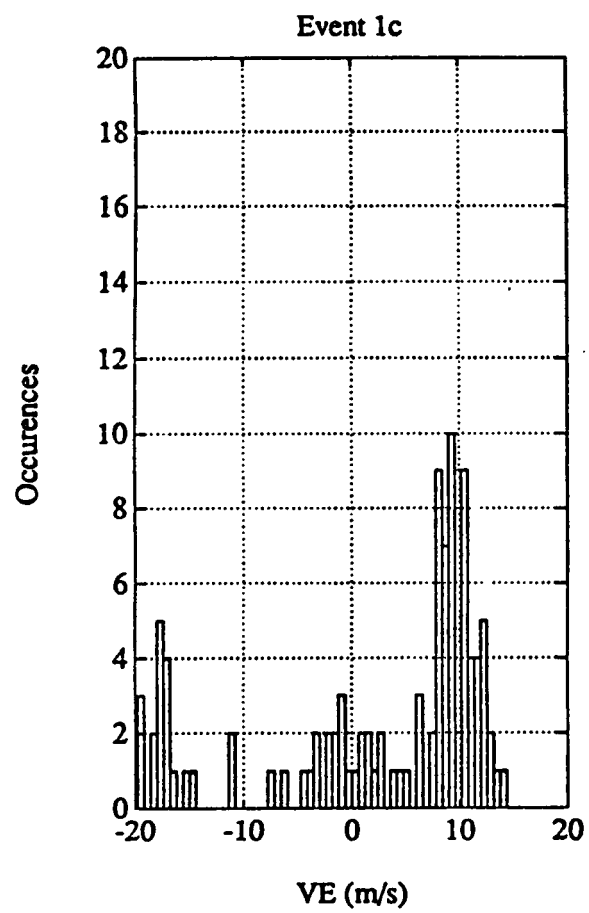


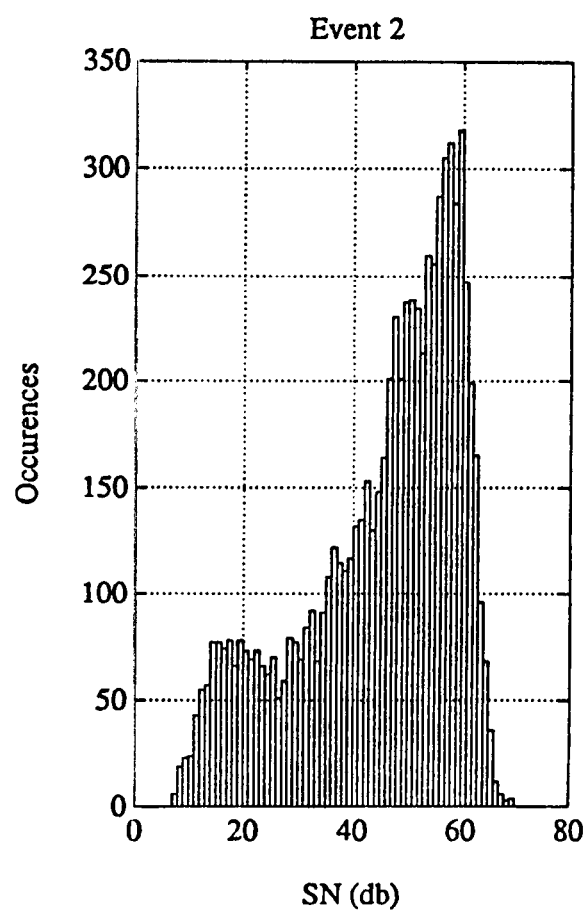
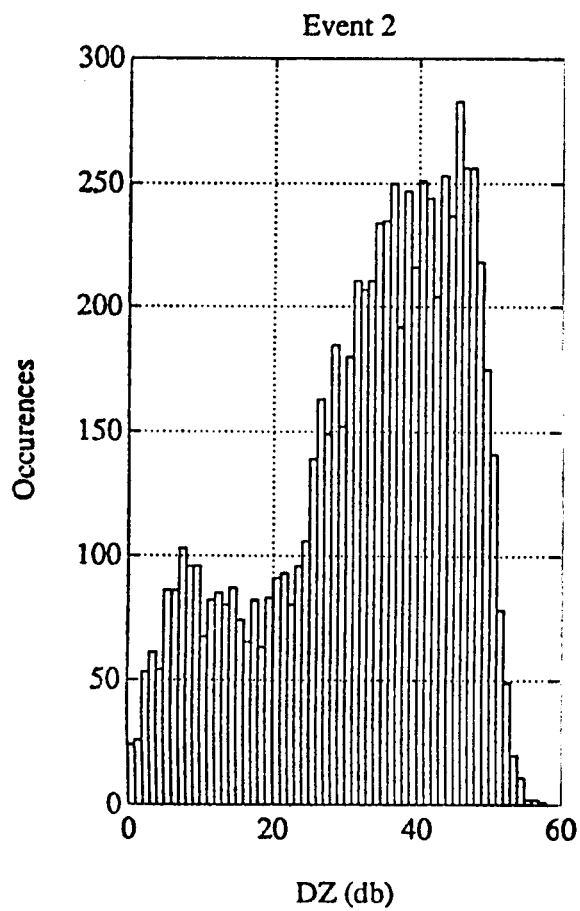
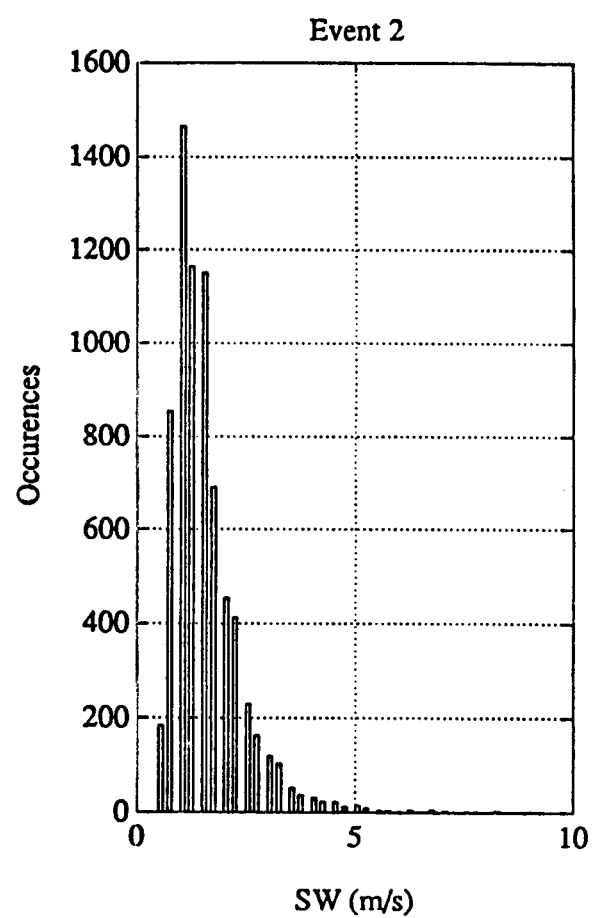
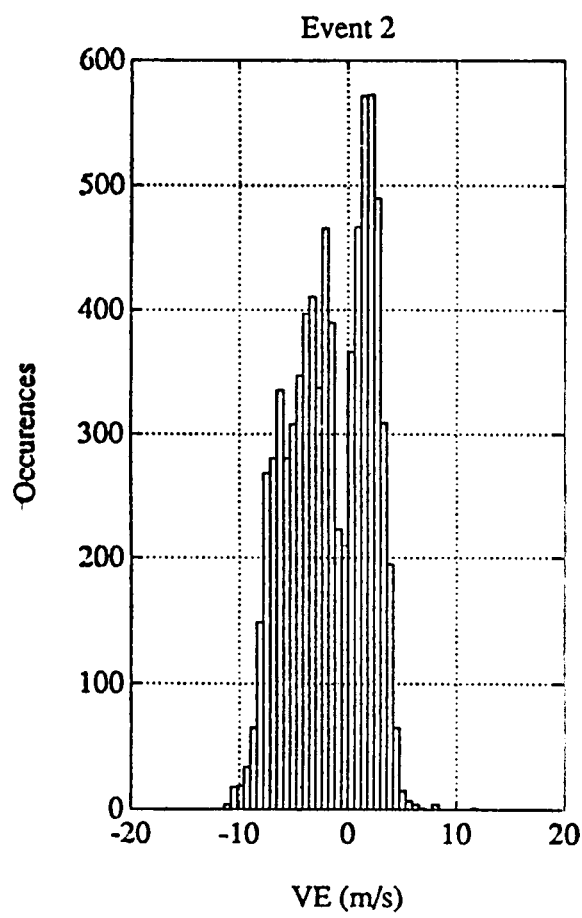


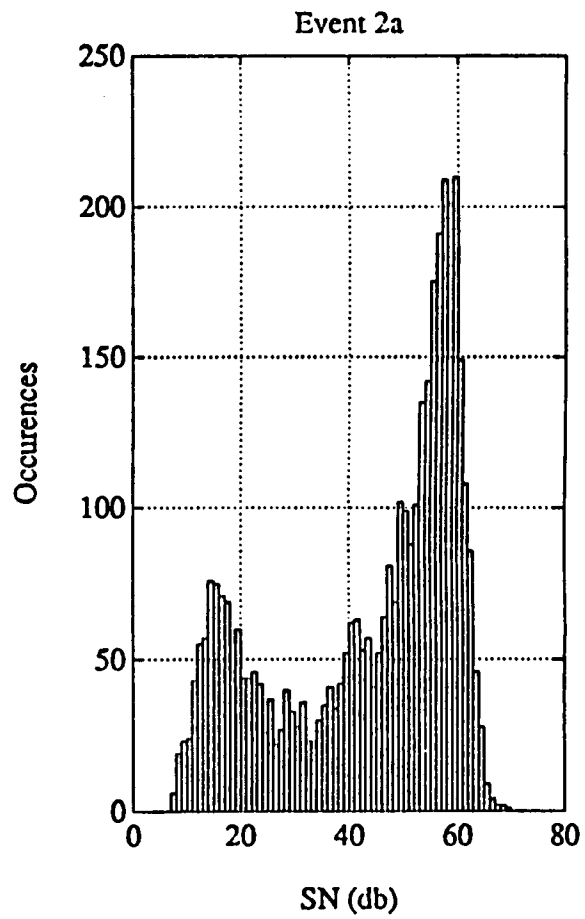
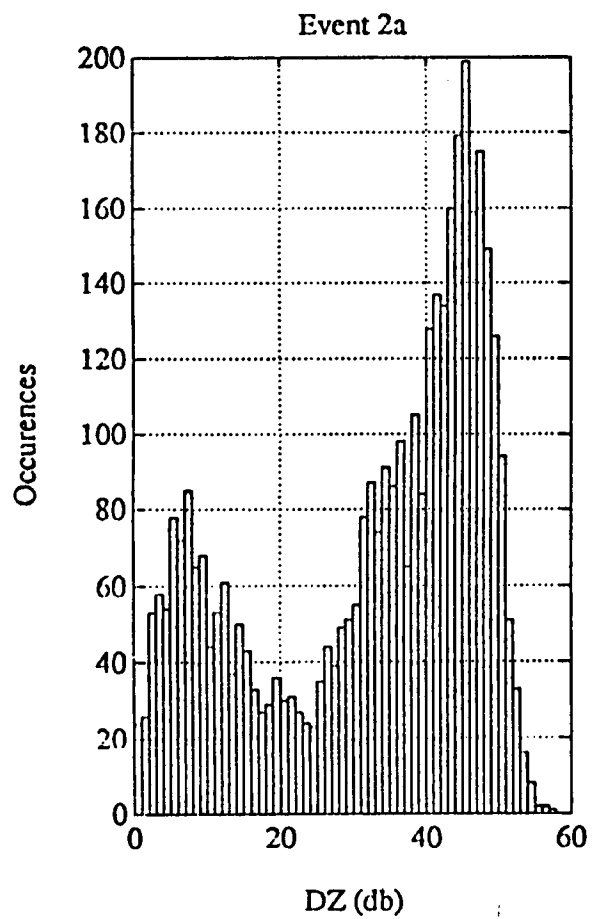
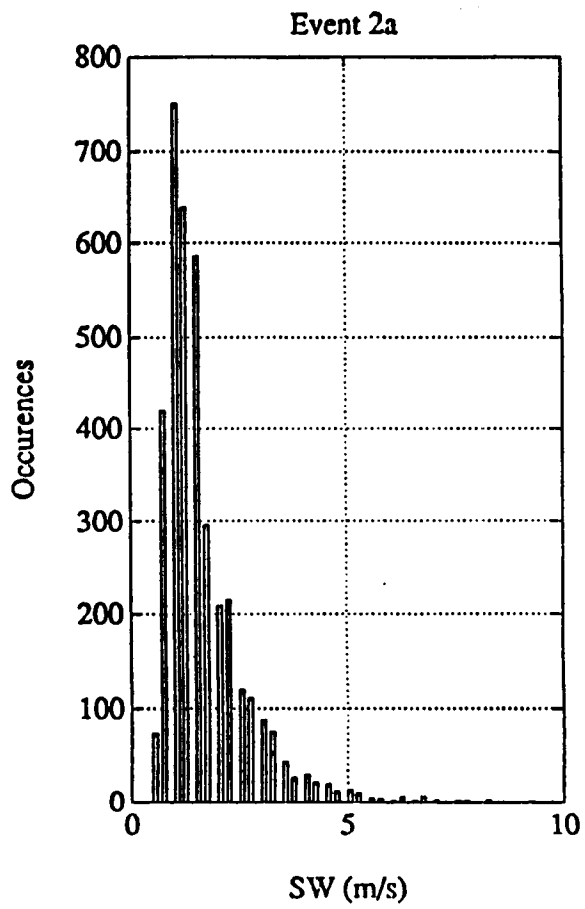
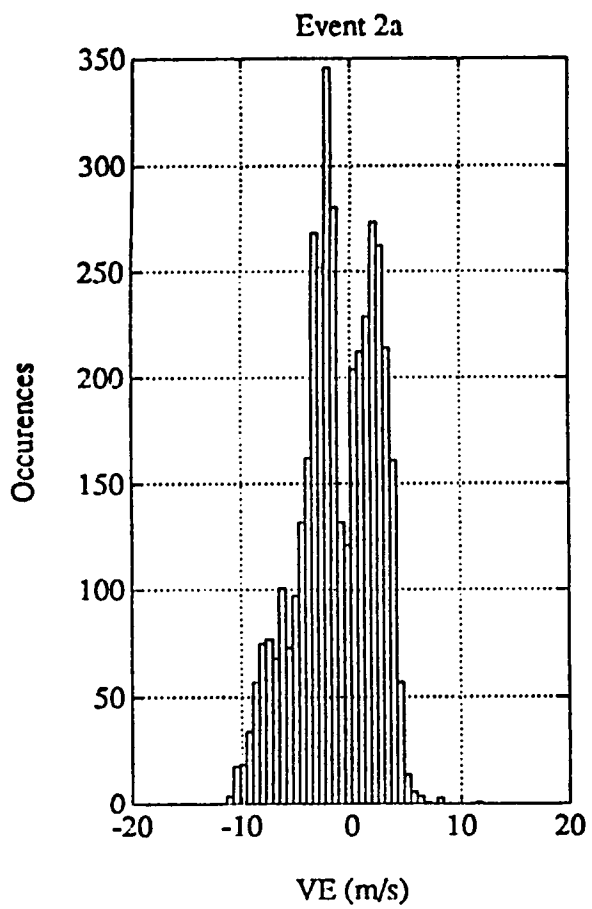


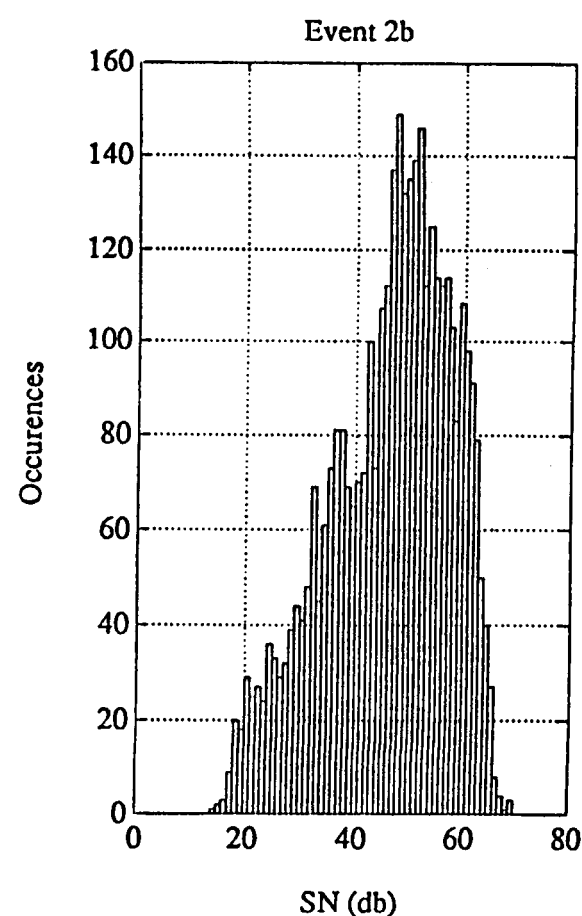
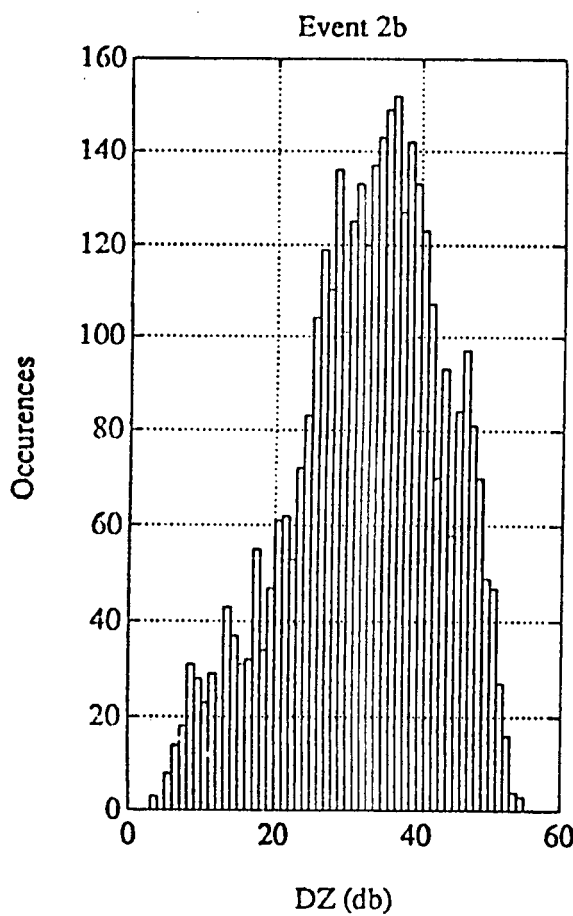
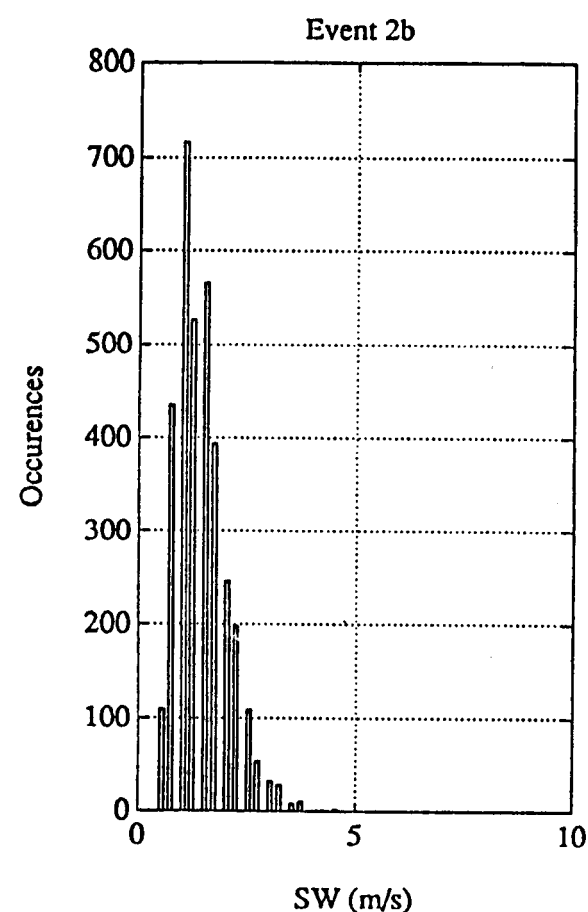
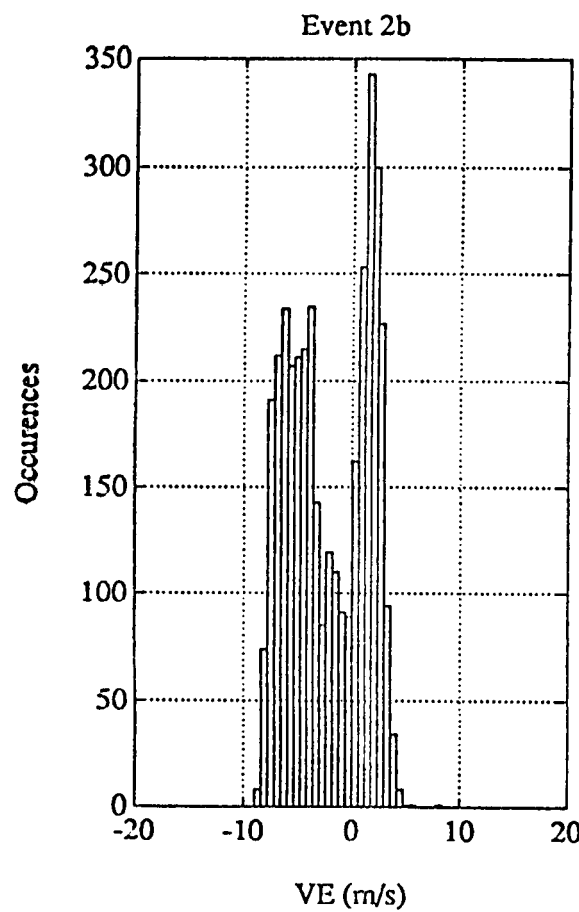


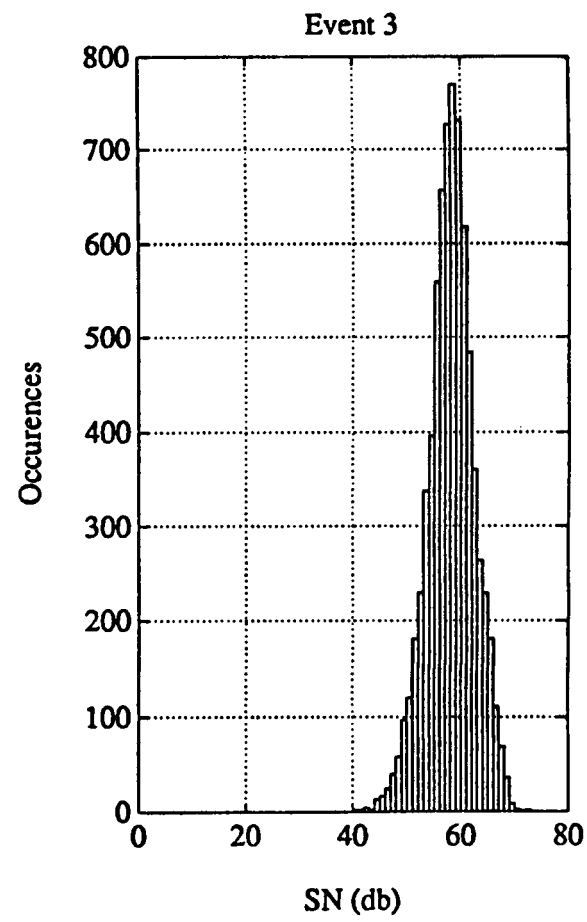
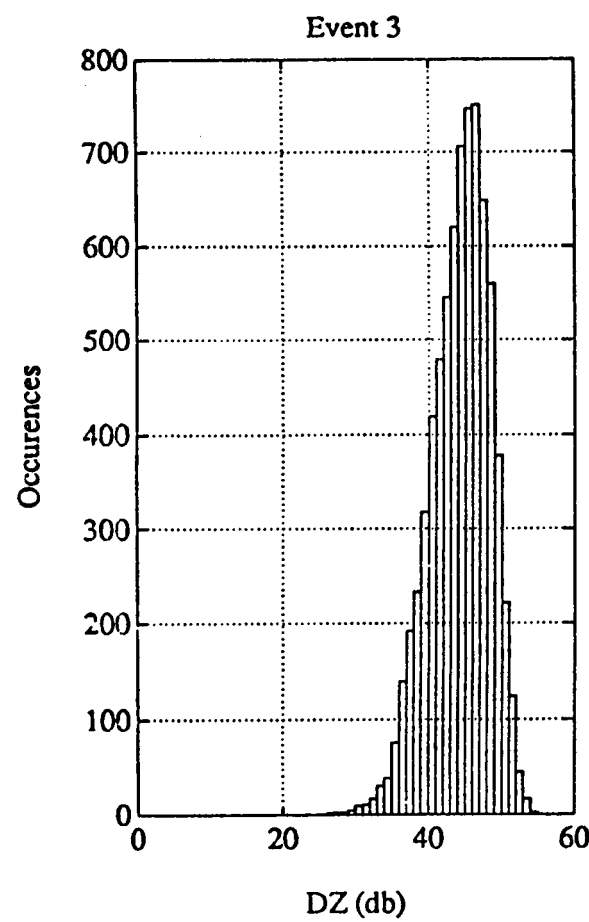
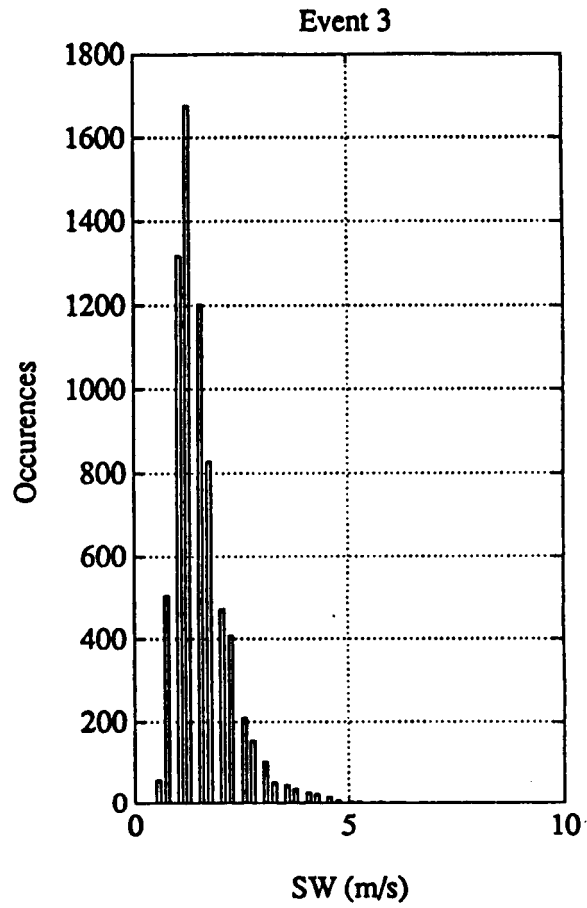
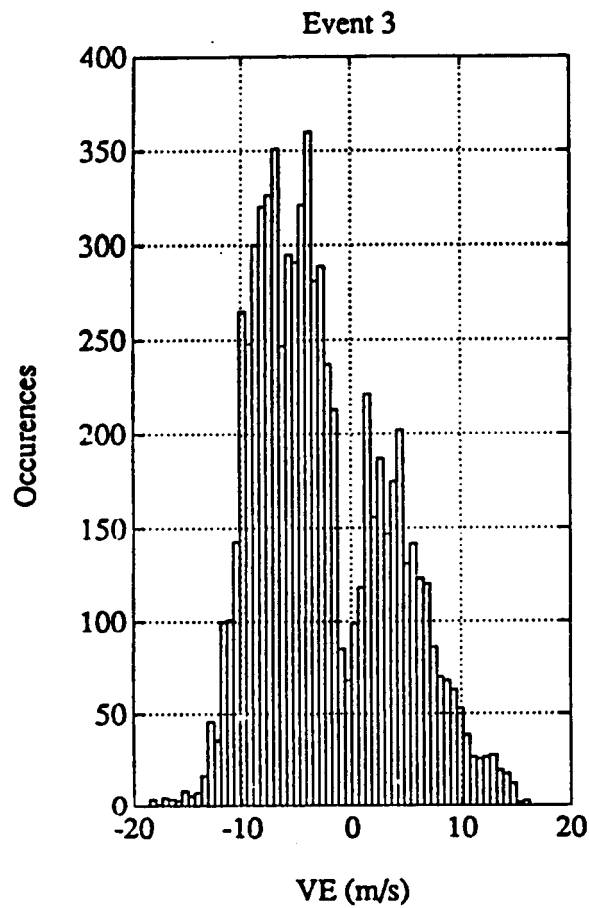


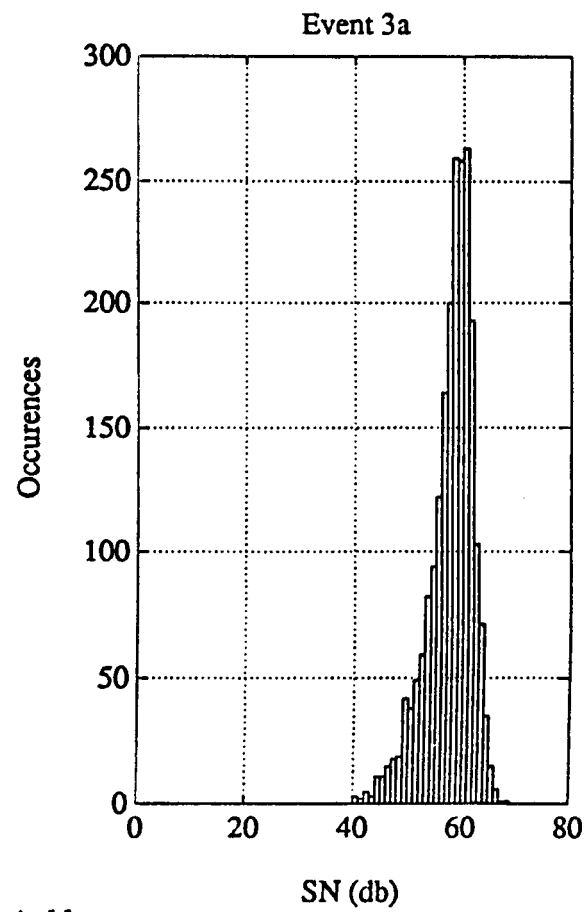
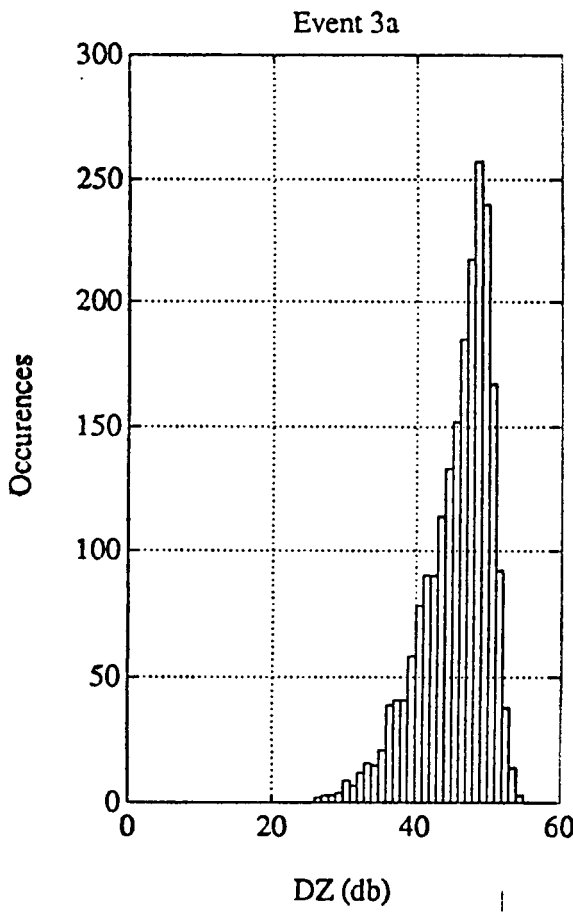
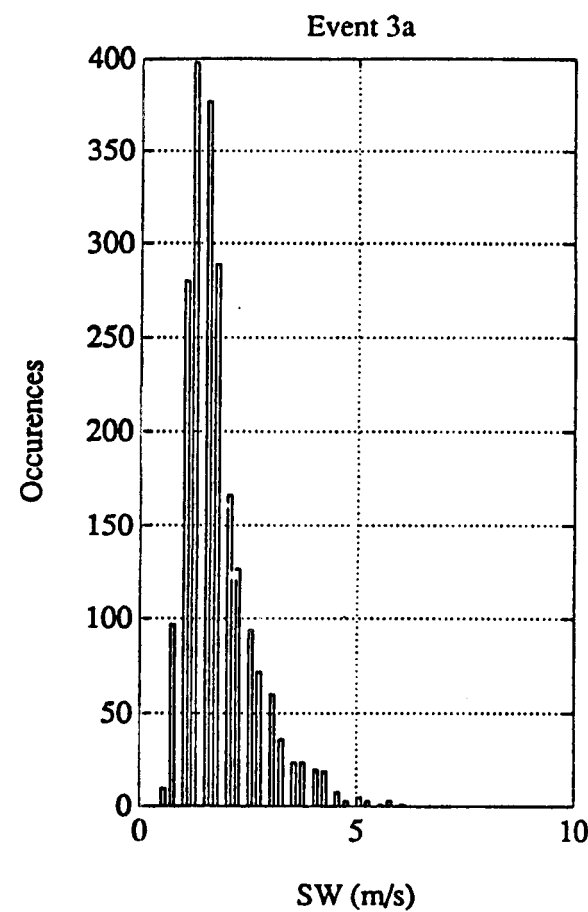
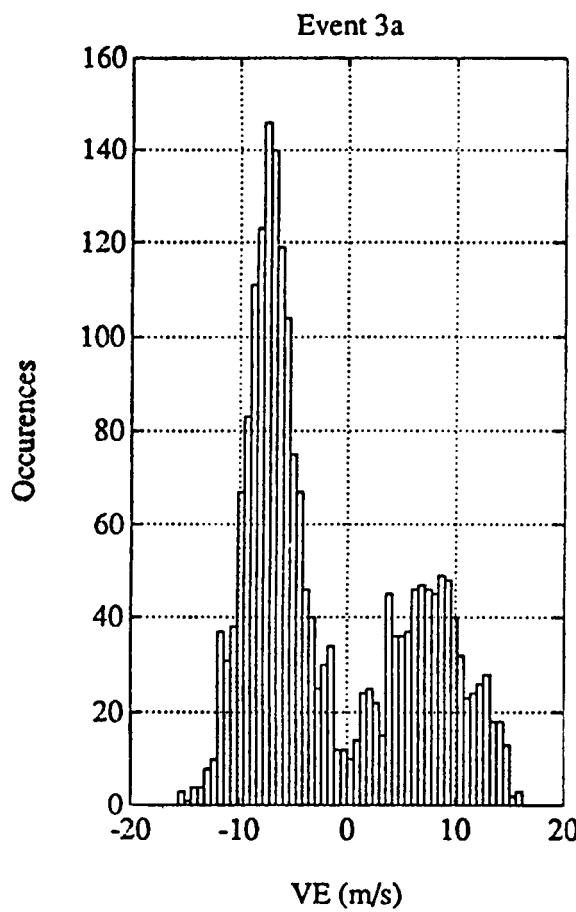


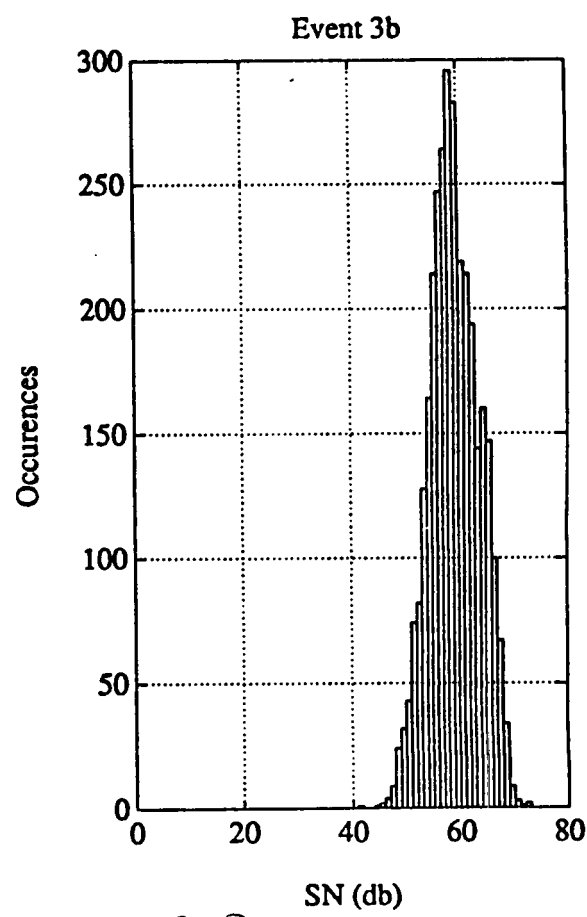
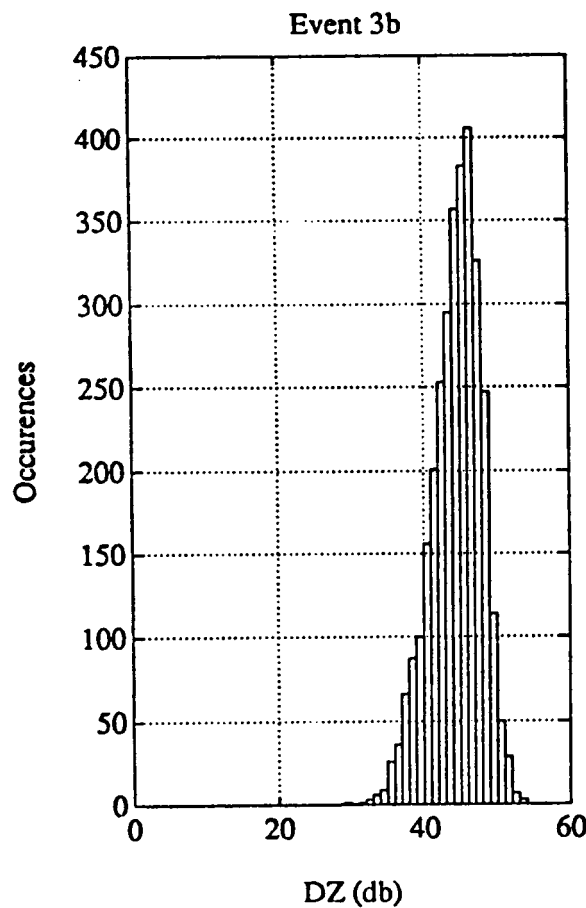
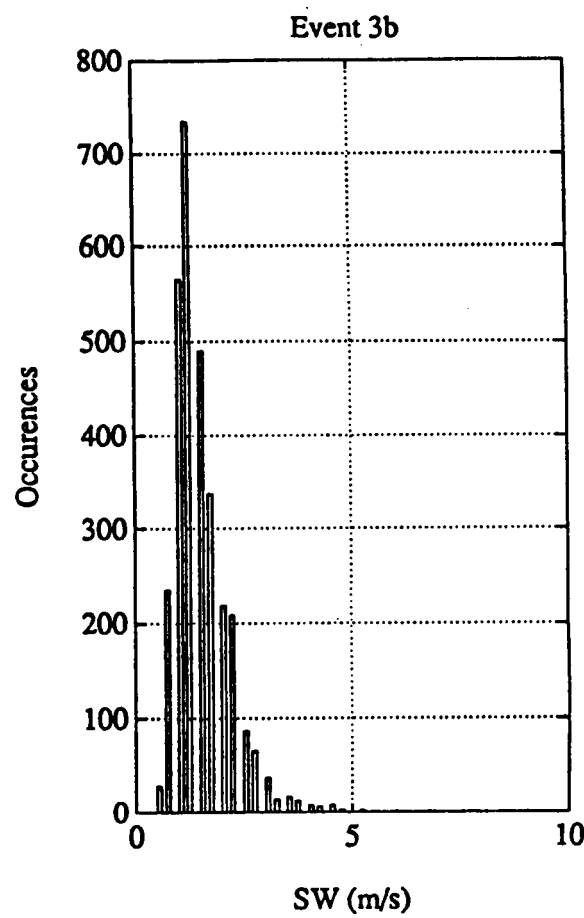
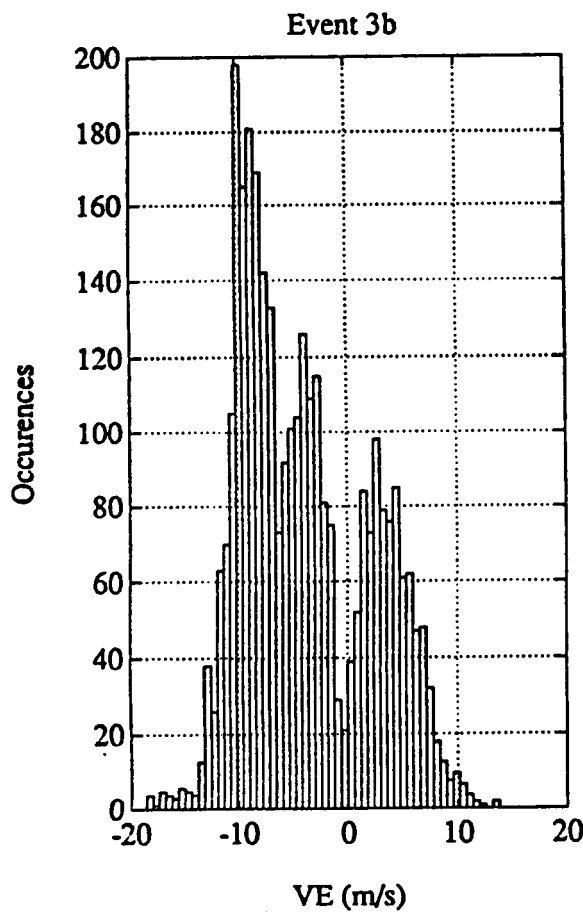


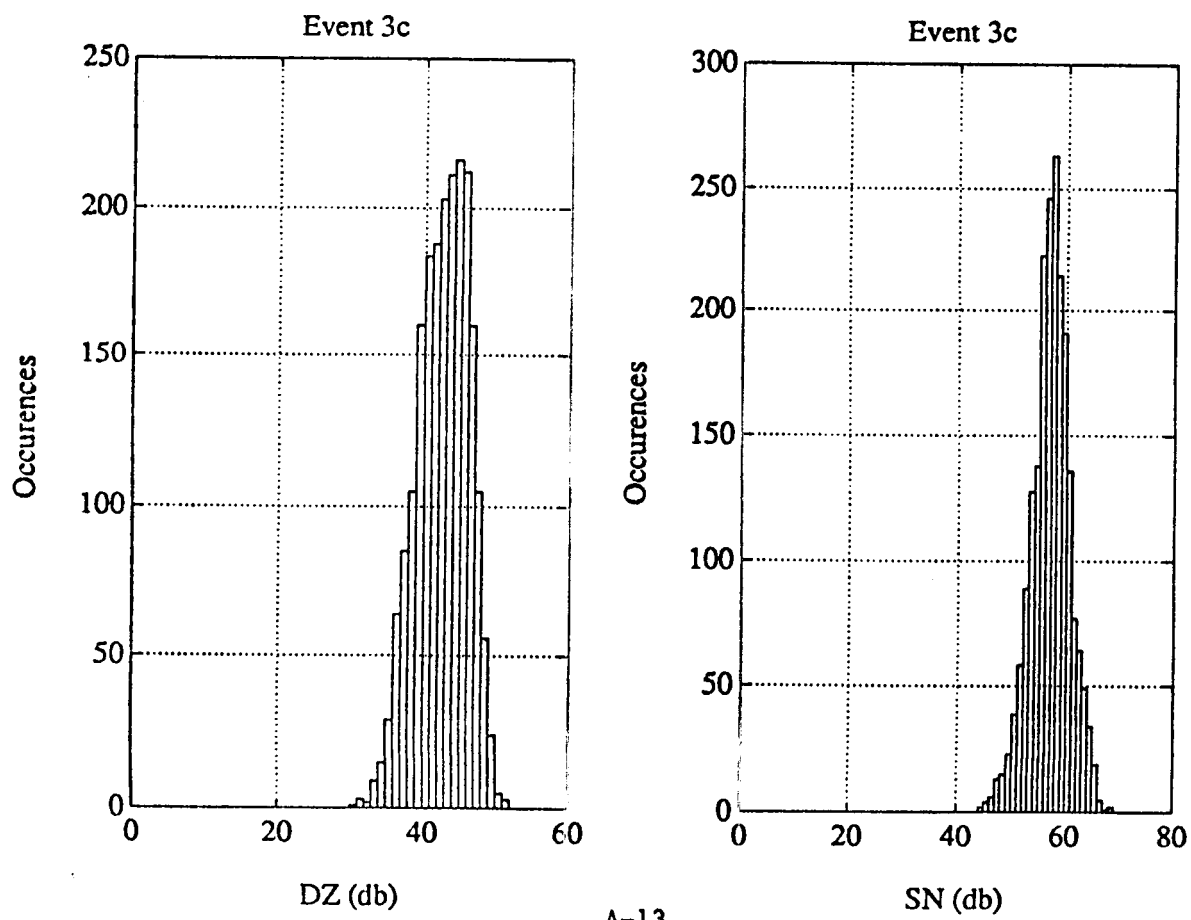
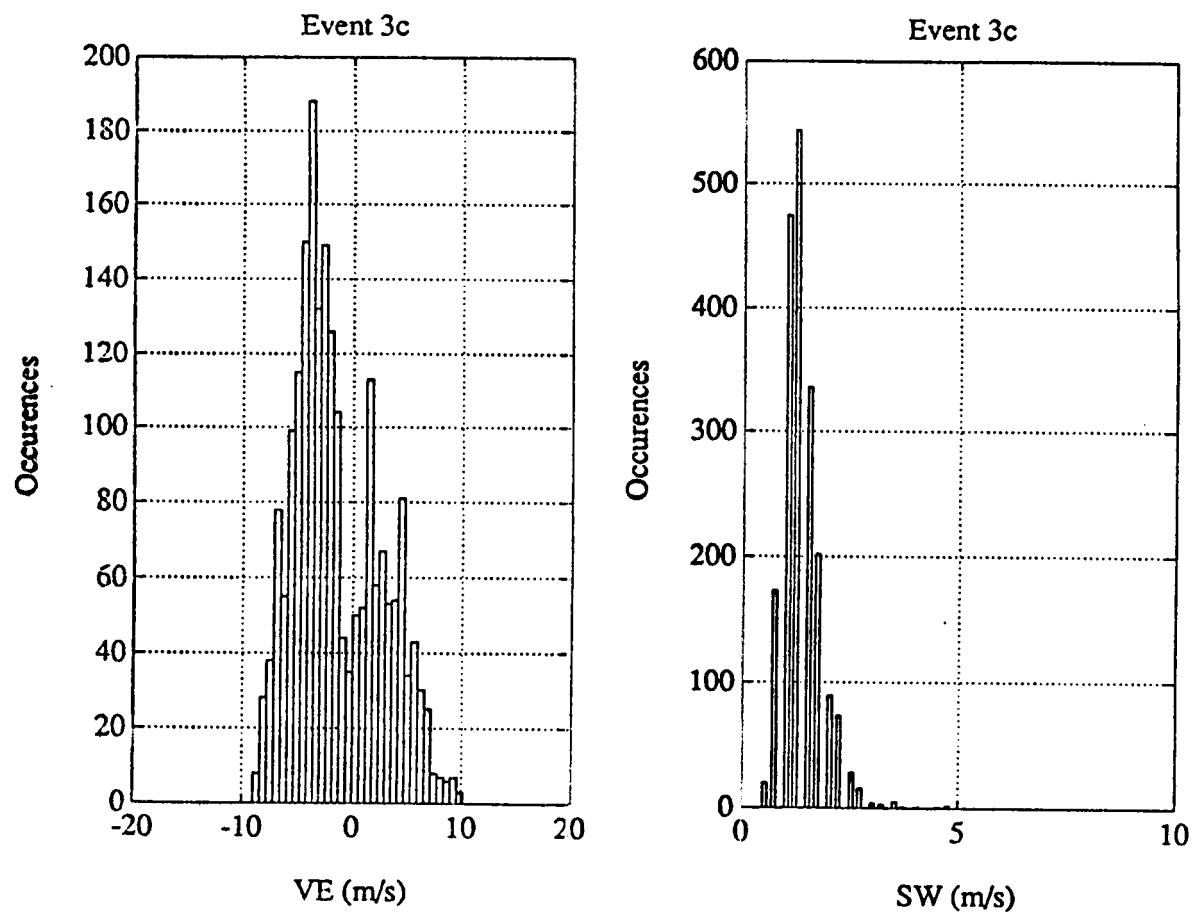


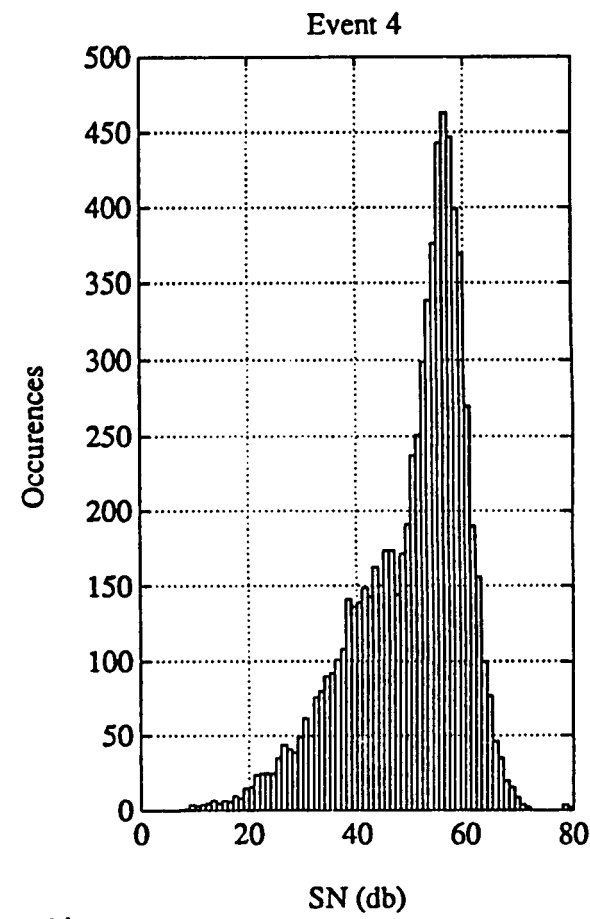
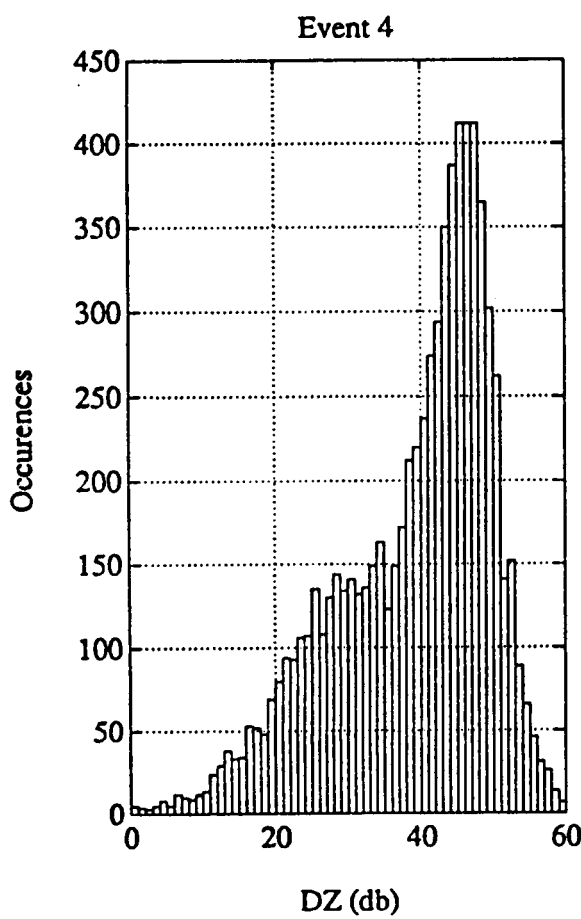
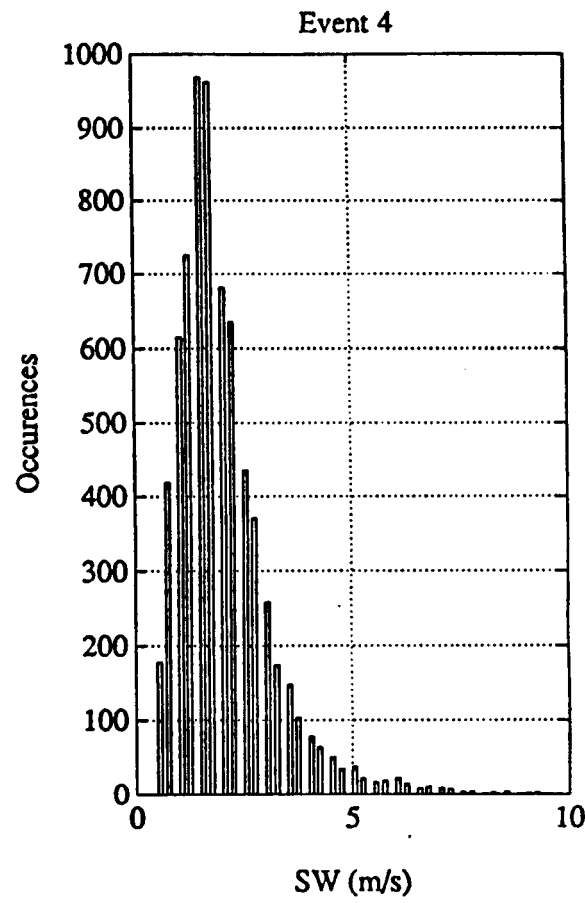
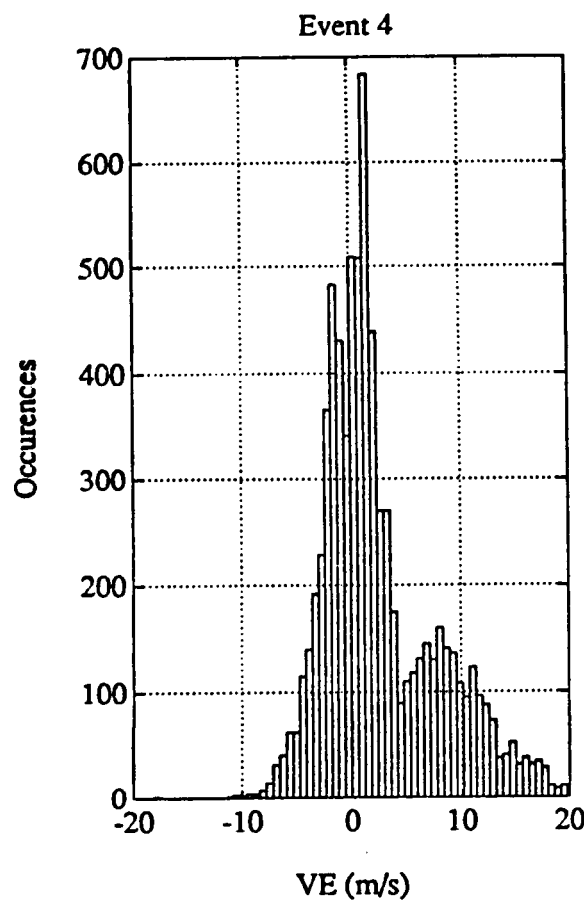


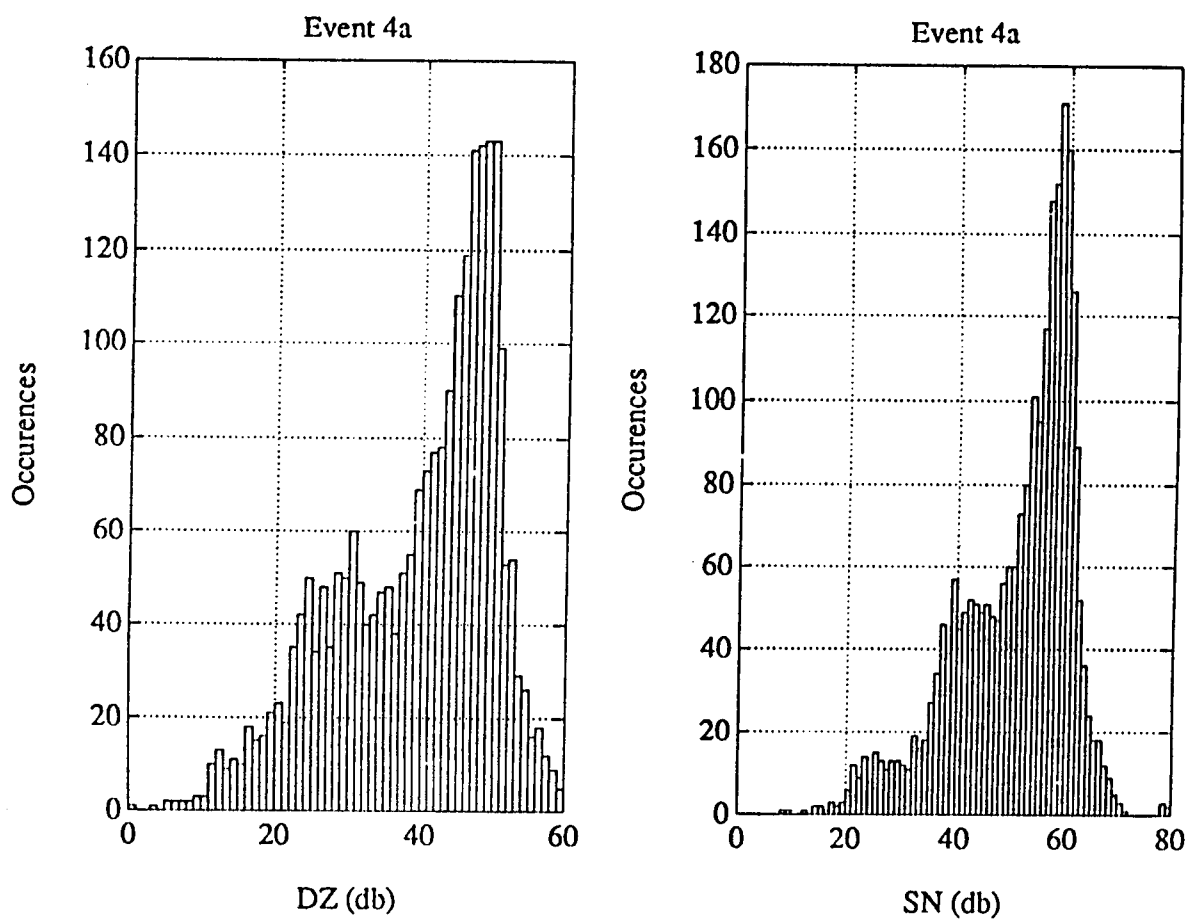
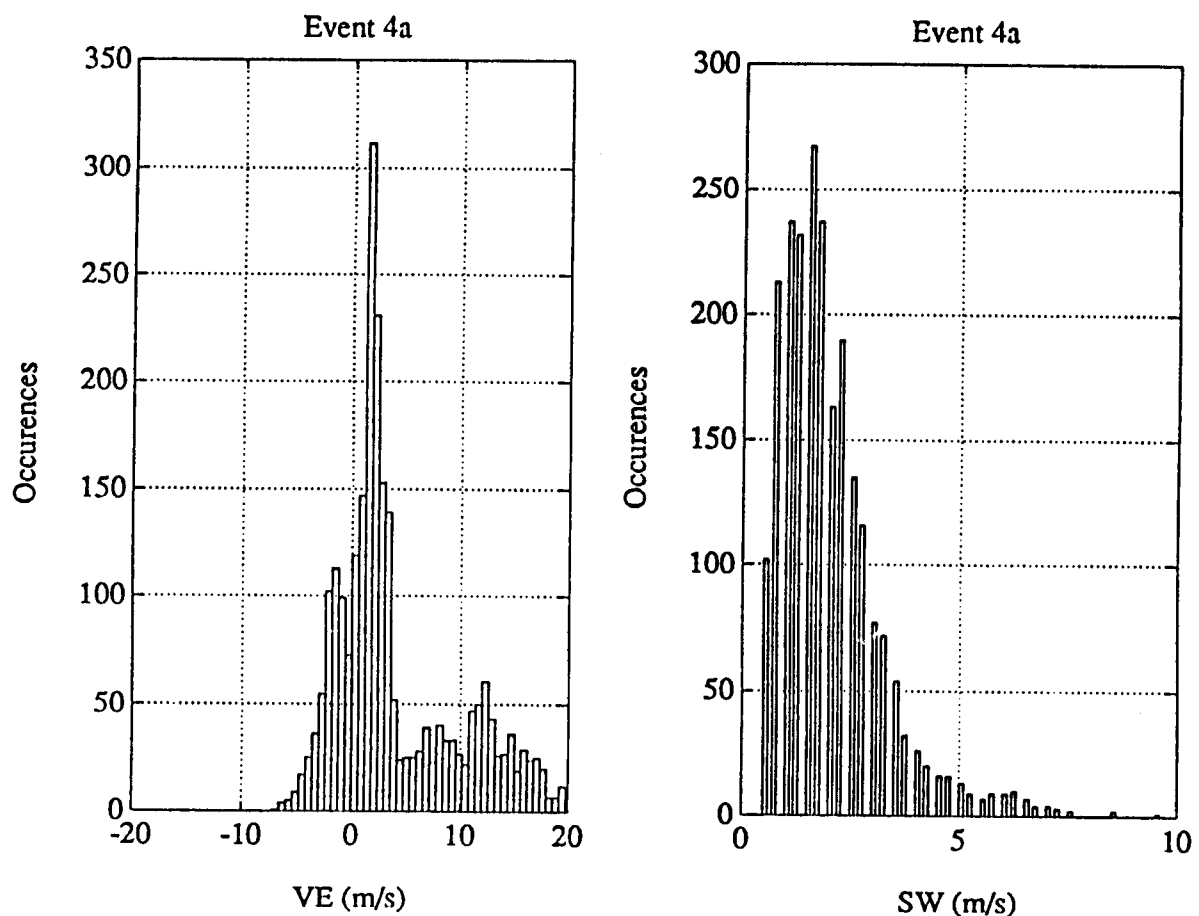


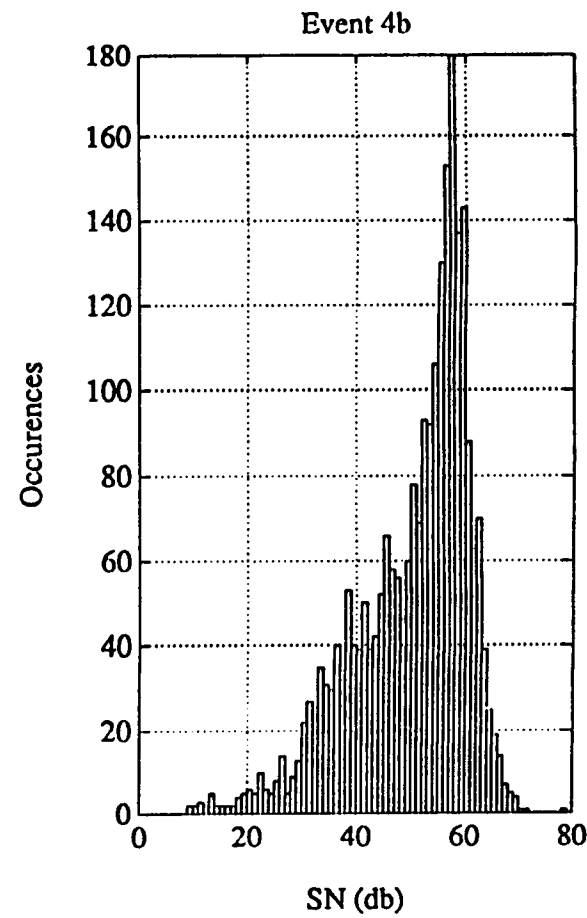
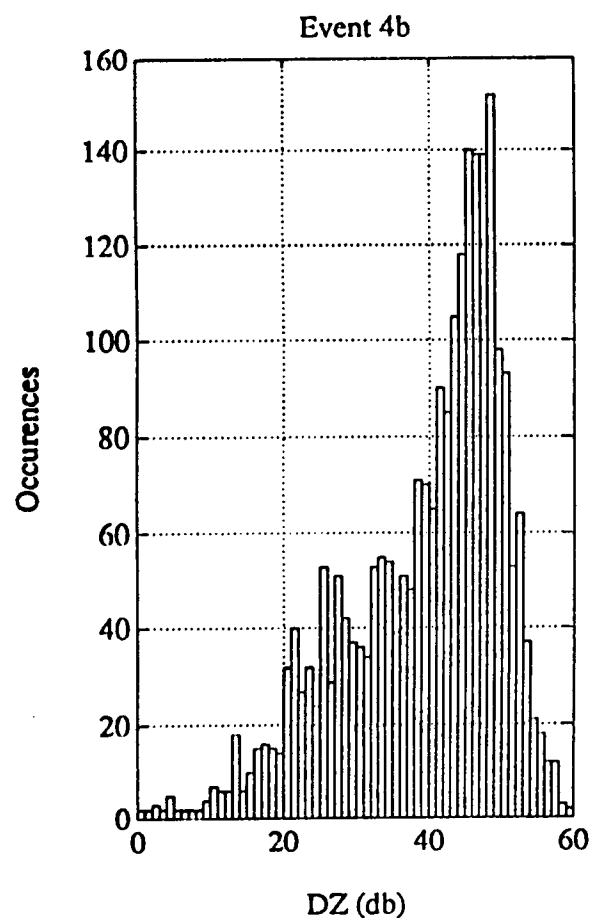
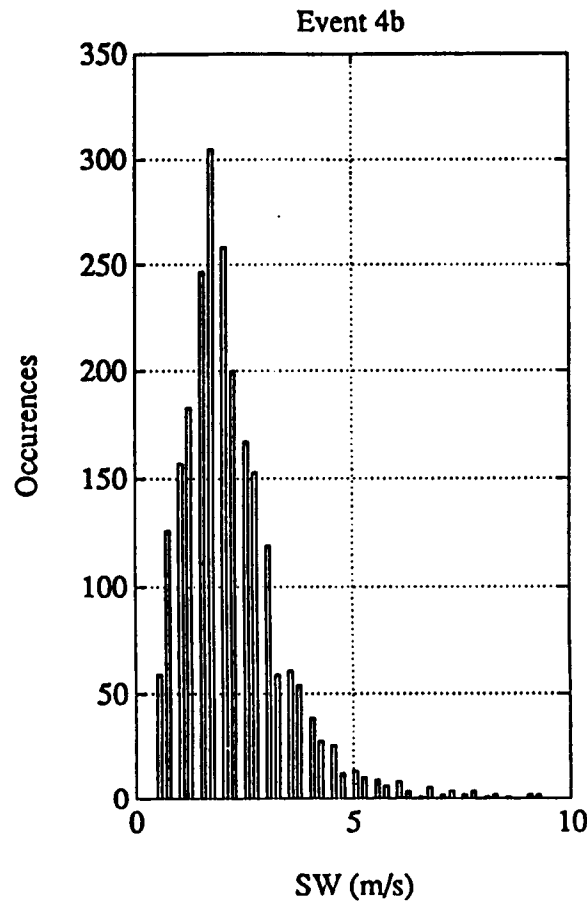
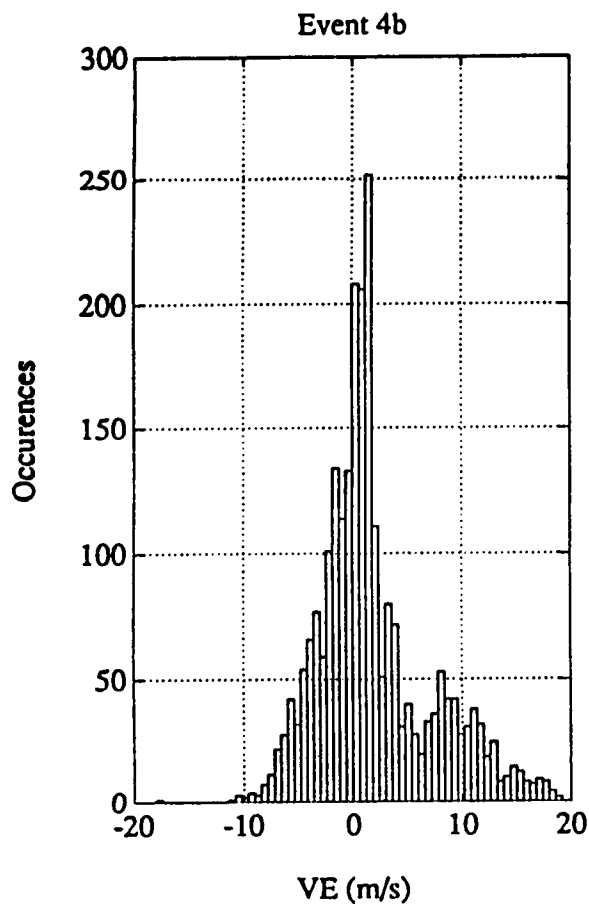


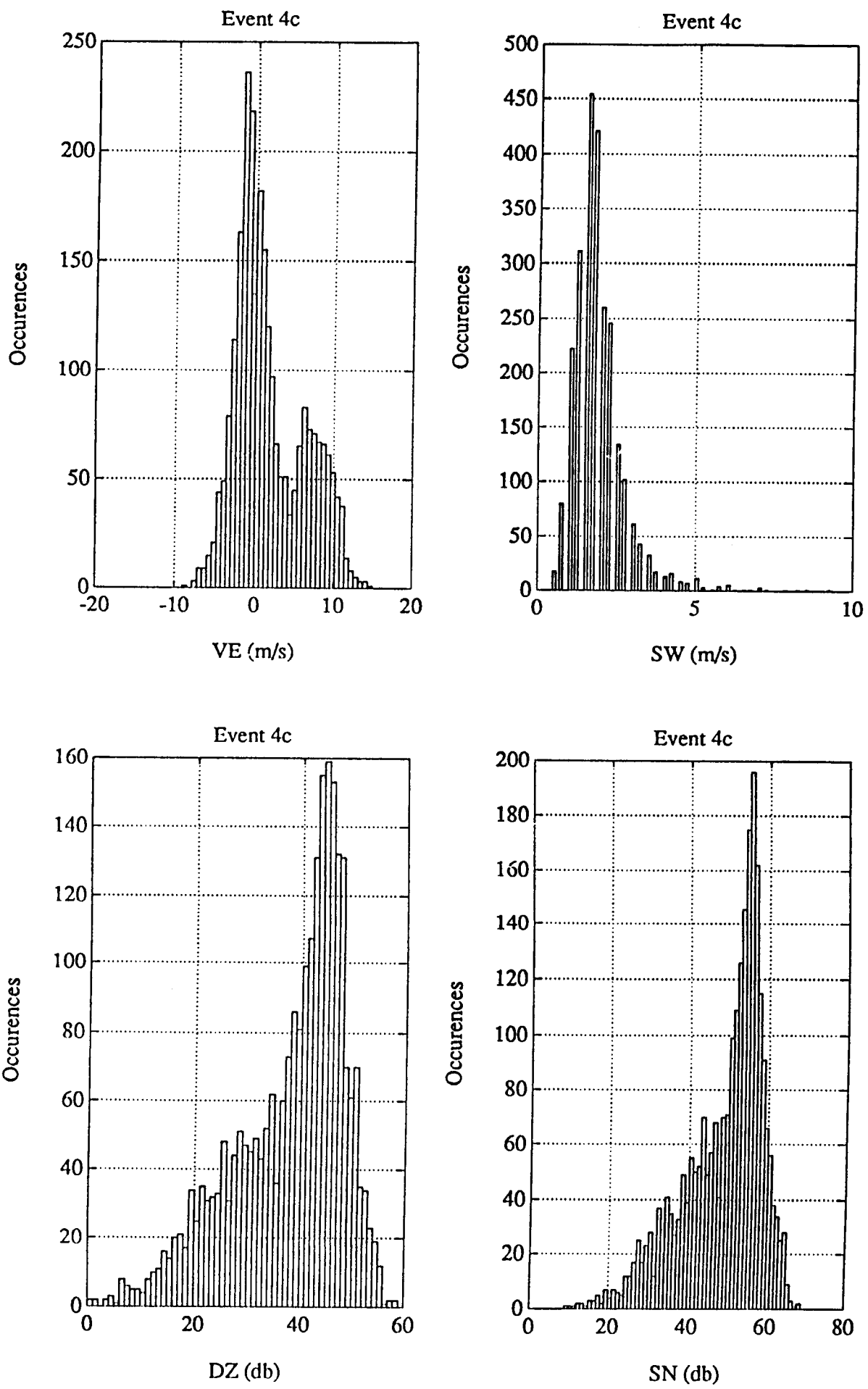


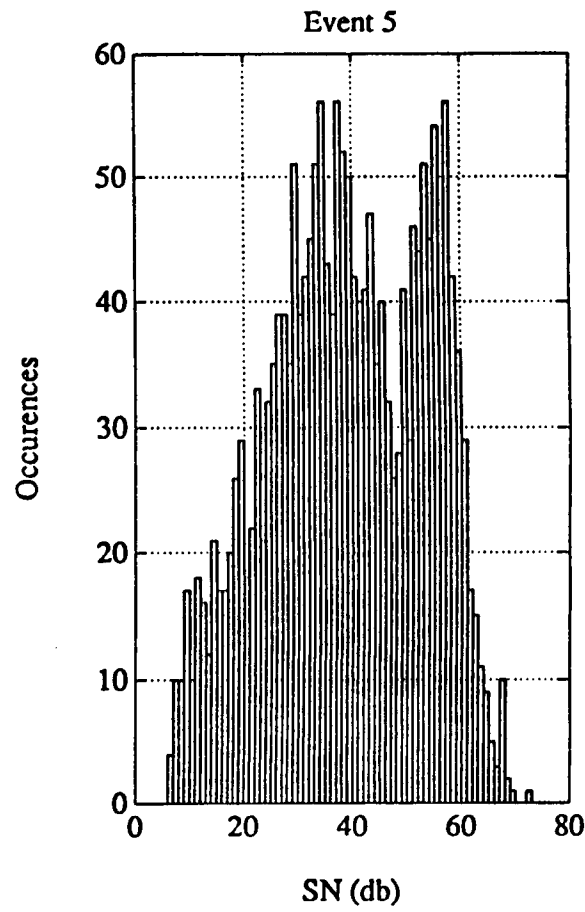
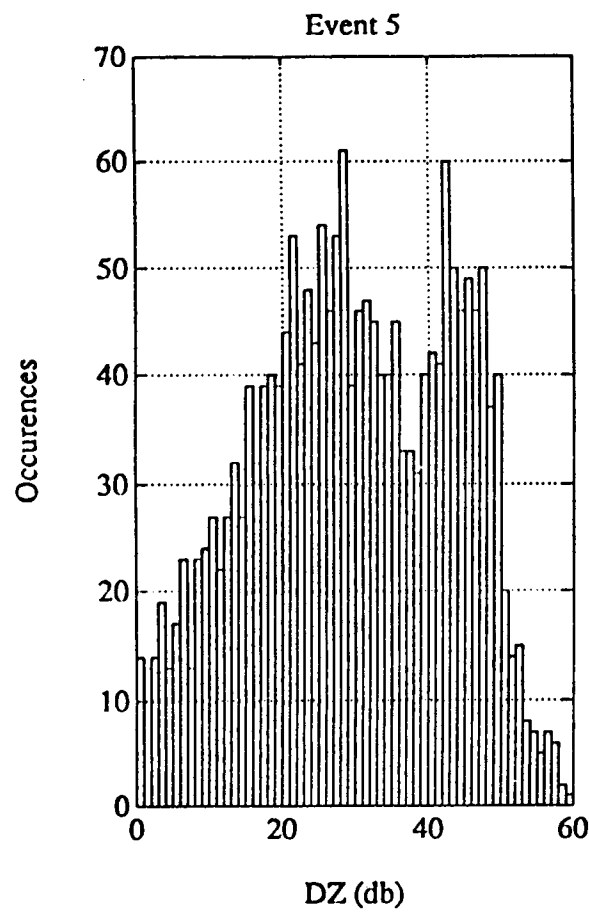
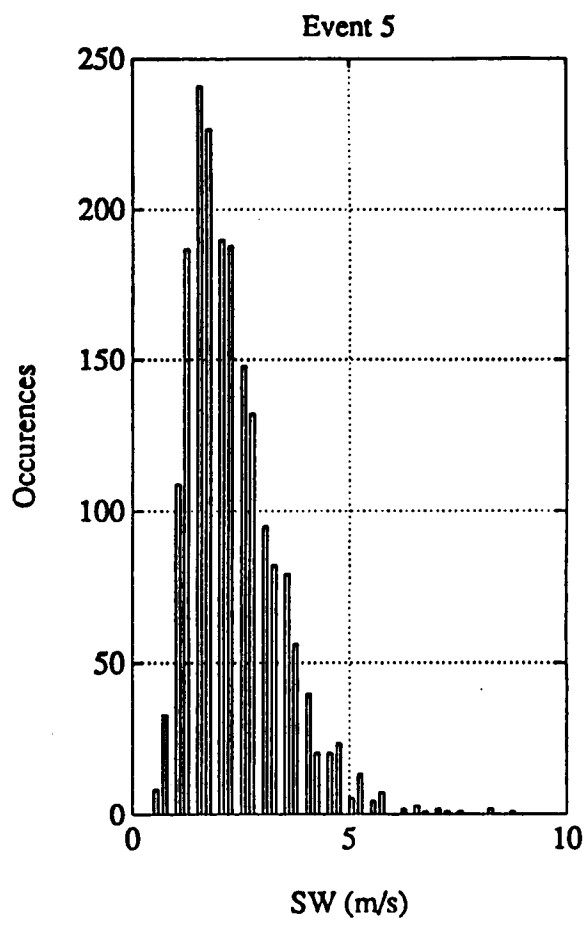
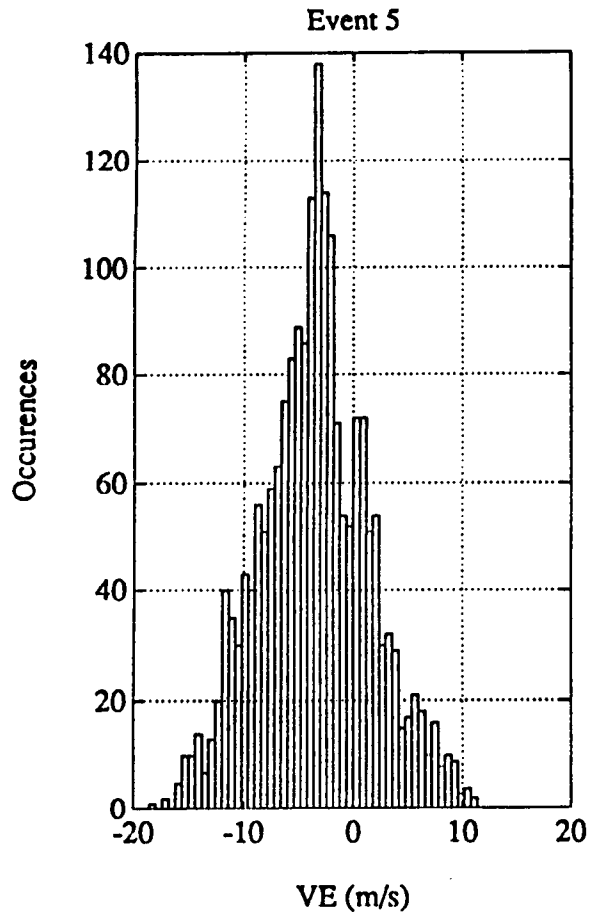


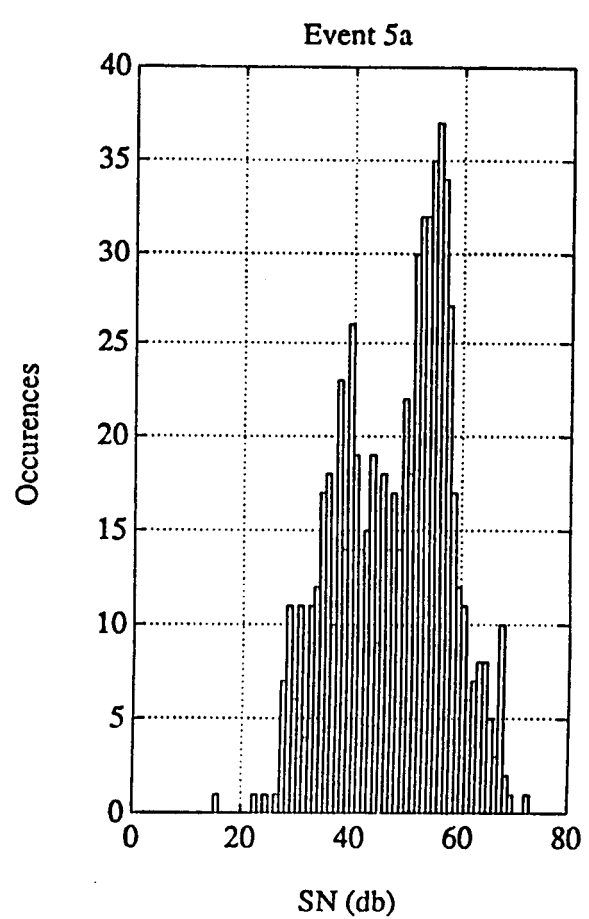
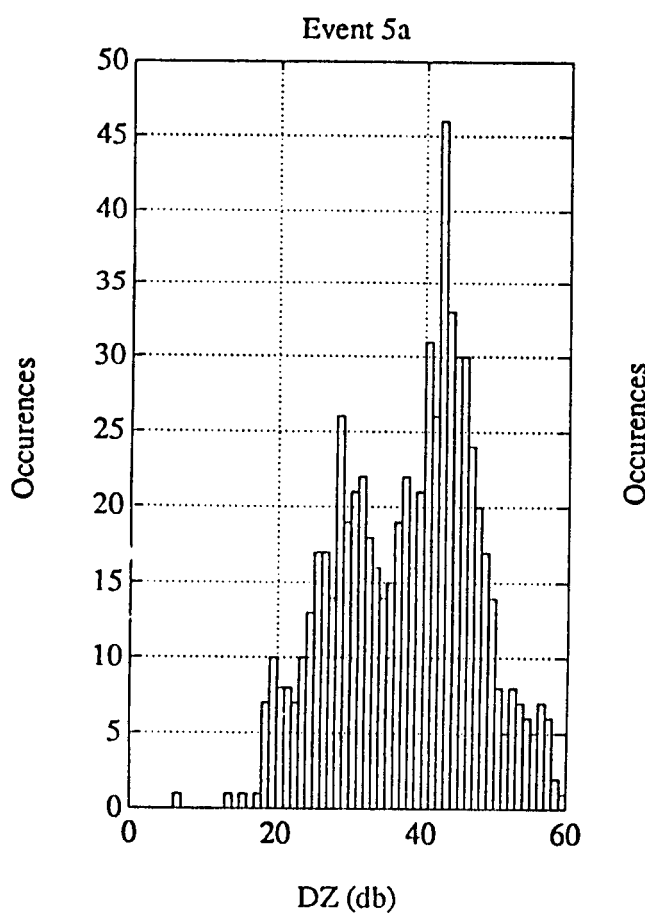
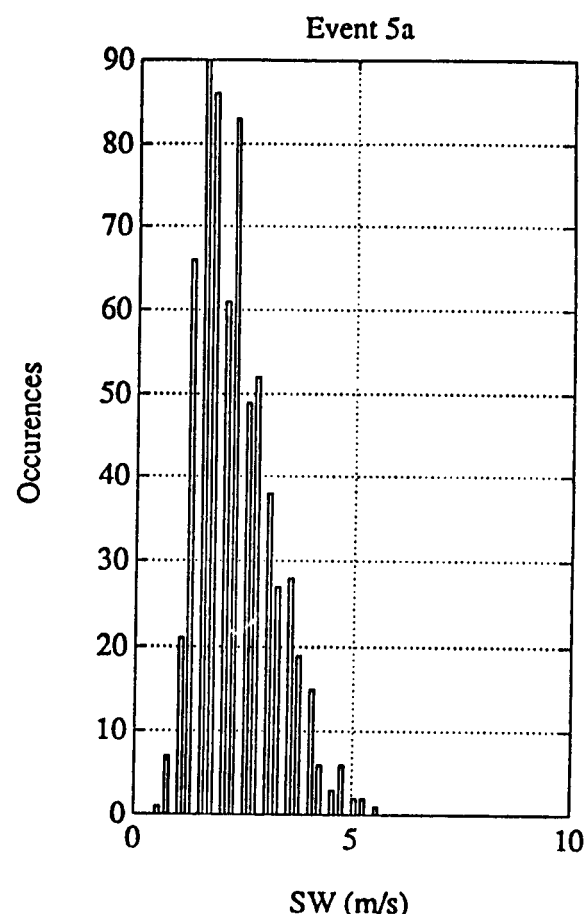
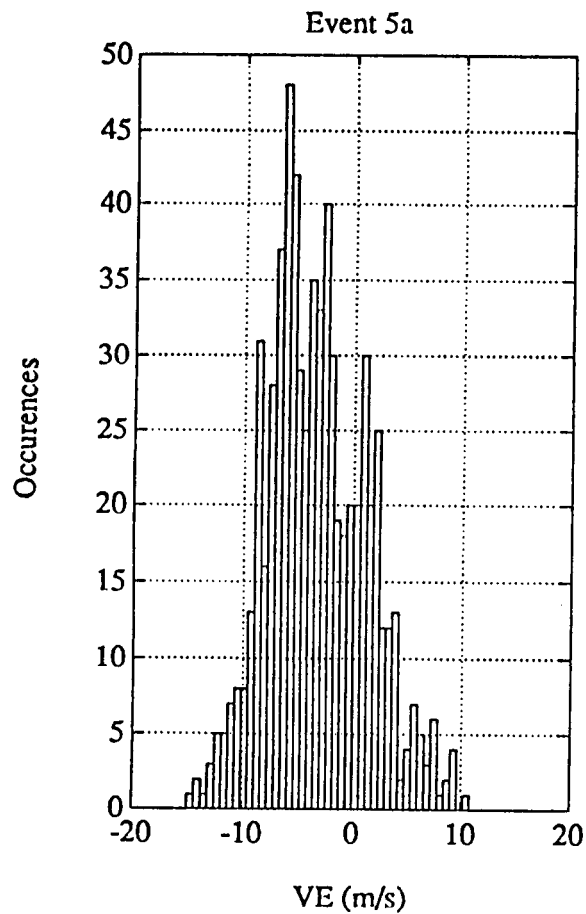


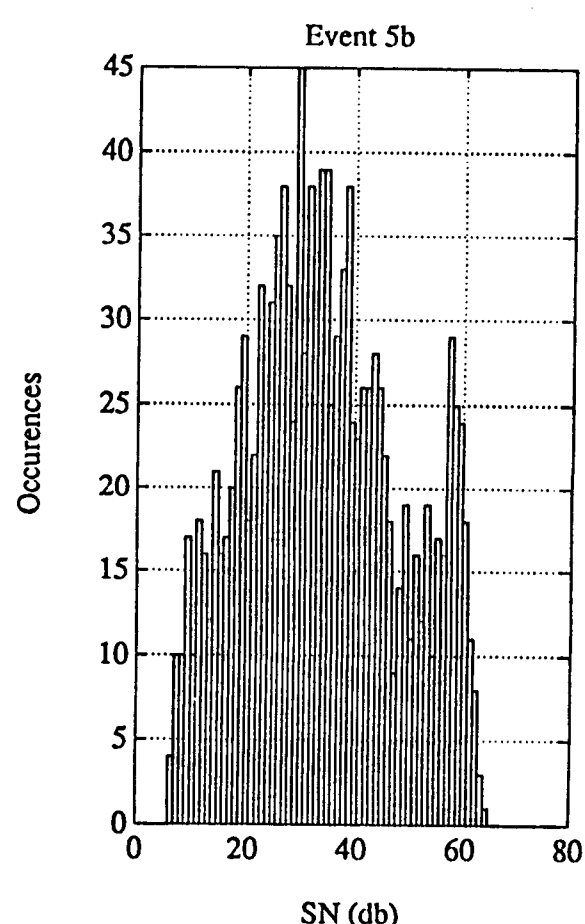
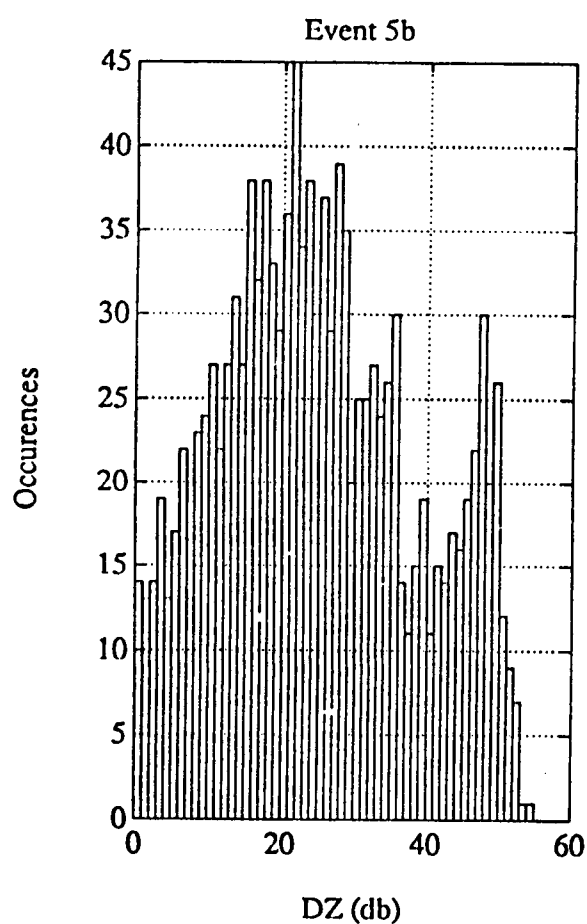
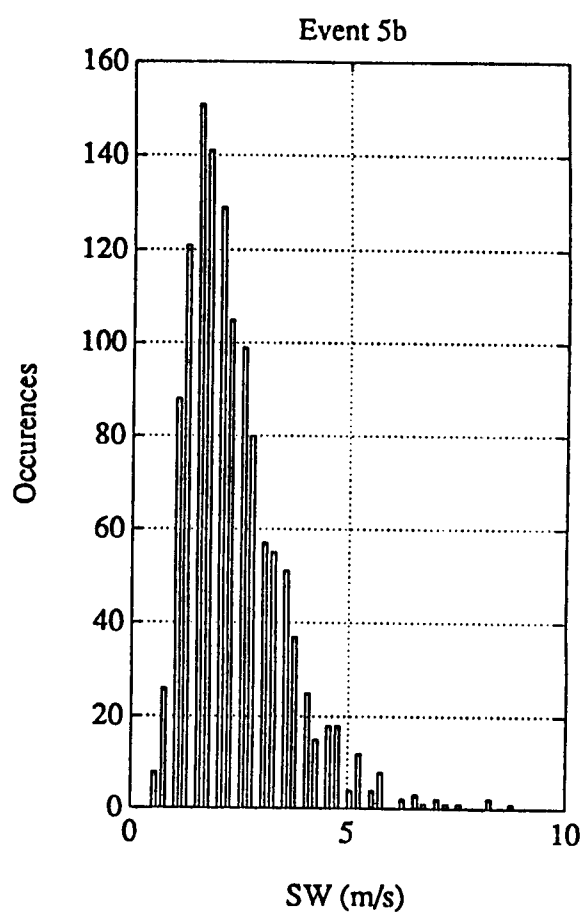
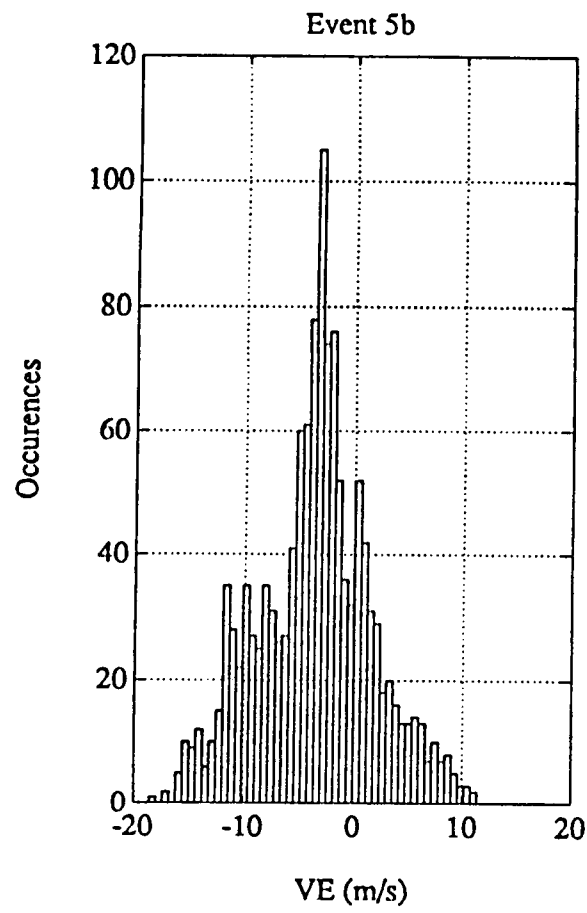


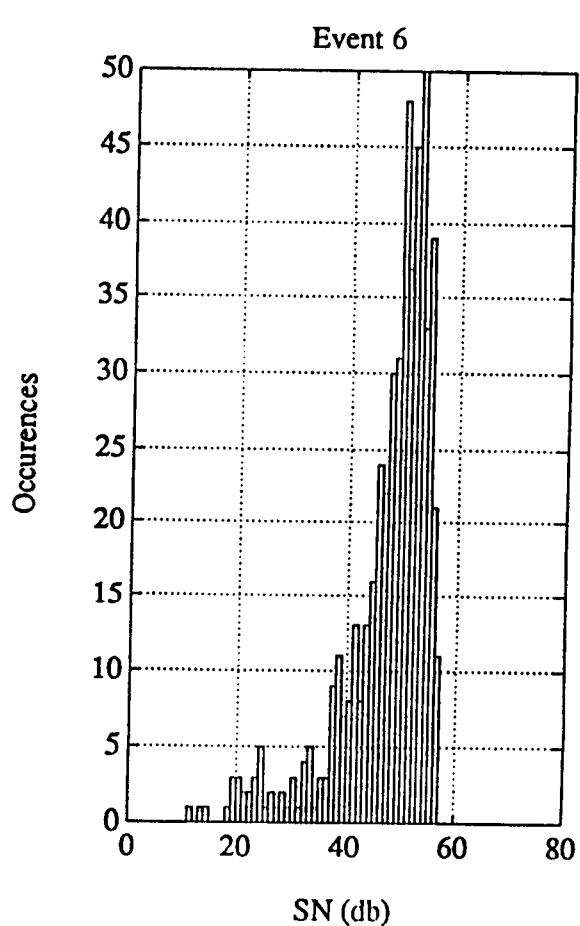
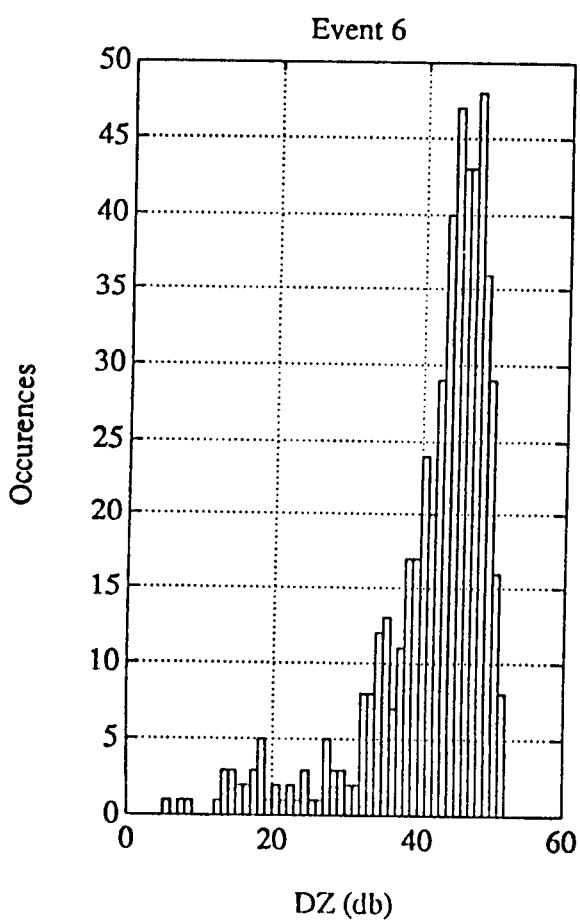
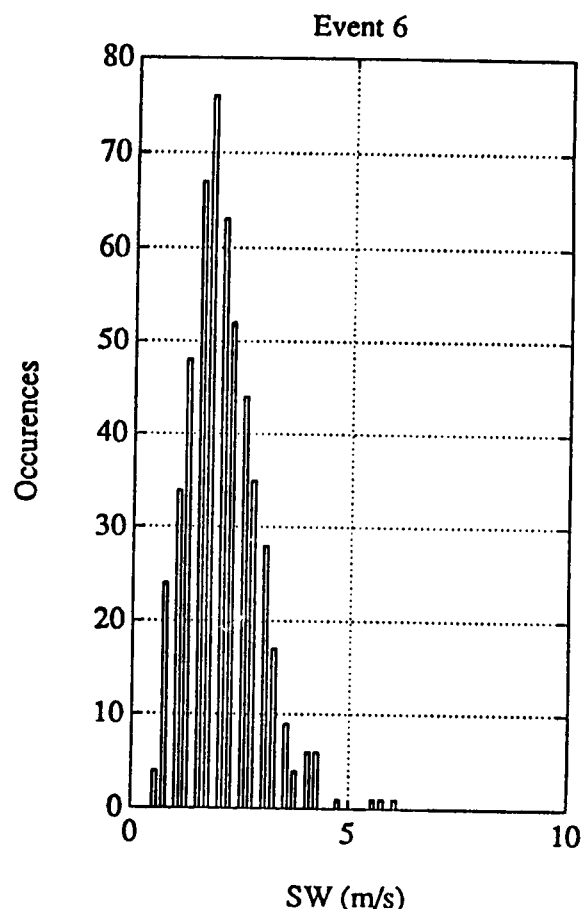
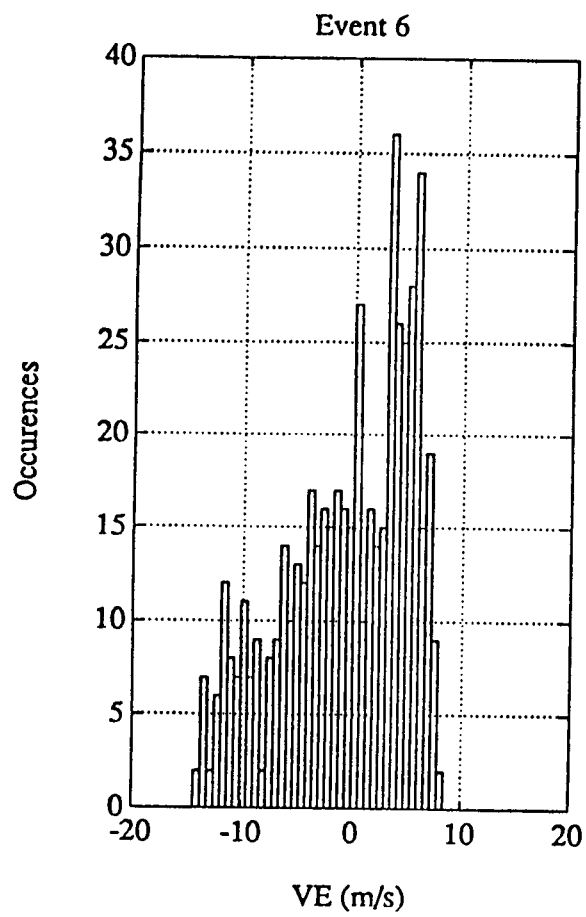


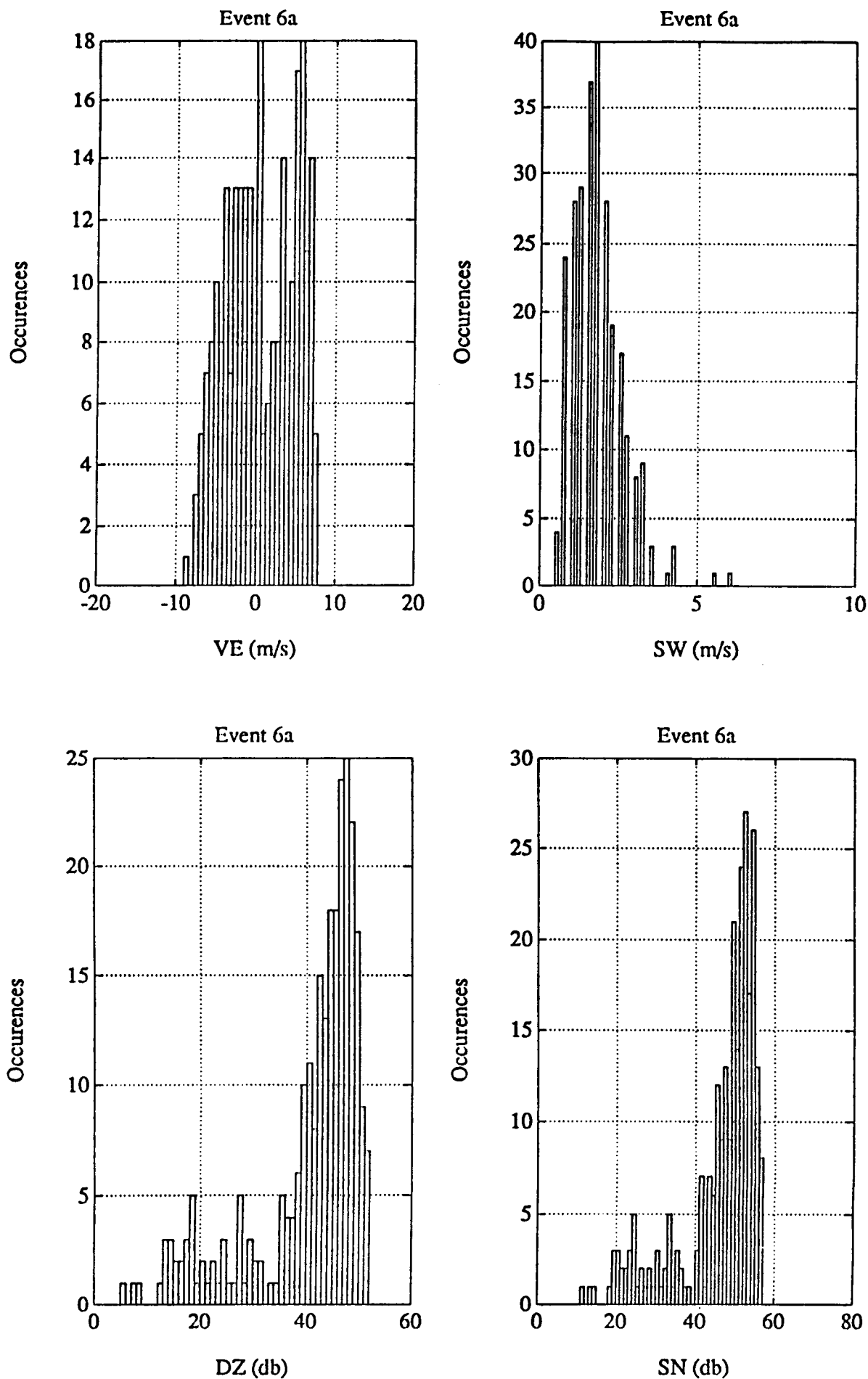


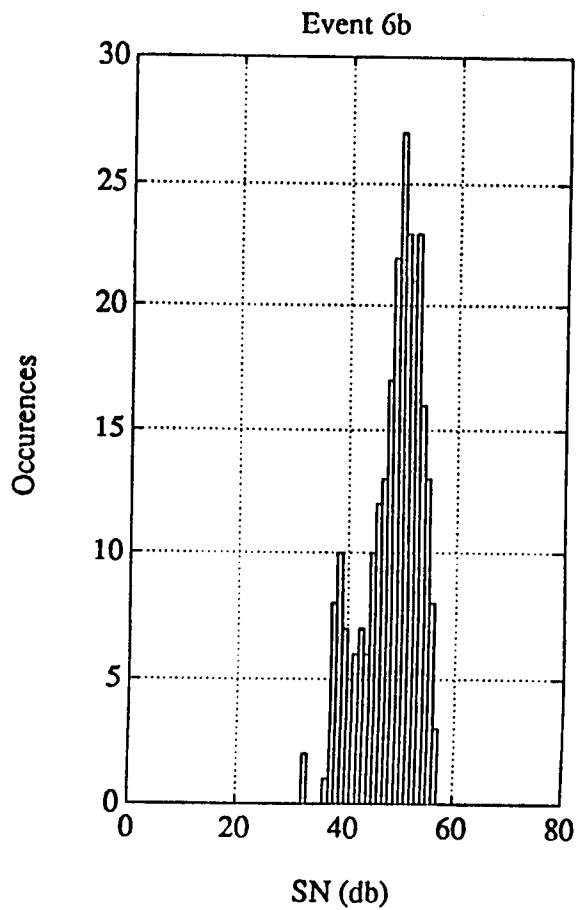
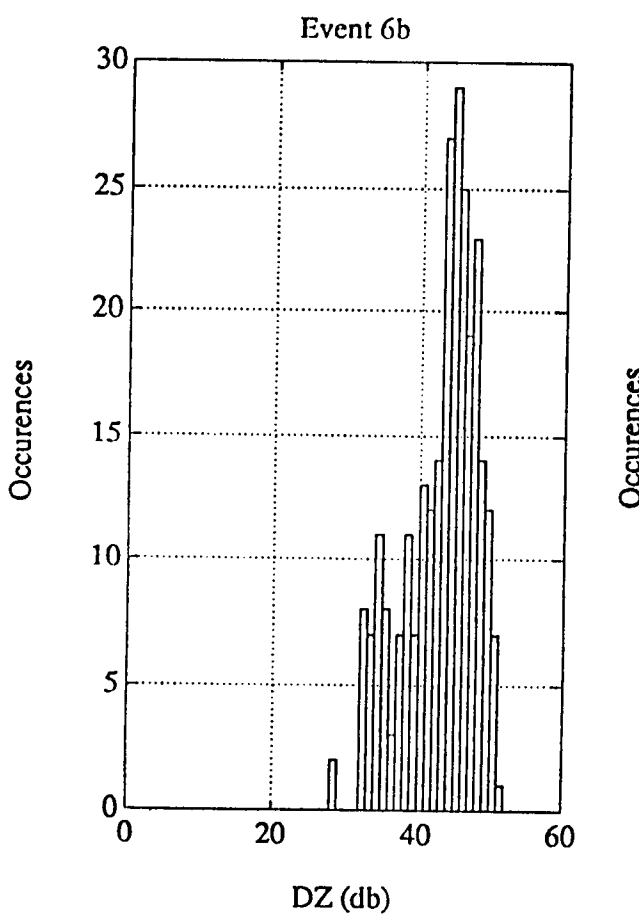
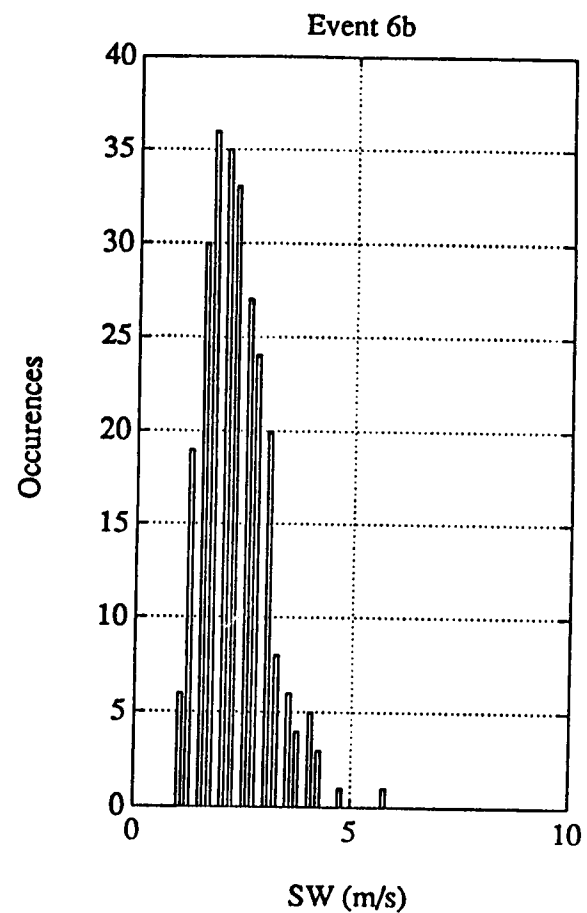
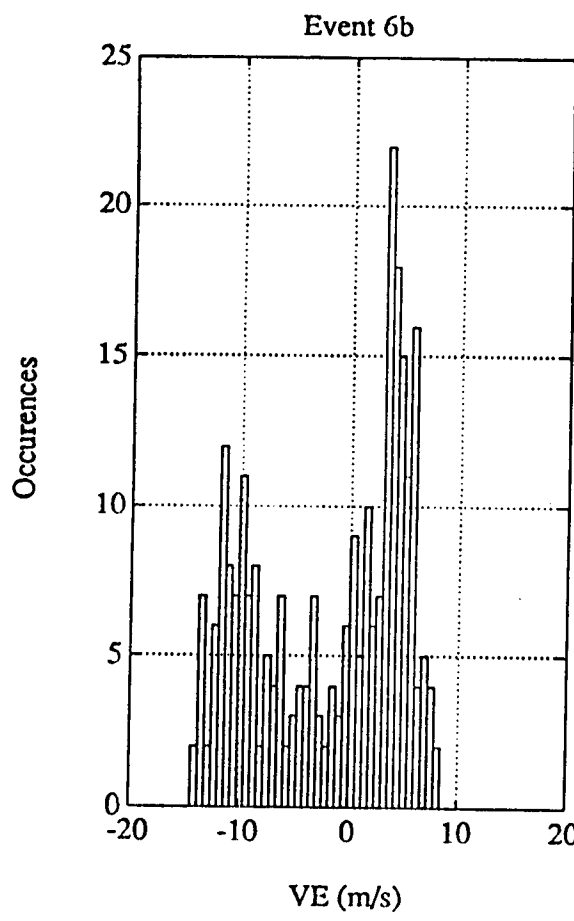


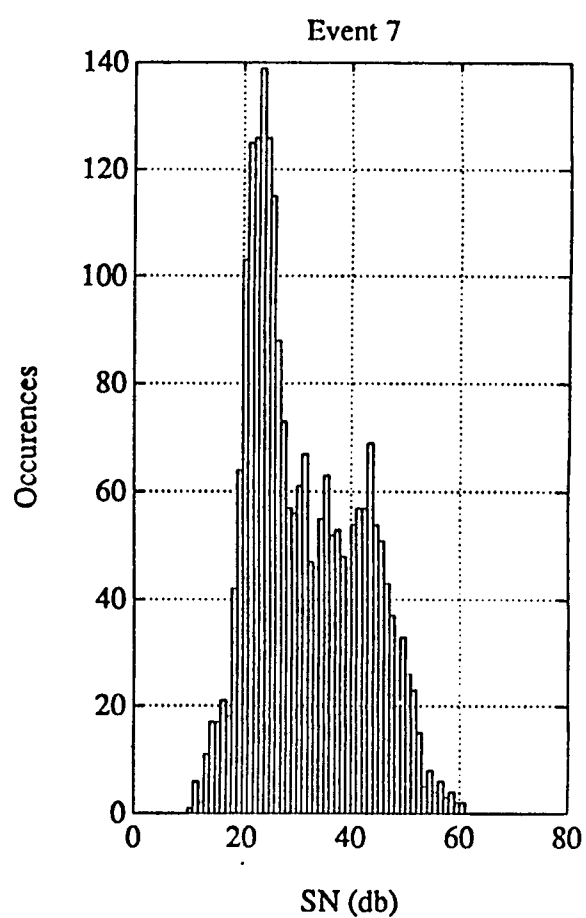
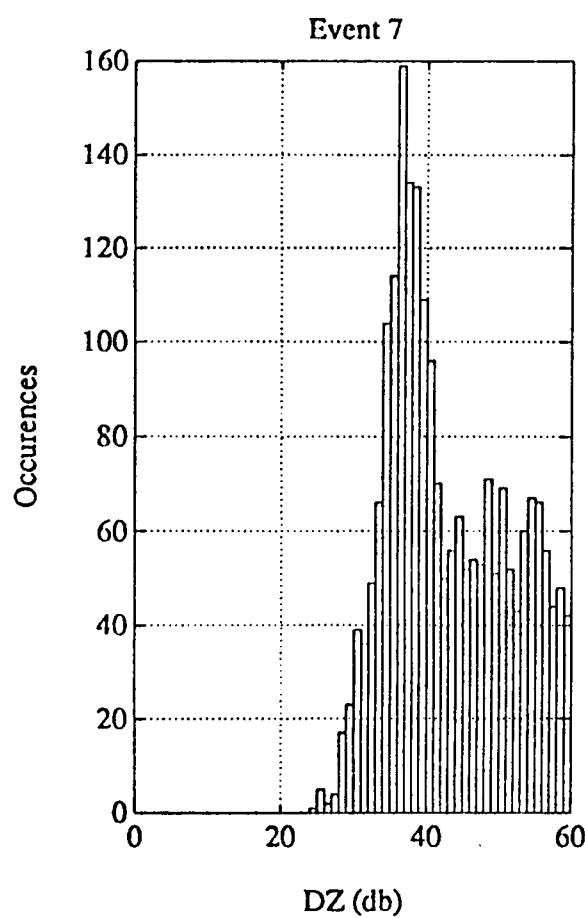
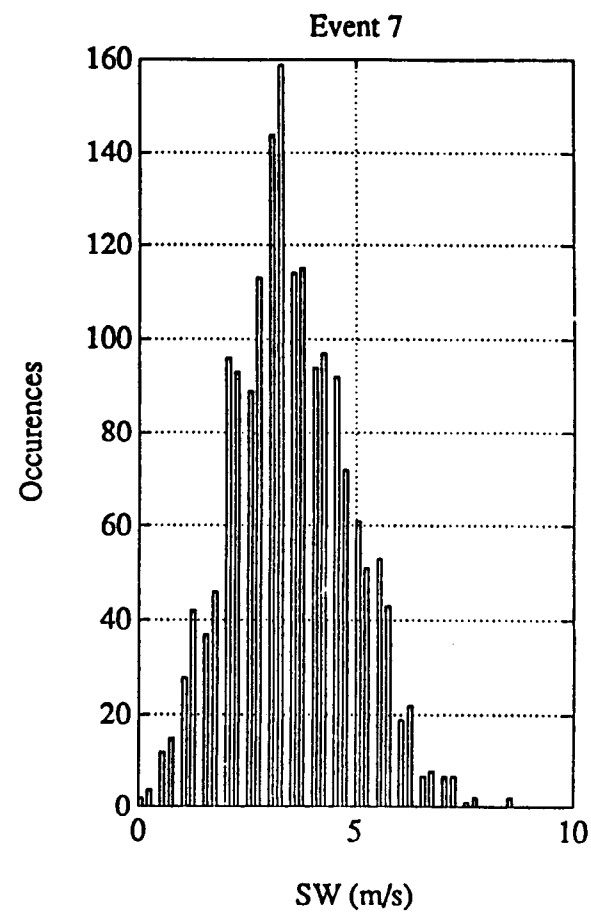
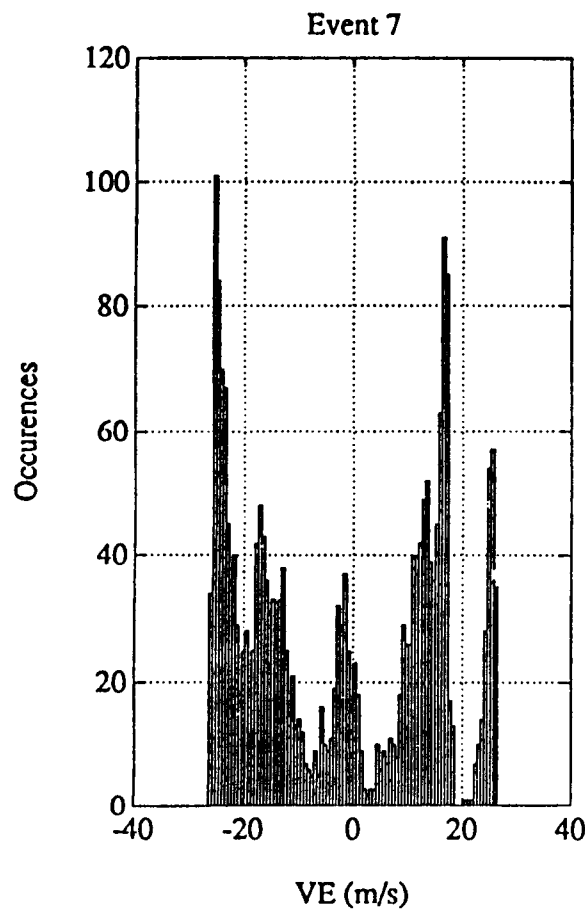


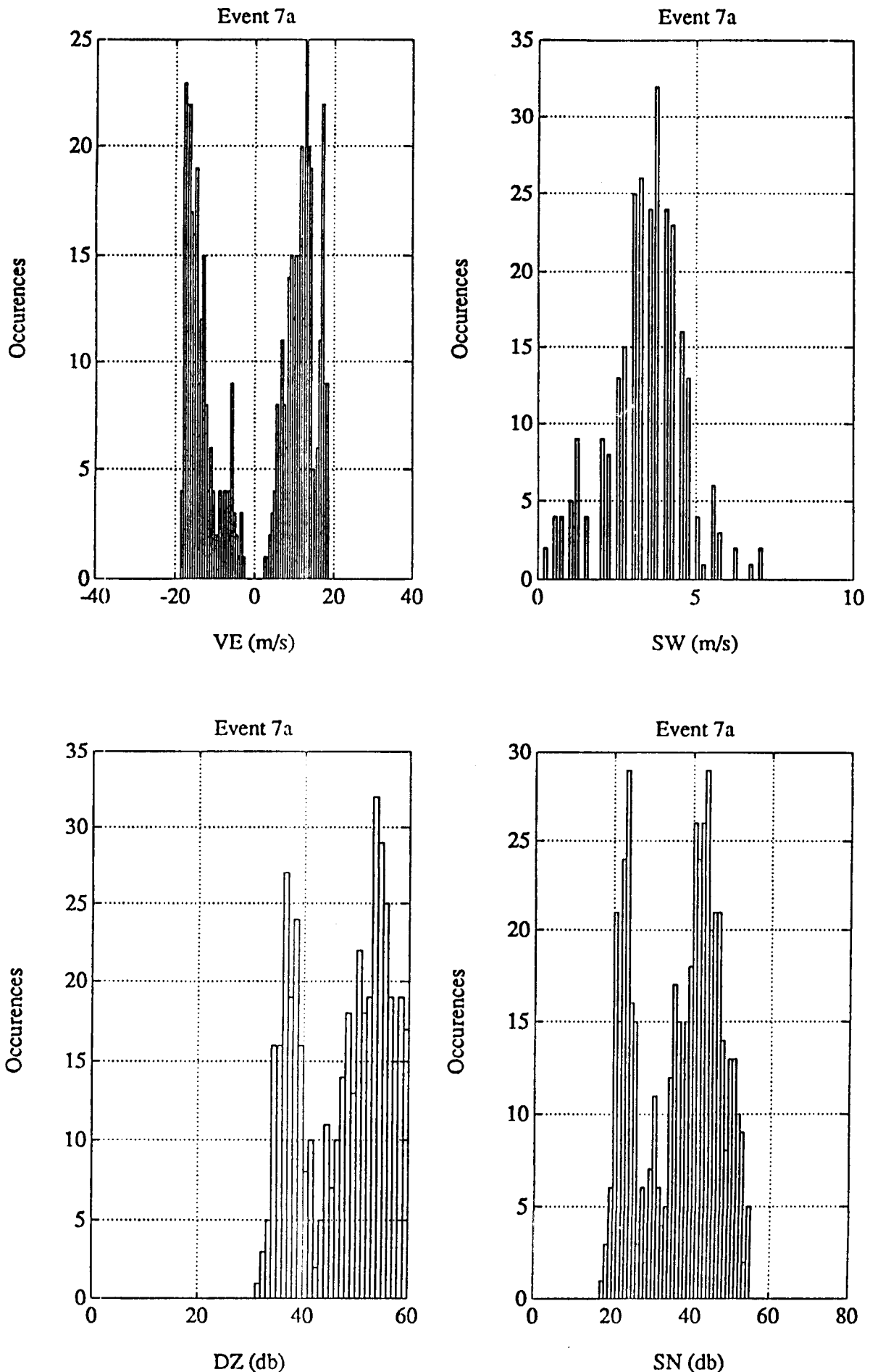


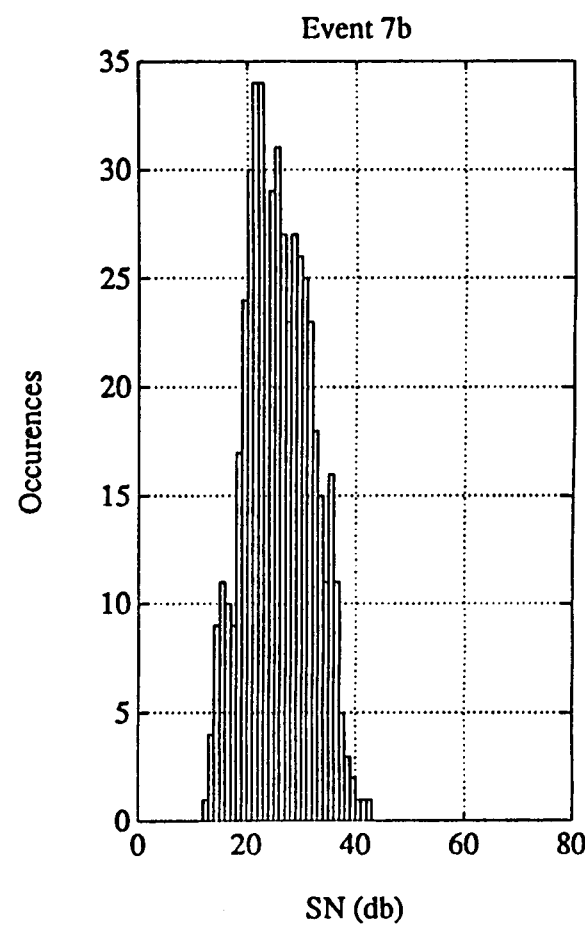
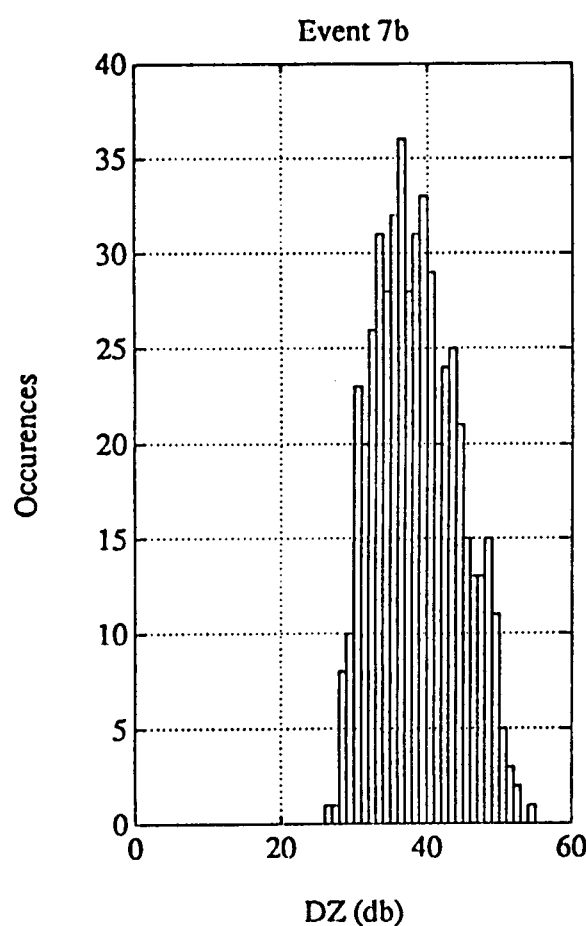
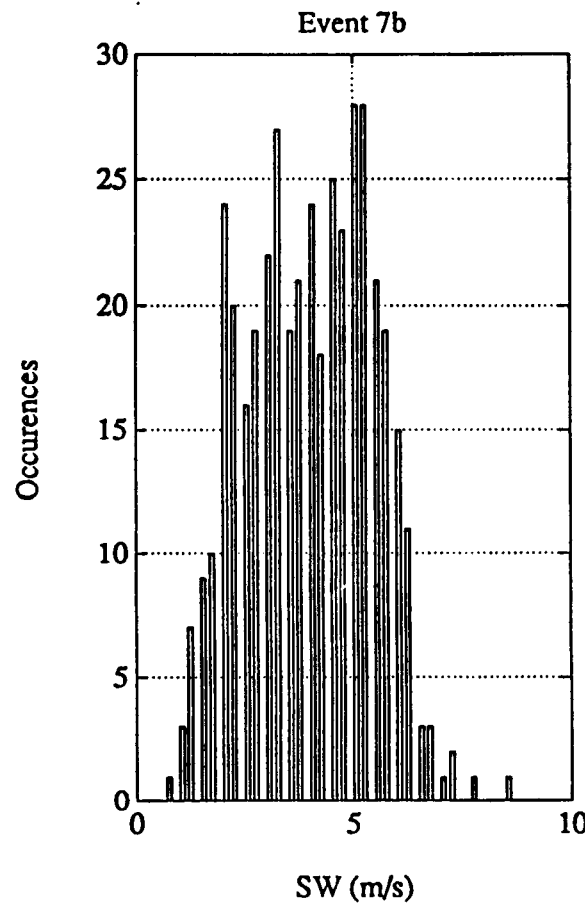
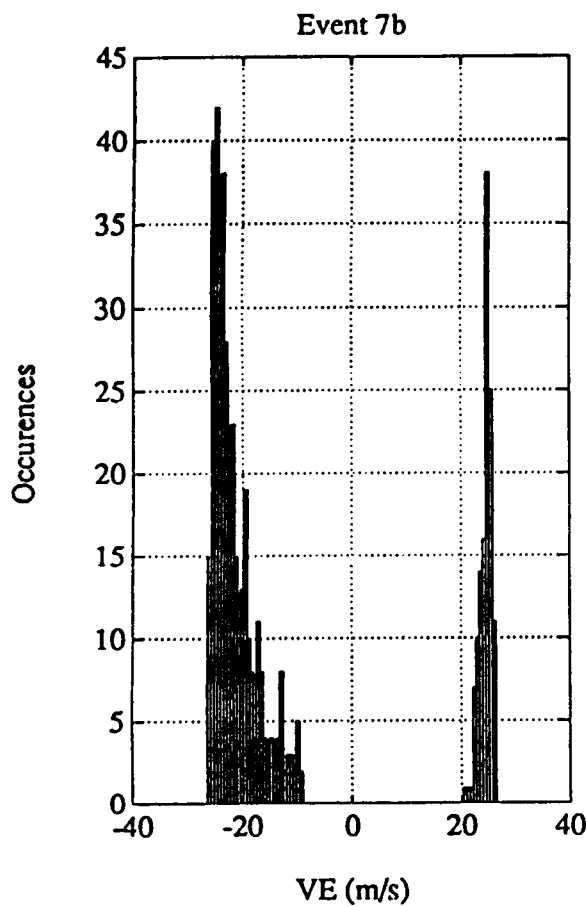


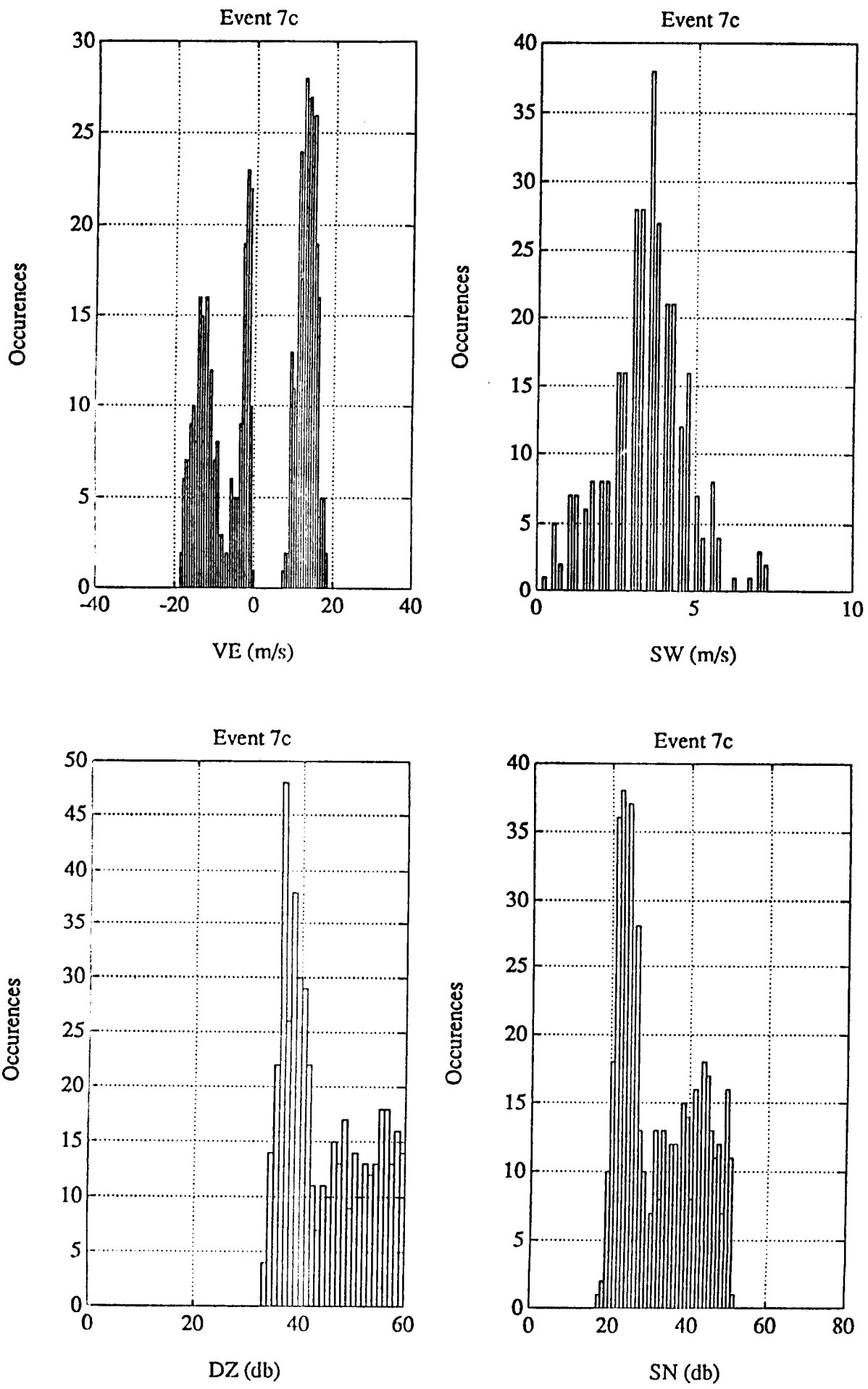


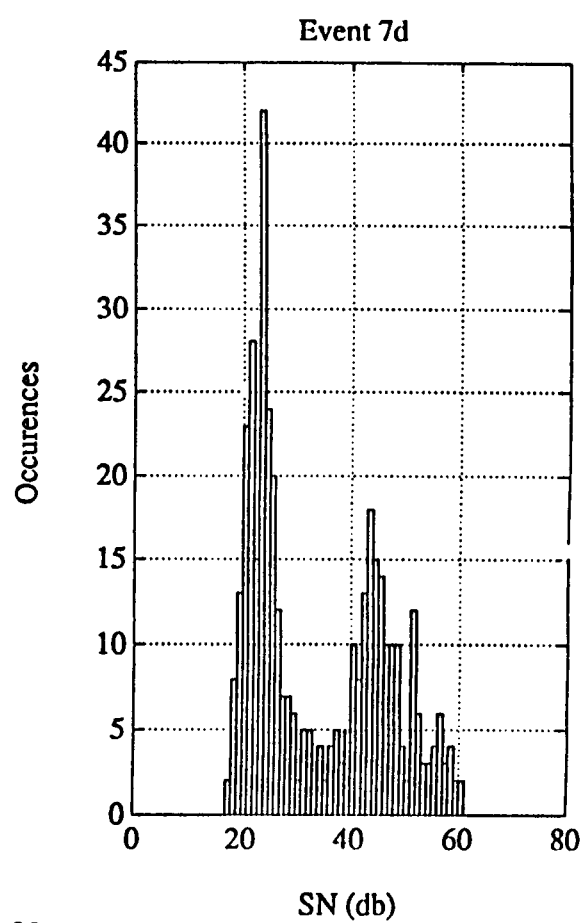
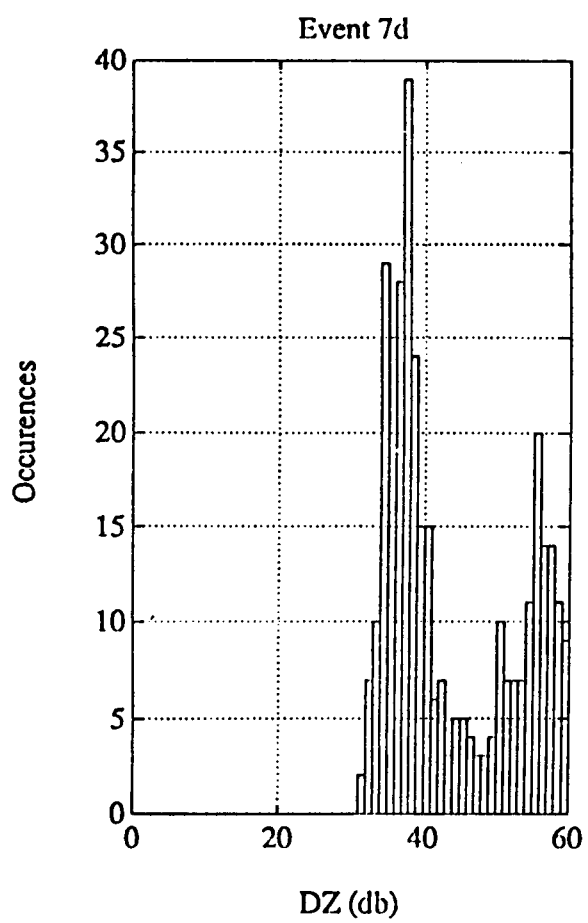
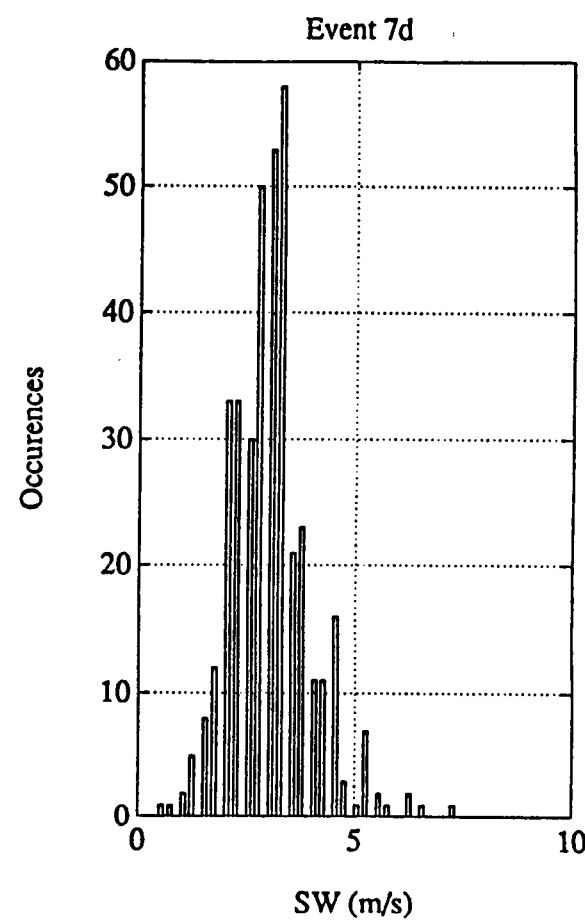
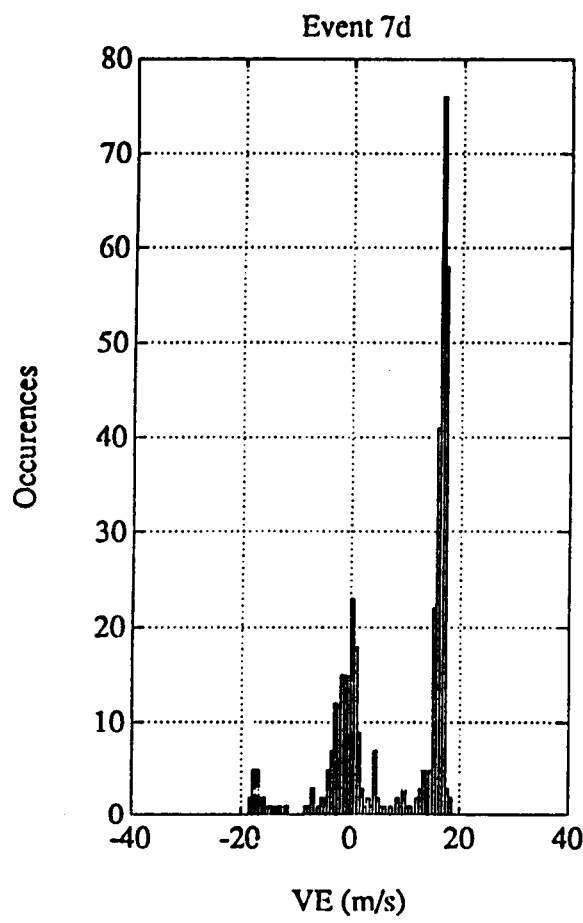


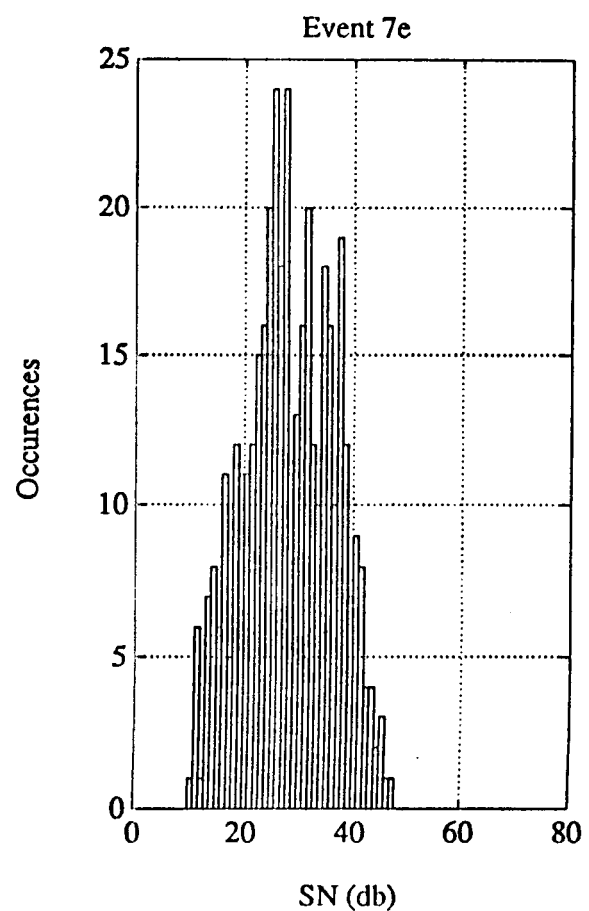
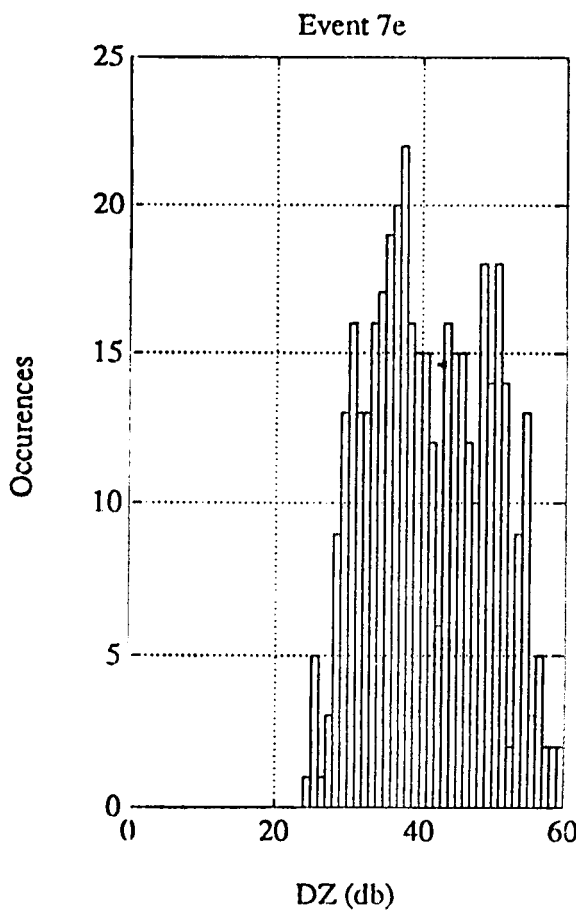
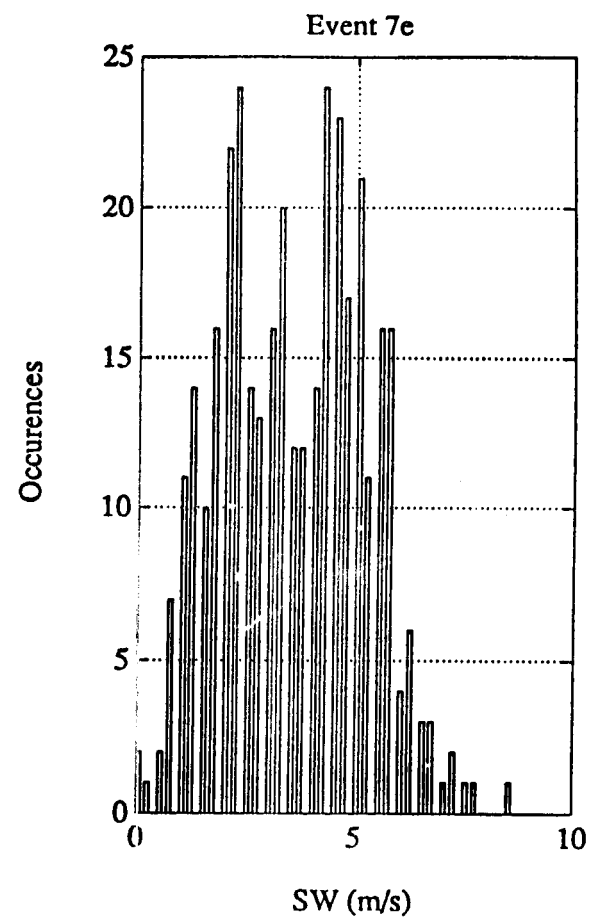
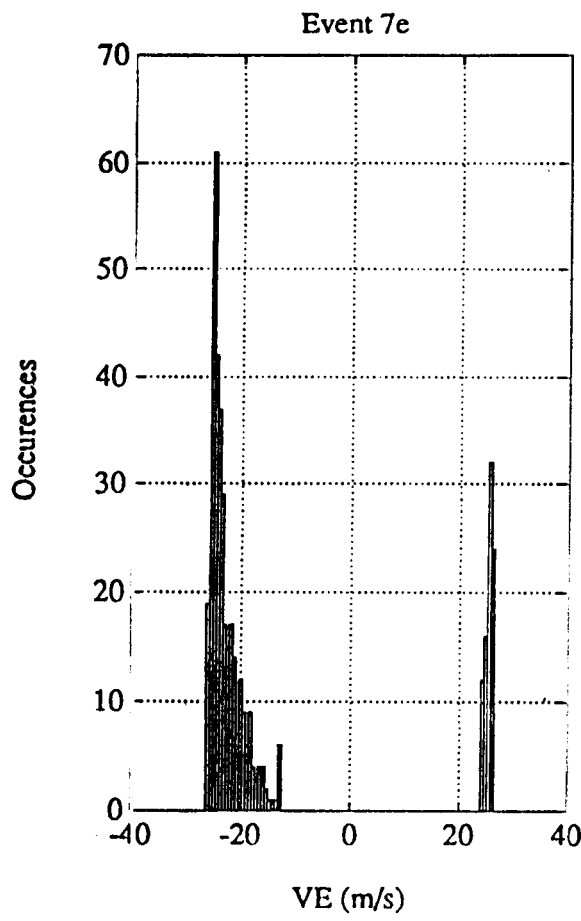


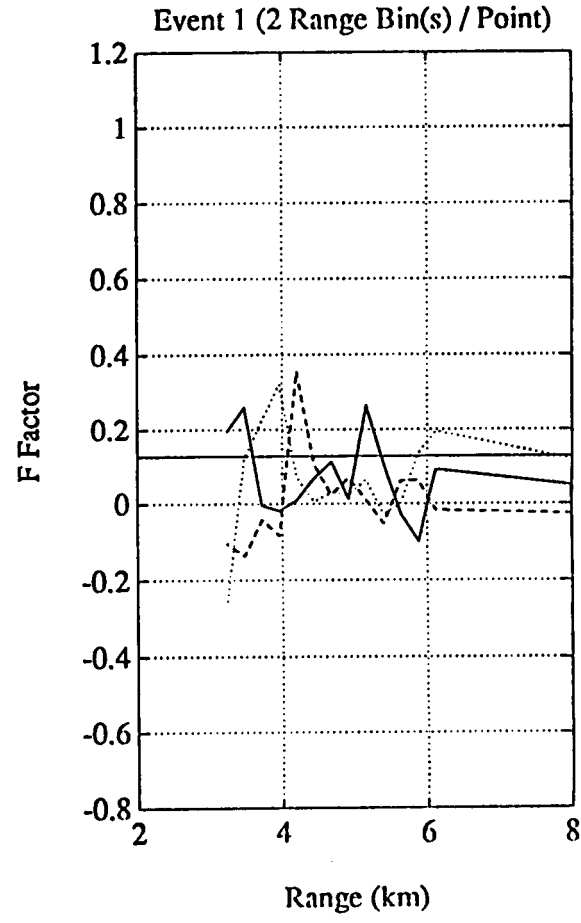
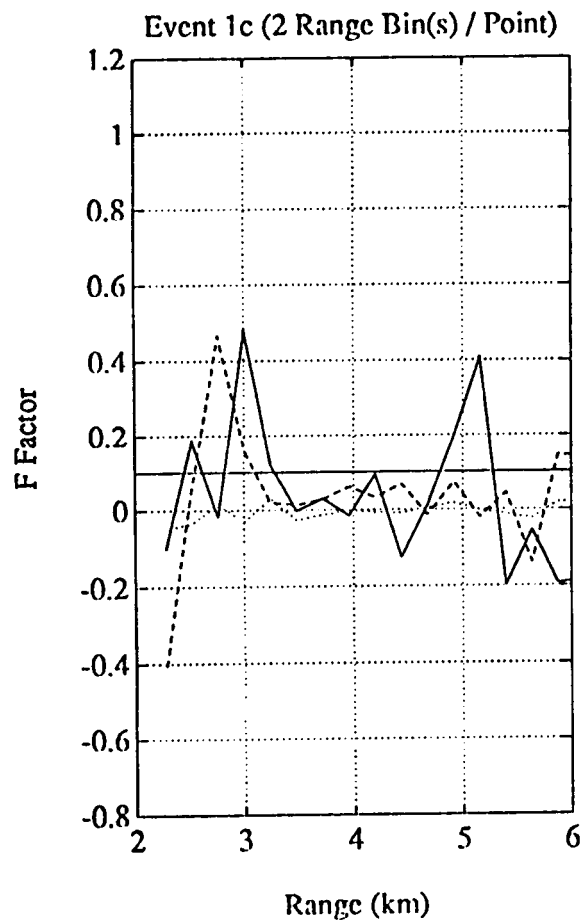
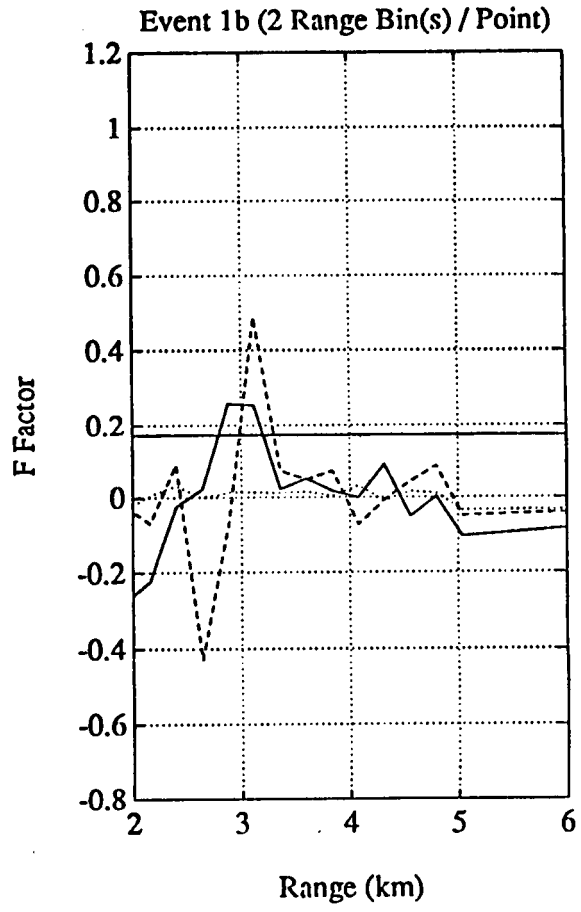
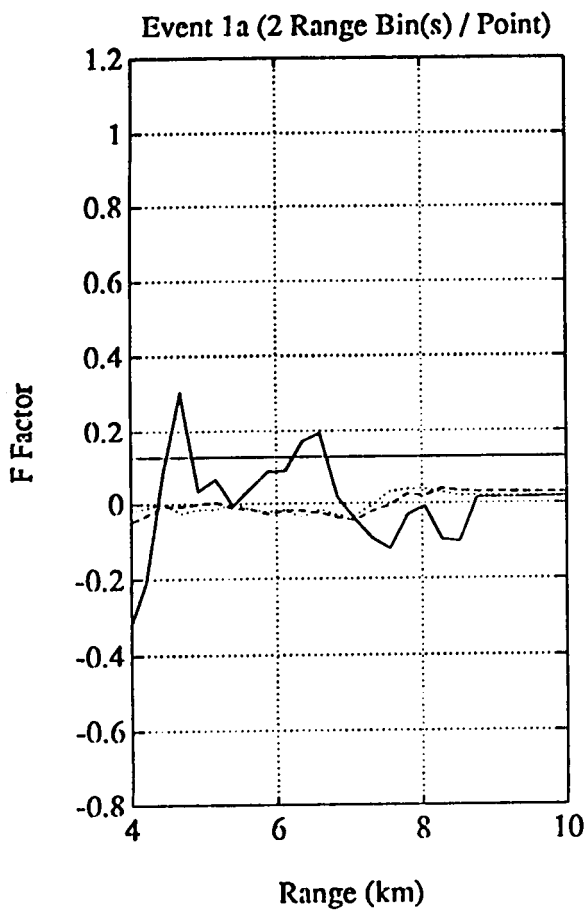


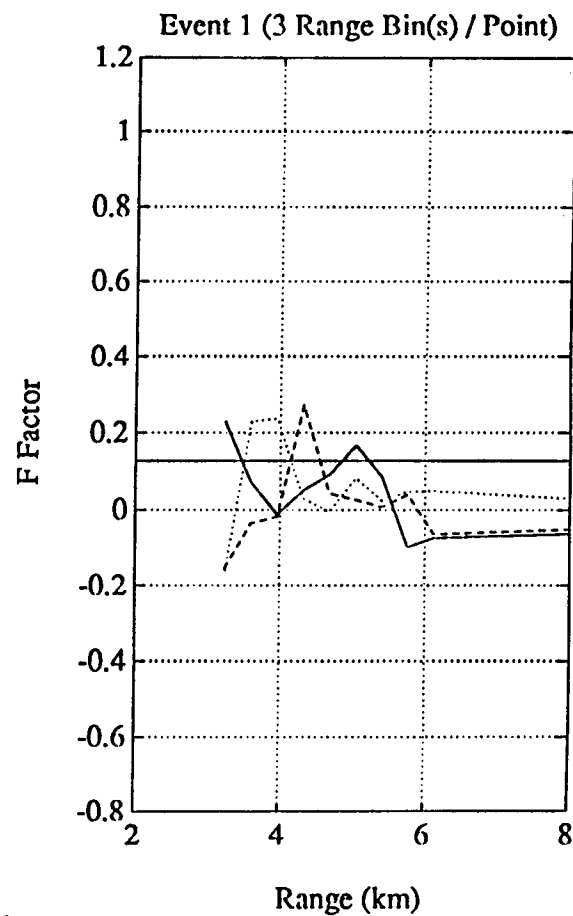
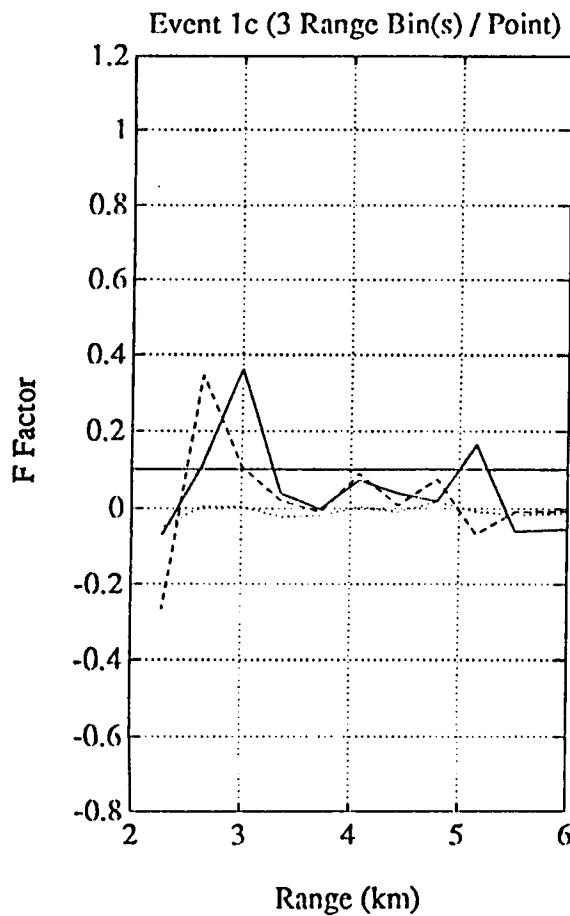
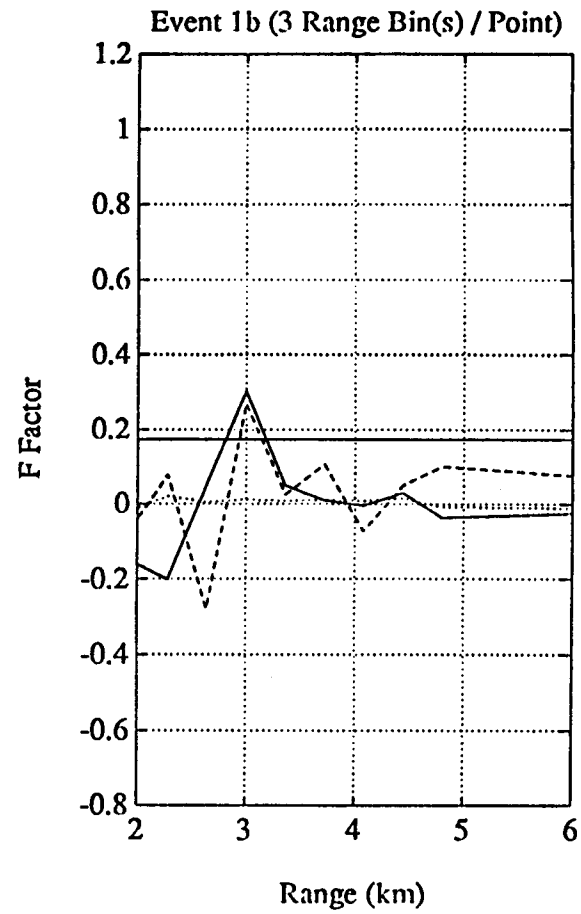
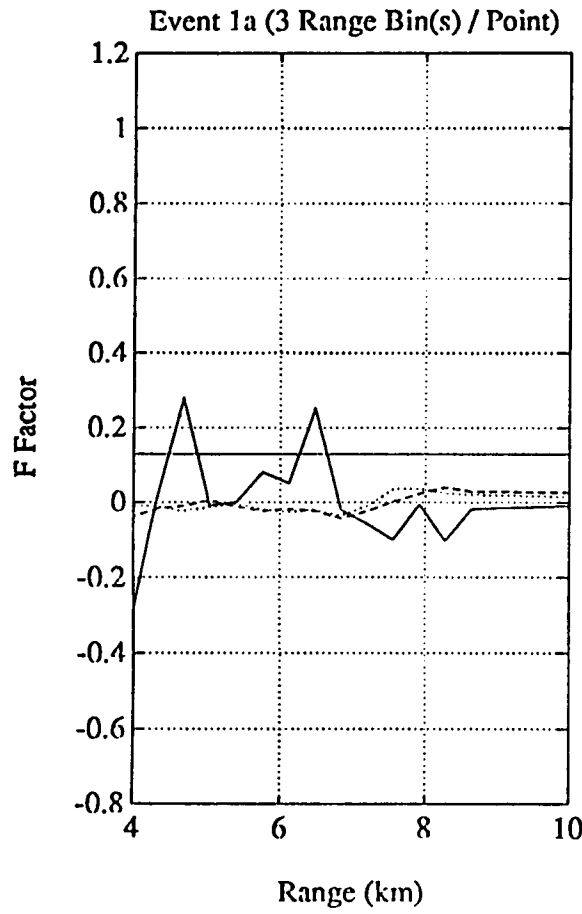


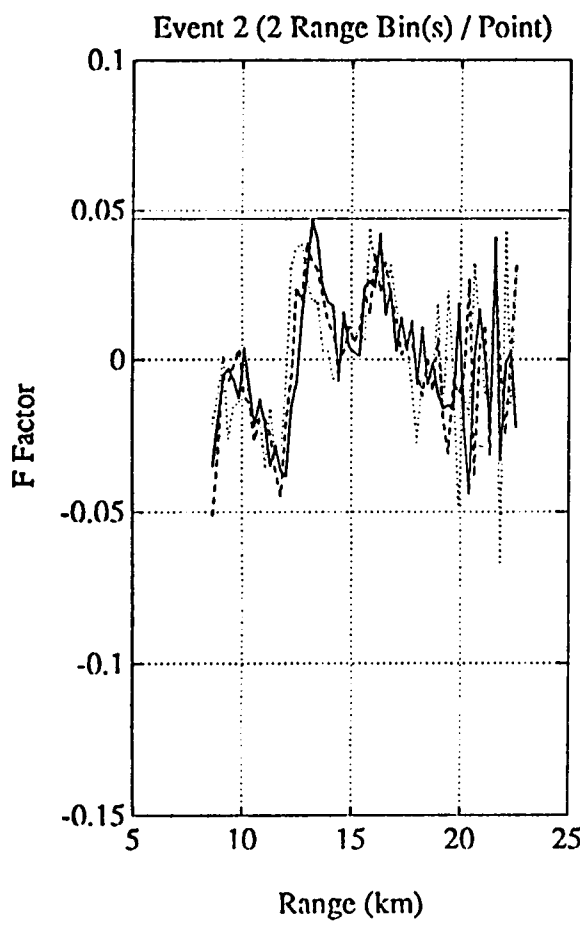
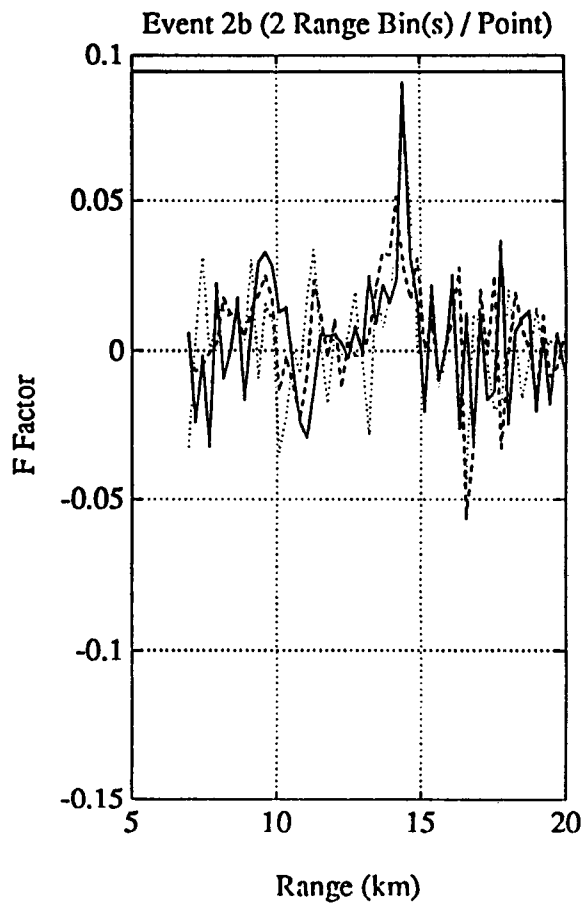
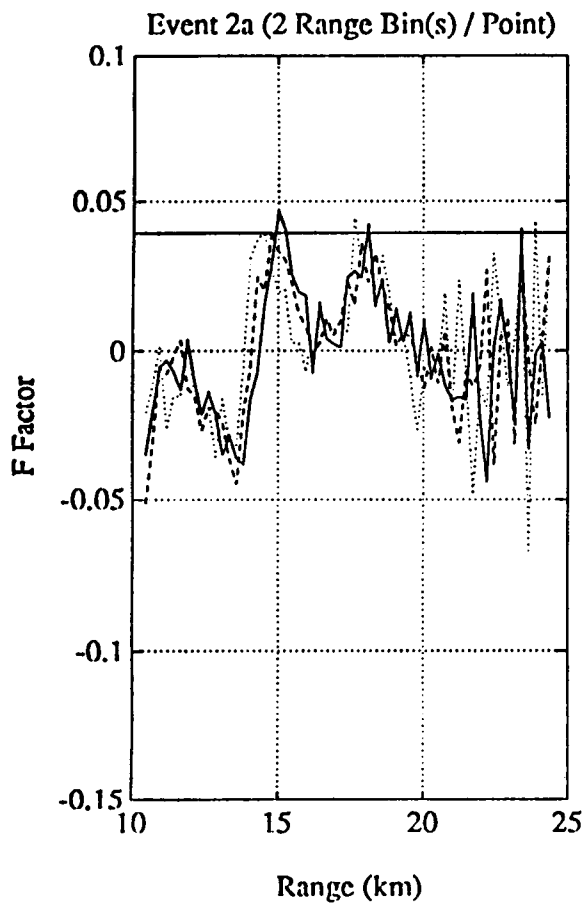


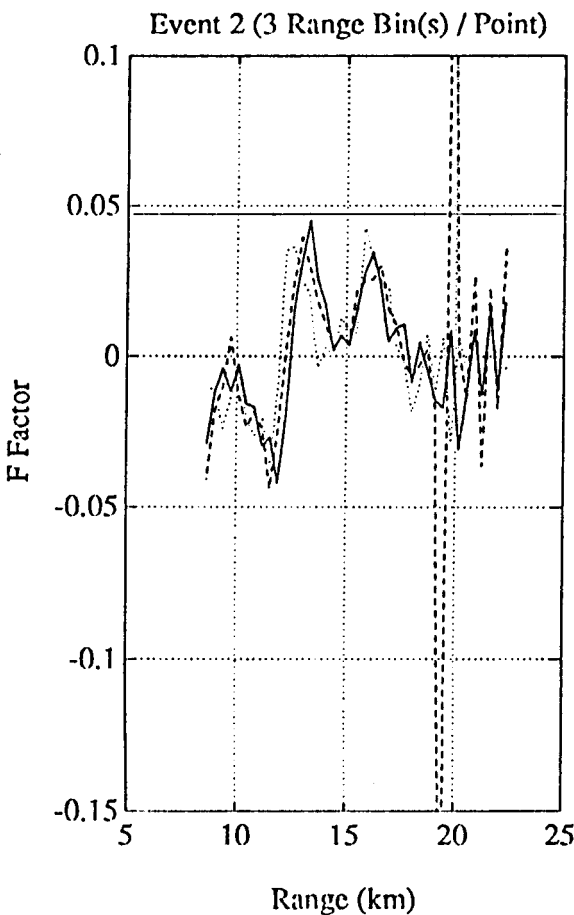
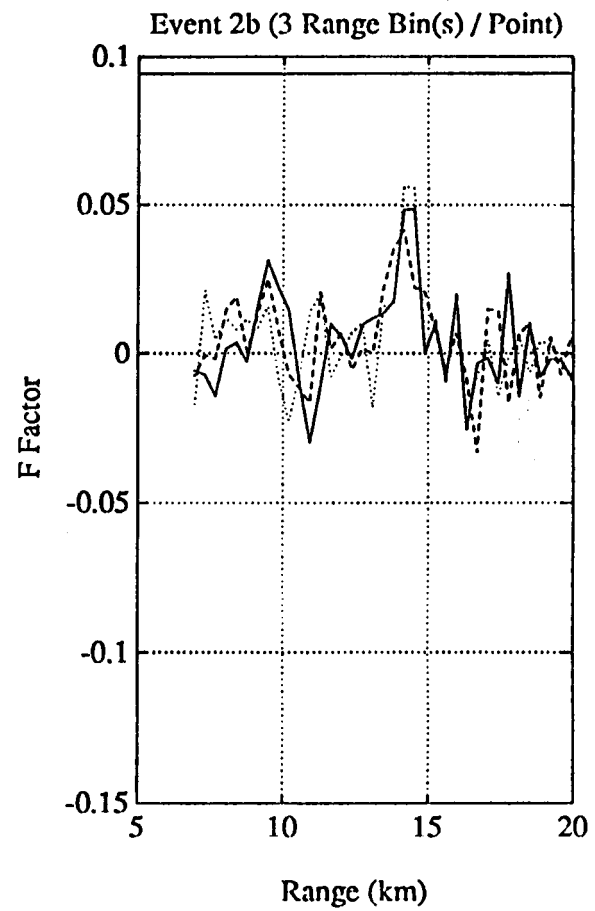
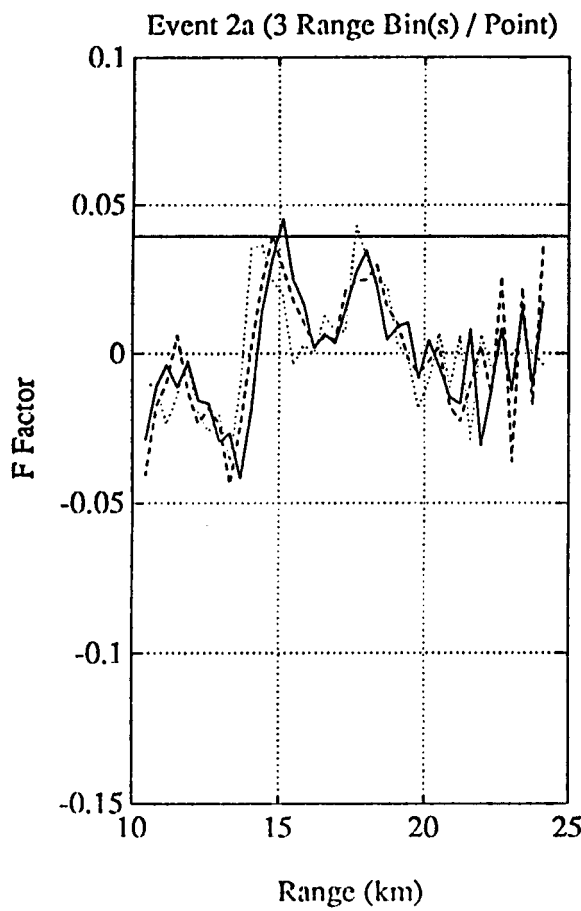


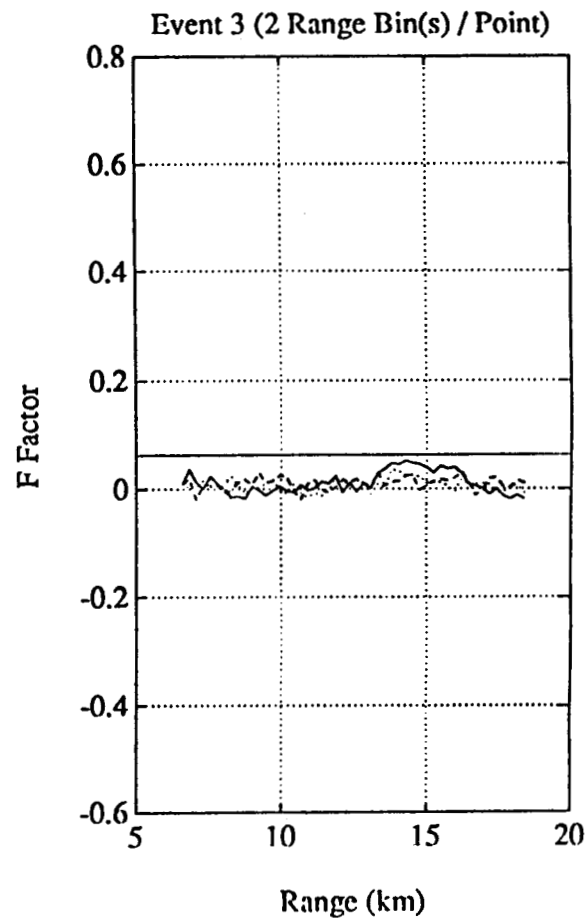
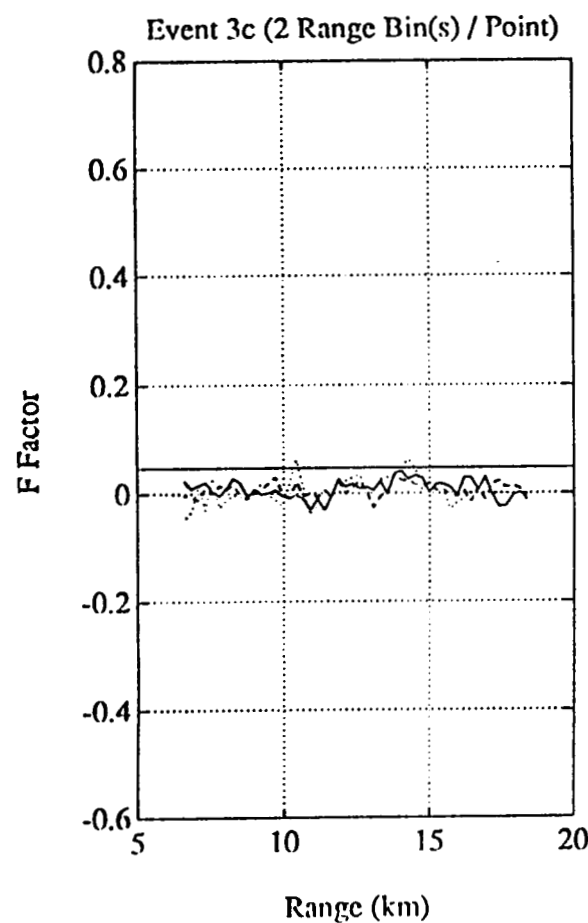
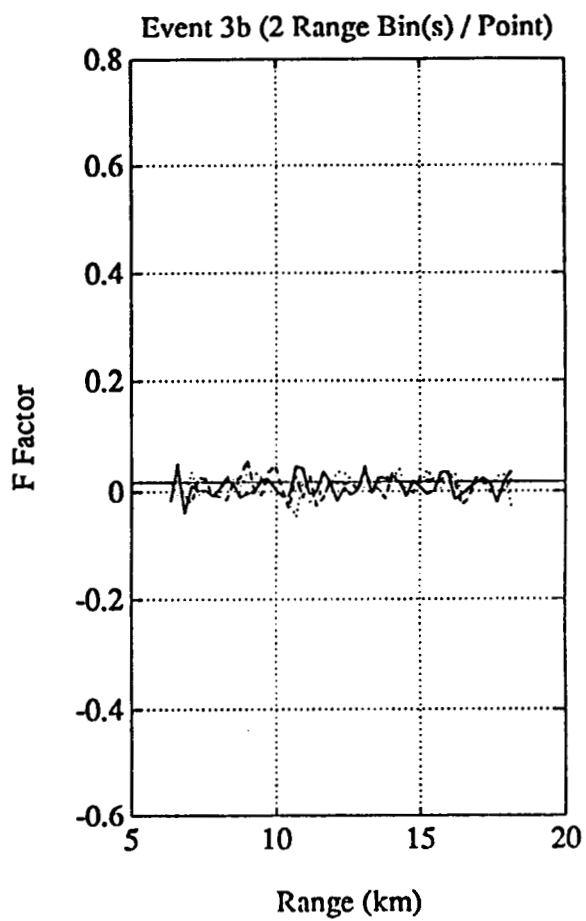
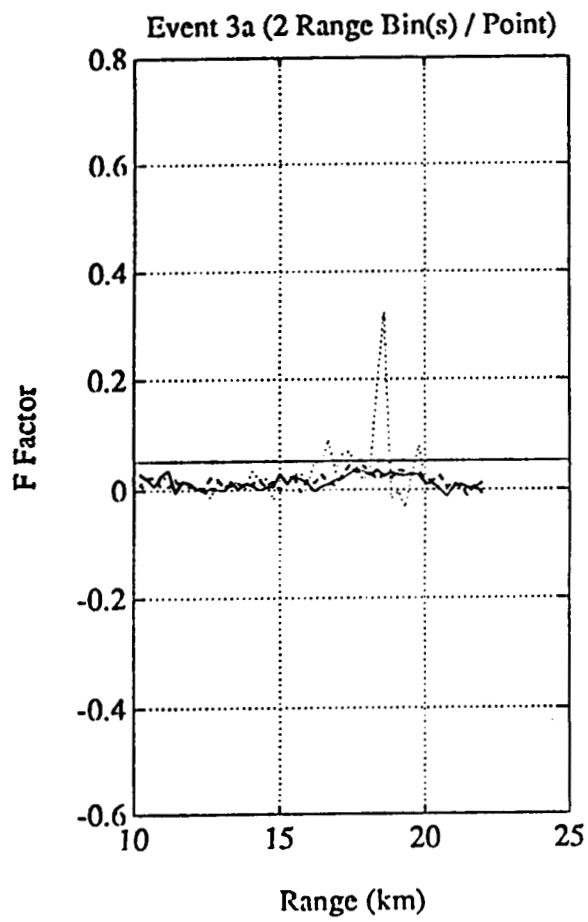


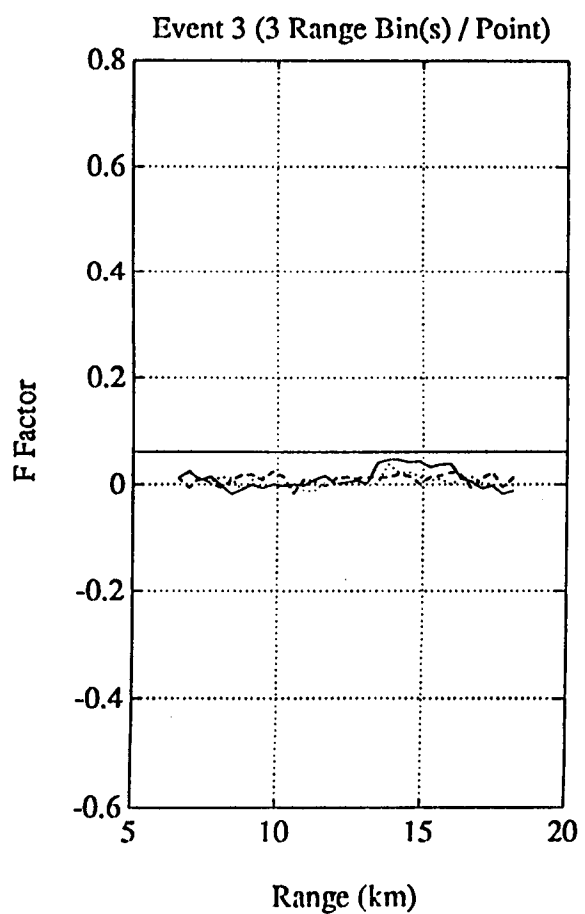
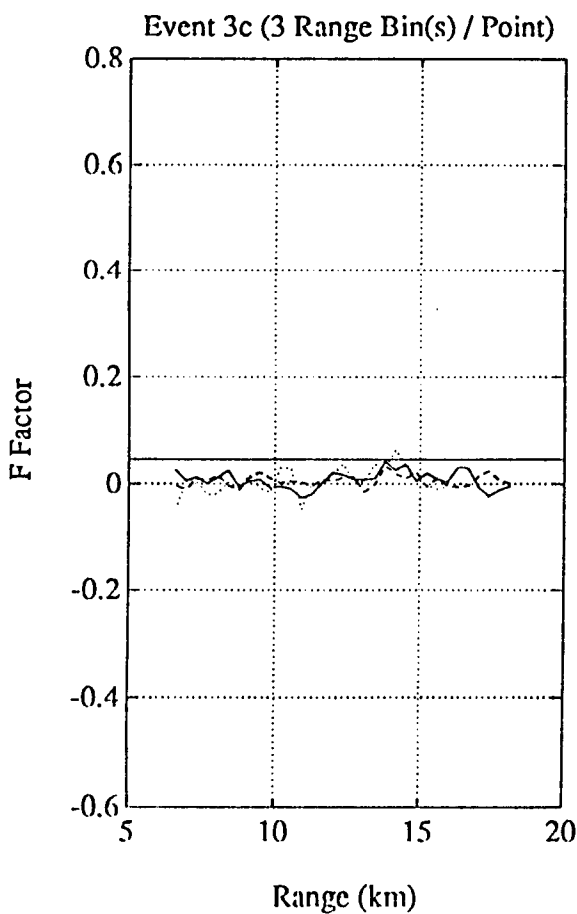
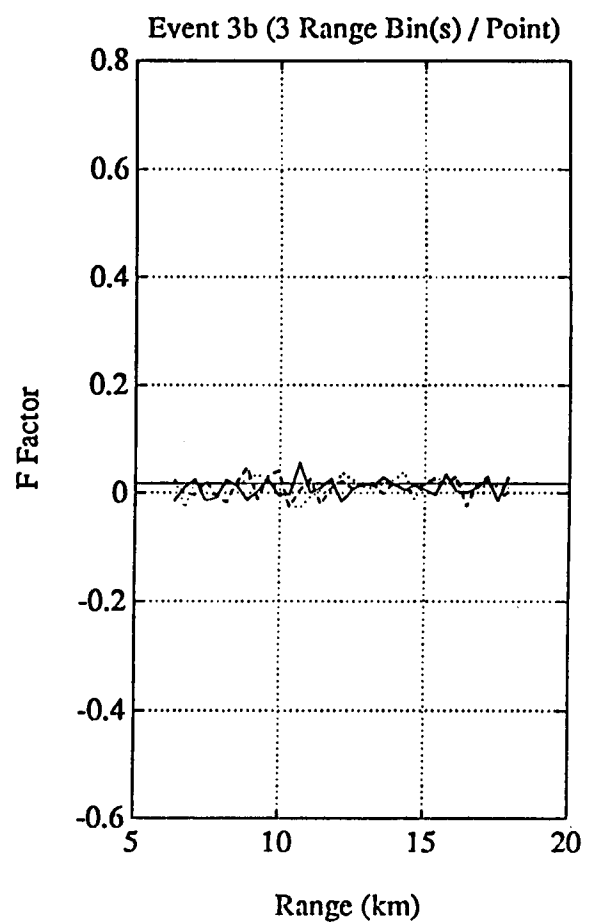
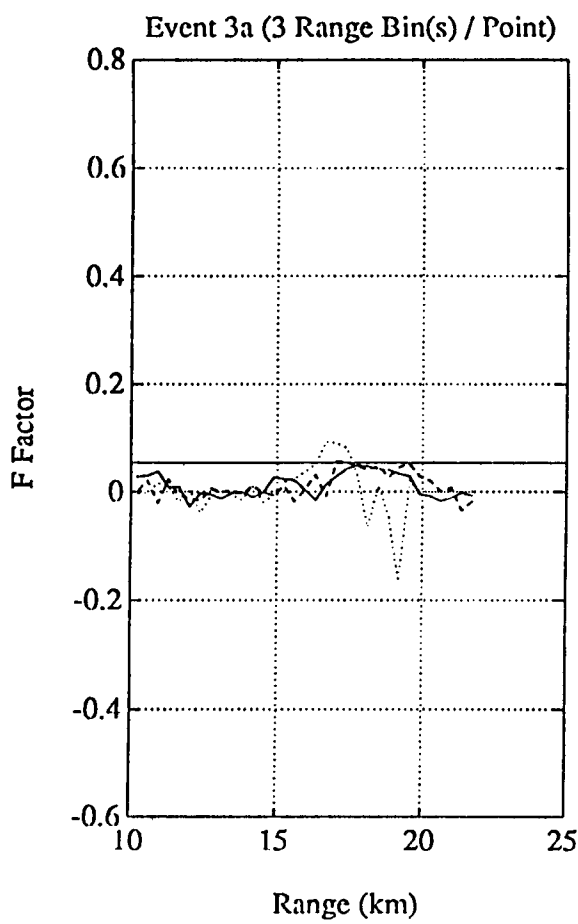


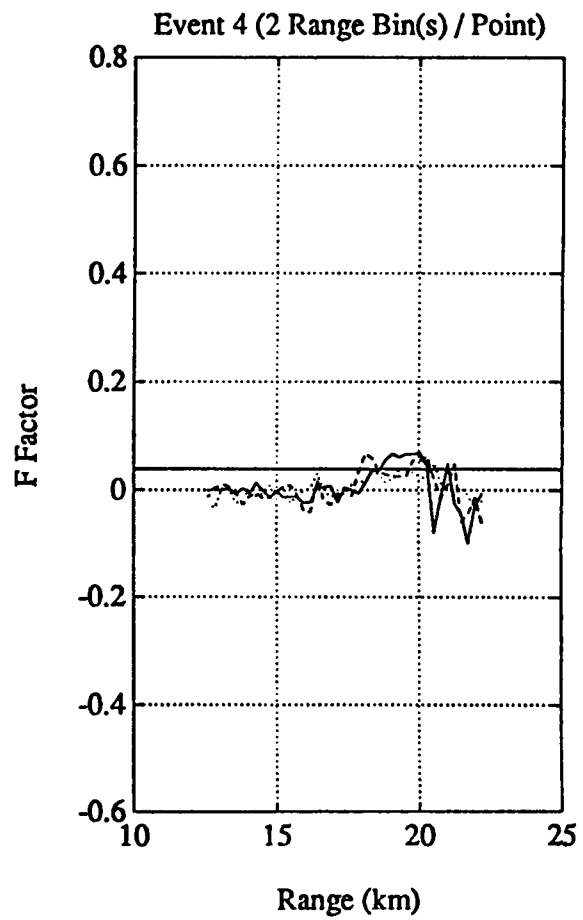
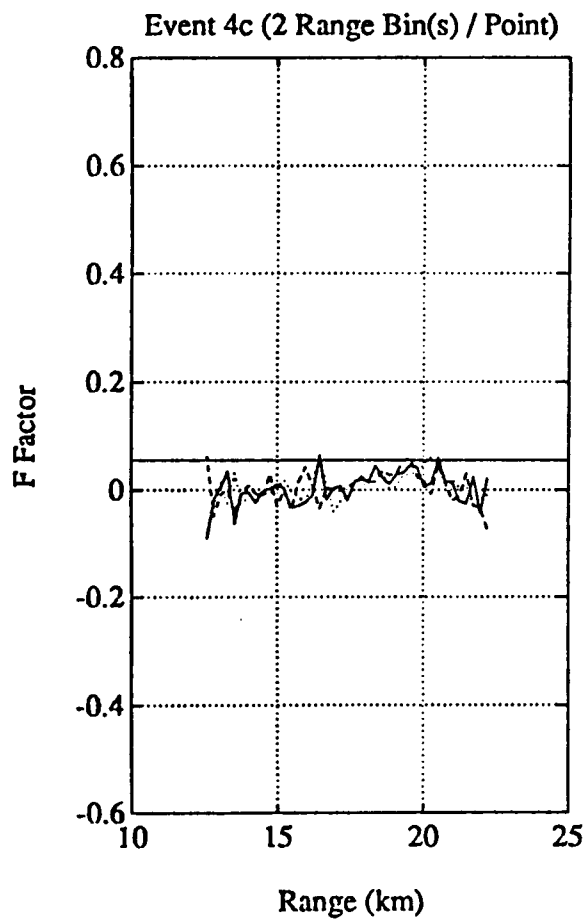
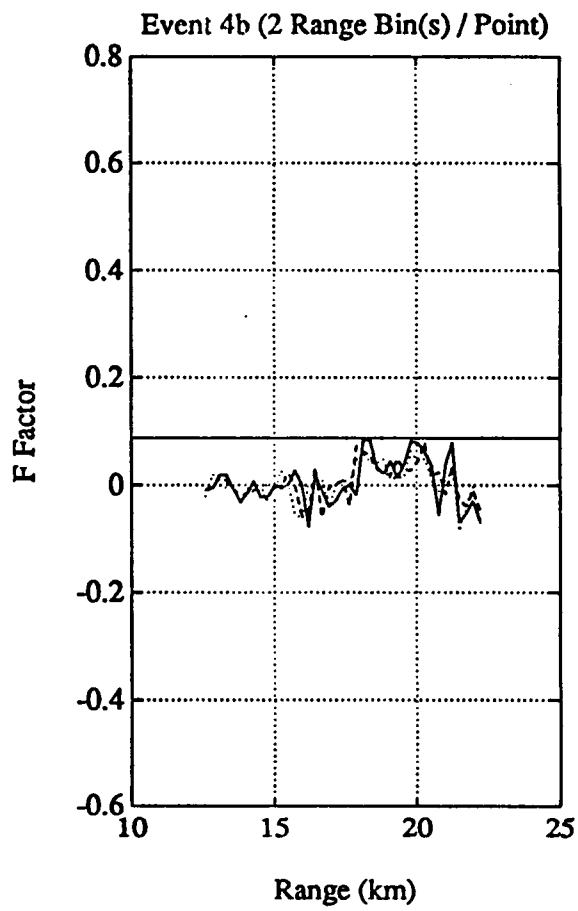
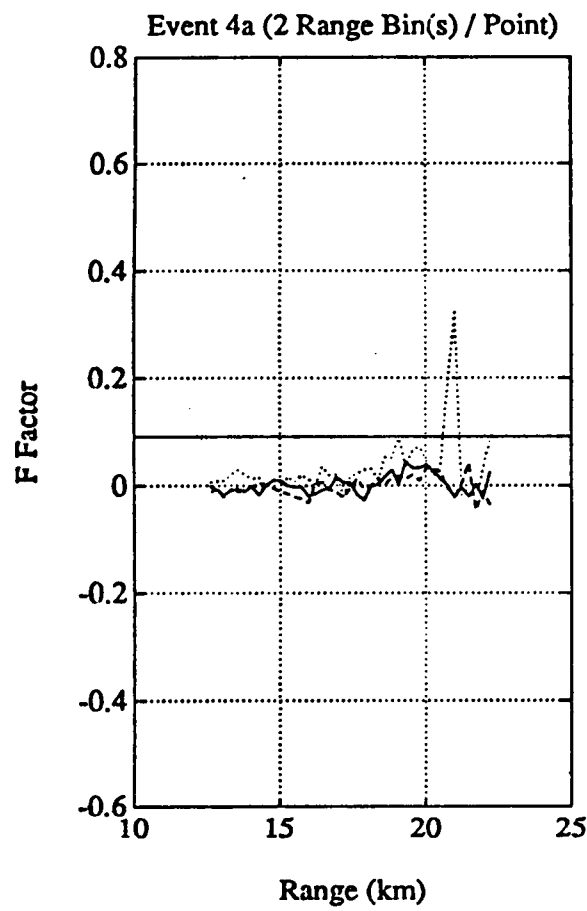


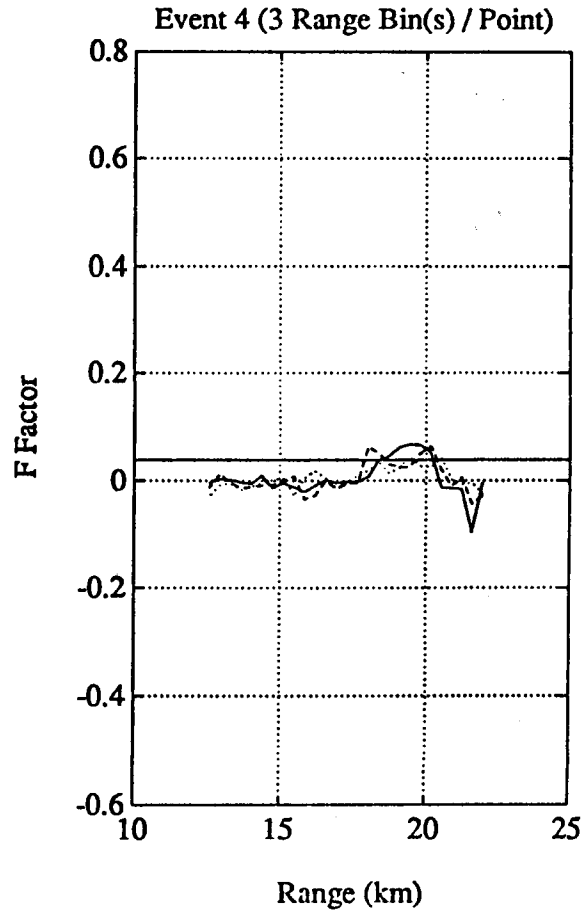
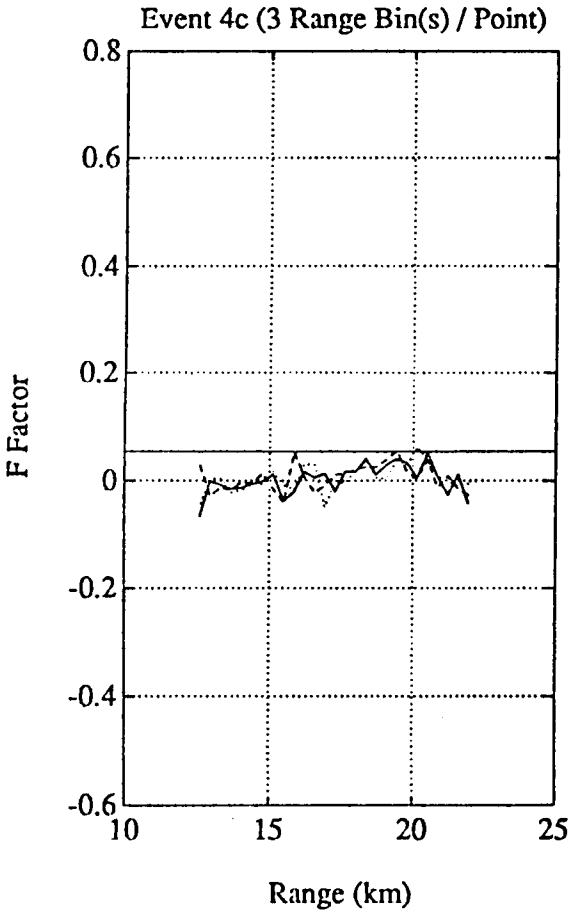
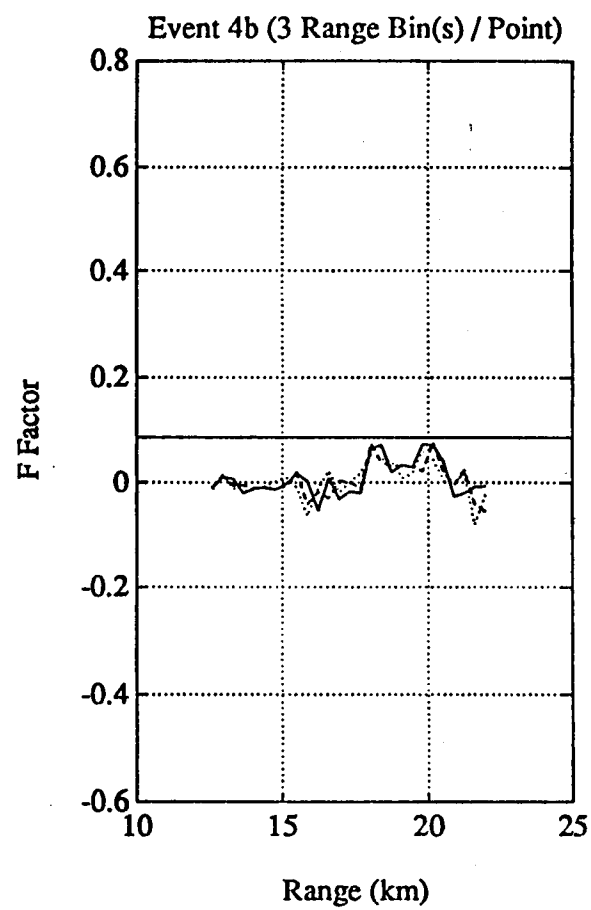
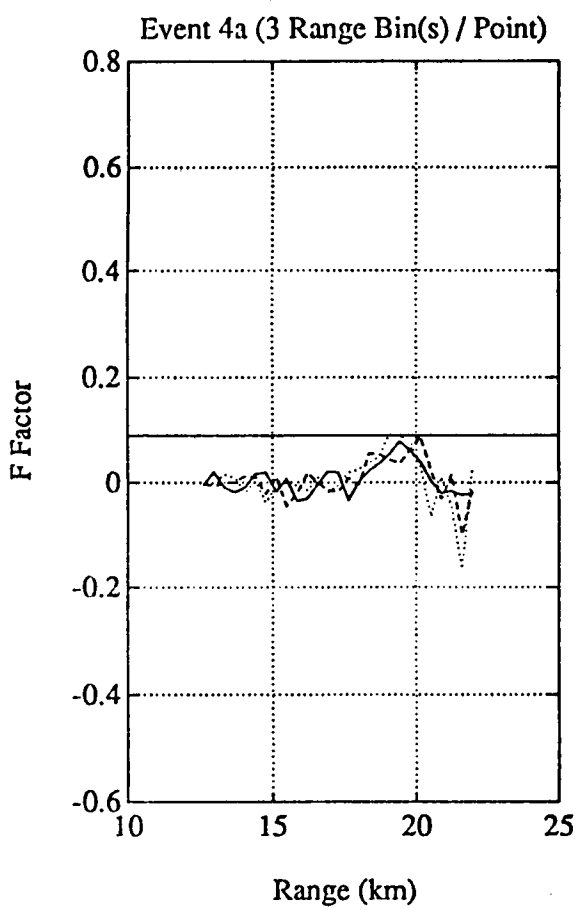


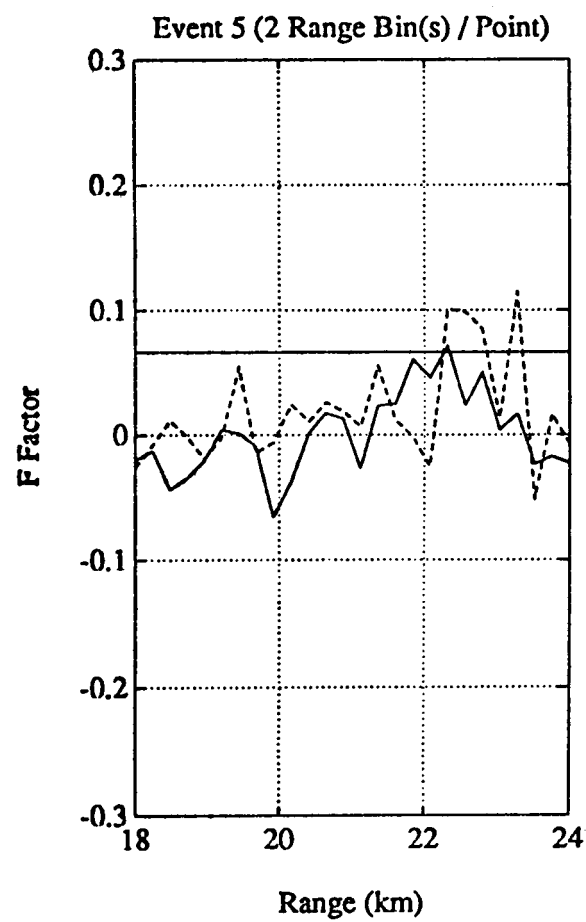
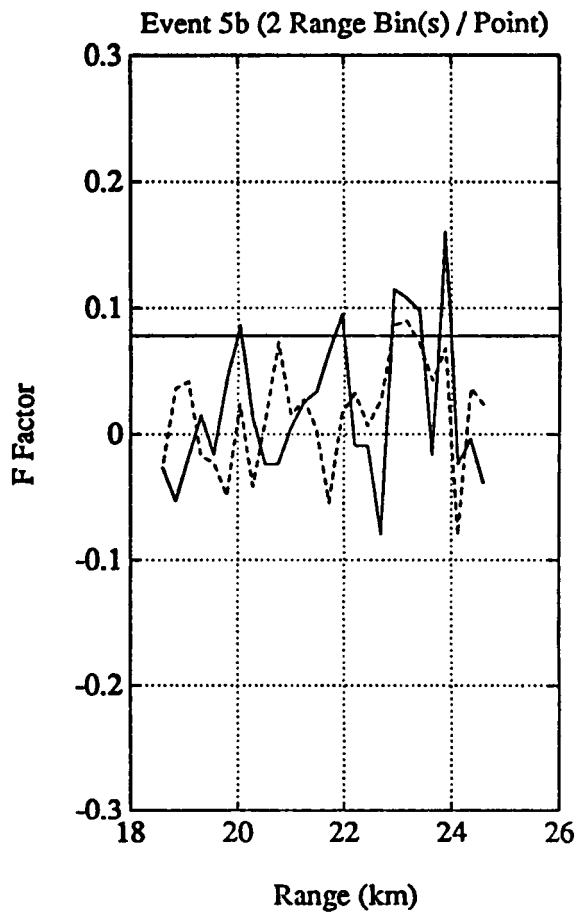
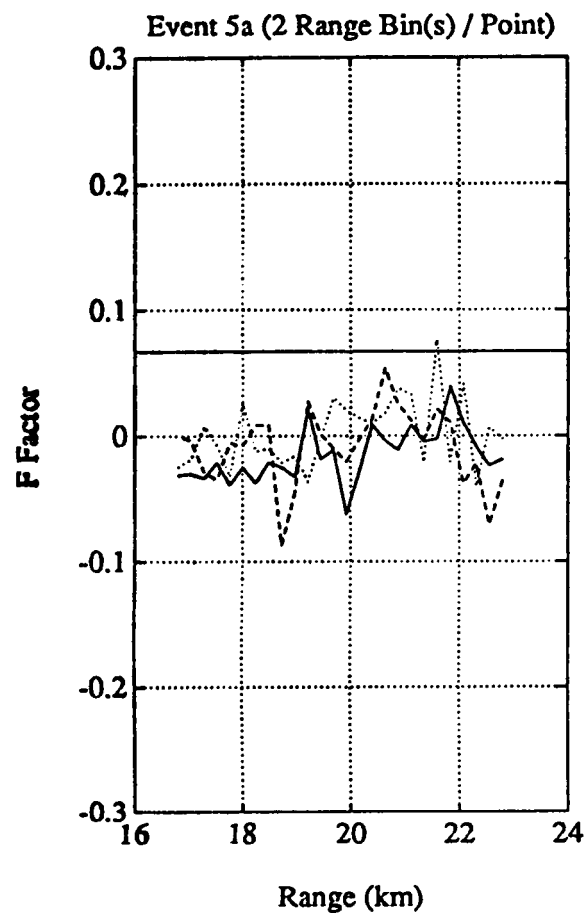


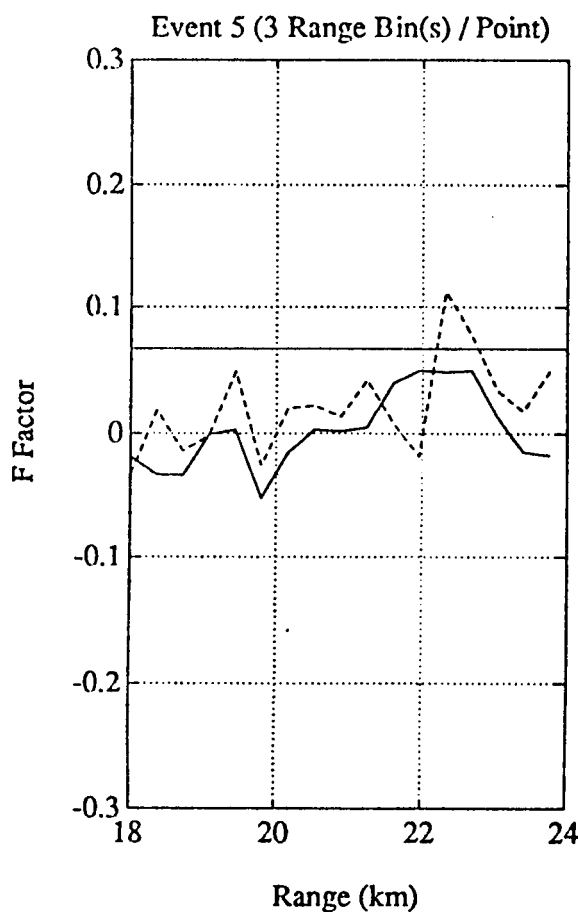
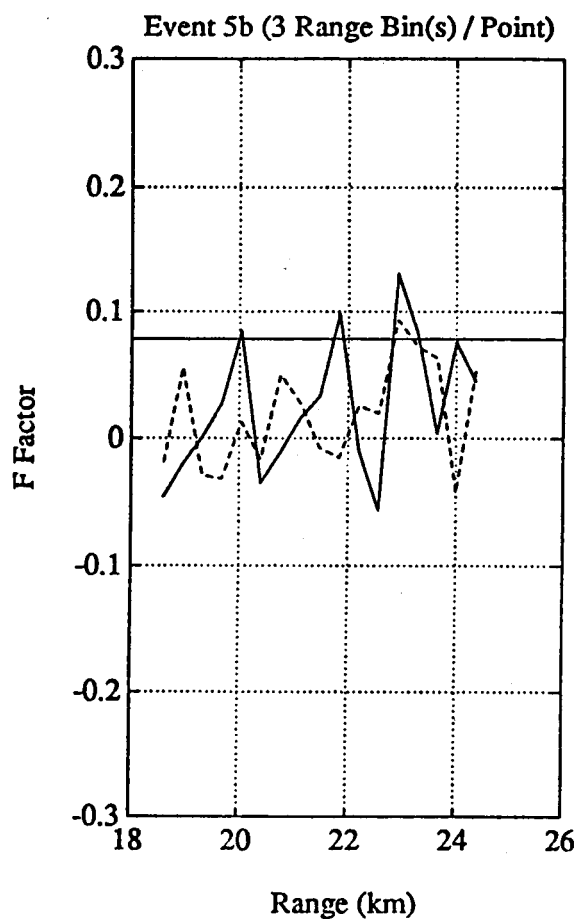
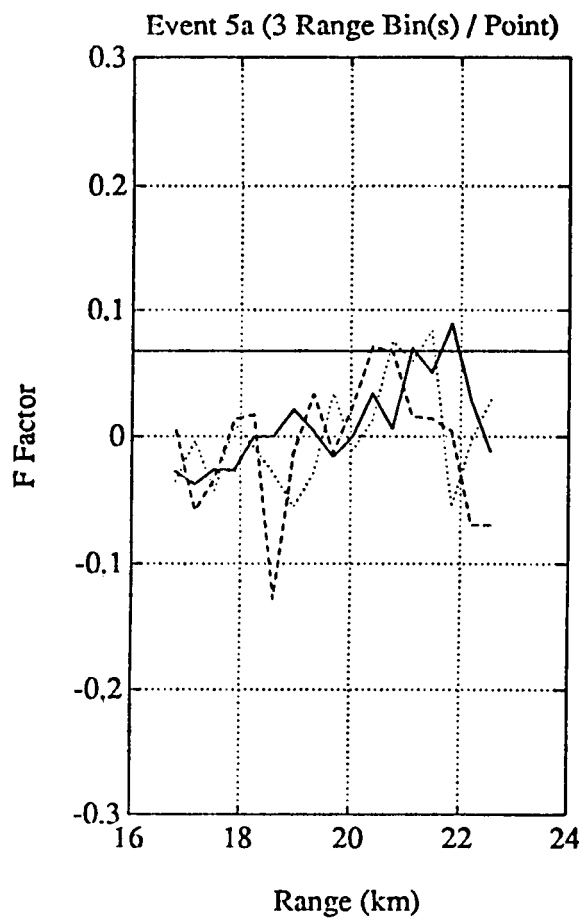


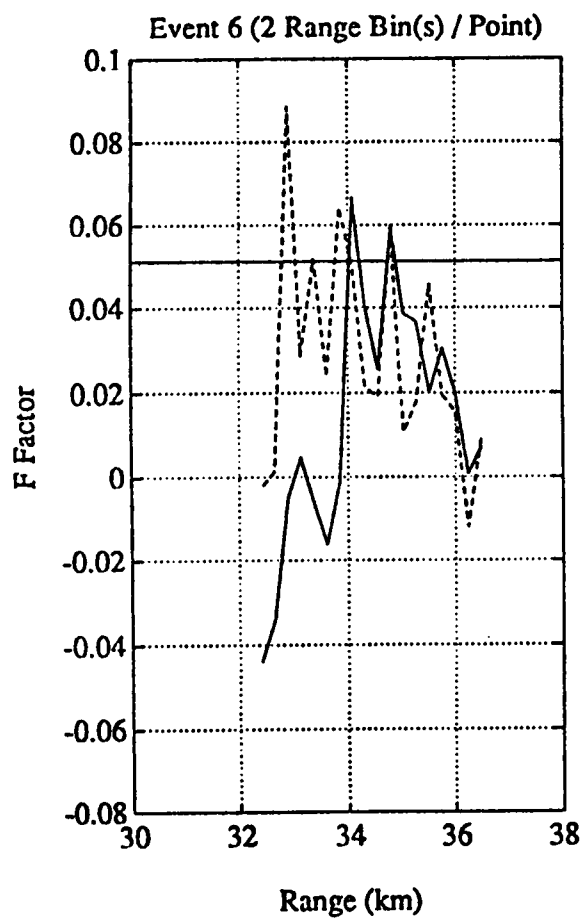
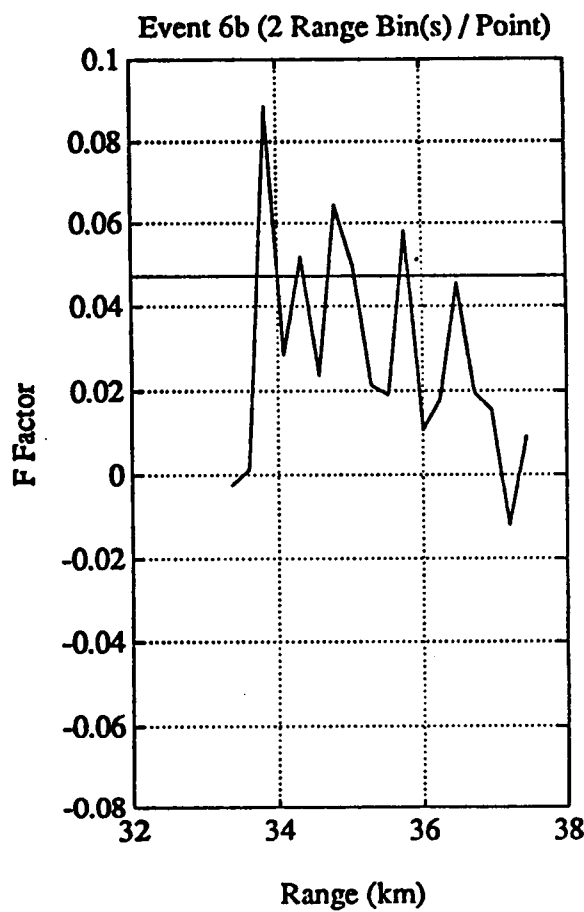
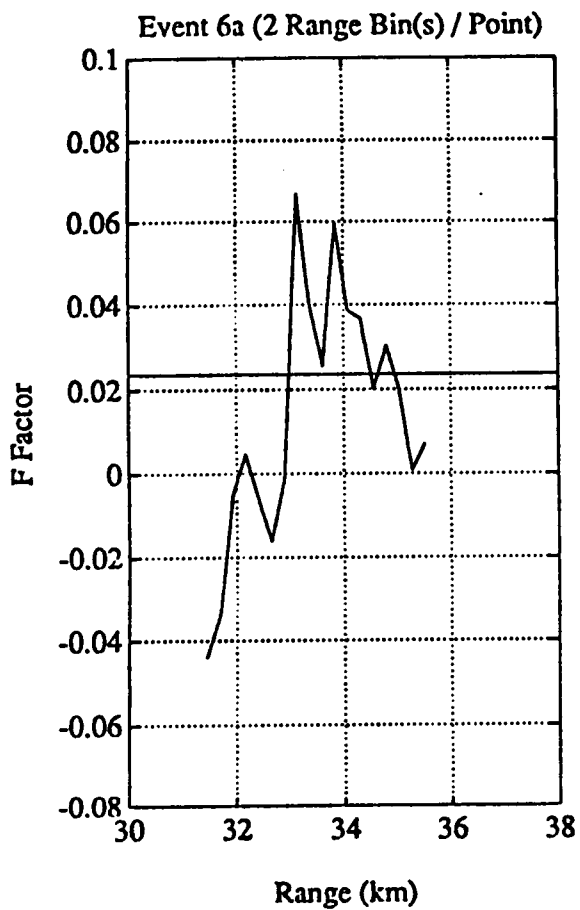


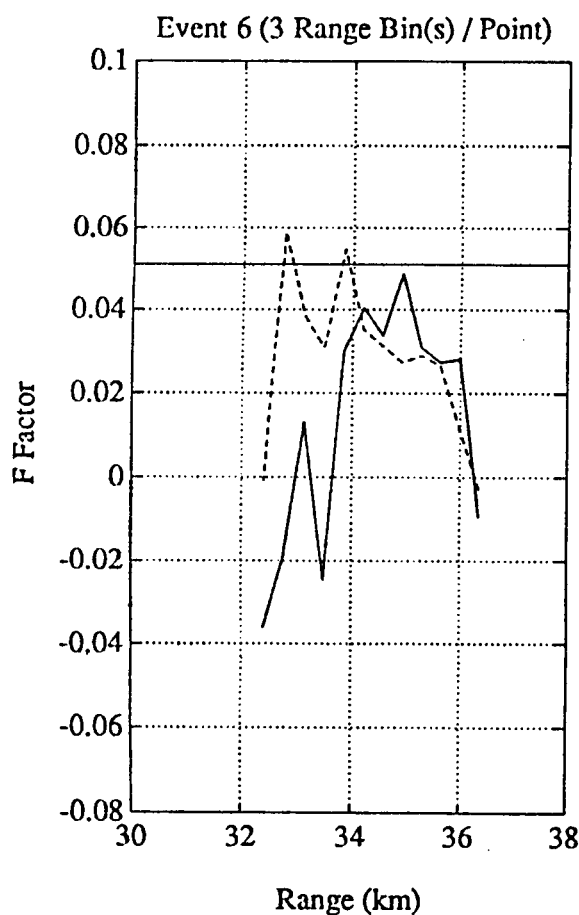
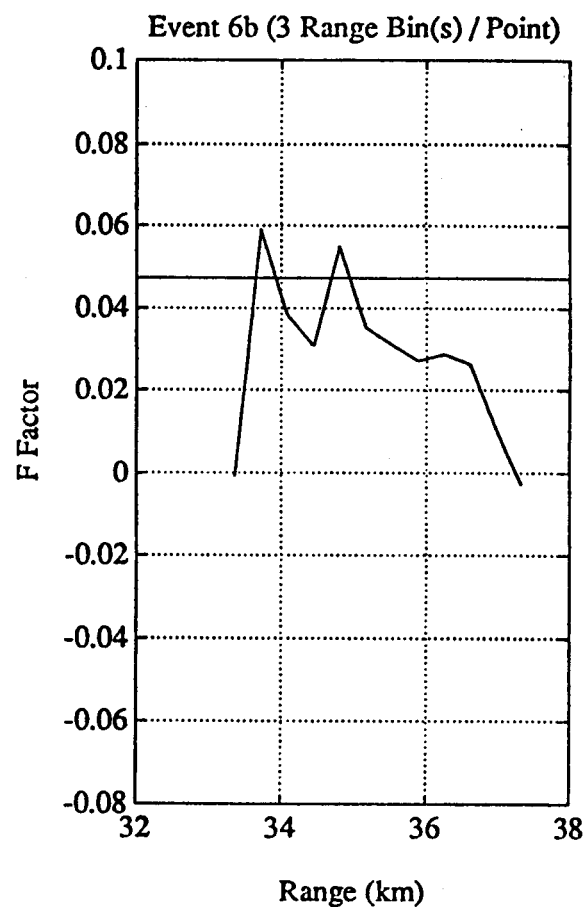
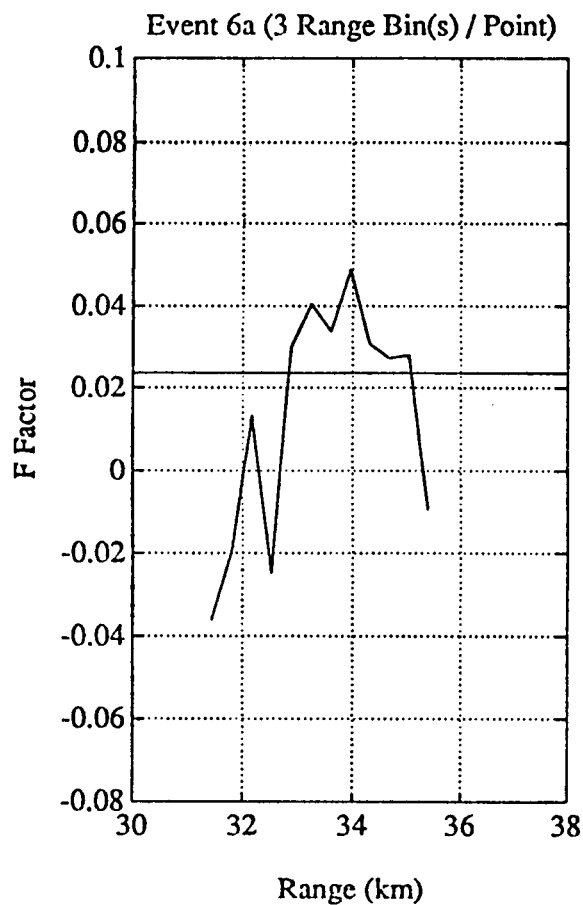


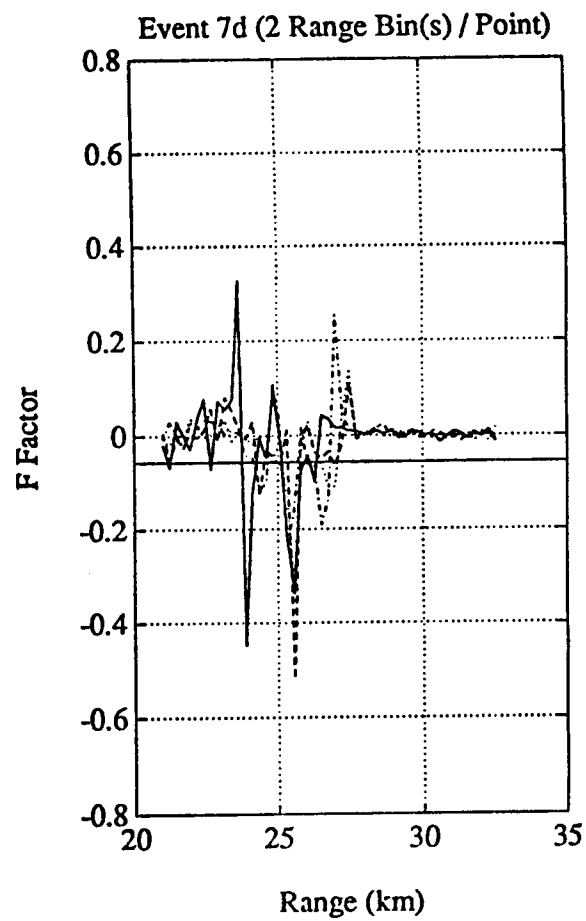
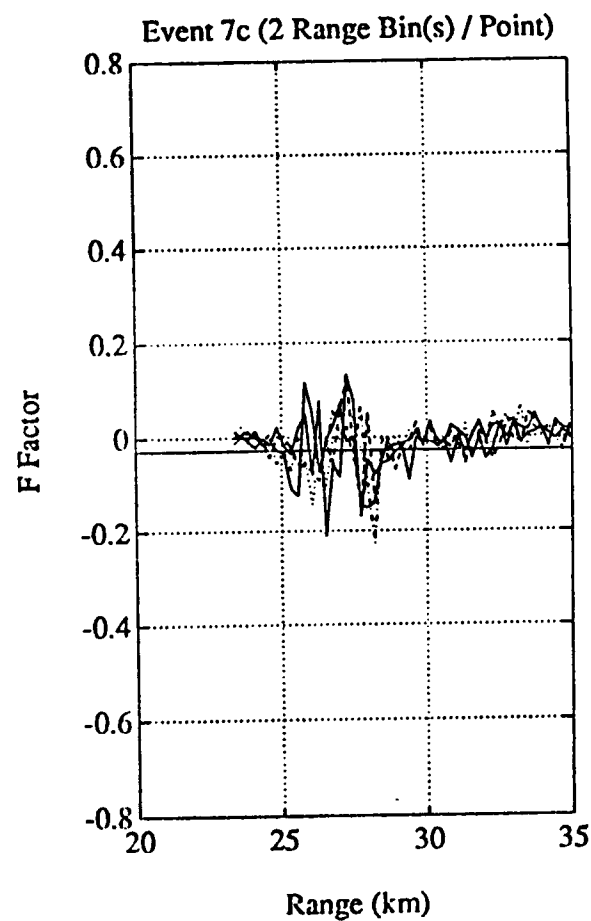
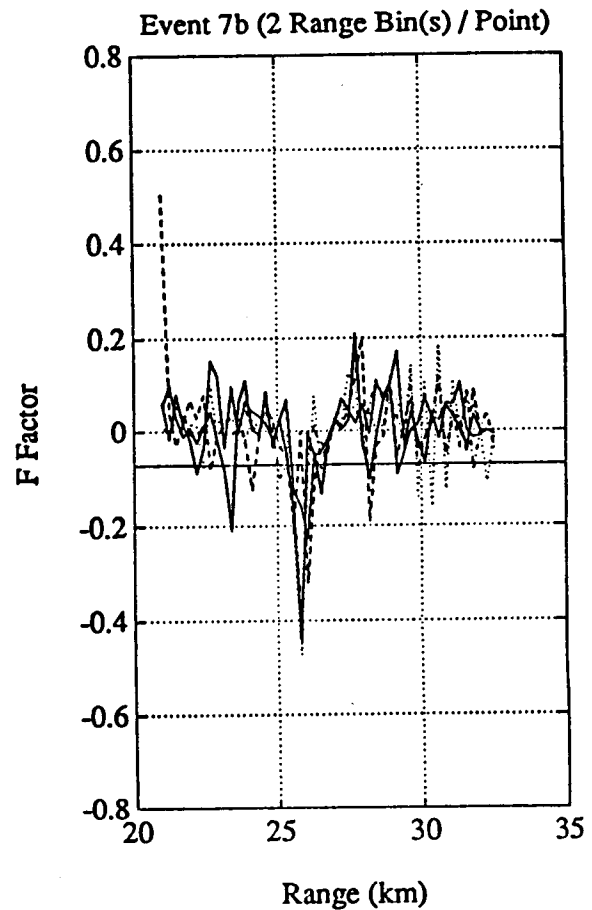
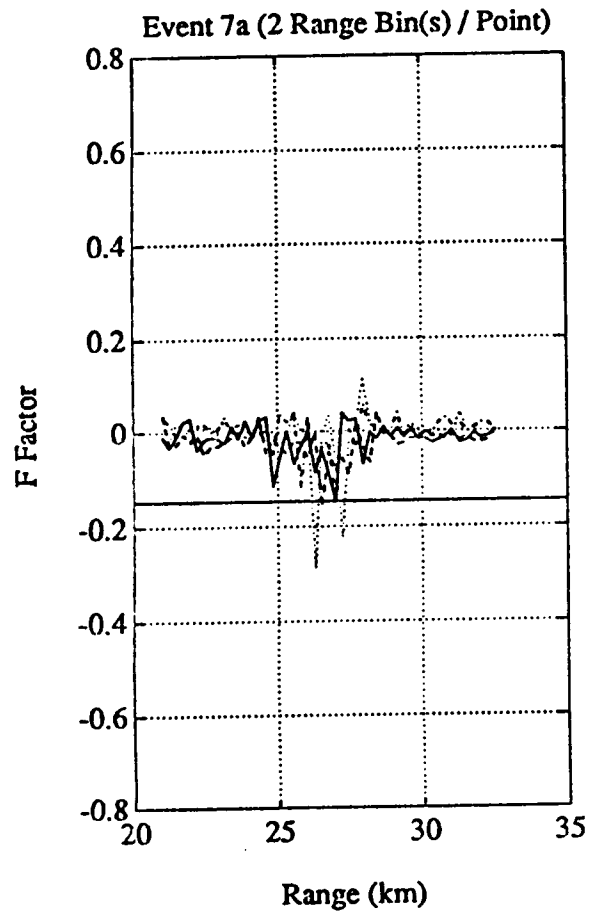


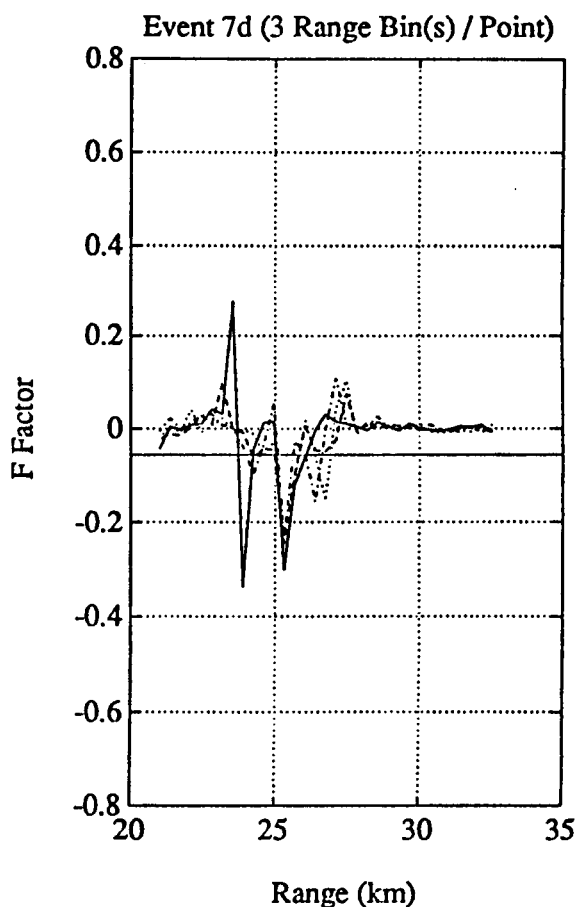
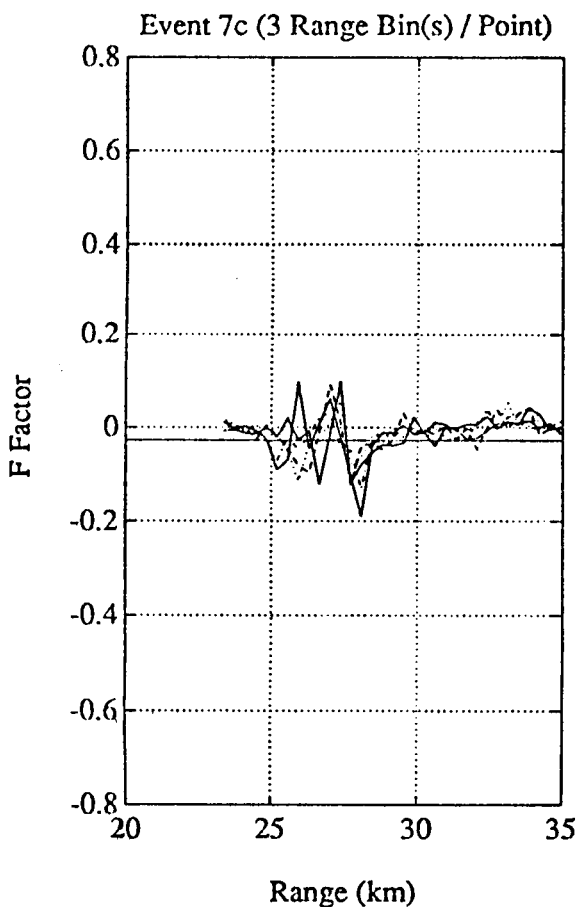
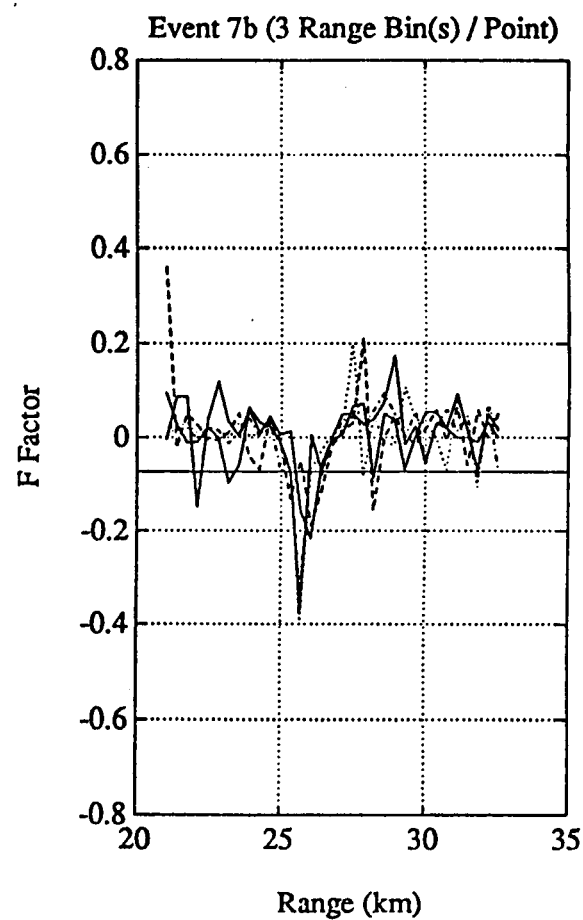
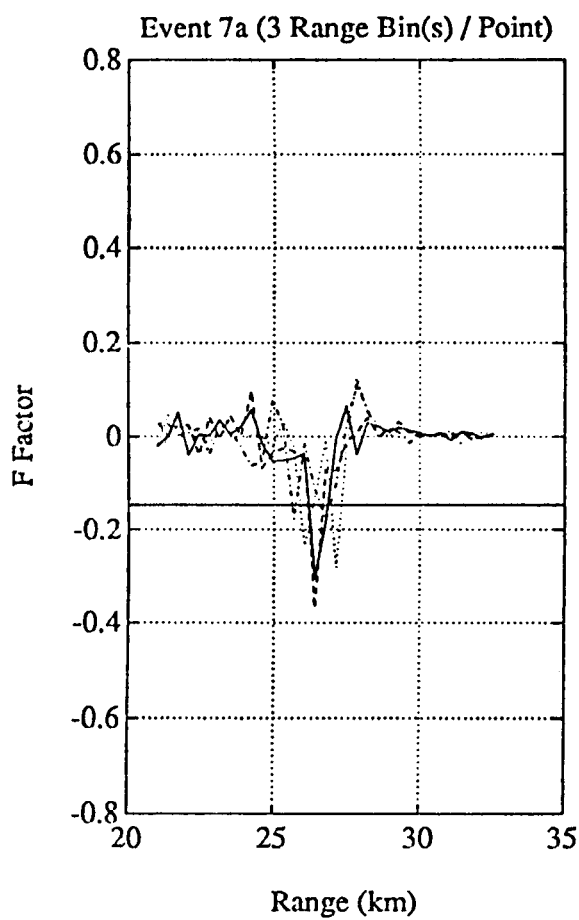


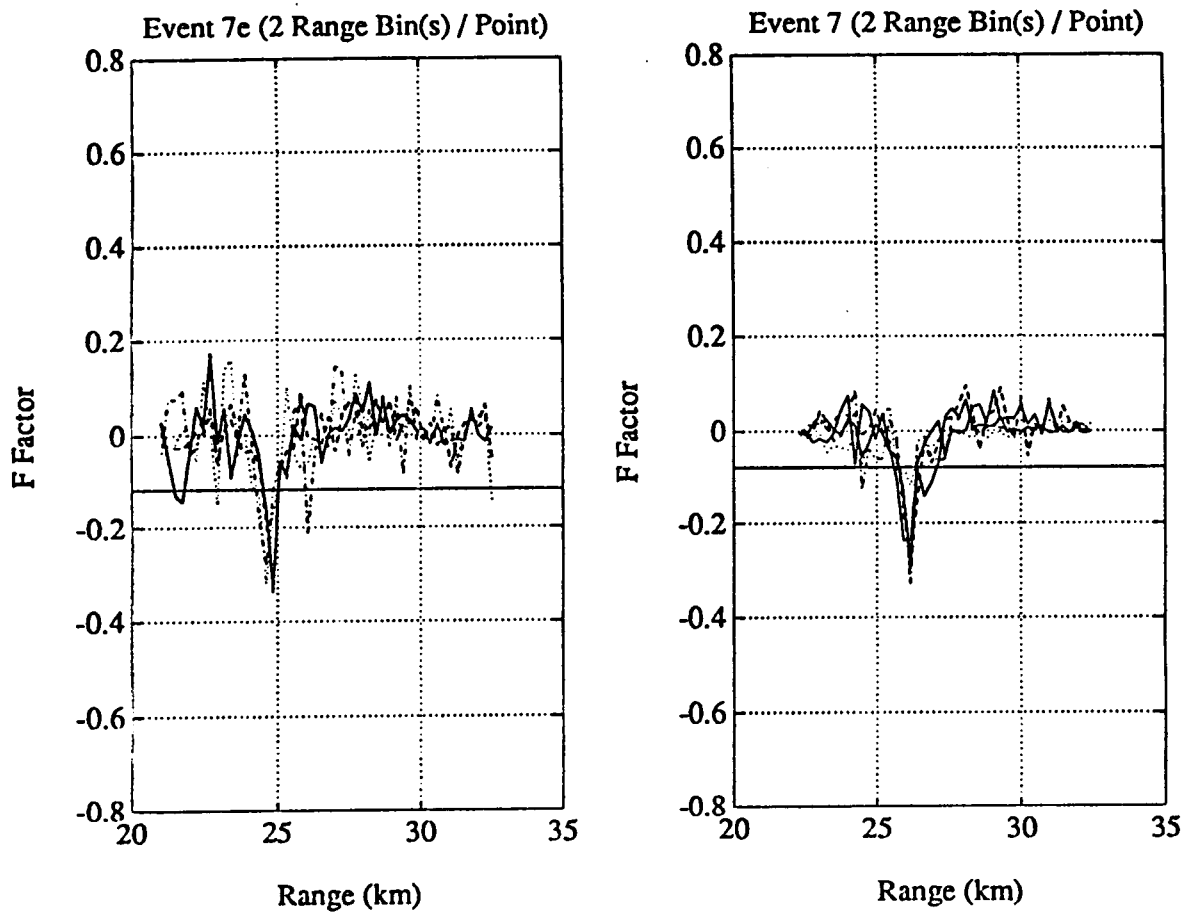


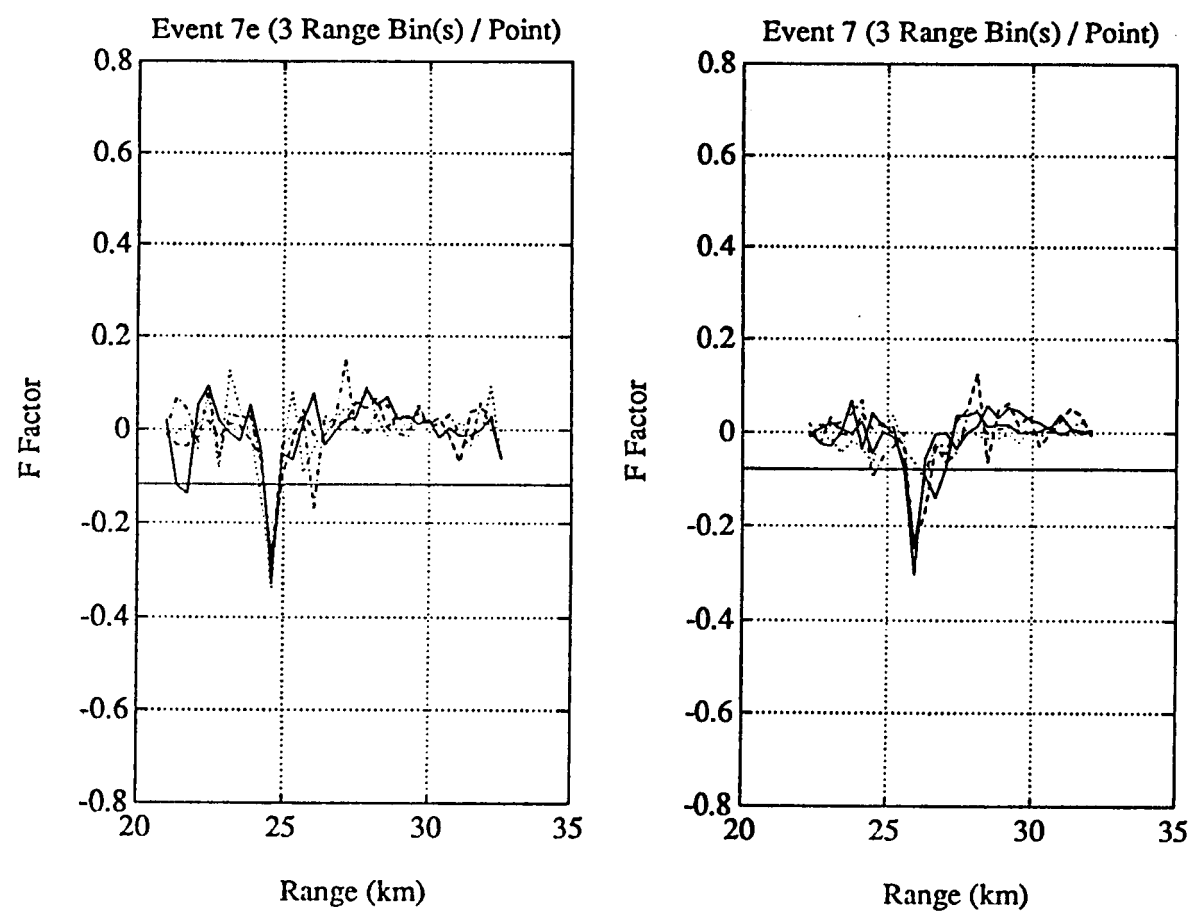


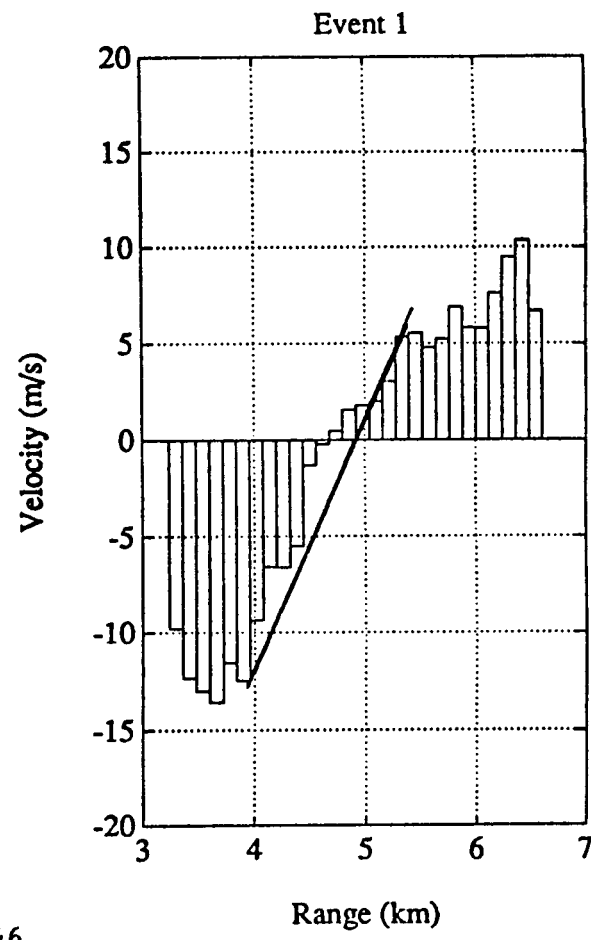
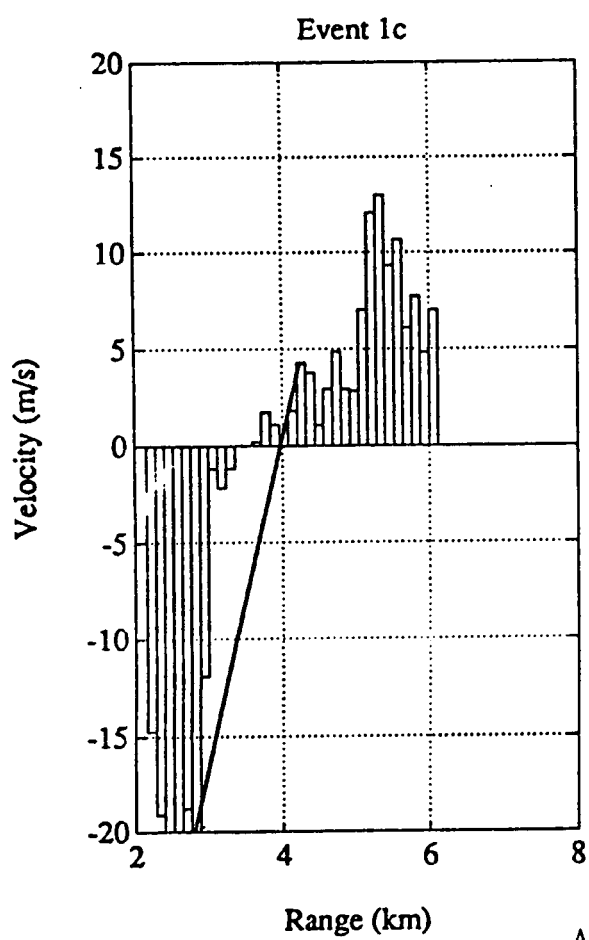
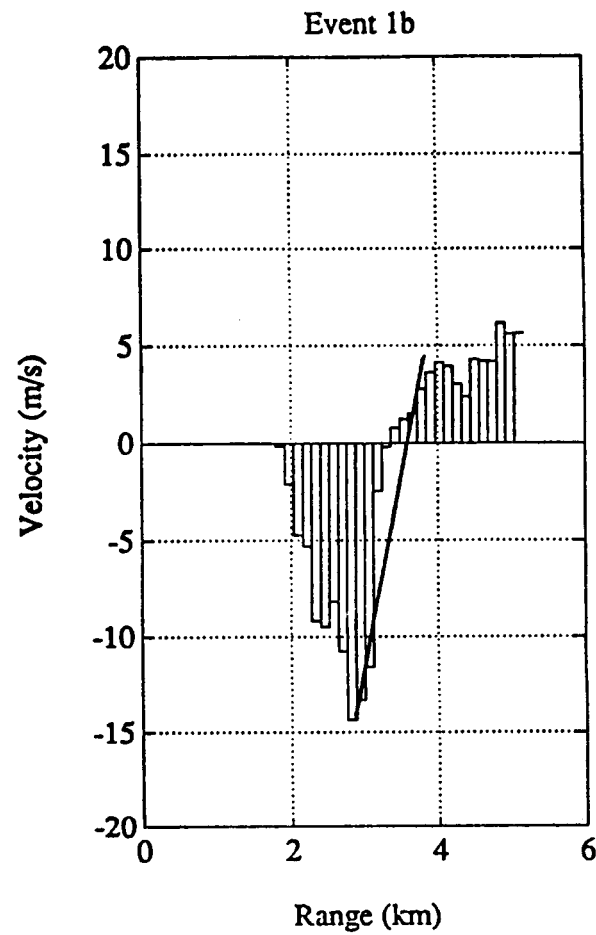
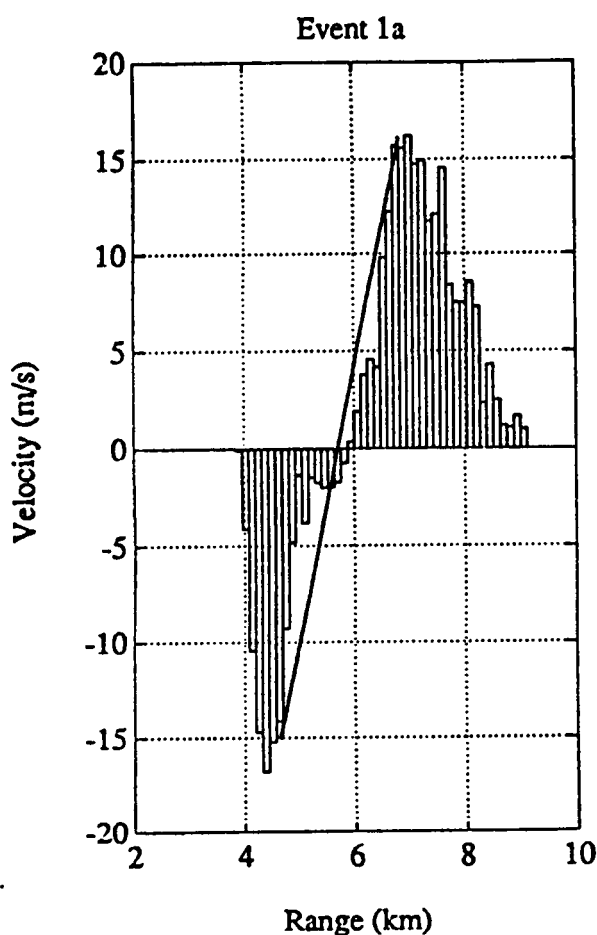


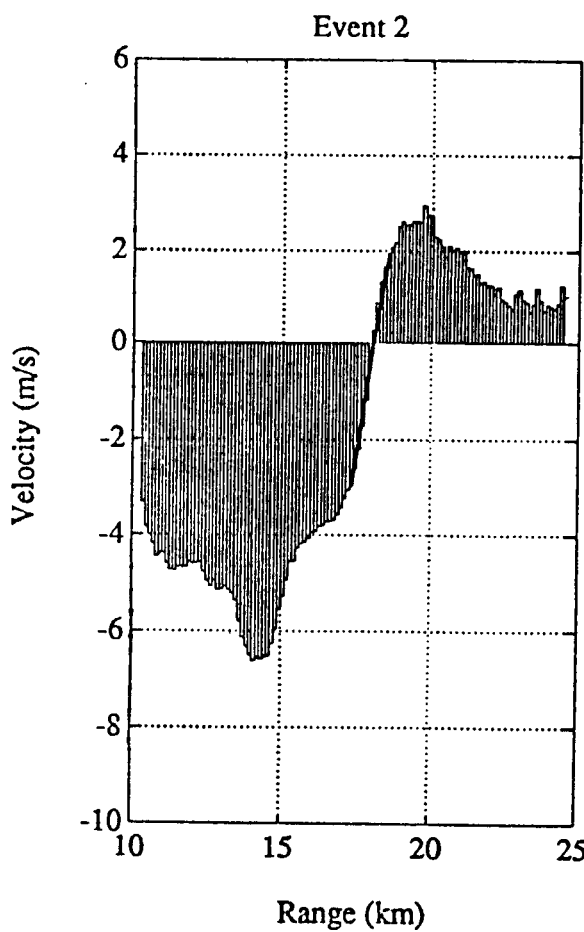
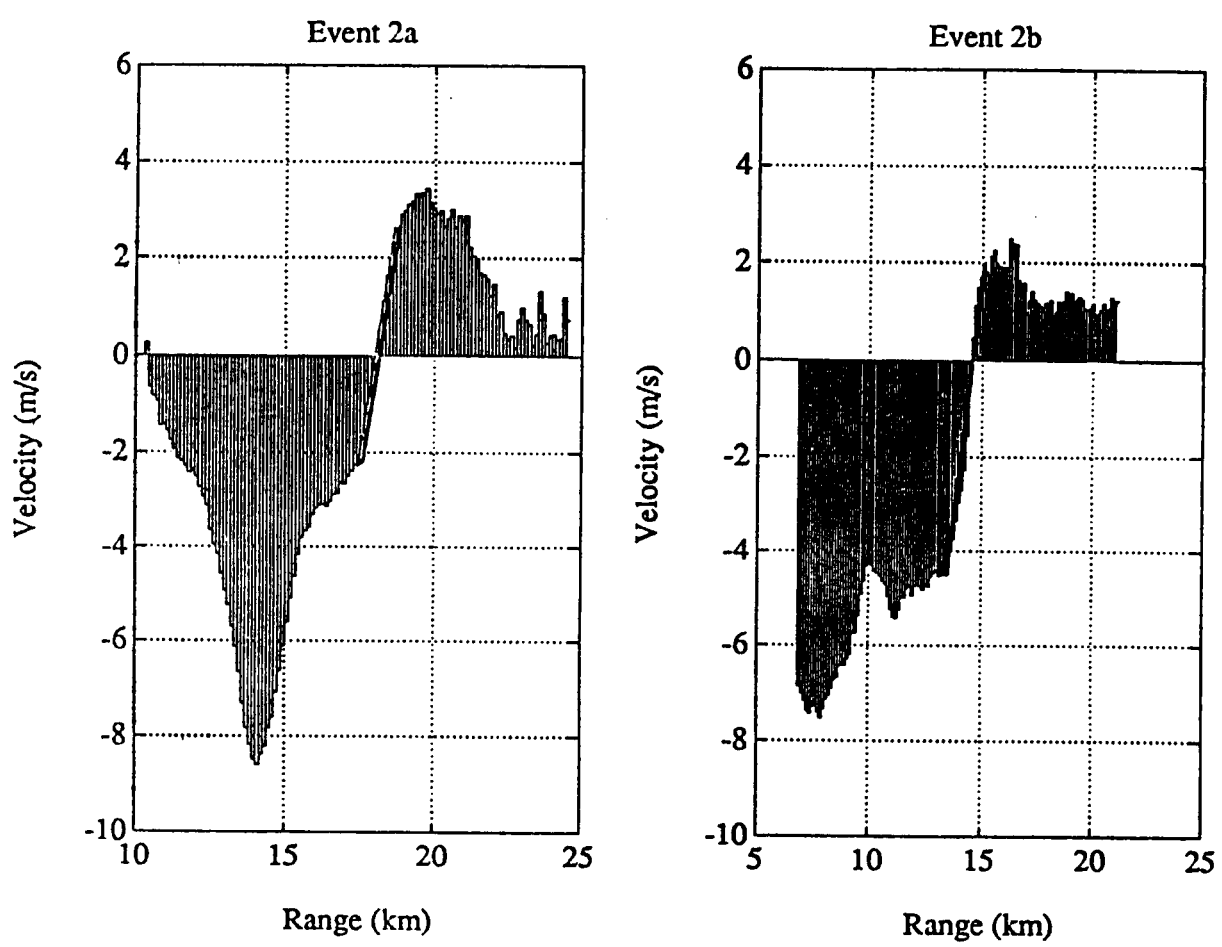


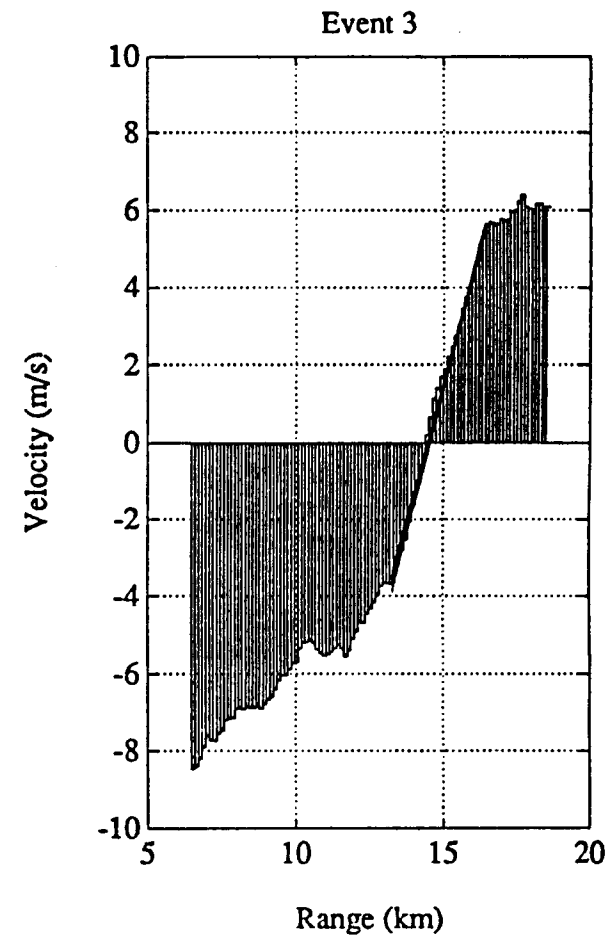
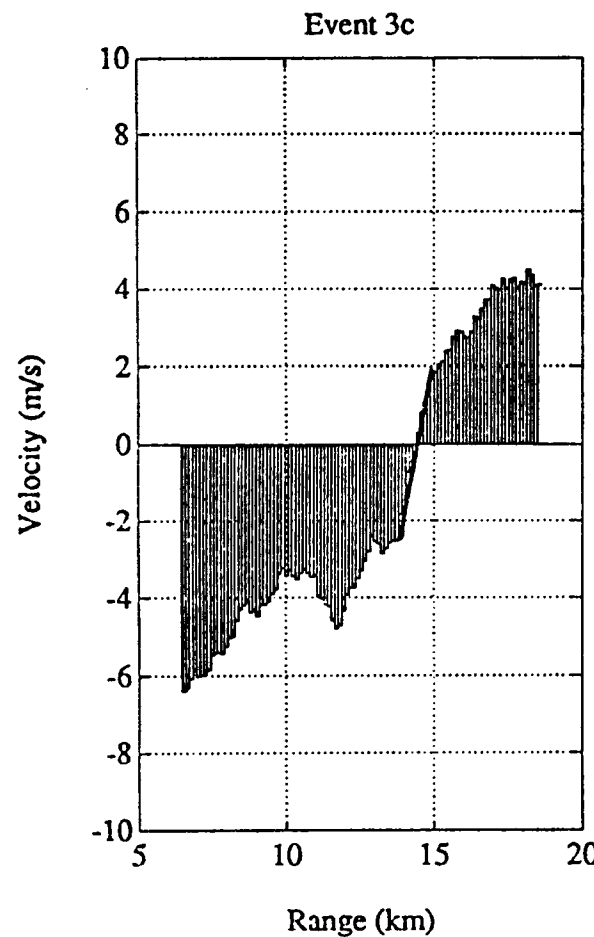
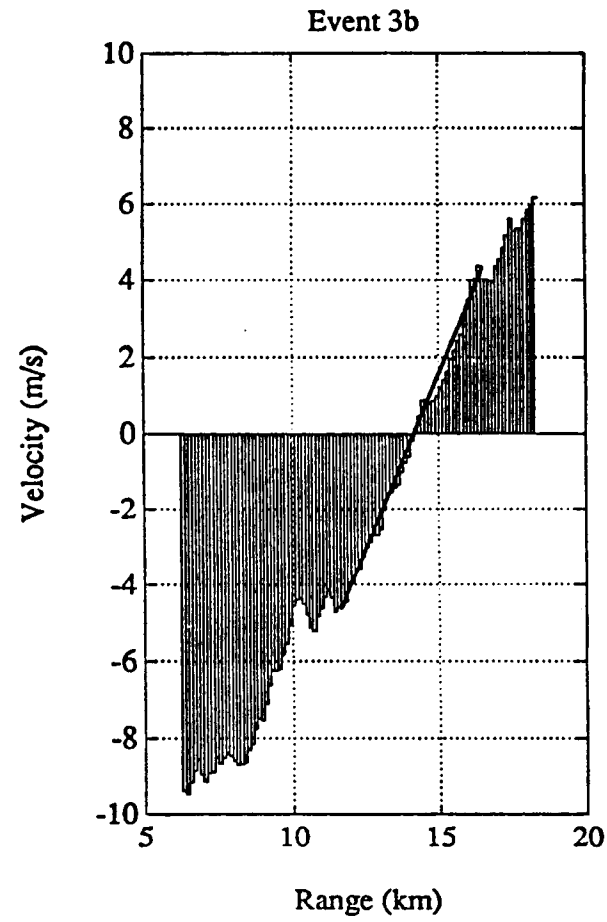
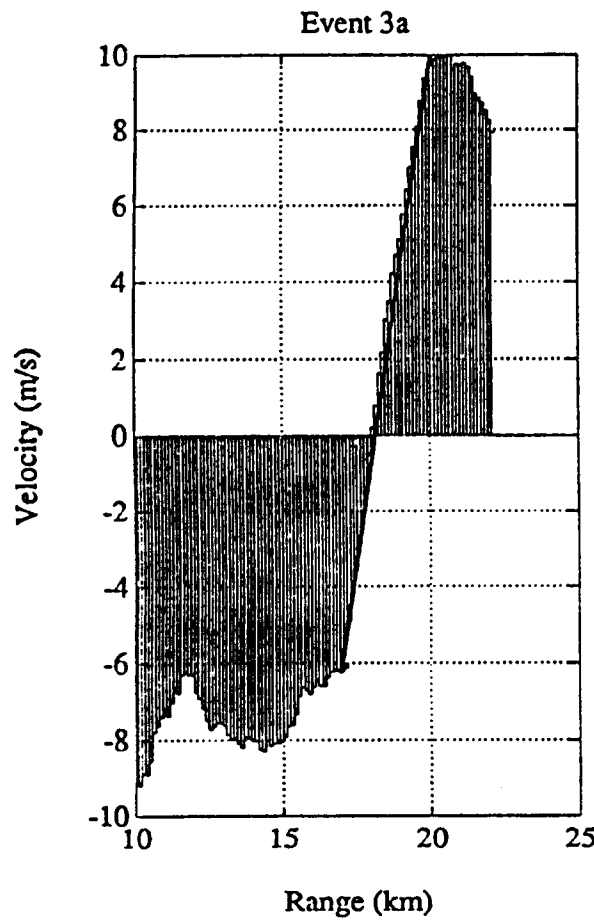


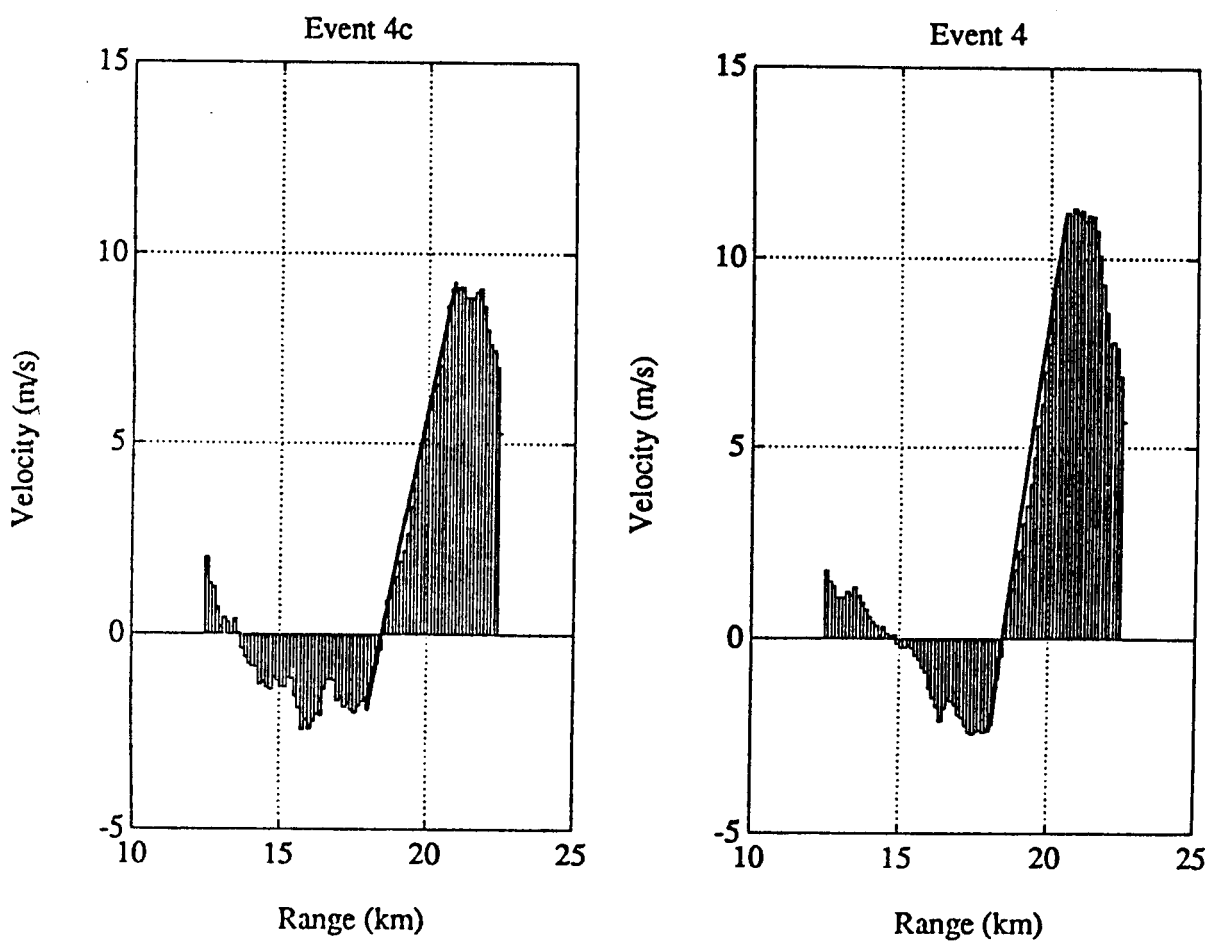
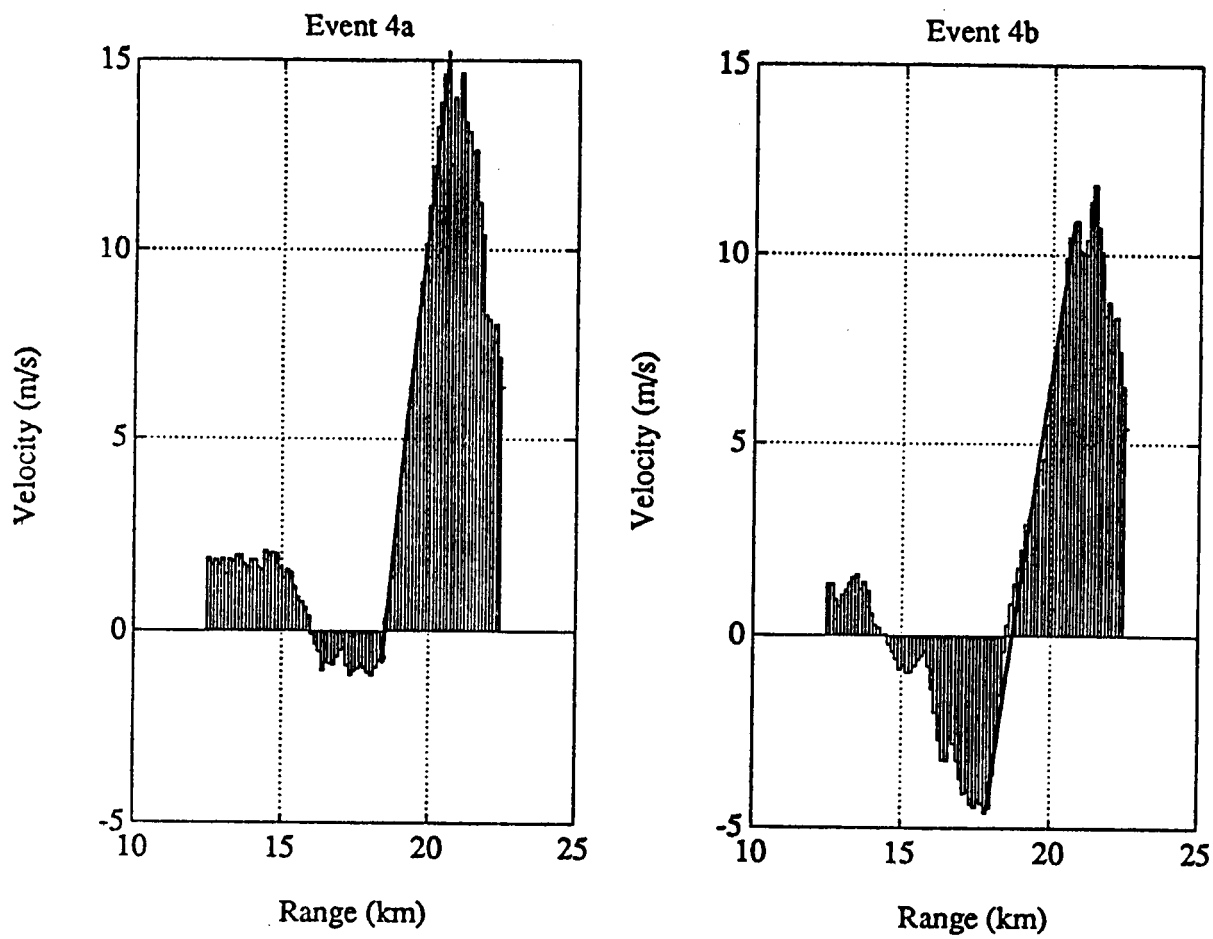


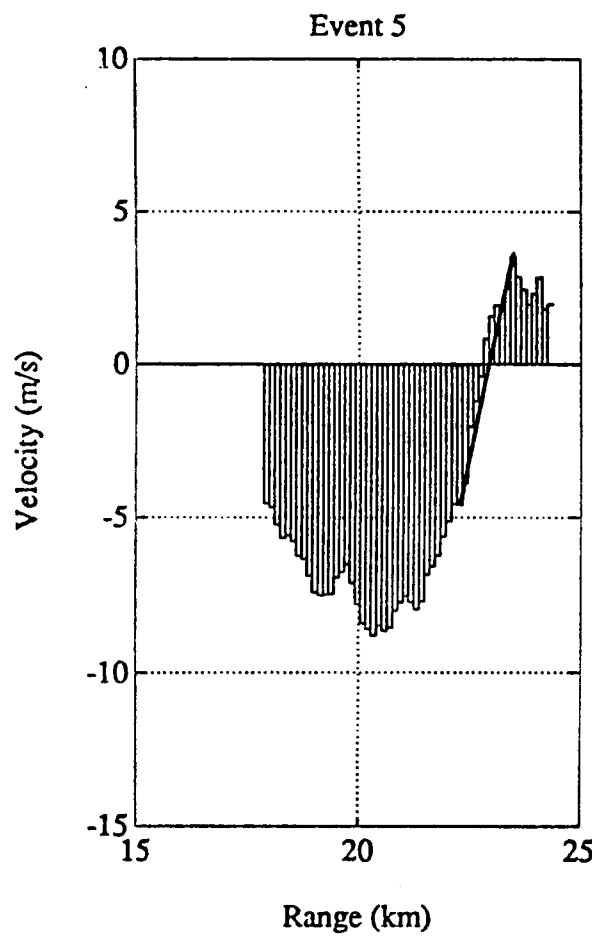
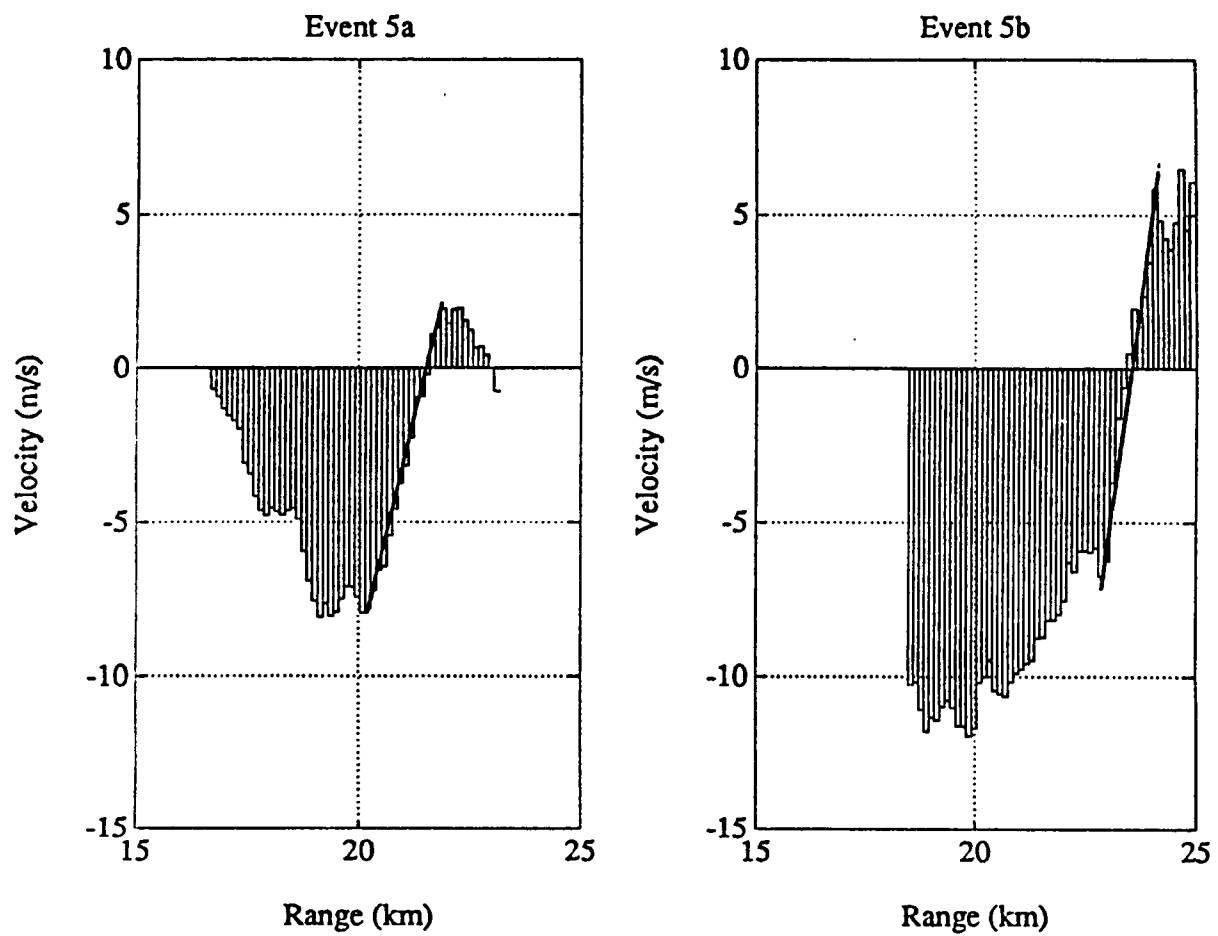


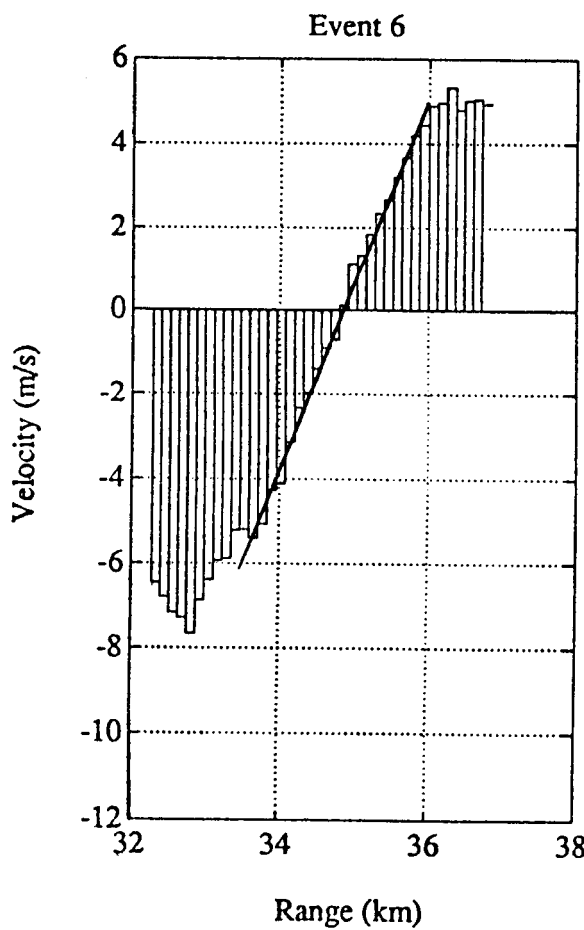
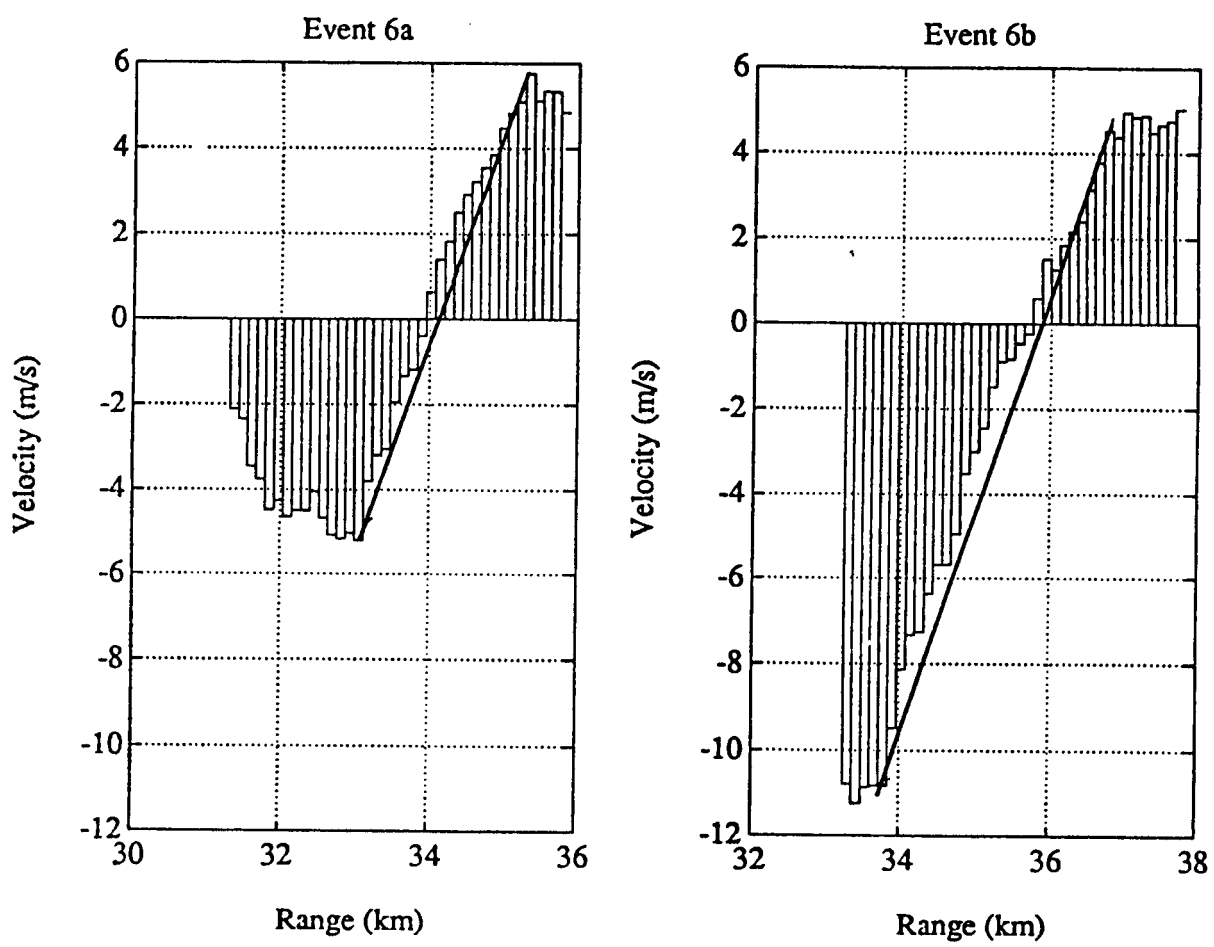


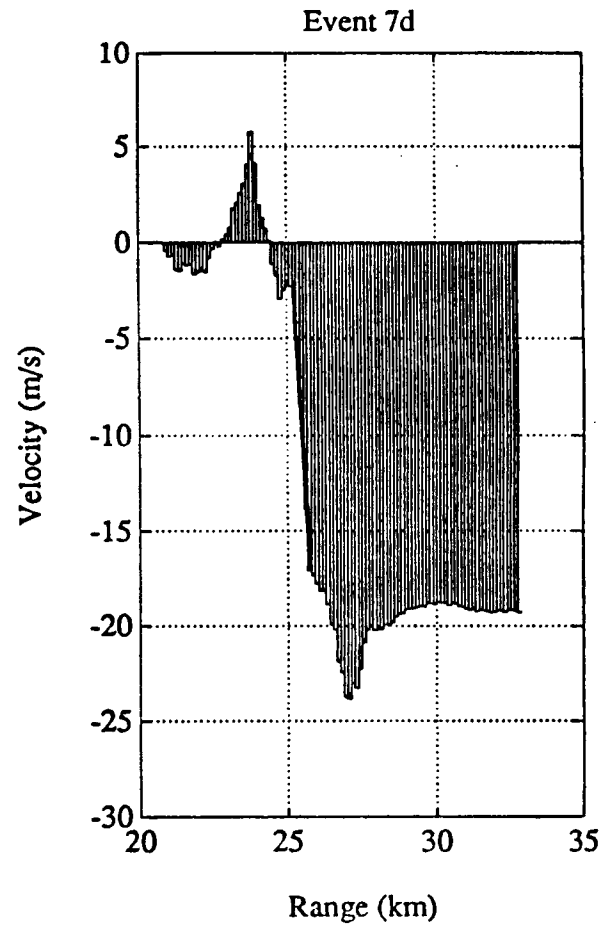
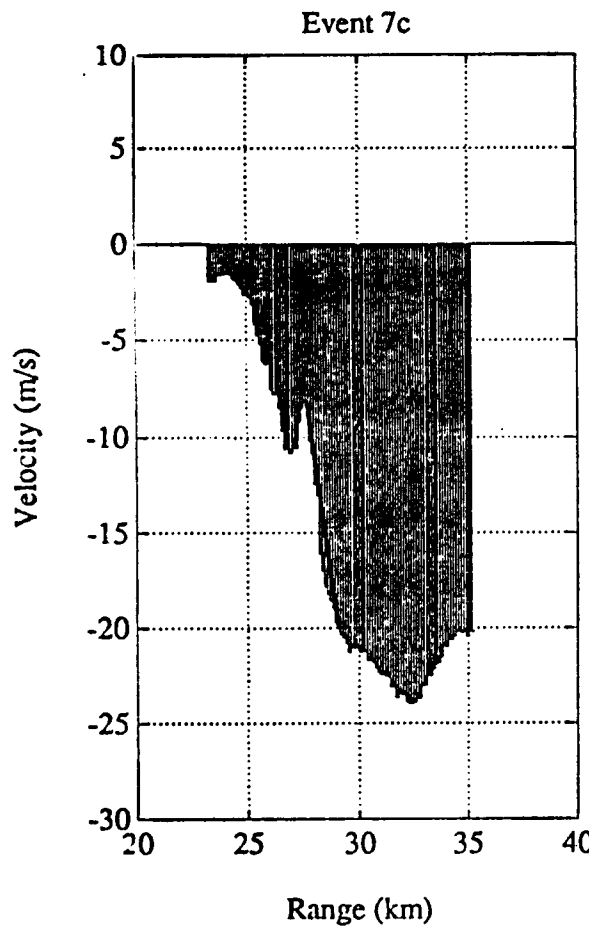
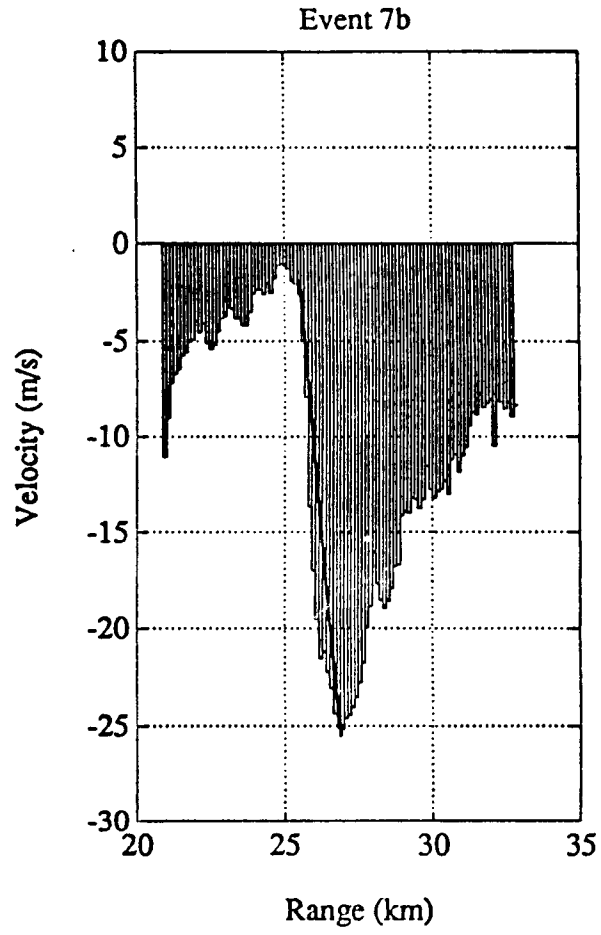
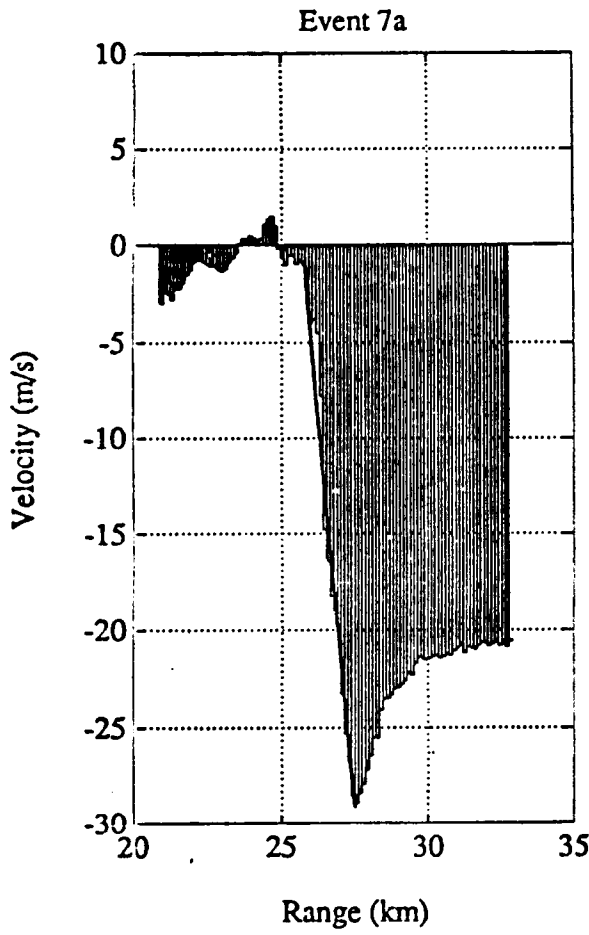


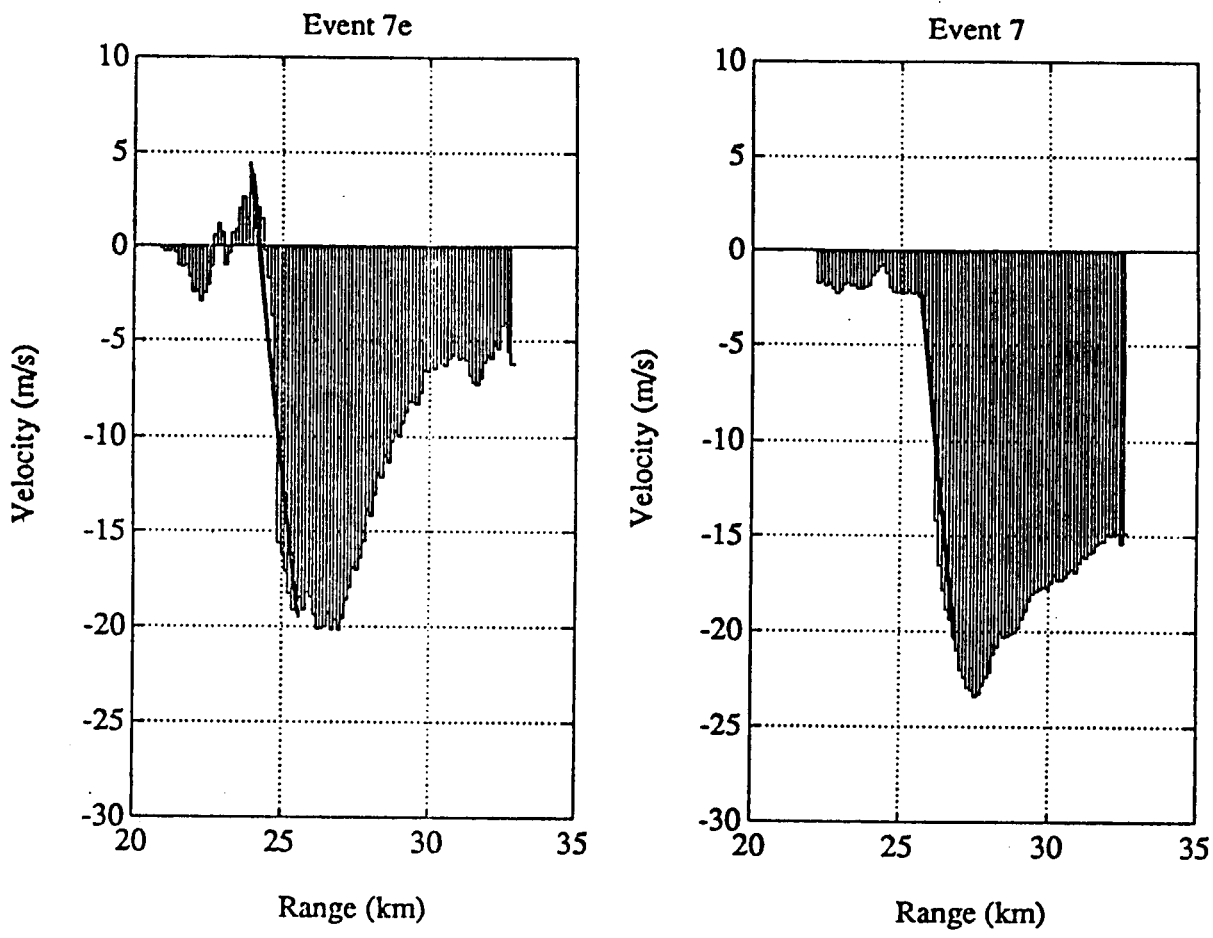


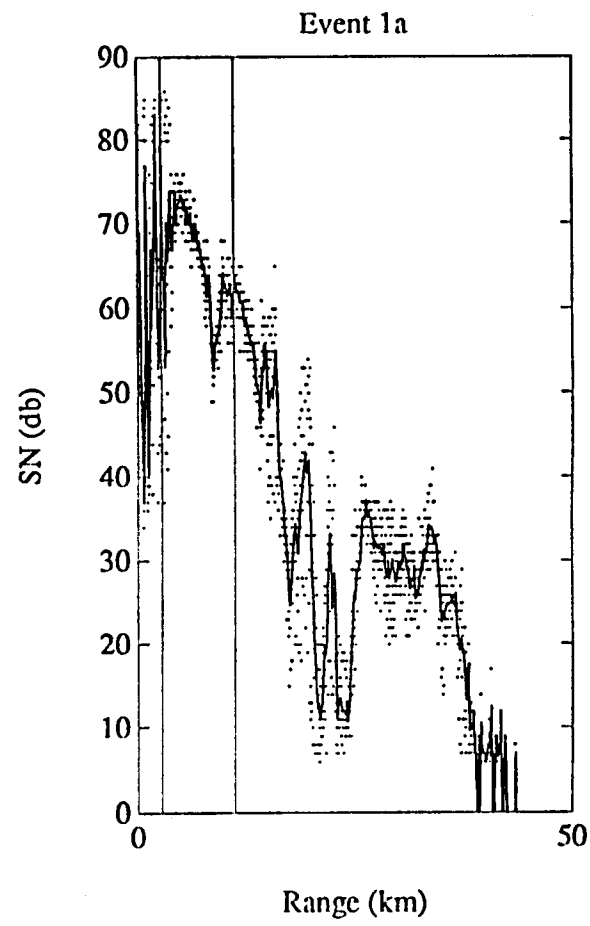
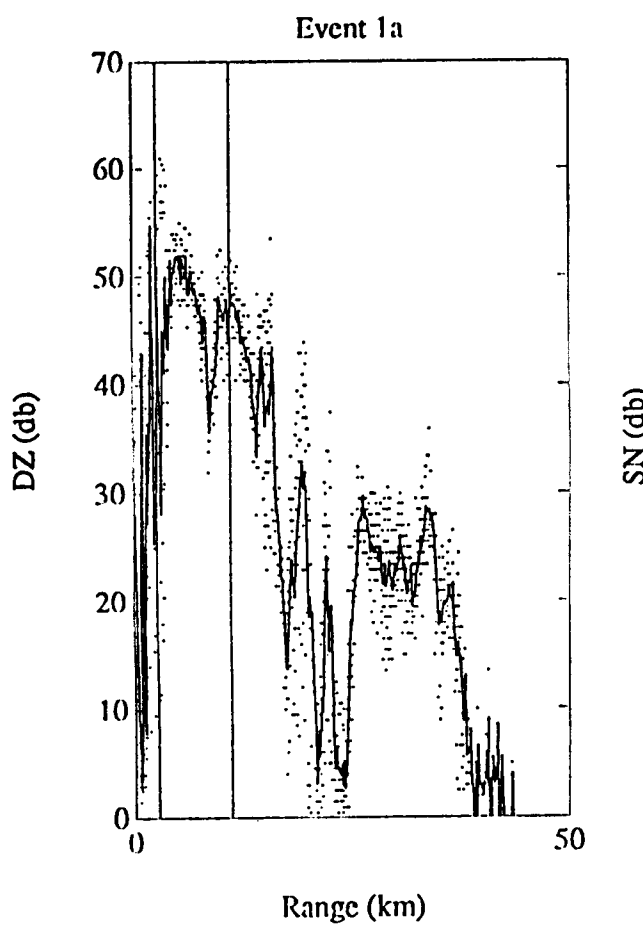
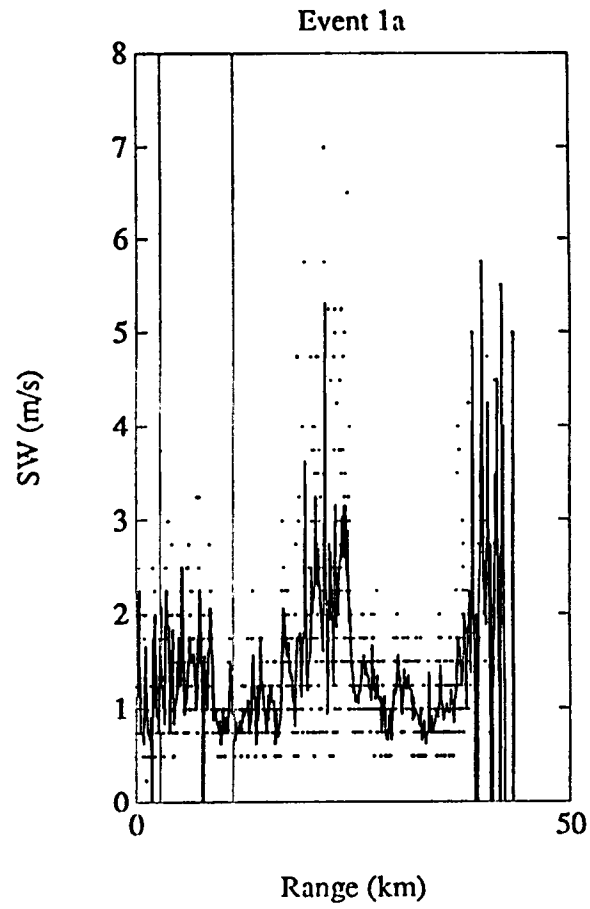
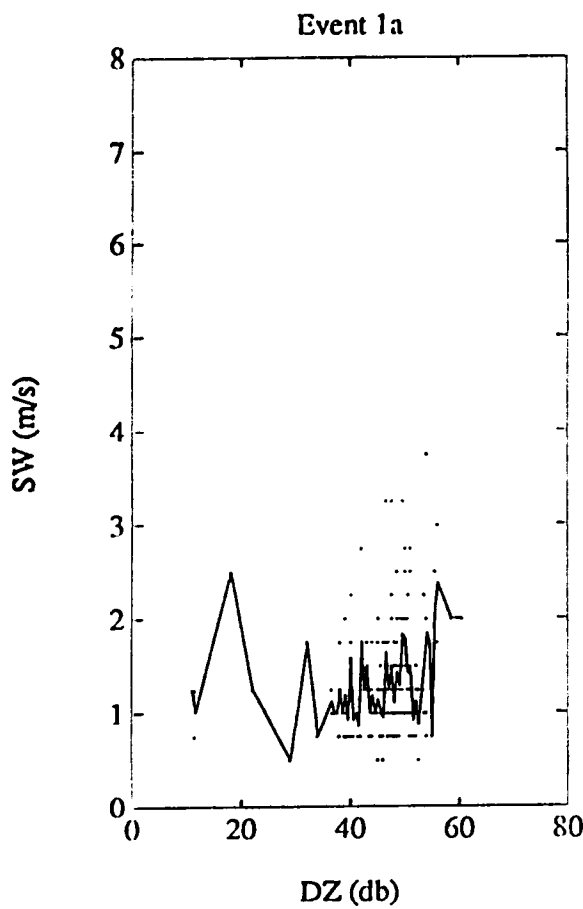


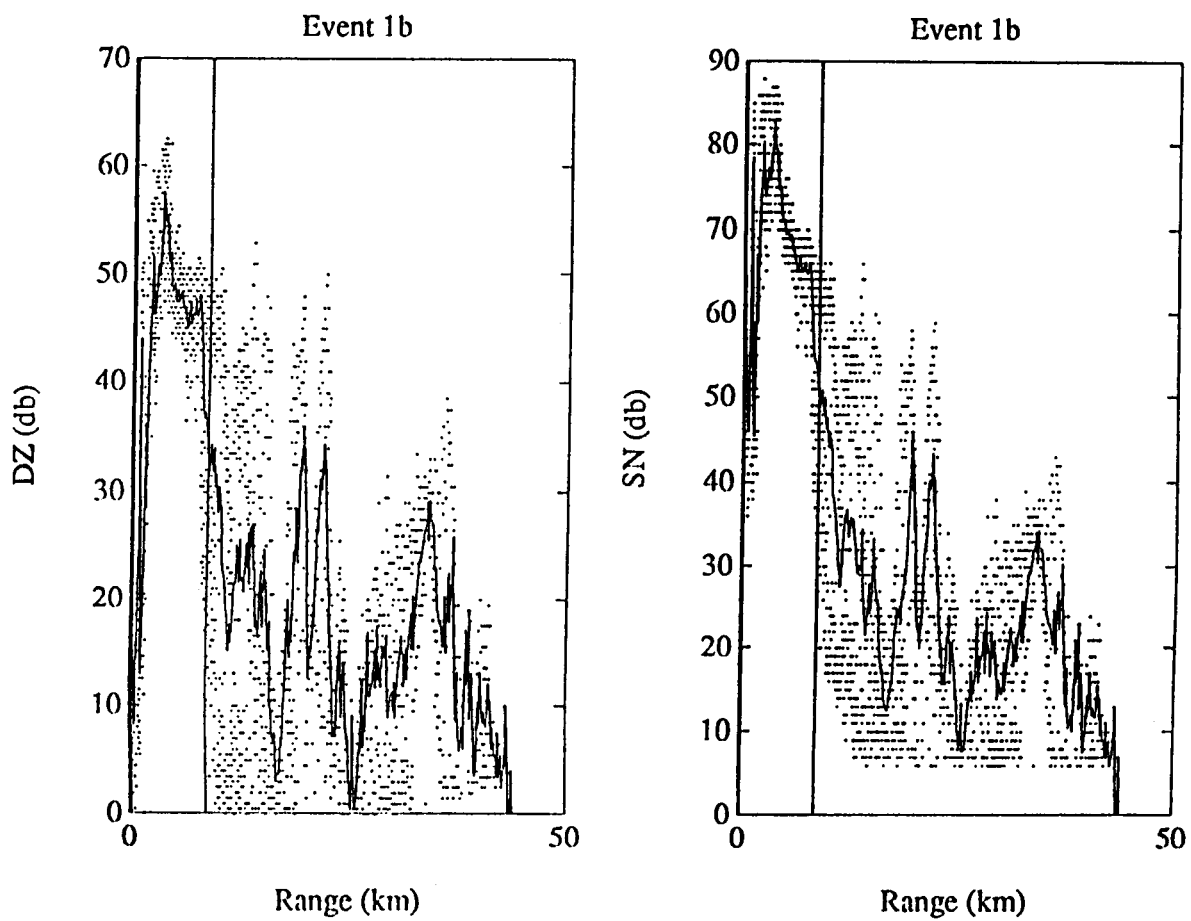
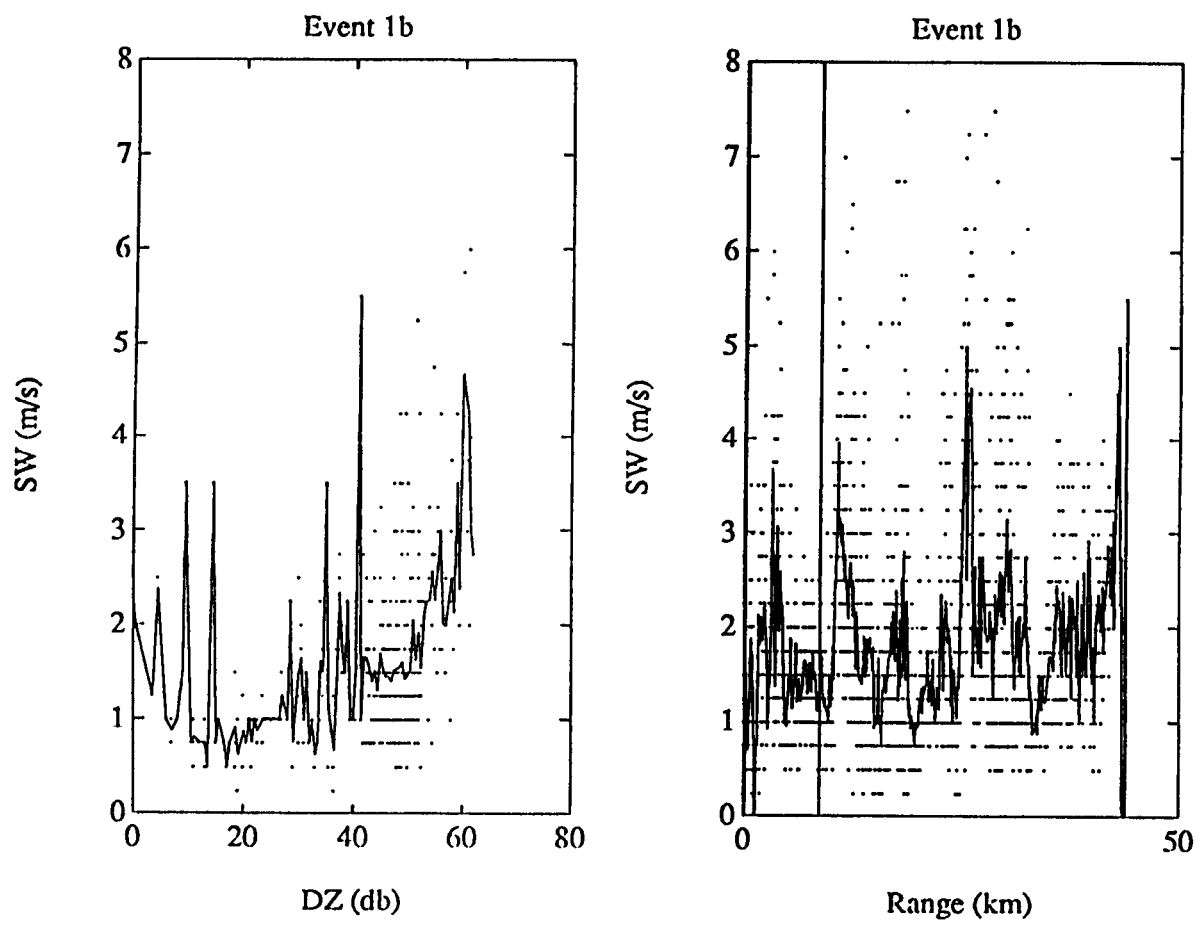


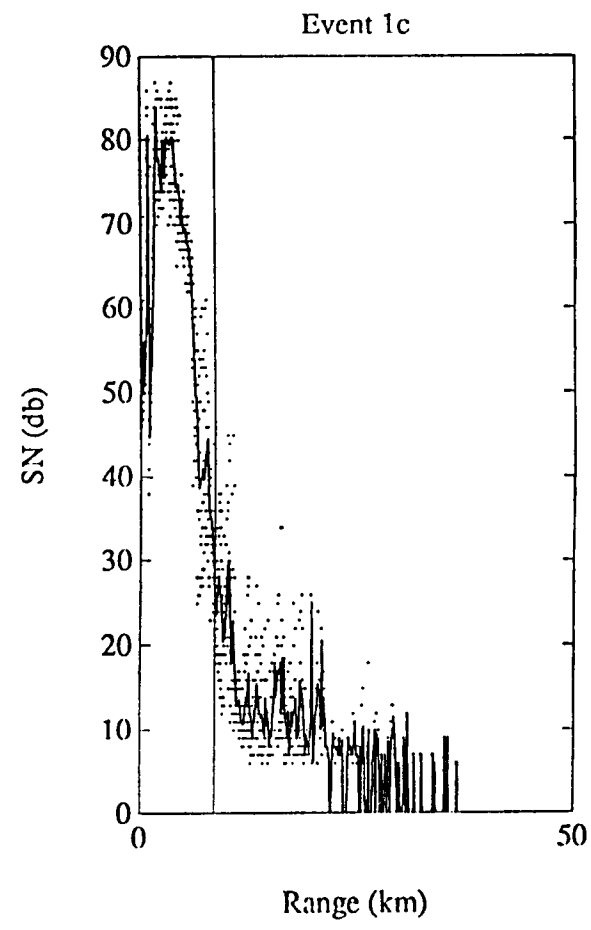
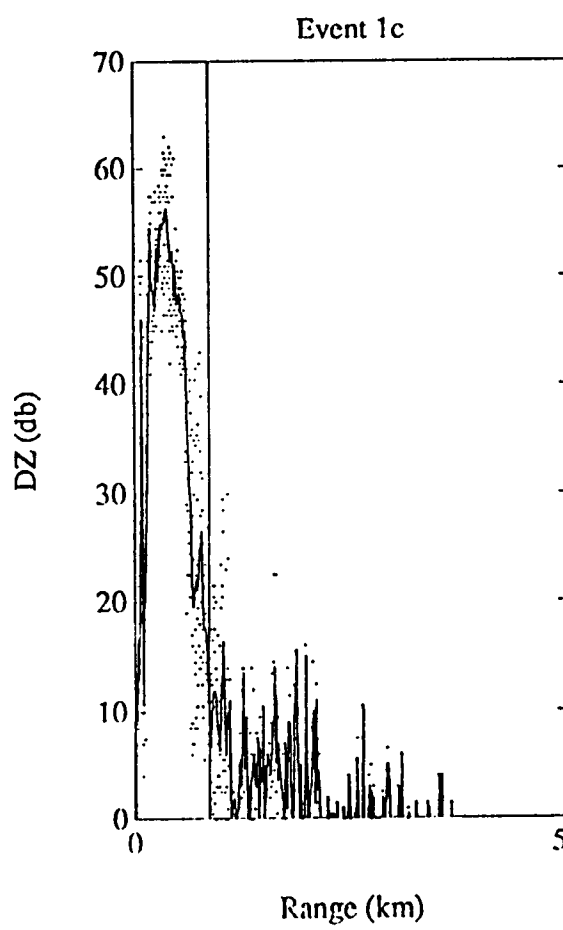
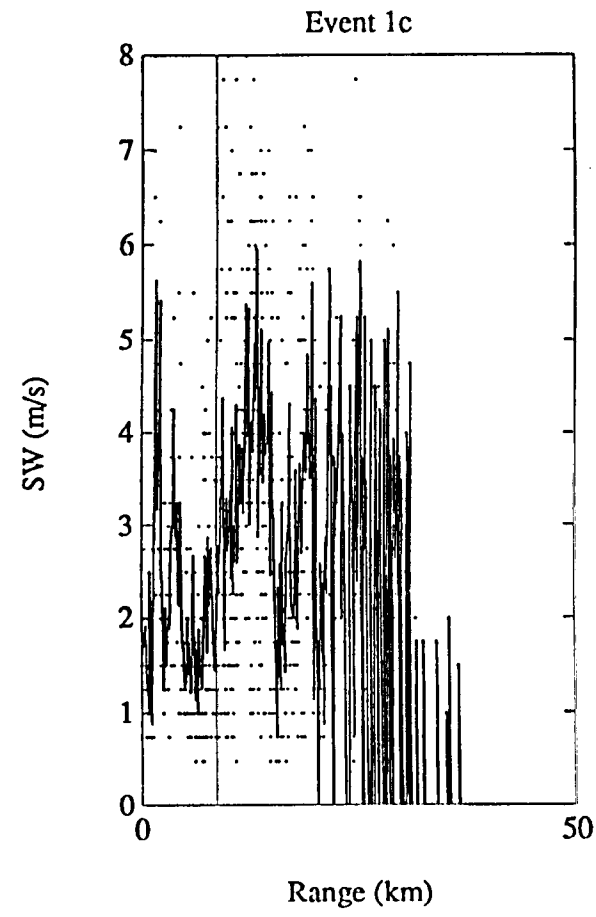
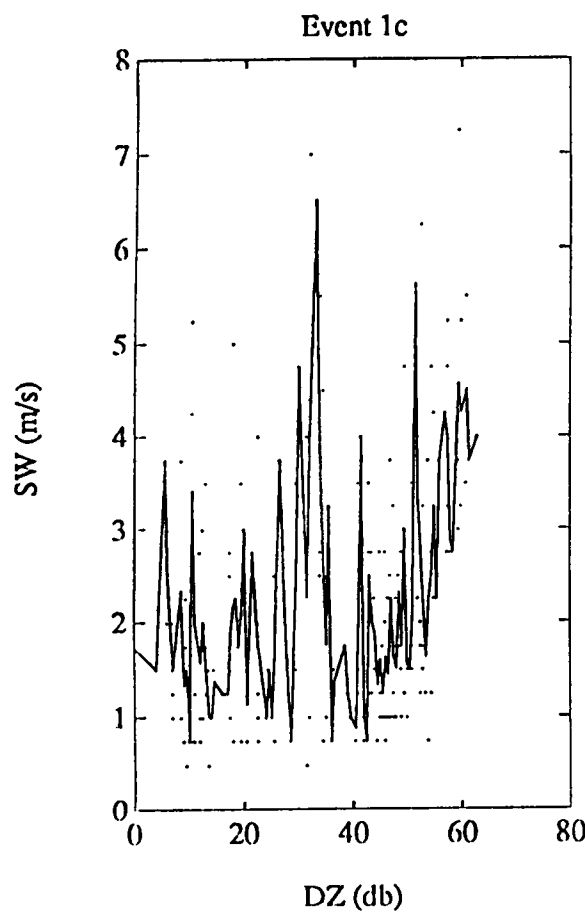


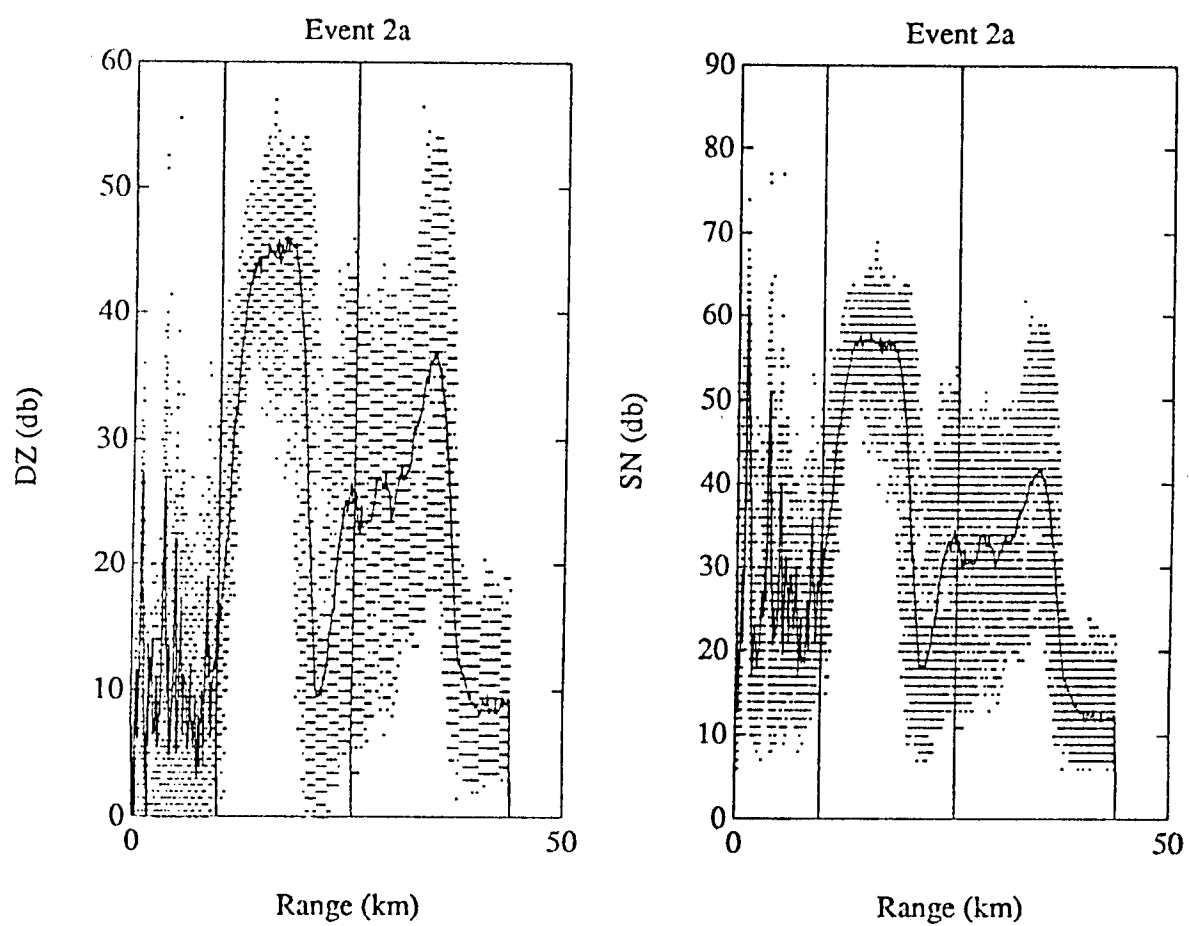
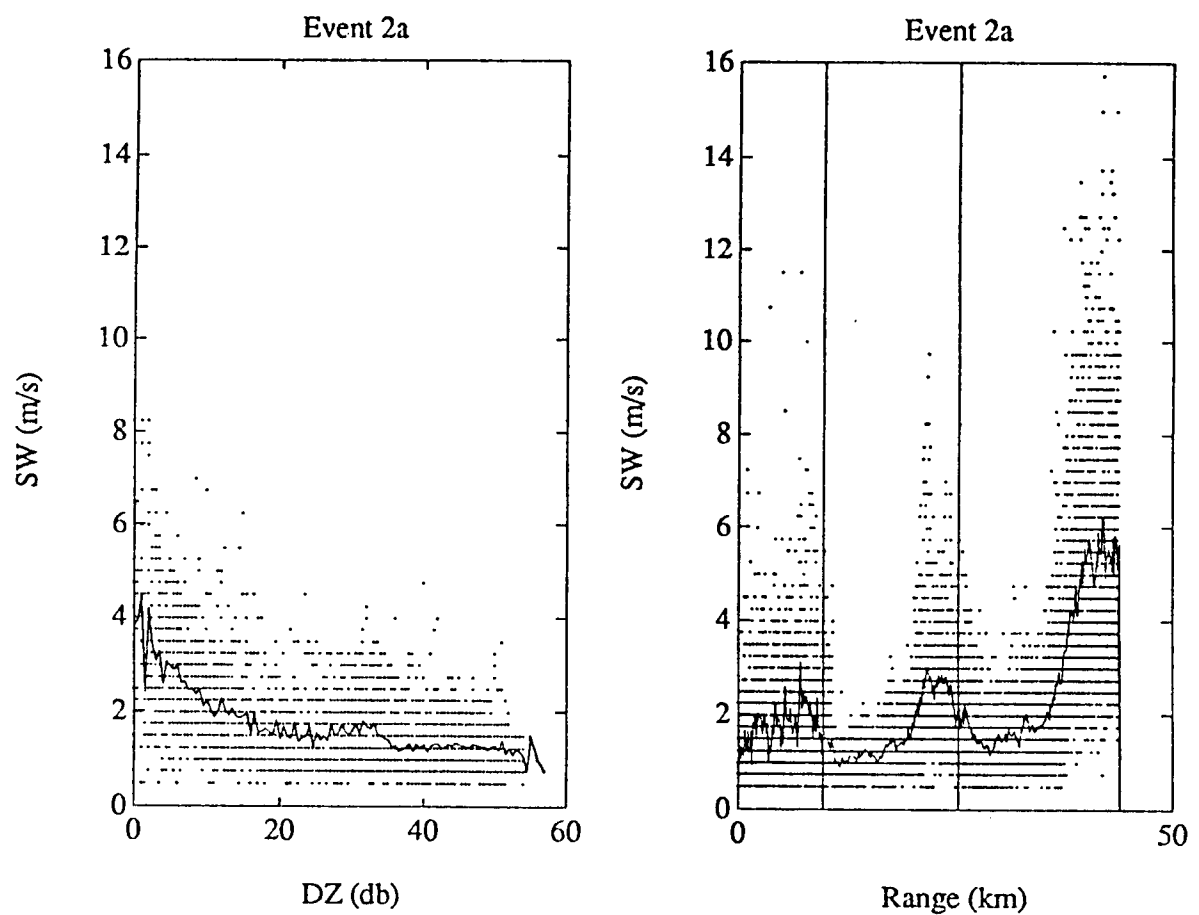


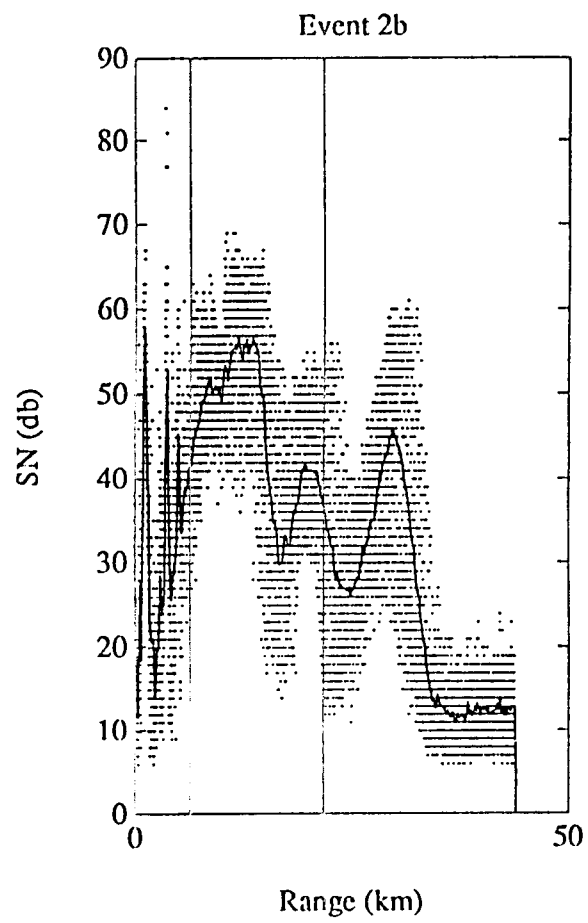
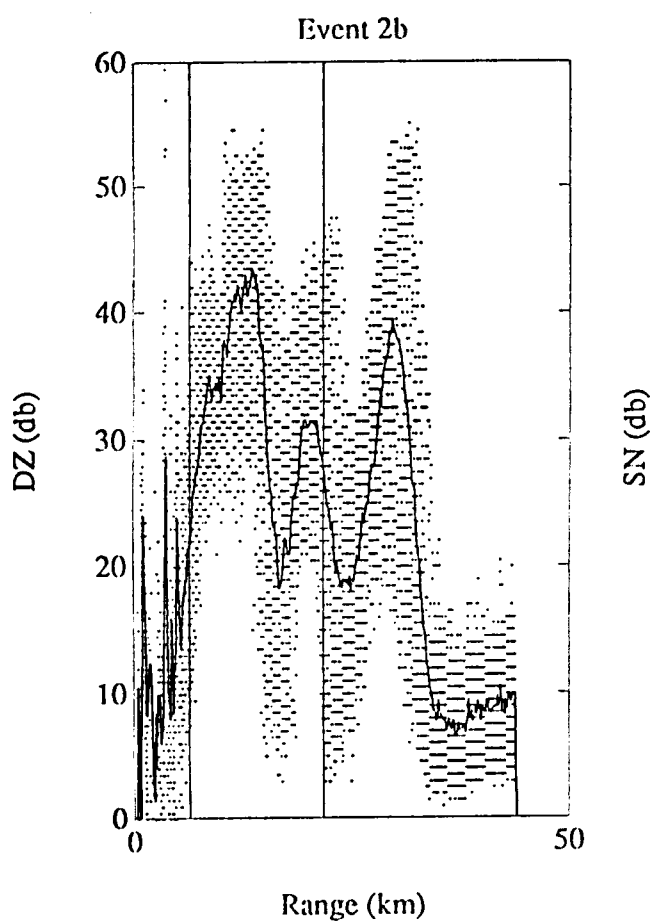
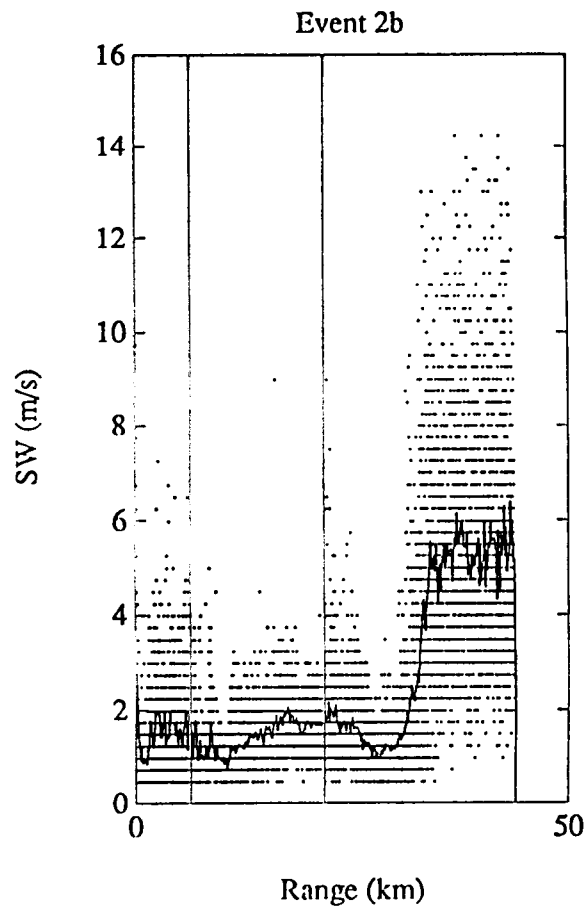
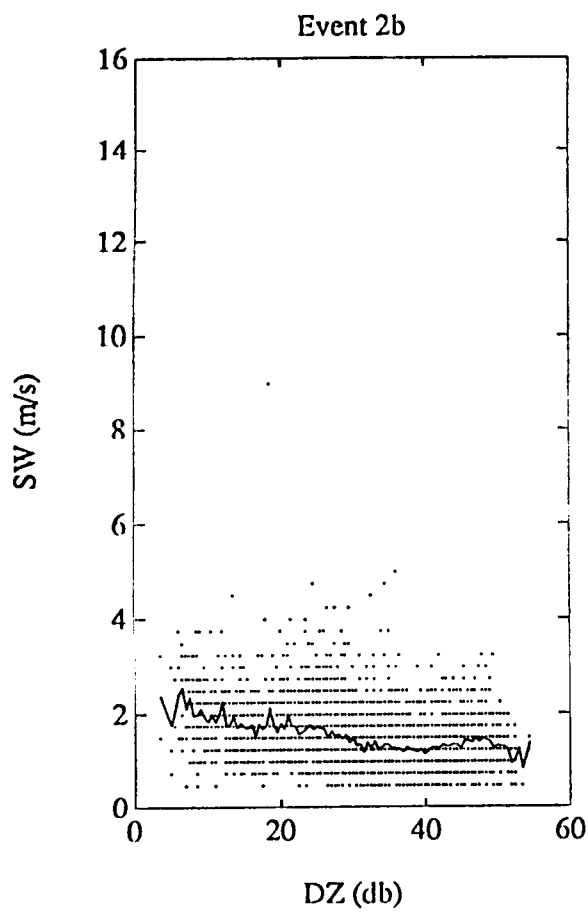


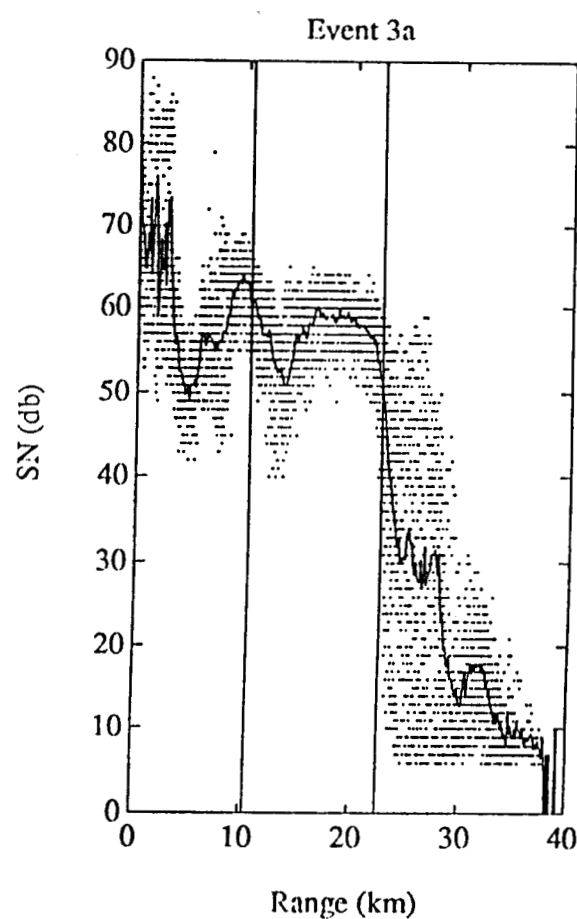
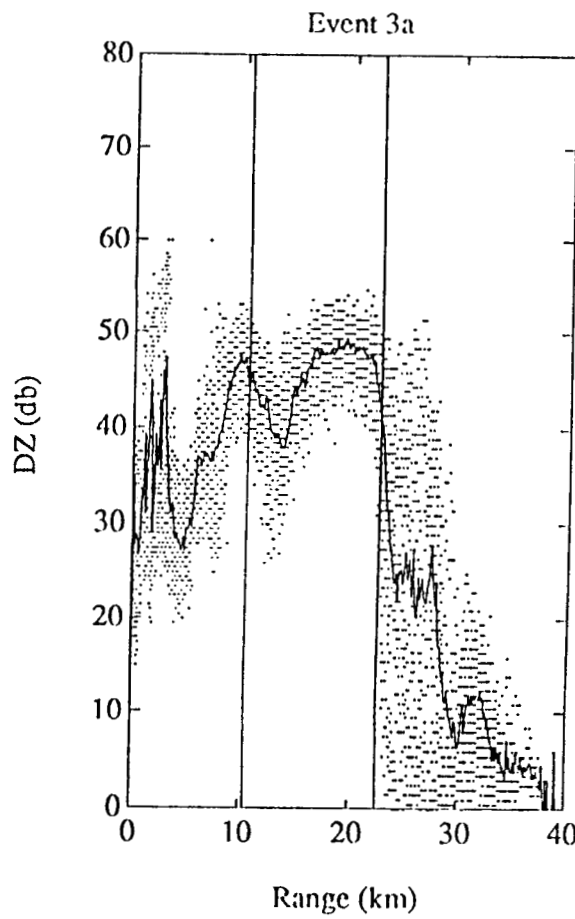
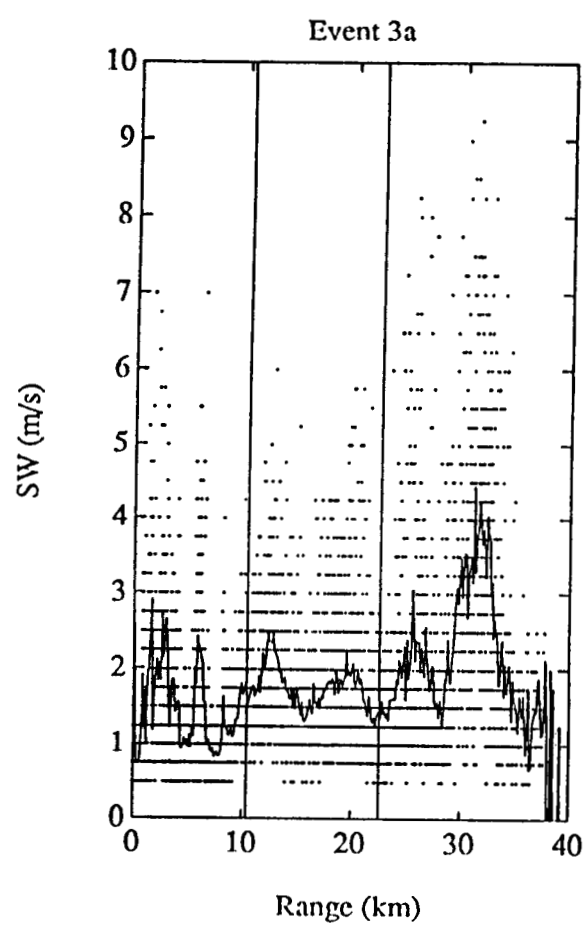
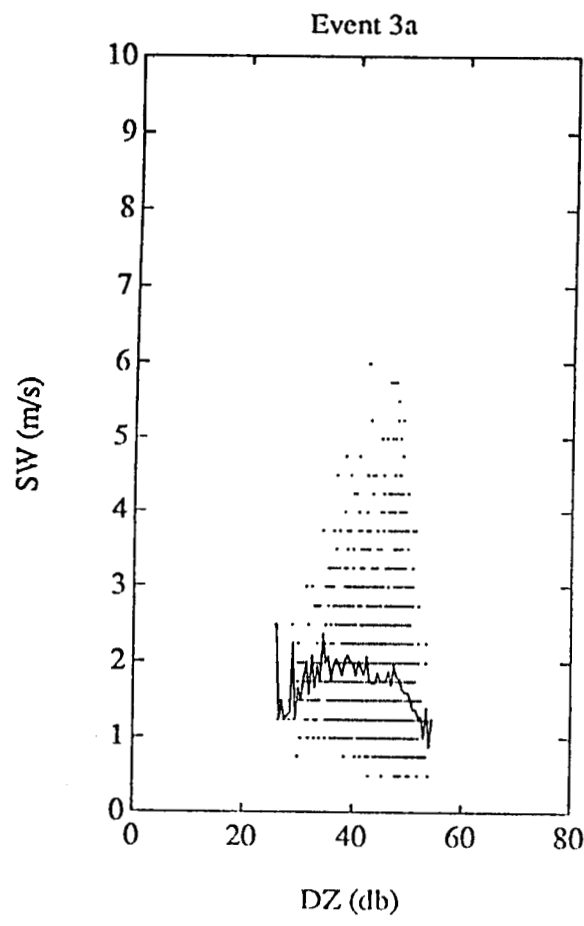


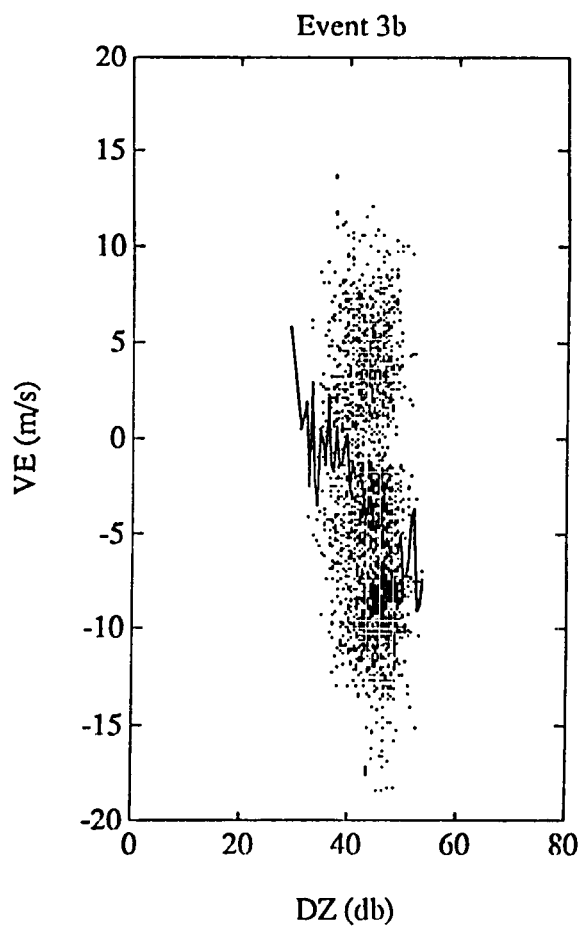
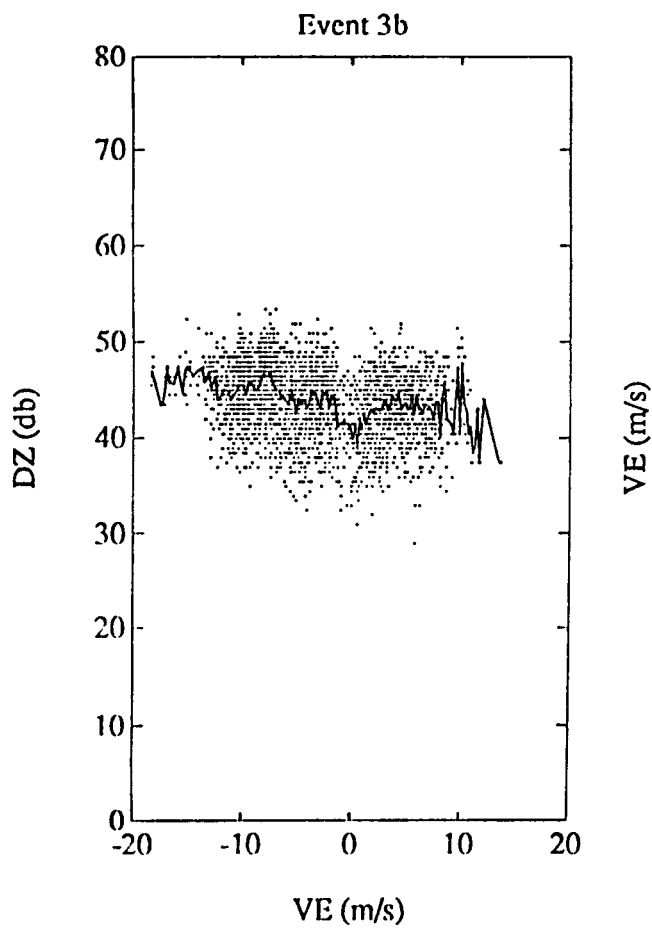
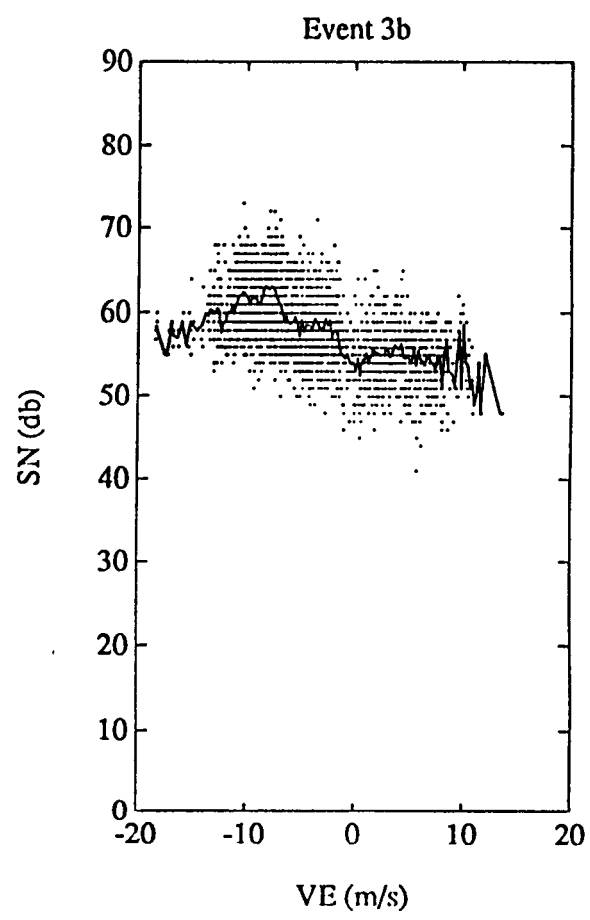
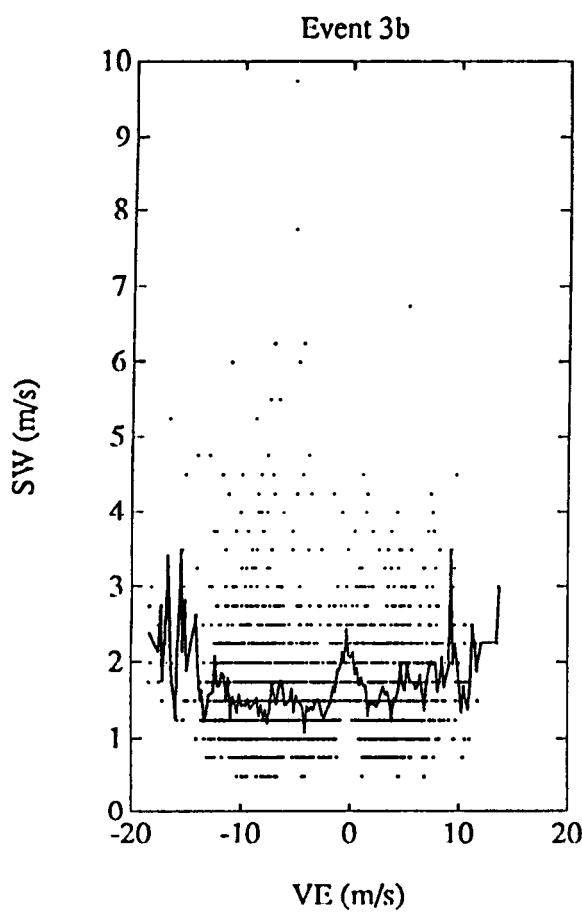


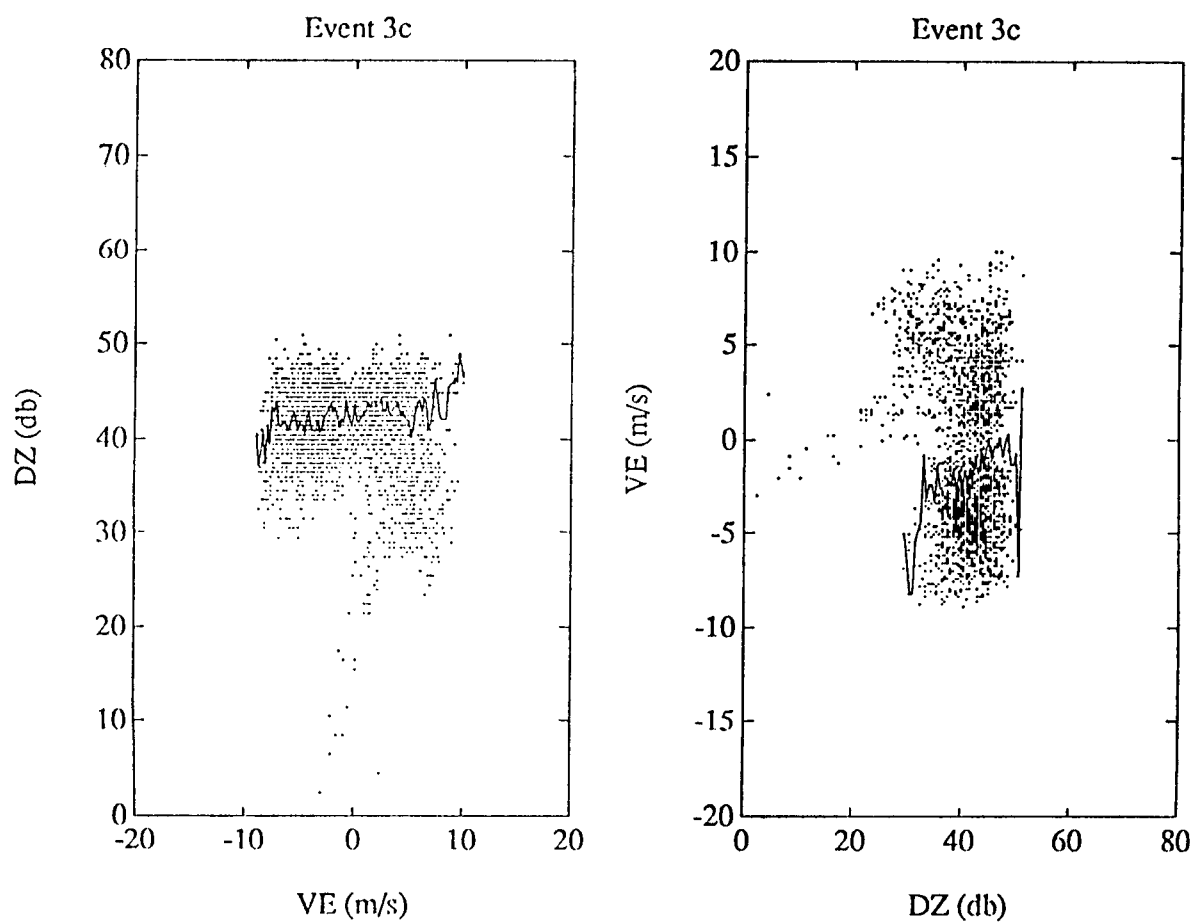
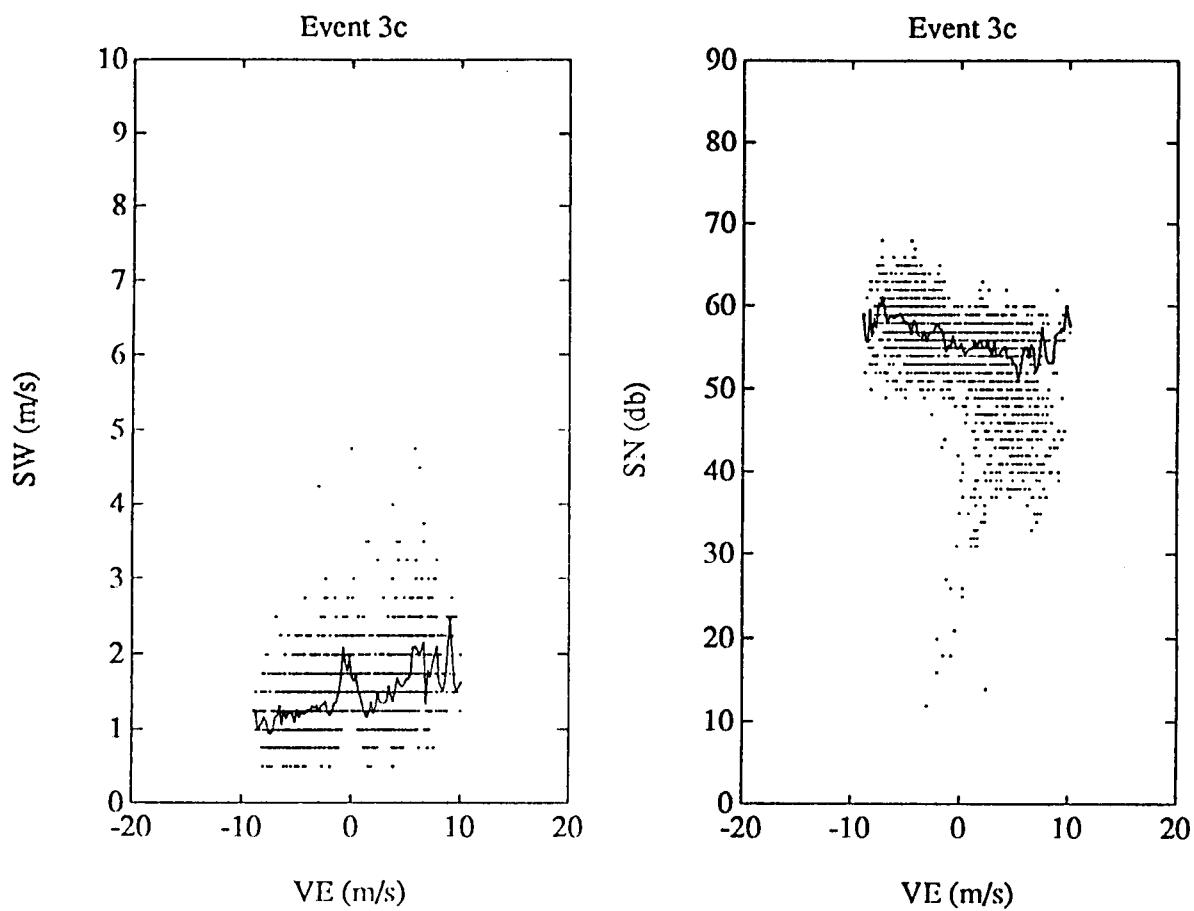


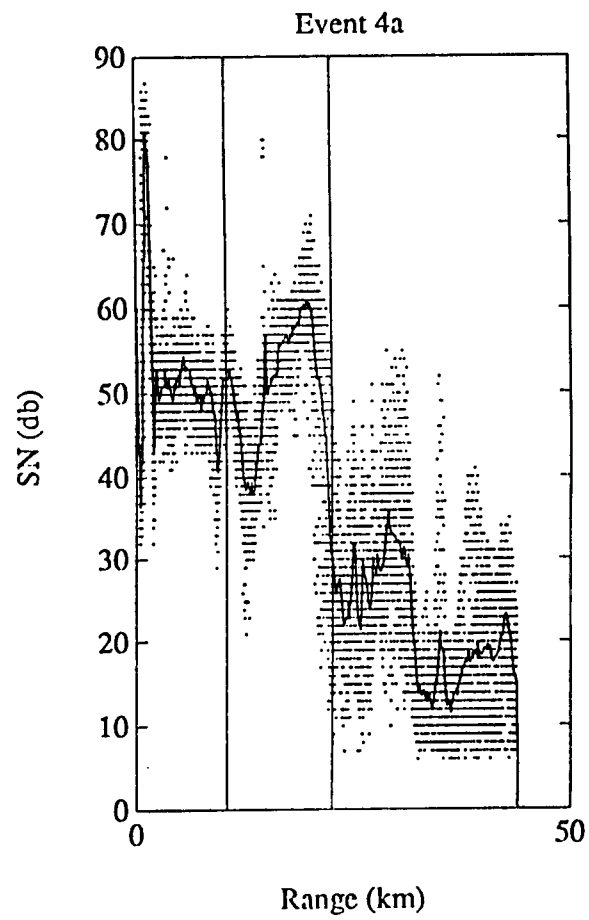
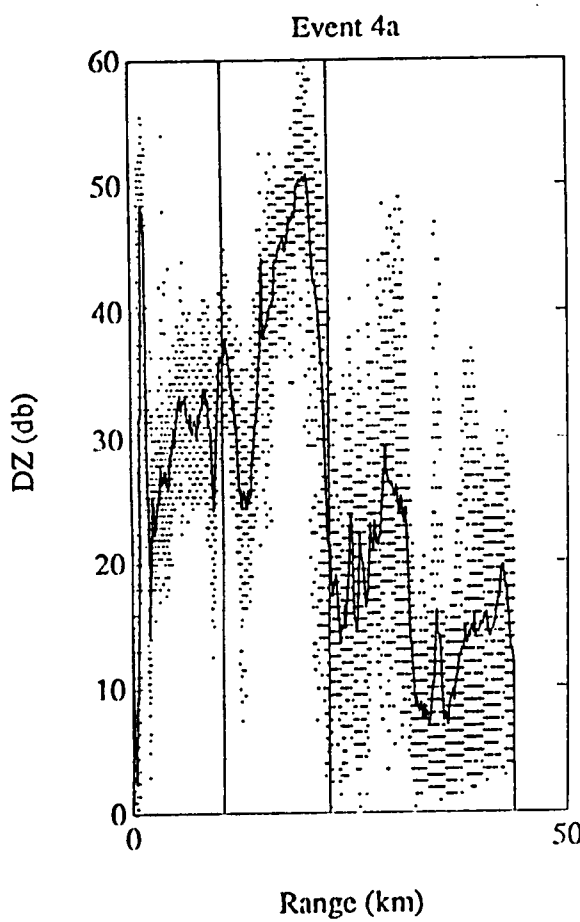
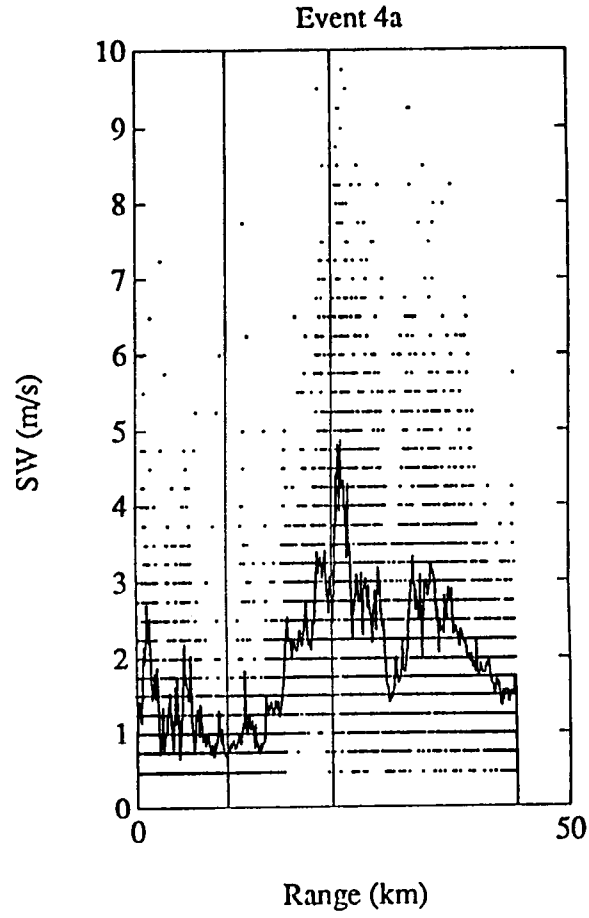
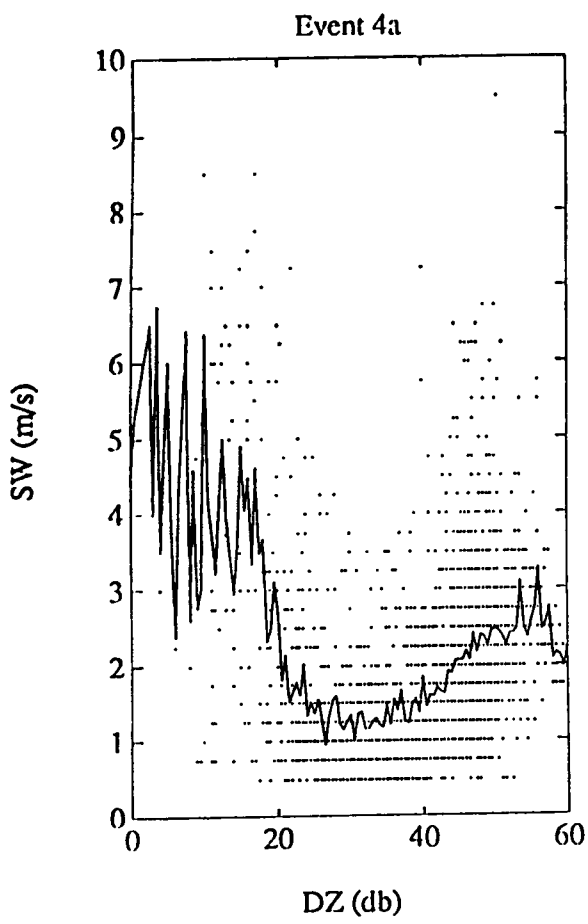


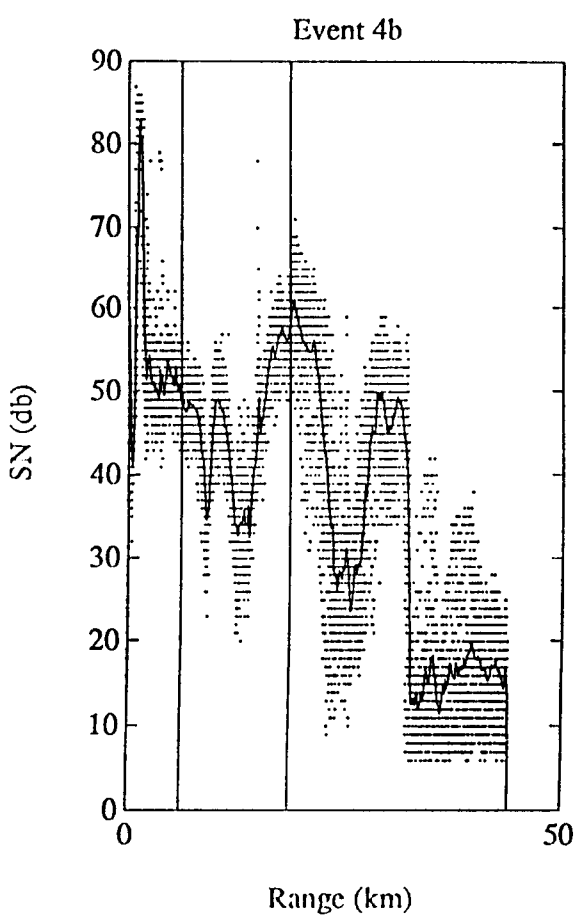
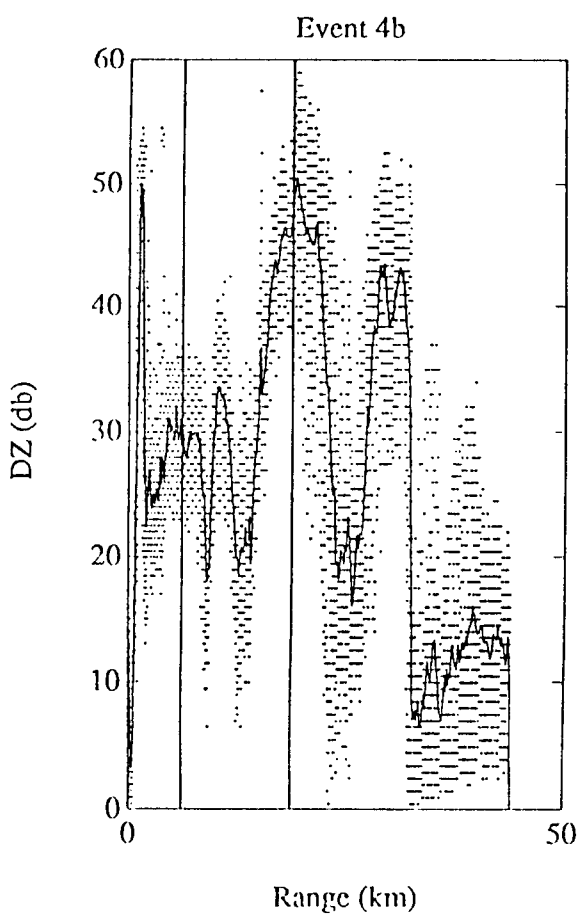
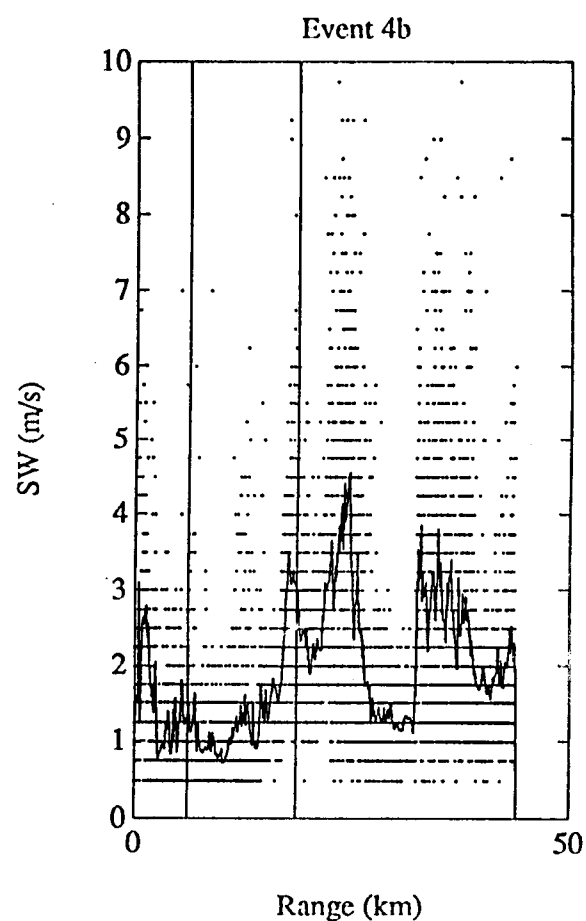
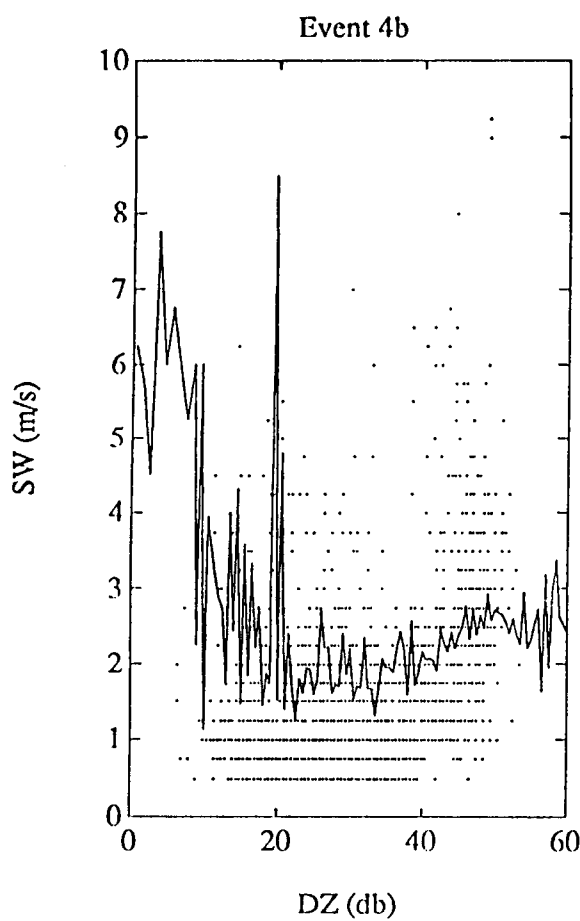


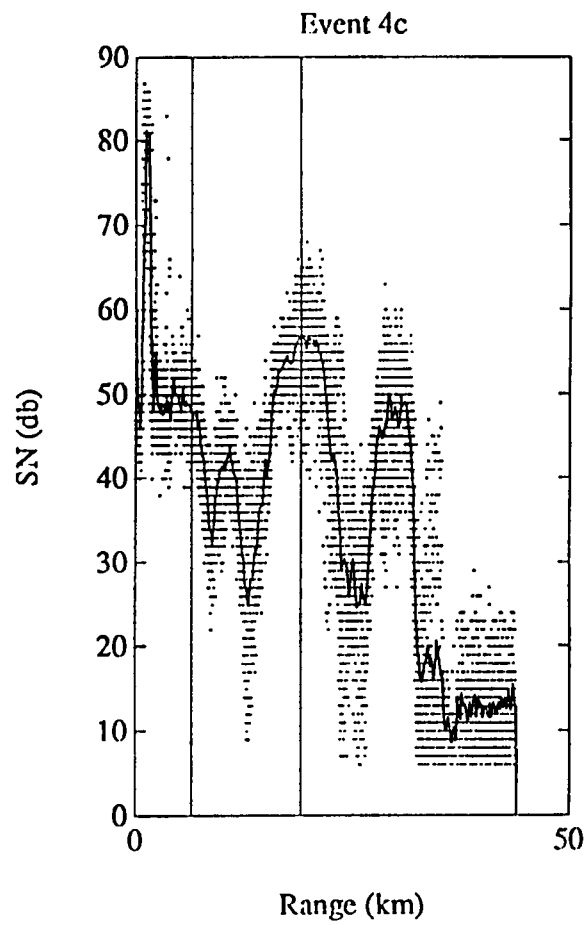
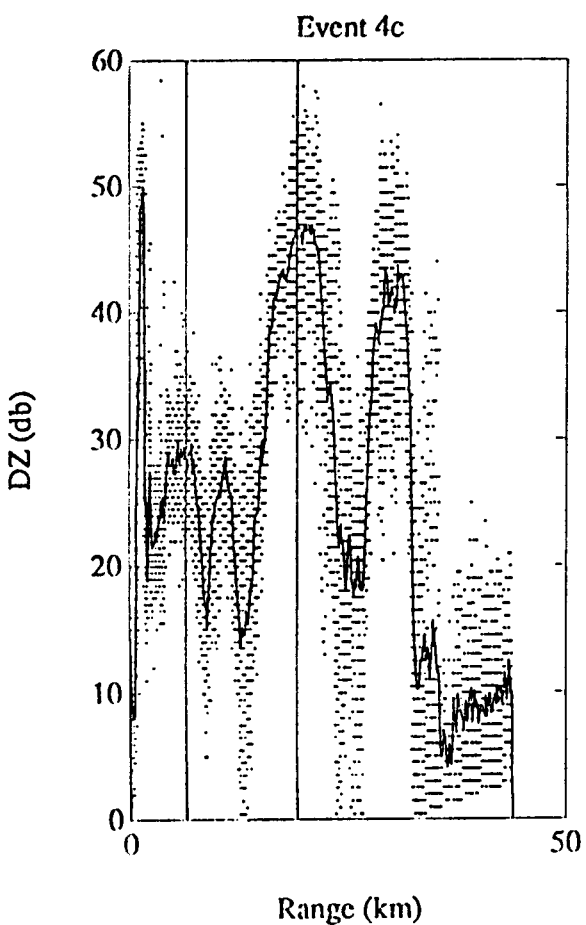
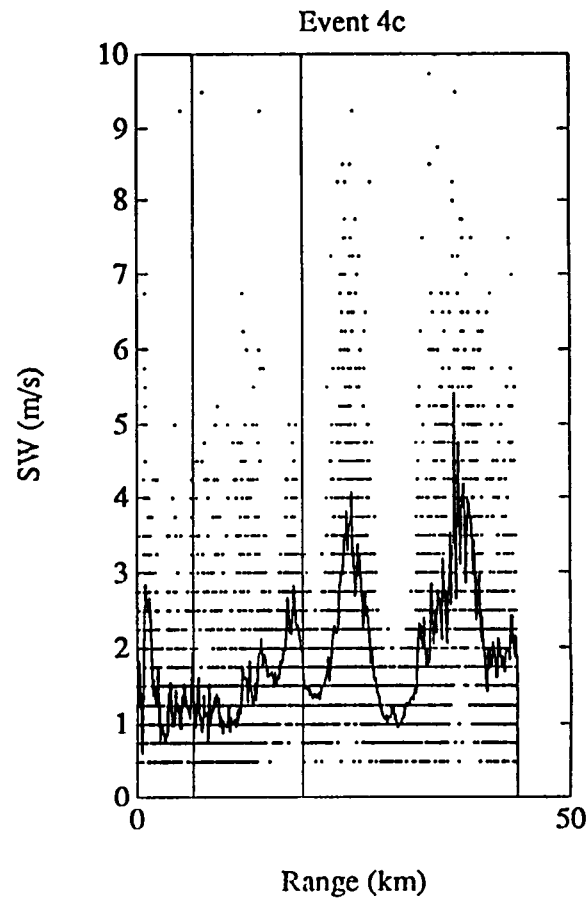
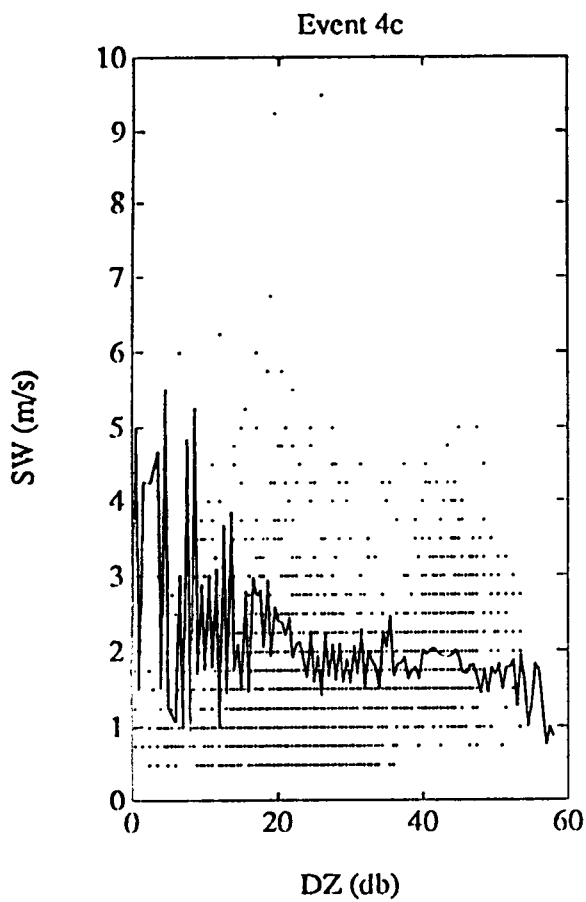


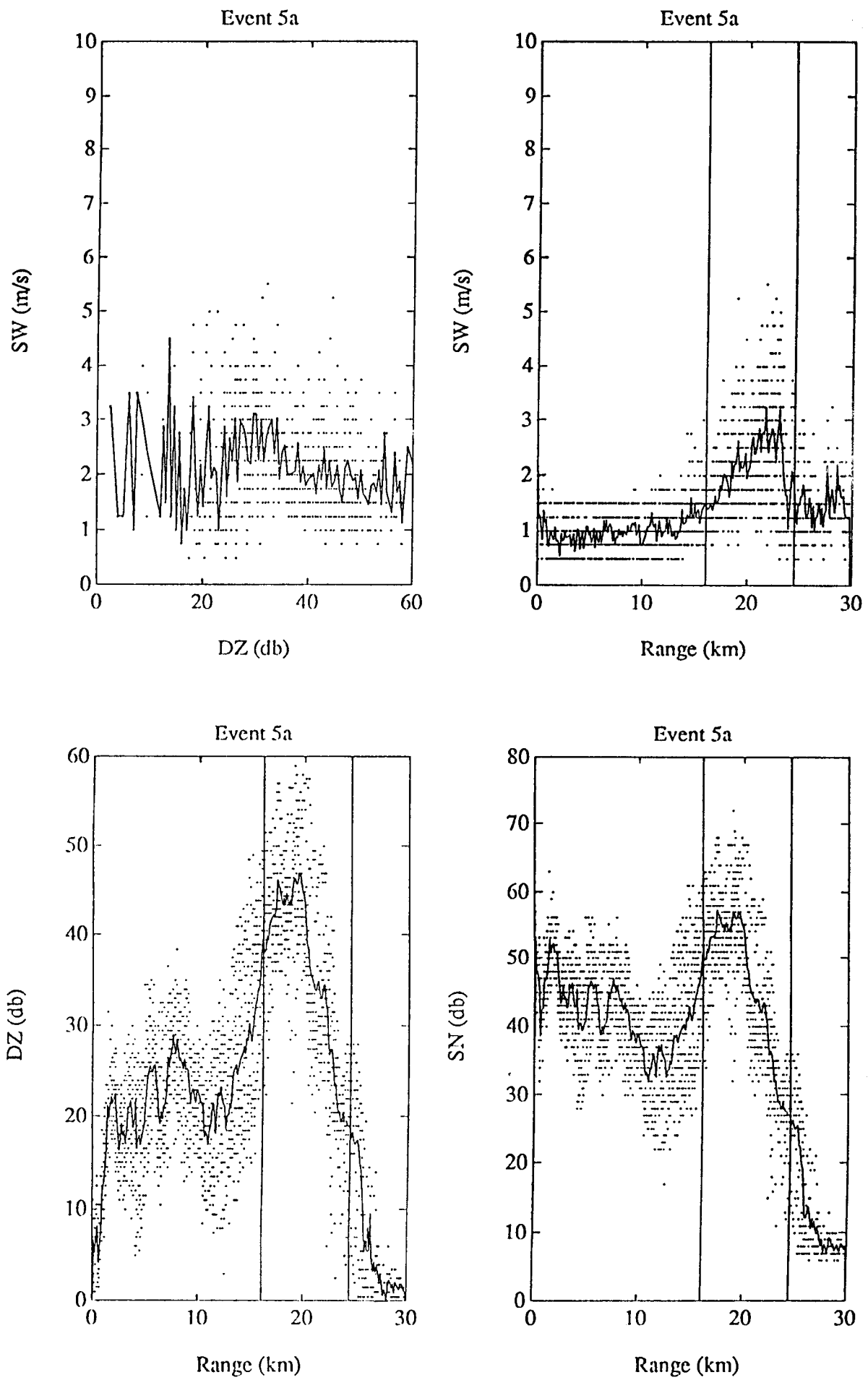


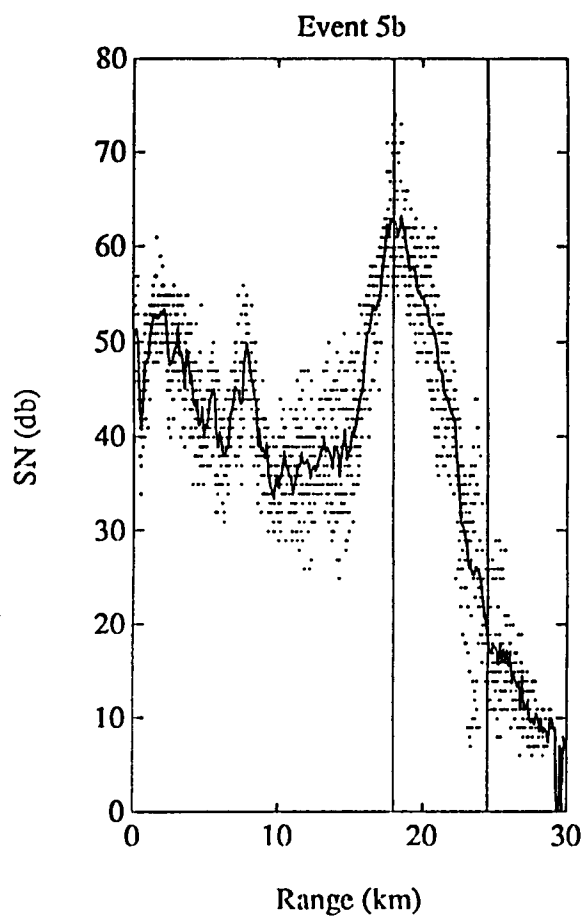
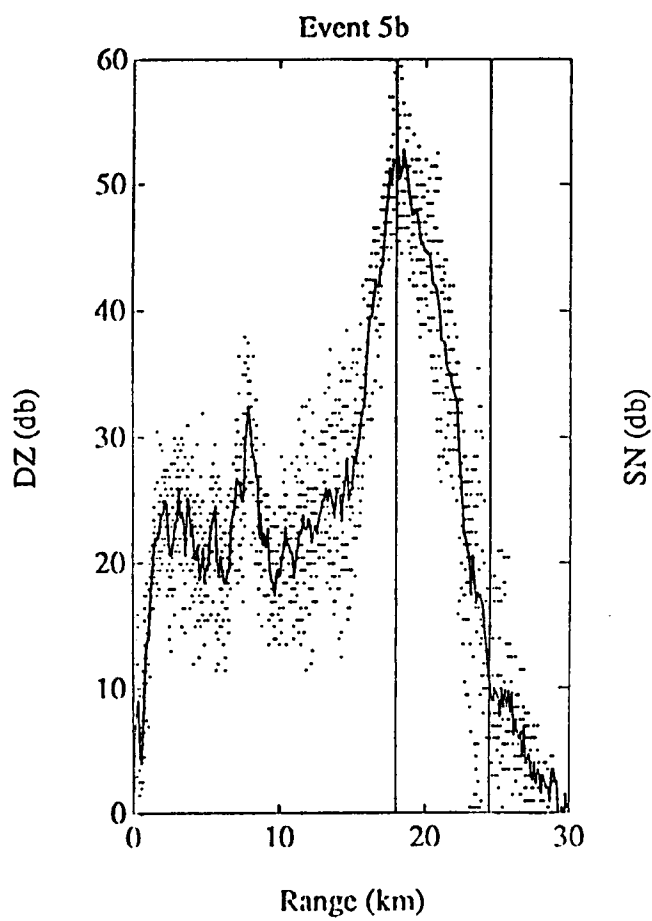
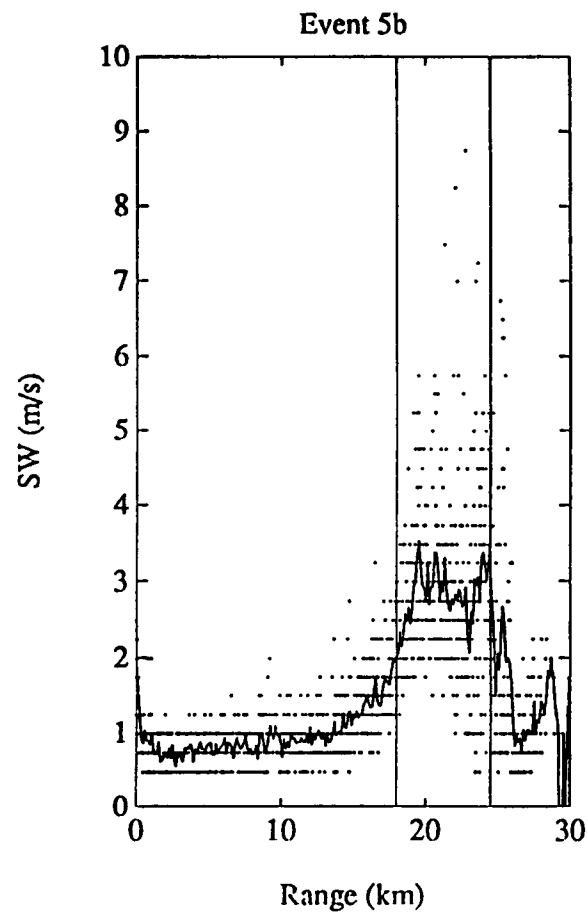
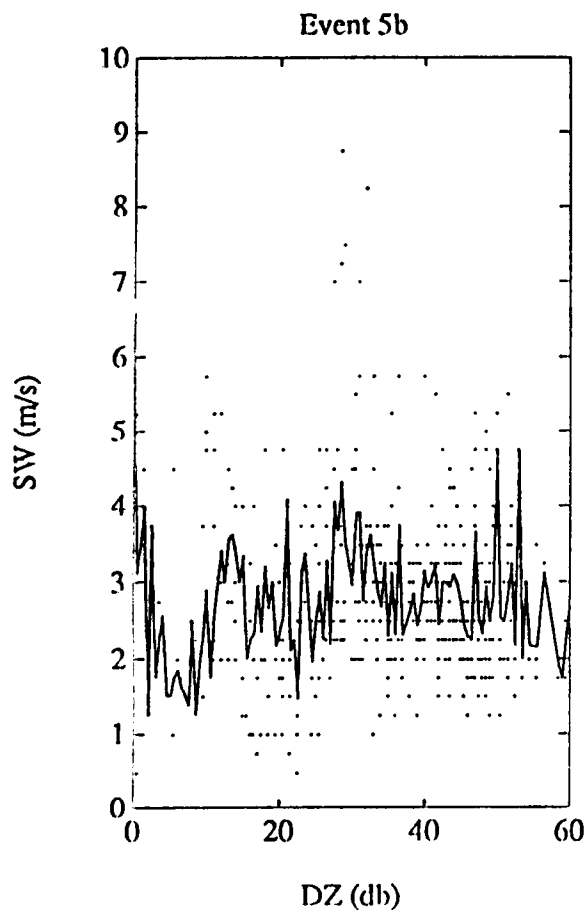


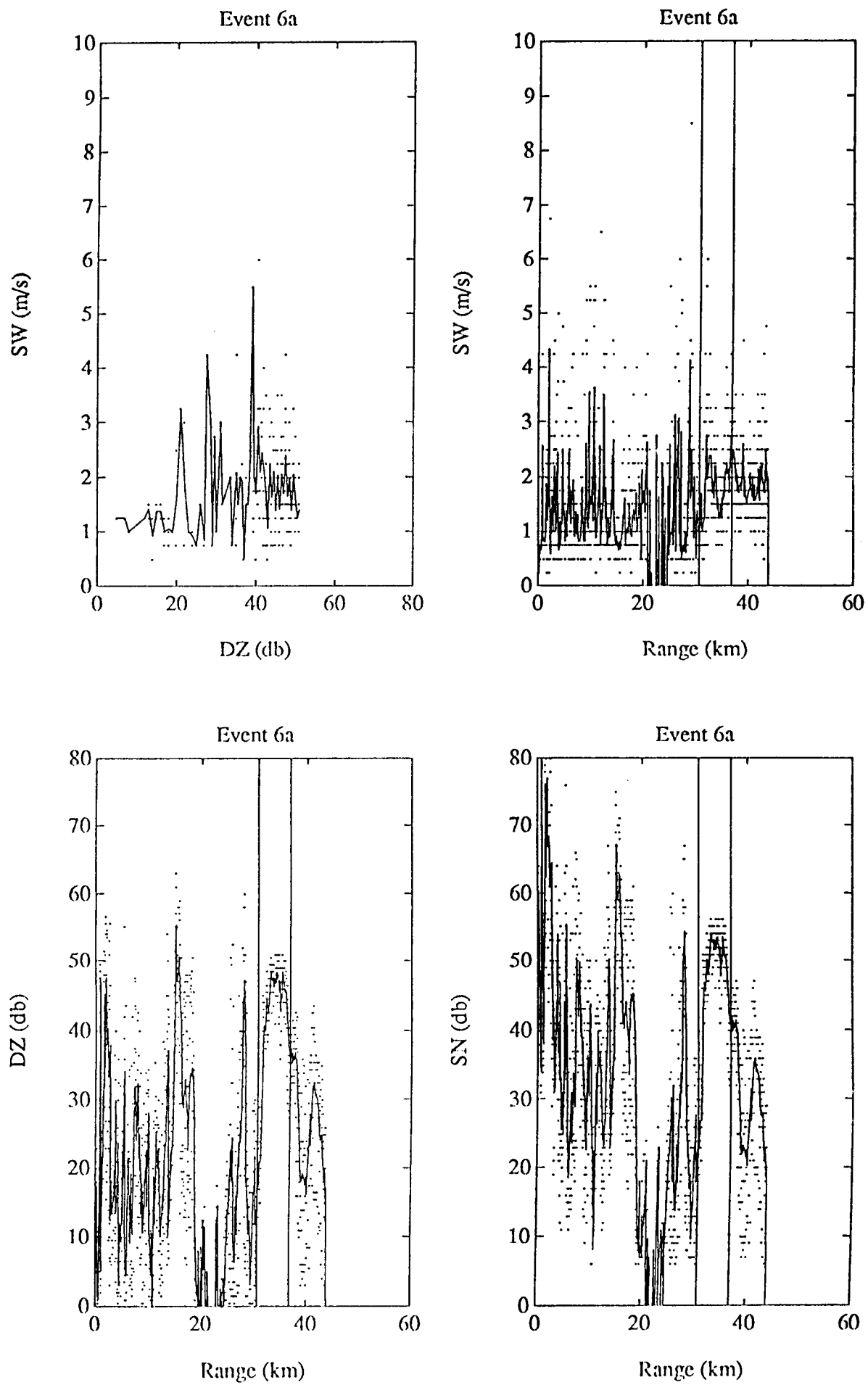


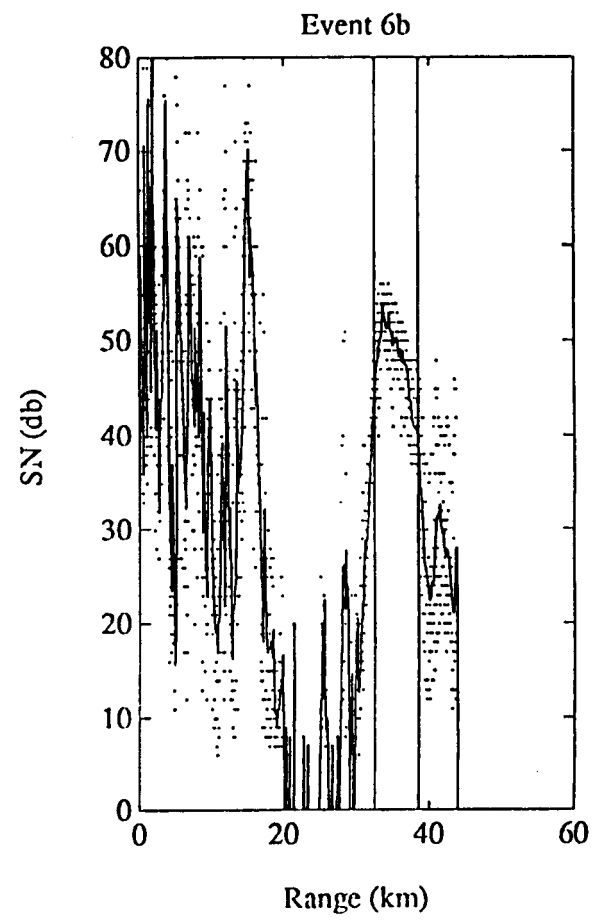
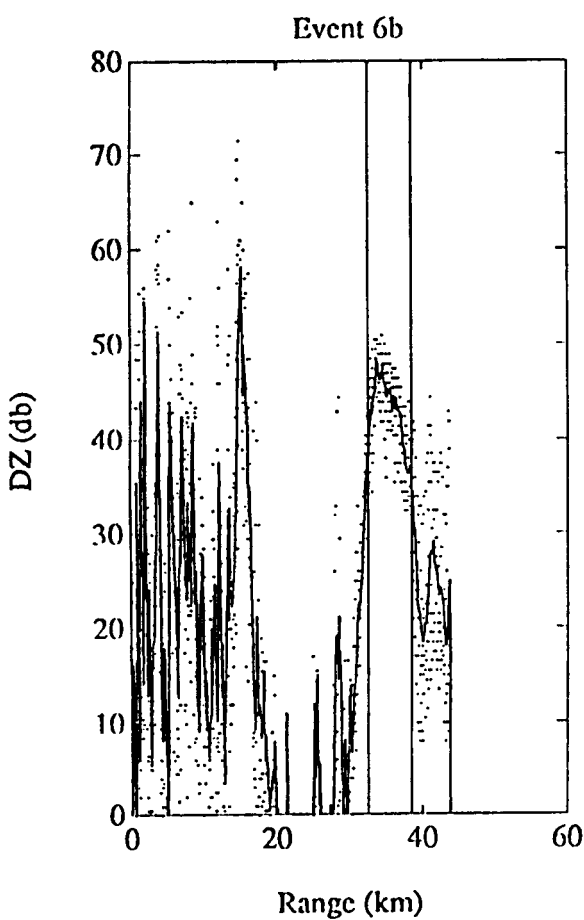
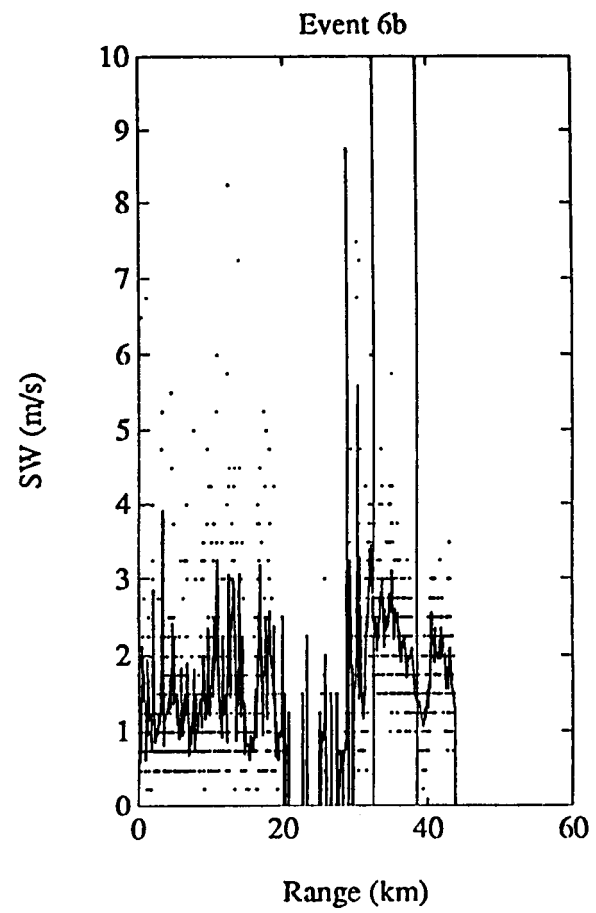
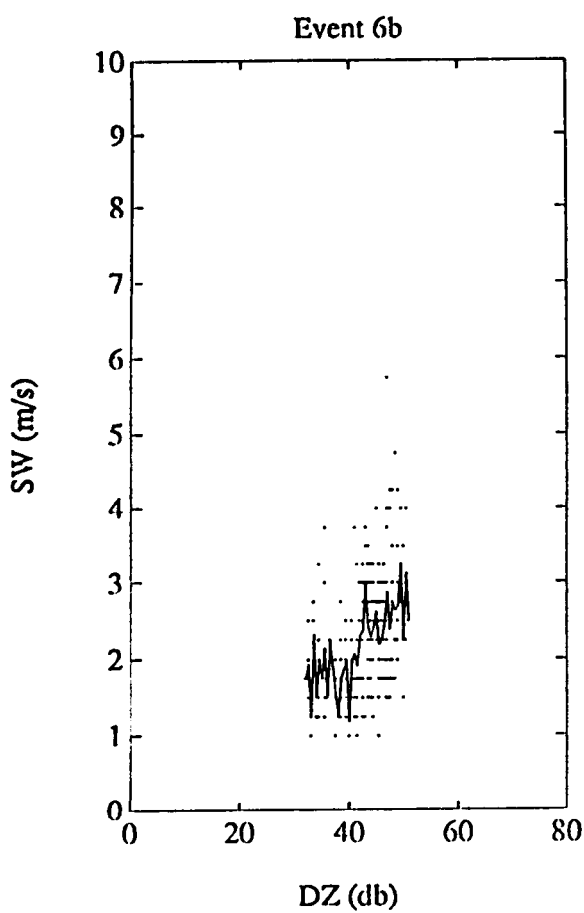


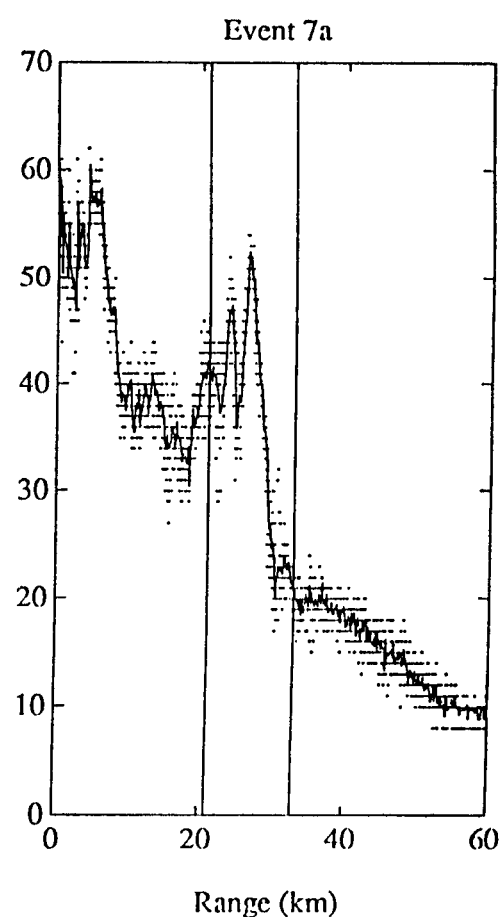
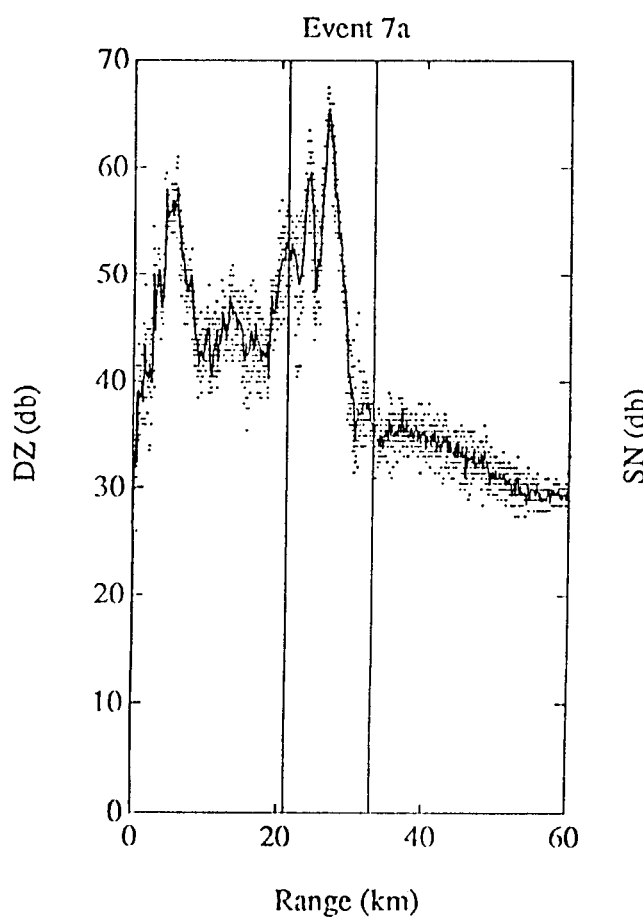
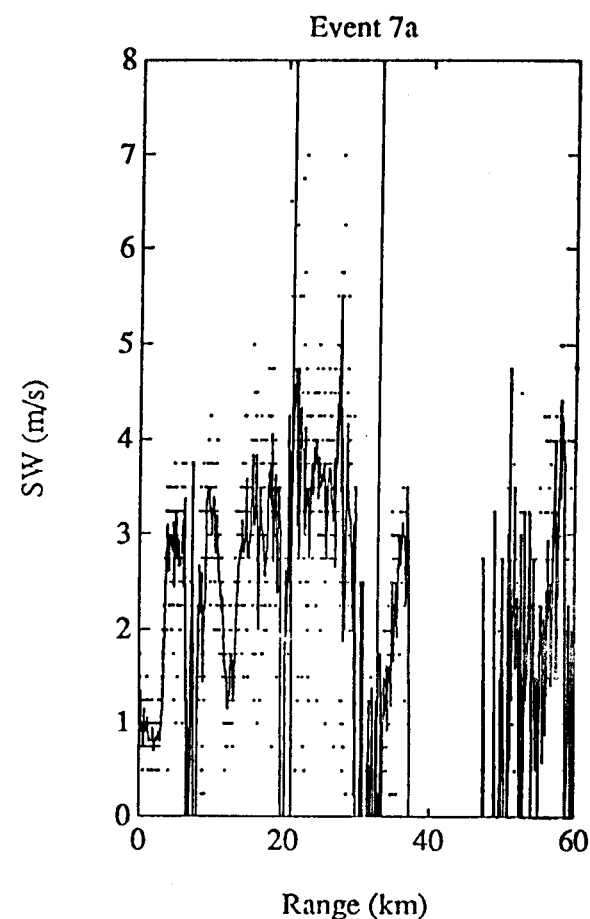
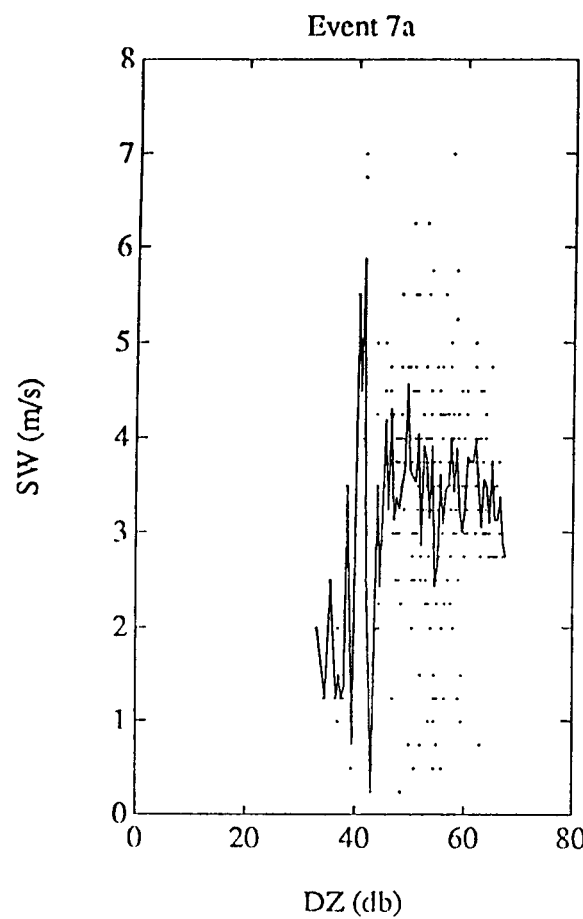


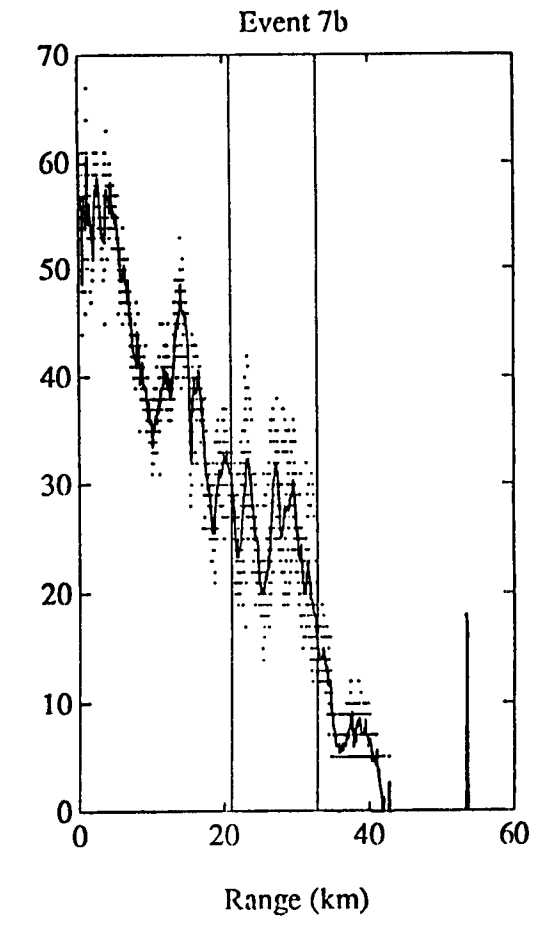
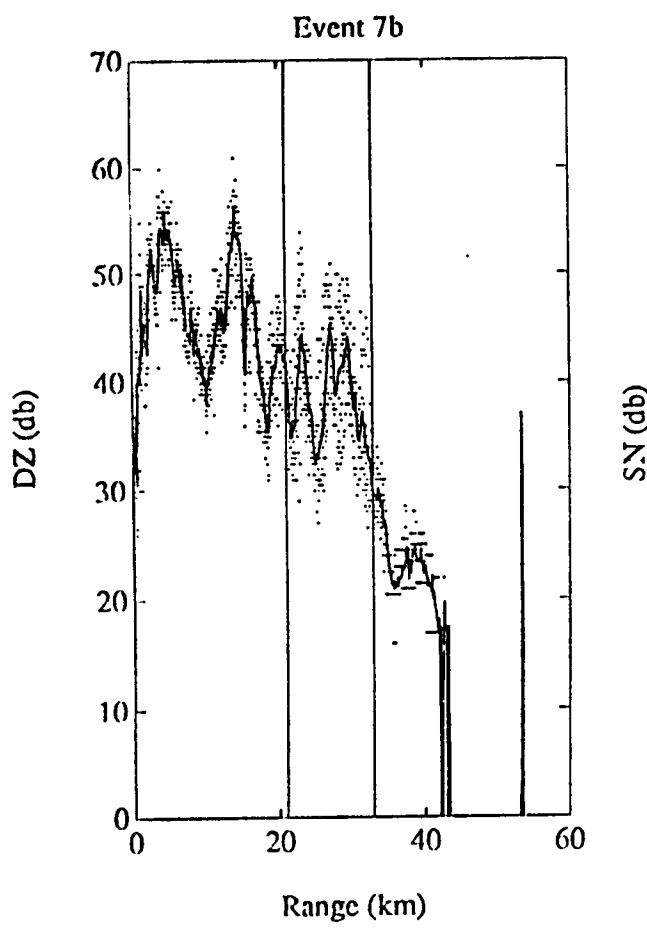
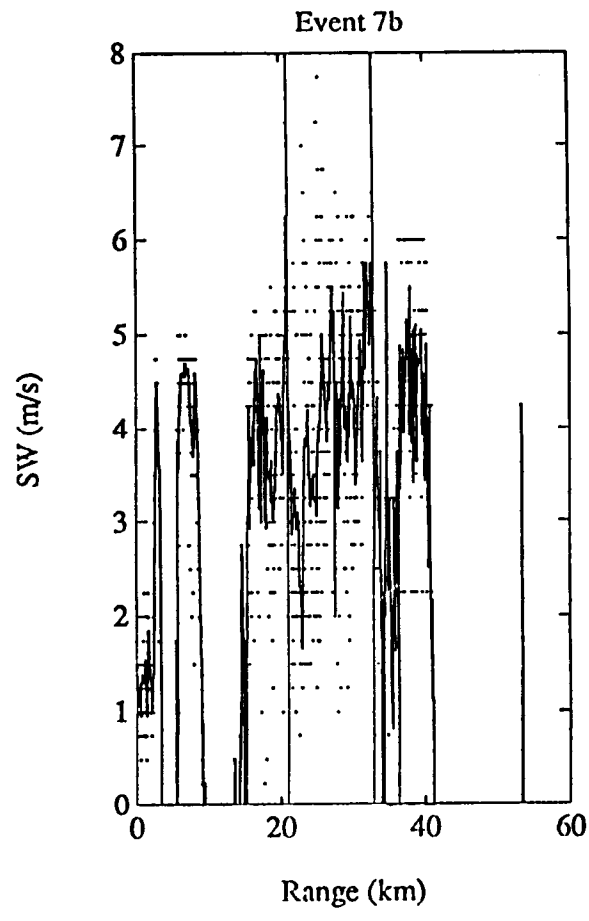
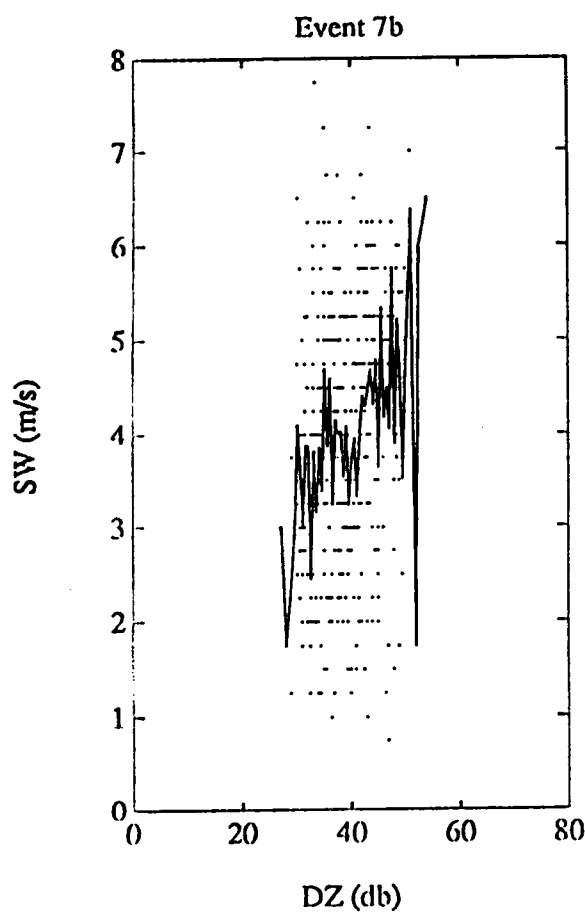


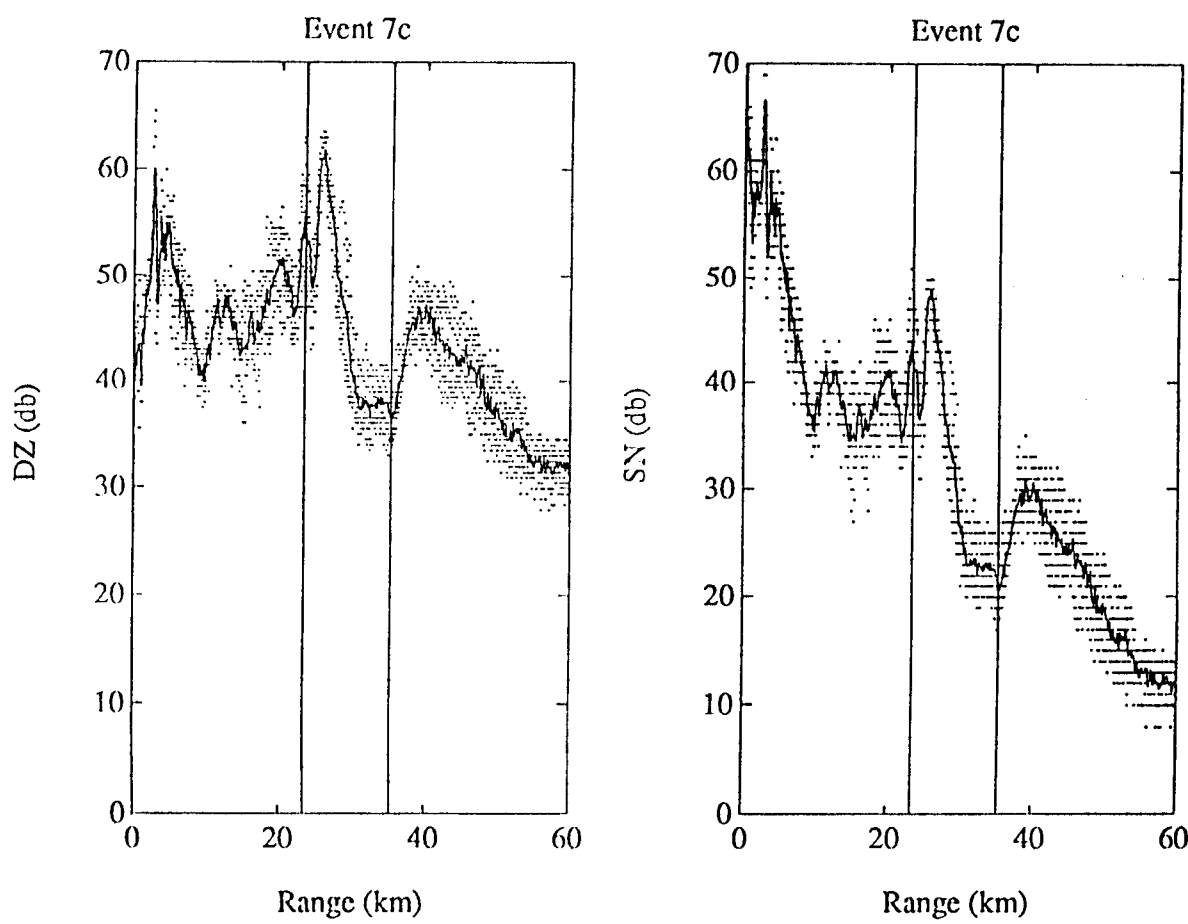
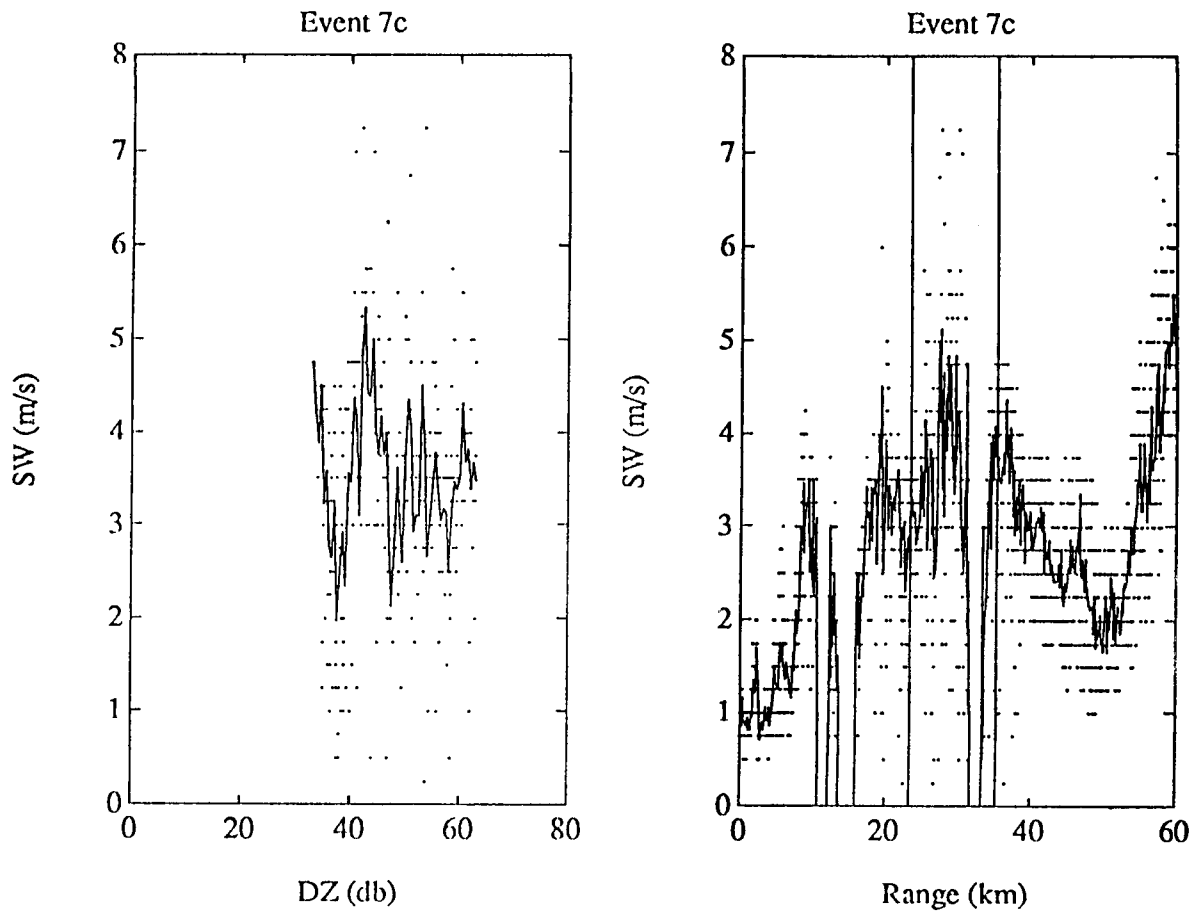


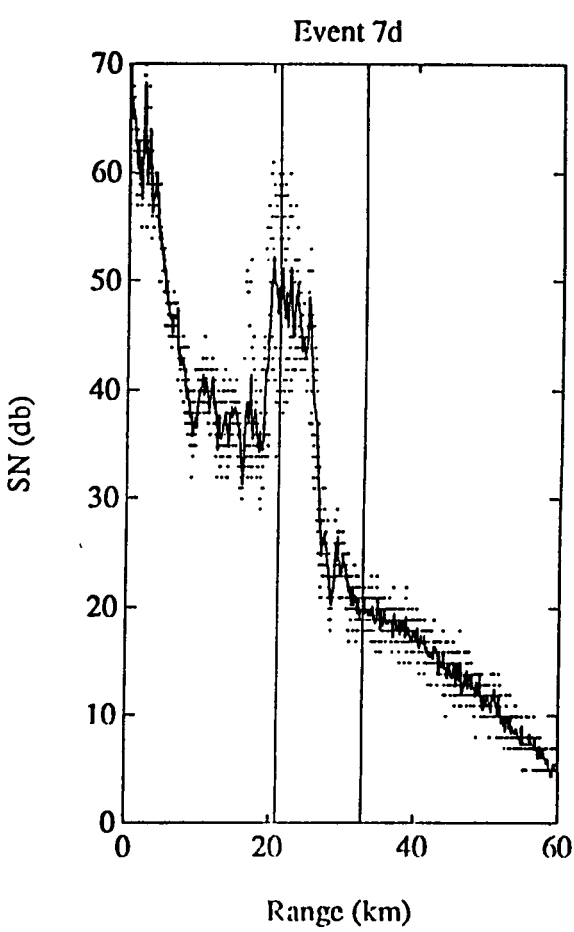
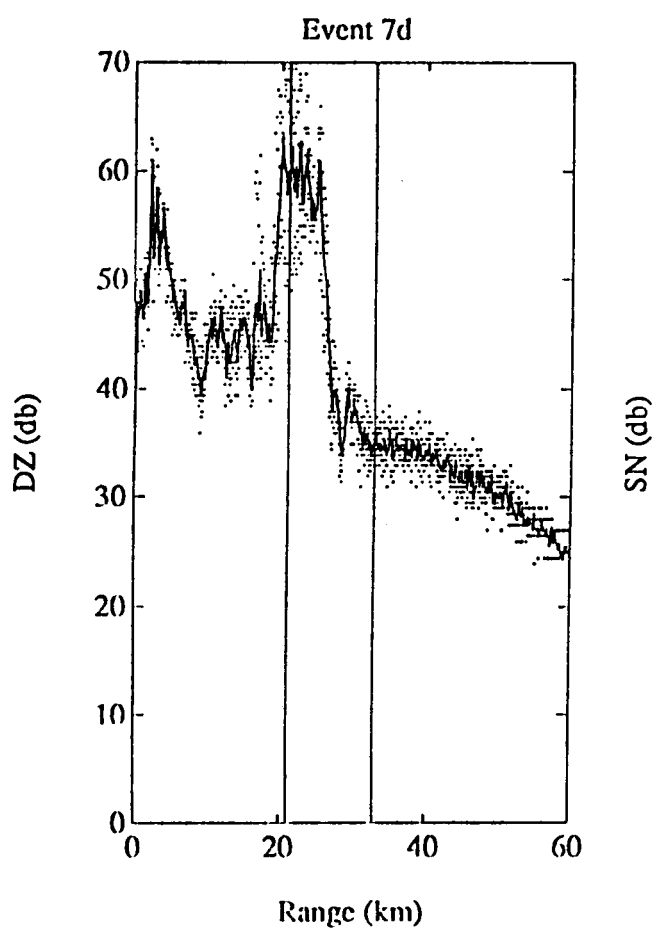
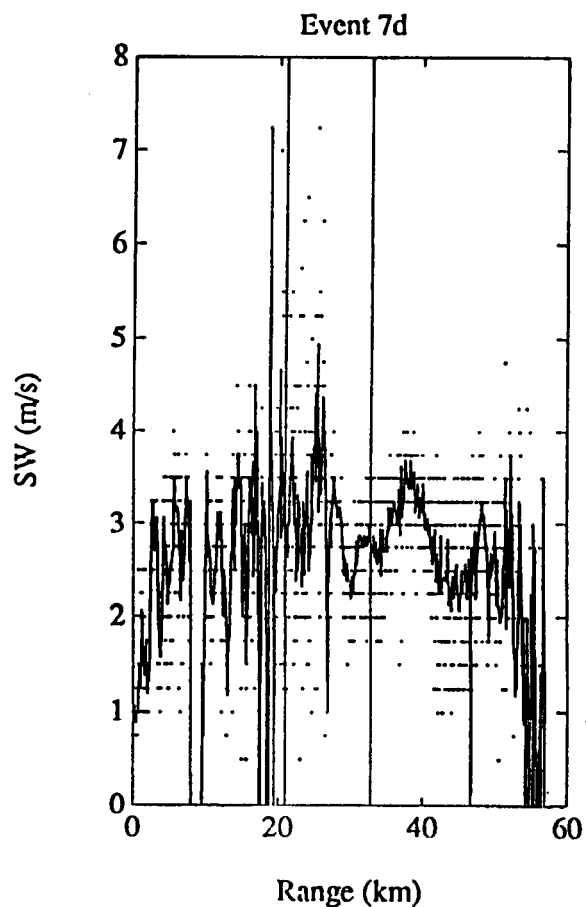
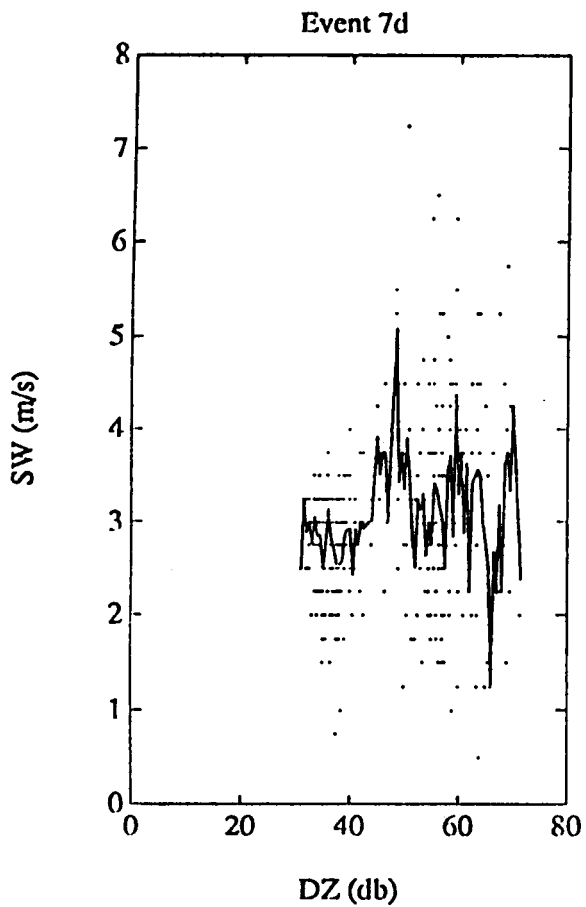


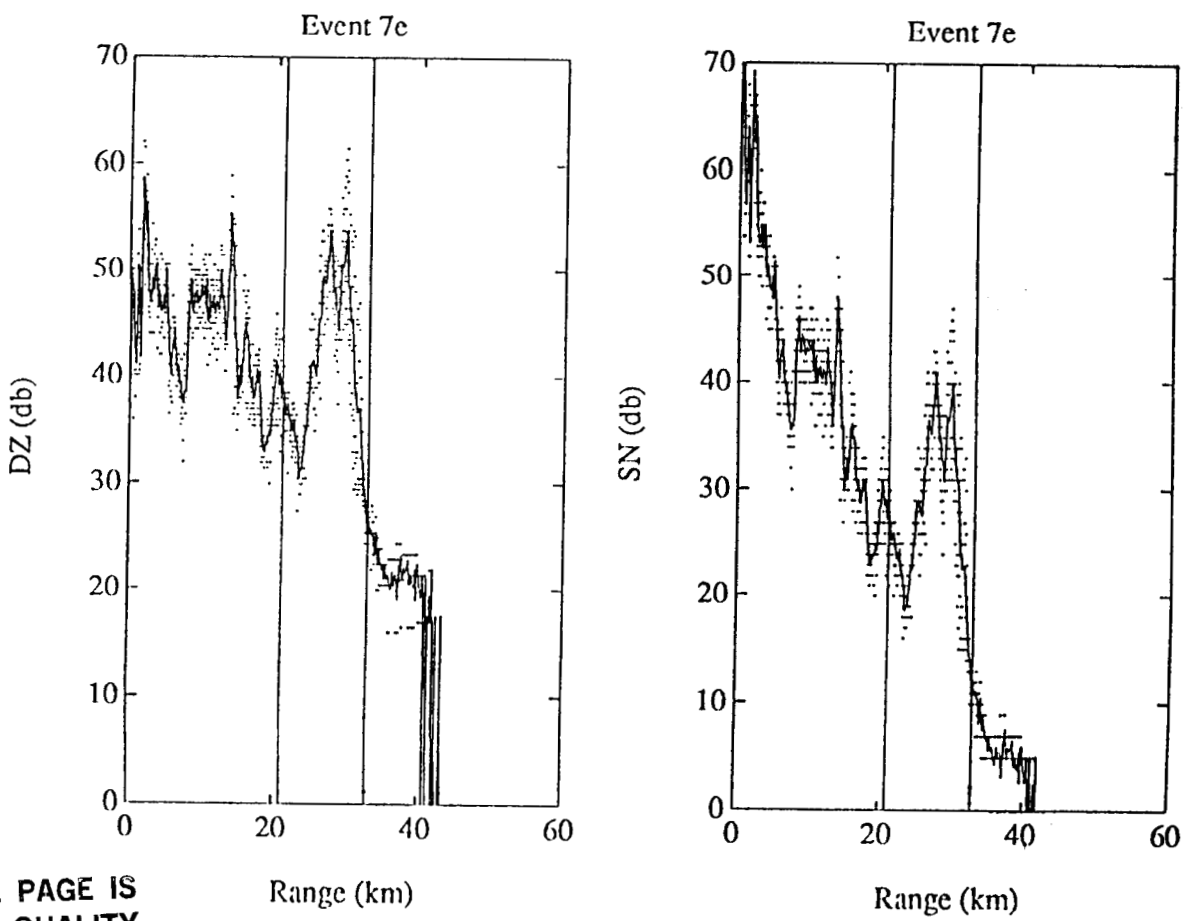
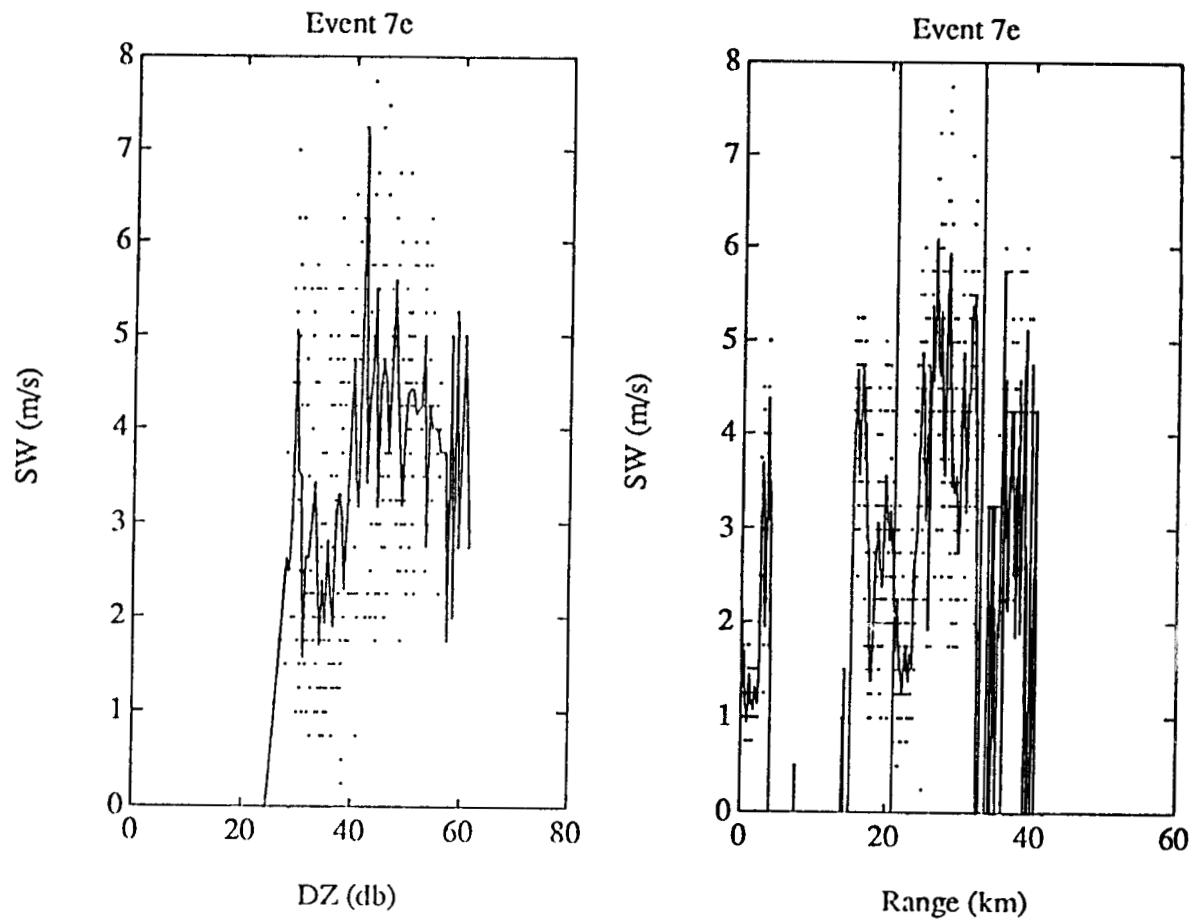




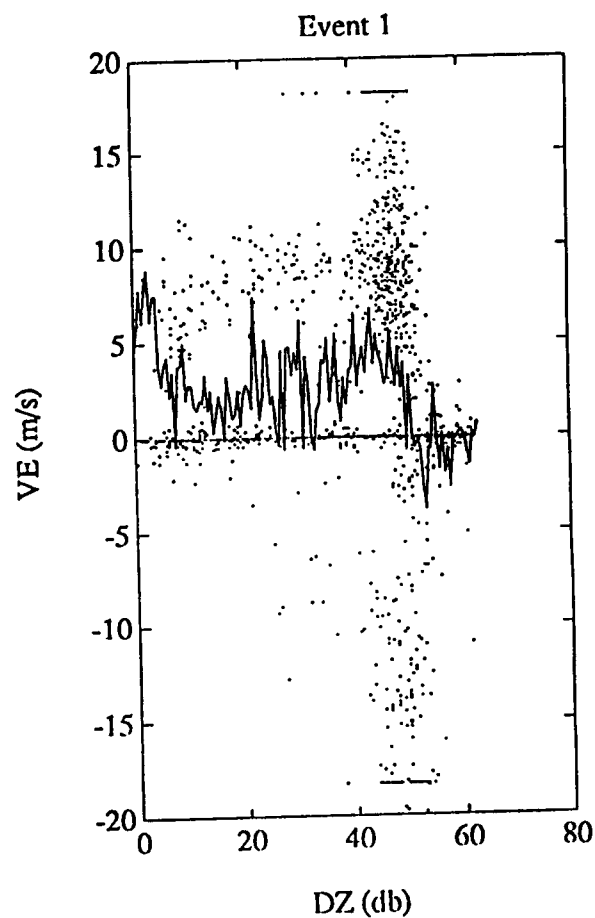
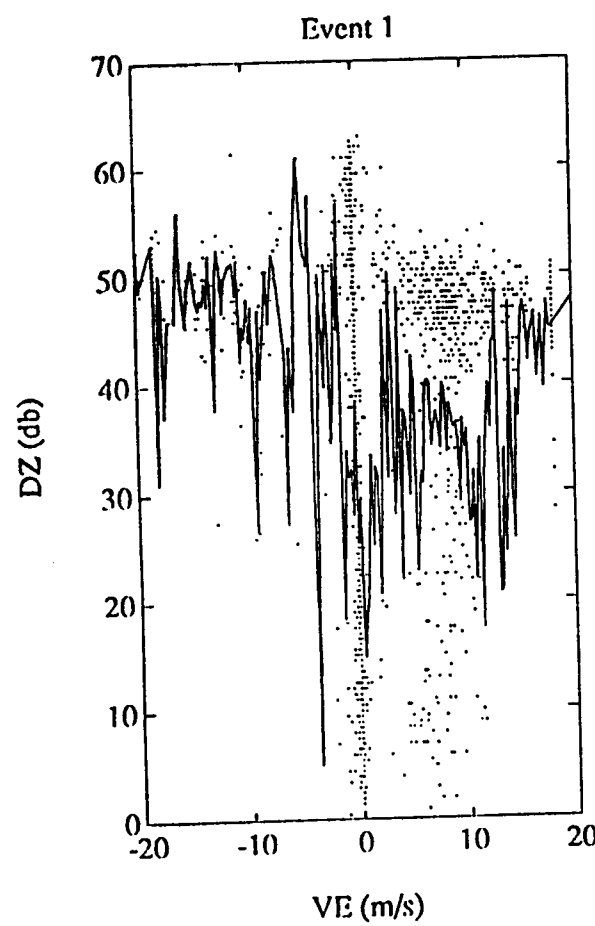
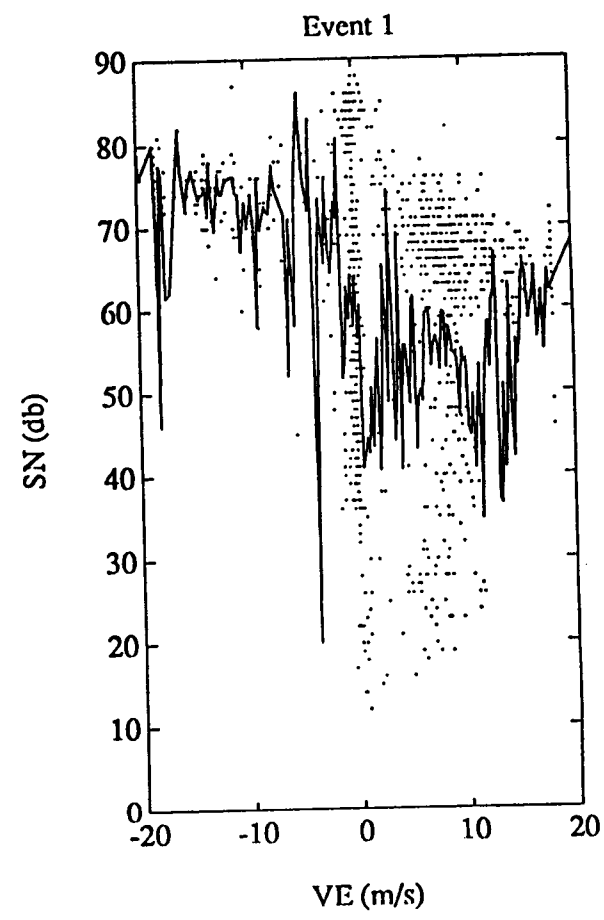
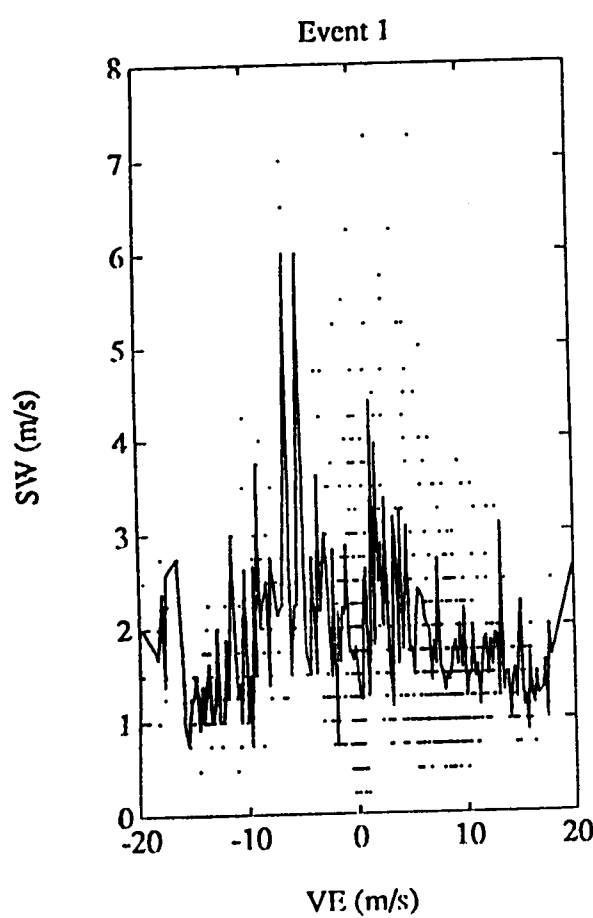


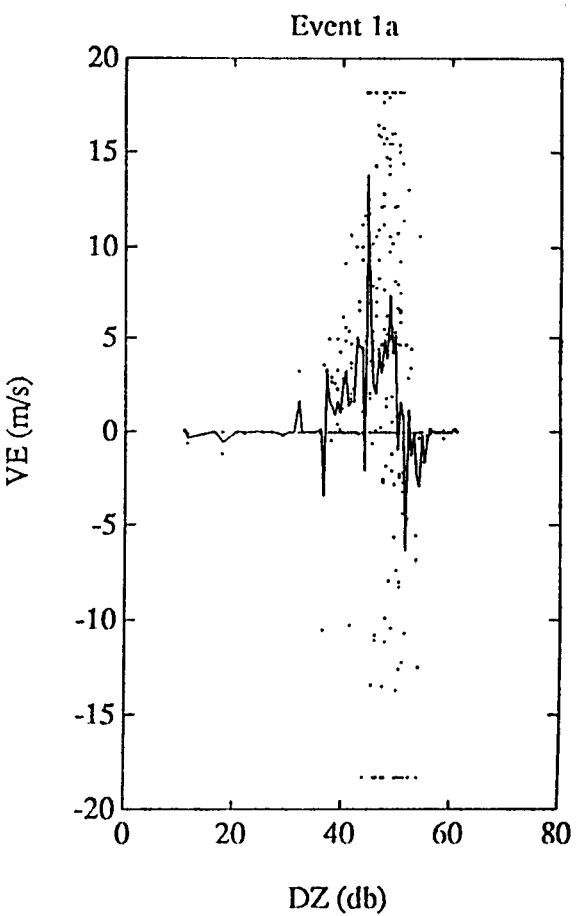
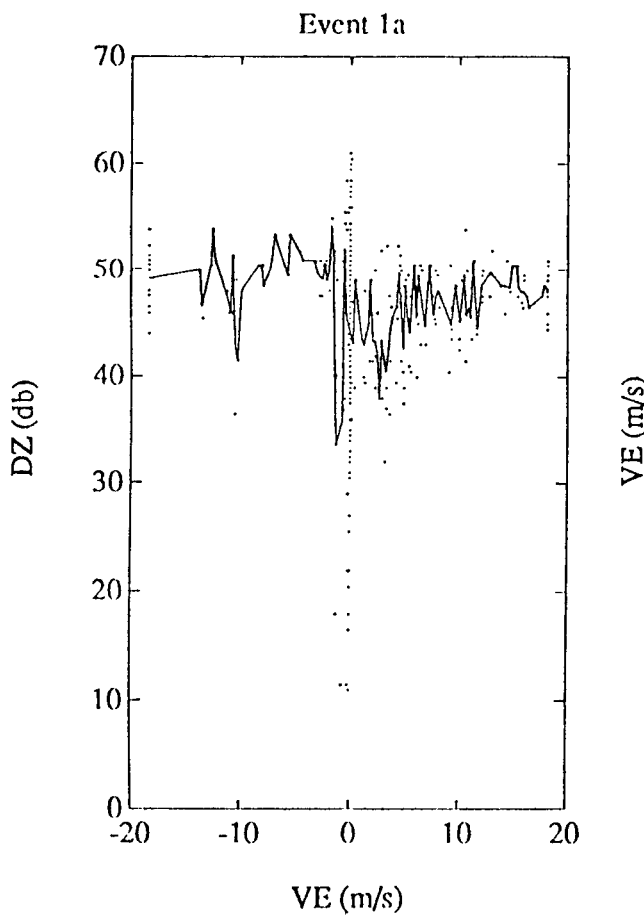
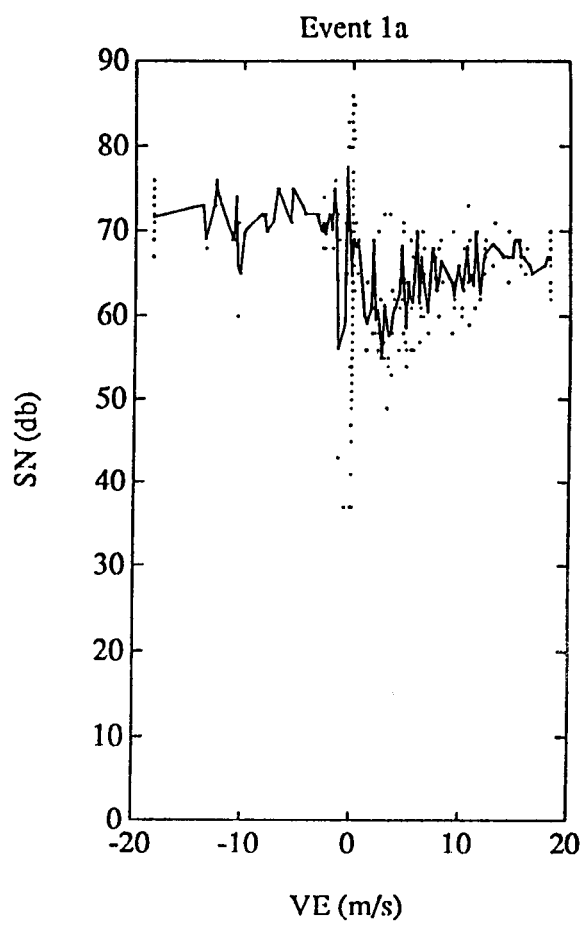
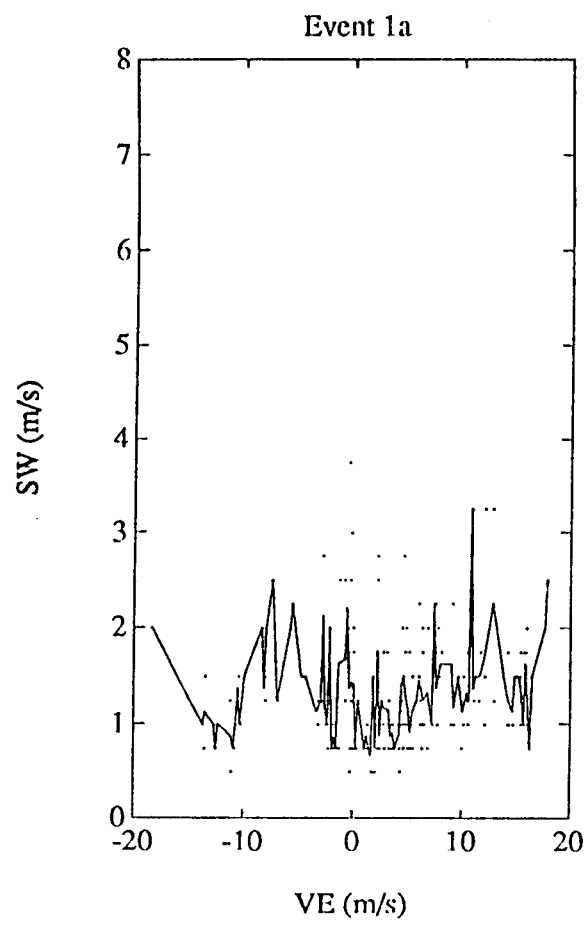


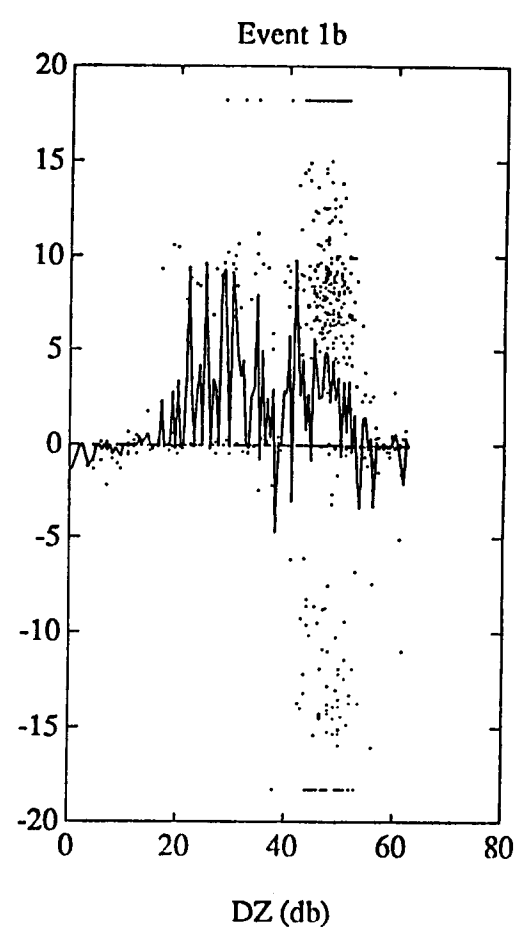
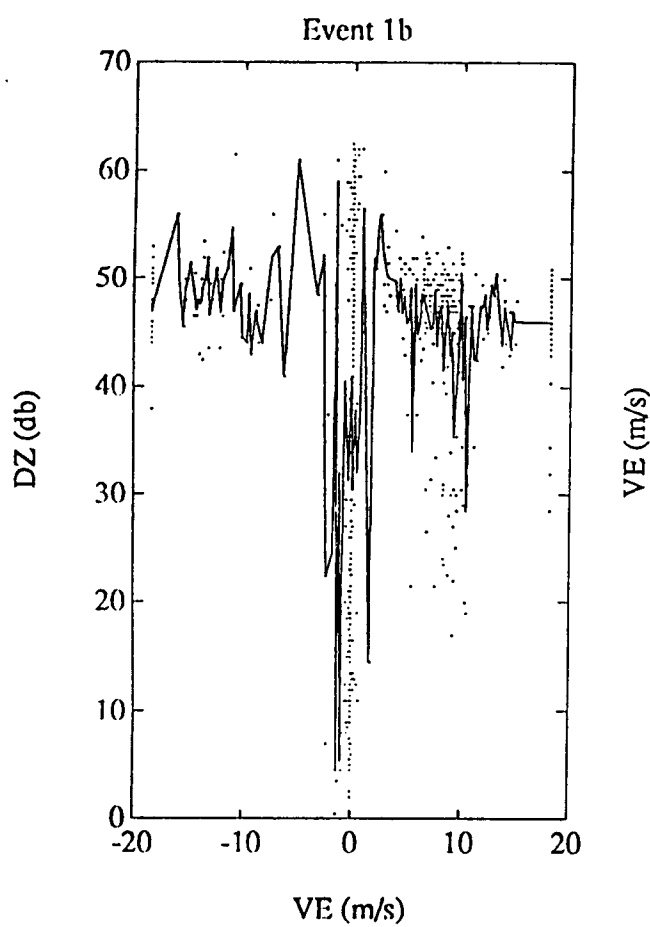
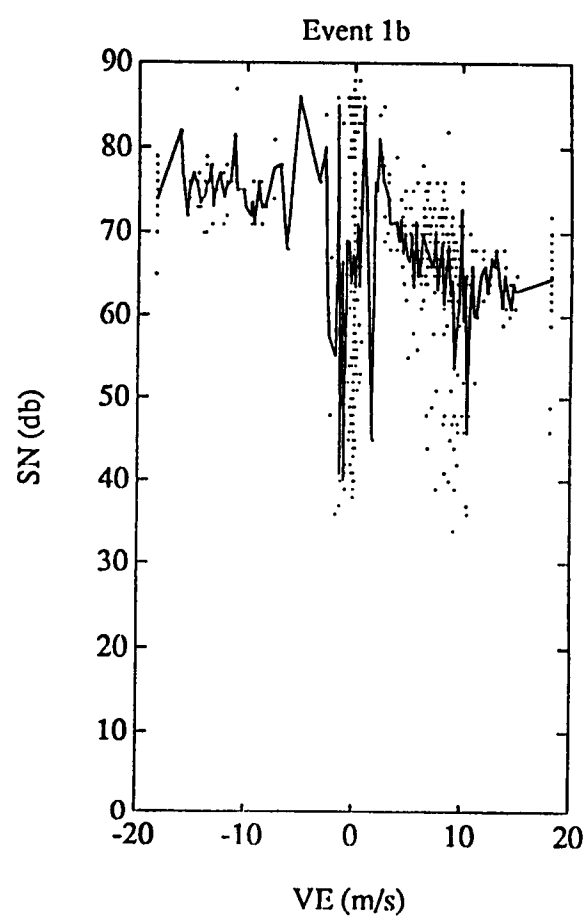
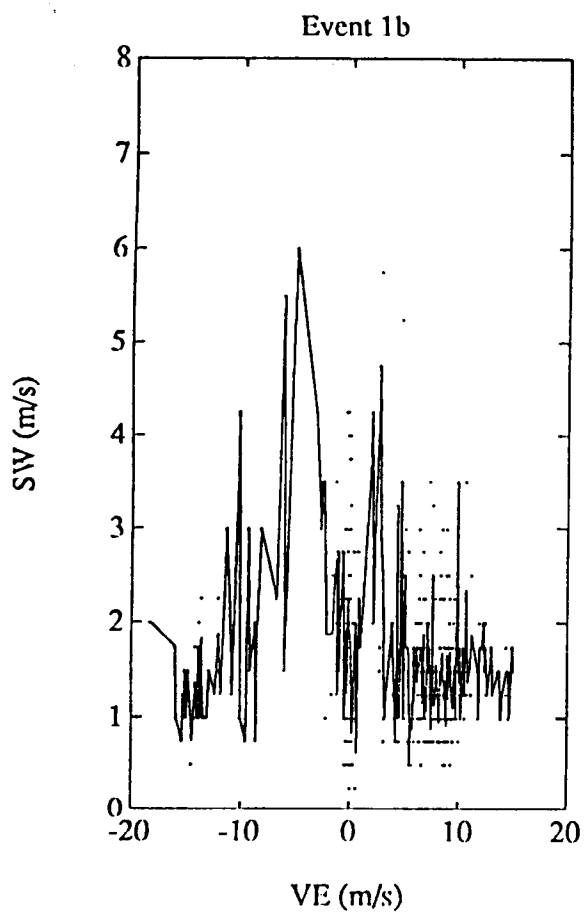


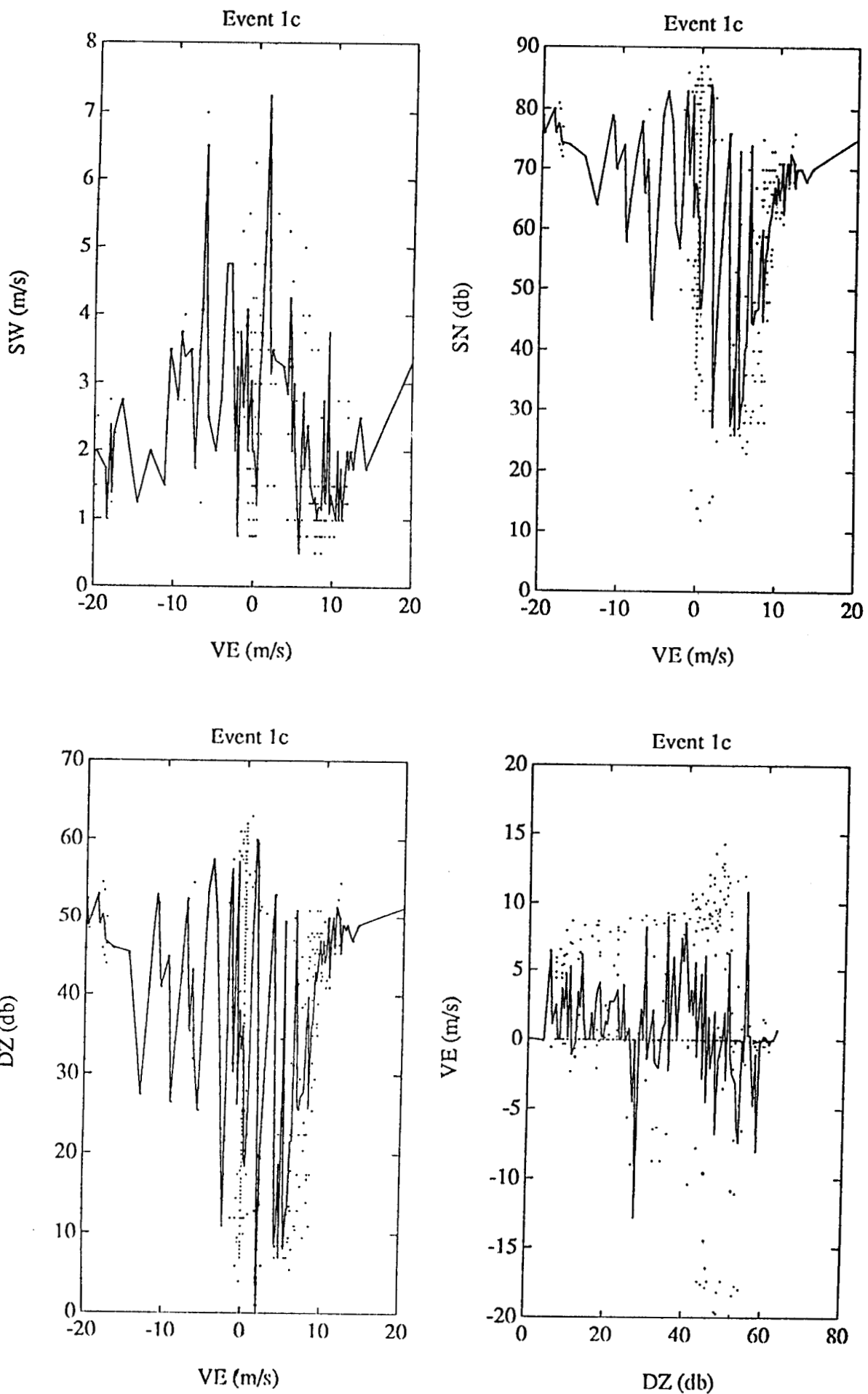


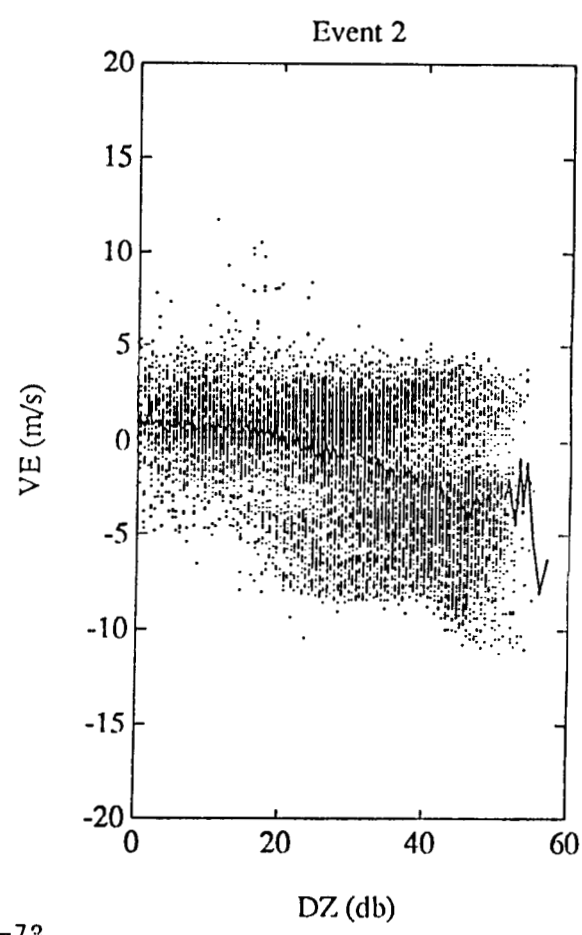
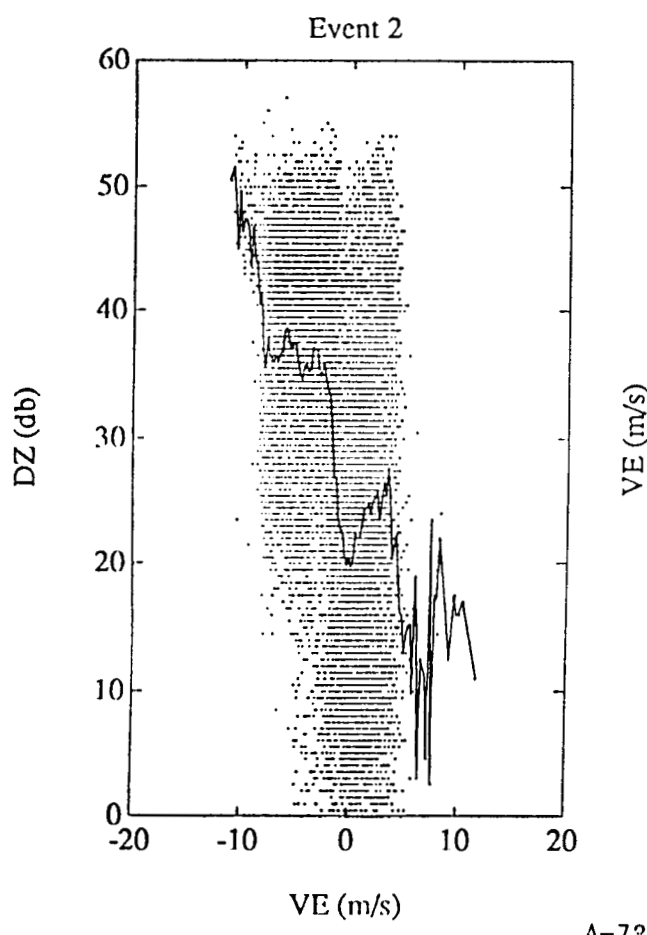
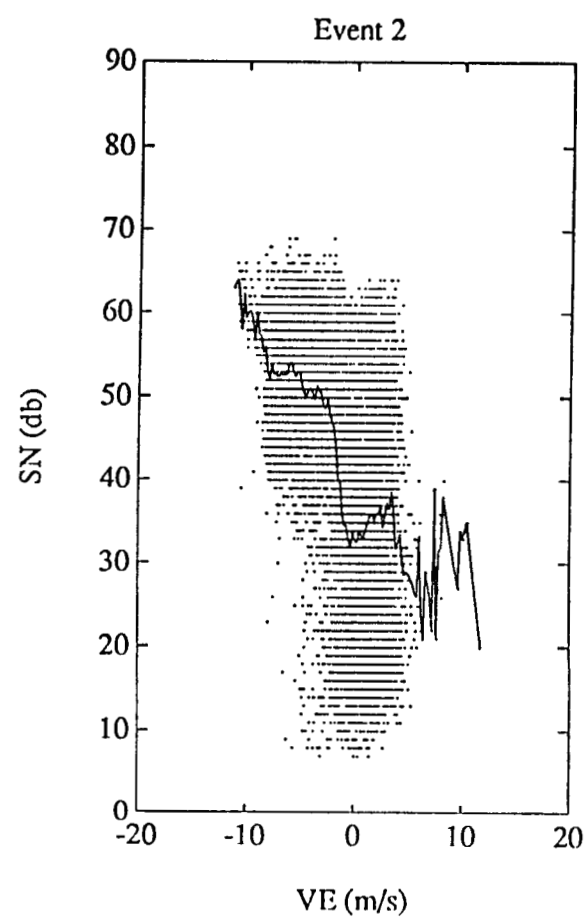
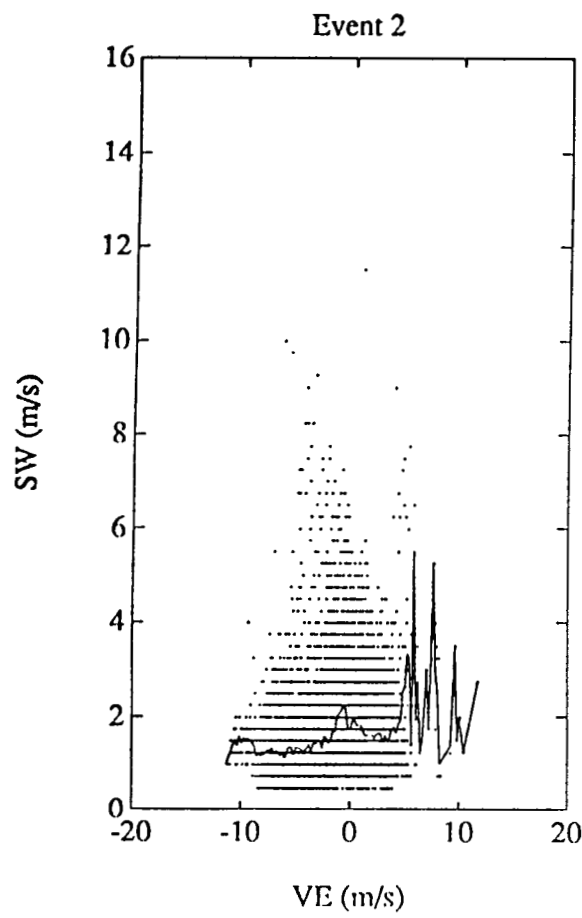
**ORIGINAL PAGE IS
OF POOR QUALITY**

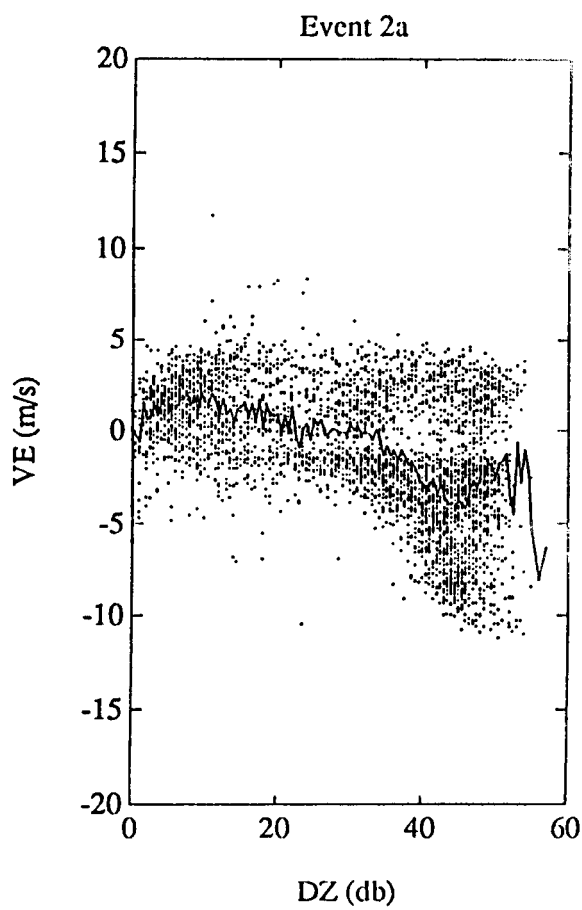
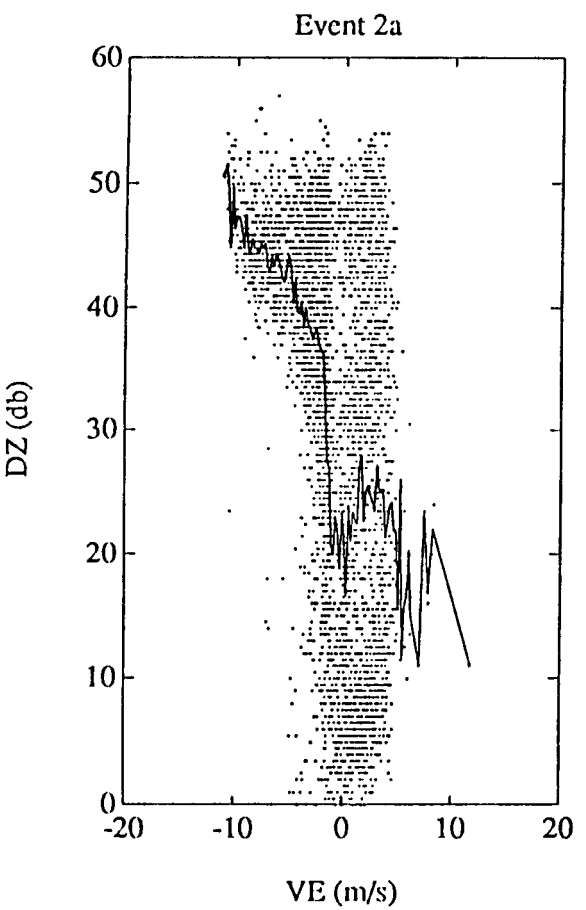
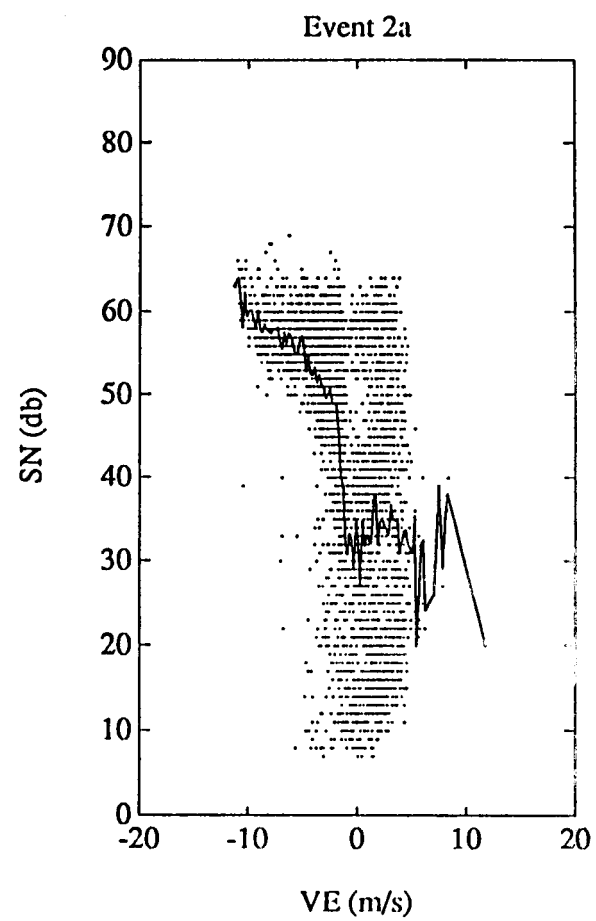
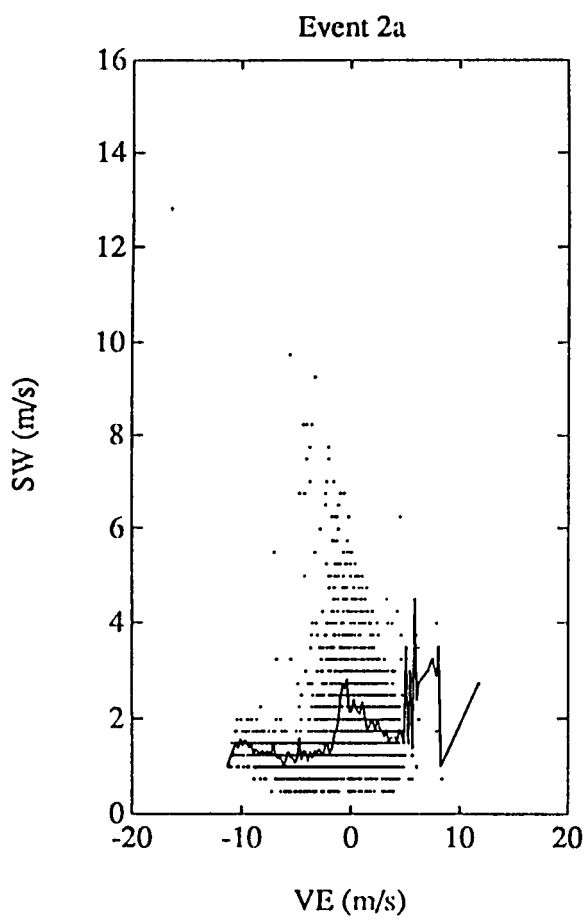


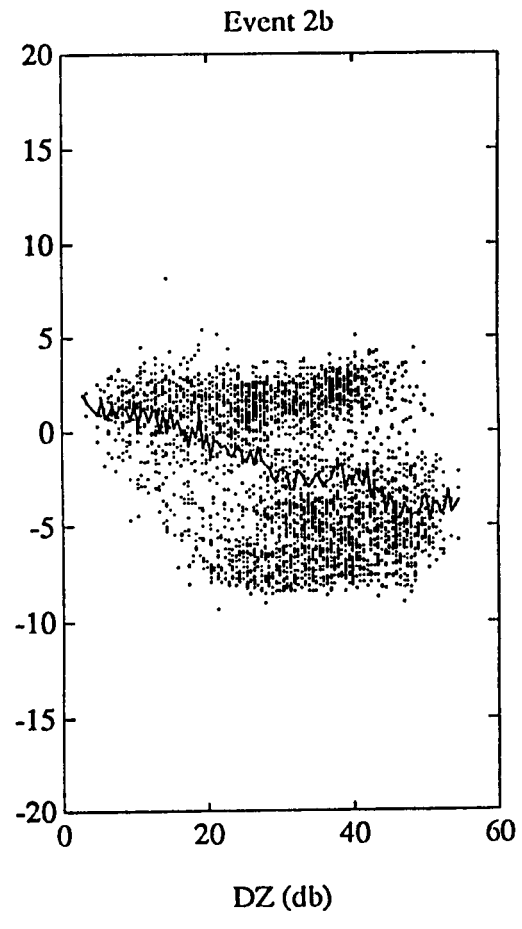
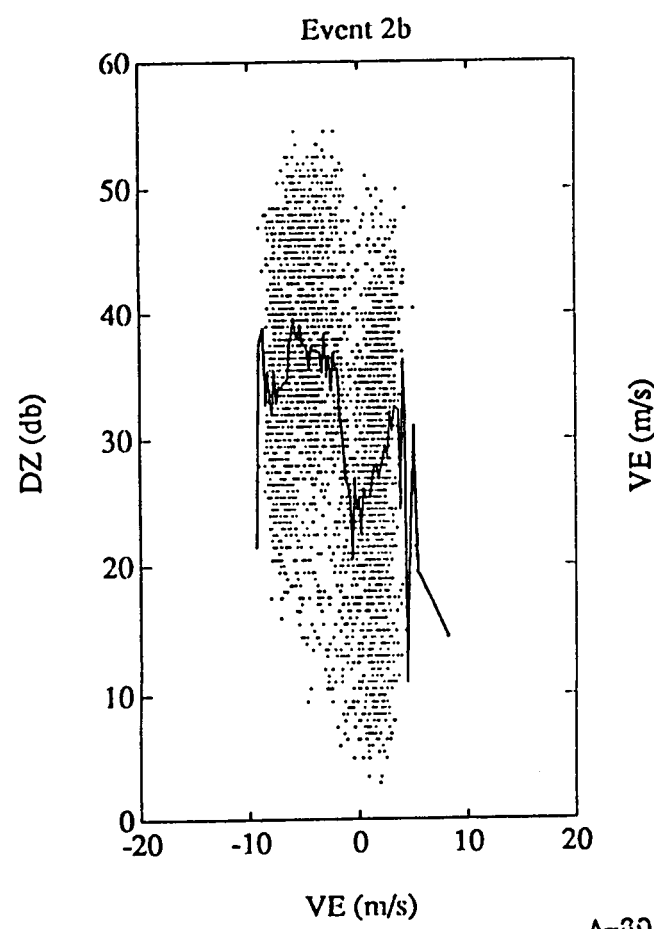
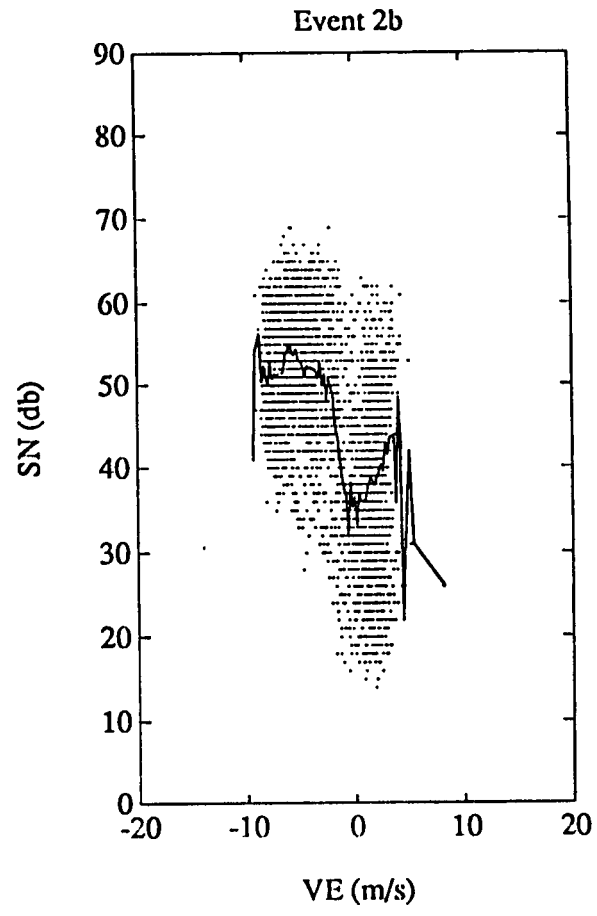
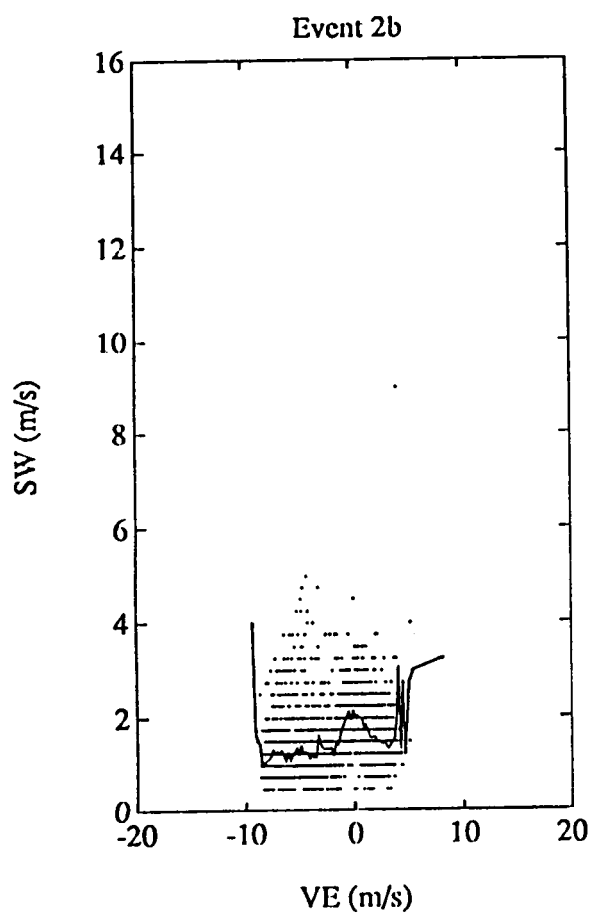


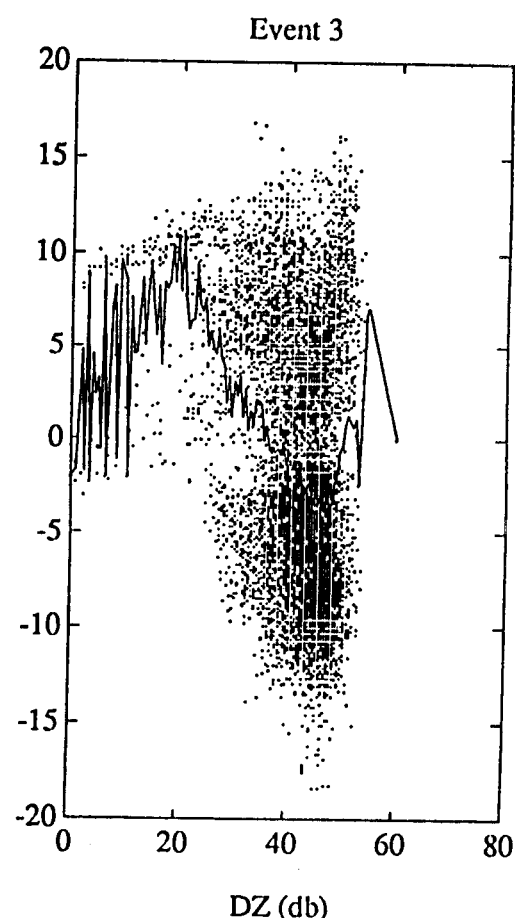
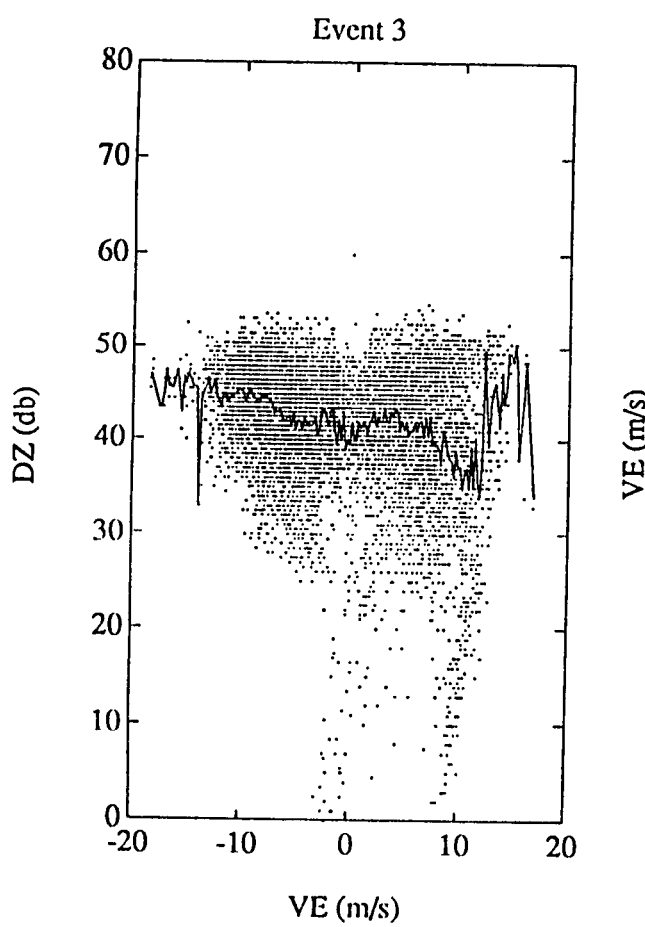
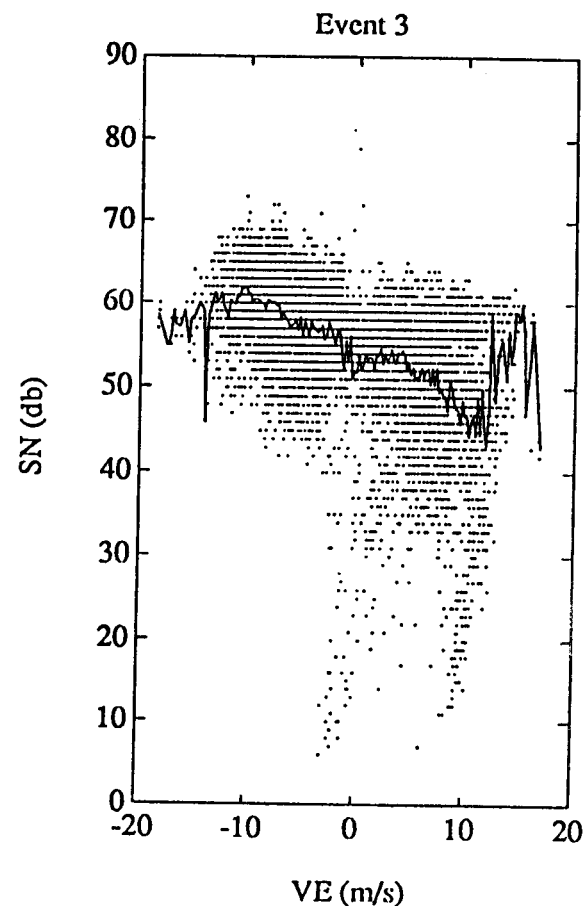
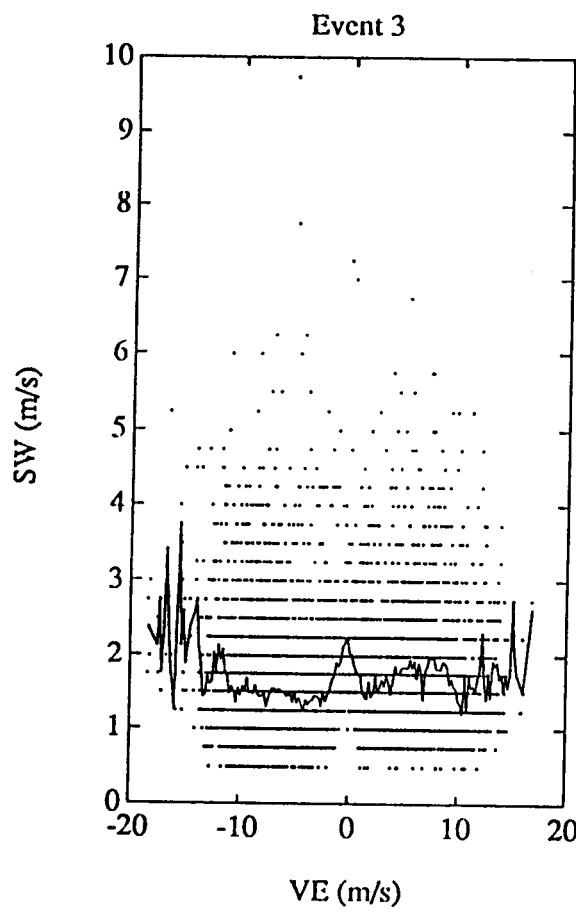


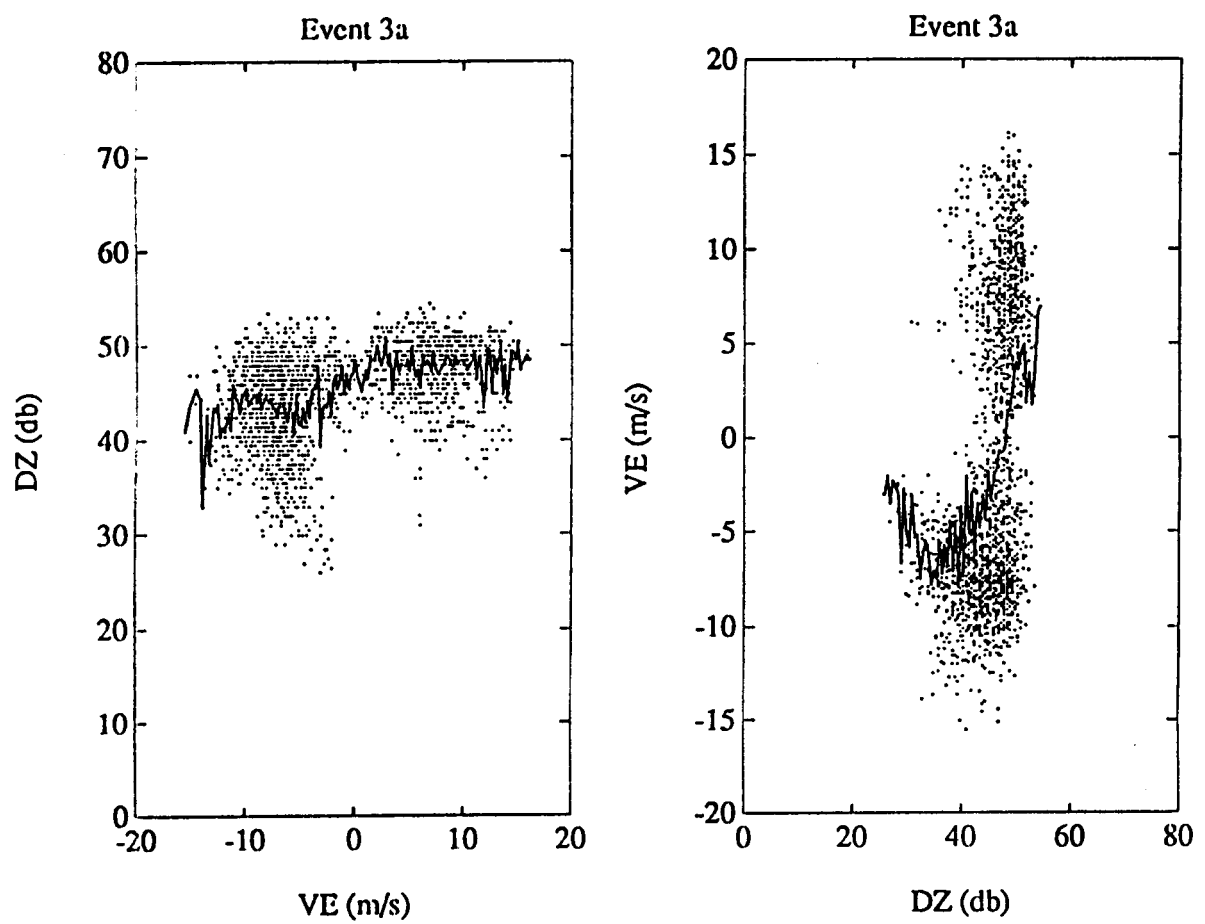
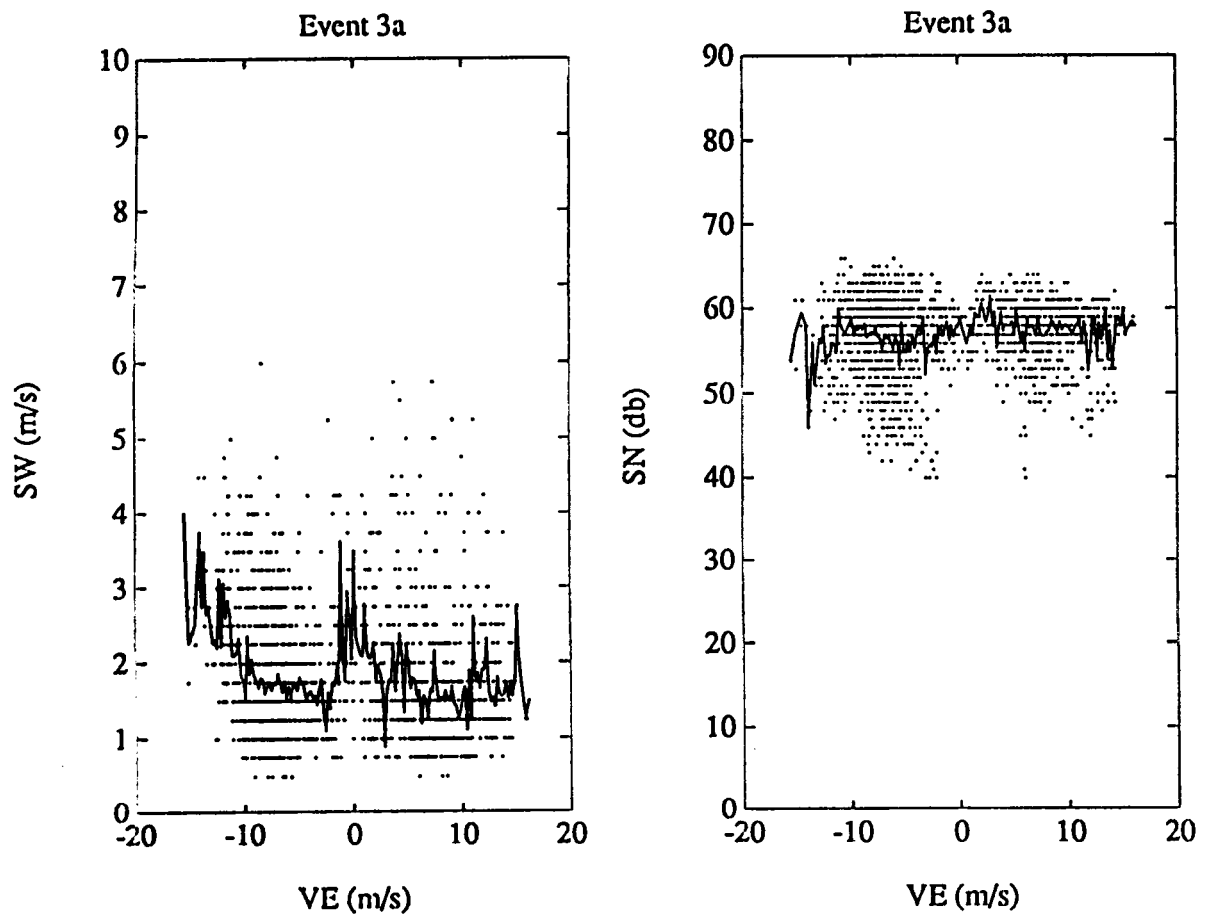


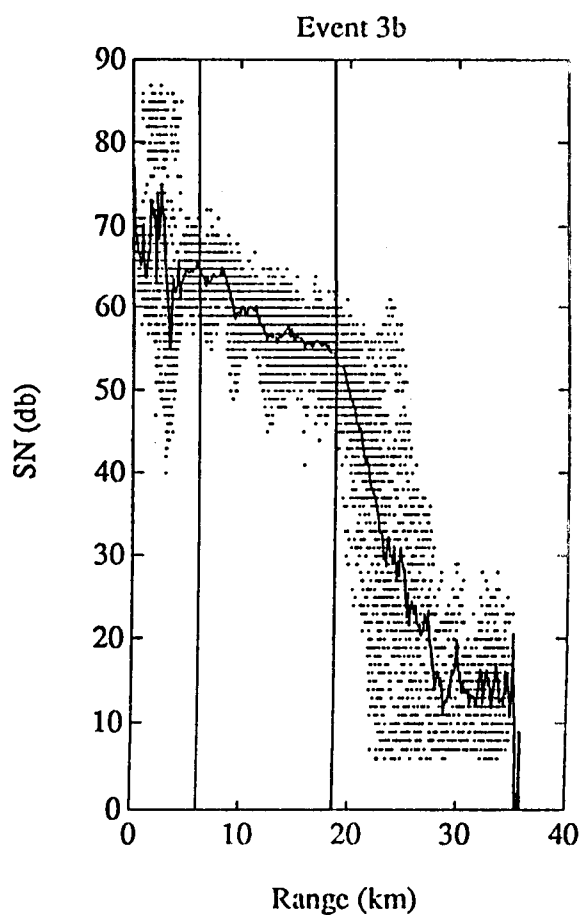
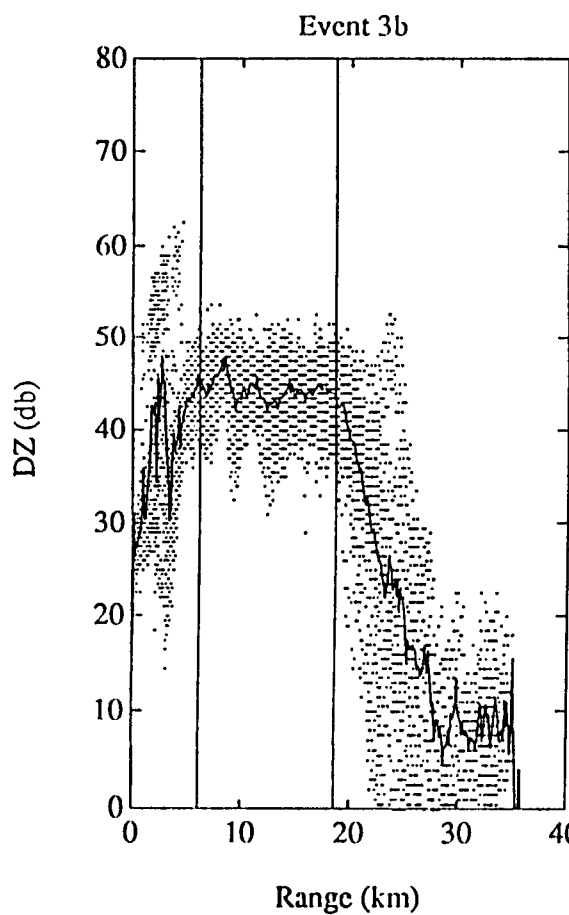
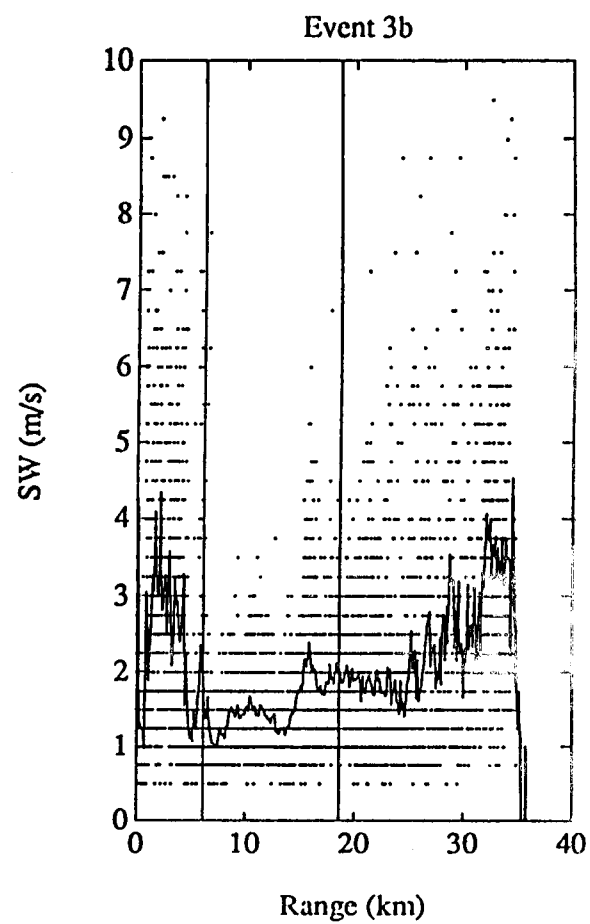
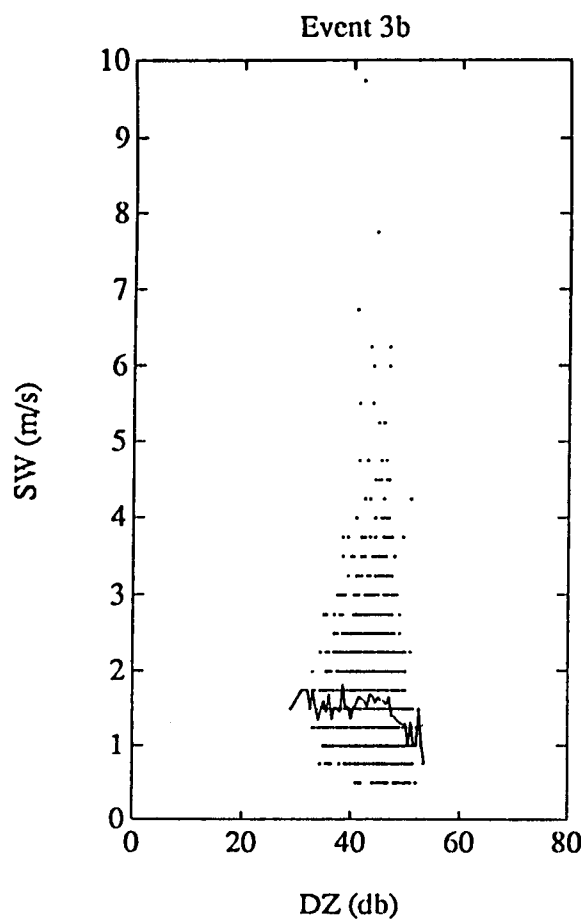


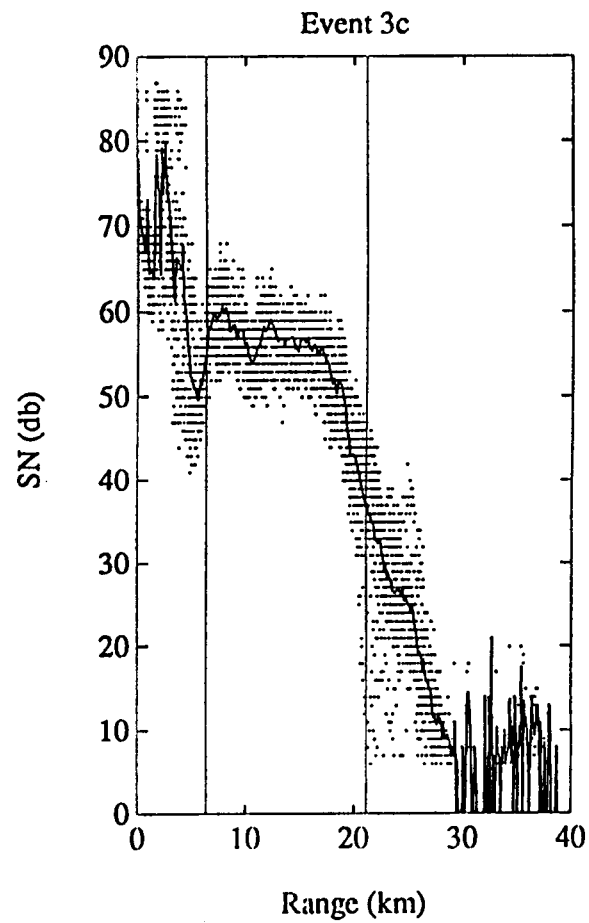
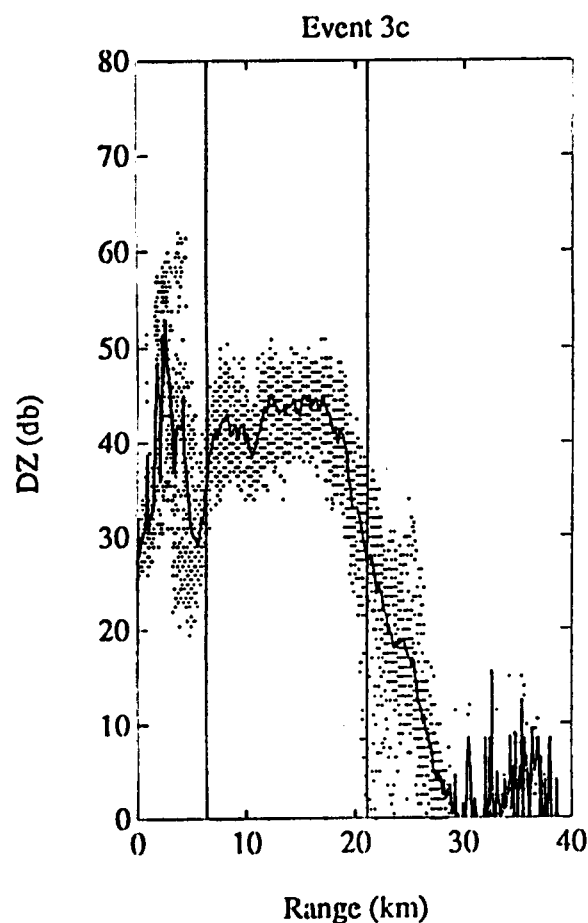
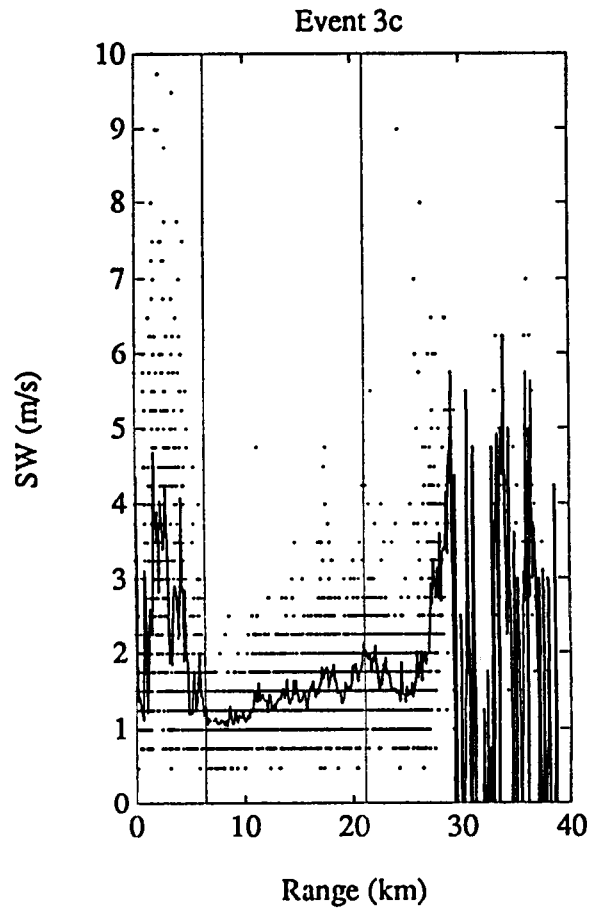
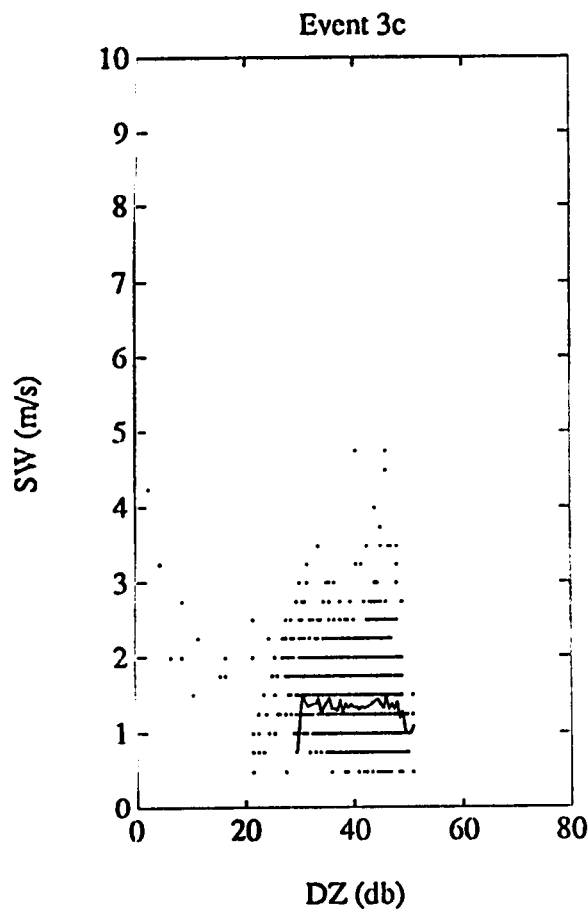


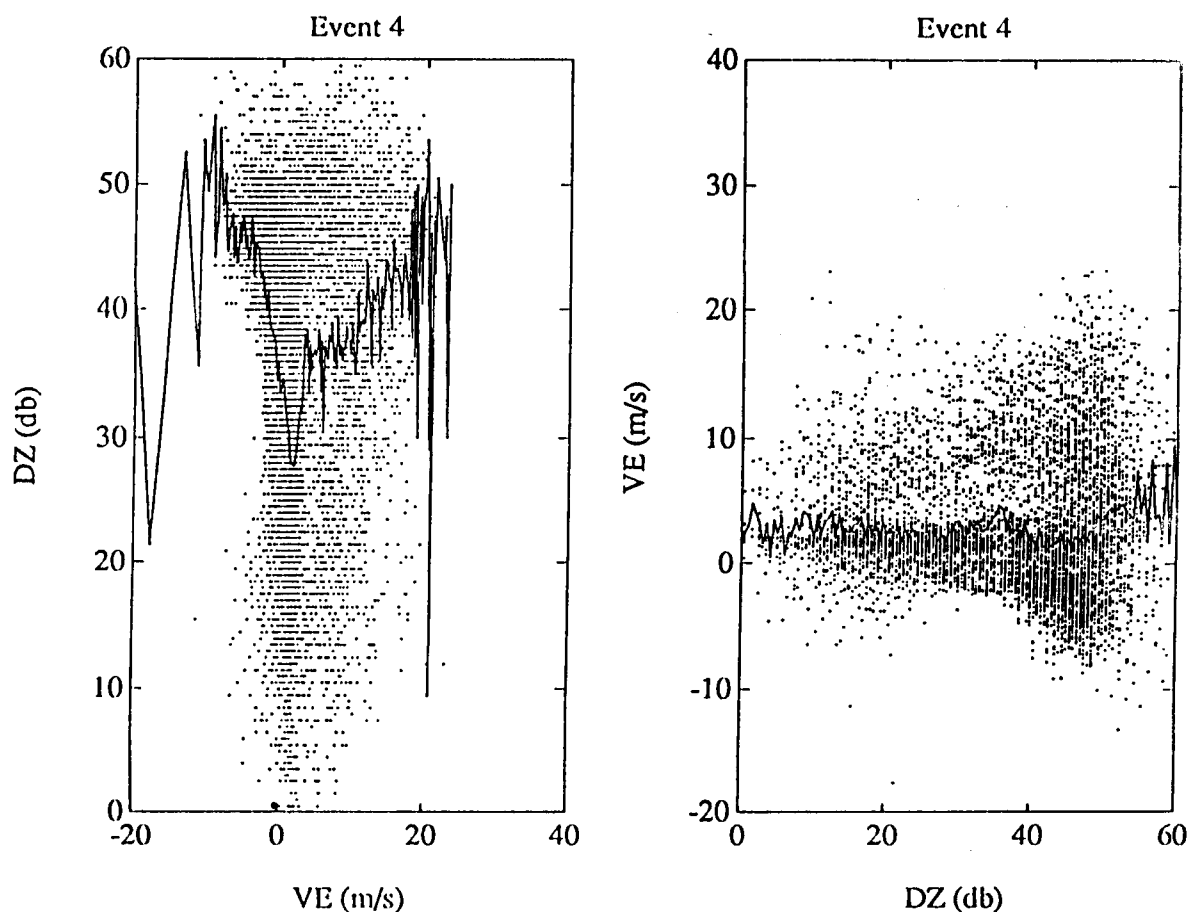
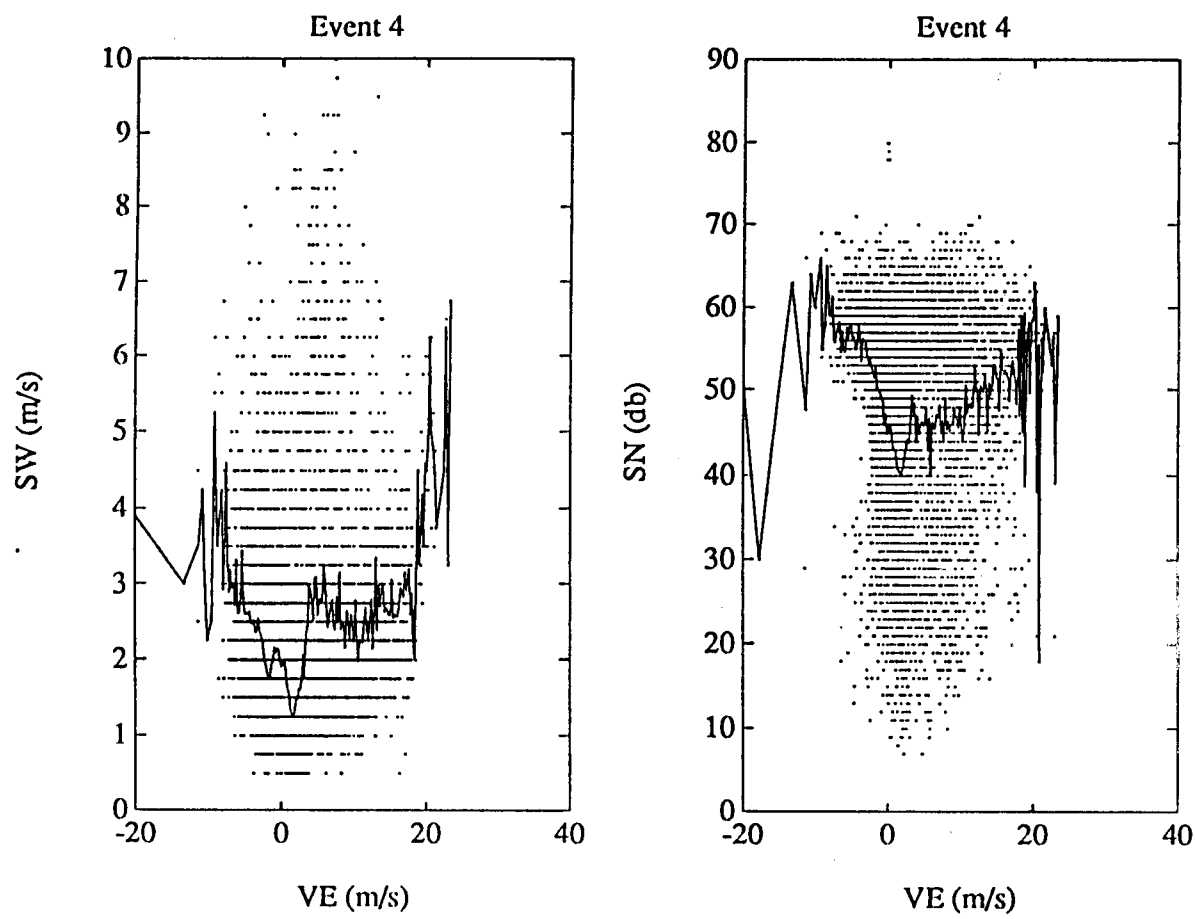


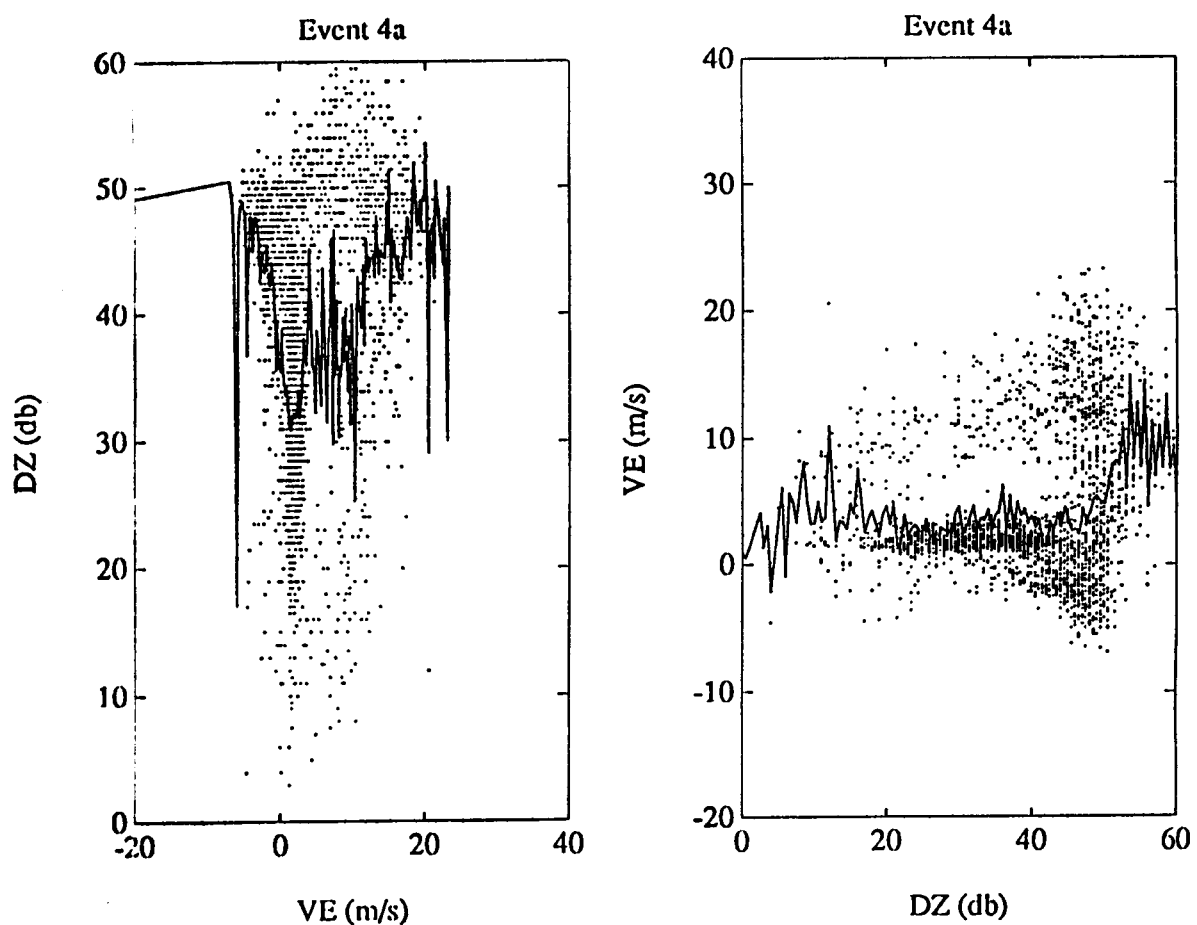
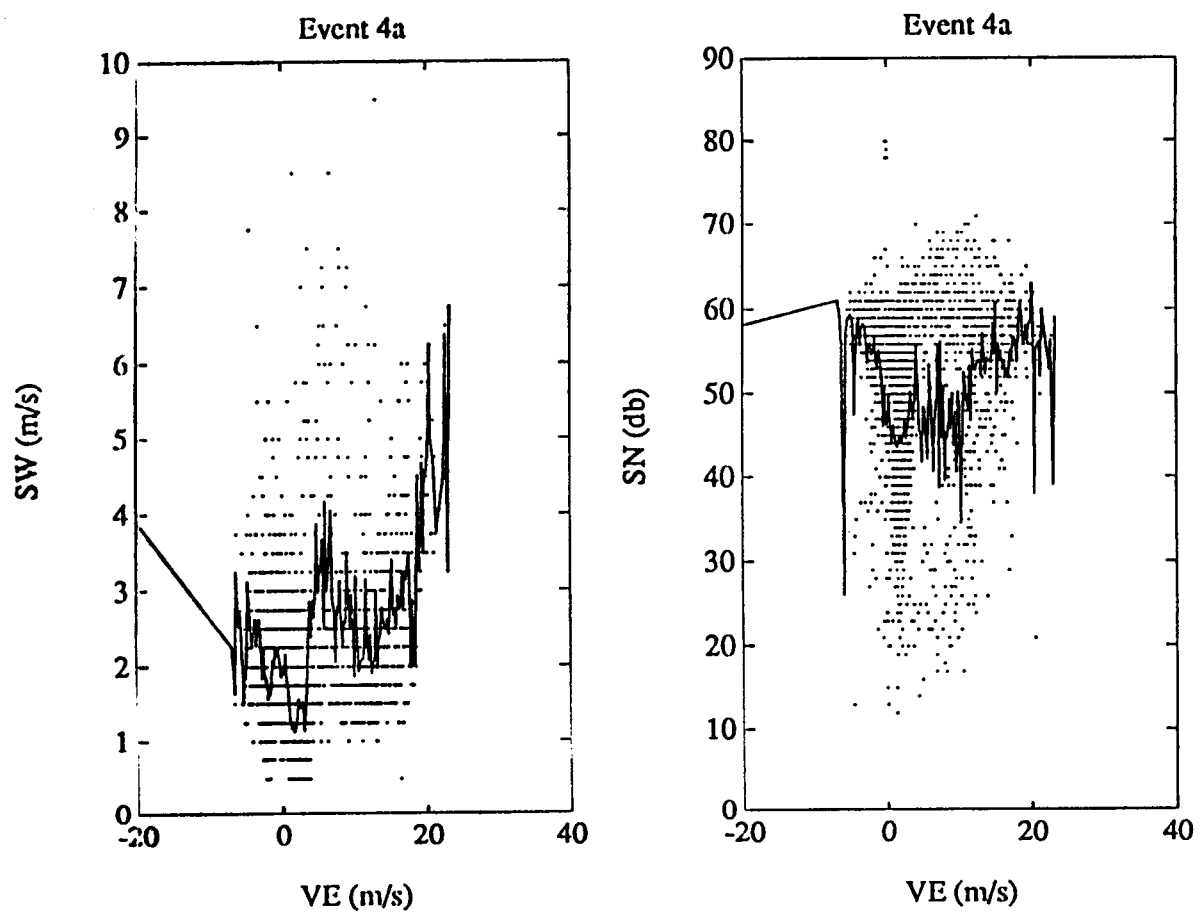


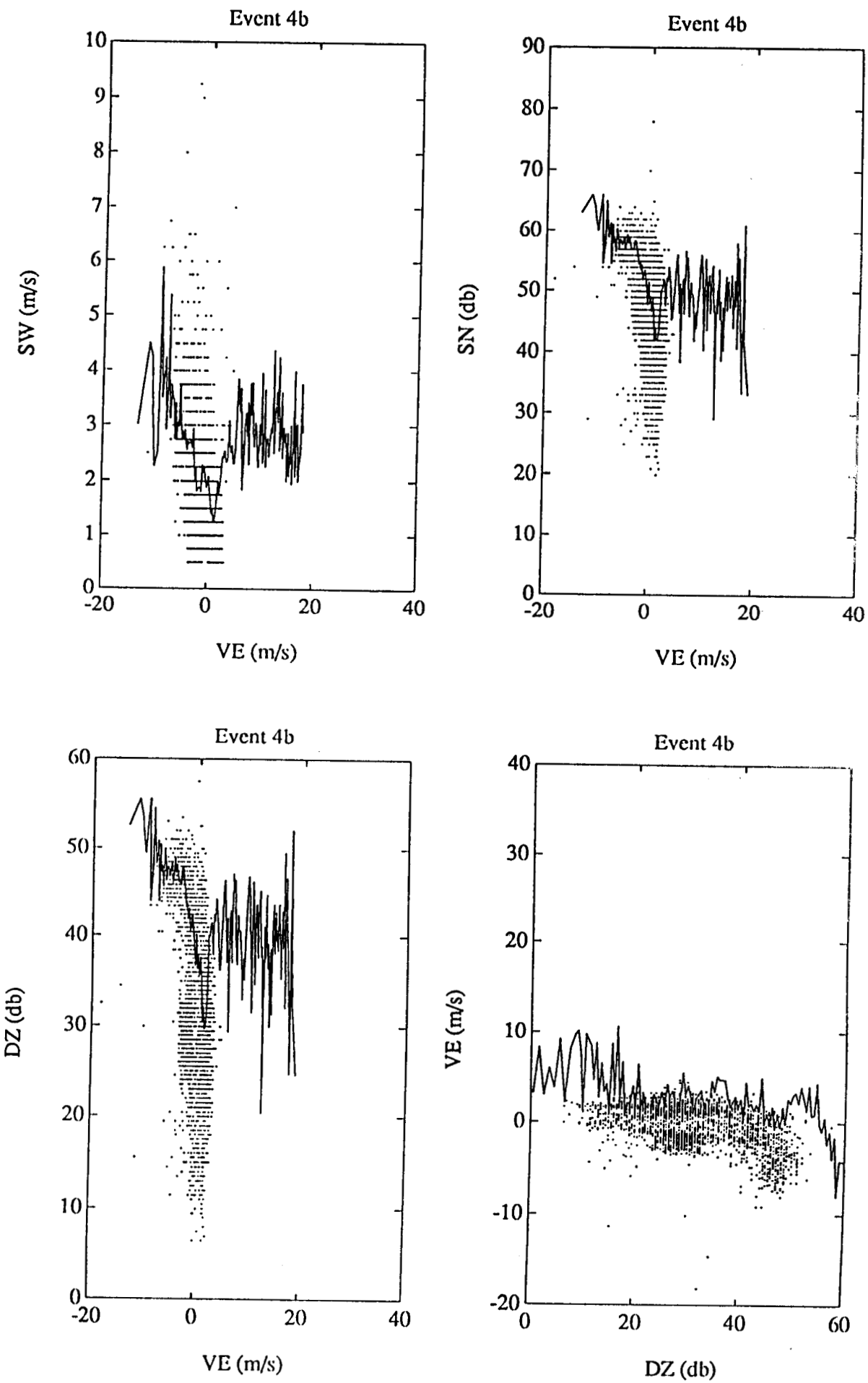


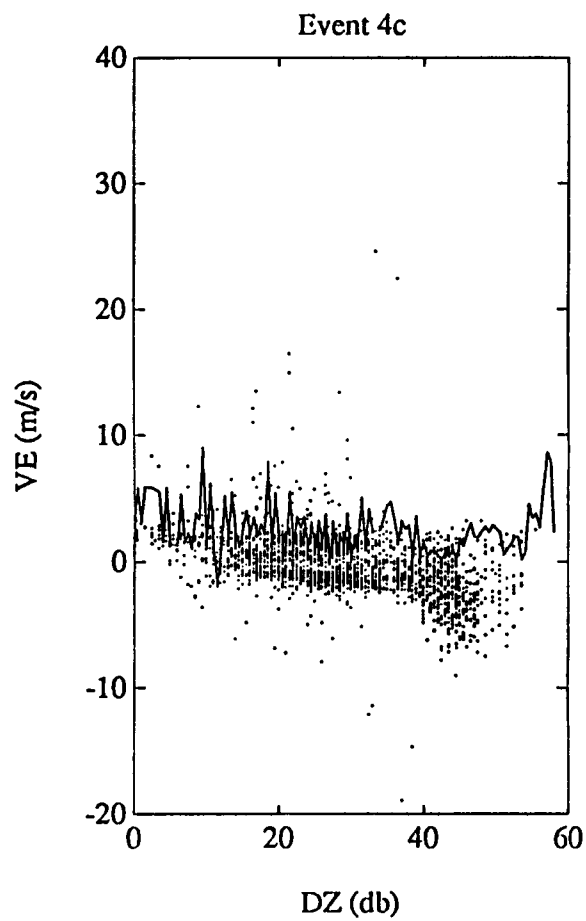
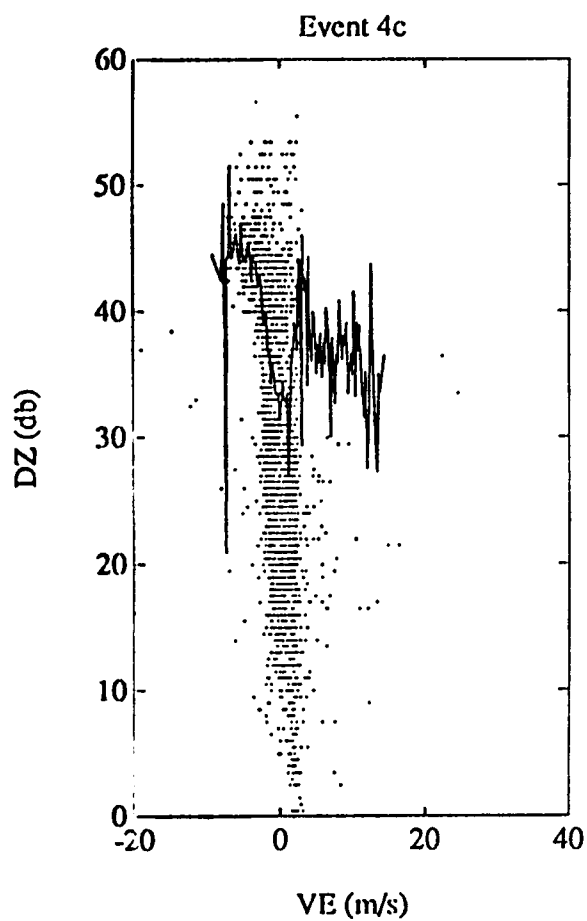
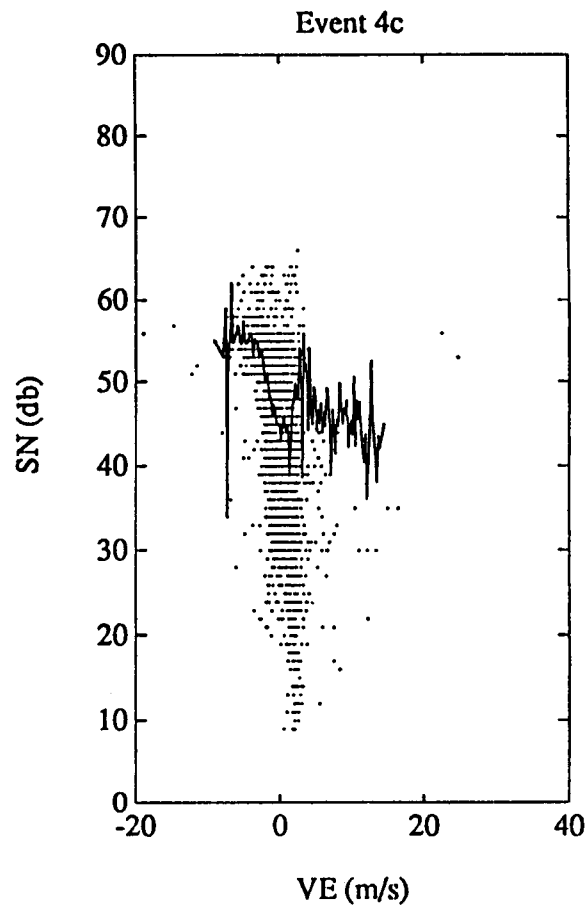
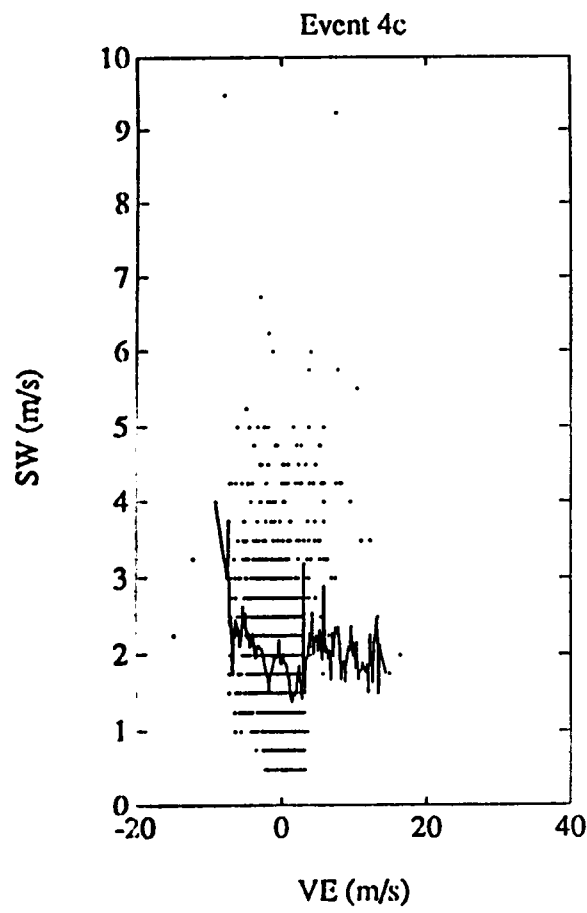


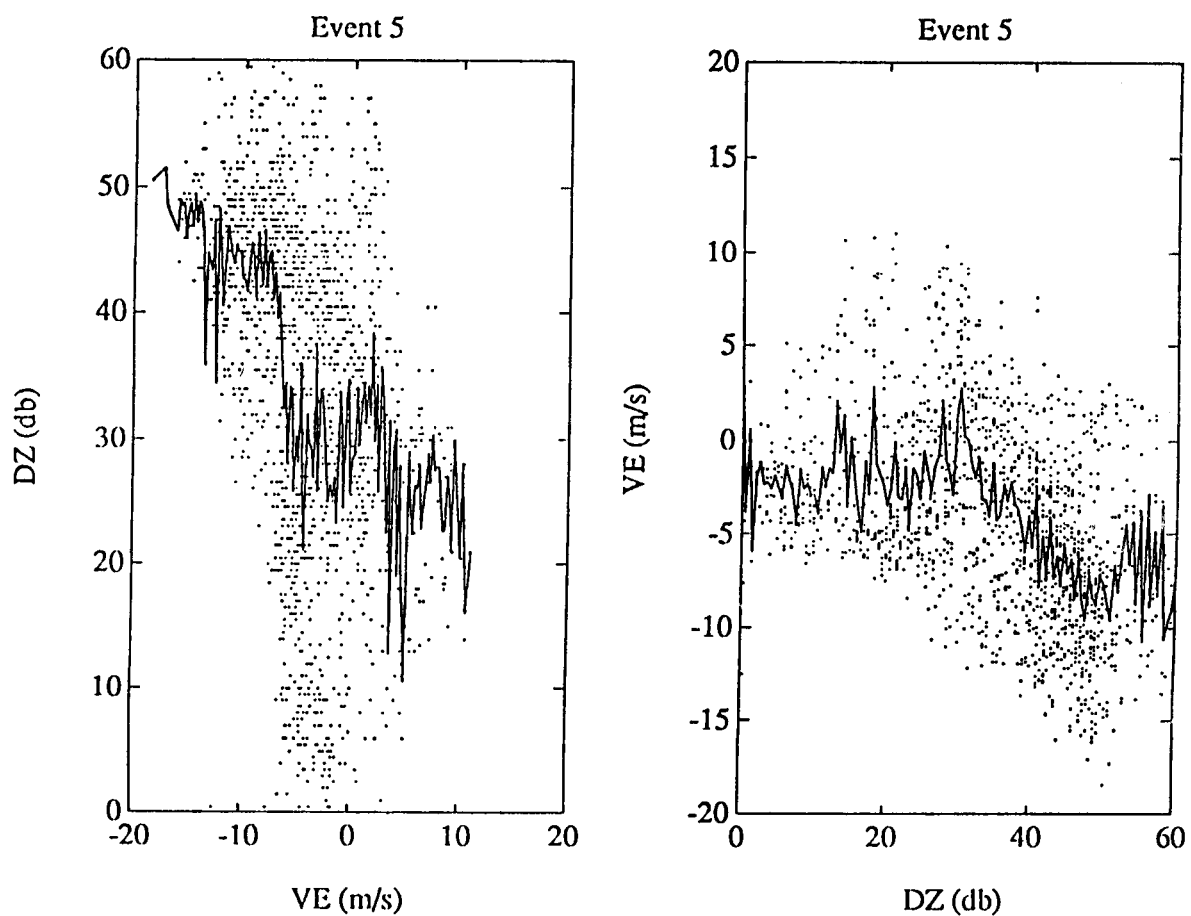
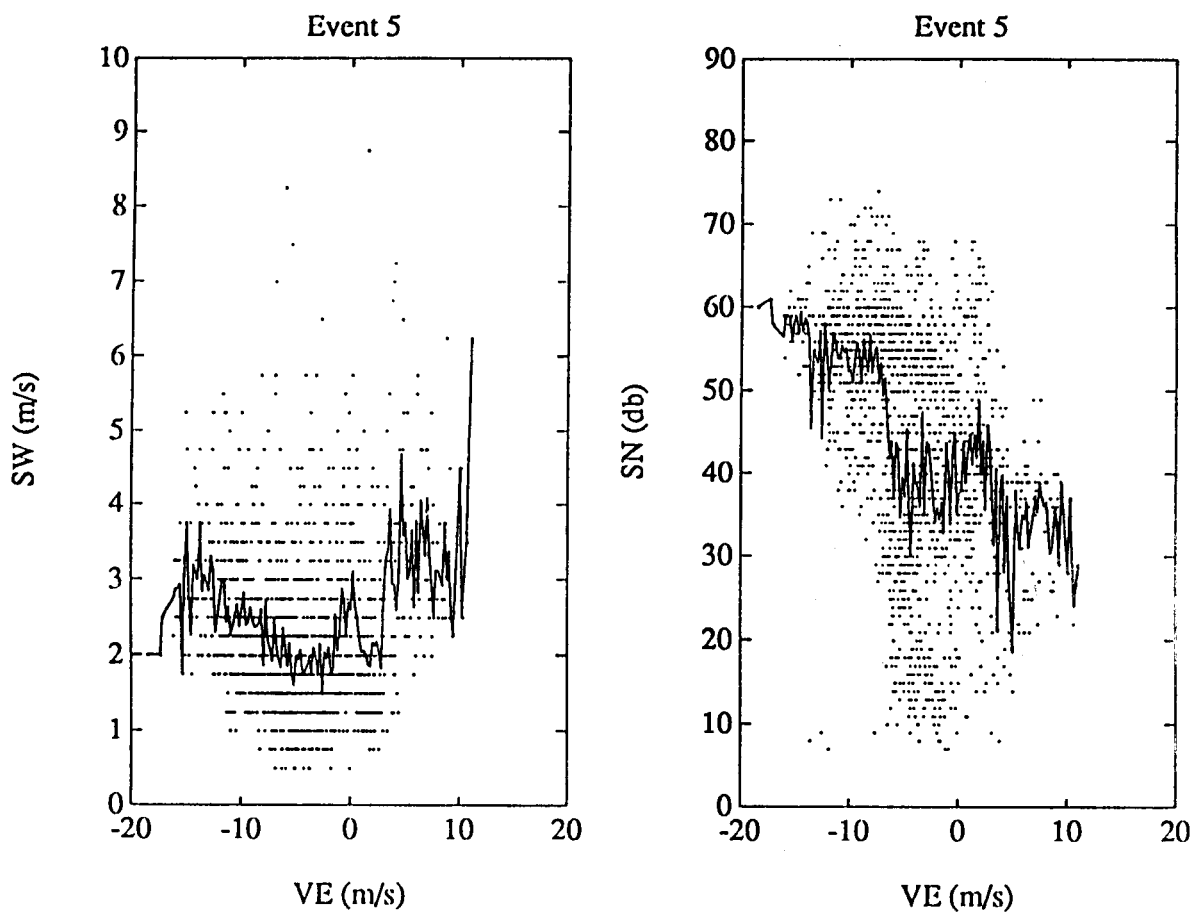


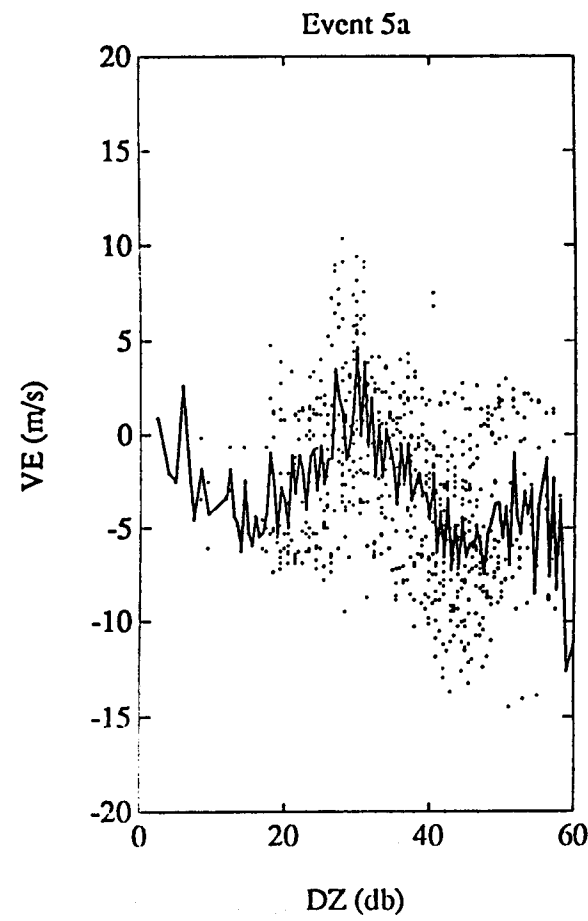
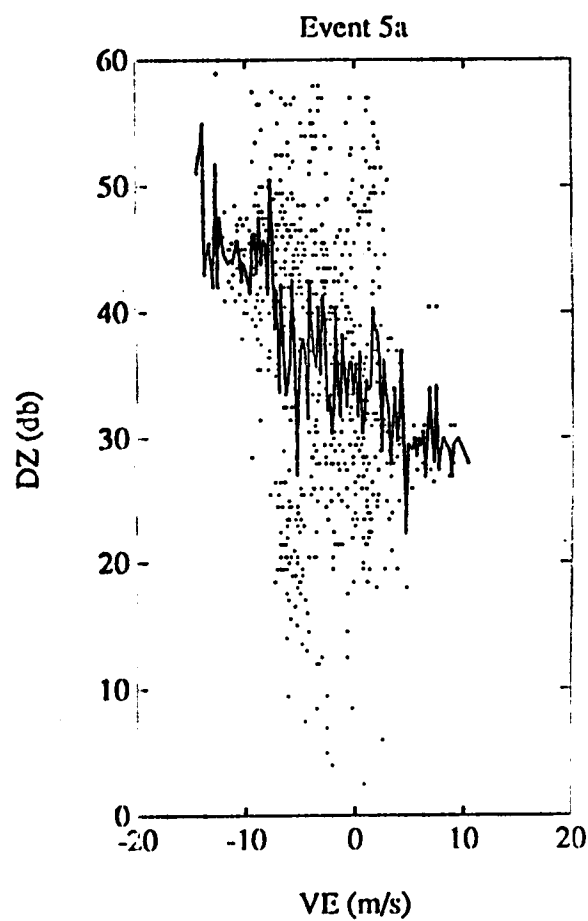
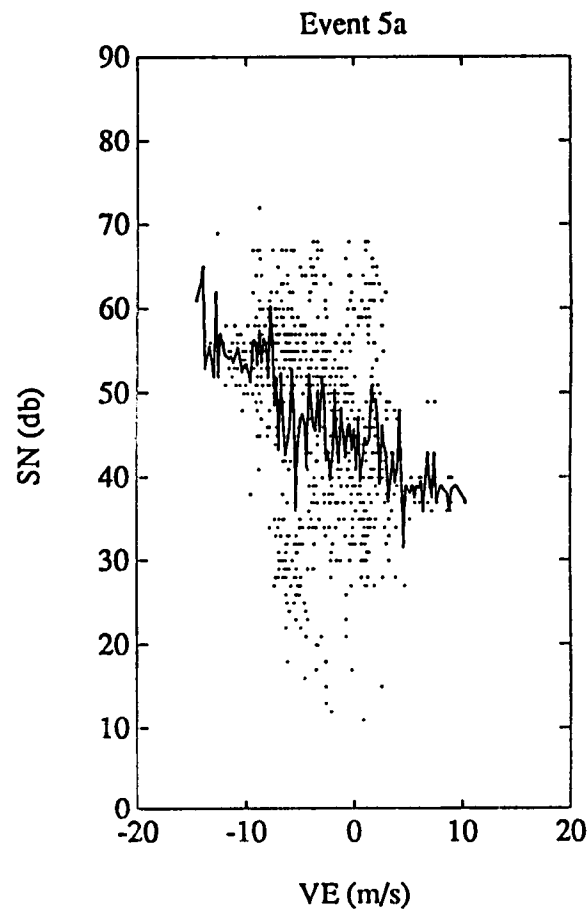
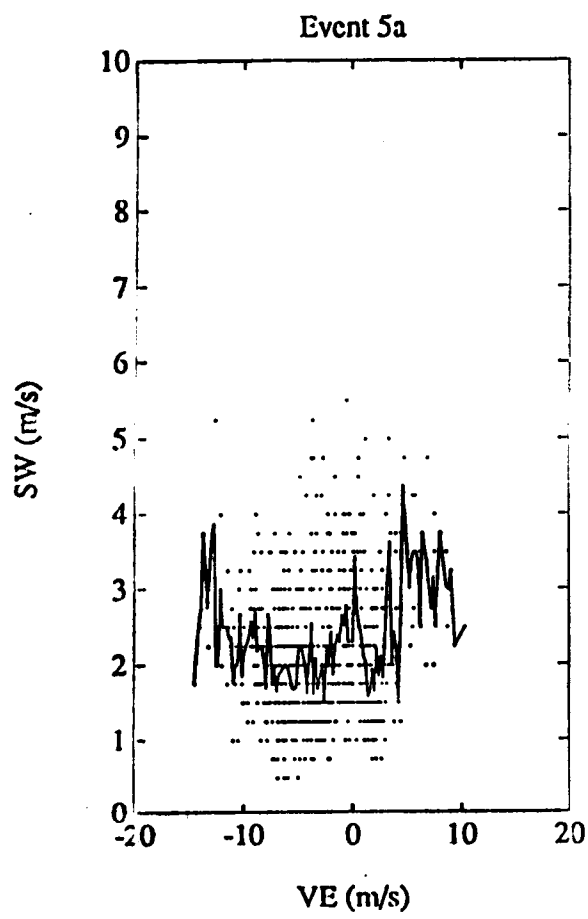


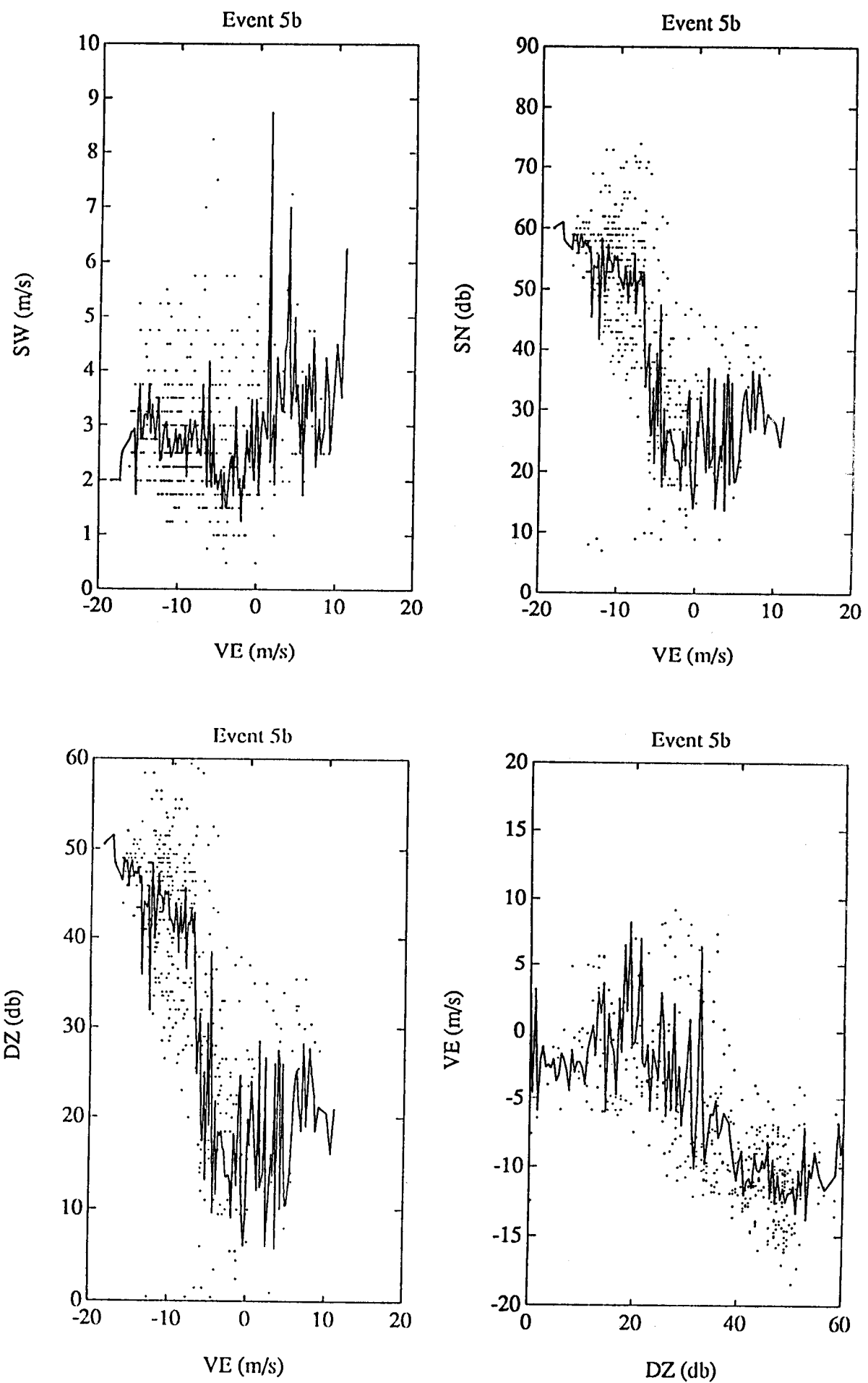


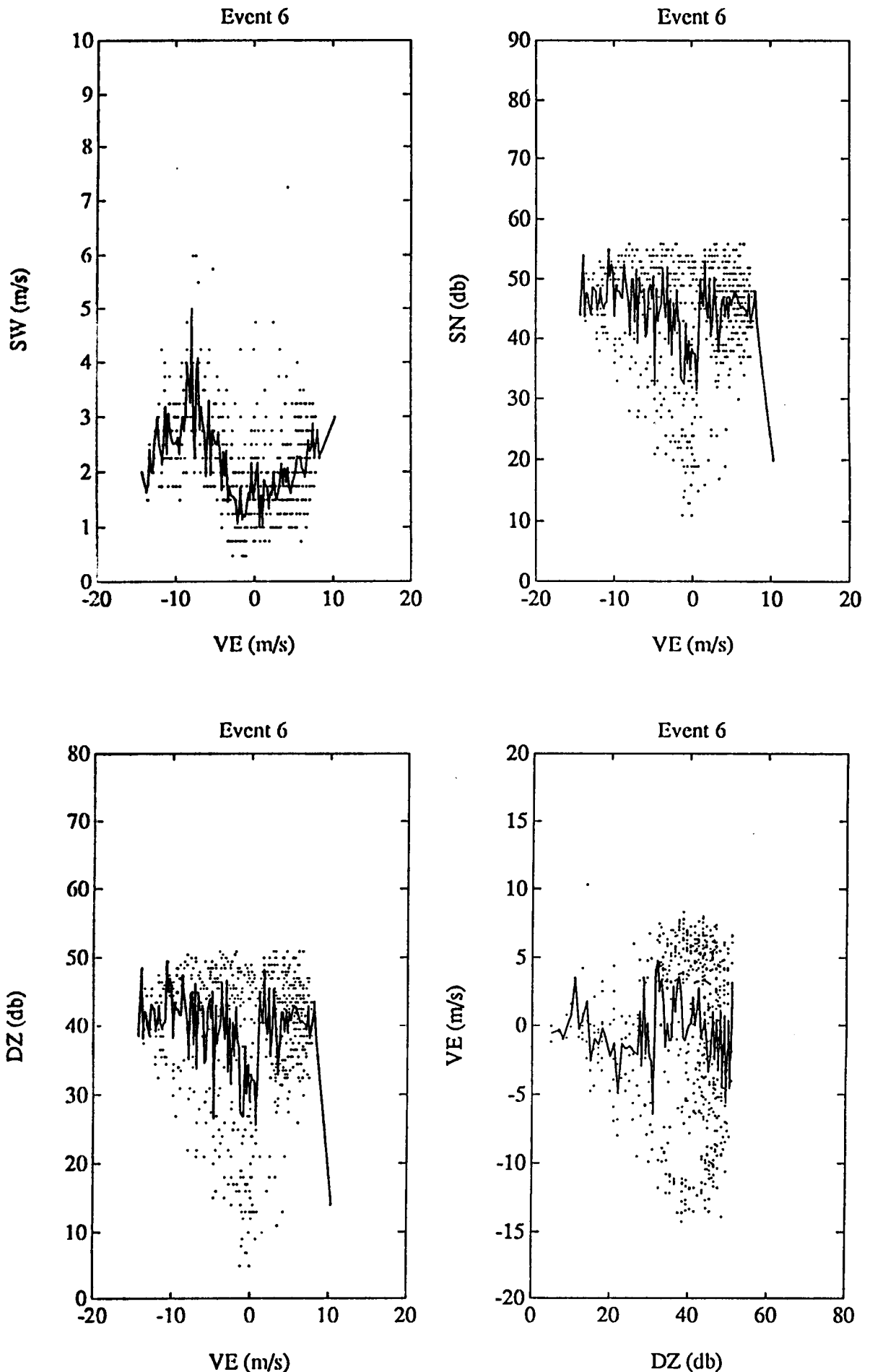


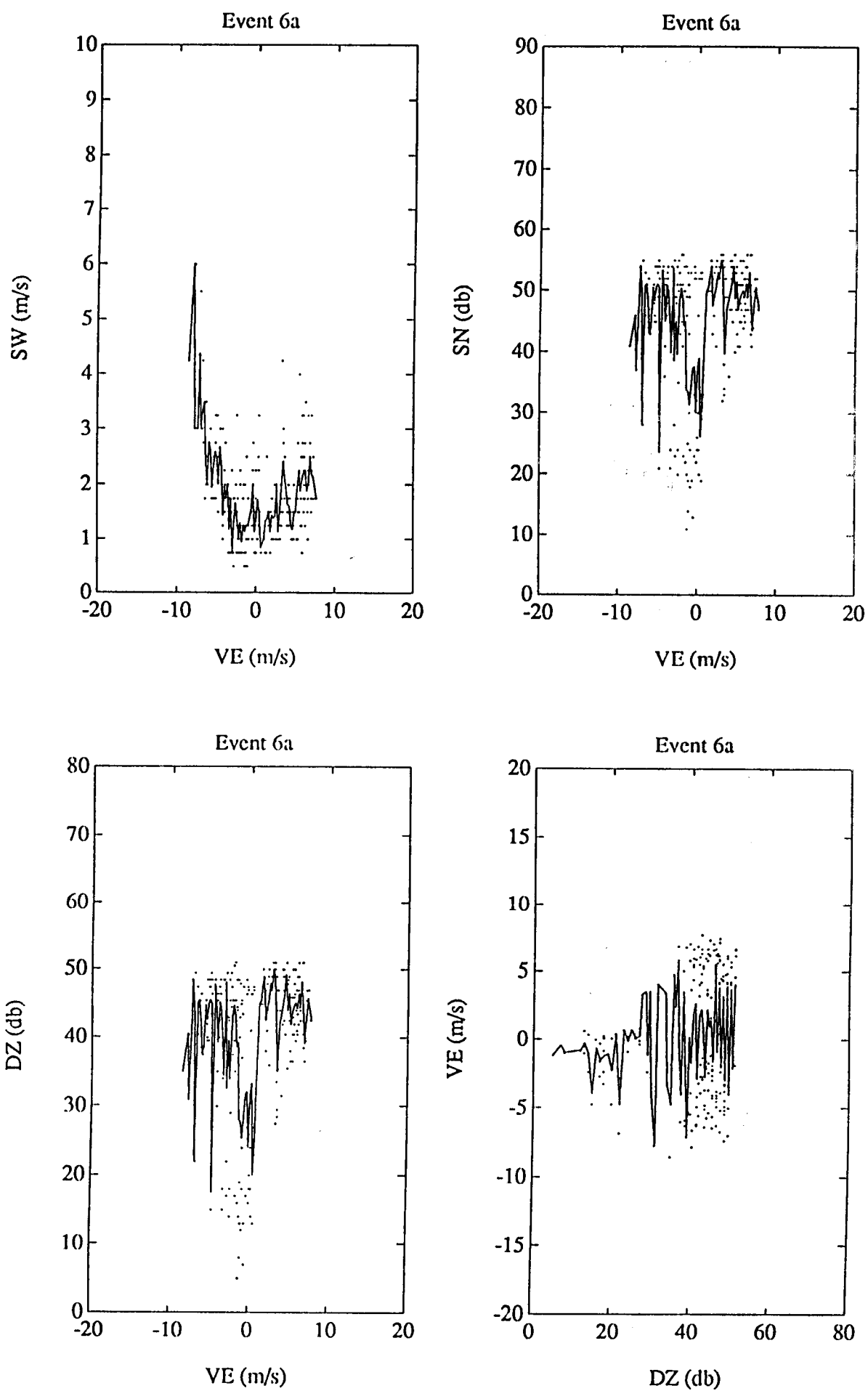


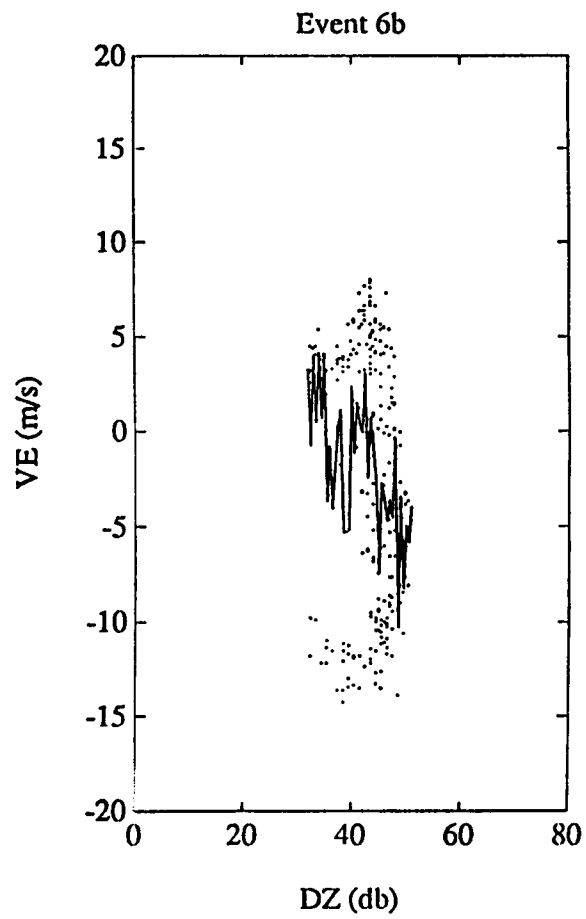
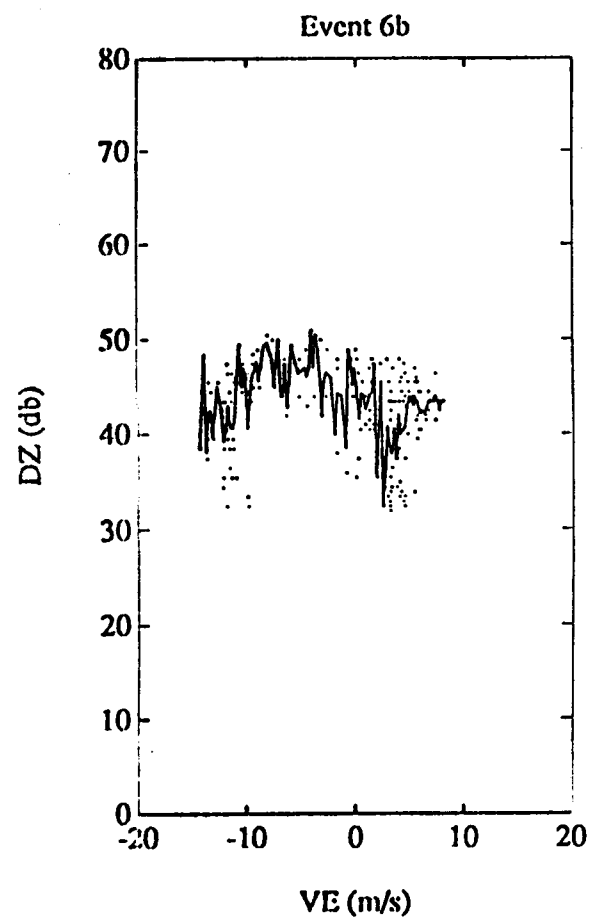
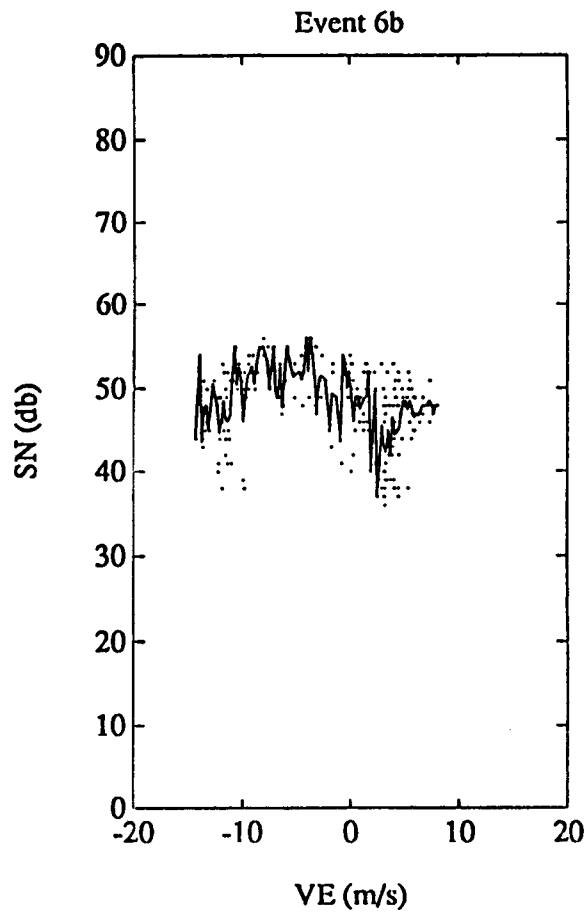
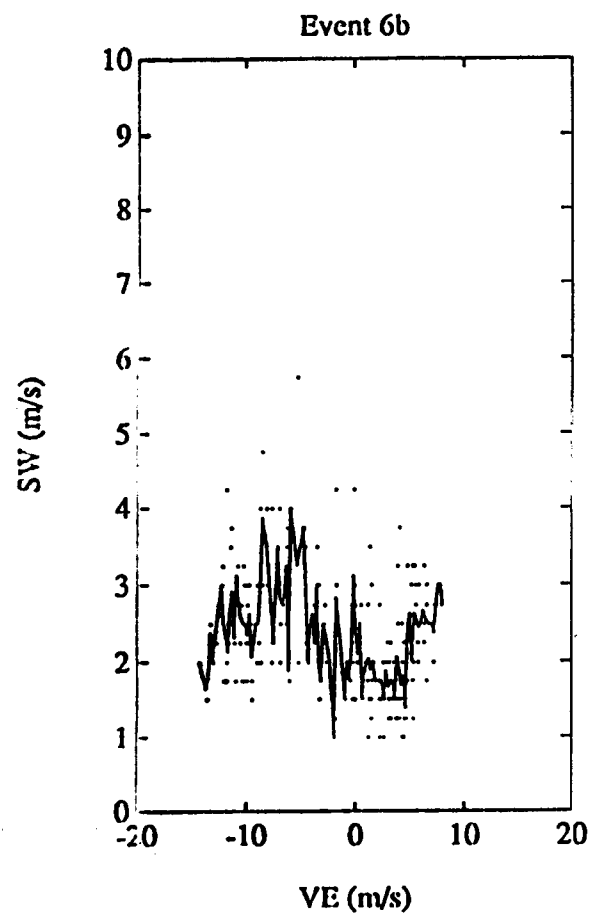


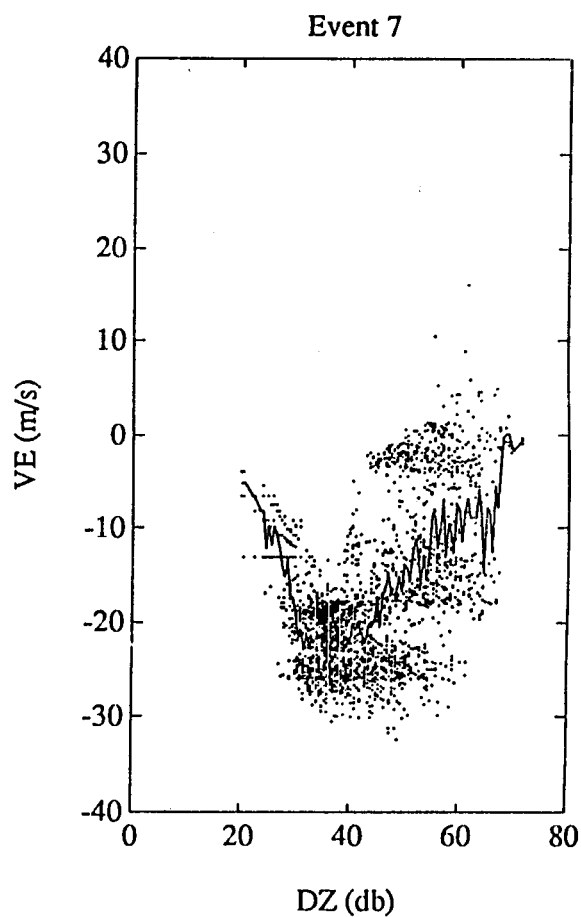
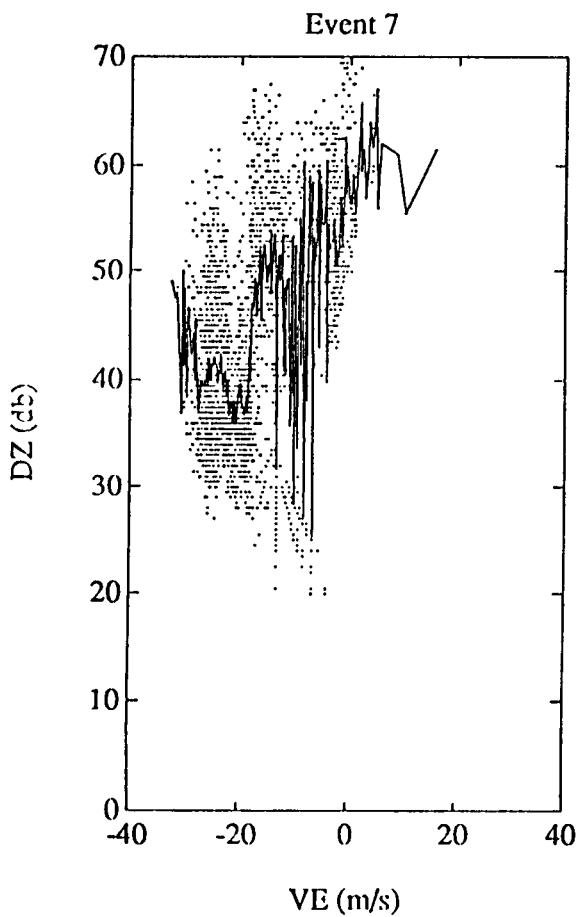
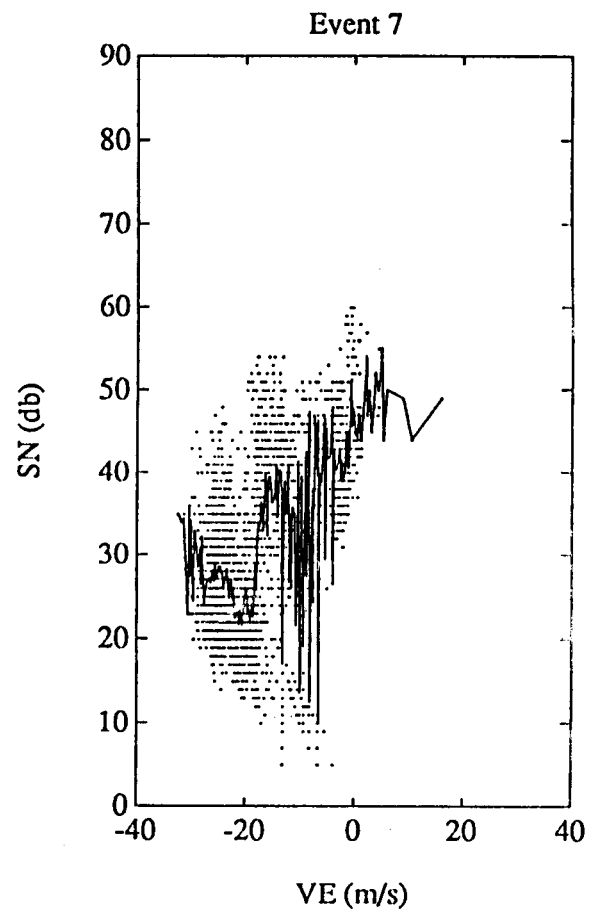
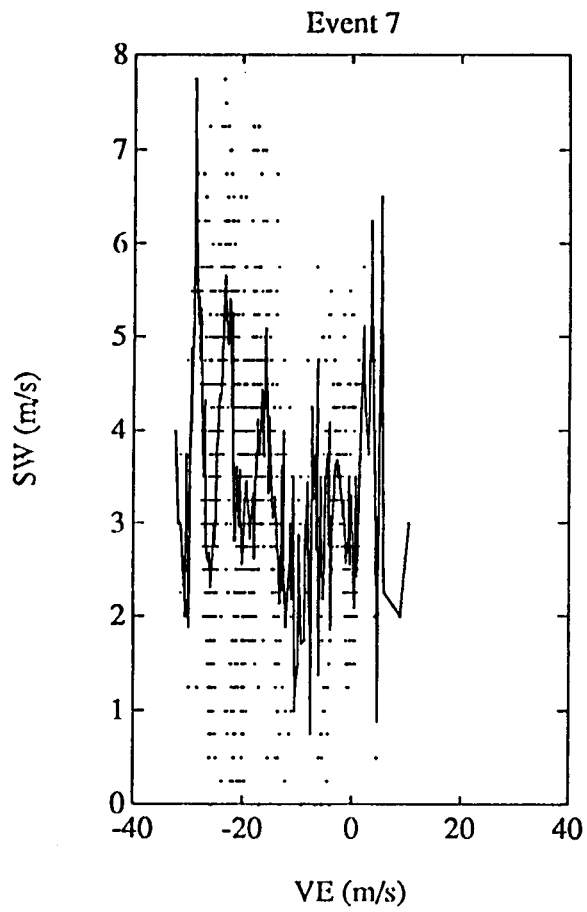


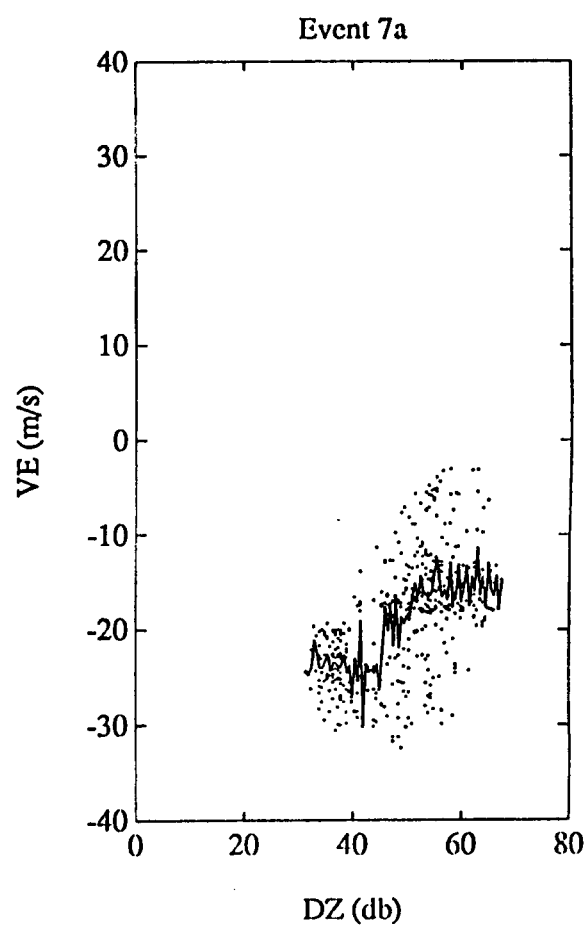
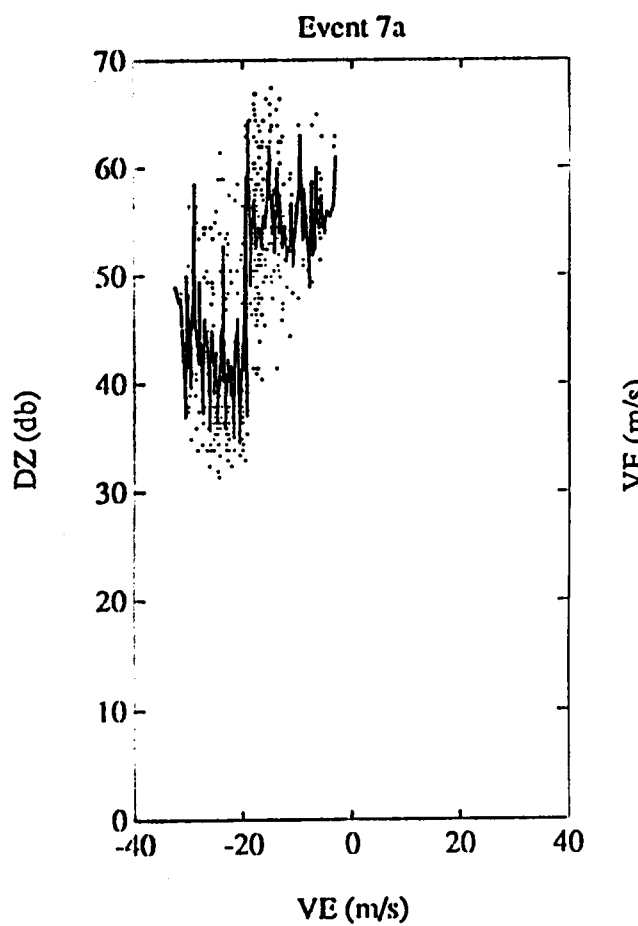
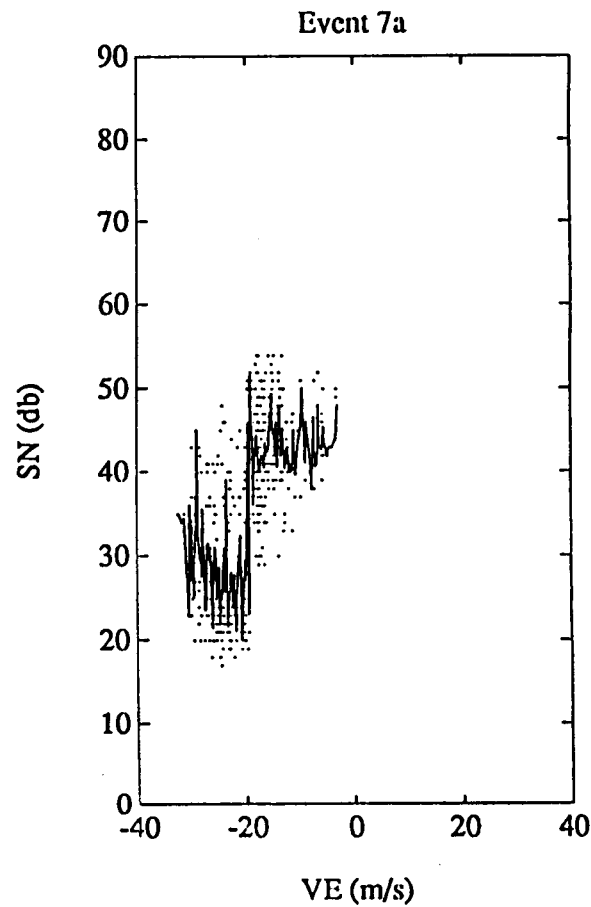
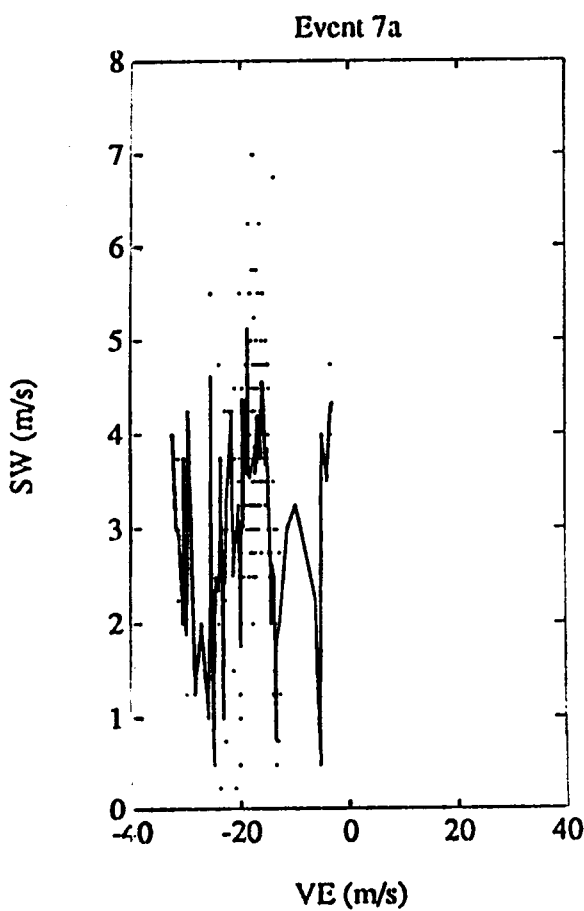


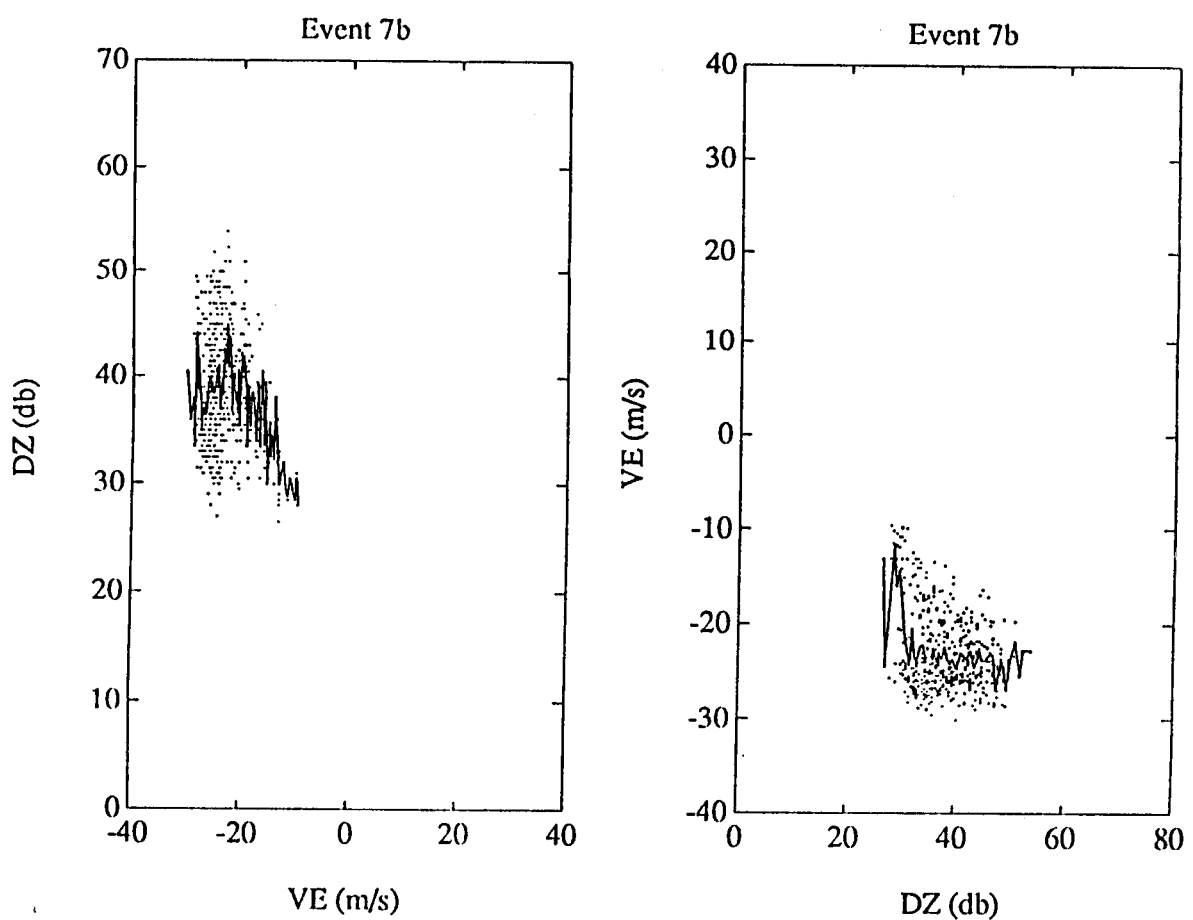
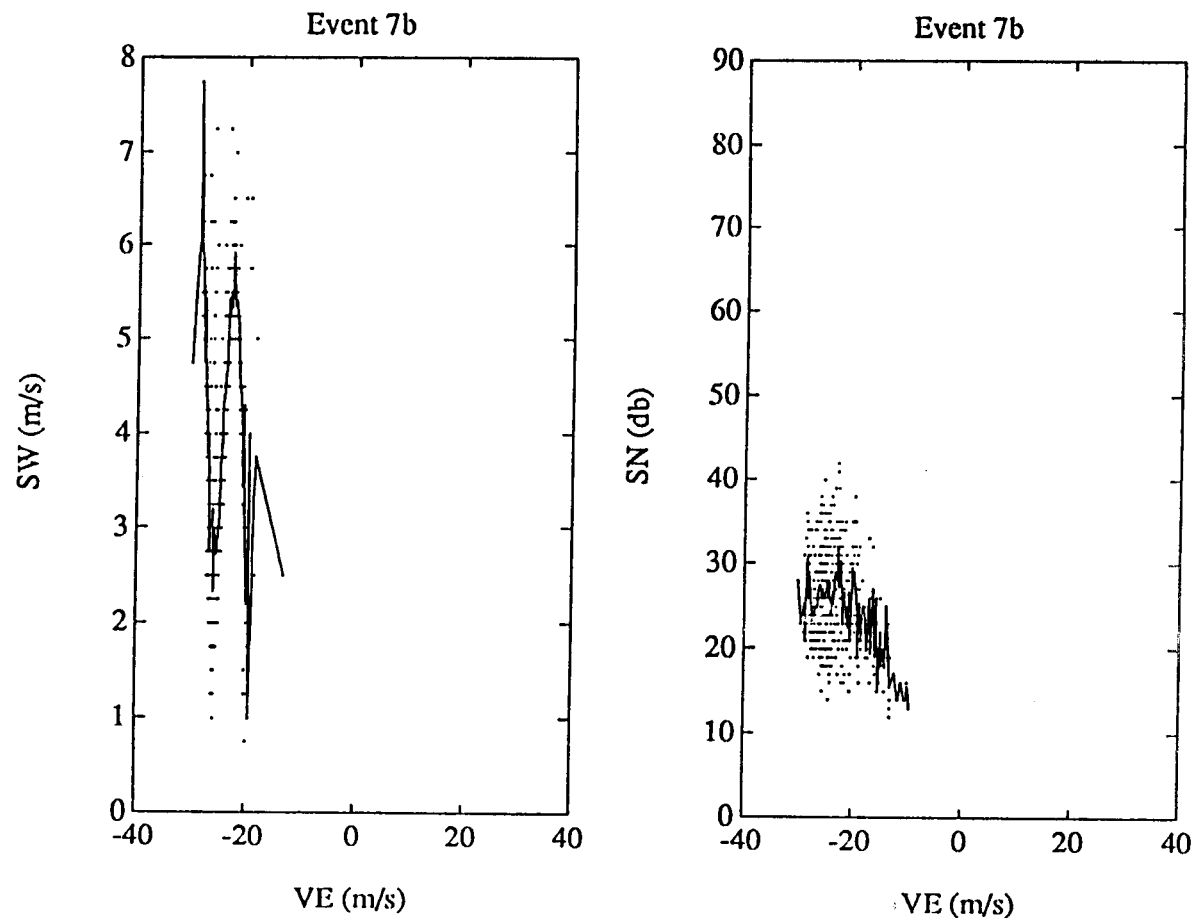


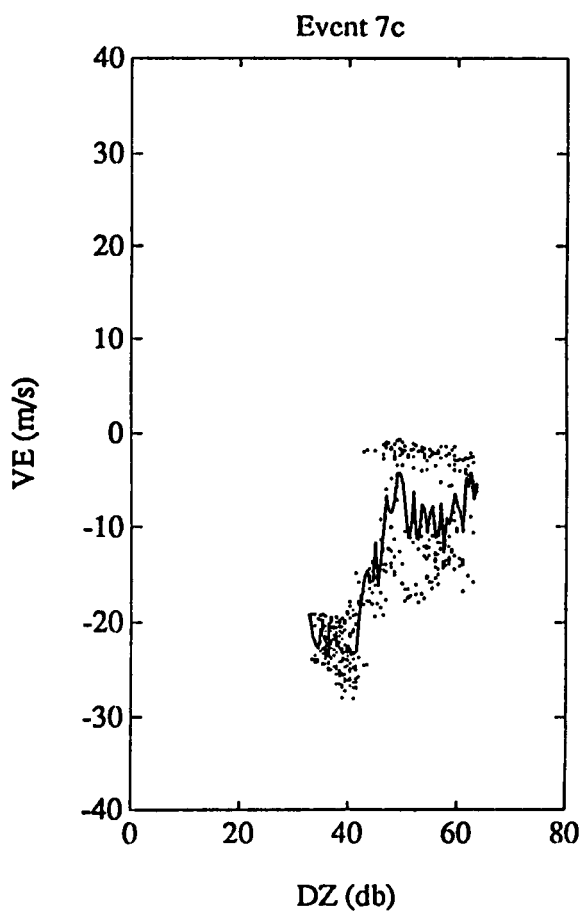
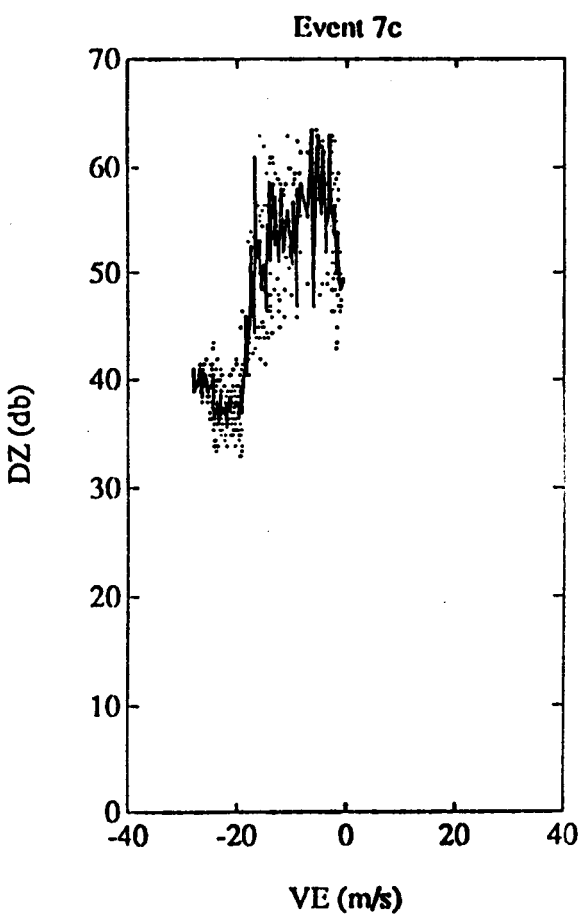
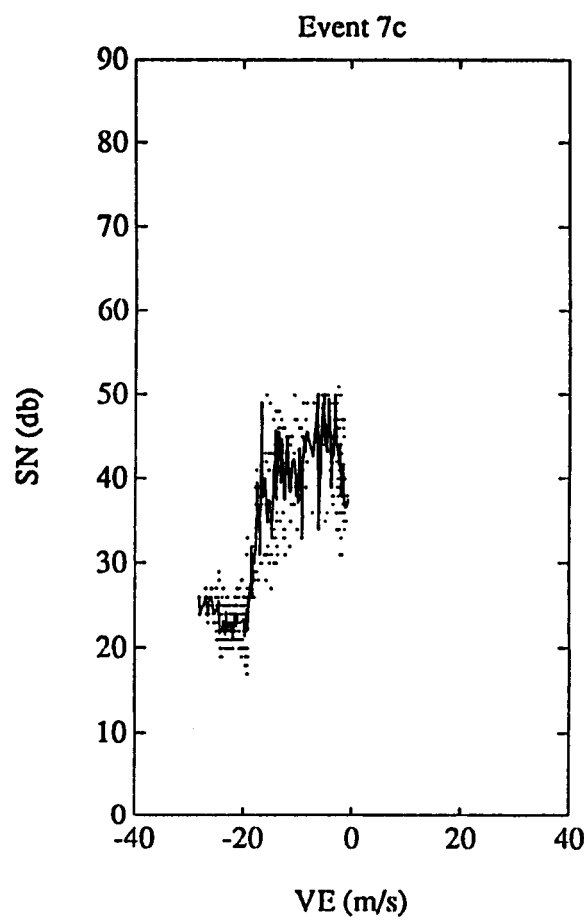
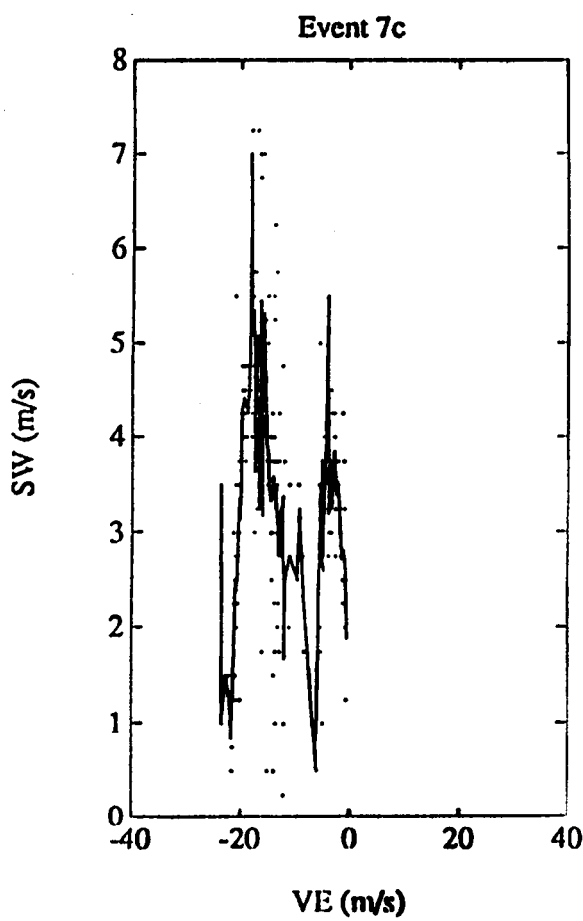


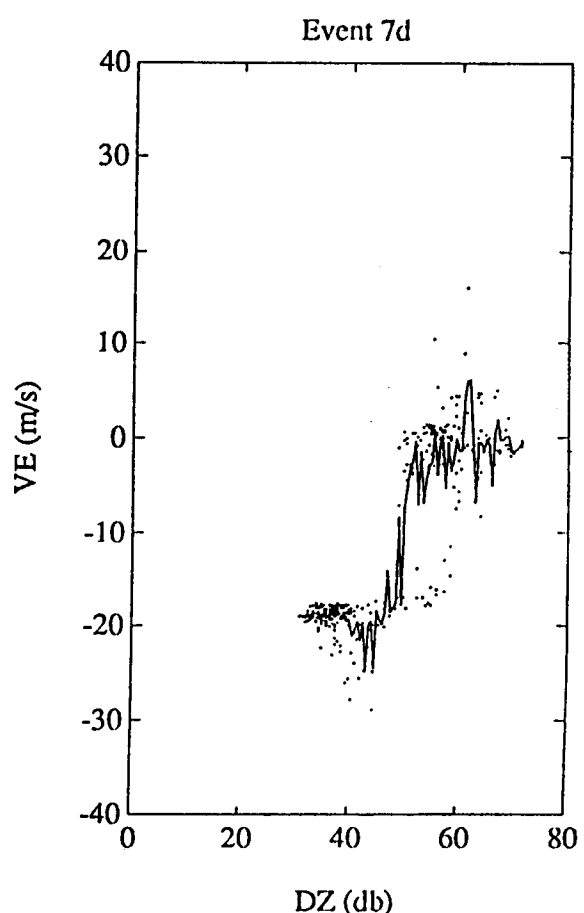
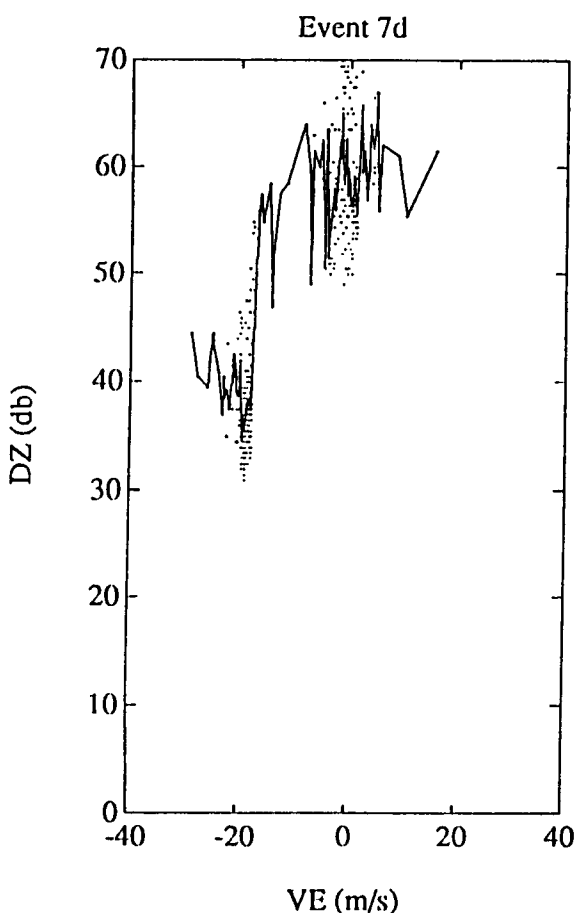
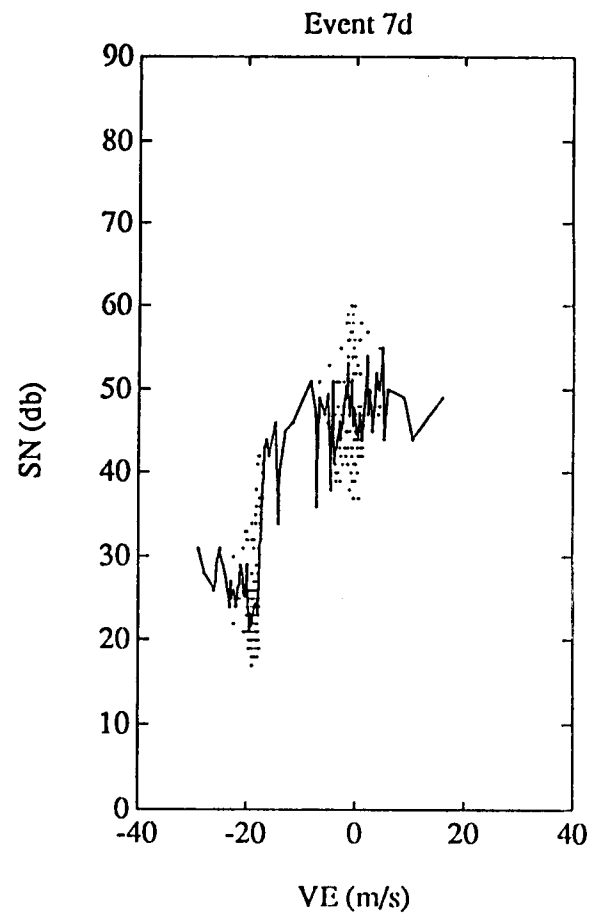
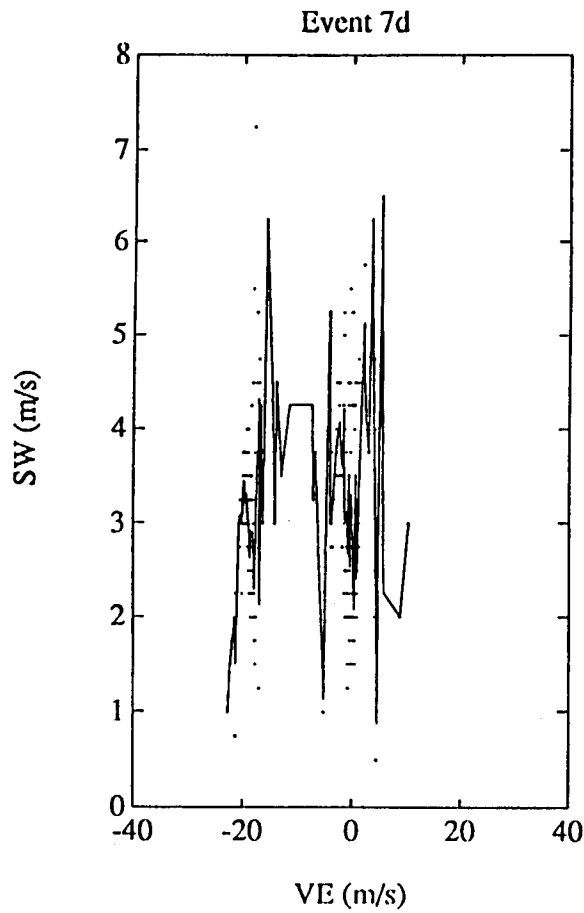


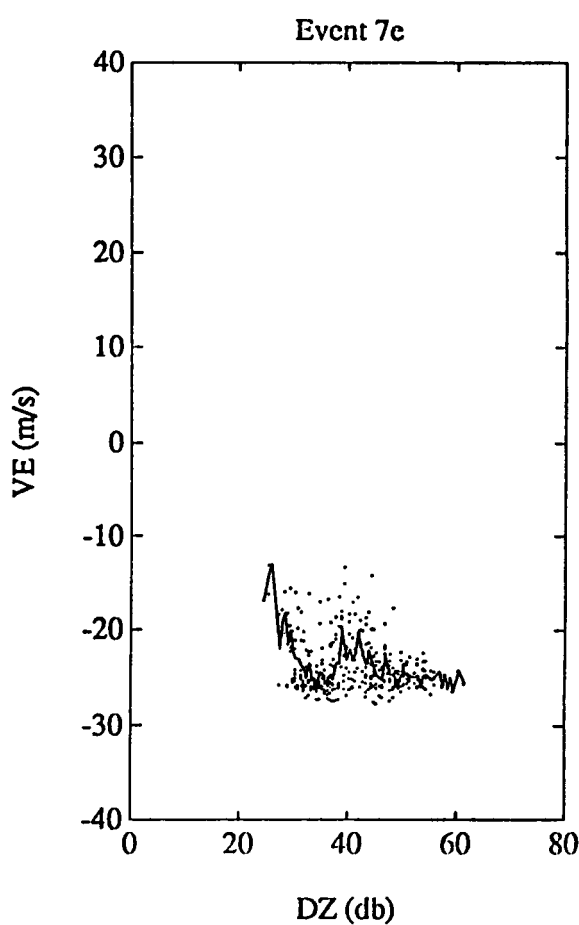
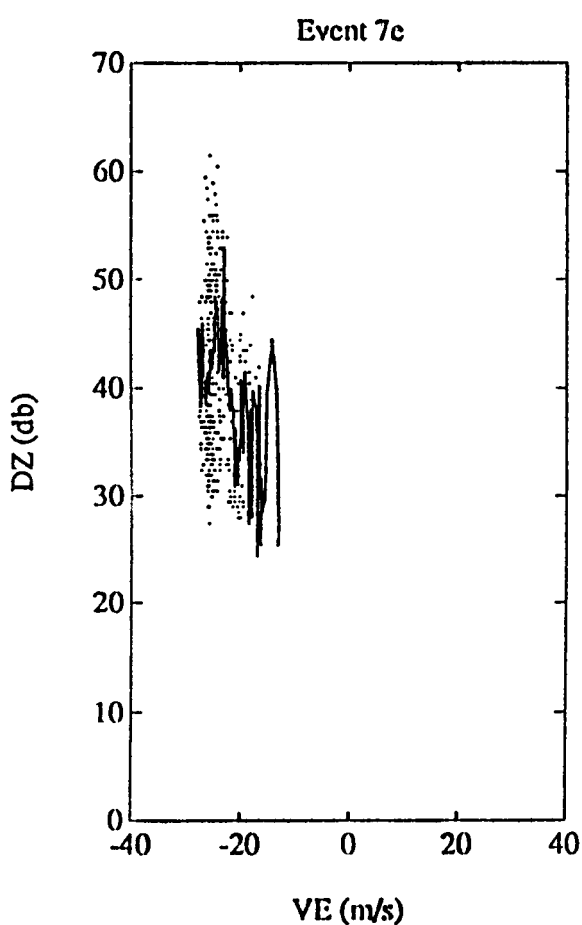
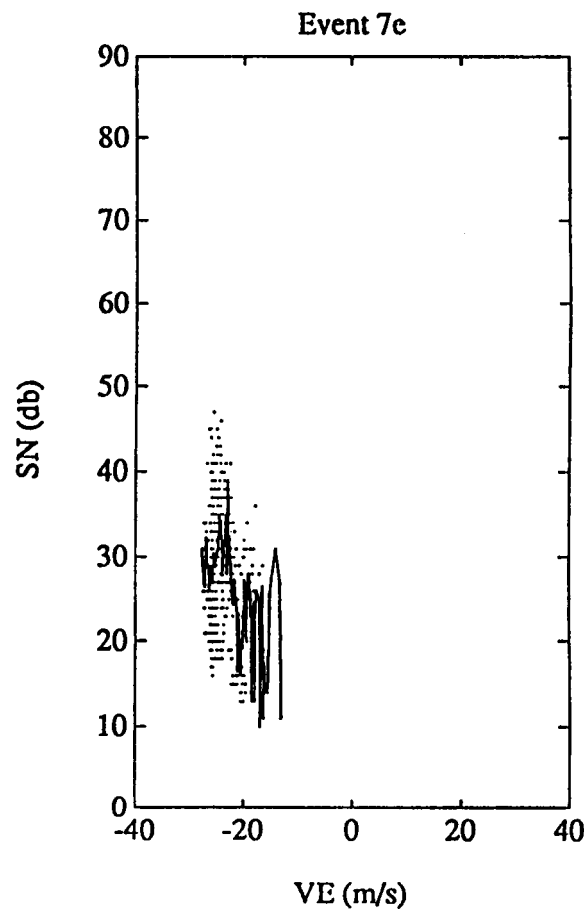
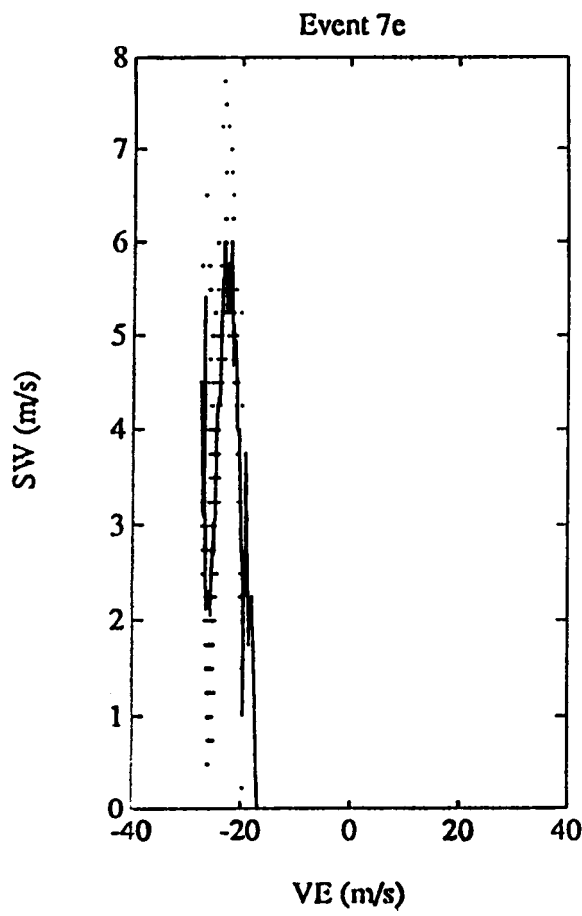


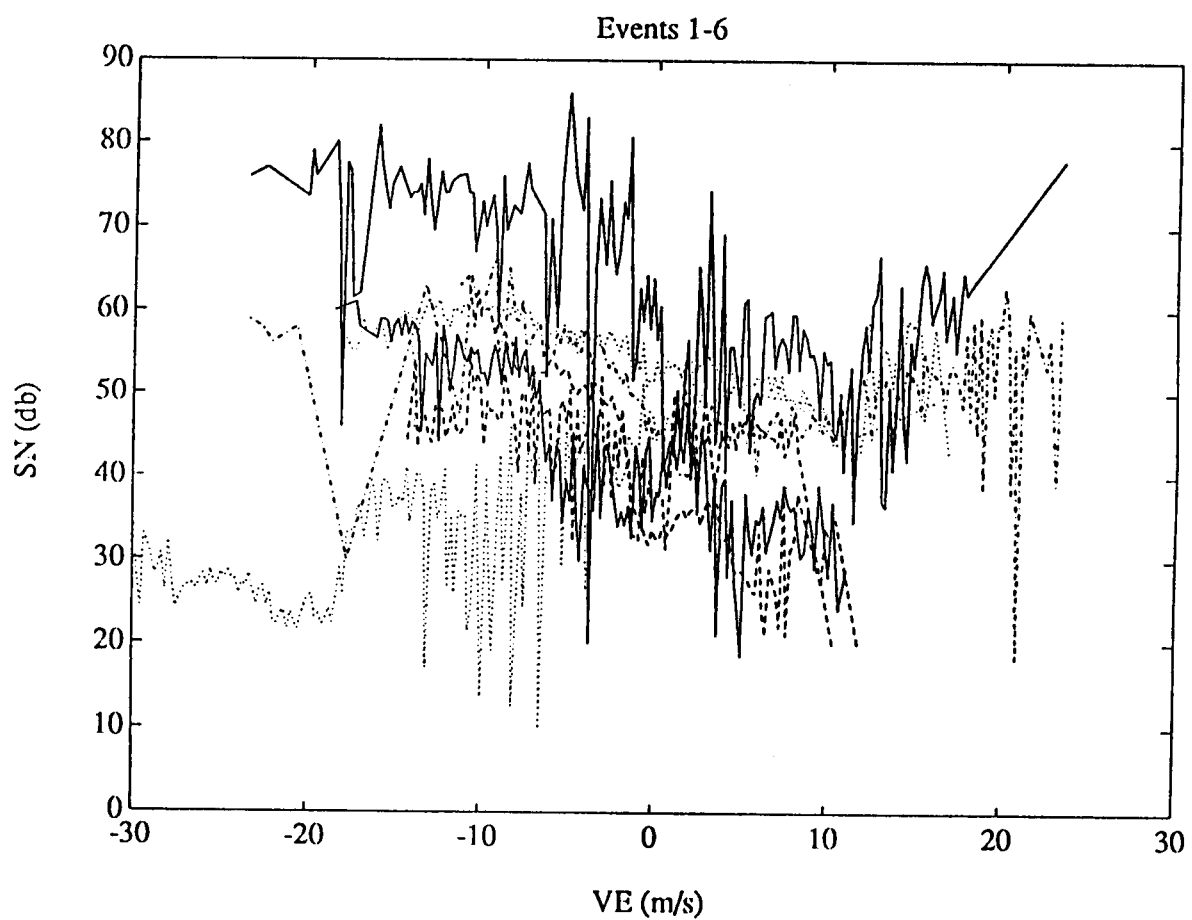
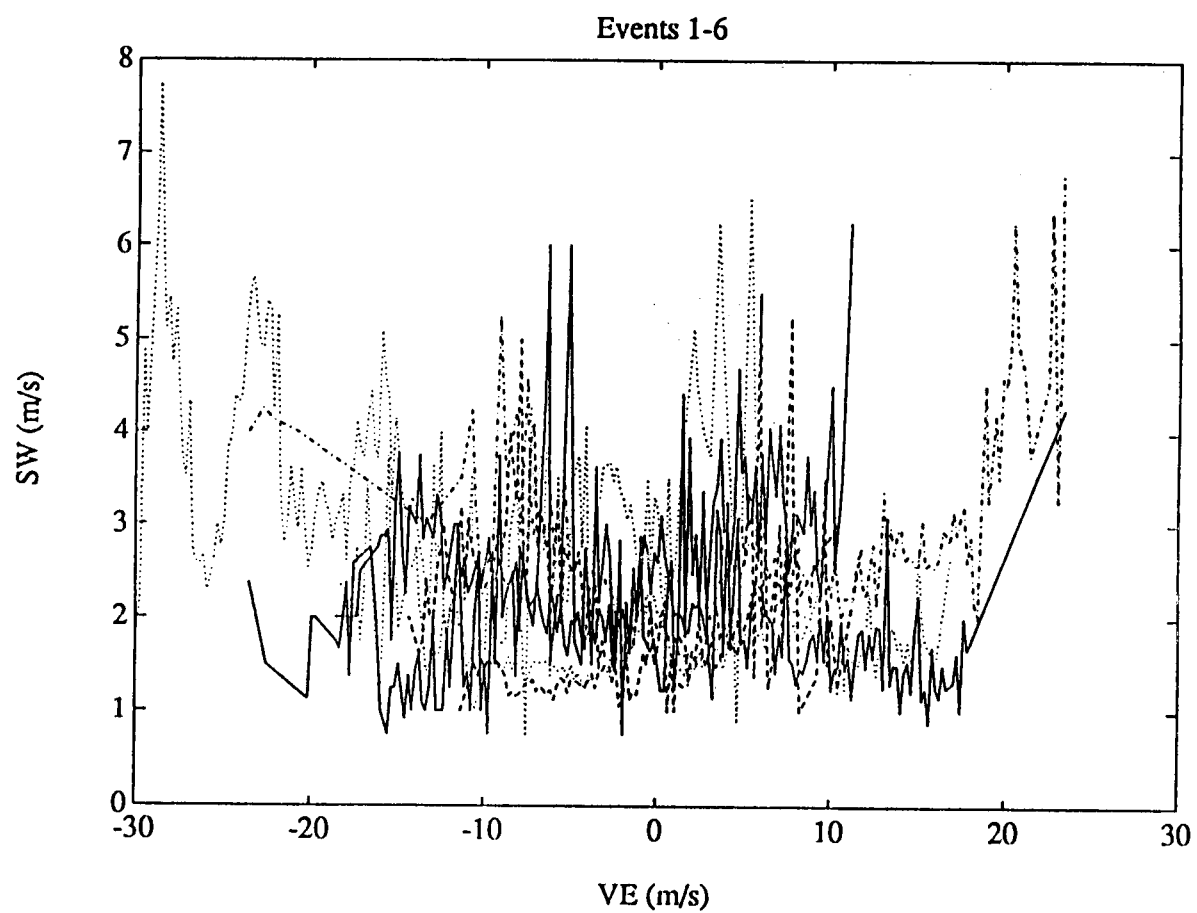




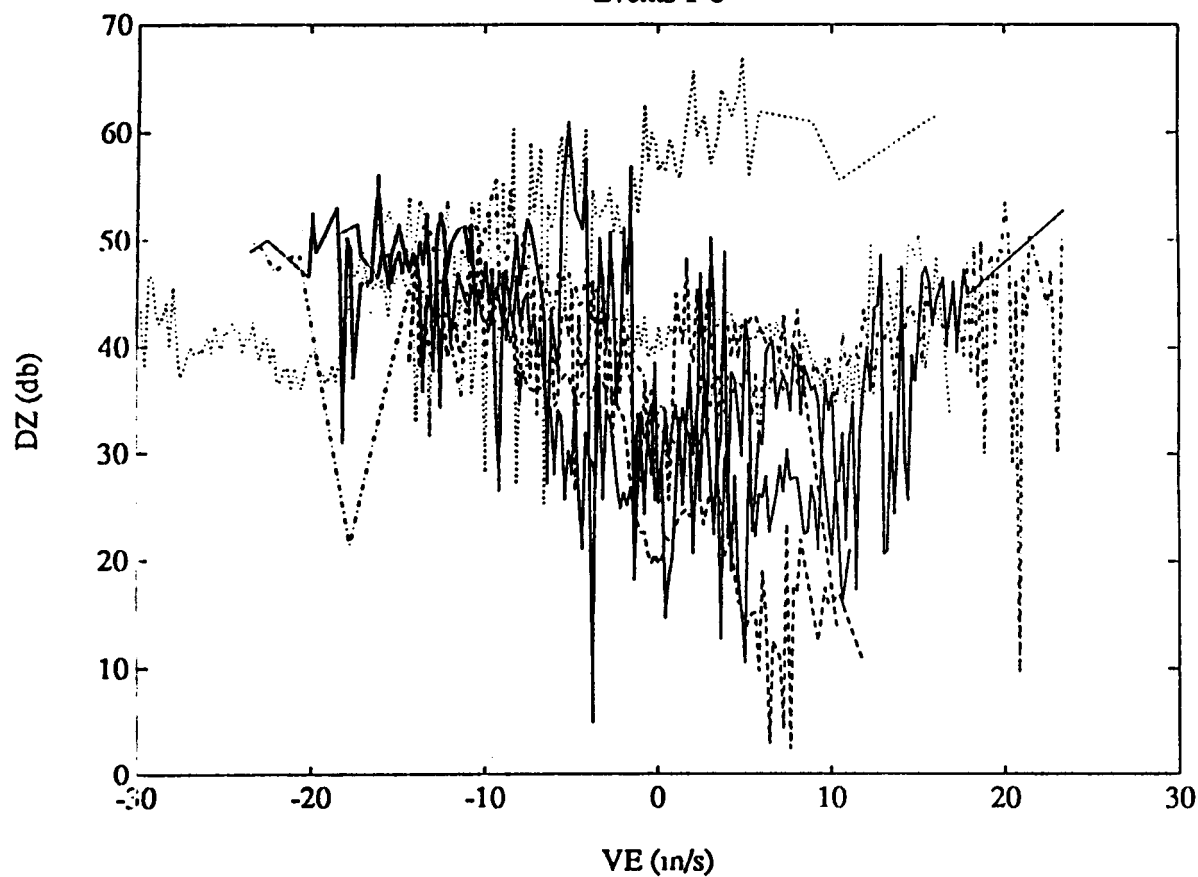




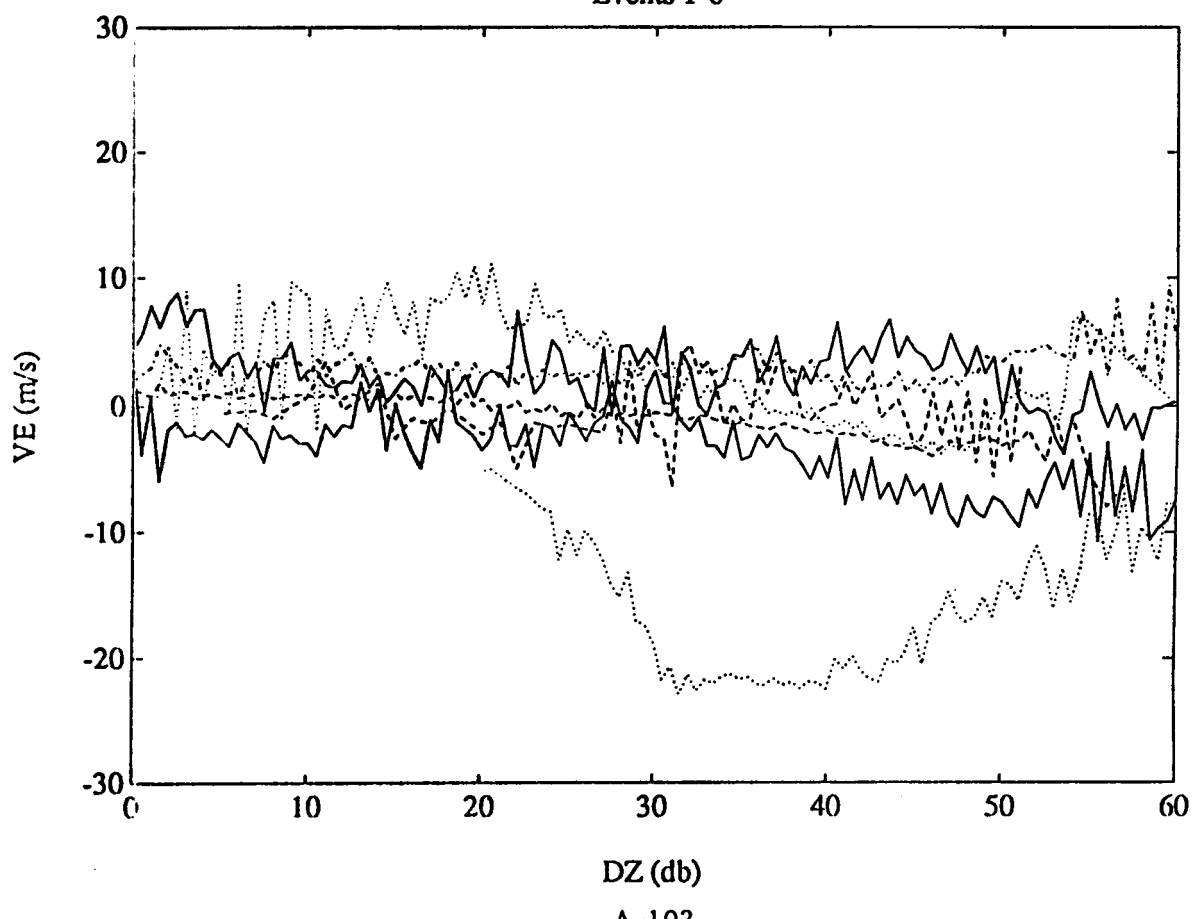




Events 1-6



Events 1-6





Report Documentation Page

1. Report No. NASA CR-181762 DOT/FAA/PS-88/19	2. Government Accession No.	3. Recipient's Catalog No.	
4. Title and Subtitle Analysis of Doppler Radar Windshear Data		5. Report Date January 1989	
7. Author(s) F. Williams, P. McKinney, and F. Ozmen		6. Performing Organization Code	
9. Performing Organization Name and Address Sierra Nevada Corporation Box 6900 Reno, NV 89513		8. Performing Organization Report No.	
12. Sponsoring Agency Name and Address National Aeronautics and Space Administration Langley Research Center Hampton, VA 23665-5225		10. Work Unit No. 505-67-41-51	
		11. Contract or Grant No. NAS1-18598	
		13. Type of Report and Period Covered Contractor Report	
		14. Sponsoring Agency Code	
15. Supplementary Notes Langley Technical Monitor: E. M. Bracalente Final Report			
16. Abstract The objective of this analysis is to process Lincoln Laboratory doppler radar data obtained during FLOWS testing at Huntsville, Alabama, in the summer of 1986, to characterize windshear events. The processing includes plotting velocity and F-factor profiles, histogram analysis to summarize statistics, and correlation analysis to demonstrate any correlation between different data fields.			
17. Key Words (Suggested by Author(s)) Windshear F-factor Spectral width microburst		18. Distribution Statement Unclassified - Unlimited Subject Category 03	
19. Security Classif. (of this report) Unclassified	20. Security Classif. (of this page) Unclassified	21. No. of pages 188	22. Price A09